



THE UNIVERSITY  
*of* ADELAIDE

Oxygen isotope and elemental  
ratios in waters and bivalves as  
tracers of hydrological change  
in the modern and past waters  
of the Coorong Lagoons, South  
Australia

Briony Kate Chamberlayne

Department of Earth Sciences  
School of Physical Sciences  
The University of Adelaide

This thesis is submitted in fulfilment of the requirements for the  
degree of Doctor of Philosophy

June 2021



---

**TABLE OF CONTENTS**

---

<b>Thesis declaration</b>	<b>iv</b>
<b>Thesis abstract</b>	<b>v</b>
<b>Acknowledgements</b>	<b>vi</b>
<b>Publications during the course of this thesis</b>	<b>vii</b>
<b>Chapter 1: Introduction and thesis outline</b>	<b>1</b>
Introduction	3
Thesis aims	14
Thesis outline	14
References	17
<b>Chapter 2: Environmental controls on the geochemistry of a short-lived bivalve in southeastern Australia</b>	<b>31</b>
Abstract	35
Introduction	36
Materials and Methods	38
Results	44
Discussion	50
Conclusions	55
Acknowledgements	56
References	57
Supplementary information	65
<b>Chapter 3: Elemental concentrations of waters and bivalves in the fresh to hypersaline Coorong Lagoons, South Australia: Implications for palaeoenvironmental studies</b>	<b>77</b>
Abstract	81
Introduction	82
Methods	83

---

**TABLE OF CONTENTS**

---

Results	87
Discussion	92
Conclusions and implications for palaeoenvironmental studies	99
Acknowledgements	100
References	101
Supplementary information	109

**Chapter 4: Controls over oxygen isotope fractionation in the waters and bivalves (*Arthritica helmsi*) of an estuarine lagoon system** **125**

Abstract	129
Introduction	130
Methods	132
Results	135
Discussion	142
Conclusions and implications for palaeoenvironmental studies	148
Acknowledgements	149
Funding	149
References	150
Supplementary information	159

**Chapter 5: Palaeohydrology of the southern Coorong Lagoon, South Australia, inferred from the oxygen isotope ratios of fossil bivalves** **177**

Abstract	181
Introduction	182
Methods	183
Results	187
Discussion	190
Conclusions	197

---

**TABLE OF CONTENTS**

---

Acknowledgements	198
References	198
Supplementary information	204
<b>Chapter 6: Key outcomes and suggestions for future research</b>	<b>209</b>
Key outcomes	211
Suggestions for future research	213
Summary	215
References	216
<b>Appendix 1: Published versions of Chapter 2, Chapter 3 and Chapter 4</b>	<b>219</b>

---

## THESIS DECLARATION

---

I certify that this work contains no material which has been accepted for the award of any other degree or diploma in my name, in any university or other tertiary institution and, to the best of my knowledge and belief, contains no material previously published or written by another person, except where due reference has been made in the text. In addition, I certify that no part of this work will, in the future, be used in a submission in my name, for any other degree or diploma in any university or other tertiary institution without the prior approval of the University of Adelaide and where applicable, any partner institution responsible for the joint-award of this degree.

I acknowledge that copyright of published works contained within this thesis resides with the copyright holder(s) of those works.

I also give permission for the digital version of my thesis to be made available on the web, via the University's digital research repository, the Library Search and also through web search engines, unless permission has been granted by the University to restrict access for a period of time.

I acknowledge the support I have received for my research through the provision of an Australian Government Research Training Program Scholarship.

Briony Kate Chamberlayne

Date: 27 June 2021

---

## THESIS ABSTRACT

---

As European land clearance and the installation of engineering controls of water flow (such as locks and barrages) have altered many estuarine ecosystems from their natural state, the range of natural variability of hydrological conditions is often poorly understood. As the instrumental record of climate and environmental monitoring in Australia is short (approximately 120 years), palaeoenvironmental archives inform our understanding of past conditions and can be useful in informing management and conservation efforts in venerable hydrological ecosystems. The geochemistry of bivalve shells preserved in sediments provides one possible archive of past hydrological conditions, though modern calibration studies are necessary prior to palaeoenvironmental applications. This thesis investigates the controls on the composition of trace elements (Sr, Mg and Ba) and stable oxygen isotope ratios ( $\delta^{18}\text{O}$ ) in the waters of the Coorong Lagoons, South Australia, alongside the incorporation of these elements and stable isotope ratios into shells of the bivalve *Arthritica helmsi*. The findings of these studies of modern populations were then applied to shells from the sediments of the Coorong South Lagoon to reconstruct hydroclimate variability for the past 1750 years.

The trace elemental ratios Mg/Ca, Sr/Ca and Ba/Ca in waters of the Coorong Lagoons were significantly correlated to salinity. In particular, the relationship between Mg/Ca was found to be consistent across different hydrological regimes and could therefore be a target as a salinity proxy in carbonate archives. However, the partitioning of trace elemental ratios into *A. helmsi* carbonate was not found to correlate with the temperature, salinity, pH, or elemental concentrations of water, indicating that biological effects likely control the incorporation of elements this species. The  $\delta^{18}\text{O}$  of contemporary waters was mostly controlled by evaporation, though water mixing also had an influence. Oxygen isotope ratios in *A. helmsi* were significantly related to both the temperature and  $\delta^{18}\text{O}$  of waters resulting in the development of a temperature-dependent fractionation equation. A  $\delta^{18}\text{O}$  record spanning 1750 years was developed from shells from sediments of the Coorong South Lagoon. This record indicates that the Coorong South Lagoon has been a highly evaporated closed system for at least the past 1750 years and that the marine dominated modern North Lagoon is not an analogue for past conditions in the South Lagoon. Furthermore multi-decadal periods of high and low precipitation/evaporation balance indicated by the  $\delta^{18}\text{O}$  record are consistent with regional hydroclimate reconstructions suggesting a common driver for hydroclimate in southeastern Australia. The outcomes of this thesis are a significant contribution to the knowledge of bivalve geochemistry as a proxy for palaeoenvironmental change, as well as past hydroclimate in the Coorong South Lagoon and surrounding region, with potential implications for modern hydrological management.

---

## ACKNOWLEDGEMENTS

---

First and foremost I would like to sincerely thank my supervisors Jon Tyler and Bronwyn Gilanders. Your unwavering support both personally and professionally has been invaluable to me. Thank you for never failing to show enthusiasm in my work, and also for your guidance and patience in assisting me in the completion of this thesis. I would also like to thank John Tibby, Deborah Haynes and Luke Mosley for your interest in my work and for sharing your knowledge and insights.

I'd like to acknowledge and thank all who assisted with data collection, especially: Mark Rollog, Rob Klæbe and Kristine Neilson for assistance with carbonate isotopic analyses; Sarah Gilbert, Ben Wade and Ken Neubauer from Adelaide Microscopy for assistance with trace elemental analyses, electron microprobe analyses and SEM imaging respectively; Tony Hall for assistance with XRD analysis; and Daniel Jardine and Jason Young from Flinders Analytical, Flinders University, for assistance with water isotope analyses. I would also like to thank everyone who accompanied me on fieldtrips to the Coorong.

I am extremely grateful to the financial support I received during my candidature. Most of the research in this thesis was made possible by generous funding from the Sir Mark Mitchell Foundation, the Field Naturalist Society of South Australia, and the Nature Conservation Society of South Australia.

Thanks to all the members of the Tyler lab group for the support, encouragement and snacks over the years. To my past and present office mates, thank you for fostering a fun, inclusive and productive work environment – special thanks to Rachel, Haidee, Martin and Asika for sharing this journey with me.

Thanks to my geology friends for sharing in the good times and the not so good times. To Richard, Alicia and Kiara, the coffee dates, pub nights and camping trips are great memories we will share forever. A special mention to Kam for always being there and supporting me in any way I need. I'd also like to thank my friends and teammates from the Wilderness Lacrosse Club and Adelaide University Football Club for the fun times and for providing an outlet from my studies.

To Mum, Dad, Nana, Emma, Georgia, Elizabeth and Jules (aka 'The Family') – I cannot thank you enough supporting me in every way possible. Lastly, to my partner Jules, thank you for everything.



**Peer-reviewed journal publications:**

**Chamberlayne, B.K.**, Tyler, J.J. and Gillanders, B.M. 2021. Elemental concentrations of waters and bivalves in the fresh to hypersaline Coorong Lagoons, South Australia: Implications for palaeoenvironmental studies. *Estuarine, Coastal and Shelf Science* 255. <https://doi.org/10.1016/j.ecss.2021.107354>

**Chamberlayne, B.K.**, Tyler, J.J., Gillanders, B.M. (2021). Controls over oxygen isotope fractionation in the waters and bivalves (*Arthritica helmsi*) of an estuarine lagoon system. *Geochemistry, Geophysics, Geosystems*, 22, e2021GC009769. <https://doi.org/10.1029/2021GC009769>

**Chamberlayne, B.K.**, Tyler, J.J., and Gillanders, B.M. 2020. Environmental Controls on the Geochemistry of a Short-Lived Bivalve in Southeastern Australian Estuaries. *Estuaries and Coasts* 43:86-101. <https://doi.org/10.1007/s12237-019-00662-7>

Shao, Y., Farkaš, J., Mosley, L., Tyler, J., Wong, H., **Chamberlayne, B.**, Raven, M., Samanta, M., Holmden, C., Gillanders, B.M., Kolevica, A., and Eisenhauer, A. 2021. Impact of salinity and carbonate saturation on stable Sr isotopes ( $\delta^{88/86}\text{Sr}$ ) in a lagoon-estuarine system. *Geochemica et Cosmochimica Acta* 293:461-476. <https://doi.org/10.1016/j.gca.2020.11.014>

**Conference abstracts:**

**Chamberlayne, B.K.**, Tyler, J.J., Gillanders, B.M., Haynes, D., Tibby, J. and Jacobsen, J. 2018. Palaeo-ecology of the Coorong Southern Lagoon inferred from geochemical signals in bivalve shells. Australian Freshwater Science Society Congress, Adelaide

**Chamberlayne, B.K.**, Tyler, J.J. and Gillanders, B.M. 2018. Assessing trace element and stable isotopic ratios as environmental recorders in short lived bivalve. Goldschmidt Geochemical Conference, Boston

**Chamberlayne, B.K.**, Tyler, J.J. and Gillanders, B.M. 2018. Using bivalve geochemistry to investigate environmental baseline characteristics of the RAMSAR listed Coorong wetland. South Australian Natural Resource Management Science Conference, Adelaide

**Chamberlayne, B.K.**, Tyler, J.J., Gillanders, B.M., Izzo, C., Haynes, D., Jacobsen, J. and Tibby, J. 2016. Geochemical signals in bivalve shells as evidence for hydroclimate variability in The Coorong Lagoon, South Australia. Australasian Quaternary Association Conference, Auckland



---

# CHAPTER 1

Introduction and Thesis Outline

---



## **1. Introduction**

Understanding the resilience of aquatic ecosystems to climate and human impacts requires a long term perspective that is rarely attainable via standard monitoring programs. This is especially true in Australia where the short instrumental record (~100 years) results in difficulty placing climate anomalies such as prolonged drought, rainfall declines, and devastating floods into the context of natural variability (Cook et al., 2016; Kiem et al., 2020). Aquatic ecosystems such as estuaries are particularly at risk of ecological decline associated with climate change (Scanes et al., 2020) due to reduced inflows of freshwater and associated increases in salinity, nutrient loads and pollution (Gillanders et al., 2011). Maintaining the ecological character of such ecosystems via management practices is best informed by a combination of modern monitoring and palaeoenvironmental data (Finlayson et al., 2016). The Coorong estuary in South Australia is one such wetland which would benefit from an improved knowledge of baseline ecological conditions and understanding of the resilience of the system to future impacts associated with the changing climate. Current management strategies are based on a relatively poor understanding of the natural range of hydrological variability in the system which in turn mirrors the broader need for data on the long term climate variability in the region. This thesis aims to develop a more robust understanding of environmental change in the Coorong Lagoon through the geochemical analysis of bivalve shells preserved in sediments.

### **1.1 The Coorong, Lower Lakes and Murray Mouth**

The Coorong, Lower Lakes and Murray Mouth (CLLMM) comprise the estuary at the terminus of Australia's Murray-Darling Basin (MDB; Figure 1a). The MDB covers 14% of Australia's land area (Figure 1a) and comprises two main rivers, the Murray and the Darling (MDBA, 2021). Around 2.2 million people live in the basin which provides around 40% of Australia's agricultural produce (MDBA, 2021). The basin is home to 16 internationally recognised wetlands, including the CLLMM (Department of Agriculture, Water and the Environment, 2021). The Coorong is a back barrier Lagoon which was formed approximately 7000 years ago with the formation of the Youngusband Peninsula which separates the lagoon from the Southern Ocean. The peninsula runs for up to 194 km, making it the longest beach in Australia (Short, 2004). The Coorong estuary runs parallel to the Youngusband Peninsula southeast from the Murray Mouth for approximately 160 km (Figure 1b), and is separated by a narrow channel at Parnka Point into two lagoons known as the North and South Lagoons (Figure 1b). For consistency with recent literature, the terms North Lagoon and South Lagoon will be capitalised throughout this thesis. The Lower Lakes comprise Lake Alexandrina and Lake Albert which are the terminal lakes of the MDB. The Coorong is classified as a reverse estuary due to a north-

south salinity gradient from fresh to hypersaline (Shao et al., 2018; Webster, 2010). Water inputs include various quantities of freshwaters from the Murray River at the northern reaches, freshwaters from the Salt Creek drainage network at the southern extremity, marine waters through the Murray Mouth, and groundwater (Shao et al. 2021).

The CLLMM is of great cultural, environmental and economic importance and as such is recognised as one of Australia’s most significant wetlands (Department of Environment and Heritage, 2009). The CLLMM region is the traditional *ruwe* (country) of the Ngarrindjeri people (Ngarrindjeri Nation & Hemming, 2019). The Lower Lakes, *Kurangk* (Coorong) and Murray Mouth form the ‘Meeting of the Waters’ and are central to the Ngarrindjeri culture. The environmental importance of the CLLMM was recognised in 1985 when the Coorong and Lower Lakes was listed as a Wetland of International Significance under the Ramsar Convention (Department for Environment and Heritage, 2000), primarily due to the number and diversity of migratory birds that visit the CLLMM each year (Paton et al., 2009) among other criteria summarised in Table 1. The CLLMM is visited by up to 170,000 shorebirds each year and provides a breeding habitat for several species (Department for Environment and

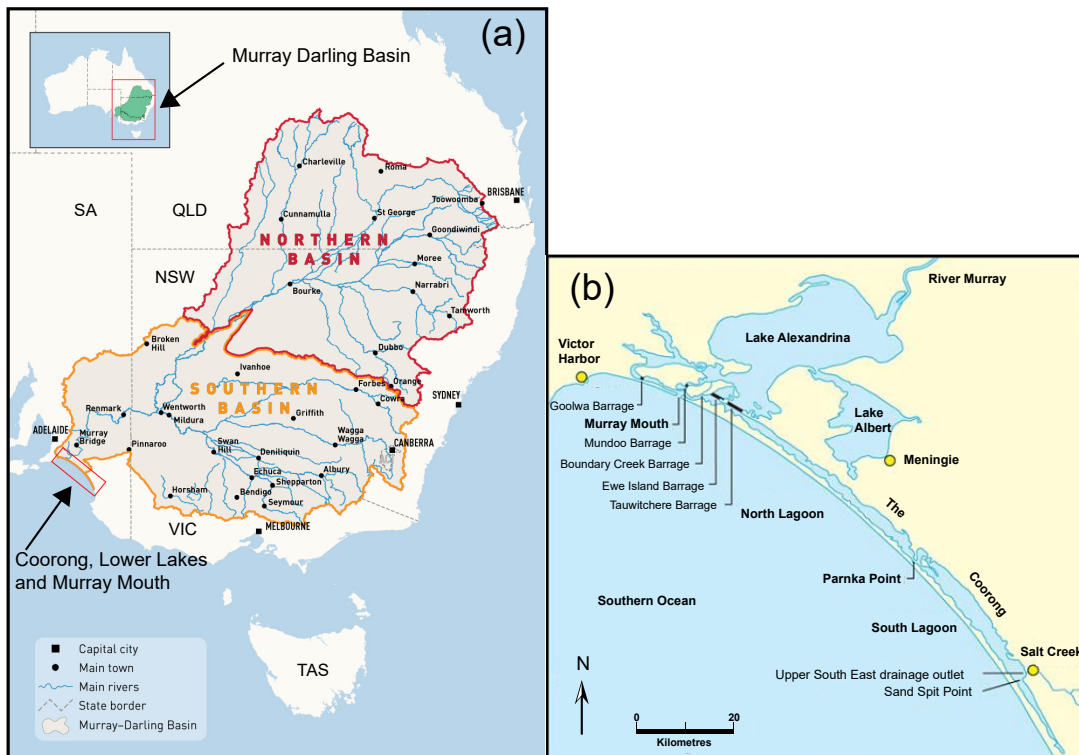


**Figure 1.** Map highlighting the location of the (a) Murray-Darling Basin in Australia (modified from MDBA (2021)) and also (b) the Coorong, Lower Lakes and Murray Mouth in South Australia (modified from Lamontagne et al. (2004)).

**Table 1.** The criteria considered for identifying Wetlands of International Importance with the criteria that the Coorong, Lake Alexandrina and Lake Albert Wetland satisfy for selection.

<b>Ramsar Sites Criteria</b>	<b>Coorong Ramsar Criteria</b>
1. A wetland should be considered internationally important if it contains a representative, rare, or unique example of a natural or near-natural wetland type found within the appropriate biogeographic region	✓
2. A wetland should be considered internationally important if it supports vulnerable, endangered, or critically endangered species or threatened ecological communities	✓
3. A wetland should be considered internationally important if it supports populations of plant and/or animal species important for maintaining the biological diversity of a particular biogeographic region	✓
4. A wetland should be considered internationally important if it supports plant and/or animal species at a critical stage in their life cycles, or provides refuge during adverse conditions	✓
5. A wetland should be considered internationally important if it regularly supports 20,000 or more waterbirds	✓
6. A wetland should be considered internationally important if it regularly supports 1% of the individuals in a population of one species or subspecies of waterbird	✓
7. A wetland should be considered internationally important if it supports a significant proportion of indigenous fish subspecies, species or families, life-history stages, species interactions and/or populations that are representative of wetland benefits and/or values and thereby contributes to global biological diversity	✓
8. A wetland should be considered internationally important if it is an important source of food for fishes, spawning ground, nursery and/or migration path on which fish stocks, either within the wetland or elsewhere, depend	✓
9. A wetland should be considered internationally important if it regularly supports 1% of the individuals in a population of one species or subspecies of wetland-dependent non-avian animal species	X

Water, 2020a). In addition, the wetland supports many nationally and internationally significant flora and fauna, including nationally threatened species (Department for Environment and Water, 2020b). Agriculture, forestry and fishing in and around the CLLMM generated \$276 million in exports in 2019/2020, while tourism spending added \$4.9 million to the economy (Regional Development Australia, 2020). Together, these industries account for almost 50% of employment in the region (Regional Development Australia, 2020).

The Coorong has in recent years experienced declining ecological health characterised by hypersalinisation and eutrophication (Kingsford et al., 2011). A combination of low rainfall and low Murray River inflow during the Millennium Drought (2001–2009; Van Dijk et al., 2013) exacerbated the Coorong’s environmental decline (Mosley et al., 2012) and led to low water levels in the Lower Lakes (Mosley et al., 2012), high salinities across the CLLMM (Leterme et al., 2015) and the exposure of thousands of hectares of acid sulfate soils (Mosley et al., 2014). The ecological disaster highlighted the Coorong’s lack of resilience to drought and the need for water security and management plans in the CLLMM. The MDB has a 200 year history of modification by infrastructure, water regulation and water extraction (Walker, 2006), including a series of barrages constructed between Lake Alexandrina and the Coorong Lagoons in the 1930s, which were built to maintain lake levels and prevent salinity incursions in response to diminished Murray River flow (Sim & Muller, 2004). Currently, management decisions are guided by the Murray Darling Basin Plan which includes objectives related to the openness of the Murray Mouth, water quality in the Coorong, and the maintenance of ecological character (MDBA 2012). In 2018, the Government of South Australia announced the Healthy Coorong, Healthy Basin project – a \$70 million commitment to restore the environmental health of the Coorong (Department for Environment and Water, 2020a). Supported by community, First Nations and scientific partnerships, the project will investigate on-ground works, management tools, research trials and investigations to secure a healthy future for the Coorong (Department for Environment and Water, 2020a).

As the instrumental record of hydrological change in the Coorong Lagoons is short, current knowledge of the long term hydrology of the two lagoons is heavily based on palaeo-environmental studies. Previous studies have examined diatom, ostracod, foraminifera and charophyte assemblages in sediment cores from the Coorong Lagoons (e.g. Cann et al., 2000; Dick et al., 2011; Fluin et al., 2007; Lower et al., 2013; Reeves et al., 2015), in addition to biogeochemical proxies such as carbon and hydrogen isotopes of sediments and lipid biomarkers (Krull et al., 2009; McKirdy et al., 2010; Tulipani et al., 2014). The majority of these concluded



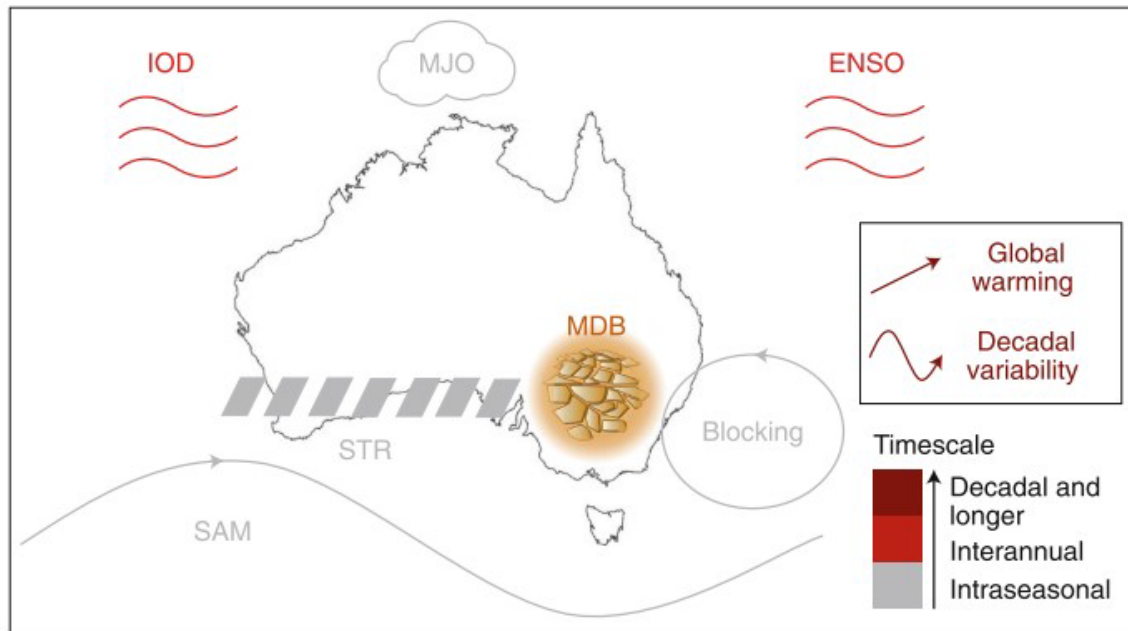


**Figure 2.** Climate drivers related to rainfall variability in the Murray-Darling Basin (MDB): Indian Ocean Dipole (IOD); Madden-Julian Oscillation (MJO); El Niño Southern Oscillation (ENSO); Southern Annular Mode (SAM); Sub-Tropical Ridge (STR) (King et al., 2020).

that the modern state of the Coorong is unusual in the context of the pre-European record (e.g. Dick et al., 2011; Lower et al., 2013; Reeves et al., 2015; Tulipani et al., 2014). Furthermore, biogeochemical evidence suggests that the North Lagoon and South Lagoon have evolved as separate systems (McKirdy et al., 2010). However, quantitative baseline conditions for the Coorong Lagoons of critical parameters such as salinity remain mostly unknown, as microflora and microfauna assemblages generally have wide environmental preferences. There is therefore a need for more robust palaeoenvironmental studies, which can assist in better defining the range of natural variability of this globally important wetland to guide restoration and conservation efforts (Finlayson et al., 2016; Saunders and Taffs, 2009). Geochemical studies of bivalve shells have the potential to contribute quantitative data on seasonal and intra-annual timescales and provide a significant contribution to the palaeoenvironmental knowledge of the Coorong.

## **1.2 Hydroclimate drivers in the Coorong and Murray Darling Basin**

Hydroclimate in the Coorong and MDB is affected by several ocean-atmosphere interactions including the Southern Annular Mode (SAM), the El Niño Southern Oscillation (ENSO), the Indian Ocean Dipole (IOD), and the position of the Sub-Tropical Ridge (STR; King et al., 2020; Murphy and Timbal, 2008; Risbey et al., 2009; Ummenhofer et al., 2009; Figure 2). These circulation patterns operate on temporal scales ranging from daily to multi-decadal (Gallant et al., 2012) and the influence of each driver varies seasonally (Risbey et al., 2009). Individual drivers rarely account for more than 20% of monthly rainfall variability (Risbey et al., 2009) due to complex interactions between the drivers themselves (Gallant et al., 2012). Furthermore, the salinity in the Coorong is also dependent on the timing of freshwater flows (Lester et al., 2011), for example, high flows in summer can reduce the evaporative enrichment of waters (Chamberlayne et al., 2021). The complexity of interactions and the variation on temporal and spatial scales makes the prediction of their influence on regional temperature and precipitation challenging (Hossain et al., 2018).

## **1.3 Bivalve Geochemistry**

One potential way to examine past change in the Coorong Lagoons is through the geochemical analysis of bivalve shells preserved in sediments. The geochemical properties of calcium carbonate minerals in the hard parts of calcifying organisms such as mollusc shells can be used to reconstruct the life and environmental histories of the organism (see Immenhauser et al., 2016 for review). The range of environments inhabited by bivalves, along with their abundant preservation in the sedimentary record, have contributed to their common use in palaeo-environmental (e.g. Alexandroff et al., 2020; Carré et al., 2014; Schöne et al., 2003) and archaeological studies (Burchell et al., 2013; Culleton et al., 2009; Hallmann et al., 2009). Bivalves accrete carbonate periodically into layers which record both signatures of hydrological conditions such as temperature, and information on growth rate and age of the individual and can therefore provide precise chronologies allowing geochemical changes to be placed into a temporal context (Clark, 1974; Jones, 1980). Long lived species can record decades to centuries worth of variation (e.g. Butler et al., 2012), while the analysis of several individuals of shorter lived species can be used to estimate the range of variability for the particular period of time captured by a sediment sample, in the context of longer term variability (e.g. Carré et al., 2013). Of the geochemical properties examined in bivalve shells, stable oxygen and carbon ratios (expressed as  $\delta^{18}\text{O}$  and  $\delta^{13}\text{C}$  respectively) and trace elemental concentrations are commonly employed to varying degrees of success.

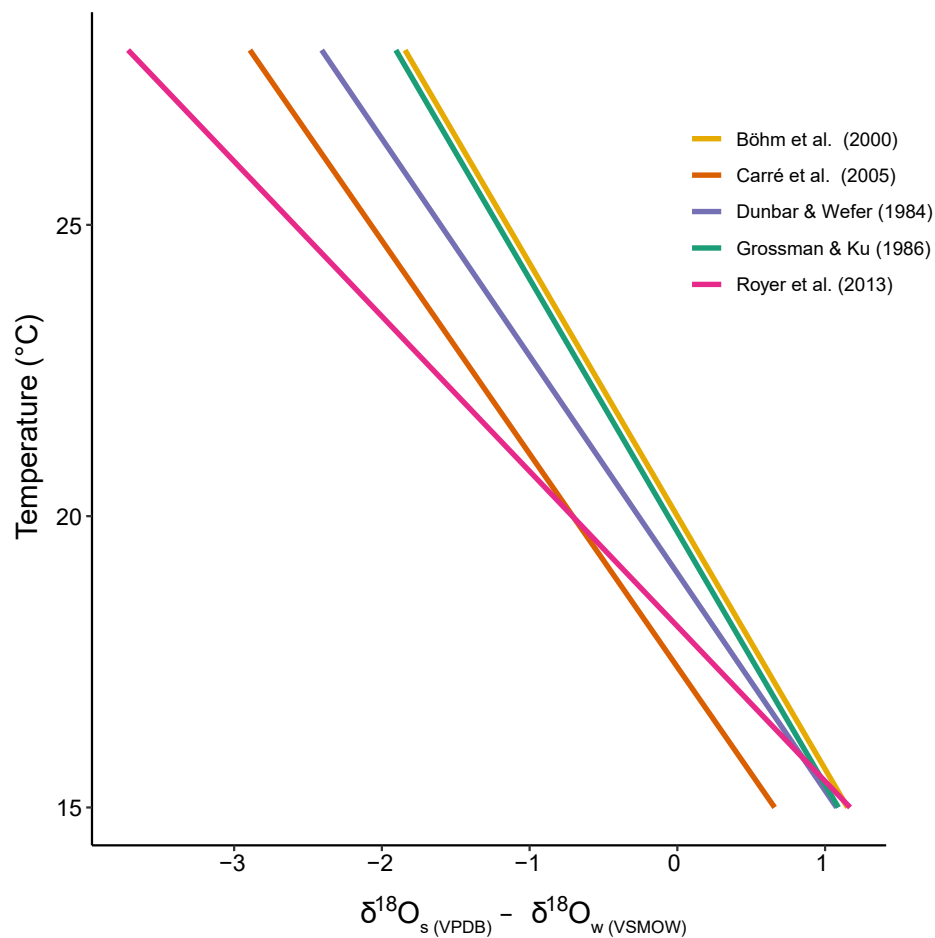


**Figure 3.** Comparison of temperature dependent oxygen isotope fractionation equations established in previous studies.

### 1.3.1 Stable isotope ratios

Following the pioneering works of Urey et al. (1951) and Epstein et al. (1953), the use of oxygen isotope ratios in biogenic carbonates has been a commonly employed technique in the reconstruction of past seawater temperature. These seminal works demonstrated that  $\delta^{18}\text{O}$  in carbonate is a function of the temperature and  $\delta^{18}\text{O}$  of the water which the organism inhabits. A number of equations, known as palaeotemperature equations, have since been developed for both calcite (Kim and O'Neil, 1997; Wanamaker et al., 2006) and aragonite carbonates (Figure 3; Böhm et al., 2000; Carré et al., 2005; Dunbar and Wefer, 1984; Grossman and Ku, 1986; Royer et al., 2013). Differences between these equations are attributed to species specific 'vital effects' which are discrepancies between the biogenic carbonate and an inorganic analogue (Epstein et al., 1951; see Weiner and Dove, 2003 for review). Vital effects can be kinetic, where the growth

rate or calcification rate of the organism drives an offset between the expected and observed isotope fractionation (Huyghe et al., 2020; Owen et al., 2008) or taxonomic where organisms exert a biological control over the isotopic composition of their carbonate (Craig, 1953; Urey et al., 1951). As such, it is now recognised that calibrations assessing the temperature dependent oxygen isotope fractionation using modern populations are required for each species of interest.

Once the relationship between temperature and oxygen isotope fractionation has been determined, oxygen isotope geochemistry has been most successfully employed as a temperature proxy in marine species (e.g. Carré et al., 2013; Featherstone et al., 2020; Schöne et al., 2004; Uvanović et al., 2021) where the  $\delta^{18}\text{O}$  of sea water is relatively invariant. In non-marine environments, interpreting shell  $\delta^{18}\text{O}$  is more complex due to changes in the  $\delta^{18}\text{O}$  of water resulting from the mixing of isotopically distinct source waters and subsequent evaporation. Oxygen isotope ratios in freshwater shells have primarily been interpreted to reflect hydrological processes such as river discharge, lake water evaporation and the  $\delta^{18}\text{O}$  of precipitation (Kelemen et al., 2017; Pfister et al., 2019; Schöne et al., 2020; Versteegh et al., 2009). Studies utilising estuarine species are less common due to the inherent difficulties of separating the effects of changing temperature and  $\delta^{18}\text{O}$  of water, which is closely linked to salinity (Gillikin et al., 2005a). Previous studies have used  $\delta^{18}\text{O}$  in estuarine shells to examine drought and flood signals (Walther and Rowley, 2013), seasonality (Culleton et al., 2009) river discharge (Dettman et al., 2004) and salinity (Ingram et al., 1996). In most cases it is recognised that quantitative reconstructions of either temperature or the  $\delta^{18}\text{O}$  composition of water from the oxygen isotope analysis of estuarine bivalves requires independent proxies for either salinity, the  $\delta^{18}\text{O}$  of water or temperature (e.g. Gillikin et al., 2005; Surge et al., 2003).

The controls on carbon isotope fractionation in biogenic carbonate are more challenging to interpret (see McConnaughey and Gillikin, 2008 for review). A high proportion of carbon isotope variation in bivalves is thought to reflect changes in the carbon isotope ratio of dissolved inorganic carbon (DIC; Goodwin et al., 2013; Lorrain et al., 2004; Owen et al., 2008; Poulain et al., 2010), while a small contribution of approximately 10% is thought to be derived from the internal respiration of particulate organic matter (Gillikin et al., 2006b; Poulain et al., 2010). Consequently, shell  $\delta^{13}\text{C}$  has been used as a proxy for salinity and water mixing given the large difference in the  $\delta^{13}\text{C}$  composition of fluvial and marine DIC (Andrus and Rich, 2008; Gillikin et al., 2006b; Vonhof et al., 2013). However, the fraction of carbon derived from metabolic

processes increases over the life stages of bivalves (Gillikin et al., 2009, 2007; Lorrain et al., 2004) making quantitative reconstructions of salinity or the  $\delta^{13}\text{C}$  of DIC difficult to achieve (Ferguson et al., 2013).

### 1.3.2 Trace element ratios

The success of trace elemental ratios Mg/Ca and Sr/Ca as palaeothermometers in corals (e.g. Corrège, 2006; Sinclair et al., 1998) and foraminifera (McConnell and Thunell, 2005; Nürnberg et al., 1996) has led to the investigation of the viability of using trace elements in bivalves as a palaeoclimate proxy. Temperature reconstructions based on Mg/Ca and Sr/Ca in biogenic carbonates are considered salinity independent (unlike  $\delta^{18}\text{O}$  based reconstructions) as the concentrations of these elements are relatively stable in waters above a salinity of 10 (Dodd and Crisp, 1982). The Mg/Ca of bivalve carbonate has been found to be temperature controlled in studies of calcitic bivalves (e.g. Freitas et al., 2005; Klein et al., 1996; Mouchi et al., 2013; Tynan et al., 2017), whereas Sr/Ca has more successfully been related to temperature in aragonitic bivalves (Dodd, 1965; Schöne et al., 2011; Yan et al., 2013; Zhao et al., 2017). However, the element partitioning into the biogenic carbonate lattice is often far from both expected equilibrium (e.g. Freitas et al., 2006; Geeza et al., 2018; Gillikin et al., 2005b; Zhao et al., 2017) and from results obtained from precipitation experiments of abiogenic carbonate (Dietzel et al., 2004; Mucci et al., 1989). Kinetic and taxonomic vital effects have been shown to disrupt element partitioning in many studies of bivalve shells (e.g. Carré et al., 2006; Vander Putten et al., 2000; Wanamaker et al., 2008; Wanamaker and Gillikin, 2018), but not always consistently. For example, growth rate has been found to correlate with Sr and Mg concentrations in several studies (e.g. Izumida et al., 2011; Lorrain et al., 2005; Takesue and van Geen, 2004) but also dismissed in others (Füllenbach et al., 2015; Zhao et al., 2017). Furthermore, the relationship between shell Sr/Ca and Mg/Ca and temperature can vary significantly among different species (Izumida et al., 2011; Mouchi et al., 2013; Surge and Walker, 2006) and among specimens of the same species (Schöne et al., 2011; Tynan et al., 2017). Therefore, while Sr/Ca and Mg/Ca ratios of bivalve carbonate presents a potential salinity independent temperature proxy, studies of modern populations are also necessary to identify whether a bivalve species accurately records temperature variation in their shell carbonate chemistry.



**Figure 4.** *Arthritica helmsi* shells with scale bar.

In addition to Mg and Sr, Ba to Ca ratios have also been explored as an environmental proxy in bivalve shells. Many studies have found Ba/Ca to be characterised by a relatively constant Ba/Ca background that is punctuated with sharp peaks which are reproducible between different individuals of the same population (e.g. Gillikin et al., 2008; Poulain et al., 2015; Stecher et al., 1996; Vander Putten et al., 2000). The background signal has been shown to reflect the Ba/Ca in water, which is in turn linked to salinity (Gillikin et al., 2006a; Izzo et al., 2016). The synchronicity of the peaks often found in Ba/Ca profiles of bivalve carbonate implies a common environmental forcing. While some studies have linked these peaks to phytoplankton blooms (Lazareth et al., 2003; Thébault et al., 2009; Vander Putten et al., 2000), others have not been able to attribute an environmental forcing (Gillikin et al., 2008; Goodwin et al., 2013; Hatch et al., 2013). Furthermore a laboratory based study of the freshwater aragonitic bivalve *Corbicula fluminea*, highlighted that a number of factors controlled barium levels in the shell, namely a combination of temperature, food supply, growth rate, and the Ba/Ca of water (Zhao et al., 2017). As such, as is the case with other trace elemental and stable isotope proxies, an examination of the controls of Ba/Ca in modern populations of a particular species is necessary prior to the interpretation of these elemental ratios as a palaeoenvironmental tracer.

#### 1.4 *Arthritica helmsi*

*Arthritica helmsi* (Galeommatoidea: Leptonidae; Figure 4) is a micro-mollusc common to southern Australian estuaries. Populations of *A. helmsi* have been observed in estuaries across Western Australia (Kanandjembo et al., 2001; Platell and Potter, 1996; Semeniuk and Wurm, 2000), Victoria (Lautenschlager et al., 2014; Matthews and Constable, 2004) and South Australia (Dittmann et al., 2015). The growth, reproduction and environmental tolerances of this species were examined in a field study conducted in the Peel-Harvey estuarine system in Western Australia between 1977 and 1980 (Wells and Threlfall, 1982a). The authors found that *A. helmsi* can grow up to 3 mm in size (Figure 4) at a rate of 0.3 mm per month and reach maturity in less than one year (Wells and Threlfall, 1982a). No annual rings were found on the shells, and only a small proportion of the population is expected to survive into a second year of life (Wells and Threlfall, 1982a). *A. helmsi* were found to reproduce continuously and were found to have many characteristics of R-selected species (Wells and Threlfall, 1982b), namely short gestational periods, short life spans and to reside and thrive in disturbed habitats. The temperature tolerance of *A. helmsi* ranged from 18 to 32 °C and the bivalves were active in waters with a salinity of 10 to at least 55 (Wells and Threlfall, 1982c).

*A. helmsi* are present in large quantities in the Holocene sedimentary profiles of the Coorong North and South Lagoons and therefore represents an ideal potential tracer for geochemically based palaeoenvironmental research (Chamberlayne, 2015). In recent years, populations of *A. helmsi* in the Coorong have been restricted to the northern reaches of the North Lagoon (Dittmann et al., 2019) due to the ecological decline of the lagoons. Monitoring of species abundance in the Coorong from 2004 to 2018 found *A. helmsi* was common in the North Lagoon except from 2009 to 2012 where occurrences were rare (Dittmann et al., 2019). To date, the degree to which *A. helmsi* shell carbonate records environmental gradients is unknown.

## 2. Thesis aims

This thesis aims to contribute to an understanding of hydrological variability in the Coorong Lagoons during the past 2000 years by developing a new palaeoenvironmental record using bivalve geochemistry. This aim will be achieved by (a) understanding the modern isotope and elemental compositions of the waters in the Coorong and Lower Lakes; (b) calibrating trace elemental and stable isotope geochemical signals in modern specimens of the bivalve *Arthritica helmsi* against modern hydrological and hydrochemical gradients; and (c) applying this calibration to sub-fossil specimens from a sediment core from the Coorong's South Lagoon to identify past conditions. The outcomes of this thesis can provide context for modern management by presenting a high-resolution record of hydrological variability which outlines natural thresholds and can inform the likely resilience of the system to a changing climate.

## 3. Thesis outline

*Chapter 2: Environmental controls on the geochemistry of a short-lived bivalve in southeastern Australian estuaries*

Chapter 2 of this thesis explores the trace elemental ratios (Mg/Ca, Sr/Ca, Sr/Li and Ba/Ca) and stable oxygen and carbon isotope ratios of 19 shells of *A. helmsi* from 14 estuaries across southeastern Australia. Specimens were sourced from museum collections and present the first geochemical analysis of shells of this species. The carbonate mineralogy of this species was determined via X-ray diffraction, and the absence of annual growth rings confirmed by scanning electron microscope and electron microprobe mapping. Sr/Ca and Mg/Ca in *A. helmsi* were negatively correlated to temperature, and both oxygen and carbon isotope values exhibited large differences between hydrological environments (i.e. terrestrial and estuarine), highlighting the potential for this species as an environmental tracer.

Chapter 2 is published as:

Chamberlayne, B.K., Tyler, J.J., and Gillanders, B.M. 2020. Environmental Controls on the Geochemistry of a Short-Lived Bivalve in Southeastern Australian Estuaries. *Estuaries and Coasts* 43:86-101. <https://doi.org/10.1007/s12237-019-00662-7>



*Chapter 3: Elemental concentrations of waters and bivalves in the fresh to hypersaline Coorong Lagoons, South Australia: Implications for palaeoenvironmental studies*

Chapter 3 builds on the results in Chapter 2 and further investigates element-to-calcium ratios as environmental tracers in *A. helmsi*. Live specimens of *A. helmsi* (n = 125) were collected along with lagoonal surface waters (n = 137) across a geographic and temporal salinity gradient from fresh to hypersaline in the Coorong Lagoons, South Australia. Mg/Ca and Sr/Ca in water exhibited logarithmic relations with salinity, while the relationship between Ba/Ca in water and salinity was best described by a negative power function. The range of element concentrations and partition coefficients in shells were similar to other studies. However, there was no correlation between element ratios in shells and element ratios in waters, temperature, pH or salinity. Therefore the incorporation of elements into shell carbonate is concluded to be heavily influenced by biological processes and is not currently suitable for palaeoenvironmental reconstruction.

Chapter 3 is published as:

Chamberlayne, B.K., Tyler, J.J. and Gillanders, B.M. 2021. Elemental concentrations of waters and bivalves in the fresh to hypersaline Coorong Lagoons, South Australia: Implications for palaeoenvironmental studies. *Estuarine, Coastal and Shelf Science* 255. <https://doi.org/10.1016/j.ecss.2021.107354>

*Chapter 4: Controls over oxygen isotope fractionation in the waters and bivalves (Arthritica helmsi) of an estuarine lagoon system*

Chapter 4 presents an investigation into the processes controlling oxygen isotope fractionation in the waters and bivalves of the Coorong Lagoons. Oxygen and carbon isotope ratios were measured in whole shells of live specimens of *A. helmsi* collected on six occasions from November 2016 to May 2018 (n = 131) alongside monthly temperature and oxygen and hydrogen isotope analyses of waters over the same time period (n = 137). Oxygen and hydrogen isotopes in waters were found to be mostly controlled by evaporation, though large freshwater inflows also had an effect in the Coorong's North Lagoon. When combined with salinity, the oxygen and hydrogen isotope ratios of waters were able to distinguish between sites with differing sources of fresh water input. A temperature-dependent fractionation equation was calibrated for *A. helmsi* which was similar to published palaeotemperature equations for other bivalve taxa. This modern calibration of oxygen isotope fractionation in *A. helmsi* coupled with our understanding

of the contemporary isotope hydrology in the Coorong Lagoons lays the foundations for future palaeoenvironmental studies utilizing this species.

Chapter 4 is published as:

Chamberlayne, B.K., Tyler, J.J., Gillanders, B.M. (2021). Control over oxygen isotope fractionation in the waters and bivalves (*Arthritica helmsi*) of an estuarine lagoon system. *Geochemistry, Geophysics, Geosystems*, 22, e2021GC009769. <https://doi.org/10.1029/2021GC009769>

*Chapter 5: Palaeohydrology of the southern Coorong Lagoon, South Australia, inferred from the oxygen isotope ratios of fossil bivalves*

Chapter 5 of this thesis applies the understanding of oxygen isotope fractionation into shells of *A. helmsi* developed in Chapter 4 to specimens extracted from a sediment core in the Coorong's South Lagoon. A 130 cm sediment core extracted from the South Lagoon was dated via 17 accelerator mass spectrometry radiocarbon dates to have a basal age of ca. 1755 years before present. Variability in the oxygen isotope composition of bivalve carbonate was interpreted to reflect multi-decadal periods of high and low evaporation/precipitation over the last 1750 years. The range of oxygen isotope values in core C18 was statistically indistinguishable from the range of values which would be expected for bivalve oxygen isotopes in the modern Coorong South Lagoon, if *A. helmsi* were to survive in the system. This implies that the contemporary hydrology of the South Lagoon, which is a restricted and highly evaporated water body, has not changed significantly over the past 1750 years. The oxygen isotope record shows coherence with other hydroclimate reconstructions for southeastern Australia, strengthening the interpretation of regional scale climate variability over the last 2 millennia, and associated forcing. This new record of hydroclimate variability in the Coorong Lagoons has implications for management and conservation efforts in this globally important wetland.

*Chapter 6: Discussion and directions for future research*

The final chapter of this thesis summarises the key findings of this thesis and offers some recommendations for future research.

#### 4. References

- Alexandroff, S.J., Butler, P.G., Hollyman, P.R., Schöne, B.R., Scourse, J.D., 2020. Late Holocene seasonal temperature variability of the western Scottish shelf (St Kilda) recorded in fossil shells of the bivalve *Glycymeris glycymeris*. *Palaeogeogr. Palaeoclimatol. Palaeoecol.* <https://doi.org/10.1016/j.palaeo.2020.110146>
- Andrus, C.F.T., Rich, K.W., 2008. A preliminary assessment of oxygen isotope fractionation and growth increment periodicity in the estuarine clam *Rangia cuneata*. *Geo-Marine Lett.* 28, 301–308. <https://doi.org/10.1007/s00367-008-0109-3>
- Böhm, F., Joachimski, M.M., Dullo, W.C., Eisenhauer, A., Lehnert, H., Reitner, J., Wörheide, G., 2000. Oxygen isotope fractionation in marine aragonite of coralline sponges. *Geochim. Cosmochim. Acta* 64, 1695–1703. [https://doi.org/10.1016/S0016-7037\(99\)00408-1](https://doi.org/10.1016/S0016-7037(99)00408-1)
- Burchell, M., Cannon, A., Hallmann, N., Schwarcz, H.P., Schöne, B.R., 2013. Refining Estimates for the season of shellfish collection on the Pacific Northwest coast: Applying high-resolution stable oxygen isotope analysis and sclerochronology. *Archaeometry* 55, 258–276. <https://doi.org/10.1111/j.1475-4754.2012.00684.x>
- Butler, P.G., Wanamaker, A.D., Scourse, J.D., Richardson, C.A., Reynolds, D.J., 2012. Variability of marine climate on the North Icelandic Shelf in a 1357-year proxy archive based on growth increments in the bivalve *Arctica islandica*. *Palaeogeogr. Palaeoclimatol. Palaeoecol.* 373, 141–151. <https://doi.org/10.1016/j.palaeo.2012.01.016>
- Cann, J.H., Bourman, R.P., Barnett, E.J., 2000. Holocene Foraminifera as Indicators of Relative Estuarine-Lagoonal and Oceanic Influences in Estuarine Sediments of the River Murray, South Australia. *Quat. Res.* 53, 378–391. <https://doi.org/10.1006/qres.2000.2129>
- Carré, M., Bentaleb, I., Blamart, D., Ogle, N., Cardenas, F., Zevallos, S., Kalin, R.M., Ortlieb, L., Fontugne, M., 2005. Stable isotopes and sclerochronology of the bivalve *Mesodesma donacium*: Potential application to Peruvian paleoceanographic reconstructions. *Palaeogeogr. Palaeoclimatol. Palaeoecol.* 228, 4–25. <https://doi.org/10.1016/j.palaeo.2005.03.045>
- Carré, M., Bentaleb, I., Bruguier, O., Ordinola, E., Barrett, N.T., Fontugne, M., 2006. Calcification rate influence on trace element concentrations in aragonitic bivalve shells: Evidences and mechanisms. *Geochim. Cosmochim. Acta* 70, 4906–4920. <https://doi.org/10.1016/j.gca.2006.07.019>
- Carré, M., Sachs, J.P., Purca, S., Schauer, A.J., Braconnot, P., Falcón, R.A., Julien, M., Lavallée, D., 2014. Holocene history of ENSO variance and asymmetry in the eastern tropical Pacific. *Science* 345, 1045–1048.
- Carré, M., Sachs, J.P., Schauer, A.J., Rodríguez, W.E., Ramos, F.C., 2013. Reconstructing El Niño–Southern Oscillation activity and ocean temperature seasonality from short-lived marine mollusk shells from Peru. *Palaeogeogr. Palaeoclimatol. Palaeoecol.* 371, 45–53. <https://doi.org/10.1016/j.palaeo.2012.12.014>
- Chamberlayne, B., 2015. Late Holocene seasonal and multicentennial hydroclimate variability

in the Coorong Lagoon, South Australia: evidence from stable isotopes and trace element profiles of bivalve molluscs, honours thesis, University of Adelaide, Adelaide.

- Chamberlayne, B.K., Tyler, J.J., Gillanders, B.M., 2021. Controls Over Oxygen Isotope Fractionation in the Waters and Bivalves (*Arthritica helmsi*) of an Estuarine Lagoon System. *Geochemistry, Geophys. Geosystems* 22, 1–18. <https://doi.org/10.1029/2021gc009769>
- Clark, G.R., 1974. Growth Lines in Invertebrate Skeletons. *Annu. Rev. Earth Planet. Sci.* 2, 77–99. <https://doi.org/10.1146/annurev.ea.02.050174.000453>
- Cook, B.I., Palmer, J.G., Cook, E.R., Turney, C.S.M., Allen, K., Fenwick, P., O'Donnell, A., Lough, J.M., Grierson, P.F., Ho, M., Baker, P.J., 2016. The paleoclimate context and future trajectory of extreme summer hydroclimate in eastern Australia. *J. Geophys. Res.* 121, 12,820–12,838. <https://doi.org/10.1002/2016JD024892>
- Corrège, T., 2006. Sea surface temperature and salinity reconstruction from coral geochemical tracers. *Palaeogeogr. Palaeoclimatol. Palaeoecol.* 232, 408–428. <https://doi.org/10.1016/j.palaeo.2005.10.014>
- Craig, H., 1953. The geochemistry of the stable carbon isotopes. *Geochim. Cosmochim. Acta* 3, 53–92. [https://doi.org/10.1016/0016-7037\(53\)90001-5](https://doi.org/10.1016/0016-7037(53)90001-5)
- Culleton, B.J., Kennett, D.J., Jones, T.L., 2009. Oxygen isotope seasonality in a temperate estuarine shell midden: a case study from CA-ALA-17 on the San Francisco Bay, California. *J. Archaeol. Sci.* 36, 1354–1363. <https://doi.org/10.1016/j.jas.2009.01.021>
- Department of Agriculture, Water and the Environment, 2021. The Ramsar Convention on Wetlands. <http://www.environment.gov.au/water/wetlands/ramsar> (accessed 17 May 2021).
- Department for Environment and Heritage, 2009. Managing for a healthy future. Murray Futures Lower Lakes & Coorong Recovery, The Coorong, Lower Lakes and Murray Mouth. [http://www.environment.sa.gov.au/managing-natural-resources/river-murray/river-restoration-and-environmental-water/Coorong\\_Lower\\_Lakes\\_Murray\\_Mouth/long-term-recovery-plan](http://www.environment.sa.gov.au/managing-natural-resources/river-murray/river-restoration-and-environmental-water/Coorong_Lower_Lakes_Murray_Mouth/long-term-recovery-plan). (accessed 18 June 2021).
- Department for Environment and Heritage, 2000. Coorong, and Lakes Alexandrina and Albert Ramsar Management Plan. South Australian Department for Environment and Heritage.
- Department for Environment and Water, 2020a. Project Coorong. <https://www.environment.sa.gov.au/topics/coorong> (accessed 17 June 2021).
- Department for Environment and Water, 2020b. Coorong and Lakes Alexandrina and Albert Wetland Ramsar Site. [https://www.environment.sa.gov.au/topics/water/water-and-the-environment/wetlands/Coorong\\_and\\_Lakes\\_Alexandrina\\_and\\_Albert\\_wetland\\_Ramsar\\_site](https://www.environment.sa.gov.au/topics/water/water-and-the-environment/wetlands/Coorong_and_Lakes_Alexandrina_and_Albert_wetland_Ramsar_site) (accessed 17 June 2021).
- Dettman, D.L., Flessa, K.W., Roopnarine, P.D., Schöne, B.R., Goodwin, D.H., 2004. The use of oxygen isotope variation in shells of estuarine mollusks as a quantitative record of seasonal and annual Colorado River discharge. *Geochim. Cosmochim. Acta* 68, 1253–

1263. <https://doi.org/10.1016/j.gca.2003.09.008>
- Dick, J., Haynes, D., Tibby, J., Garcia, A., Gell, P., 2011. A history of aquatic plants in the Coorong, a Ramsar-listed coastal wetland, South Australia. *J. Paleolimnol.* 46, 623–635. <https://doi.org/10.1007/s10933-011-9510-4>
- Dietzel, M., Gussone, N., Eisenhauer, A., 2004. Co-precipitation of Sr<sup>2+</sup> and Ba<sup>2+</sup> with aragonite by membrane diffusion of CO<sub>2</sub> between 10 and 50 °C. *Chem. Geol.* 203, 139–151. <https://doi.org/10.1016/j.chemgeo.2003.09.008>
- Dittmann, S., Baring, R., Baggalley, S., Cantin, A., Earl, J., Gannon, R., Keuning, J., Mayo, A., Navong, N., Nelson, M., Noble, W., Ramsdale, T., 2015. Drought and flood effects on macrobenthic communities in the estuary of Australia's largest river system. *Estuar. Coast. Shelf Sci.* 165, 36–51. <https://doi.org/10.1016/j.ecss.2015.08.023>
- Dittmann, S., Gordillo, O.L., Baring, R., 2019. Benthic Macroinvertebrate survey 2018-2019 report Coorong, Lower Lakes and Murray Mouth Icon Site. Report for the Department of Environment and Water and the Murray-Darling Basin Authority. Flinders University, Adelaide.
- Dodd, J.R., 1965. Environmental control of strontium and magnesium in *Mytilus*. *Geochim. Cosmochim. Acta* 29, 385–398. [https://doi.org/10.1016/0016-7037\(65\)90035-9](https://doi.org/10.1016/0016-7037(65)90035-9)
- Dodd, J.R., Crisp, E.L., 1982. Non-linear variation with salinity of Sr/Ca and Mg/Ca ratios in water and aragonitic bivalve shells and implications for paleosalinity studies. *Palaeogeogr. Palaeoclimatol. Palaeoecol.* 38, 45–56.
- Dunbar, R.B., Wefer, G., 1984. Stable isotope fractionation in benthic foraminifera from the Peruvian continental margin. *Mar. Geol.* 59, 215–225. [https://doi.org/10.1016/0025-3227\(84\)90094-X](https://doi.org/10.1016/0025-3227(84)90094-X)
- Epstein, S., Buchsbaum, R., Lowenstam, H., Urey, H.C., 1953. Revised Carbonate-Water Isotopic Temperature Scale. *Geol. Soc. Am. Bull.* 64, 1315–1325. [https://doi.org/10.1130/0016-7606\(1953\)64](https://doi.org/10.1130/0016-7606(1953)64)
- Epstein, S., Buchsbaum, R., Lowenstam, H., Urey, H.C., 1951. Carbonate-water isotopic temperature scale. *Bull. Geol. Soc. Am.* 62, 417–426.
- Featherstone, A.M., Butler, P.G., Schöne, B.R., Peharda, M., Thébaud, J., 2020. A 45-year sub-annual reconstruction of seawater temperature in the Bay of Brest, France, using the shell oxygen isotope composition of the bivalve *Glycymeris glycymeris*. *The Holocene* 30, 3–12. <https://doi.org/10.1177/0959683619865592>
- Ferguson, J.E., Johnson, K.R., Santos, G., Meyer, L., Tripathi, A., 2013. Investigating δ<sup>13</sup>C and Δ<sup>14</sup>C within *Mytilus californianus* shells as proxies of upwelling intensity. *Geochemistry, Geophys. Geosystems* 14, 1856–1865. <https://doi.org/10.1002/ggge.20090>
- Finlayson, C.M., Clarke, S.J., Davidson, N.C., Gell, P., 2016. Role of palaeoecology in describing the ecological character of wetlands. *Mar. Freshw. Res.* 67, 687–694. <https://doi.org/10.1071/MF15293>
- Fluin, J., Gell, P., Haynes, D., Tibby, J., Hancock, G., 2007. Palaeolimnological evidence for

- the independent evolution of neighbouring terminal lakes, the Murray Darling Basin, Australia. *Hydrobiologia* 591, 117–134. <https://doi.org/10.1007/s10750-007-0799-y>
- Freitas, P., Clarke, L.J., Kennedy, H., Richardson, C., Abrantes, F., 2005. Mg/Ca, Sr/Ca, and stable-isotope ( $^{18}\text{O}$  and  $^{13}\text{C}$ ) ratio profiles from the fan mussel *Pinna nobilis*: Seasonal records and temperature relationships. *Geochemistry, Geophys. Geosystems* 6. <https://doi.org/10.1029/2004GC000872>
- Freitas, P.S., Clarke, L.J., Kennedy, H., Richardson, C.A., Abrantes, F., 2006. Environmental and biological controls on elemental (Mg/Ca, Sr/Ca and Mn/Ca) ratios in shells of the king scallop *Pecten maximus*. *Geochim. Cosmochim. Acta* 70, 5119–5133. <https://doi.org/10.1016/j.gca.2006.07.029>
- Füllenbach, C.S., Schöne, B.R., Mertz-Kraus, R., 2015. Strontium/lithium ratio in aragonitic shells of *Cerastoderma edule* (Bivalvia) - A new potential temperature proxy for brackish environments. *Chem. Geol.* 417, 341–355. <https://doi.org/10.1016/j.chemgeo.2015.10.030>
- Gallant, A.J.E., Kiem, A.S., Verdon-Kidd, D.C., Stone, R.C., Karoly, D.J., 2012. Understanding hydroclimate processes in the Murray-Darling Basin for natural resources management. *Hydrol. Earth Syst. Sci.* 16, 2049–2068. <https://doi.org/10.5194/hess-16-2049-2012>
- Geeza, T.J., Gillikin, D.P., Goodwin, D.H., Evans, S.D., Watters, T., Warner, N.R., 2018. Controls on magnesium, manganese, strontium, and barium concentrations recorded in freshwater mussel shells from Ohio. *Chem. Geol.* 1–12. <https://doi.org/10.1016/j.chemgeo.2018.01.001>
- Gillanders, B.M., Elsdon, T.S., Halliday, I.A., Jenkins, G.P., Robins, J.B., Valesini, F.J., 2011. Potential effects of climate change on Australian estuaries and fish utilising estuaries: A review. *Mar. Freshw. Res.* 62, 1115–1131. <https://doi.org/10.1071/MF11047>
- Gillikin, D.P., De Ridder, F., Ulens, H., Elskens, M., Keppens, E., Baeyens, W., Dehairs, F., 2005a. Assessing the reproducibility and reliability of estuarine bivalve shells (*Saxidomus giganteus*) for sea surface temperature reconstruction: Implications for paleoclimate studies. *Palaeogeogr. Palaeoclimatol. Palaeoecol.* 228, 70–85. <https://doi.org/10.1016/j.palaeo.2005.03.047>
- Gillikin, D.P., Dehairs, F., Lorrain, A., Steenmans, D., Baeyens, W., André, L., 2006a. Barium uptake into the shells of the common mussel (*Mytilus edulis*) and the potential for estuarine paleo-chemistry reconstruction. *Geochim. Cosmochim. Acta* 70, 395–407. <https://doi.org/10.1016/j.gca.2005.09.015>
- Gillikin, D.P., Hutchinson, K.A., Kumai, Y., 2009. Ontogenic increase of metabolic carbon in freshwater mussel shells (*Pyganodon cataracta*). *J. Geophys. Res. Biogeosciences* 114, 1–6. <https://doi.org/10.1029/2008JG000829>
- Gillikin, D.P., Lorrain, A., Bouillon, S., Willenz, P., Dehairs, F., 2006b. Stable carbon isotopic composition of *Mytilus edulis* shells: relation to metabolism, salinity  $\delta^{13}\text{C}$  DIC and phytoplankton. *Org. Geochem.* 37, 1371–1382. <https://doi.org/10.1016/j.orggeochem.2006.03.008>

- Gillikin, D.P., Lorrain, A., Meng, L., Dehairs, F., 2007. A large metabolic carbon contribution to the  $\delta^{13}\text{C}$  record in marine aragonitic bivalve shells. *Geochim. Cosmochim. Acta* 71, 2936–2946. <https://doi.org/10.1016/j.gca.2007.04.003>
- Gillikin, D.P., Lorrain, A., Navez, J., Taylor, J.W., André, L., Keppens, E., Baeyens, W., Dehairs, F., 2005b. Strong biological controls on Sr/Ca ratios in aragonitic marine bivalve shells. *Geochemistry, Geophys. Geosystems* 6. <https://doi.org/10.1029/2004GC000874>
- Gillikin, D.P., Lorrain, A., Paulet, Y.M., André, L., Dehairs, F., 2008. Synchronous barium peaks in high-resolution profiles of calcite and aragonite marine bivalve shells. *Geo-Marine Lett.* 28, 351–358. <https://doi.org/10.1007/s00367-008-0111-9>
- Goodwin, D.H., Gillikin, D.P., Roopnarine, P.D., 2013. Preliminary evaluation of potential stable isotope and trace element productivity proxies in the oyster *Crassostrea gigas*. *Palaeogeogr. Palaeoclimatol. Palaeoecol.* 373, 88–97. <https://doi.org/10.1016/j.palaeo.2012.03.034>
- Grossman, E.L., Ku, T.-L., 1986. Oxygen and carbon isotope fractionation in biogenic aragonite: Temperature effects. *Chem. Geol.* 59, 59–74. [https://doi.org/10.1016/0168-9622\(86\)90057-6](https://doi.org/10.1016/0168-9622(86)90057-6)
- Hallmann, N., Burchell, M., Schöne, B.R., Irvine, G. V., Maxwell, D., 2009. High-resolution sclerochronological analysis of the bivalve mollusk *Saxidomus gigantea* from Alaska and British Columbia: techniques for revealing environmental archives and archaeological seasonality. *J. Archaeol. Sci.* 36, 2353–2364. <https://doi.org/10.1016/j.jas.2009.06.018>
- Hatch, M.B.A., Schellenberg, S.A., Carter, M.L., 2013. Ba/Ca variations in the modern intertidal bean clam *Donax gouldii*: An upwelling proxy? *Palaeogeogr. Palaeoclimatol. Palaeoecol.* 373, 98–107. <https://doi.org/10.1016/j.palaeo.2012.03.006>
- Hossain, I., Rasel, H.M., Imteaz, M.A., Mekanik, F., 2018. Long-term seasonal rainfall forecasting: efficiency of linear modelling technique. *Environ. Earth Sci.* 77, 1–10. <https://doi.org/10.1007/s12665-018-7444-0>
- Huyghe, D., Emmanuel, L., de Rafelis, M., Renard, M., Ropert, M., Labourdette, N., Lartaud, F., 2020. Oxygen isotope disequilibrium in the juvenile portion of oyster shells biases seawater temperature reconstructions. *Estuar. Coast. Shelf Sci.* 240, 106777. <https://doi.org/10.1016/j.ecss.2020.106777>
- Immenhauser, A., Schöne, B.R., Hoffmann, R., Niedermayr, A., 2016. Mollusc and brachiopod skeletal hard parts: intricate archives of their marine environment. *Sedimentology* 63, 1–59. <https://doi.org/10.1111/sed.12231>
- Ingram, B.L., Conrad, M.E., Ingle, J.C., 1996. Stable isotope and salinity systematics in estuarine waters and carbonates: San Francisco Bay. *Geochim. Cosmochim. Acta* 60, 455–467. [https://doi.org/10.1016/0016-7037\(95\)00398-3](https://doi.org/10.1016/0016-7037(95)00398-3)
- Izumida, H., Yoshimura, T., Suzuki, A., Nakashima, R., Ishimura, T., Yasuhara, M., Inamura, A., Shikazono, N., Kawahata, H., 2011. Biological and water chemistry controls on Sr/Ca, Ba/Ca, Mg/Ca and  $\delta^{18}\text{O}$  profiles in freshwater pearl mussel *Hyriopsis* sp.

- Palaeogeogr. Palaeoclimatol. Palaeoecol. 309, 298–308. <https://doi.org/10.1016/j.palaeo.2011.06.014>
- Izzo, C., Manetti, D., Doubleday, Z.A., Gillanders, B.M., 2016. Calibrating the element composition of *Donax deltoides* shells as a palaeo-salinity proxy. Palaeogeogr. Palaeoclimatol. Palaeoecol. 484, 89–96. <https://doi.org/10.1016/j.palaeo.2016.11.038>
- Jones, D.T., 1980. Annual Cycle of Shell Growth Increment Formation in Two Continental Shelf Bivalves and its Paleocologic Significance. Paleobiology 6, 331–340.
- Kanandjembo, A.N., Platell, M.E., Potter, I.C., 2001. The benthic macroinvertebrate community of the upper reaches of an Australian estuary that undergoes marked seasonal changes in hydrology. Hydrol. Process. 15, 2481–2501. <https://doi.org/10.1002/hyp.296>
- Kelemen, Z., Gillikin, D.P., Graniero, L.E., Havel, H., Darchambeau, F., Borges, A. V., Yambélé, A., Bassirou, A., Bouillon, S., 2017. Calibration of hydroclimate proxies in freshwater bivalve shells from Central and West Africa. Geochim. Cosmochim. Acta 208, 41–62. <https://doi.org/10.1016/j.gca.2017.03.025>
- Kiem, A.S., Vance, T.R., Tozer, C.R., Roberts, J.L., Dalla Pozza, R., Vitkovsky, J., Smolders, K., Curran, M.A.J., 2020. Learning from the past – Using palaeoclimate data to better understand and manage drought in South East Queensland (SEQ), Australia. J. Hydrol. Reg. Stud. 29, 100686. <https://doi.org/10.1016/j.ejrh.2020.100686>
- Kim, S.-T., O’Neil, J.R., 1997. Equilibrium and nonequilibrium oxygen isotope effects in synthetic carbonates. Geochim. Cosmochim. Acta 61, 3461–3475. [https://doi.org/10.1016/S0016-7037\(97\)00169-5](https://doi.org/10.1016/S0016-7037(97)00169-5)
- King, A.D., Pitman, A.J., Henley, B.J., Ukkola, A.M., Brown, J.R., 2020. The role of climate variability in Australian drought. Nat. Clim. Chang. 10, 173–183. <https://doi.org/10.1038/s41558-020-0712-5>
- Kingsford, R.T., Walker, K.F., Lester, R.E., Young, W.J., Fairweather, P.G., Sammut, J., Geddes, M.C., 2011. A Ramsar wetland in crisis the Coorong, lower lakes and Murray mouth, Australia. Mar. Freshw. Res. 62, 255–265. <https://doi.org/10.1071/MF09315>
- Klein, R.T., Lohmann, K.C., Thayer, C.W., 1996. Bivalve skeletons record sea-surface temperature and  $\delta^{18}\text{O}$  via Mg/Ca and  $^{18}\text{O}/^{16}\text{O}$  ratios. Geology 24, 415–418.
- Krull, E., Haynes, D., Lamontagne, S., Gell, P., McKirdy, D., Hancock, G., McGowan, J., Smernik, R., 2009. Changes in the chemistry of sedimentary organic matter within the Coorong over space and time. Biogeochemistry 92, 9–25. <https://doi.org/10.1007/s10533-008-9236-1>
- Lamontagne, S., McEwan, K., Webster, I., Ford, P., Leaney F., Walker, G., 2004. Coorong, Lower Lakes and Murray Mouth: knowledge gaps and knowledge needs for delivering better ecological outcomes, Water for a Healthy Country National Research Flagship, CSIRO, Canberra.
- Lautenschlager, A.D., Matthews, T.G., Quinn, G.P., 2014. Utilization of organic matter by invertebrates along an estuarine gradient in an intermittently open estuary. Estuar. Coast.



- Shelf Sci. 149, 232–243. <https://doi.org/10.1016/j.ecss.2014.08.020>
- Lazareth, C.E., Vander Putten, E., André, L., Dehairs, F., 2003. High-resolution trace element profiles in shells of the mangrove bivalve *Isognomon ephippium*: A record of environmental spatio-temporal variations? *Estuar. Coast. Shelf Sci.* 57, 1103–1114. [https://doi.org/10.1016/S0272-7714\(03\)00013-1](https://doi.org/10.1016/S0272-7714(03)00013-1)
- Lester, R.E., Fairweather, P.G., Heneker, T.M., Higham, J.S., Muller, K.L., 2011. Specifying an environmental water requirement for the Coorong and Lakes Alexandrina and Albert: a first iteration, Government of South Australia, Adelaide, S.Aust.
- Leterme, S.C., Allais, L., Jendyk, J., Hemraj, D.A., Newton, K., Mitchell, J., Shana, M., 2015. Drought conditions and recovery in the Coorong wetland, South Australia in 1997–2013. *Estuar., Coast. Shelf Sci.* 163, 175–184. <https://doi.org/10.1016/j.ecss.2015.06.009>
- Lorrain, A., Gillikin, D.P., Paulet, Y.M., Chauvaud, L., Le Mercier, A., Navez, J., André, L., 2005. Strong kinetic effects on Sr/Ca ratios in the calcitic bivalve *Pecten maximus*. *Geology* 33, 965–968. <https://doi.org/10.1130/G22048.1>
- Lorrain, A., Paulet, Y.M., Chauvaud, L., Dunbar, R., Mucciarone, D., Fontugne, M., 2004.  $\delta^{13}\text{C}$  variation in scallop shells: Increasing metabolic carbon contribution with body size? *Geochim. Cosmochim. Acta* 68, 3509–3519. <https://doi.org/10.1016/j.gca.2004.01.025>
- Lower, C.S., Cann, J.H., Haynes, D., 2013. Microfossil evidence for salinity events in the Holocene Coorong Lagoon, South Australia. *Aust. J. Earth Sci.* 60, 573–587. <https://doi.org/10.1080/08120099.2013.823112>
- Matthews, T.G., Constable, A.J., 2004. Effect of flooding on estuarine bivalve populations near the mouth of the Hopkins River, Victoria, Australia. *J.Mar.Biol.Assn.Uk* 84, 633–639. <https://doi.org/10.1017/S0025315404009671h>
- McConnaughey, T.A., Gillikin, D.P., 2008. Carbon isotopes in mollusk shell carbonates. *Geo-Marine Lett.* 28, 287–299. <https://doi.org/10.1007/s00367-008-0116-4>
- McConnell, M.C., Thunell, R.C., 2005. Calibration of the planktonic foraminiferal Mg/Ca paleothermometer: Sediment trap results from the Guaymas Basin, Gulf of California. *Paleoceanography* 20, 1–18. <https://doi.org/10.1029/2004PA001077>
- McKirdy, D.M., Thorpe, C.S., Haynes, D.E., Grice, K., Krull, E., Halverson, G.P., Webster, L.J., 2010. The biogeochemical evolution of the Coorong during the mid- to late Holocene: An elemental, isotopic and biomarker perspective. *Org. Geochem.* 41, 96–110.
- MDBA (Murray-Darling Basin Authority), 2021, The Murray-Darling Basin and why it's important. <https://www.mdba.gov.au/importance-murray-darling-basin> (accessed 17 May 2021).
- MDBA (Murray-Darling Basin Authority), 2012. Murray-Darling Basin Authority (MDBA) Water Act 2007 — Basin Plan 2012 (Murray-Darling Basin Authority, Canberra)
- Mosley, L.M., Fitzpatrick, R.W., Palmer, D., Leyden, E., Shand, P., 2014. Changes in acidity and metal geochemistry in soils, groundwater, drain and river water in the Lower Murray River after a severe drought. *Sci. Total Environ.* 485–486, 281–291. <https://doi.org/10.1016/j.scitotenv.2014.08.020>

org/10.1016/j.scitotenv.2014.03.063

- Mosley, L.M., Zammit, B., Leyden, E., Heneker, T.M., Hipsey, M.R., Skinner, D., Aldridge, K.T., 2012. The Impact of Extreme Low Flows on the Water Quality of the Lower Murray River and Lakes (South Australia). *Water Resour. Manag.* 26, 3923–3946. <https://doi.org/10.1007/s11269-012-0113-2>
- Mouchi, V., de Raféllis, M., Lartaud, F., Fialin, M., Verrecchia, E., 2013. Chemical labelling of oyster shells used for time-calibrated high-resolution Mg/Ca ratios: A tool for estimation of past seasonal temperature variations. *Palaeogeogr. Palaeoclimatol. Palaeoecol.* 373, 66–74. <https://doi.org/10.1016/j.palaeo.2012.05.023>
- Mucci, A., Canuel, R., Zhong, S., 1989. The solubility of calcite and aragonite in sulfate-free seawater and the seeded growth kinetics and composition of the precipitates at 25°C. *Chem. Geol.* 74, 309–320. [https://doi.org/10.1016/0009-2541\(89\)90040-5](https://doi.org/10.1016/0009-2541(89)90040-5)
- Murphy, B.F., Timbal, B., 2008. A review of recent climate variability and climate change in southeastern Australia. *Int. J. Climatol.* 28, 859–879.
- Ngarrindjeri Nation, Hemming, S., 2019. Ngarrindjeri Nation Yarluwar-Ruwe Plan: Caring for Ngarrindjeri Country and Culture: Kungun Ngarrindjeri Yunnan (Listen to Ngarrindjeri People Talking, in: Mosley, L., Ye, Q., Shepherd, S., Hemming, S., Fitzpatrick, R. (Eds.), *Natural History of the Coorong, Lower Lakes and Murray Mouth Region (Yarluwar-Ruwe)*. University of Adelaide Press, Adelaide, pp. 3–21.
- Nürnberg, D., Bijma, J., Hemleben, C., 1996. Assessing the reliability of magnesium in foraminiferal calcite as a proxy for water mass temperatures. *Geochim. Cosmochim. Acta* 60, 803–814. [https://doi.org/10.1016/0016-7037\(95\)00446-7](https://doi.org/10.1016/0016-7037(95)00446-7)
- Owen, E.F., Wanamaker, A.D., Feindel, S.C., Schöne, B.R., Rawson, P.D., 2008. Stable carbon and oxygen isotope fractionation in bivalve (*Placopecten magellanicus*) larval aragonite. *Geochim. Cosmochim. Acta* 72, 4687–4698. <https://doi.org/10.1016/j.gca.2008.06.029>
- Paton, D.C., Rogers, D.J., Hill, B.M., Bailey, C.P., Ziembicki, M., 2009. Temporal changes to spatially stratified waterbird communities of the Coorong, South Australia: Implications for the management of heterogenous wetlands. *Anim. Conserv.* 12, 408–417. <https://doi.org/10.1111/j.1469-1795.2009.00264.x>
- Pfister, L., Grave, C., Beisel, J.N., McDonnell, J.J., 2019. A global assessment of freshwater mollusk shell oxygen isotope signatures and their relation to precipitation and stream water. *Sci. Rep.* 9, 1–6. <https://doi.org/10.1038/s41598-019-40369-0>
- Platell, M.E., Potter, I.C., 1996. Influence of water depth, season, habitat and estuary location on the macrobenthic fauna of a seasonally closed estuary. *J. Mar. Biol. Assoc. United Kingdom* 76, 1–21. <https://doi.org/10.1017/S0025315400028988>
- Poulain, C., Gillikin, D.P., Thébault, J., Munaron, J.M., Bohn, M., Robert, R., Paulet, Y.M., Lorrain, A., 2015. An evaluation of Mg/Ca, Sr/Ca, and Ba/Ca ratios as environmental proxies in aragonite bivalve shells. *Chem. Geol.* 396, 42–50. <https://doi.org/10.1016/j.chemgeo.2014.12.019>

- Poulain, C., Lorrain, A., Mas, R., Gillikin, D.P., Dehairs, F., Robert, R., Paulet, Y.M., 2010. Experimental shift of diet and DIC stable carbon isotopes: Influence on shell  $\delta^{13}\text{C}$  values in the Manila clam *Ruditapes philippinarum*. *Chem. Geol.* 272, 75–82. <https://doi.org/10.1016/j.chemgeo.2010.02.006>
- Reeves, J.M., Haynes, D., García, A., Gell, P.A., 2015. Hydrological Change in the Coorong Estuary, Australia, Past and Present: Evidence from Fossil Invertebrate and Algal Assemblages. *Estuaries and Coasts* 38, 2101–2116. <https://doi.org/10.1007/s12237-014-9920-4>
- Regional Development Australia, 2020. RDA Murraylands and Riverland economic profile. <https://economy.id.com.au/rda-murraylands-riverland/tourism-value?WebID=110&sEndYear=2012> (accessed 18 June 2021).
- Risbey, J.S., Pook, M.J., McIntosh, P.C., Wheeler, M.C., Hendon, H.H., 2009. On the remote drivers of rainfall variability in Australia. *Mon. Weather Rev.* 137, 3233–3253. <https://doi.org/10.1175/2009MWR2861.1>
- Royer, C., Thébault, J., Chauvaud, L., Olivier, F., 2013. Structural analysis and paleoenvironmental potential of dog cockle shells (*Glycymeris glycymeris*) in Brittany, northwest France. *Palaeogeogr. Palaeoclimatol. Palaeoecol.* 373, 123–132. <https://doi.org/10.1016/j.palaeo.2012.01.033>
- Saunders, K.M., Taffs, K.H., 2009. Palaeoecology: A tool to improve the management of Australian estuaries. *J. Environ. Manage.* 90, 2730–2736. <https://doi.org/10.1016/j.jenvman.2009.03.001>
- Scanes, E., Scanes, P.R., Ross, P.M., 2020. Climate change rapidly warms and acidifies Australian estuaries. *Nat. Commun.* 11, 1–11. <https://doi.org/10.1038/s41467-020-15550-z>
- Schöne, B.R., Flessa, K.W., Dettman, D.L., Goodwin, D.H., 2003. Upstream dams and downstream clams: Growth rates of bivalve mollusks unveil impact of river management on estuarine ecosystems (Colorado River Delta, Mexico). *Estuar. Coast. Shelf Sci.* 58, 715–726. [https://doi.org/10.1016/S0272-7714\(03\)00175-6](https://doi.org/10.1016/S0272-7714(03)00175-6)
- Schöne, B.R., Freyre Castro, A.D., Fiebig, J., Houk, S.D., Oschmann, W., Kröncke, I., 2004. Sea surface water temperatures over the period 1884–1983 reconstructed from oxygen isotope ratios of a bivalve mollusk shell (*Arctica islandica*, southern North Sea). *Palaeogeogr. Palaeoclimatol. Palaeoecol.* 212, 215–232. <https://doi.org/10.1016/j.palaeo.2004.05.024>
- Schöne, B.R., Meret, A.E., Baier, S.M., Fiebig, J., Esper, J., McDonnell, J., Pfister, L., 2020. Freshwater pearl mussels from northern Sweden serve as long-term, high-resolution stream water isotope recorders. *Hydrol. Earth Syst. Sci.* 24, 673–696. <https://doi.org/10.5194/hess-24-673-2020>
- Schöne, B.R., Zhang, Z., Radermacher, P., Thébault, J., Jacob, D.E., Nunn, E. V., Maurer, A.-F., 2011. Sr/Ca and Mg/Ca ratios of ontogenetically old, long-lived bivalve shells (*Arctica islandica*) and their function as paleotemperature proxies. *Palaeogeogr. Palaeoclimatol. Palaeoecol.* 302, 52–64. <https://doi.org/10.1016/j.palaeo.2010.03.016>

- Semeniuk, V., Wurm, P.A.S., 2000. Mollusc of the Leschenault Inlet estuary: their diversity, distribution, and population dynamics. *J. R. Soc. West. Aust.* 83, 377–418.
- Shao, Y., Farkaš, J., Holmden, C., Mosley, L., Kell-Duivesteyn, I., Izzo, C., Reis-Santos, P., Tyler, J., Törber, P., Frýda, J., Taylor, H., Haynes, D., Tibby, J., Gillanders, B.M., 2018. Calcium and strontium isotope systematics in the lagoon-estuarine environments of South Australia: Implications for water source mixing, carbonate fluxes and fish migration. *Geochim. Cosmochim. Acta* 239, 90–108. <https://doi.org/10.1016/j.gca.2018.07.036>
- Shao, Y., Farkaš, J., Mosley, L., Tyler, J., Wong, H., Chamberlayne, B.K., Raven, M., Samanta, M., Holmden, C., Gillanders, B.M., Kolevica, A., Eisenhauer, A., 2021. Impact of salinity and carbonate saturation on stable Sr isotopes ( $\delta^{88/86}\text{Sr}$ ) in a lagoon-estuarine system. *Geochim. Cosmochim. Acta* 293, 461–476. <https://doi.org/10.1016/j.gca.2020.11.014>
- Short, A. D., 2004. *Beaches of the South Australian Coast and Kangaroo Island: A guide to their nature, characteristics, surf and safety* (346 pp). Sydney: Sydney University Press.
- Sim, T. & Muller, K.L., 2004. *A fresh history of the Lakes: Wellington to barrages, 1800s to 1935.* River Murray Catchment Water Management Board, Strathalbyn.
- Sinclair, D.J., Kinsley, L., McCulloch, M.T., 1998. High resolution analysis of trace elements in corals by laser ablation ICP-MS. *Geochim. Cosmochim. Acta* 62, 1889–1901. [https://doi.org/10.1016/S0016-7037\(98\)00112-4](https://doi.org/10.1016/S0016-7037(98)00112-4)
- Stecher, H.A., Krantz, D.E., Lord, C.J., Luther, G.W., Bock, K.W., 1996. Profiles of strontium and barium in *Mercenaria mercenaria* and *Spisula solidissima* shells. *Geochim. Cosmochim. Acta* 60, 3445–3456. [https://doi.org/10.1016/0016-7037\(96\)00179-2](https://doi.org/10.1016/0016-7037(96)00179-2)
- Surge, D., Walker, K.J., 2006. Geochemical variation in microstructural shell layers of the southern quahog (*Mercenaria campechiensis*): Implications for reconstructing seasonality. *Palaeogeogr. Palaeoclimatol. Palaeoecol.* 237, 182–190. <https://doi.org/10.1016/j.palaeo.2005.11.016>
- Surge, D.M., Lohmann, K.C., Goodfriend, G.A., 2003. Reconstructing estuarine conditions: Oyster shells as recorders of environmental change, Southwest Florida. *Estuar. Coast. Shelf Sci.* 57, 737–756. [https://doi.org/10.1016/S0272-7714\(02\)00370-0](https://doi.org/10.1016/S0272-7714(02)00370-0)
- Takesue, R.K., van Geen, A., 2004. Mg/Ca, Sr/Ca, and stable isotopes in modern and Holocene *Protothaca staminea* shells from a northern California coastal upwelling region. *Geochim. Cosmochim. Acta* 68, 3845–3861. <https://doi.org/10.1016/j.gca.2004.03.021>
- Thébault, J., Chauvaud, L., L'Helguen, S., Clavier, J., Barats, A., Jacquet, S., Pécheyran, C., Amouroux, D., 2009. Barium and molybdenum records in bivalve shells: Geochemical proxies for phytoplankton dynamics in coastal environments? *Limnol. Oceanogr.* 54, 1002–1014. <https://doi.org/10.4319/lo.2009.54.3.1002>
- Tulipani, S., Grice, K., Krull, E., Greenwood, P., Revill, A.T., 2014. Salinity variations in the northern Coorong Lagoon, South Australia: Significant changes in the ecosystem following human alteration to the natural water regime. *Org. Geochem.* 75, 74–86.
- Tynan, S., Opdyke, B.N., Walczak, M., Eggins, S., Dutton, A., 2017. Assessment of Mg/Ca in *Saccostrea glomerata* (the Sydney rock oyster) shell as a potential temperature record. *Palaeogeogr. Palaeoclimatol. Palaeoecol.* 484, 79–88. <https://doi.org/10.1016/j.palaeo.2016.08.009>

- Ummenhofer, C.C., England, M.H., McIntosh, P.C., Meyers, G.A., Pook, M.J., Risbey, J.S., Gupta, A. Sen, Taschetto, A.S., 2009. What causes southeast Australia's worst droughts? *Geophys. Res. Lett.* 36, 1–5. <https://doi.org/10.1029/2008GL036801>
- Urey, H.C., Lowenstam, H.A., Epstein, S., McKinney, C.R., 1951. Measurement of paleotemperatures and temperatures of the Upper Cretaceous of England, Denmark and the Southeastern United States. *Bull. Geol. Soc. Am.* 62, 399–416.
- Uvanović, H., Schöne, B.R., Markulin, K., Janeković, I., Peharda, M., 2021. Venerid bivalve *Venus verrucosa* as a high-resolution archive of seawater temperature in the Mediterranean Sea. *Palaeogeogr. Palaeoclimatol. Palaeoecol.* 561, 110057. <https://doi.org/10.1016/j.palaeo.2020.110057>
- Van Dijk, A.I.J.M., Beck, H.E., Crosbie, R.S., De Jeu, R.A.M., Liu, Y.Y., Podger, G.M., Timbal, B., Viney, N.R., 2013. The Millennium Drought in southeast Australia (2001–2009): Natural and human causes and implications for water resources, ecosystems, economy, and society. *Water Resour. Res.* 49, 1040–1057. <https://doi.org/10.1002/wrcr.20123>
- Vander Putten, E., Dehairs, F., Keppens, E., Baeyens, W., 2000. High resolution distribution of trace elements in the calcite shell layer of modern *Mytilus edulis*: Environmental and biological controls. *Geochim. Cosmochim. Acta* 64, 997–1011.
- Versteegh, E.A.A., Troelstra, S.R., Vonhof, H.B., Kroon, D., 2009. Oxygen Isotope Composition of Bivalve Seasonal Growth Increments and Ambient Water in the Rivers Rhine and Meuse. *Palaios* 24, 497–504. <https://doi.org/10.2110/palo.2008.p08-071r>
- Vonhof, H.B., Joordens, J.C.A., Noback, M.L., van der Lubbe, J.H.J.L., Feibel, C.S., Kroon, D., 2013. Environmental and climatic control on seasonal stable isotope variation of freshwater molluscan bivalves in the Turkana Basin (Kenya). *Palaeogeogr. Palaeoclimatol. Palaeoecol.* 383–384, 16–26. <https://doi.org/10.1016/j.palaeo.2013.04.022>
- Walther, B.D., Rowley, J.L., 2013. Drought and flood signals in subtropical estuaries recorded by stable isotope ratios in bivalve shells. *Estuar. Coast. Shelf Sci.* 133, 235–243. <https://doi.org/10.1016/j.ecss.2013.08.032>
- Wanamaker, A.D., Gillikin, D.P., 2018. Strontium, magnesium, and barium incorporation in aragonitic shells of juvenile *Arctica islandica* : Insights from temperature controlled experiments. *Chem. Geol.* 0–1. <https://doi.org/10.1016/j.chemgeo.2018.02.012>
- Wanamaker, A.D., Kreutz, K.J., Borns, H.W., Introne, D.S., Feindel, S., Barber, B.J., 2006. An aquaculture-based method for calibrated bivalve isotope paleothermometry. *Geochemistry, Geophys. Geosystems* 7, 1–13. <https://doi.org/10.1029/2005GC001189>
- Wanamaker, A.D., Kreutz, K.J., Wilson, T., Borns, H.W., Introne, D.S., Feindel, S., 2008. Experimentally determined Mg/Ca and Sr/Ca ratios in juvenile bivalve calcite for *Mytilus edulis*: Implications for paleotemperature reconstructions. *Geo-Marine Lett.* 28, 359–368. <https://doi.org/10.1007/s00367-008-0112-8>
- Webster, I.T., 2010. The hydrodynamics and salinity regime of a coastal lagoon - The Coorong, Australia - Seasonal to multi-decadal timescales. *Estuar. Coast. Shelf Sci.* 90, 264–274. <https://doi.org/10.1016/j.ecss.2010.09.007>
- Weiner, S., Dove, P.M., 2003. An Overview of Biomineralization Processes and the Problem of the Vital Effect. *Rev. Mineral. Geochemistry* 54, 1–29. <https://doi.org/10.2113/0540001>

- Wells, F.E., Threlfall, T.J., 1982a. Density Fluctuations , Growth and Dry Tissue Production of *Hydrococcus Brazieri* (Tenison Woods, 1876) and *Arthritica semen* (Menke, 1843) in Peel Inlet, Western Australia. J. Molluscan Stud. 48, 310–320.
- Wells, F.E., Threlfall, T.J., 1982b. Reproductive strategies of *Hydrococcus brazieri* (Tenison Woods , 1876) and *Arthritica semen* (Menke, 1843) in Peel Inlet , Western Australia. J. Malacol. Soc. Aust. 5, 157–166.
- Wells, F.E., Threlfall, T.J., 1982c. Salinity and temperture tolerance of *Hydrococcus brazieri* (T. Woods, 1876) and *Arthritica semen* (Menke, 1843) from the Peel-Harvey estuarine system, Western Australia. J. Malacol. Soc. Aust. 5, 151–156.
- Yan, H., Shao, D., Wang, Y., Sun, L., 2013. Sr/Ca profile of long-lived *Tridacna gigas* bivalves from South China Sea: A new high-resolution SST proxy. Geochim. Cosmochim. Acta 112, 52–65. <https://doi.org/10.1016/j.gca.2013.03.007>
- Zhao, L., Schöne, B.R., Mertz-Kraus, R., 2017. Controls on strontium and barium incorporation into freshwater bivalve shells (*Corbicula fluminea*). Palaeogeogr. Palaeoclimatol. Palaeoecol. 465, 386–394. <https://doi.org/10.1016/j.palaeo.2015.11.040>







---

# CHAPTER 2

This chapter is published as:

Chamberlayne, B.K., Tyler, J.J., and Gillanders, B.M. 2020. Environmental Controls on the Geochemistry of a Short-Lived Bivalve in Southeastern Australian Estuaries. *Estuaries and Coasts* 43:86-101. <https://doi.org/10.1007/s12237-019-00662-7>

Supplementary information concerning this chapter follows the text.

---



# Statement of Authorship

Title of Paper	Environmental controls on the geochemistry of a short-lived bivalve in southeastern Australian estuaries
Publication Status	<input checked="" type="checkbox"/> Published <input type="checkbox"/> Accepted for Publication <input type="checkbox"/> Submitted for Publication <input type="checkbox"/> Unpublished and Unsubmitted work written in manuscript style
Publication Details	Chamberlayne, B.K., Tyler, J.J., and Gillanders, B.M. 2020. Environmental Controls on the Geochemistry of a Short-Lived Bivalve in Southeastern Australian Estuaries. Estuaries and Coasts 43:86-101. <a href="https://doi.org/10.1007/s12237-019-00662-7">https://doi.org/10.1007/s12237-019-00662-7</a>

## Principal Author

Name of Principal Author (Candidate)	Briony Chamberlayne		
Contribution to the Paper	Conceptualisation, procurement and preparation of samples for analysis, statistical analysis, figure production, manuscript preparation and editing.		
Overall percentage (%)	80		
Certification:	This paper reports on original research I conducted during the period of my Higher Degree by Research candidature and is not subject to any obligations or contractual agreements with a third party that would constrain its inclusion in this thesis. I am the primary author of this paper.		
Signature		Date	20/06/2021

## Co-Author Contributions

By signing the Statement of Authorship, each author certifies that:

- i. the candidate's stated contribution to the publication is accurate (as detailed above);
- ii. permission is granted for the candidate to include the publication in the thesis; and
- iii. the sum of all co-author contributions is equal to 100% less the candidate's stated contribution.

Name of Co-Author	Jonathan Tyler		
Contribution to the Paper	Provided guidance and assistance in conceptualisation, data analysis and interpretation. Manuscript editing.		
Signature		Date	21/Jun/2021

Name of Co-Author	Bronwyn Gillanders		
Contribution to the Paper	Provided guidance and assistance in conceptualisation, data analysis and interpretation. Manuscript editing.		
Signature		Date	23 June 2021



## Environmental Controls on the Geochemistry of a Short-Lived Bivalve in Southeastern Australian Estuaries

### Abstract

Geochemical signals in bivalve carbonate hold the potential to record environmental change over timescales from months to centuries, however not all bivalves provide reliable proxy records and modern studies are essential to calibrate these relationships prior to use in palaeoenvironmental reconstruction. In this study 19 shells of the estuarine bivalve *Arthritica helmsi*, from 14 sites in southeastern Australia, were obtained from museum collections and analysed for trace elemental (Sr/Ca, Mg/Ca, Sr/Li and Ba/Ca) and stable isotopic ratios ( $^{18}\text{O}/^{16}\text{O}$  and  $^{13}\text{C}/^{12}\text{C}$ ). Mean Sr/Ca and Mg/Ca exhibited significant negative correlations to temperature ( $R^2 = 0.49$ ,  $p = 0.001$ ;  $R^2 = 0.25$ ,  $p = 0.02$ ) in agreement with previously published models for trace element partitioning into inorganic aragonite. In addition, the within-shell range of Sr/Ca and Mg/Ca, as measured by laser ablation ICP-MS, correlated to the temperature range ( $R^2 = 0.22$ ,  $p = 0.03$ ;  $R^2 = 0.46$ ,  $p = 0.002$  respectively). Sr/Li ratios were also negatively correlated to temperature ( $R^2 = 0.34$ ,  $p = 0.008$ ) however a significant difference in the model coefficients with previous studies indicates this proxy should be applied with caution. Both oxygen and carbon isotope values exhibited large differences between shells from terrestrial, estuarine and marine waters suggesting that these stable isotopes hold potential to record large environmental changes such as sea level changes or freshening/salinization in estuarine environments. This study presents the first geochemical study of *Arthritica helmsi* highlighting its potential as an environmental tracer.

## 1. Introduction

The shell chemistry of living and fossil bivalves has emerged as a useful tool for reconstructing various palaeo-hydrological variables including temperature (e.g. Hart and Blusztajn, 1998; Schöne et al., 2004), salinity (e.g. Gillikin et al., 2005a; Izzo et al., 2016), aquatic productivity (e.g. Wanamaker et al., 2009; Goodwin et al., 2013) and anthropogenic pollution (e.g. Krause-Nehring et al., 2012; O’Neil and Gillikin, 2014). Bivalves are particularly useful for such reconstructions as they periodically accrete carbonate, are widely dispersed, and are abundant in archaeological and sedimentary deposits (Schöne and Gillikin 2013). Depending on the lifespan of the species, reconstructions can represent seasonal to centennial timescales. As such, multiple specimens of one species can provide material for reconstructions spanning millennia (Butler et al. 2009), allowing a unique perspective not only on long-term climate variability, but also on how patterns of seasonal climate variability evolve alongside long-term climate on multicentennial timescales (Schöne and Fiebig, 2009; Carré et al., 2013). To date, many of these studies have focussed on marine taxa, however an increasing number of studies have addressed freshwater, brackish and estuarine environments (Surge and Lohmann, 2008; Kelemen et al., 2017; Geeza et al., 2018).

Several geochemical tracers have been employed to reconstruct climate and environmental variables in bivalves with perhaps the most successful being oxygen isotope ratios as a water temperature proxy, particularly in marine environments (Urey et al., 1951; Mook, 1971; Grossman and Ku, 1986; Carré et al., 2014). However, this proxy can be difficult in freshwater or estuarine environments due to the need to constrain the oxygen isotope composition of water (Epstein and Mayeda 1953). When the oxygen isotope composition of water cannot be measured, it is often estimated from its relationship with salinity (e.g. Schöne et al., 2004; Carré et al., 2013), or is assumed to be constant over the lifetime of the shell (e.g. Andrus and Rich, 2008). Alternatively, it can also be estimated from climate models in marine environments (Tindall et al., 2010; Bougeois et al., 2014). These approaches present challenges for calibration studies and environmental reconstructions in non-marine aquatic ecosystems, such as estuaries, where isotopically distinct water end members mix to an unknown proportion and monitoring data are scarce.

To overcome these challenges, a search for independent temperature and salinity proxies has been a focus of recent studies. Element to calcium ratios for Mg/Ca and Sr/Ca remain relatively constant in waters with a salinity above 10 (Dodd, J R and Crisp 1982) and so the incorporation of these elements into biogenic carbonates is thought to be temperature controlled. These elements have been successfully used in corals to reconstruct temperature (e.g. McCulloch et al., 1996; Mitsuguchi et al., 1996), where partition coefficients are generally close to 1 (Weber

1973). However, lower partition coefficients observed in bivalves (Gillikin et al., 2006; Izumida et al., 2011; Zhao et al., 2017; Geeza et al., 2018) support the conclusions of many studies that incorporation of trace elements into bivalve carbonate is strongly affected by vital and kinetic effects (Urey et al., 1951; Elliot et al., 2009; Wanamaker and Gillikin, 2018; see Schöne, 2008 for review). Despite this, many studies have successfully calibrated shell Sr/Ca or Mg/Ca against temperature (Surge and Walker, 2006; Freitas et al., 2012; Mouchi et al., 2013; Tynan et al., 2016), although these relationships can differ greatly between species or even specimens within the same species (Hart and Blusztajn 1998; Lorrain et al. 2005; Schöne et al. 2011). In addition to temperature proxies, bivalve Ba/Ca has been explored as a potential salinity proxy (Gillikin et al., 2006; Gillikin et al., 2008; Poulain et al., 2015). The Ba/Ca ratio of bivalves is closely related to the Ba/Ca ratio of water which shares a relationship to salinity in estuarine and near shore environments (Gillikin et al., 2006a; Izzo et al., 2016). Furthermore, the carbon isotope ratio of bivalve carbonate is in part dependent on the dissolved inorganic carbonate of ambient water and as such has been investigated as a proxy for carbon processes such as upwelling (Ferguson et al. 2013) and productivity (Goodwin et al. 2013). However both Ba/Ca and carbon isotopes are prone to metabolic and kinetic effects which make interpretation complex (McConnaughey and Gillikin 2008). Recently, there has been some success in overcoming the challenge of biological effects with the development of alternative proxies such as Sr/Li where Sr/Ca and Li/Ca are normalised to lessen the influence of vital effects (Füllenbach et al. 2015).

As the reliability of the relationship between geochemical proxies and carbonate chemistry can vary between species, it is important to validate the technique through modern calibration prior to application in palaeoenvironmental studies. In these calibration studies, the carbonate chemistry of modern populations can be compared to known hydrological conditions assisting with validation of the technique and identification of species specific relationships. Modern field-based calibration studies, however, can be both time consuming and costly, requiring frequent travel and the deployment of monitoring equipment. In addition, the seasonal and inter-annual range of variability at an individual location can often be relatively small, compared to the range of variability often measured in palaeoenvironmental studies. To supplement temporal calibration studies, space-for-time substitution is a viable alternative (Tyler et al. 2008). In this respect, museum bivalve collections are a potentially valuable resource with which to preliminarily explore modern climate-geochemistry relationships. Museum archives present a wealth of readily available specimens, often collected across a wide geographical/environmental gradient. However, a lack of information upon collection, varying storage methods, and obtaining reliable instrumental environmental information also mean that museum archived specimens are not without their challenges.

The aim of this study was to investigate the utility of the short lived micromollusc *Arthritica helmsi* (Galeommatoidea: Leptonidae) shells as a proxy for environmental geochemical processes. *A. helmsi* is widely abundant in southern Australian estuarine environments and has been found in great quantities in some sedimentary profiles, e.g. in the Coorong Lagoon, South Australia (Chamberlayne, 2015). Although the mollusc is short lived, the abundance of the fossils in such environments presents the opportunity to develop sub-annual records of hydrological change in the context of multi-centennial records based on multiple individuals. Museum samples collected across a range of locations in southeastern Australia were used for calibration against environmental data covering the tolerances of this species. Specifically, the aims of this research were to: (1) examine intra-shell and intra-population geochemical variation in specimens across a temporal and environmental gradient; and (2) determine relationships between shell geochemical composition and environmental parameters.

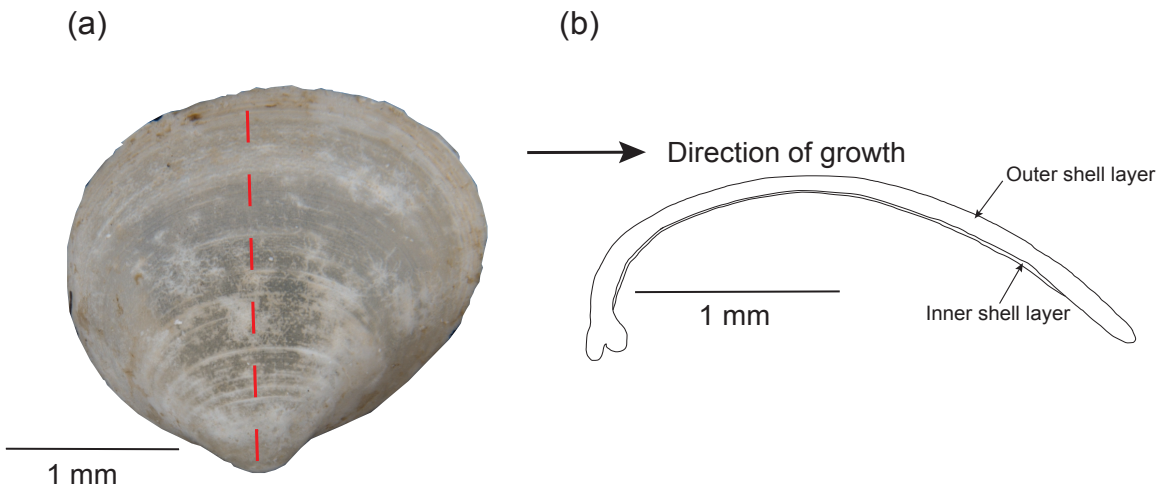


**Fig 1.** (a) *A. helmsi* shell showing the maximum growth axis (red dashed line). (b) Cross section of *A. helmsi* showing the inner and outer aragonite layers and the direction of growth. Scale bars are 1 mm.

## 2. Materials and methods

### 2.1 Specimens

*Arthritica helmsi* (Figure 1) are endemic to southern Australian estuaries and are well adapted to these dynamic environments. Field based studies found that *A. helmsi* are active in salinities ranging from 15-55 with a temperature tolerance of 18-32 °C and can survive for short periods of time outside of these optimal conditions (Wells and Threlfall, 1982a). The absence of discrete breeding periods can lead to population densities exceeding 8,000 individuals/m<sup>2</sup> in favourable conditions (Wells and Threlfall, 1982b, 1982c). Growth is continuous at approximately 0.3 mm/month occurring over their lifetime of ~1 year and there is an absence of visible growth rings (Wells and Threlfall, 1982b).



**Table 1.** Shown are collection location, latitude and longitude, date of collection, how samples were preserved, size of shells, whether shells were alive at the time of collection and the water source.

<b>Shell ID</b>	<b>Location</b>	<b>Latitude</b>	<b>Longitude</b>	<b>Date of Collection</b>	<b>Preservation</b>	<b>Size (mm)</b>
AM 1	Merricks Creek	-38.4	145.15	19/02/1990	Dry	1.8
AM 2	Simpsons Bay	-34.08	151.13	10/08/1975	Dry	1.68
AM 3	Trunketabella Creek	-36.05	150.05	28/11/1989	Dry	2.1
AM 4	Simpsons Bay	-34.08	151.14	22/09/1972	Dry	1.7
AM 5	Yowaka River	-36.96	149.87	28/11/1989	Dry	1.9
AM 6	Tuross Inlet	-36.08	150.13	8/08/1974	Dry	2
AM 7	Clyde River	-35.67	150.15	12/10/1974	Dry	2.3
AM 8	Wagonga Inlet	-36.22	150.12	17/09/1974	Dry	2
AM 9	Lake Macquarie	-32.97	151.63	18/09/1953	Dry	2.16
AM 10	Swan Bay	-38.26	144.63	18/09/1973	Dry	2
TM 1	North Oyster Bay	-42.67	148.05	10/01/1967	Dry	1.1
TM 2	North Oyster Bay	-42.67	148.05	10/01/1967	Dry	0.9
TM 3	North Oyster Bay	-42.67	148.05	10/01/1967	Dry	1.4
VM 1	Corner Inlet	-38.9	146.32	21/11/1983	Ethanol 70%	2.4
VM 2	Port Welshpool	-38.7	146.45	20/11/1983	Ethanol 70%	1.5
VM 3	Port Welshpool	-38.7	146.45	22/11/1983	Ethanol 70%	2.4
VM 4	Sea Elephant Lagoon	-39.82	144.12	8/03/1980	Ethanol 70%	2.2
VM 5	Sea Elephant Lagoon	-39.82	144.12	8/03/1980	Ethanol 70%	2.5
VM 6	Painkalac Creek	-38.47	144.1	23/11/1957	Dry	2

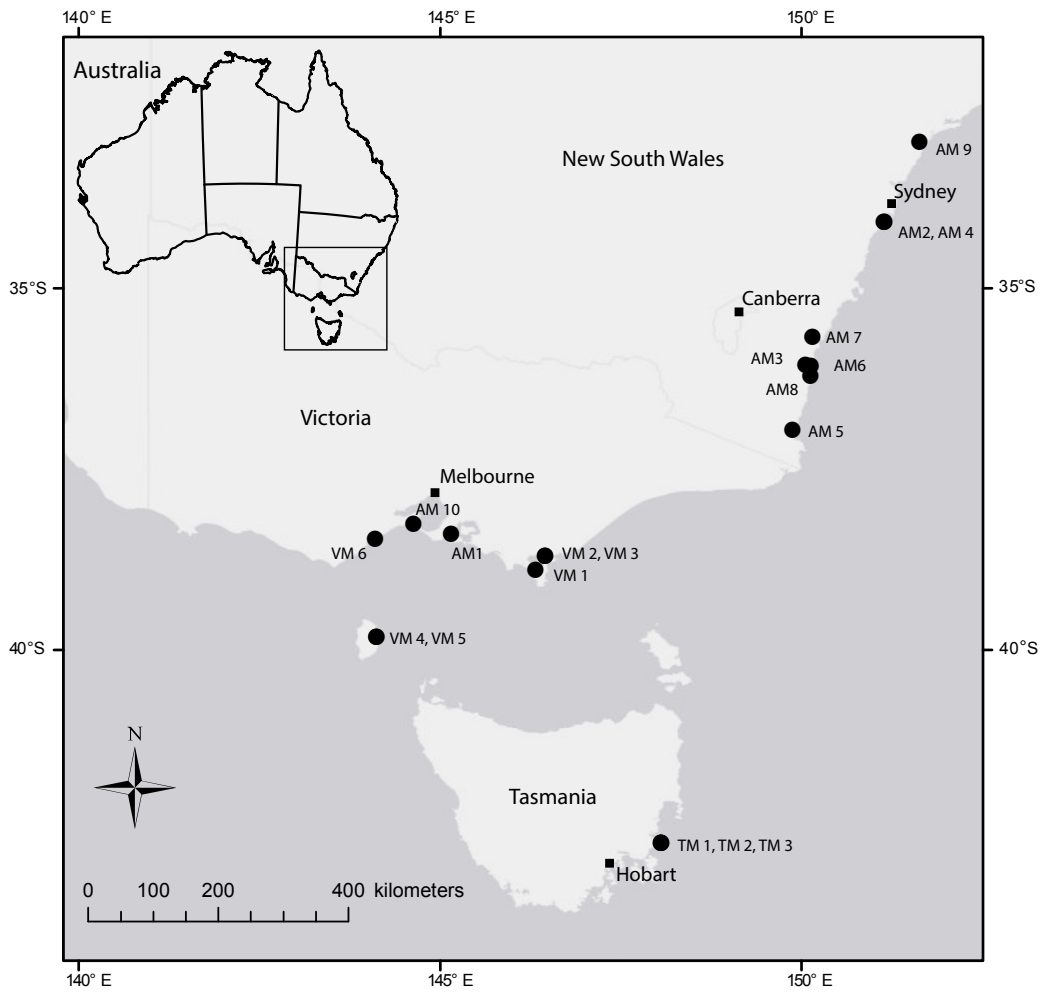


**Fig 2.** Map of south eastern Australia showing the location *A. helmsi* collection sites outlined in Table 1.

The specimens used in this study were obtained from collections at The Australian Museum (AM; Sydney), Museum Victoria (VM; Melbourne) and Tasmanian Museum and Art Gallery (TM; Hobart). To be included in the analyses, the location and timing of collection must have been recorded; 19 shells from 14 sites along the temperate coast of southern Australia met these criteria (Table 1; Figure 2). Samples from the Australian Museum were specified as being collected live, but specimens from Museum Victoria and Tasmanian Museum and Art Gallery did not specify whether the organisms were live upon collection. Consequently, shells which were not preserved well or showed signs of transport were not included for analysis. For subsequent analyses we assumed that all samples were live at collection. Each shell was classified as growing in either terrestrial, marine or estuarine waters based on the collection location (Table 1).

## 2.2 Geochemical analyses

### 2.2.1 Sample preparation

Shells had been stored either dry or in ethanol following collection, although the exact pre-treatment procedures of each collection were unknown (Table 1). Shells were mechanically cleaned in ultra-pure water with a resistivity of 18.2 M $\Omega$  at 25 °C and a pH of 7 before being placed in a drying oven overnight at 30 °C. In order to estimate the age of each shell, the length of the maximum growing axis was measured with digital callipers. Due to the small size of the shell, one whole valve from each shell was crushed for whole shell stable isotope analysis. The other valve was embedded in epoxy resin spiked with 40 ppm indium to enable distinction between the shell carbonate and resin. Shells were then sectioned to approximately 0.8 mm along the growth axis using a Buehler Isomet Low Speed Saw with diamond edge blades. Sections were polished on fine lapping paper to a thickness of 0.5 mm before being adhered to slides with indium spiked thermoplastic glue.

### 2.2.2 Shell microstructure and mineralogy

Polished thin sections were quantitatively mapped using a Cameca SXFive Electron Microprobe running the PeakSite software, and equipped with 5 WDS X-Ray detectors. Beam conditions were set at an accelerating voltage of 15 kV and 100 nA, utilising a focussed beam. Mapped area dimensions ranged from 0.8-2 mm in both x and y axes, at a pixel resolution of 2  $\mu$ m. Pixel dwell time in all maps was set to 100 ms. Calibration and quantitative data reduction of maps was carried out in Probe for EPMA, distributed by Probe Software Inc. Colour images of the maps were processed in Surfer 10® distributed by Golden Software. Calibration was performed on certified natural standards of calcite, dolomite, and Celestine from Astimex.

Each sample was mapped for 3 elements (Mg, Ca and Sr). Mg was mapped on 3 separate TAP crystals and aggregated for enhanced detection limits. Map quantification was conducted in CalcImage, a module of Probe for EPMA. Stoichiometric C was entered into the map quantification calculations for accurate matrix corrections. Background subtraction on the maps was performed via the Mean Atomic Number (MAN) background correction (Donovan and Tingle, 1996; Donovan and Armstrong, 2014), omitting the need for a second pass “off-peak” map acquisition. Following this each pixel goes through full ZAF corrected quantification identical to traditional spot analysis. The average minimum detection limits (99 % CI) in wt% for the quantitative maps were: Mg (0.02), Ca (0.05), Sr (0.16).

Polished thin sections of *A. helmsi* were examined using a FEI Quanta 450 FEG Scanning Electron Microscope (SEM) at Adelaide Microscopy, The University of Adelaide. Thin sections were carbon coated prior to analysis. Images captured are backscattered electron images taken

using a 15 kV beam voltage and a spot size of 4.

The carbonate mineralogy of *A. helmsi* was determined using a Bruker D8 Advance X-ray diffractometer located at the Mawson Laboratories, The University of Adelaide. Approximately 1 g of powdered sample (>100 valves) was loaded into a sample holder with vibration to minimise orientation. Sample rotation was 30 rotations per minute, scanning 2 theta from 5 to 65 degrees with a Cu source operating at 40 kV and 40 amps.

### 2.2.3 Trace element ratio analysis

The elemental concentrations of specimens were determined using a New Wave Q-Switched Nd YAG 213 nm UV laser coupled with an Agilent 7500cs ICP-MS at Adelaide Microscopy, The University of Adelaide. Concentrations of  $^7\text{Li}$ ,  $^{24}\text{Mg}$ ,  $^{88}\text{Sr}$ ,  $^{138}\text{Ba}$  and  $^{43}\text{Ca}$  were measured in addition to  $^{44}\text{Ca}$  as an internal standard and  $^{115}\text{In}$  as an indicator of resin contamination. To measure instrument drift, external standards NIST SRM 612 and the USGS carbonate standard MACS-3 were analysed periodically resulting in a mean coefficient of variation of <4% for all elements analysed. Trace element time series were produced through continuous ablation of transects along the outer margin of the shell. Samples were pre-ablated with a 40  $\mu\text{m}$  diameter spot size prior to ablation with a 30  $\mu\text{m}$  spot size at 10  $\mu\text{m}/\text{second}$  scan speed with a repetition rate of 10 Hz. Data reduction was performed in Iolite (Hellstrom et al. 2008; Paton et al. 2011) and elements are expressed as ratios to Ca. To reduce the effect of instrumental noise, elemental profiles were smoothed with a 7-point running mean and 7-point running median (Sinclair et al. 1998).

### 2.2.4 Stable oxygen and carbon isotopes

A sub-sample of approximately 100  $\mu\text{g}$  crushed whole shell carbonate powder was used for stable isotope analysis. Samples were flushed with helium and then acidified with 105% phosphoric acid at 70°C using a Nu Instruments GasPrep, with resultant  $\text{CO}_2$  analysed for  $^{18}\text{O}/^{16}\text{O}$  and  $^{13}\text{C}/^{12}\text{C}$  with a Nu Instruments Horizon continuous flow isotope ratio mass spectrometer. Repeat measurements of laboratory standards ANU-P3 ( $\delta^{18}\text{O} = -0.32 \text{‰}$ ,  $\delta^{13}\text{C} = +2.2 \text{‰}$ ), UAC-1 ( $\delta^{18}\text{O} = -18.4 \text{‰}$ ,  $\delta^{13}\text{C} = -15.0 \text{‰}$ ) and IAEA CO-8 ( $\delta^{18}\text{O} = -22.7 \text{‰}$ ,  $\delta^{13}\text{C} = -5.76 \text{‰}$ ) had an analytical precision of  $\pm 0.1 \text{‰}$ . Isotope results are reported relative to the Vienna Pee Dee Belemnite (VPDB) international standard using the standard delta ( $\delta$ ) notation in parts per thousand (‰):

$$\delta = \left( \frac{R_{\text{sample}} - R_{\text{standard}}}{R_{\text{standard}}} \right) \times 1000 \quad (1)$$

where R is the isotope ratio ( $^{18}\text{O}/^{16}\text{O}$  or  $^{13}\text{C}/^{12}\text{C}$ ). The oxygen isotope ratio of source water was estimated for each sample from their relationship with temperature and the  $\delta^{18}\text{O}$  of carbonate using the equation of Böhm et al. (2000).

$$\delta^{18}\text{O}_w = \frac{T-(20.0 \pm 0.2)}{(4.42 \pm 0.1)} + \delta^{18}\text{O}_s \quad \text{for } 3^\circ\text{C} < T < 28^\circ\text{C} \quad (2)$$

where  $\delta^{18}\text{O}_w$  is the oxygen isotope value of water,  $\delta^{18}\text{O}_s$  is the oxygen isotope value of shell aragonite, and T is the temperature in degrees celsius.

### 2.3 Climate data

Elemental and isotopic compositions of the shells were regressed against local environmental data sourced from the Scientific Information for Land Owners (SILO) data base (Jeffrey et al. 2001) as instrumental climate and environmental data from the sites at the time of collection was not available. The SILO data base provides ‘Patched Point’ daily estimates for a range of climate variables interpolated from observational climate records from the Australian Bureau of Meteorology. The number of days of climate data used in the regression for each shell was determined through an estimate of the number of days the shell had lived based on shell length and a growth rate of 0.3 mm/month, based on previous research (Wells and Threlfall, 1982a).

**Table 2.** Temperature and precipitation information for the lifespan of each shell sourced from the SILO database.

Shell ID	Age (days)	Average temperature (°C)	Temperature Range (°C)	Total Precipitation (mm)
AM 1	180	15.77	9.81	356.60
AM 2	168	15.80	8.89	929.80
AM 3	210	13.65	9.14	523.40
AM 4	170	15.77	9.81	356.60
AM 5	190	12.42	9.52	452.60
AM 6	200	16.02	8.00	1168.30
AM 7	230	14.61	9.09	1495.10
AM 8	200	13.85	8.10	1195.80
AM 9	216	16.24	10.37	703.90
AM 10	200	12.39	7.95	302.90
TM 1	110	12.37	8.75	191.30
TM 2	90	12.82	8.99	152.50
TM 3	140	11.76	8.41	294.00
VM 1	240	11.81	6.33	801.20
VM 2	140	11.42	7.44	392.60
VM 3	230	11.63	7.09	719.70
VM 4	220	13.68	6.03	644.10
VM 5	250	13.32	5.88	699.40
VM 6	200	11.46	8.56	332.30

### 3. Results

#### 3.1 Climate data

SILO data from the collection sites exhibited a 4.8 °C range in average air temperature and a 1342.5 mm range in total precipitation during the time periods defined by the age of the shell (Table 2). As air temperatures are usually correlated to water temperatures over time (McCombie, 1959; Livingstone and Lotter, 1998; Wurster and Patterson, 2001), the SILO air temperature was used as an approximation of water temperatures in these locations. The salinity and oxygen isotope composition of water was not measured at the time of bivalve sampling, therefore the total rainfall amount from SILO was used as a proxy for the degree of freshwater – marine mixing, which in turn is often manifest in the salinity and  $\delta^{18}\text{O}$  of estuarine waters (Bar-Matthews et al. 2003). Temperature and precipitation both varied in response to latitude with the sites at higher latitudes experiencing higher temperatures and rainfall than those at lower latitudes (Figure S1; supplementary material).

#### 3.3 Geochemical data

##### 3.3.1 Shell microstructure and mineralogy

Element maps show MgO to have varied from ~ 0.01-0.20 wt% and SrO to have varied from ~0.05-0.60 wt % (Figure 3a and b). SrO is more variable in the specimen than MgO and both elements show sections of higher concentration along the inner margin. CaO values for majority of the shell ranged from ~50-53 wt% but there are portions which exhibit much lower (~47 wt%) concentration. These sections appear to occur alongside cracks in the shell. There does not appear to be any evidence of banding in any element map.

SEM images display a massive ultrastructure with a lack of banding (Figure 3d, e and f). Both the umbo region (Figure 3e) and the ventral margin (Figure 3f) show a uniform composition with some cracking. These cracks correspond to regions of increased magnesium and strontium and lower calcium observed in Figures 3a, b and c.

The XRD pattern from a bulk sample of several individuals of *A. helmsi* corresponds with the intensity and spacing of aragonite (Figure S2; supplementary material). Trace amounts (<0.5%) of calcite were also present in the sample but were so minor that *A. helmsi* can be considered aragonitic.

##### 3.3.2 Shell trace elemental ratios

Trace elemental data showed variation both within and between shells (Table 3; Figures S3-

S10; supplementary material). Mean Mg/Ca ratios varied from 0.287 mmol/mol in shell AM 9 (Lake Macquarie) to 0.754 mmol/mol in shell AM 10 (Swan Bay). The largest intra-shell range was 1.15 mmol/mol in shell VM 4 from Sea Elephant Lagoon which also had the highest maximum value of 1.39 mmol/mol. Mean shell Sr/Ca ratios ranged from 1.24 – 2.22 mmol/mol in shells VM 1 (Corner Inlet) and VM 6 (Painkalac Creek) respectively. Shell VM 6 also had the highest recorded value of Sr/Ca at 2.81 mmol/mol, while shell VM 3 (Port Welshpool) had the lowest maximum value (1.50 mmol/mol) and also the lowest intra-shell range (0.369 mmol/mol) of all shells. Shells VM 2 and VM 6 had considerably higher mean Sr/Li values (1226 and 1283 mmol/mol respectively). The intra-shell range of Sr/Li values was highly variable with the largest being 2365 mmol/mol in AM 5 (Yowaka River) and the smallest being 339.8 mmol/mol in AM 2 from Simpsons Bay. Intra-shell ranges were also variable in Ba/Ca ratios which ranged from 0.797  $\mu\text{mol/mol}$  in TM 3 (North Oyster Bay) to 33.3  $\mu\text{mol/mol}$  in AM 8 (Wagonga Inlet). Mean values were also highly variable and the shells with the highest and lowest means also had the highest and lowest minimum values of Ba/Ca (shells AM 1 and VM 5). Maximum values are more variable than minimum values in all trace elemental ratios. All continuous transects had peaks that were randomly distributed throughout the shells (Figure S3-S6; supplementary material). In some specimens these peaks appear cyclical, particularly for Sr/Ca and Mg/Ca elemental ratios.

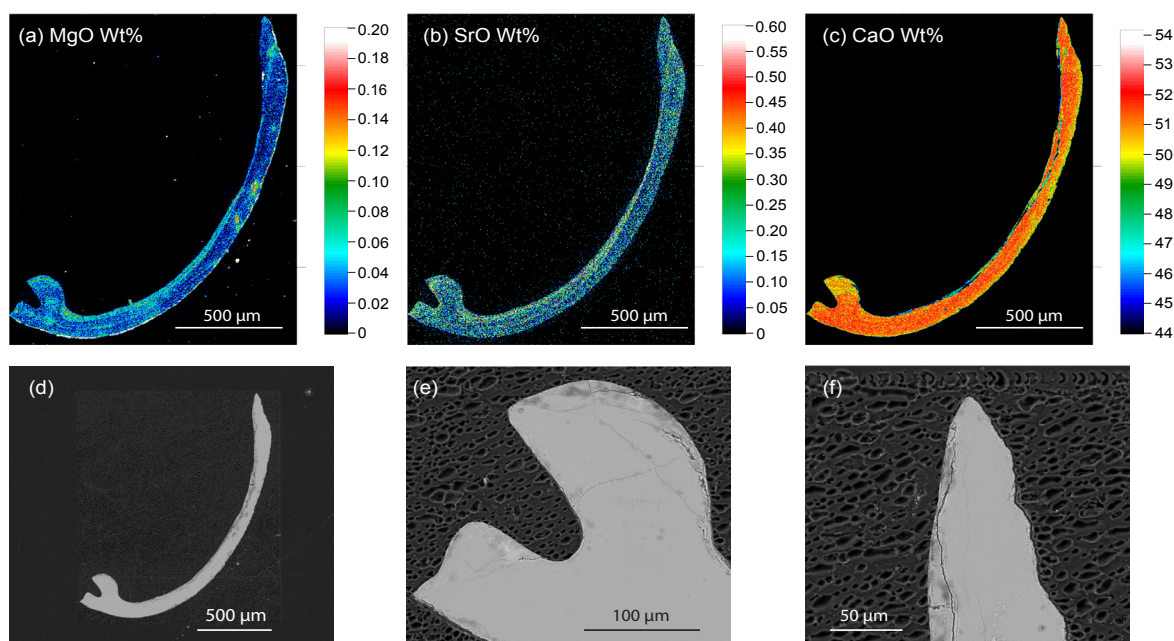


**Fig 3.** Trace element concentrations and microstructures in a thin section of *A. helmsi*; (a) MgO wt%, (b) SrO wt% and (c) CaO wt%. (d-e) SEM images showing a massive ultrastructure in the whole shell (d), umbo region (e) and ventral margin (f).

**Table 3.** Average, minimum and maximum Sr/Ca, Mg/Ca, Sr/Li and Ba/Ca for *A. helmsi* specimens. Whole shell  $\delta^{18}\text{O}$  and  $\delta^{13}\text{C}$  and predicted water  $\delta^{18}\text{O}$ .  $\sigma$  = standard deviation.

Shell ID	Average $\pm 1\sigma$ /minimum/maximum									
	Sr/Ca (mmol/mol)	Mg/Ca (mmol/mol)	Sr/Li (mmol/mol)	Ba/Ca ( $\mu\text{mol/mol}$ )	$\delta^{18}\text{O}_{\text{shell}}$	$\delta^{13}\text{C}_{\text{shell}}$	$\delta^{18}\text{O}_{\text{water}}$			
AM 1	1.39 $\pm$ 0.14/1.13/1.71	0.35 $\pm$ 0.06/0.25/0.50	550.4 $\pm$ 191.0/277.8/1602.6	11.70 $\pm$ 2.60/8.19/17.79	-0.55 $\pm$ 0.03	-0.28 $\pm$ 0.04	-1.14 $\pm$ 0.07			
AM 2	1.28 $\pm$ 0.13/1.08/1.63	0.43 $\pm$ 0.09/0.29/0.65	284.8 $\pm$ 52.6/132.5/472.3	1.65 $\pm$ 0.62/0.83/3.09	0.67 $\pm$ 0.04	-10.81 $\pm$ 0.03	0.09 $\pm$ 0.07			
AM 3	1.71 $\pm$ 0.15/1.36/1.97	0.44 $\pm$ 0.07/0.27/0.54	650.8 $\pm$ 181.9/311.9/1364.1	2.77 $\pm$ 0.82/1.49/5.28	-1.34 $\pm$ 0.02	-9.75 $\pm$ 0.05	-2.41 $\pm$ 0.08			
AM 4	1.40 $\pm$ 0.08/1.24/1.64	0.51 $\pm$ 0.10/0.36/0.83	321.4 $\pm$ 99.0/136.5/627.6	2.96 $\pm$ 0.62/1.65/4.15	0.50 $\pm$ 0.10	0.09 $\pm$ 0.04	-0.09 $\pm$ 0.07			
AM 5	1.79 $\pm$ 0.17/1.52/2.24	0.40 $\pm$ 0.07/0.25/0.58	721.7 $\pm$ 361.0/194.3/2560.1	6.87 $\pm$ 3.29/1.96/15.21	-1.40 $\pm$ 0.26	-2.71 $\pm$ 0.42	-2.74 $\pm$ 0.09			
AM 6	1.37 $\pm$ 0.16/1.02/1.94	0.44 $\pm$ 0.22/0.21/1.26	391.1 $\pm$ 152.5/203.6/1132.3	2.20 $\pm$ 1.00/0.65/5.28	0.61 $\pm$ 0.09	1.20 $\pm$ 0.05	0.08 $\pm$ 0.07			
AM 7	1.73 $\pm$ 0.17/1.40/2.08	0.59 $\pm$ 0.10/0.39/0.80	426.1 $\pm$ 128.9/211.3/907.7	5.72 $\pm$ 2.95/2.09/20.86	2.31 $\pm$ 0.07	-4.32 $\pm$ 0.04	1.46 $\pm$ 0.07			
AM 8	1.32 $\pm$ 0.24/0.97/2.10	0.55 $\pm$ 0.09/0.42/1.06	231.80 $\pm$ 116.7/82.4/522.6	9.00 $\pm$ 4.19/2.66/33.35	0.32 $\pm$ 0.05	1.75 $\pm$ 0.03	-0.70 $\pm$ 0.08			
AM 9	1.49 $\pm$ 0.18/1.25/1.92	0.29 $\pm$ 0.04/0.21/0.38	348.5 $\pm$ 90.2/67.9/739.5	2.21 $\pm$ 0.39/1.51/3.11	1.42 $\pm$ 0.05	1.66 $\pm$ 0.06	0.94 $\pm$ 0.07			
AM 10	1.45 $\pm$ 0.25/1.16/2.42	0.75 $\pm$ 0.23/0.37/1.23	266.5 $\pm$ 131.4/149.5/725.4	2.02 $\pm$ 0.54/1.10/3.34	1.73 $\pm$ 0.05	0.02 $\pm$ 0.05	0.38 $\pm$ 0.09			
TM 1	1.57 $\pm$ 0.14/1.33/1.94	0.49 $\pm$ 0.18/0.23/0.91	538.9 $\pm$ 174.2/244.0/1158.8	4.45 $\pm$ 0.84/2.44/5.83	0.93 $\pm$ 0.09	2.10 $\pm$ 0.05	-0.43 $\pm$ 0.09			
TM 2	1.91 $\pm$ 0.16/1.59/2.35	0.53 $\pm$ 0.15/0.35/1.04	433.0 $\pm$ 93.2/261.5/754.7	1.30 $\pm$ 0.36/0.75/3.37	1.39 $\pm$ 0.26	1.78 $\pm$ 0.23	0.14 $\pm$ 0.08			
TM 3	1.87 $\pm$ 0.11/1.64/2.27	0.63 $\pm$ 0.11/0.47/0.95	562.3 $\pm$ 106.6/357.3/966.8	1.18 $\pm$ 0.17/0.92/1.72	1.71 $\pm$ 0.11	2.85 $\pm$ 0.01	0.22 $\pm$ 0.09			
VM 1	1.24 $\pm$ 0.15/1.00/1.77	0.34 $\pm$ 0.11/0.20/0.62	298.5 $\pm$ 79.2/171.5/530.1	0.95 $\pm$ 0.17/0.63/1.51	0.67 $\pm$ 0.05	0.85 $\pm$ 0.05	-0.81 $\pm$ 0.09			
VM 2	2.06 $\pm$ 0.26/1.64/2.64	0.53 $\pm$ 0.21/0.27/1.02	1226.4 $\pm$ 345.3/802.3/2563.5	1.83 $\pm$ 0.36/1.31/2.73	1.91 $\pm$ 0.06	1.06 $\pm$ 0.05	0.34 $\pm$ 0.09			
VM 3	1.31 $\pm$ 0.09/1.13/1.50	0.35 $\pm$ 0.09/0.22/0.52	370.5 $\pm$ 155.6/173.9/868.9	1.75 $\pm$ 0.28/1.21/2.64	2.31 $\pm$ 0.04	-0.29 $\pm$ 0.04	0.79 $\pm$ 0.09			
VM 4	1.45 $\pm$ 0.20/1.10/1.93	0.67 $\pm$ 0.30/0.24/1.39	588.7 $\pm$ 288.3/196.7/2362.3	1.12 $\pm$ 0.21/0.60/1.62	1.01 $\pm$ 0.07	-0.91 $\pm$ 0.01	-0.05 $\pm$ 0.08			
VM 5	1.39 $\pm$ 0.23/1.03/1.97	0.41 $\pm$ 0.14/0.20/0.73	487.2 $\pm$ 225.6/219.3/1490.3	0.88 $\pm$ 0.25/0.49/1.59	1.43 $\pm$ 0.06	-0.81 $\pm$ 0.07	0.29 $\pm$ 0.08			
VM 6	2.22 $\pm$ 0.20/1.58/2.81	0.62 $\pm$ 0.14/0.39/0.91	1283.7 $\pm$ 344.5/622.3/2231.8	6.60 $\pm$ 1.44/3.25/10.91	0.35 $\pm$ 0.03	-6.38 $\pm$ 0.09	-1.21 $\pm$ 0.09			



There were two collection dates where multiple shells were analysed. Shells TM 1, TM 2 and TM 3 from North Oyster Bay, and shells VM 4 and VM 5 from Sea Elephant Lagoon, allowing intra-population comparison. Within-shell trace element patterns from the same location show similar trends but were not correlated in time (Figure 4). All shells show similar ranges of trace element ratios with the exception of Ba/Ca in TM 1 where the values were significantly higher than those of TM 2 and TM 3 (Figure 4).

### 3.3.3 Shell and water isotopes

Whole shell  $\delta^{18}\text{O}$  values varied between shells with values ranging from -1.40 ‰ in shell AM 5 from Yowaka River to 2.31 ‰ in shell VM 3 from Port Welshpool with an average of  $0.84 \pm 0.08$  ‰ (Table 3). The average  $\delta^{13}\text{C}$  value was  $-1.21 \pm 0.07$  ‰; values ranged from -10.81 ‰ to 2.85 ‰ in shells AM 3 from Trunketabella Creek and TM 3 from North Oyster Bay respectively (Table 3).  $\delta^{18}\text{O}$  and  $\delta^{13}\text{C}$  of shells showed a positive co-variation ( $R^2 = 0.32$ ,  $p = 0.011$ ; Figure S11, supplementary material). Calculated source water  $\delta^{18}\text{O}$  ranged from -3.11 ‰ at Yowaka River to 1.09 ‰ at Clyde River which are realistic values for estuarine waters (Table 3).

### 3.3.4 Geochemical – environmental data relationships

Initial comparisons between shell geochemistry and environmental data indicated no correlations, however the analyses were consistently skewed by two samples, VM 1 and VM 3 which exhibited markedly lower Sr/Ca, Mg/Ca and Sr/Li data (Figure 5). These samples are two of six samples that were stored in ethanol, which may offer one explanation for their anomalous values; these samples may also not have been living upon collection (Table 1). When the samples were removed from the analyses, significant relationships emerge between temperature and trace element ratios. These relationships are summarised in Table 4. Temperature was significantly negatively correlated with Sr/Ca ( $R^2 = 0.49$ ,  $p = 0.001$ ), Mg/Ca ( $R^2 = 0.25$ ,  $p = 0.023$ ) and Sr/Li ( $R^2 = 0.34$ ,  $p = 0.009$ ; Figure 5). The predicted temperature range based on lifespan was also negatively correlated to the range of intrashell Sr/Ca ( $R^2 = 0.22$ ,  $p = 0.003$ ) and Mg/Ca ( $R^2 = 0.45$ ,  $p = 0.002$ ; Figure 6). The effect of including/excluding ethanol stored shells in the analysis was mixed. For Mg/Ca the correlation with temperature increased from  $R^2 = 0.25$  to  $R^2 = 0.31$ , however for all other geochemical data, the correlation decreased when all ethanol stored shells were excluded. Similarly, there were mixed results when removing shells which were not specified as live collected. The only relationship to improve when these shells were excluded was Sr/Ca range and temperature range which improved from  $R^2 = 0.22$  to  $R^2 = 0.53$ . Ba/Ca ratios did not correlate with any trace element or environmental data.

Shell  $\delta^{18}\text{O}$  and  $\delta^{13}\text{C}$  values did not exhibit any correlation with either temperature or rainfall, but values could be grouped based on the classification of water source for the site from which they

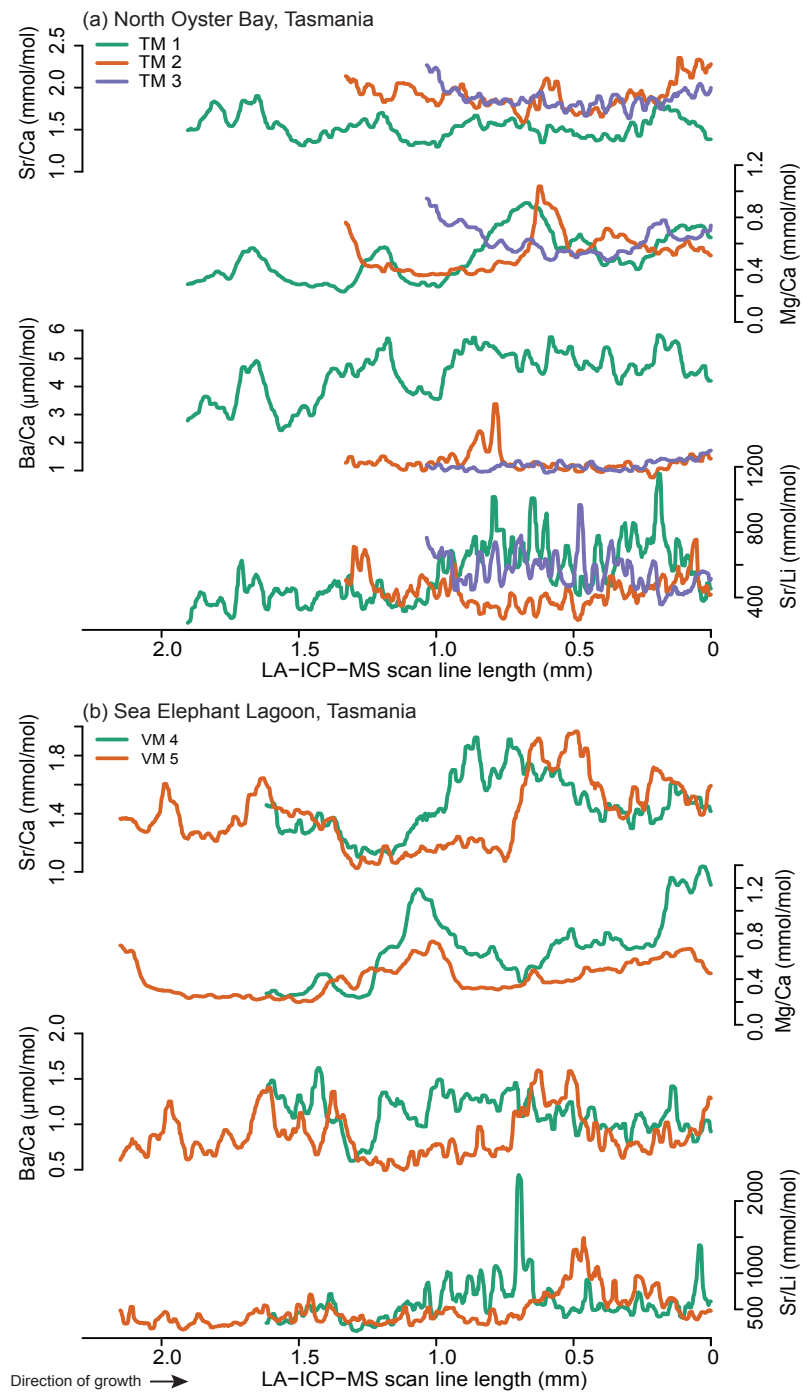


**Fig 4.** Sr/Ca, Mg/Ca, Ba/Ca and Sr/Li profiles across outer layer of shells of the same collection from (a) North Oyster Bay and (b) Sea Elephant Lagoon. The ventral margin of each shell (0 mm) represents the most recent growth before collection.

were collected (Figure 7). Higher values for both  $\delta^{18}\text{O}$  and  $\delta^{13}\text{C}$  were measured from sites for which waters were terrestrially derived to those which had marine waters. Terrestrially sourced sites showed a greater range in both  $\delta^{18}\text{O}$  and  $\delta^{13}\text{C}$  (3.71 ‰, 8.1 ‰) compared to estuarine (1.11 ‰, 2.66 ‰) and marine waters (1.41 ‰, 3.13 ‰). Mean  $\delta^{13}\text{C}$  values of -6.8 ‰, 0.31 ‰ and 1.16 ‰ for terrestrial, estuarine and marine waters respectively indicated terrestrial waters were isotopically distinct from the estuarine and marine waters. Mean  $\delta^{18}\text{O}$  shell values also showed an increase from terrestrial (-0.126 ‰) to estuarine (0.843 ‰) to marine waters (1.28 ‰). However, the range of shell  $\delta^{18}\text{O}$  values in each category indicated that terrestrial waters were not distinct from estuarine and marine waters (Figure 7). This trend was mirrored in the inferred source water  $\delta^{18}\text{O}$  where mean values also increased from terrestrial (-1.58 ‰) to estuarine (-0.47 ‰) to marine (-0.17 ‰) waters, although a large range of terrestrial values (-3.11 ‰ – 4.20 ‰) meant that terrestrial waters were not distinct from estuarine and marine waters.

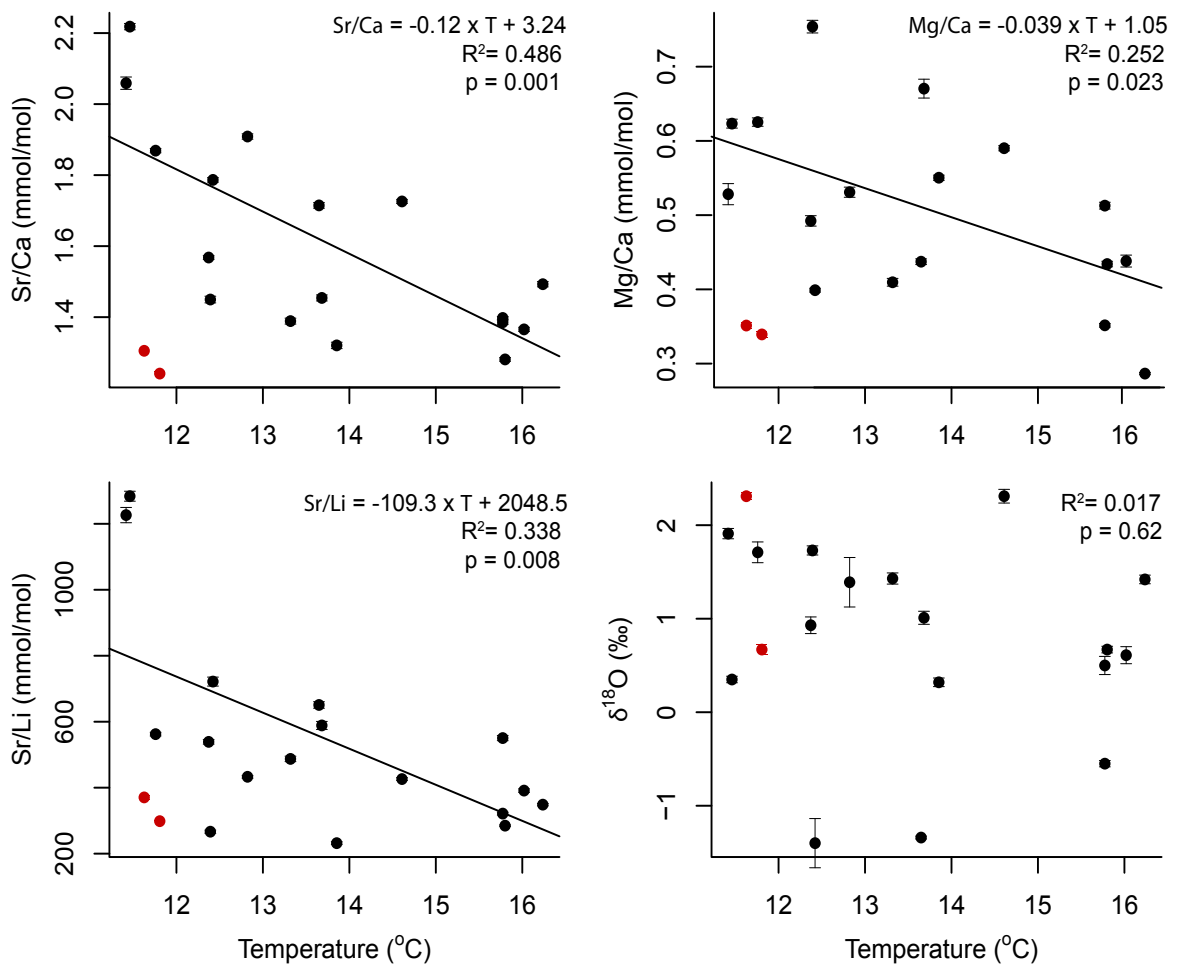


**Fig 5.** Mean Sr/Ca, Mg/Ca and Sr/Li concentrations from shell transects and whole shell  $\delta^{18}\text{O}$  versus temperature in individual *A. helmsi* shells. Samples in red (VM 1 and VM 3) are excluded from all linear models. Error bars are  $\pm$  SE.

#### 4. Discussion

Museum bivalve collections offer great potential for calibrating shell geochemistry-environment relationships, facilitating access to specimens collected across a wide geographic and temporal gradient with a relatively minimal cost and time expense. This is particularly beneficial when exploring the geochemical signatures in hitherto unstudied bivalve species, such as *Arthritica helmsi*, which is an abundant and cosmopolitan species in southern Australia. However museum specimen collection and storage methods can add complications for geochemical analyses. For example, storage in ethanol and several pre-treatment options have been shown to alter both isotopic ratios and trace elemental ratios in biogenic carbonates (Milton and Chenery, 1998; Krause-Nehring et al., 2011; Schöne et al., 2017). Furthermore, a lack of detailed records on the conditions of specimens at the time of collection, as well as a lack of environmental variable data for the specific habitat and lifespan of the individual specimen, mean that museum collections are, at best, a useful source of preliminary information. In the present study, it was difficult to constrain the influence of the sample treatment and storage, providing a potential source of error. Nevertheless, three of the four trace element ratios investigated (Sr/Ca, Mg/Ca and Sr/Li) were exhibited significant correlations with air temperature, conforming to expected relationships based on other bivalve taxa (Füllenbach et al. 2015; Zhao et al. 2017). In addition, both oxygen and carbon isotope ratios broadly varied with water source, demonstrating that the geochemistry of *A. helmsi* has potential as an environmental tracer, albeit subject to further refinement of these relationships.

##### 4.1 Trace elemental ratios

Temperature was found to be most strongly correlated with Sr/Ca in *A. helmsi*, particularly when samples stored in ethanol were excluded, whereby shells from colder waters were found to have higher strontium concentrations than those from warmer waters. This negative relationship is consistent with both inorganic precipitation experiments (Dietzel et al. 2004; Gaetani and Cohen 2006) and some other bivalve species (Dodd, J. Robert 1965; Schöne et al. 2011; Yan et al. 2013; Füllenbach et al. 2015; Zhao et al. 2017). However the slope of the relationship between temperature and Sr/Ca in *A. helmsi* is significantly greater (-0.12) than that of other bivalves (-0.06, Yan et al., 2013; -0.02, Füllenbach et al., 2015; -0.02, Zhao et al., 2017) and synthetic aragonite (-0.04, Dietzel et al., 2004). Temperature was also found to be negatively correlated to Mg/Ca in *A. helmsi* shells in agreement with inorganic aragonite (Gaetani and Cohen 2006). There are few studies which find a temperature control of Mg/Ca in aragonitic bivalves, with the majority concluding that Mg/Ca ratios primarily reflect a physiological control (e.g. Elliot

**Table 4.** Relationship between geochemical analyses and temperature variables. Shown are the equations for the models of best fit and the r squared values.

Analysis	Variable	Relationship	R <sup>2</sup>
Sr/Ca mean	Temperature mean	$Sr/Ca = -0.12 \times T + 3.24$	0.486
Sr/Ca range	Temperature range	$Sr/Ca = -0.11 \times T + 1.70$	0.222
Mg/Ca mean	Temperature mean	$Mg/Ca = -0.039 \times T + 1.05$	0.252
Mg/Ca range	Temperature range	$Mg/Ca = -0.158 \times T + 1.91$	0.455
Sr/Li mean	Temperature mean	$Sr/Li = -109.3 \times T + 2048.5$	0.338
Sr/Li range	Temperature range	No relationship	0.047
Ba/Ca mean	Temperature mean	No relationship	0.012
Ba/Ca range	Temperature range	No relationship	0.026
$\delta^{18}O_{shell}$	Temperature mean	No relationship	0.017

et al., 2009; Poulain et al., 2015; Wanamaker and Gillikin, 2018). Mg/Ca has more successfully been applied as a temperature tracer in calcitic shells, however in these studies the regressions have positive slopes (e.g. Vander Putten et al., 2000; Wanamaker et al., 2008; Freitas et al., 2012; Tynan et al., 2016). It is possible that the correlation here is in fact an indirect link between temperature and metabolism or growth rate. To resolve these questions, further culture or field based studies are required.

Temperature reconstructions from shell Sr/Ca and Mg/Ca are reliant on the notion that water Sr/Ca and Mg/Ca are stable above salinities of ~10 PSU (Dodd and Crisp 1982). Water Sr/Ca in particular has been shown to be strongly reflected in bivalve Sr/Ca in both marine (Lorens and Bender 1980) and freshwater bivalves (Zhao et al. 2017; Geeza et al. 2018). The range of Sr/Ca in *A. helmsi* (~1-3 mmol/mol) compares well to other studies (~0.5-3 mmol/mol, Lorens and Bender, 1980; ~1-6 mmol/mol, Geeza et al., 2018; ~1-4 mmol/mol, Zhao et al., 2017) and so we would expect the distribution coefficient ( $K_D^{Sr/Ca}$ ) to compare well given that Sr/Ca of water should be relatively stable. This would result in  $K_D^{Sr/Ca}$  values in the range of 0.16 (Geeza et al. 2018) to 0.23 (Lorens and Bender 1980; Zhao et al. 2017) which are well below that of abiogenic aragonite (Gaetani and Cohen 2006). However, due to a lack of instrumental salinity or water chemistry measurements in this study, we cannot be sure of past salinity variations in these estuarine sites. It is reasonable to expect that most sites have seasonally variable water chemistry, in addition to periods of low salinity which could cause imprecise estimates of distribution coefficients and temperature reconstructions, particularly at those sites with large terrestrial influences (AM 1, AM 3, AM 5, AM 7 and VM 6). A further complication

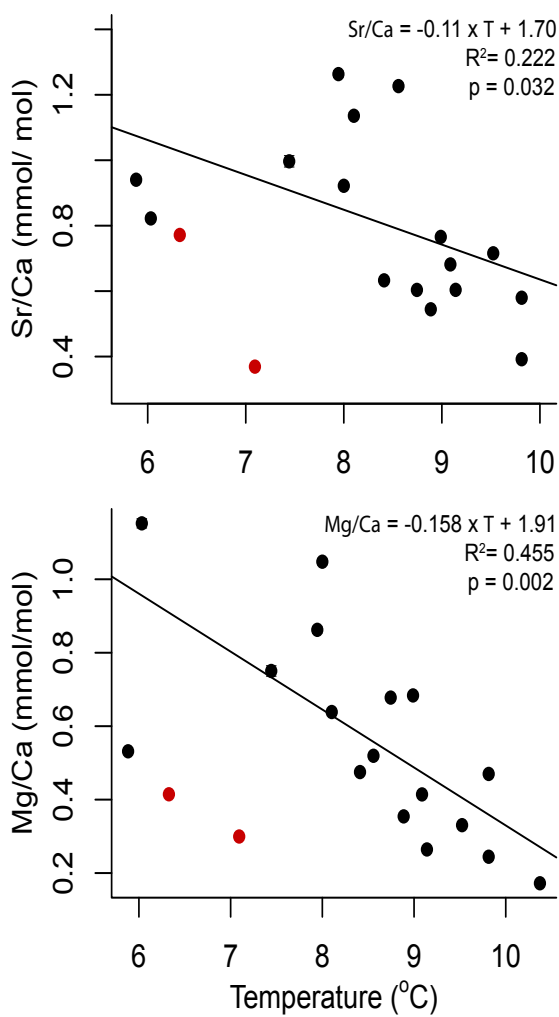


**Fig 6.** Range of Sr/Ca and Mg/Ca concentrations versus range of temperature experienced by individual *A. helmsi* shells. Samples in red (VM 1 and VM 3) are excluded from all linear models.

relationship between average temperature and Sr/Li, however the equation of this relationship ( $Sr/Li = -109.3 \times T + 2048.5$ ,  $R^2 = 0.34$ ) differs significantly from that of Füllenbach et al. (2015;  $Sr/Li = -12.3 \times T + 319$ ,  $R^2 = 0.81$ ). There was also no relationship between the range of air temperature at each site and the range of Sr/Li values. Although the difference between our observed relationship and that of Füllenbach et al. (2015) could be explained by differences in the Li and Sr concentrations of the host waters, Sr/Li also explained less variance than Sr/Ca suggesting that other factors, for example the poor constraint on water temperatures at the time of growth, represent larger sources of uncertainty than vital effects in this study. Therefore, while a significant relationship between Sr/Li and temperature was found in *A. helmsi*, caution should be used with this proxy, particularly given the large differences in slope to that of previous studies.

is the low tolerance of *A. helmsi* to salinities <10 PSU (Wells and Threlfall 1982a), meaning that bivalves in these environments may have been more seasonal in their growth habits than at other sites.

Recently, the Sr/Li ratio of biogenic carbonate has been investigated as a temperature proxy in brackish environments due to its potential to reduce the influence of vital effects (Füllenbach et al. 2015). By normalising Sr/Ca to Li/Ca, Füllenbach et al. (2015) observed a reduction in scatter and an increase in the sensitivity to temperature. Similar methods have been successfully applied in foraminifera and corals (Bryan and Marchitto 2008; Case et al. 2010; Montagna et al. 2014), however not all studies with molluscs have demonstrated significant correlations between Li/Ca and water temperature (Graniero et al. 2017). The exact mechanism of lithium incorporation into aragonite is not well understood, though it is likely that this occurs via the substitution of  $Li^+$  for  $Ca^{2+}$  to form lithium carbonate  $Li_2CO_3$  (Thébault, Schöne, et al. 2009; Hathorne et al. 2013). Here we find a statistically significant

Shell Ba/Ca has been proposed as a salinity or productivity proxy in many bivalve species as it has been strongly correlated to the Ba/Ca of waters (Gillikin et al., 2006; Elliot et al., 2009; Poulain et al., 2015; Izzo et al., 2016). In agreement to empirical studies with inorganic aragonite (Dietzel et al. 2004; Gaetani and Cohen 2006), previous studies have also found a strong correlation between Ba/Ca and temperature (Geeza et al. 2018; Wanamaker and Gillikin 2018), however these correlations have been attributed to co-variance with growth rates and thus discounted as a pure temperature effect. Our results showed no response of Ba/Ca to temperature or precipitation, but instead shell Ba/Ca was highly variable among specimens from the same collection location. Many studies have found that within-shell Ba/Ca transects are characterised by a relatively flat background signal with sharp peaks (Gillikin et al., 2008; Thébault et al., 2009; Hatch et al., 2013); this pattern was not found consistently in this study. This evidence does not support the use of Ba/Ca as an environmental proxy in *A. helmsi*.

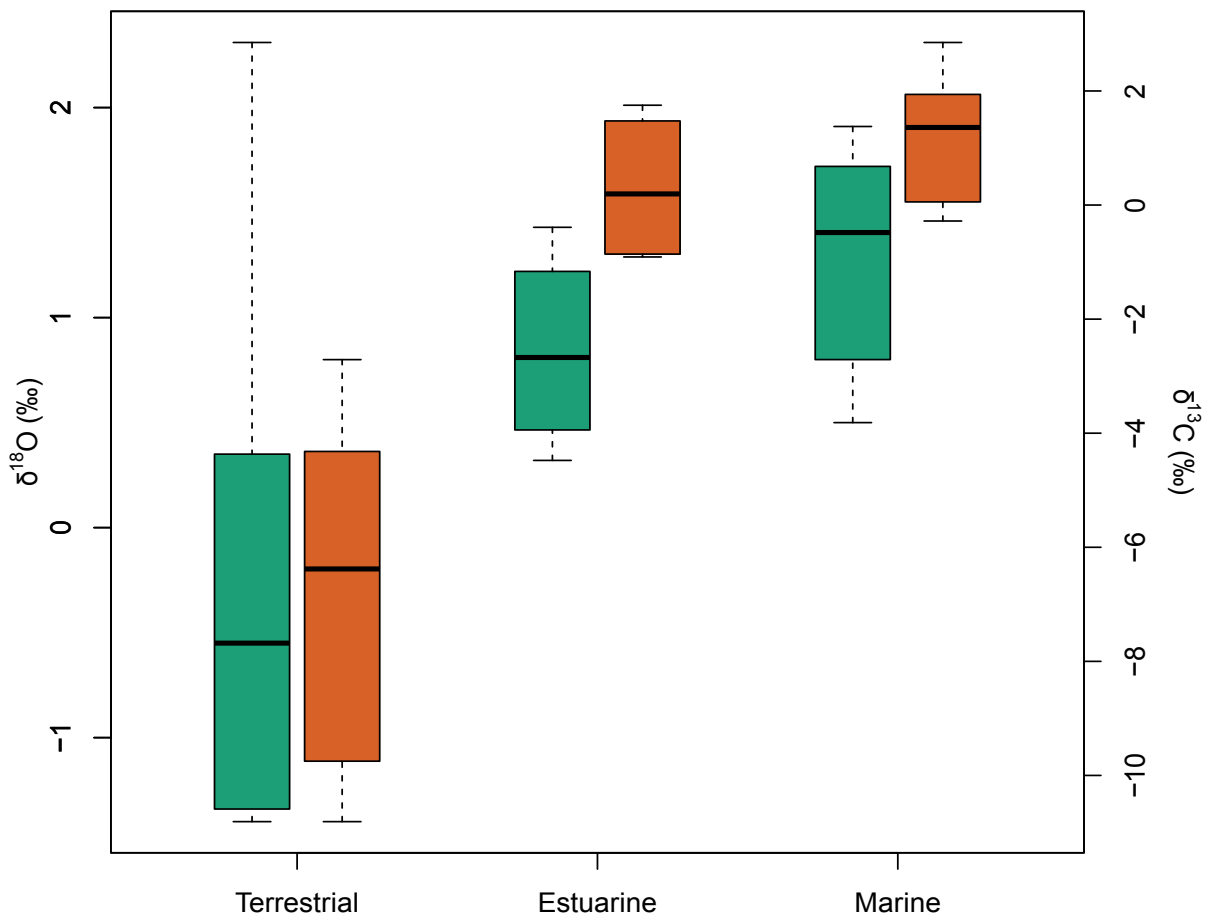


**Fig 7.** Oxygen (green) and carbon (orange) isotopes of *A. helmsi* shells grouped per the source waters of their environment. Whiskers show the upper and lower values, interquartile range is indicated by the box and the horizontal line inside the box indicates the median value. Terrestrial n = 5, Estuarine n = 4, Marine n = 8. Values from shells VM1 and VM 3 are excluded.

Investigation of element:Ca profiles of shells from the same collections illustrated similar patterns in Sr/Ca and Mg/Ca between shells, however these patterns appear to have a phase offset between samples. The similar patterns and values (particularly in shells VM 4 and VM 5) suggest that individual shells are responding to the same forcing, while the offset indicates that either shells were not living when collected or that there is a difference in growth rate between the two shells. As these shells are different sizes and therefore have different inferred ages, it is possible that as in other species, individuals experience varying growth rates and vital effects through ontogeny (Schöne et al. 2011). If this were the case, a faster growing individual would deposit more carbonate which could explain the phase offset. However, field based studies on *A. helmsi* suggesting a constant growth rate (Wells and Threlfall 1982c) are supported in this study by a lack of imaging evidence for growth lines. The impact of growth rate on elemental ratios in bivalves is unclear as many studies report it as being both significant (e.g. Takesue and van Geen, 2004; Lorrain et al., 2005; Izumida et al., 2011; Wanamaker and Gillikin, 2018) and insignificant (e.g. Stecher et al., 1996; Füllenbach et al., 2015; Geeza et al., 2018). The conditions of the current study do not allow conclusions on the role of growth rate on element incorporation. As such, we cannot be sure of the cause of this phase offset, particularly given we cannot guarantee the age of each specimen or whether the specimens were live collected. Shell microstructure has also been linked to trace element ratios with higher Sr/Ca values occurring at circatidal (Füllenbach et al. 2017) and diurnal (Sano et al. 2012) growth lines. However, the homogeneous shell architecture in this species indicates that it is possible that the potentially seasonal patterns observed in some individuals are driven by environmental variation rather than microstructure.

## 4.2 Stable isotopes

Deciphering the relationship between stable isotopes and the environment was hindered in this study due to our lack of control over the source water  $\delta^{18}\text{O}$ ,  $\delta^{13}\text{C}$ , DIC and salinity. Nevertheless, when bivalve stable isotope ratios are grouped by environmental water source, distinct isotopic differences were revealed. Both  $\delta^{18}\text{O}$  and  $\delta^{13}\text{C}$  exhibited higher values in marine environments and the range of values decreased moving from terrestrial (freshwater) through to marine influenced environments. This suggests that both ratios reflect a common environmental forcing, most likely the mixing of isotopically distinct marine and fresh waters in coastal environments. The  $\delta^{18}\text{O}$  of bivalves reflects the temperature and isotopic composition of the water in which they grew (Epstein et al. 1953); as there is no correlation between temperature or any trace elemental ratios and shell  $\delta^{18}\text{O}$  it is clear that  $\delta^{18}\text{O}$  of waters is the dominant control, as in other estuarine studies (Dettman et al. 2004; Andrus and Rich 2008). Water oxygen isotopic values



often correlate with salinity (Fry 2002) and so the variation observed in this study likely records a combination of water mixing and evaporation, accounting for the large variation, particularly in terrestrial influenced sites.

Shell  $\delta^{13}\text{C}$  is also related to salinity through the strong relationship between salinity and dissolved inorganic carbon (DIC) (Fry, 2002; Gillikin et al., 2006b; Poulain et al., 2010). It has been experimentally confirmed that the carbon incorporated into bivalve carbonate is sourced from both water DIC and metabolic DIC from food (Poulain et al. 2010). However, the same study found a strong relationship between bivalve  $\delta^{13}\text{C}$  and the  $\delta^{13}\text{C}$  of DIC ( $R^2 = 0.77$ ), supporting the conclusions of previous studies that aquatic molluscs derive the majority of their carbon from ambient DIC (McConnaughey and Gillikin 2008; Owen et al. 2008; Poulain et al. 2010). In addition to salinity, DIC is influenced by water source as fluvially transported DIC typically has a lower  $\delta^{13}\text{C}$  than marine DIC due to the presence of  $\text{CO}_2$  derived from the decomposition of terrestrial plants (McConnaughey and Gillikin 2008). This isotopic offset between water sources is observed in this study where bivalves from terrestrial waters (rivers and creeks) exhibit lower  $\delta^{13}\text{C}$  compared to bivalves from estuarine and marine environments. Similar results are reported by previous studies which found distinct differences in  $\delta^{13}\text{C}$  in bivalves from riverine and deltaic environments (Vanhof et al. 2013) and within shells transplanted from a marine to an estuarine environment (Gillikin et al., 2006b). While  $\delta^{13}\text{C}$  appears to respond to environmental changes, age related trends and uncertainties regarding the influence of metabolic DIC make quantitative salinity or DIC reconstruction from  $\delta^{13}\text{C}_{\text{shell}}$  difficult (Gillikin et al., 2006b; Gillikin et al., 2007; Poulain et al., 2010; Butler et al., 2011). Our results support those of previous studies that large changes in bivalve  $\delta^{13}\text{C}$  can reflect large changes in the  $\delta^{13}\text{C}$  of DIC and therefore differences in environment with respect to salinity and the mixing of fresh/marine water source (Gillikin et al., 2006b; Vanhof et al., 2013; Lacey et al., 2018). As a consequence, stable isotope ratios  $\delta^{18}\text{O}$  and  $\delta^{13}\text{C}$  of *A. helmsi* offer potential to determine large scale changes in environment which could be potentially useful for inferring the marine-freshwater mixing regime in palaeo-estuarine settings, or for studies of sea level change.

## 5. Conclusions

This study presents the first geochemical analysis of aragonitic shells of the bivalve *Arthritica helmsi*, a short lived micro-mollusc common to southern Australian estuaries. Several trace elemental ratios were significantly correlated to temperature – namely average Sr/Ca, Mg/Ca and Sr/Li ratios – and stable isotope tracers  $\delta^{18}\text{O}$  and  $\delta^{13}\text{C}$  broadly recorded large environmental differences. Trace element transects through individual shells from the same collection revealed similar patterns in Sr/Ca and Mg/Ca but timing of peaks did not correspond suggesting a phase

offset or that one individual was not living when collected. In part, the uncertainties exhibited by this study are due to poorly constrained environmental data, including the water chemistry, temperature, salinity and isotopic composition of the water at the time of shell growth. Further uncertainty arises from a lack of detailed knowledge of when the shells were growing and whether some shells may have been dead at time of collection. As a consequence, although analysis of museum specimens provides a valuable first look at the geographical trends in the geochemistry of bivalve shells, further research under more controlled conditions is required. Nevertheless, this study demonstrates interesting patterns in the geochemistry of *A. helmsi* shells, suggesting that geochemical analysis of fossil shells of this species has potential as a tracer of past climates, hydrology and ecology.

### **Acknowledgements**

The authors would like to acknowledge Kirrily Moore from the Tasmanian Museum and Art Gallery, Chris Rowley from Museum Victoria, and Mandy Reid from The Australian Museum for providing samples for this study. Sarah Gilbert, Mark Rollog, Ben Wade, Tony Hall and Ken Neubauer are thanked for their assistance with trace elemental analyses, stable isotope analyses, electron microprobe analyses, XRD analysis and SEM imaging respectively. This research was supported by a grant from the Sir Mark Mitchell Foundation, South Australia.

**References**

- Andrus, C.F.T., and Rich, K.W. 2008. A preliminary assessment of oxygen isotope fractionation and growth increment periodicity in the estuarine clam *Rangia cuneata*. *Geo-Marine Letters* 28: 301–308. doi:10.1007/s00367-008-0109-3.
- Bar-Matthews, M., Ayalon, A., Gilmour, M., Matthews, A., and Hawkesworth, C.J. 2003. Sea-land oxygen isotopic relationships from planktonic foraminifera and speleothems in the Eastern Mediterranean region and their implication for paleorainfall during interglacial intervals. *Geochimica et Cosmochimica Acta* 67: 3181–3199.
- Böhm, F., Joachimski, M.M., Dullo, W.C., Eisenhauer, A., Lehnert, H., Reitner, J., and Wörheide, G. 2000. Oxygen isotope fractionation in marine aragonite of coralline sponges. *Geochimica et Cosmochimica Acta* 64: 1695–1703. doi:10.1016/S0016-7037(99)00408-1.
- Bougeois, L., de Rafélis, M., Reichart, G.J., de Nooijer, L.J., Nicollin, F., and Dupont-Nivet, G. 2014. A high resolution study of trace elements and stable isotopes in oyster shells to estimate central asian middle eocene seasonality. *Chemical Geology* 363: 200–212. doi:10.1016/j.chemgeo.2013.10.037.
- Bryan, S.P., and Marchitto, T.M. 2008. Mg/Ca-temperature proxy in benthic foraminifera: New calibrations from the Florida Straits and a hypothesis regarding Mg/Li. *Paleoceanography* 23: 1–17. doi:10.1029/2007PA001553.
- Butler, P.G., Richardson, C.A., Scourse, J.D., Witbaard, R., Schöne, B.R., Fraser, N.M., Wanamaker, A.D., Bryant, C.L., Harris, I., and Robertson, I. 2009. Accurate increment identification and the spatial extent of the common signal in five *Arctica islandica* chronologies from the Fladen Ground, northern North Sea. *Paleoceanography* 24: 1–18. doi:10.1029/2008PA001715.
- Butler, P.G., Wanamaker, A.D., Scourse, J.D., Richardson, C.A., and Reynolds, D.J. 2011. Long-term stability of  $\delta^{13}\text{C}$  with respect to biological age in the aragonite shell of mature specimens of the bivalve mollusk *Arctica islandica*. *Palaeogeography, Palaeoclimatology, Palaeoecology* 302: 21–30. doi:10.1016/j.palaeo.2010.03.038.
- Carré, M., Sachs, J.P., Purca, S., Schauer, A.J., Braconnot, P., Falcón, R.A., Julien, M., and Lavallée, D. 2014. Holocene history of ENSO variance and asymmetry in the eastern tropical Pacific. *Science* 345: 1045–1048.
- Carré, M., Sachs, J.P., Schauer, A.J., Rodríguez, W.E., and Ramos, F.C. 2013. Reconstructing El Niño-Southern Oscillation activity and ocean temperature seasonality from short-lived marine mollusk shells from Peru. *Palaeogeography, Palaeoclimatology, Palaeoecology* 371: 45–53. doi:10.1016/j.palaeo.2012.12.014.
- Case, D.H., Robinson, L.F., Auro, M.E., and Gagnon, A.C. 2010. Environmental and biological controls on Mg and Li in deep-sea scleractinian corals. *Earth and Planetary Science Letters* 300: 215–225. doi:10.1016/j.epsl.2010.09.029.
- Chamberlayne, B.K. 2015. Late Holocene seasonal and multicentennial hydroclimate variability in the Coorong Lagoon, South Australia: evidence from stable isotopes and trace element profiles of bivalve molluscs (unpublished honours thesis), The University of Adelaide,

Adelaide, Australia

- Dettman, D.L., Flessa, K.W., Roopnarine, P.D., Schöne, B.R., and Goodwin, D.H. 2004. The use of oxygen isotope variation in shells of estuarine mollusks as a quantitative record of seasonal and annual Colorado River discharge. *Geochimica et Cosmochimica Acta* 68: 1253–1263. doi:10.1016/j.gca.2003.09.008.
- Dietzel, M., Gussone, N., and Eisenhauer, A. 2004. Co-precipitation of Sr<sup>2+</sup> and Ba<sup>2+</sup> with aragonite by membrane diffusion of CO<sub>2</sub> between 10 and 50 °C. *Chemical Geology* 203: 139–151. doi:10.1016/j.chemgeo.2003.09.008.
- Dodd, J. Robert. 1965. Environmental control of strontium and magnesium in *Mytilus*. *Geochimica et Cosmochimica Acta* 29: 385–398. doi:10.1016/0016-7037(65)90035-9.
- Dodd, J R, and Crisp, E.L. 1982. Non-linear variation with salinity of Sr/Ca and Mg/Ca ratios in water and aragonitic bivalve shells and implications for paleosalinity studies. *Palaeogeography Palaeoclimatology Palaeoecology* 38: 45–56.
- Donovan, J.J., and Armstrong, J.T. 2014. A New EPMA Method For Fast Trace Element Analysis In Simple Matrices. *Microscopy and Microanalysis* 20: 724–725. doi:10.1017/S1431927614005340.
- Donovan, J.J., and Tingle, T.N. 1996. An improved mean atomic number background correction for quantitative microanalysis. *Microscopy and Microanalysis*. doi:10.1017/S1431927696210013.
- Elliot, M., Welsh, K., Chilcott, C., McCulloch, M., Chappell, J., and Ayling, B. 2009. Profiles of trace elements and stable isotopes derived from giant long-lived *Tridacna gigas* bivalves: Potential applications in paleoclimate studies. *Palaeogeography, Palaeoclimatology, Palaeoecology* 280: 132–142. doi:10.1016/j.palaeo.2009.06.007.
- Epstein, S., Buchsbaum, R., Lowenstam, H. a, and Urey, H.C. 1953. Revised Carbonate-Water Isotopic Temperature Scale. *Geological Society of America Bulletin* 64: 1315–1325. doi:10.1130/0016-7606(1953)64.
- Epstein, S., and Mayeda, T. 1953. Variation of O<sup>18</sup> content of waters from natural sources. *Geochimica et Cosmochimica Acta* 4: 213–224.
- Ferguson, J.E., Johnson, K.R., Santos, G., Meyer, L., and Tripathi, A. 2013. Investigating δ<sup>13</sup>C and Δ<sup>14</sup>C within *Mytilus californianus* shells as proxies of upwelling intensity. *Geochemistry, Geophysics, Geosystems* 14: 1856–1865. doi:10.1002/ggge.20090.
- Freitas, P.S., Clarke, L.J., Kennedy, H., and Richardson, C.A. 2012. The potential of combined Mg/Ca and δ<sup>18</sup>O measurements within the shell of the bivalve *Pecten maximus* to estimate seawater δ<sup>18</sup>O composition. *Chemical Geology* 291: 286–293. doi:10.1016/j.chemgeo.2011.10.023.
- Fry, B. 2002. Conservative mixing of stable isotopes across estuarine salinity gradients: A conceptual framework for monitoring watershed influences on downstream fisheries production. *Estuaries* 25: 264–271. doi:10.1007/BF02691313.
- Füllenbach, C.S., Schöne, B.R., and Mertz-Kraus, R. 2015. Strontium/lithium ratio in aragonitic

- shells of *Cerastoderma edule* (Bivalvia) - A new potential temperature proxy for brackish environments. *Chemical Geology* 417: 341–355. doi:10.1016/j.chemgeo.2015.10.030.
- Füllenbach, C.S., Schöne, B.R., Shirai, K., Takahata, N., Ishida, A., and Sano, Y. 2017. Minute co-variations of Sr/Ca ratios and microstructures in the aragonitic shell of *Cerastoderma edule* (Bivalvia) – Are geochemical variations at the ultra-scale masking potential environmental signals? *Geochimica et Cosmochimica Acta* 205: 256–271. doi:10.1016/j.gca.2017.02.019.
- Gaetani, G.A., and Cohen, A.L. 2006. Element partitioning during precipitation of aragonite from seawater: A framework for understanding paleoproxies. *Geochimica et Cosmochimica Acta* 70: 4617–4634. doi:10.1016/j.gca.2006.07.008.
- Geeza, T.J., Gillikin, D.P., Goodwin, D.H., Evans, S.D., Watters, T., and Warner, N.R. 2018. Controls on magnesium, manganese, strontium, and barium concentrations recorded in freshwater mussel shells from Ohio. *Chemical Geology*. 1–12. doi:10.1016/j.chemgeo.2018.01.001.
- Gillikin, D.P., Dehairs, F., Lorrain, A., Steenmans, D., Baeyens, W., and André, L. 2006. Barium uptake into the shells of the common mussel (*Mytilus edulis*) and the potential for estuarine paleo-chemistry reconstruction. *Geochimica et Cosmochimica Acta* 70: 395–407. doi:10.1016/j.gca.2005.09.015.
- Gillikin, D.P., Lorrain, A., Bouillon, S., Willenz, P., and Dehairs, F. 2006. Stable carbon isotopic composition of *Mytilus edulis* shells: relation to metabolism, salinity,  $\delta^{13}\text{C}_{\text{DIC}}$  and phytoplankton. *Organic Geochemistry* 37: 1371–1382. doi:10.1016/j.orggeochem.2006.03.008.
- Gillikin, D.P., Lorrain, A., Meng, L., and Dehairs, F. 2007. A large metabolic carbon contribution to the  $\delta^{13}\text{C}$  record in marine aragonitic bivalve shells. *Geochimica et Cosmochimica Acta* 71: 2936–2946. doi:10.1016/j.gca.2007.04.003.
- Gillikin, David Paul, Lorrain, A., Paulet, Y.M., André, L., and Dehairs, F. 2008. Synchronous barium peaks in high-resolution profiles of calcite and aragonite marine bivalve shells. *Geo-Marine Letters* 28: 351–358. doi:10.1007/s00367-008-0111-9.
- Gillikin, David Paul, De Ridder, F., Ulens, H., Elskens, M., Keppens, E., Baeyens, W., and Dehairs, F. 2005. Assessing the reproducibility and reliability of estuarine bivalve shells (*Saxidomus giganteus*) for sea surface temperature reconstruction: Implications for paleoclimate studies. *Palaeogeography, Palaeoclimatology, Palaeoecology* 228: 70–85. doi:10.1016/j.palaeo.2005.03.047.
- Goodwin, D.H., Gillikin, D.P., and Roopnarine, P.D. 2013. Preliminary evaluation of potential stable isotope and trace element productivity proxies in the oyster *Crassostrea gigas*. *Palaeogeography, Palaeoclimatology, Palaeoecology* 373: 88–97. doi:10.1016/j.palaeo.2012.03.034.
- Graniero, L.E., Surge, D., Gillikin, D.P., Briz, I., and Álvarez, M. 2017. Assessing elemental ratios as a paleotemperature proxy in the calcite shells of patelloid limpets. *Palaeogeography, Palaeoclimatology, Palaeoecology* 465: 376–385. doi:10.1016/j.palaeo.2016.10.021.

- Grossman, E.L., and Ku, T.-L. 1986. Oxygen and carbon isotope fractionation in biogenic aragonite: Temperature effects. *Chemical Geology: Isotope Geoscience section* 59: 59–74. doi:10.1016/0168-9622(86)90057-6.
- Hart, S.R., and Blusztajn, J. 1998. Clams As Recorders of Ocean Ridge Volcanism and Hydrothermal Vent Field Activity. *Science* 280: 883–886.
- Hatch, M.B.A., Schellenberg, S.A., and Carter, M.L. 2013. Ba / Ca variations in the modern intertidal bean clam *Donax gouldii* : An upwelling proxy? *Palaeogeography, Palaeoclimatology, Palaeoecology* 373: 98–107. doi:10.1016/j.palaeo.2012.03.006.
- Hathorne, E.C., Felis, T., Suzuki, A., Kawahata, H., and Cabioch, G. 2013. Lithium in the aragonite skeletons of massive *Porites* corals: A new tool to reconstruct tropical sea surface temperatures. *Paleoceanography* 28: 143–152. doi:10.1029/2012PA002311.
- Hellstrom, J., Paton, C., Woodhead, J., and Hergt, J. 2008. Iolite: software for spatially resolved LA-(quad and MC) ICPMS analysis. In *Laser Ablation ICP-MS in the Earth Sciences: Current practices and Outstanding Issues*, ed. Sylvester, P., 343. Mineralogical Association of Canada short course volume 40.
- Izumida, H., Yoshimura, T., Suzuki, A., Nakashima, R., Ishimura, T., Yasuhara, M., Inamura, A., Shikazono, N., and Kawahata, H. 2011. Biological and water chemistry controls on Sr/Ca, Ba/Ca, Mg/Ca and  $\delta^{18}\text{O}$  profiles in freshwater pearl mussel *Hyriopsis* sp. *Palaeogeography, Palaeoclimatology, Palaeoecology* 309: 298–308. doi:10.1016/j.palaeo.2011.06.014.
- Izzo, C., Manetti, D., Doubleday, Z.A., and Gillanders, B.M. 2016. Calibrating the element composition of *Donax deltoides* shells as a palaeo-salinity proxy. *Palaeogeography, Palaeoclimatology, Palaeoecology* 484: 89–96. doi:10.1016/j.palaeo.2016.11.038.
- Jeffrey, S.J., Carter, J.O., Moodie, K.B., and Beswick, A.R. 2001. Using spatial interpolation to construct a comprehensive archive of Australian climate data. *Environmental Modelling and Software* 16: 309–330. doi:10.1016/S1364-8152(01)00008-1.
- Kelemen, Z., Gillikin, D.P., Graniero, L.E., Havel, H., Darchambeau, F., Borges, A. V., Yambélé, A., Bassirou, A., and Bouillon, S. 2017. Calibration of hydroclimate proxies in freshwater bivalve shells from Central and West Africa. *Geochimica et Cosmochimica Acta* 208: 41–62. doi:10.1016/j.gca.2017.03.025.
- Krause-Nehring, J., Brey, T., and Thorrold, S.R. 2012. Centennial records of lead contamination in northern Atlantic bivalves (*Arctica islandica*). *Marine Pollution Bulletin* 64: 233–240. doi:10.1016/j.marpolbul.2011.11.028.
- Krause-Nehring, J., Kligel, A., Nehrke, G., Brellocks, B., and Brey, T. 2011. Impact of sample pretreatment on the measured element concentrations in the bivalve *Arctica islandica*. *Geochemistry, Geophysics, Geosystems* 12. doi:10.1029/2011GC003630.
- Lacey, J.H., Leng, M.J., Peckover, E.N., Dean, J.R., Wilke, T., Francke, A., Zhang, X., Masi, A., and Wagner, B. 2018. Investigating the environmental interpretation of oxygen and carbon isotope data from whole and fragmented bivalve shells. *Quaternary Science Reviews* 194: 55–61. doi:10.1016/j.quascirev.2018.06.025.

- Livingstone, D.M., and Lotter, A.F. 1998. The relationship between air and water temperatures in lakes of the Swiss Plateau: a case study with palaeolimnological implication. *Journal of Paleolimnology* 19: 181–198. doi:10.1023/a:1007904817619.
- Lorens, R.B., and Bender, M.L. 1980. The impact of solution chemistry on *Mytilus edulis* calcite and aragonite. *Geochimica et Cosmochimica Acta* 44: 1265–1278. doi:10.1016/0016-7037(80)90087-3.
- Lorrain, A., Gillikin, D.P., Paulet, Y.M., Chauvaud, L., Le Mercier, A., Navez, J., and André, L. 2005. Strong kinetic effects on Sr/Ca ratios in the calcitic bivalve *Pecten maximus*. *Geology* 33: 965–968. doi:10.1130/G22048.1.
- McCombie, A.M. 1959. Some Relations Between Air Temperatures and the Surface Water Temperatures of Lakes. *Limnology and Oceanography* 4: 252–258. doi:10.4319/lo.1959.4.3.0252.
- McConnaughey, T.A., and Gillikin, D.P. 2008. Carbon isotopes in mollusk shell carbonates. *Geo-Marine Letters* 28: 287–299. doi:10.1007/s00367-008-0116-4.
- McCulloch, M., Mortimer, G., Esat, T., Xianhua, L., Pillans, B., and Chappell, J. 1996. High resolution windows into early Holocene climate: Sr/Ca coral records from the Huon Peninsula. *Earth and Planetary Science Letters* 138: 169–178. doi:10.1016/0012-821X(95)00230-A.
- Milton, D.A., and Chenery, S.R. 1998. The effect of otolith storage methods on the concentrations of elements detected by laser-ablation ICPMS. *Journal of Fish Biology* 53: 785–794. doi:10.1006/jfbi.1998.0745.
- Mitsuguchi, T., Matsumoto, E., Abe, O., Uchida, T., and Isdale, P.J.. 1996. Mg / Ca Thermometry in Coral Skeletons. *Science* 274: 961–963.
- Montagna, P., McCulloch, M., Douville, E., López Correa, M., Trotter, J., Rodolfo-Metalpa, R., Dissard, D., et al. 2014. Li/Mg systematics in scleractinian corals: Calibration of the thermometer. *Geochimica et Cosmochimica Acta* 132: 288–310. doi:10.1016/j.gca.2014.02.005.
- Mook, W.G. 1971. Paleotemperatures and chlorinities from stable carbon and oxygen isotopes in shell carbonate. *Palaeogeography, Palaeoclimatology, Palaeoecology* 9: 245–263. doi:10.1016/0031-0182(71)90002-2.
- Mouchi, V., de Rafélis, M., Lartaud, F., Fialin, M., and Verrecchia, E. 2013. Chemical labelling of oyster shells used for time-calibrated high-resolution Mg/Ca ratios: A tool for estimation of past seasonal temperature variations. *Palaeogeography, Palaeoclimatology, Palaeoecology* 373: 66–74. doi:10.1016/j.palaeo.2012.05.023.
- O’Neil, D.D., and Gillikin, D.P. 2014. Do freshwater mussel shells record road-salt pollution? *Scientific Reports* 4: 7168. doi:10.1038/srep07168.
- Owen, E.F., Wanamaker, A.D., Feindel, S.C., Schöne, B.R., and Rawson, P.D. 2008. Stable carbon and oxygen isotope fractionation in bivalve (*Placopecten magellanicus*) larval aragonite. *Geochimica et Cosmochimica Acta* 72: 4687–4698. doi:10.1016/j.gca.2008.06.029.

- Paton, C., Hellstrom, J., Paul, B., Woodhead, J., and Hergt, J. 2011. Iolite: Freeware for the visualisation and processing of mass spectrometric data. *Journal of Analytical Atomic Spectrometry* 26: 2508. doi:10.1039/c1ja10172b.
- Poulain, C., Gillikin, D.P., Thébault, J., Munaron, J.M., Bohn, M., Robert, R., Paulet, Y.M., and Lorrain, A. 2015. An evaluation of Mg/Ca, Sr/Ca, and Ba/Ca ratios as environmental proxies in aragonite bivalve shells. *Chemical Geology* 396: 42–50. doi:10.1016/j.chemgeo.2014.12.019.
- Poulain, C., Lorrain, A., Mas, R., Gillikin, D.P., Dehairs, F., Robert, R., and Paulet, Y.M. 2010. Experimental shift of diet and DIC stable carbon isotopes: Influence on shell  $\delta^{13}\text{C}$  values in the Manila clam *Ruditapes philippinarum*. *Chemical Geology* 272: 75–82. doi:10.1016/j.chemgeo.2010.02.006.
- Vander Putten, E., Dehairs, F., Keppens, E., and Baeyens, W. 2000. High resolution distribution of trace elements in the calcite shell layer of modern *Mytilus edulis*: Environmental and biological controls. *Geochimica et Cosmochimica Acta* 64: 997–1011.
- Sano, Y., Kobayashi, S., Shirai, K., Takahata, N., Matsumoto, K., Watanabe, T., Sowa, K., and Iwai, K. 2012. Past daily light cycle recorded in the strontium/calcium ratios of giant clam shells. *Nature Communications* 3:761 doi:10.1038/ncomms1763.
- Schöne, B.R. 2008. The curse of physiology - Challenges and opportunities in the interpretation of geochemical data from mollusk shells. *Geo-Marine Letters* 28: 269–285. doi:10.1007/s00367-008-0114-6.
- Schöne, B.R., and Fiebig, J. 2009. Seasonality in the North Sea during the Allerød and Late Medieval Climate Optimum using bivalve sclerochronology. *International Journal of Earth Sciences* 98: 83–98.
- Schöne, B.R., Freyre Castro, A.D., Fiebig, J., Houk, S.D., Oschmann, W., and Kröncke, I. 2004. Sea surface water temperatures over the period 1884–1983 reconstructed from oxygen isotope ratios of a bivalve mollusk shell (*Arctica islandica*, southern North Sea). *Palaeogeography, Palaeoclimatology, Palaeoecology* 212: 215–232. doi:10.1016/j.palaeo.2004.05.024.
- Schöne, B.R., and Gillikin, D.P. 2013. Unraveling environmental histories from skeletal diaries - Advances in sclerochronology. *Palaeogeography, Palaeoclimatology, Palaeoecology* 373: 1–5. doi:10.1016/j.palaeo.2012.11.026.
- Schöne, B.R., Schmitt, K., and Maus, M. 2017. Effects of sample pretreatment and external contamination on bivalve shell and Carrara marble  $\delta^{18}\text{O}$  and  $\delta^{13}\text{C}$  signatures. *Palaeogeography, Palaeoclimatology, Palaeoecology* 484: 22–32. doi:10.1016/j.palaeo.2016.10.026.
- Schöne, B.R., Zhang, Z., Radermacher, P., Thébault, J., Jacob, D.E., Nunn, E. V., and Maurer, A.-F. 2011. Sr/Ca and Mg/Ca ratios of ontogenetically old, long-lived bivalve shells (*Arctica islandica*) and their function as paleotemperature proxies. *Palaeogeography, Palaeoclimatology, Palaeoecology* 302: 52–64. doi:10.1016/j.palaeo.2010.03.016.
- Sinclair, D.J., Kinsley, L., and McCulloch, M.T. 1998. High resolution analysis of trace elements



- in corals by laser ablation ICP-MS. *Geochimica Et Cosmochimica Acta* 62: 1889–1901. doi:10.1016/S0016-7037(98)00112-4.
- Stecher, H.A., Krantz, D.E., Lord, C.J., Luther, G.W., and Bock, K.W. 1996. Profiles of strontium and barium in *Mercenaria mercenaria* and *Spisula solidissima* shells. *Geochimica et Cosmochimica Acta* 60: 3445–3456. doi:10.1016/0016-7037(96)00179-2.
- Surge, D., and Lohmann, K.C. 2008. Evaluating Mg/Ca ratios as a temperature proxy in the estuarine oyster, *Crassostrea virginica*. *Journal of Geophysical Research* 113: 1–9.
- Surge, D., and Walker, K.J. 2006. Geochemical variation in microstructural shell layers of the southern quahog (*Mercenaria campechiensis*): Implications for reconstructing seasonality. *Palaeogeography, Palaeoclimatology, Palaeoecology* 237: 182–190. doi:10.1016/j.palaeo.2005.11.016.
- Takesue, R.K., and van Geen, A. 2004. Mg/Ca, Sr/Ca, and stable isotopes in modern and Holocene *Protothaca staminea* shells from a northern California coastal upwelling region. *Geochimica et Cosmochimica Acta* 68: 3845–3861. doi:10.1016/j.gca.2004.03.021.
- Thébault, J., Chauvaud, L., L'Helguen, S., Clavier, J., Barats, A., Jacquet, S., Pécheyran, C., and Amouroux, D. 2009. Barium and molybdenum records in bivalve shells: Geochemical proxies for phytoplankton dynamics in coastal environments? *Limnology and Oceanography* 54: 1002–1014. doi:10.4319/lo.2009.54.3.1002.
- Thébault, J., Schöne, B.R., Hallmann, N., Barth, M., and Nunn, E. V. 2009. Investigation of Li/Ca variations in aragonitic shells of the ocean quahog *Arctica islandica*, northeast Iceland. *Geochemistry, Geophysics, Geosystems* 10. doi:10.1029/2009GC002789.
- Tindall, J., Flecker, R., Valdes, P., Schmidt, D.N., Markwick, P., and Harris, J. 2010. Modelling the oxygen isotope distribution of ancient seawater using a coupled ocean-atmosphere GCM: Implications for reconstructing early Eocene climate. *Earth and Planetary Science Letters* 292: 265–273. doi:10.1016/j.epsl.2009.12.049.
- Tyler, J.J., Leng, M.J., Sloane, H.J., Sachse, D., and Gleixner, G. 2008. Oxygen isotope ratios of sedimentary biogenic silica reflect the European transcontinental climate gradient. *Journal of Quaternary Science* 23: 341–350. doi:10.1002/jqs.
- Tynan, S., Opdyke, B.N., Walczak, M., Eggins, S., and Dutton, A. 2016. Assessment of Mg / Ca in *Saccostrea glomerata* ( the Sydney rock oyster ) shell as a potential temperature record. *Palaeogeography, Palaeoclimatology, Palaeoecology* 484: 79-88. doi:10.1016/j.palaeo.2016.08.009.
- Urey, H.C., Lowenstam, H.A., Epstein, S., and McKinney, C.R. 1951. Measurement of paleotemperatures and temperatures of the Upper Cretaceous of England, Denmark and the Southeastern United States. *Bulletin of the Geological Society of America* 62: 399–416.
- Vonhof, H.B., Joordens, J.C.A., Noback, M.L., van der Lubbe, J.H.J.L., Feibel, C.S., and Kroon, D. 2013. Environmental and climatic control on seasonal stable isotope variation of freshwater molluscan bivalves in the Turkana Basin (Kenya). *Palaeogeography, Palaeoclimatology, Palaeoecology* 383–384: 16–26. doi:10.1016/j.palaeo.2013.04.022.

- Wanamaker, A.D., and Gillikin, D.P. 2018. Strontium, magnesium, and barium incorporation in aragonitic shells of juvenile *Arctica islandica*: Insights from temperature controlled experiments. *Chemical Geology* doi:10.1016/j.chemgeo.2018.02.012.
- Wanamaker, A.D., Kreutz, K.J., Schöne, B.R., Maasch, K.A., Pershing, A.J., Borns, H.W., Introne, D.S., and Feindel, S. 2009. A late Holocene paleo-productivity record in the western Gulf of Maine, USA, inferred from growth histories of the long-lived ocean quahog (*Arctica islandica*). *International Journal of Earth Sciences* 98: 19–29.
- Wanamaker, A.D., Kreutz, K.J., Wilson, T., Borns, H.W., Introne, D.S., and Feindel, S. 2008. Experimentally determined Mg/Ca and Sr/Ca ratios in juvenile bivalve calcite for *Mytilus edulis*: Implications for paleotemperature reconstructions. *Geo-Marine Letters* 28: 359–368. doi:10.1007/s00367-008-0112-8.
- Weber, J.N. 1973. Incorporation of strontium into reef coral skeletal carbonate. *Geochimica et Cosmochimica Acta* 37: 2173–2190. doi:10.1016/0016-7037(73)90015-X.
- Wells, F.E., and Threlfall, T.J. 1982a. Salinity and temperature tolerance of *Hydrococcus brazieri* (T. Woods, 1876) and *Arthritica semen* (Menke, 1843) from the Peel-Harvey estuarine system, Western Australia. *Journal of the Malacological Society of Australia* 5: 151–156.
- Wells, F.E., and Threlfall, T.J. 1982b. Reproductive strategies of *Hydrococcus brazieri* (Tenison Woods, 1876) and *Arthritica semen* (Menke, 1843) in Peel Inlet, Western Australia. *Journal of the Malacological Society of Australia* 5: 157–166.
- Wells, F.E., and Threlfall, T.J. 1982c. Density Fluctuations, Growth and Dry Tissue Production of *Hydrococcus Brazieri* (Tenison Woods, 1876) and *Arthritica semen* (Menke, 1843) in Peel Inlet, Western Australia. *Journal of Molluscan Studies* 48: 310–320.
- Wurster, C.M., and Patterson, W.P. 2001. Seasonal variation in stable oxygen and carbon isotope values recovered from modern lacustrine freshwater molluscs: Paleoclimatological implications for sub-weekly temperature records. *Journal of Paleolimnology* 26: 205–218. doi:10.1023/A:1011194011250.
- Yan, H., Shao, D., Wang, Y., and Sun, L. 2013. Sr/Ca profile of long-lived *Tridacna gigas* bivalves from South China Sea: A new high-resolution SST proxy. *Geochimica et Cosmochimica Acta* 112: 52–65. doi:10.1016/j.gca.2013.03.007.
- Zhao, L., Schöne, B.R., and Mertz-Kraus, R. 2017. Controls on strontium and barium incorporation into freshwater bivalve shells (*Corbicula fluminea*). *Palaeogeography, Palaeoclimatology, Palaeoecology* 465: 386–394. doi:10.1016/j.palaeo.2015.11.040.

## Supplementary Information

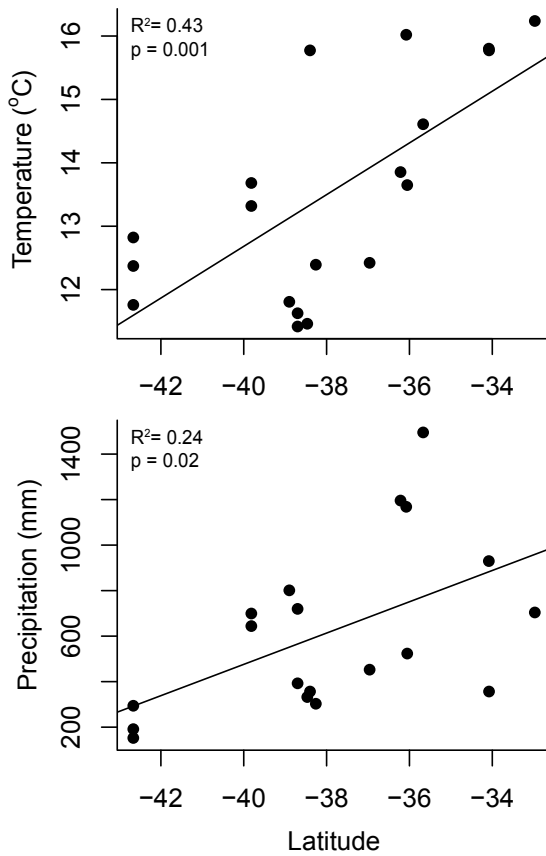


**Fig S1.** Temperature and precipitation versus latitude for sample sites. Linear relationship (solid line) and coefficient of variation ( $R^2$ ) are shown.

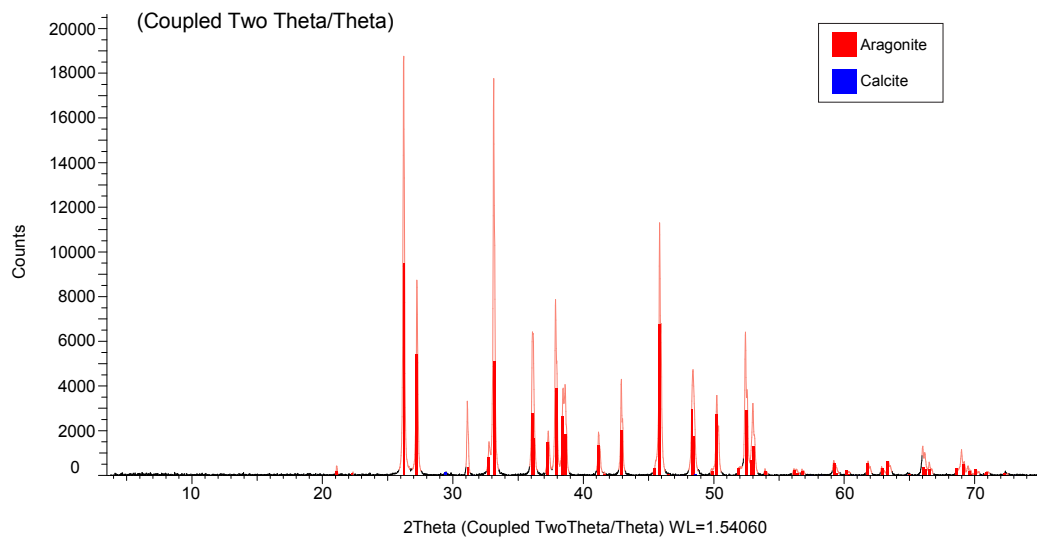


**Fig S2.** *A. helmsi* XRD profile. Bivalve carbonate peaks (pink) are overlain with the aragonite spectra (red) and calcite spectra (blue).

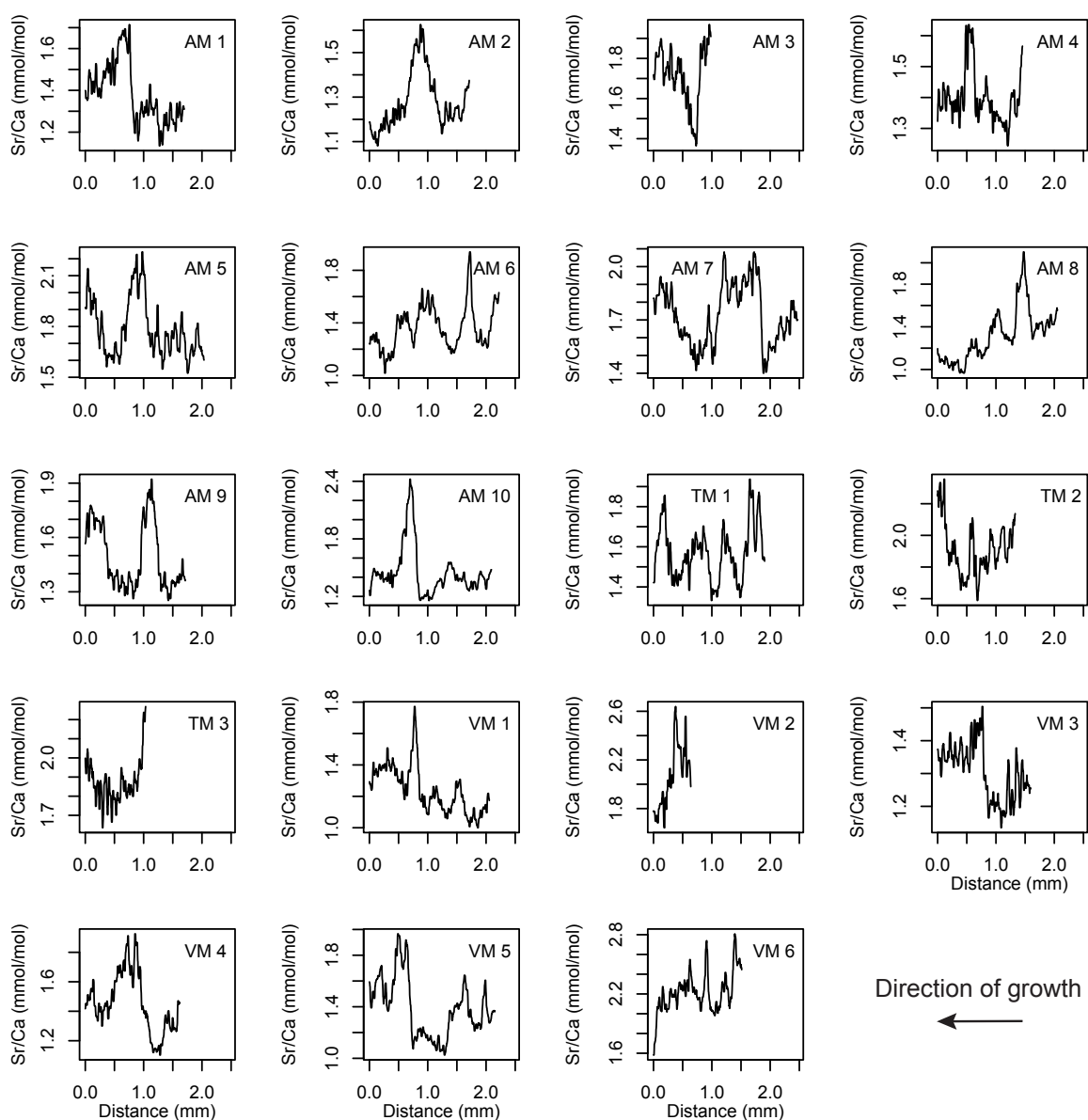


**Fig S3.** Sr/Ca profiles across outer layer of *A. helmsi* shells. The ventral margin of each shell (0 mm) represents the most recent growth before collection.

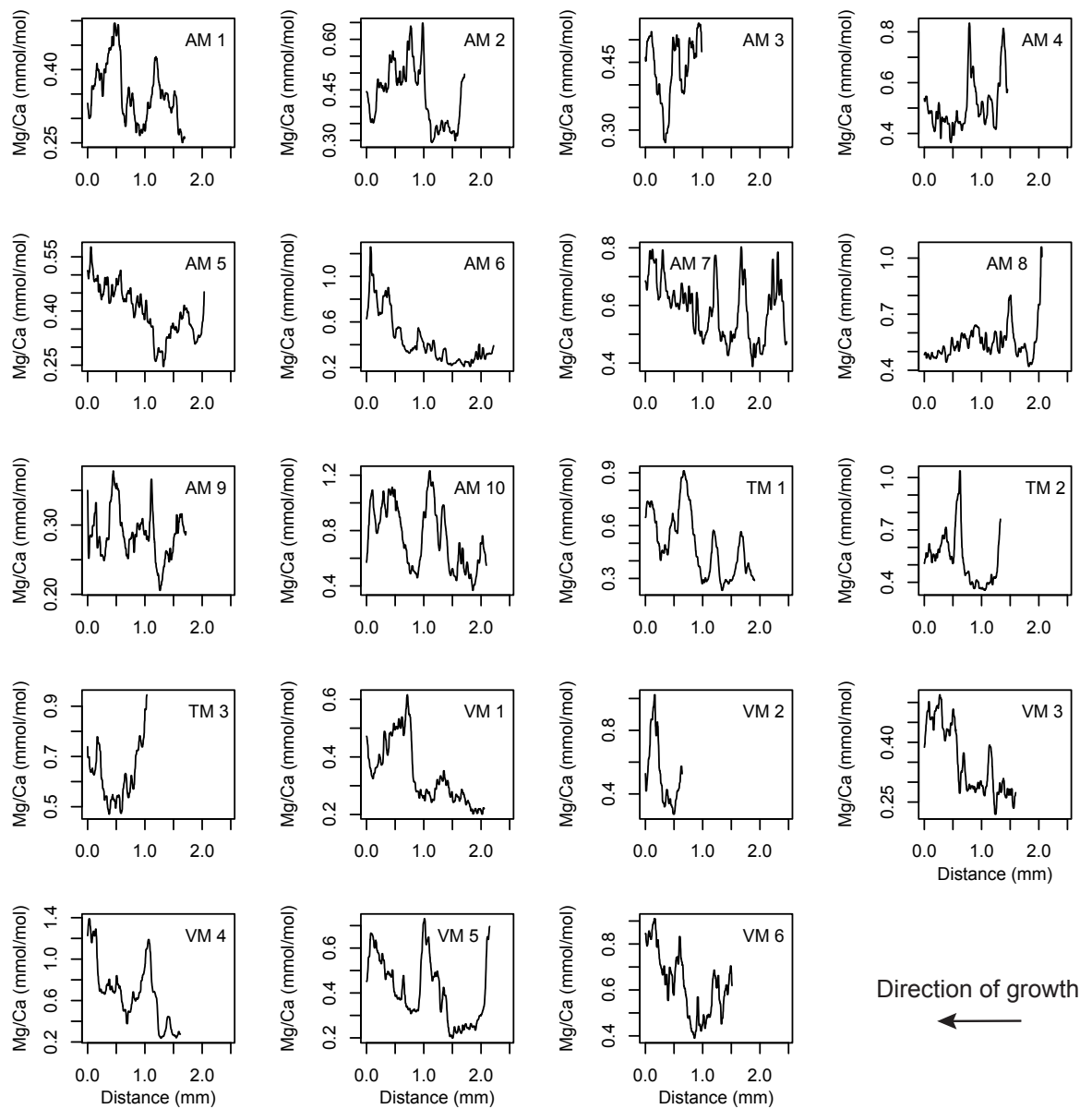


**Fig S4.** Mg/Ca profiles across outer layer of *A. helmsi* shells. The ventral margin of each shell (0 mm) represents the most recent growth before collection.

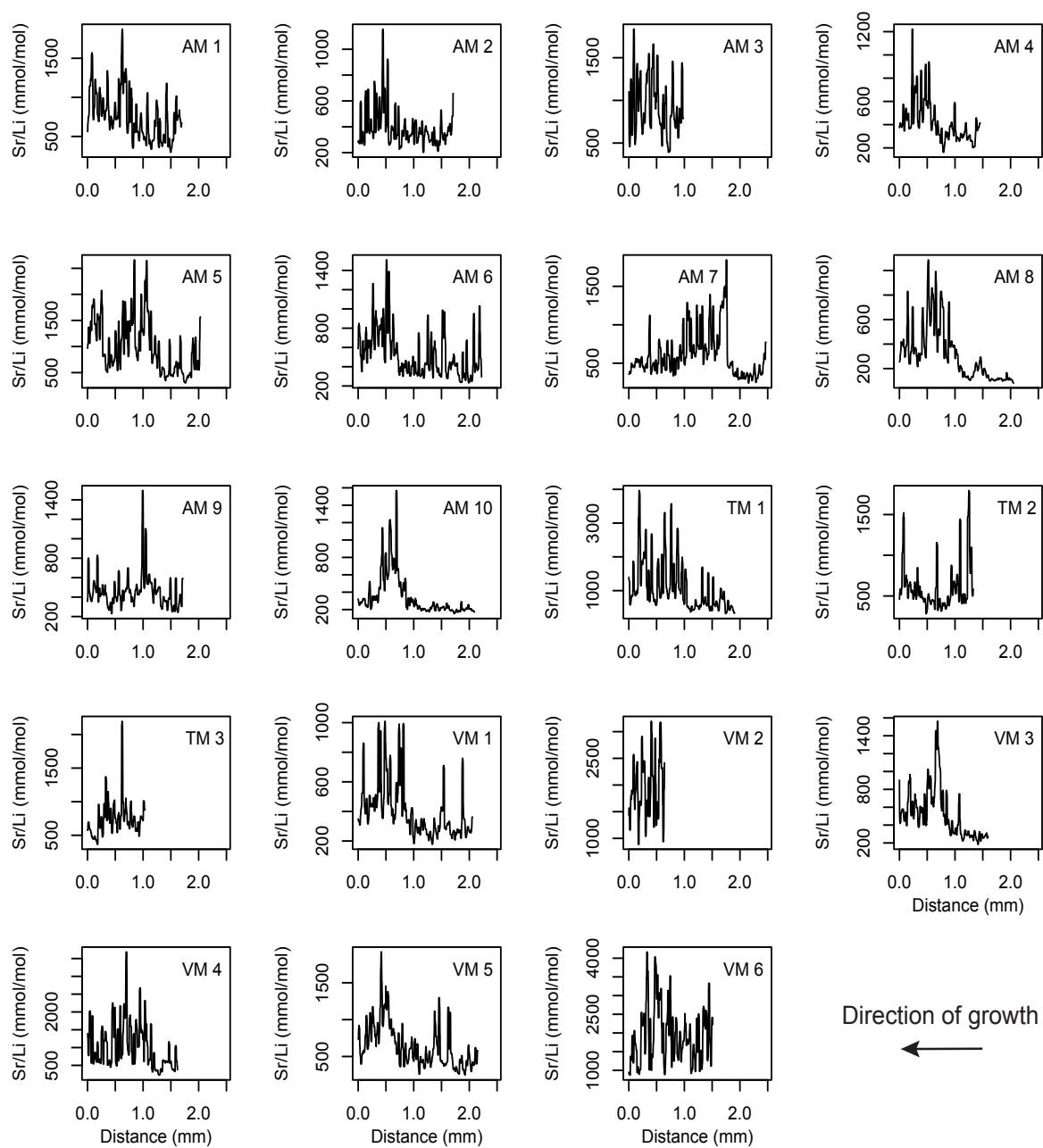


**Fig S5.** Sr/Li profiles across outer layer of *A. helmsi* shells. The ventral margin of each shell (0 mm) represents the most recent growth before collection.

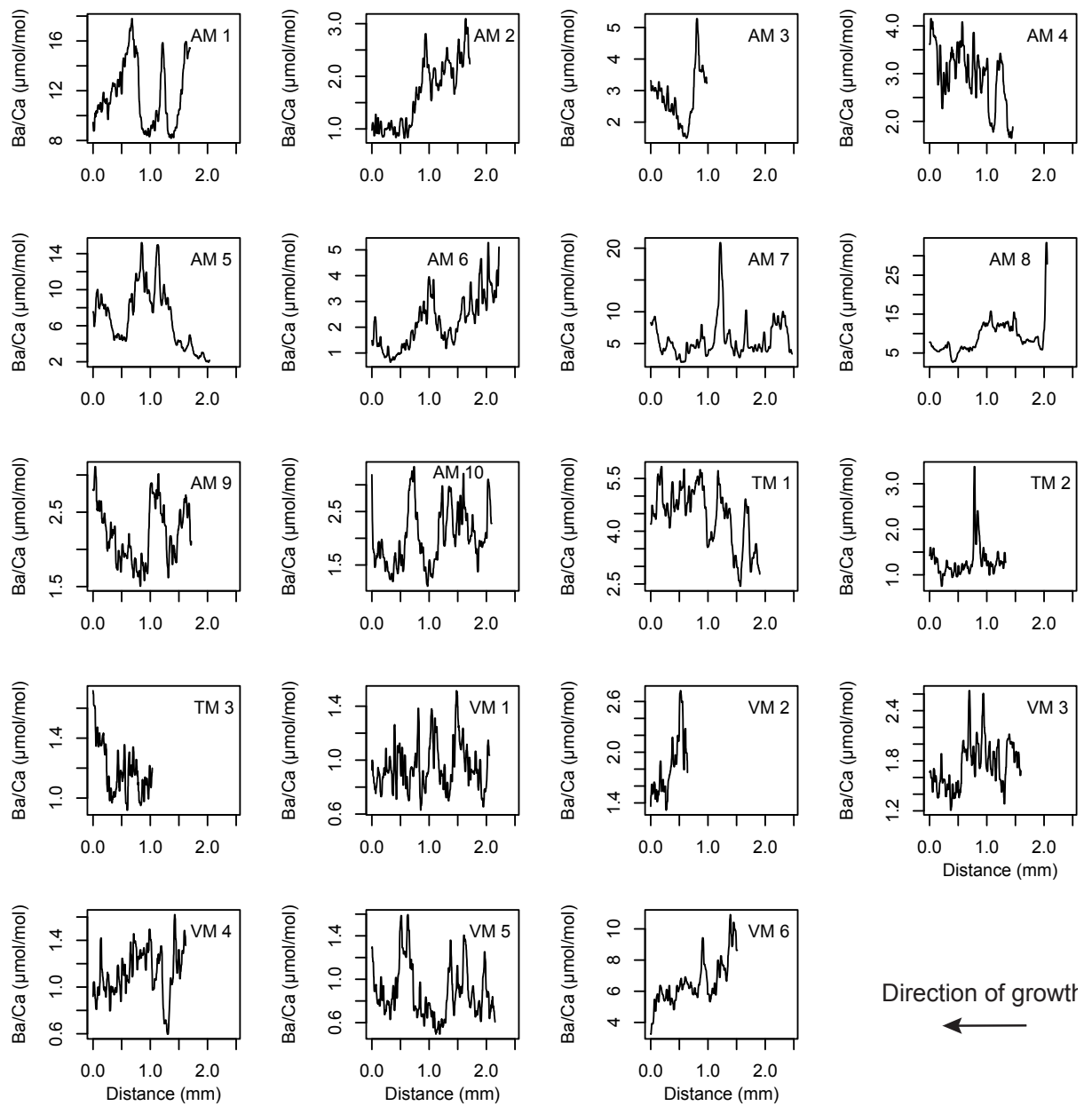


**Fig S6.** Ba/Ca profiles across outer layer of *A. helmsi* shells. The ventral margin of each shell (0 mm) represents the most recent growth before collection.

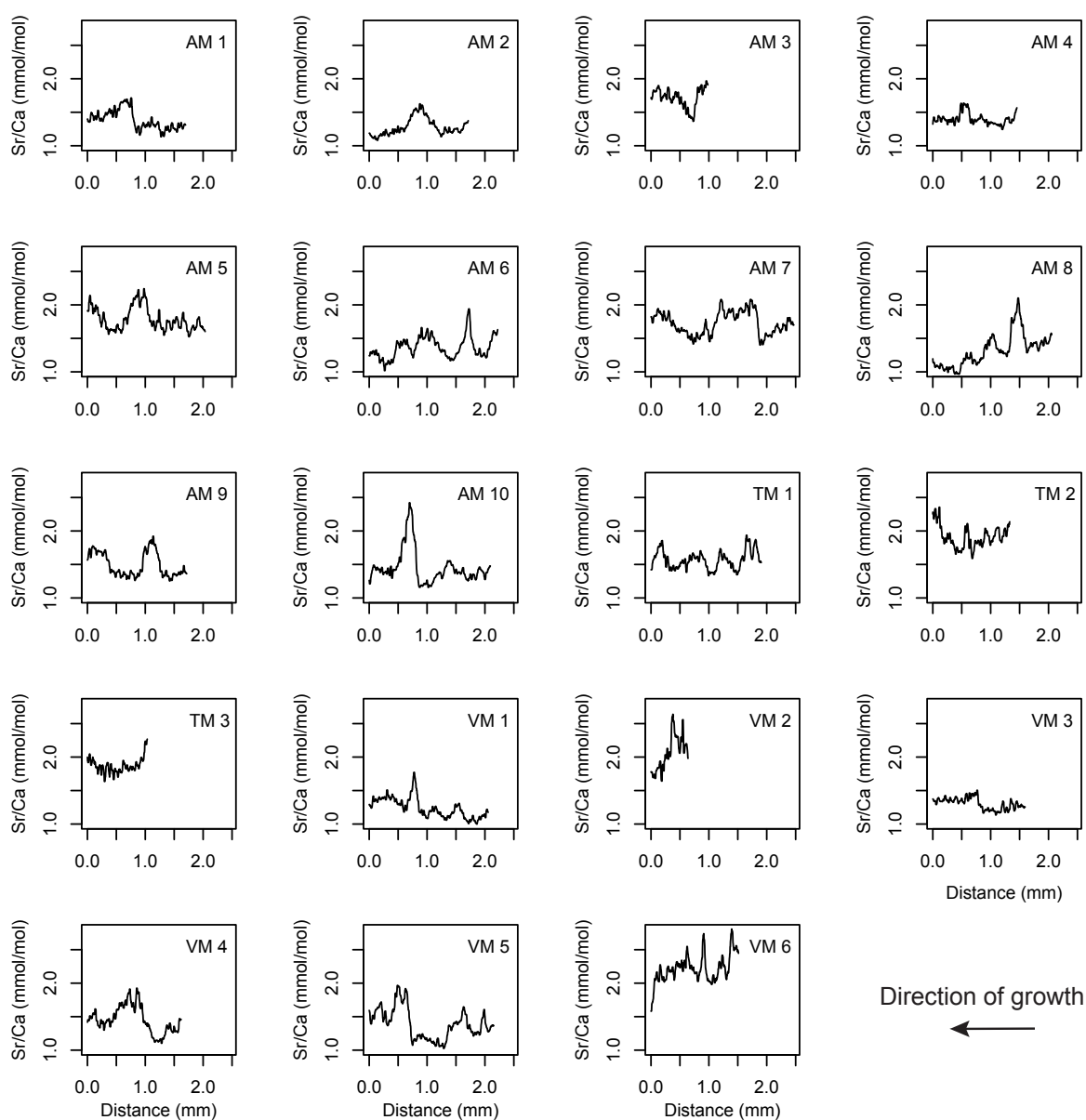


**Fig S7.** Sr/Ca profiles across outer layer of *A. helmsi* shells with equivalent y-axis across all specimens. The ventral margin of each shell (0 mm) represents the most recent growth before collection.



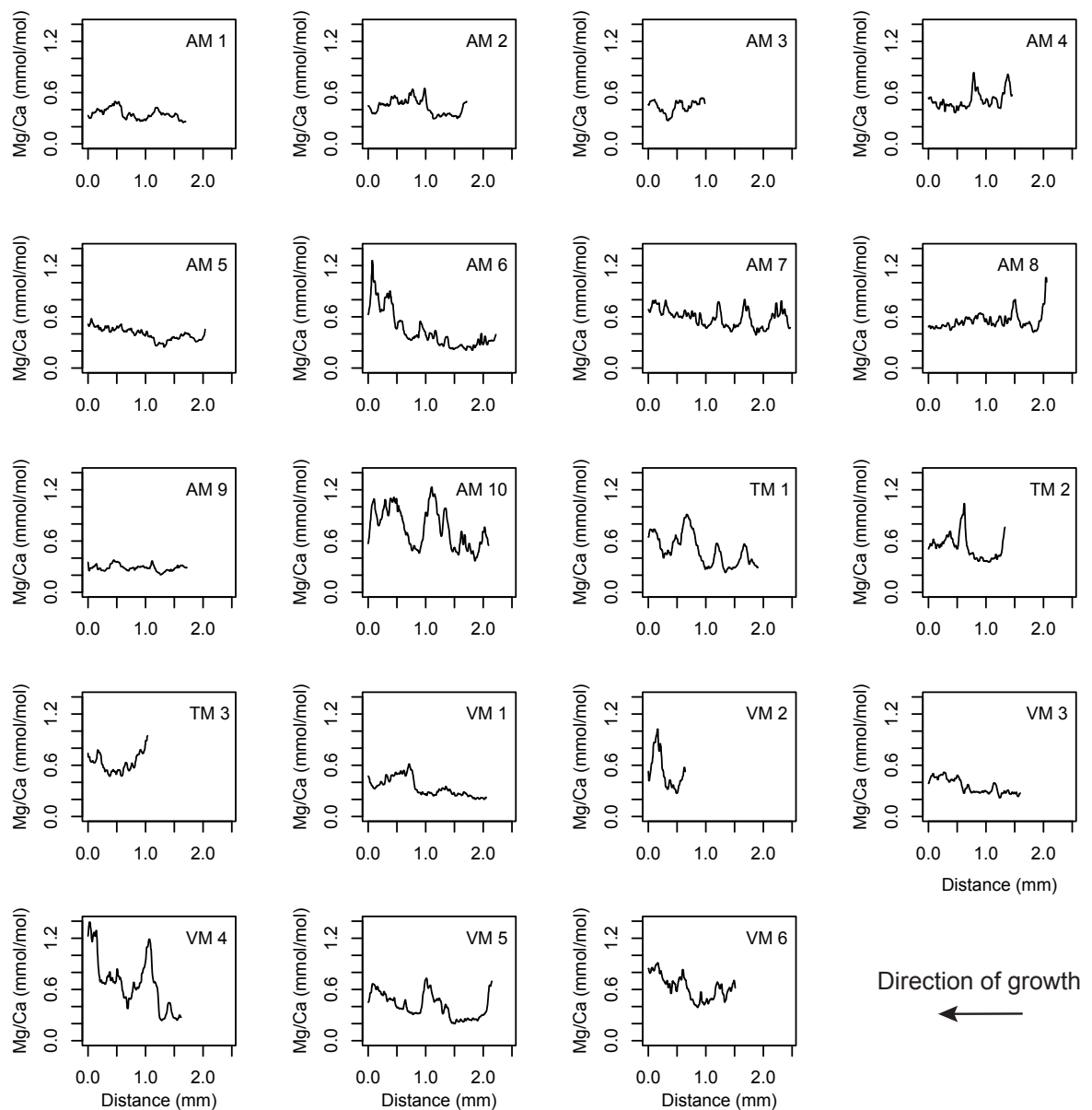


**Fig S8.** Mg/Ca profiles across outer layer of *A. helmsi* shells with equivalent y-axis across all specimens. The ventral margin of each shell (0 mm) represents the most recent growth before collection.

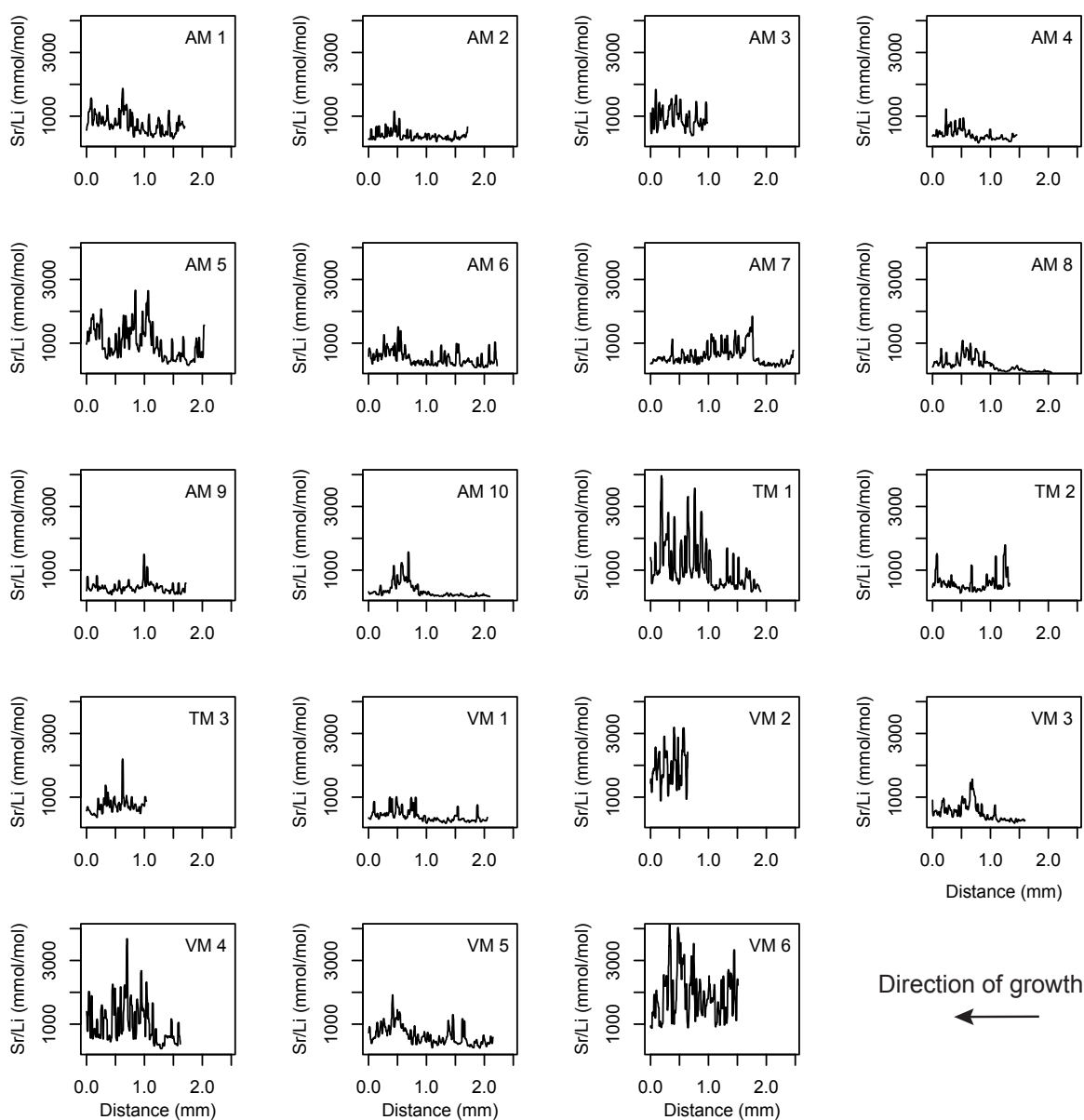


**Fig S9.** Sr/Li profiles across outer layer of *A. helmsi* shells with equivalent y-axis across all specimens. The ventral margin of each shell (0 mm) represents the most recent growth before collection.

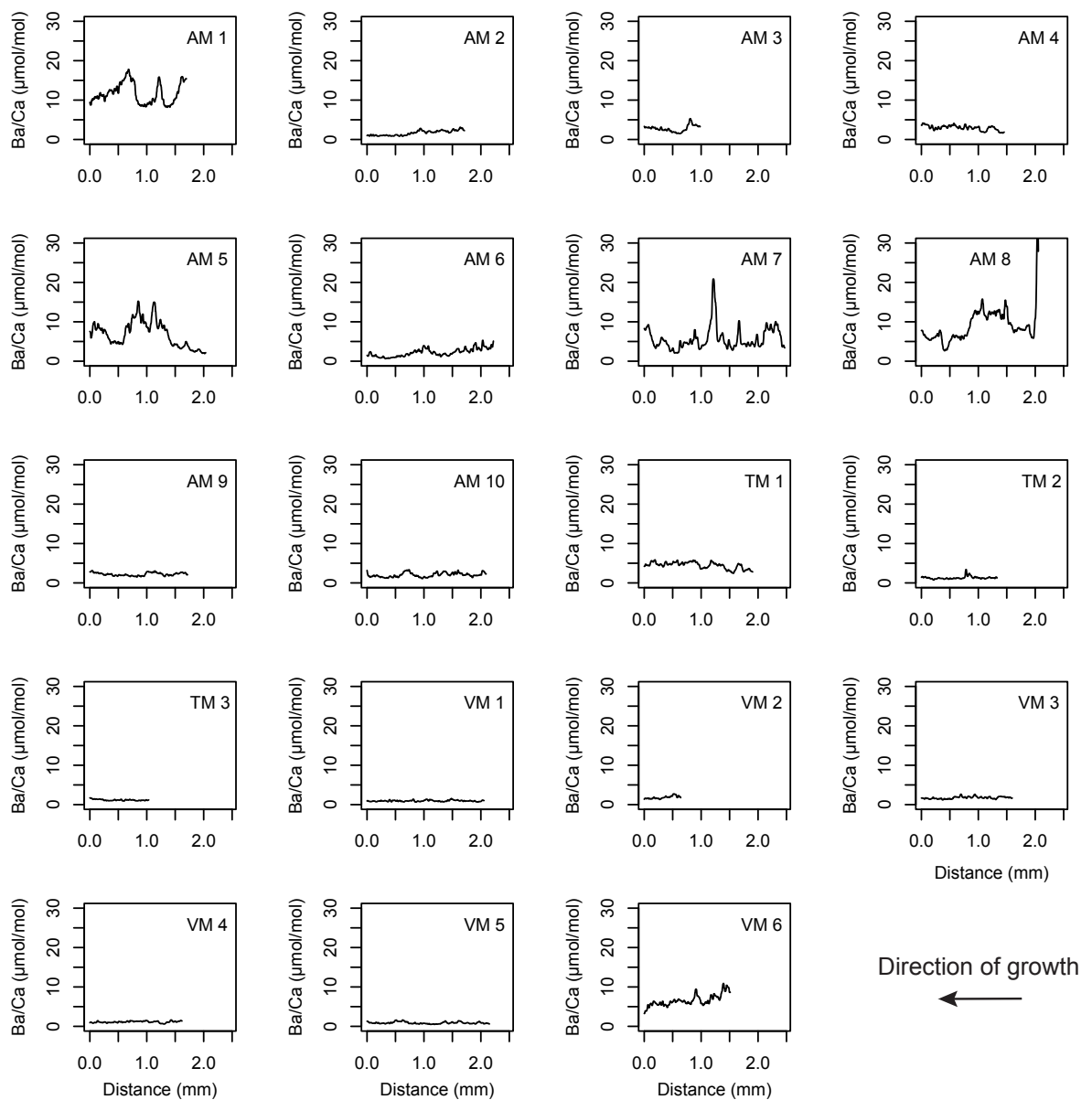


**Fig S10.** Ba/Ca profiles across outer layer of *A. helmsi* shells with equivalent y-axis across all specimens. The ventral margin of each shell (0 mm) represents the most recent growth before collection.

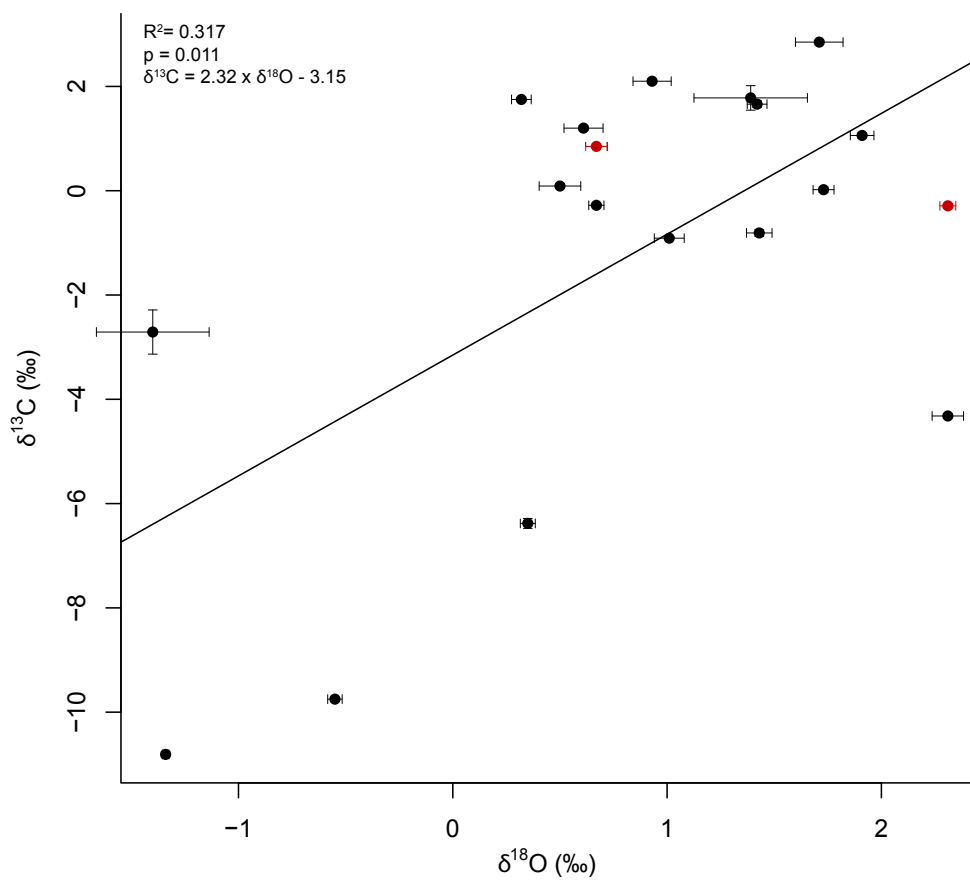


**Fig S11.** Whole shell  $\delta^{18}\text{O}$  versus  $\delta^{13}\text{C}$  for *A. helmsi* shells. Samples in red (VM 1 and VM 3) are excluded from all linear models. Error bars are  $\pm$  SE.





---

# CHAPTER 3

This chapter is published as:

Chamberlayne, B.K., Tyler, J.J., Gillanders, B.M., 2021. Elemental concentrations of waters and bivalves across a salinity gradient in the Coorong Lagoons, South Australia: Implications for palaeoenvironmental studies. *Estuar. Coastal Shelf Sci.* 255, <https://doi.org/10.1016/j.ecss.2021.107354>

Supplementary information concerning this chapter follows the text.

---





# Statement of Authorship

Title of Paper	Elemental concentrations of waters and bivalves in the fresh to hypersaline Coorong Lagoons, South Australia: Implications for palaeoenvironmental studies
Publication Status	<input checked="" type="checkbox"/> Published <input type="checkbox"/> Accepted for Publication <input type="checkbox"/> Submitted for Publication <input type="checkbox"/> Unpublished and Unsubmitted work written in manuscript style
Publication Details	Chamberlayne, B.K., Tyler, J.J. and Gillanders, B.M. 2021. Elemental concentrations of waters and bivalves in the fresh to hypersaline Coorong Lagoons, South Australia: Implications for palaeoenvironmental studies. Estuarine, Coastal and Shelf Science 255. <a href="https://doi.org/10.1016/j.ecss.2021.107354">https://doi.org/10.1016/j.ecss.2021.107354</a>

## Principal Author

Name of Principal Author (Candidate)	Briony Chamberlayne		
Contribution to the Paper	Conceptualisation, procurement and preparation of samples for analysis, statistical analysis, figure production, manuscript preparation and editing.		
Overall percentage (%)	80		
Certification:	This paper reports on original research I conducted during the period of my Higher Degree by Research candidature and is not subject to any obligations or contractual agreements with a third party that would constrain its inclusion in this thesis. I am the primary author of this paper.		
Signature		Date	20/06/2021

## Co-Author Contributions

By signing the Statement of Authorship, each author certifies that:

- i. the candidate's stated contribution to the publication is accurate (as detailed above);
- ii. permission is granted for the candidate to include the publication in the thesis; and
- iii. the sum of all co-author contributions is equal to 100% less the candidate's stated contribution.

Name of Co-Author	Jonathan Tyler		
Contribution to the Paper	Provided guidance and assistance in conceptualisation, data analysis and interpretation. Manuscript editing.		
Signature		Date	21/Jun/2021

Name of Co-Author	Bronwyn Gillanders		
Contribution to the Paper	Provided guidance and assistance in conceptualisation, data analysis and interpretation. Manuscript editing.		
Signature		Date	23 June 2021



## Elemental concentrations of waters and bivalves in the fresh to hypersaline Coorong Lagoons, South Australia: Implications for palaeoenvironmental studies

### Abstract

Element-to-calcium ratios of bivalve shells are potentially useful proxies for environmental change, provided the relationship between the environmental variable and element ratio are calibrated using modern specimens. In this study we investigate the utility of trace elemental ratios in the estuarine micromollusc *Arthritica helmsi* as (palaeo)environmental proxies. Sr/Ca, Mg/Ca and Ba/Ca ratios were measured in waters (n = 137) and live bivalves (n = 125) were collected along a salinity gradient from fresh to hypersaline in the Coorong Lagoon and Lake Alexandrina, at the terminus of the Murray River, South Australia. Water Mg, Sr and Ca exhibited linear relationships with salinity, while Ba showed no relationship. Mg/Ca and Sr/Ca in water both showed positive logarithmic responses to increasing salinity, while the response of Ba/Ca was best explained by a negative power function. The Sr concentration and Sr/Ca of water collected between 2016 and 2018 were elevated compared to a previous study conducted between 2007 and 2008, possibly due to a higher river flow regime in the more recent period. The range of Sr/Ca, Mg/Ca and Ba/Ca measured in *A. helmsi* were in agreement with previous studies, as were the range of partition coefficients. However, the incorporation of Sr/Ca, Mg/Ca and Ba/Ca did not correlate with water elemental ratios, temperature, salinity or pH and are therefore likely to be more heavily influenced by biological processes. As a consequence, while the elemental composition of other carbonate fossils within the Coorong system may hold potential to reconstruct past climate and environmental change, the trace element geochemistry of *A. helmsi* aragonite shells, and possibly other similar micro- bivalve molluscs, should be treated with caution as a palaeoenvironmental tracer.

## 1. Introduction

The geochemical signals preserved in bivalve shell carbonate provide a potential archive of climate variability spanning months to millennia depending on the species (Schöne and Surge, 2014). Following the success of trace elemental ratios, notably Mg/Ca and Sr/Ca, as palaeothermometers in corals and other carbonate biominerals (e.g. Corrège, 2006; Mitsuguchi et al., 1996; Sinclair et al., 1998), the usefulness of these ratios as environmental recorders in bivalve species has been extensively studied in recent years (see Gillikin, 2019). Much of this growing body of research focusses on marine taxa (e.g. Carré et al., 2006; Elliot et al., 2009; Schöne et al., 2011), while a smaller body of work explores bivalve carbonate proxies in freshwater (e.g. Geeza et al., 2018; Izumida et al., 2011; Zhao et al., 2017) and estuarine species (e.g. Gillikin et al., 2006; Lazareth et al., 2003; Surge et al., 2003). Continuous profiles of chemical change in shell carbonate are possible due to the sequential nature of growth, which can be analysed using high resolution techniques such as laser ablation – inductively coupled plasma – mass spectrometry (LA-ICP-MS). Such techniques record seasonal (Durham et al., 2017) and even daily (Poulain et al., 2015) cycles in bivalve carbonate geochemistry which can be used to provide baselines for natural seasonal variability, or record sudden events such as discharges or pollution to waterways (e.g. Krause-Nehring et al., 2012; O’Neil and Gillikin, 2014).

Strontium, magnesium and barium are three commonly examined metals in bivalve shells and have been employed as proxies for environmental conditions with mixed success. Mg/Ca and Sr/Ca have been extensively tested as temperature proxies (e.g. Freitas et al., 2005; Poulain et al., 2015; Schöne et al., 2011; Wanamaker and Gillikin, 2018), though many studies have found that these ratios are controlled by biological effects such as metabolism and growth rate (e.g. Gillikin et al., 2005a; Lorrain et al., 2005; Vander Putten et al., 2000). However, some species have been shown to reliably record temperature variation in their Mg/Ca (Freitas et al., 2012; Tynan et al., 2017) and Sr/Ca ratios (Yan et al., 2013; Zhao et al., 2017). Ba/Ca ratios display a relatively invariable background interrupted by sharp peaks (Gillikin et al., 2008), which have been related to phytoplankton blooms in several studies (e.g. Elliot et al., 2009; Thébault et al., 2009). Ba/Ca in bivalves also correlates with Ba/Ca of the ambient waters that the bivalve grew in (Izzo et al., 2016; Poulain et al., 2015), which often co-vary with salinity (Walther and Nims, 2015). Though many studies have had success reconstructing various environmental variables from elemental ratios in bivalves, other studies have uncovered intra-population heterogeneity at the micro-metre scale (Schöne et al., 2013). In addition, uncertainties around element partitioning in juveniles and fast growing species have also hindered the interpretation of elemental patterns in bivalve carbonate (Wanamaker and Gillikin, 2018). The conflicting results of previous studies of bivalve taxa highlight the need for species specific calibrations.

This is especially important in estuarine environments where water chemistries are dynamic and determined by mixing from various distinct water sources as well as processes such as evaporation, in contrast to relatively stable marine waters (Walther and Nims, 2015). It is therefore essential to understand the drivers of water chemistry in such systems to rigorously interpret the signals in biogenic carbonates (Elsdon and Gillanders, 2006).

In this study, we examine the Sr/Ca, Mg/Ca and Ba/Ca patterns in the micro-mollusc *Arthritica helmsi* to compare to the chemical and physical properties of the ambient waters. Abundant in south eastern Australian estuaries and also in the sediment record (Chamberlayne, 2015; Kanandjembo et al., 2001; Matthews and Constable, 2004; Semeniuk and Wurm, 2000), *A. helmsi* is an aragonitic micro-mollusc with a broad environmental tolerance (Wells and Threlfall, 1982a), short life span of ~1 year (Wells and Threlfall, 1982b), and continuous growth (Chamberlayne et al., 2020; Wells and Threlfall, 1982b). A previous geochemical analysis of this species from museum collections showed promising correlations between Sr/Ca and Mg/Ca and temperature (Chamberlayne et al., 2020), although water chemistry data were not available for that study. Consequently, there was a need for a more detailed investigation into trace element incorporation into *A. helmsi* with tighter constraints over the physical conditions and water chemistry during growth.

The objectives of this study were to: (i) determine the controls and stability of elemental chemistry in the waters of the Coorong Lagoons collected over an 18 month period; (ii) obtain high-resolution records of element-to-calcium variation within individuals of *Arthritica helmsi*; (iii) compare element-to-calcium signals within contemporary specimens; and (iv) compare carbonate elemental data to the physical and chemical properties of host waters.

## 2. Methods

### 2.1 Study site

The Coorong is a ~130 km long, narrow estuarine coastal lagoon system located at the terminus of Australia's Murray Darling Basin (Figure 1). A constricted channel at Parnka Point separates the estuary into the North Lagoon and the South Lagoon, which are characterised by a north-south salinity gradient (Geddes and Butler, 1984; Gillanders and Munro, 2012). The North Lagoon is connected to the Murray River via Lake Alexandrina (Figure 1) and also receives inflows of tidal marine waters, while the South Lagoon receives freshwater surface flows from the South East Drainage Network at Salt Creek. Groundwater inputs are an additional water input of varying quantity along the length of the lagoons (Haese et al., 2008; Shao et al., 2018). A series of barrages constructed in the 1940s control the release of freshwater from Lake

Alexandrina to the North Lagoon (Figure 1). Daily salinity and temperature monitoring data for Pelican Point and Long Point for the sampling period were sourced from the WaterConnect website (Government of South Australia, 2020).

## **2.2 Water sampling and analysis**

Surface waters were collected from 9 sites along Lake Alexandrina, the Coorong and Murray Mouth (Figure 1) approximately monthly from November 2016 to May 2018 (n= 137 samples in total). The location and date for each sample collection are summarised in Table S1. A single measurement of water temperature, salinity and pH was measured using a Hanna Instruments HI-98194 multiparameter probe at each site during each sampling time, and water samples were collected in hydrochloric acid washed 250 mL HDPE bottles for trace element analyses. Water samples were filtered through 2 µm cellulose nitrate filters and acidified to 2% with nitric acid before being refrigerated prior to analysis.

Water samples were analysed for major and trace element concentration at Adelaide Microscopy, University of Adelaide, with an Agilent 8900x inductively coupled plasma-mass spectrometer (ICP-MS). The plasma conditions were: RF power 1550W, sample depth 10 µm and total Ar carrier gas flow rate 1.05 L/min, with a Micro Mist nebuliser and Scott Type spray chamber. The collision cell was run in He mode (4 mL/min He gas flow) for the majority of elements (Mg, Sr and Ba). Ca was analysed with oxygen (30% flow rate) in the collision cell and the MO<sup>+</sup> reaction products measured: <sup>44</sup>Ca □ <sup>44</sup>Ca<sup>16</sup>O at mass 60. On-line addition of indium was used as the internal standard. A series of mixed element calibration solutions (10, 50, 100, 200, 300, 500, 1000 ppb) were used for quantification. The IAPSO sea water reference material (OSIL) was used as a quality control standard. Samples were diluted with ultra-pure water acidified to 2% with nitric acid by a factor of 10, 20, 40, 50, 80, 100 or 120 times depending on sample salinity. 15% of samples were analysed in triplicate; the mean precision for triplicate samples was <1% for Mg and Sr; 1.8% for Ca; and 5.2 % for Ba.

## **2.3 Shell collection and analysis**

Shells were collected from the sediment water interface from five sites (Mundoo Channel, Pelican Point, Mark Point, Mulbin Yerrok and Long Point) in the North Lagoon of the Coorong (Figure 1) on six occasions between March 2017 and May 2018. Between 1 and 8 individual live shells were collected from each site at each sampling time, totalling 125 individuals (Table S2). Digital callipers were used to measure the length of the maximum growth axis. Residual

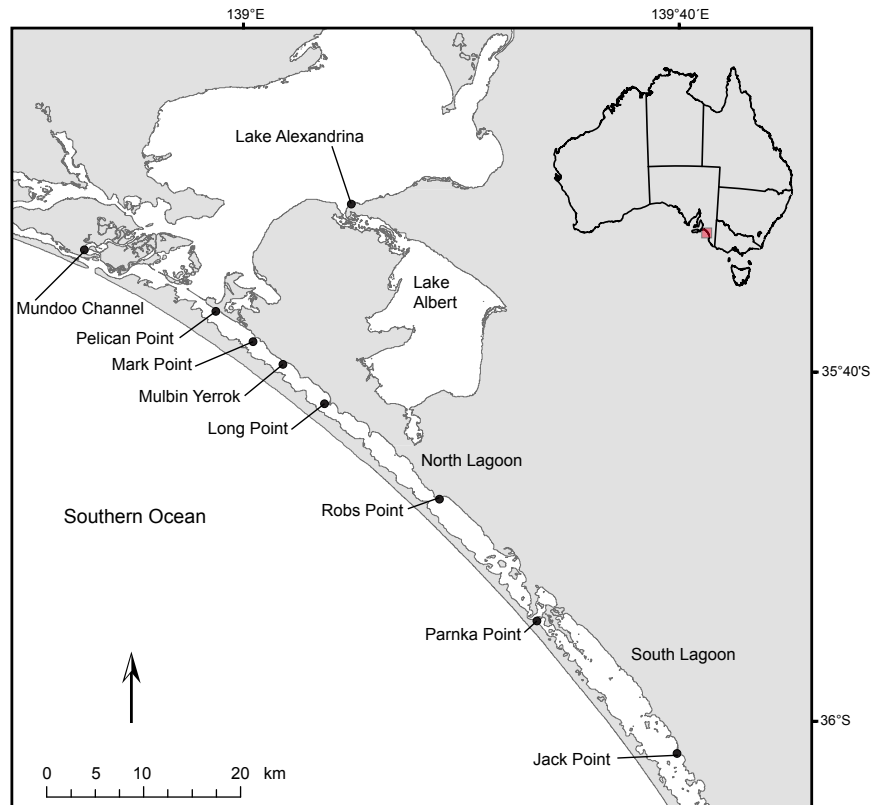


**Figure 1.** Sampling locations in Lake Alexandrina and the Coorong Lagoons at the terminus of the River Murray.

organic matter was then removed via treatment with an 18%  $\text{H}_2\text{O}_2$  solution which was buffered to pH 8 using 0.5 M sodium hydroxide (Falster et al., 2018). The shells were then rinsed in ultra-pure water with a resistivity of 18.2  $\text{M}\Omega$  at 25 °C and a pH of 7 and dried for 12 hours at 30 °C. One valve from each individual shell ( $n=125$ ) was embedded in indium spiked epoxy resin (40 ppm) and sectioned along the maximum growth axis to approximately 0.8 mm using a Buehler Isomet Low Speed Saw with diamond edge blades. Shell sections were polished to a thickness of approximately 0.5 mm on progressively finer grades of lapping film (30, 9, 3  $\mu\text{m}$ ) and then adhered to slides with indium spiked thermoplastic glue.

To investigate physical representations of growth increments in *A. helmsi* two sectioned shells were immersed in Mutvei's solution following the methods of Schöne et al. (2005). Briefly, the Mutvei's solution was prepared using 100 ml 1% acetic acid, 100 ml 25% glutaraldehyde and ~2 g Alcian blue powder. The solution was heated to 40 °C and the samples were immersed for 30 minutes under constant stirring. The samples were then rinsed with demineralised water and allowed to air-dry before examination using light microscopy.

Trace element profiles for Mg, Sr, Ba and Ca were obtained using LA-ICP-MS at Adelaide Microscopy, University of Adelaide, using a New Wave Q-Switched Nd YAG 213 nm UV laser coupled with an Agilent 7500cs ICP-MS. Beam intensities of  $^{24}\text{Mg}$ ,  $^{88}\text{Sr}$ ,  $^{138}\text{Ba}$  and  $^{43}\text{Ca}$  were measured, in addition to  $^{44}\text{Ca}$  as an internal standard and  $^{115}\text{In}$  as an indicator of resin contamination. Pre-ablation with a 40  $\mu\text{m}$  diameter spot size along the outer margin of the shell preceded ablation transects of a 30  $\mu\text{m}$  diameter with repetition rate of 10 Hz at 10  $\mu\text{m}/\text{second}$  scan speed. Transects were collected for each individual shell ( $n=125$ ) and spanned from the ventral margin to the umbo region. The length of individual transects ranged from 1.1 mm to 2.5 mm. The glass standard NIST SRM 612 and the USGS carbonate standard MACS-3 were analysed periodically to account for instrumental drift. The mean coefficient of variation of repeated measures was 1.08 % for Mg, 1.06 % for Sr and 1.29 % for Ba. Data reduction was performed in Iolite (Hellstrom et al., 2008; Paton et al., 2011). Transects of elemental concentrations were smoothed with a 7-point running mean and 7-point running median (Sinclair et al., 1998) and are expressed as ratios to Ca.

## 2.4 Calculation of partition coefficients

The relationship between the chemical composition of the bivalve carbonate and the chemical composition of the ambient water in which those bivalves grew can be quantified as a partition coefficient ( $D_{\text{Me}} = R_{\text{carb}}/R_{\text{water}}$ ) where  $R_{\text{carb}}$  is the metal to calcium ratio in the shell and  $R_{\text{water}}$  is the metal to calcium ratio in the water.

As the exact lifespan and growth rate of each specimen is unknown, two methods were employed when calculating partition coefficients and when comparing to water chemistry. Firstly, we estimated the lifespan of each shell based on its size and an assumed growth rate of 0.3 mm/month as estimated by Wells and Threlfall (1982b). Average water element ratios, temperature, salinity and pH for the lifespan of each shell were then calculated to the nearest month based on this age estimation. The second approach was to take the last 10  $\mu\text{m}$  of each individual shell elemental transect ( $n=125$ ) at the ventral margin as a representation of the growth occurring immediately prior to the collection of the shell. The resulting metal to calcium ratio of the shell was then used in conjunction with the metal to calcium ratio of the water measured on the day of collection to calculate coefficients which represent a more constrained time period. The partition coefficients obtained from the two approaches were compared using a one-way ANOVA in R (R Core Team, 2020).



### 3. Results

#### 3.1 Elements in water

Dissolved element concentrations for Coorong waters and their uncertainties are summarised in Table S1. Concentrations of dissolved Mg, Sr and Ca of water samples all showed conservative relations with salinity (Figure 2; Table 1), in agreement with data previously collected for the Coorong Lagoons by Gillanders and Munro (2012). Maximum concentrations of these elements were recorded at Jack Point in the South Lagoon (Figure 1; Table S1); Mg and Ca maximum concentrations were measured in March 2018 while the maximum Sr concentration occurred in February 2018. Minimum concentrations for Mg, Sr and Ca were all recorded at Lake Alexandrina in March 2018. In contrast to a previous study by Gillanders and Munro (2012), there was no relationship found between Ba concentration and salinity (Figure 2). The maximum value for Ba was recorded in Lake Alexandrina in August 2017, while the minimum concentration was recorded at Pelican Point in November 2016.

Mg/Ca, Sr/Ca and Ba/Ca all exhibited non-linear relationships with salinity (Figure 3; Table 1). Mg/Ca and Sr/Ca exhibited a positive logarithmic correlation with salinity ( $r^2 = 0.932$  and  $r^2 = 0.927$  respectively), while Ba/Ca exhibited a negative power correlation with salinity ( $r^2 = 0.906$ ; Table 1). Maximum values for Mg/Ca and Sr/Ca were measured at the South Lagoon site Jack Point in February 2018 (Table S1). Minimum values for Mg/Ca and Sr/Ca both occurred in December 2016 at Mundoo Channel and Pelican Point respectively. Both Ba/Ca maximum and minimum values were measured in the North Lagoon with the maximum value in August 2017 at Lake Alexandrina, while the minimum value was measured at Mundoo Channel in September 2017.

**Table 1.** Relationships between elemental data, and salinity for all sites. Shown are the equations for the models of best fit and the corresponding r-squared values.

Vs. Salinity	Equation	$r^2$
Mg (ppm)	$y = 35.65 \times \text{salinity} + 19.58$	0.979
Sr (ppm)	$y = 0.28 \times \text{salinity} + 0.14$	0.980
Ba (ppb)	No Relationship	
Ca (ppm)	$y = 9.88 \times \text{salinity} + 68.70$	0.978
Mg/Ca (mol/mol)	$y = 0.892 \times \ln(\text{salinity}) + 1.722$	0.932
Sr/Ca (mmol/mol)	$y = 1.74 \times \ln(\text{salinity}) + 4.403$	0.927
Ba/Ca ( $\mu\text{mol/mol}$ )	$y = 466.51 \times (\text{salinity}^{-0.62})$	0.906

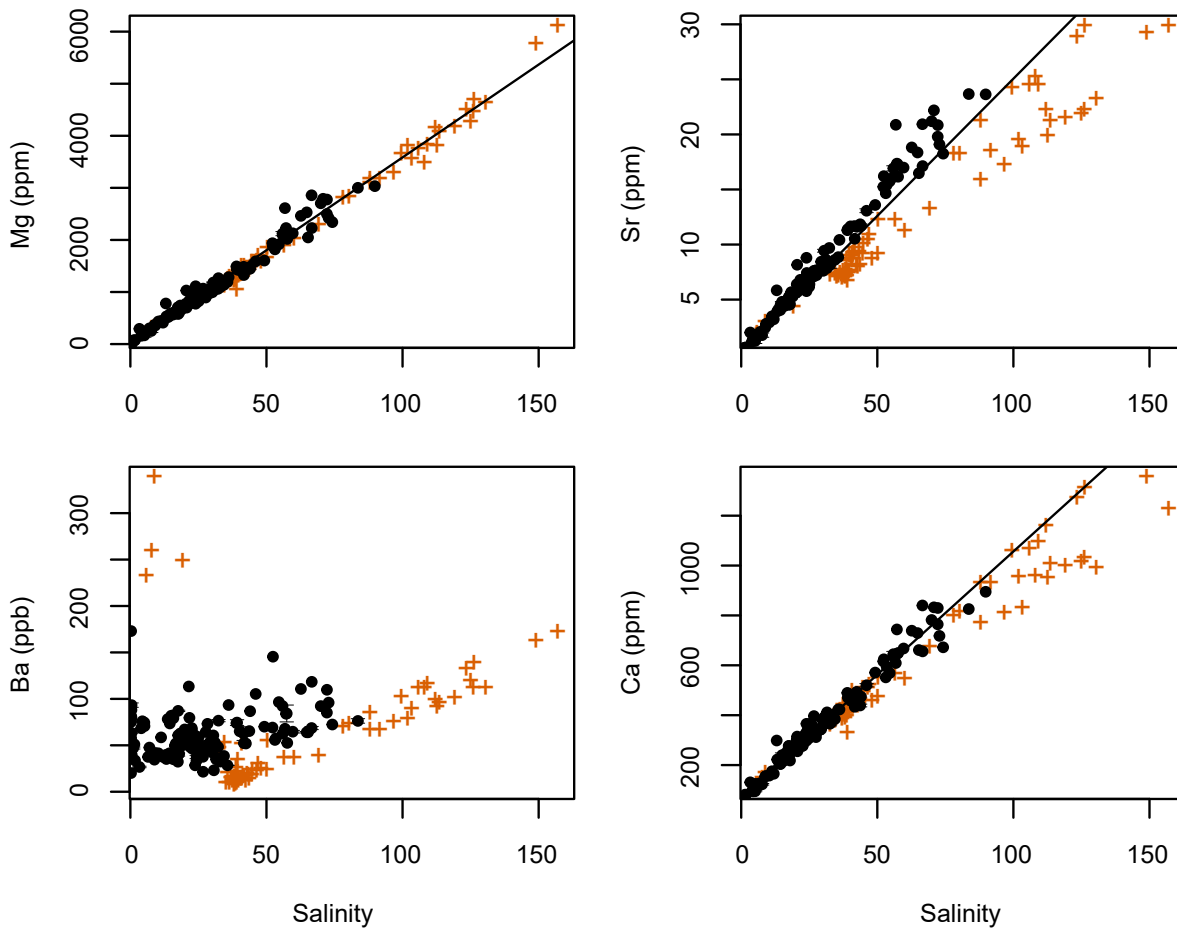


**Figure 2.** Water elemental concentration against salinity for samples from all sites collected between November 2016 and May 2018 (black circles). Also depicted are elemental concentrations against salinity from Gillanders and Munro (2012) for Coorong waters collected between May 2007 and June 2008 (orange crosses). Error bars indicate  $\pm 1$  SE.

### 3.2 Elements in shells

Staining with Mutvei's solution showed no evidence of incremental growth. Examination of stained sections of *A. helmsi* showed a consistent structure with no visible growth lines. The average, standard deviation, minimum and maximum values of Sr/Ca, Mg/Ca and Ba/Ca ratios measured in shells are provided in Table S2. In summary, average Sr/Ca ranged from 1.39 mmol/mol in shell LP0317-2 to 3.06 mmol/mol in shell LP1017-2. Shell LP1017-2 also recorded the highest intra-shell range of Sr/Ca (7.59 mmol/mol). The average Sr/Ca in the last 10  $\mu\text{m}$  of the ventral margin ranged from 1.27 to 4.78 mmol/mol in shells LP0317-1 and MP1017-4 respectively. The average Mg/Ca ranged from 0.26 to 1.61 mmol/mol in shells MC0317-1 and MC0518-4 respectively. The intra-shell range of Mg/Ca was lowest in shell PP0317-2 (0.38 mmol/mol) and highest in shell MC0518-4 (4.45 mmol/mol). Mg/Ca in the ventral margin of

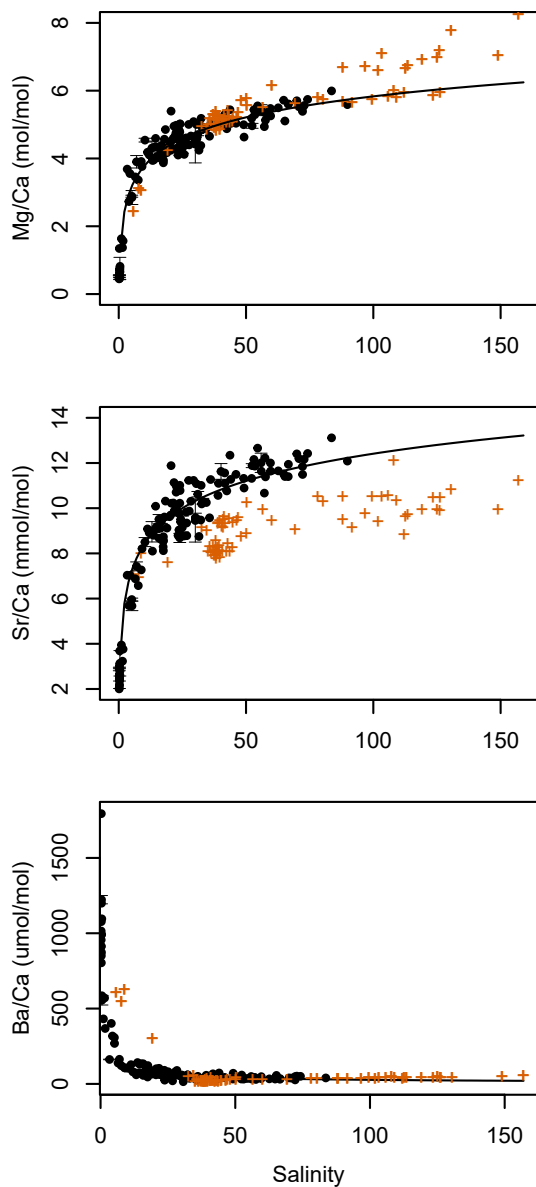


**Figure 3.** Elemental ratios plotted against salinity for all samples collected in the Coorong between November 2016 and May 2018 (black circles). Also shown are elemental ratios against salinity from Gillanders and Munro (2012) for Coorong waters collected between May 2007 and June 2008 (orange crosses). Error bars indicate  $\pm 1$  SE.

both shell averaged ( $r^2 = 0.165$ ;  $p = <0.001$ ) and ventral margin ( $r^2 = 0.036$ ;  $p = 0.029$ ) values. The intra-shell range of shell elemental ratios did not correlate to any environmental variable. In addition, there were no obvious differences between samples when separated into high ( $>35$ ) and low ( $<35$ ) salinities (Figure 4; Figure 5).

shells ranged from 0.26 to 2.43 mmol/mol in shells MC0317-1 and PP0518-3 respectively. Ba/Ca in the ventral margin ranged from 1.9 to 30  $\mu\text{mol/mol}$  in shells LP0317-1 and PP0118-7 respectively, while the average Ba/Ca ranged from 2.8 to 22  $\mu\text{mol/mol}$  in shells LP0317-2 and PP0817-1 respectively. The intra-shell range of Ba/Ca values ranged from 6.1  $\mu\text{mol/mol}$  in shell MC0317-1 to 75  $\mu\text{mol/mol}$  in shell PP0817-3. Shells with the lowest average and range of metal/calcium ratios were all collected in March 2017 from various sites, while shells recording the highest averages and intra-shell ranges were more varied in the timing of their collection. Average and ventral margin shell elemental ratios were regressed against water metal/calcium ratios, temperature, pH and salinity to assess controls on the incorporation of elements into shells (Figure 4; Figure 5). Weak but statistically significant relationships were found between shell average  $\text{Mg/Ca}_{\text{carb}}$  and  $\text{Mg/Ca}_{\text{water}}$  ( $r^2 = 0.075$ ;  $p = 0.003$ ) and  $\text{Ba/Ca}_{\text{carb}}$  and  $\text{Ba/Ca}_{\text{water}}$  ( $r^2 = 0.160$ ;  $p = <0.001$ ; Table 2). Similar relationships were not observed when comparing metal/calcium ratios between waters and the ventral margin of the shells (Table 2). Both the average ( $r^2 = 0.039$ ;  $p = 0.035$ ) and the ventral margin ( $r^2 = 0.046$ ;  $p = 0.016$ ) Ba/Ca ratios were weakly correlated to temperature. Ventral margin  $\text{Sr/Ca}_{\text{carb}}$  and  $\text{Ba/Ca}_{\text{carb}}$  showed weak but significant relationships to pH.  $\text{Ba/Ca}_{\text{carb}}$  was significantly correlated to salinity for

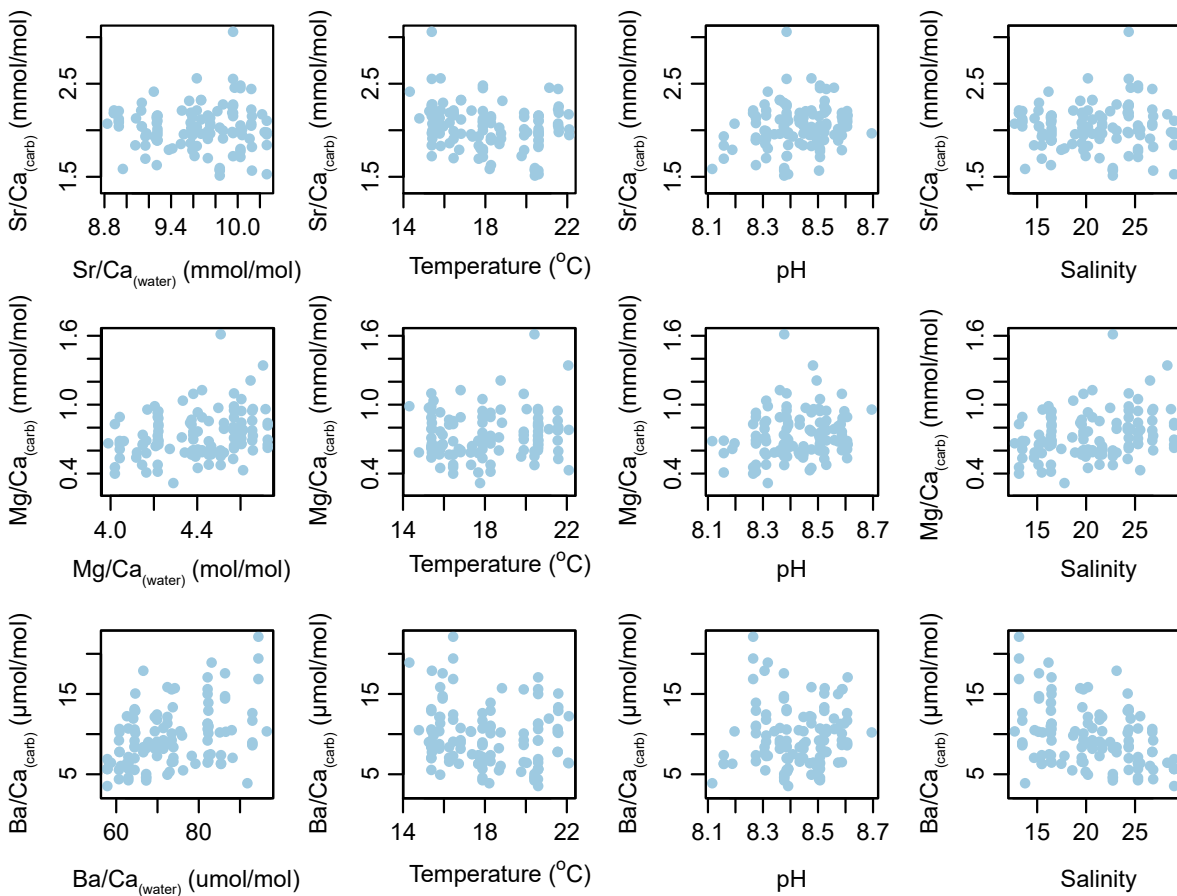


**Figure 4.** Average element/calcium ratio in *A. helmsi* vs. water element/calcium ratio, temperature, pH and salinity.

Continuous laser ablation transects allow the comparison of signals between contemporary specimens. As an example, trace elemental transects from four shells collected on the same occasion from Pelican Point and Long Point are compared in Figure 6. Also shown is the salinity and temperature from nearby logging stations plotted over a period of time estimated as the maximum possible lifespan of the shells. Trace elemental transects from all shells showed a similar range of values and some but not all peaks were displayed across multiple specimens (Figure 6). There did not appear to be similarity between any element to calcium ratio in shells from Pelican Point or Long Point and salinity or temperature from the corresponding site (Figure 6).

### 3.3 Partition Coefficients

Strontium partition coefficients ranged from 0.14 to 0.75 for whole shell average values and from 0.13 to 0.74 for ventral margin values. The partition coefficients for average magnesium concentrations ranged from 0.00006 to 0.001, while for ventral margin values of magnesium

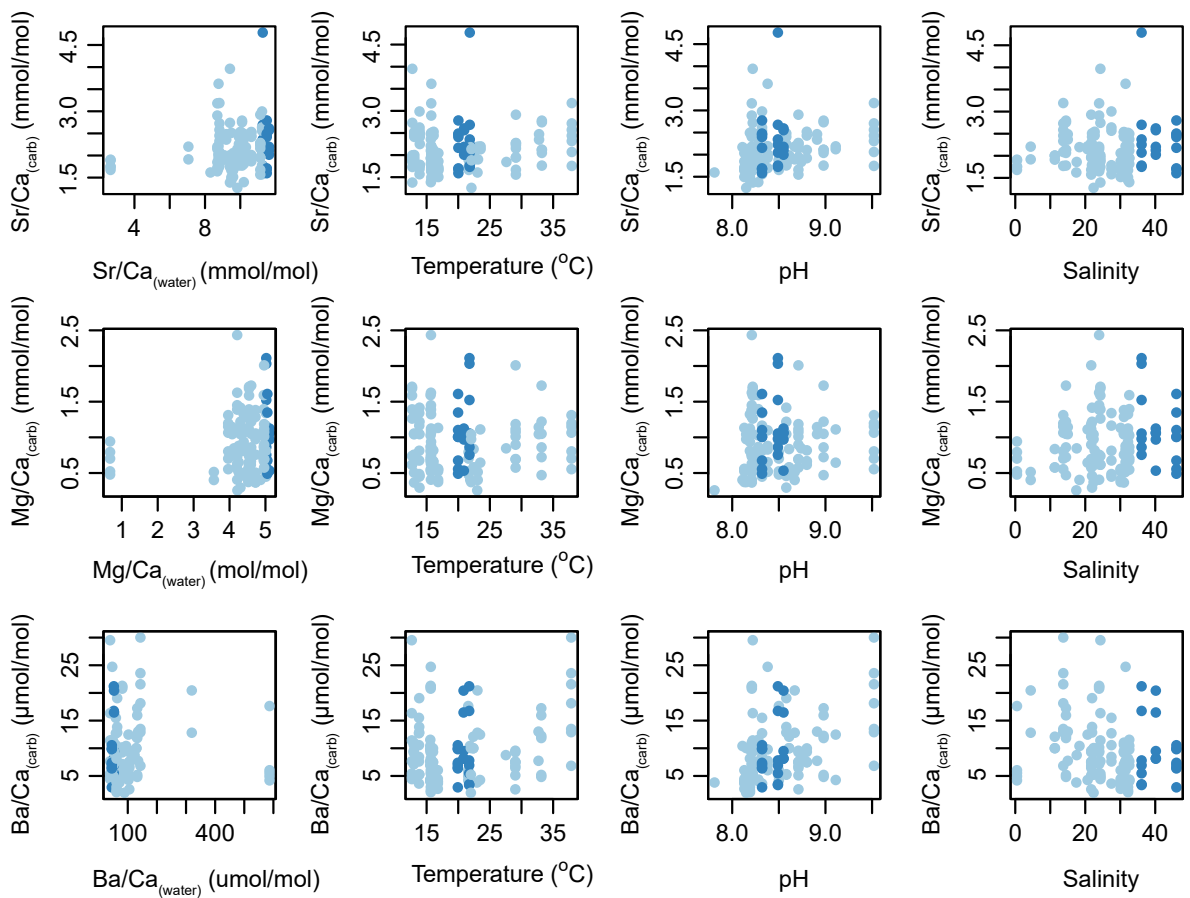


**Figure 5.** Ventral margin element/calcium ratio in *A. helmsi* vs. water element/calcium ratio, temperature, pH and salinity. Light blue points represent samples where salinity < 35 and dark blue points are samples where salinity is > 35.

the range was 0.00006 to 0.0014. The barium partition coefficients ranged from 0.007 to 0.37 and from 0.007 to 0.79 for average and ventral margin samples respectively. The strontium and magnesium partition coefficients of five shells collected from Mundoo Channel in October 2017 plotted outside 1.5 times the interquartile range for all data (Figure 7), while the outliers in the barium data were from various sites and collection times. The partition coefficients did not vary significantly when calculated from average or ventral margin element/calcium ratios for strontium ( $F = 1.29$ ,  $p = 0.26$ ) or barium ( $F = 0.024$ ,  $p = 0.88$ ). The partition coefficients for magnesium were higher when calculated using ventral margin Mg/Ca than when using average Mg/Ca ( $F = 5.31$ ,  $p = 0.022$ ). The strontium and magnesium partition coefficients were not correlated with temperature, while both average and ventral margin Ba partition coefficients showed a weak but significant relationship with temperature ( $r^2 = 0.296$ ;  $p = < 0.001$  and  $r^2 = 0.094$ ;  $p = < 0.001$  respectively; Table 2).

#### 4. Discussion

This study examined patterns in elemental concentrations in the waters of the Coorong Lagoons and of a resident bivalve species *A. helmsi*. Abundantly preserved in sediments, geochemical analyses of the fossil shells of *A. helmsi* offer a potential proxy for palaeo-environmental reconstruction, particularly due to the interest in the past environmental condition of the Ramsar listed Coorong system. Our results show that over a salinity gradient of ~0 to 90, concentrations of Mg and Sr in waters responded conservatively to changes in salinity. The Mg/Ca and Sr/Ca ratios in waters displayed a strong positive non-linear relationship with salinity, while Ba/Ca was found to have a negative non-linear relationship with salinity. These patterns remained largely consistent over time, and during wetter and drier climates, as observed when comparing the newly collected data with a previous study conducted from 2007 – 2008 by Gillanders and Munro (2012). However, trace elemental ratios measured in live collected specimens of *A. helmsi* exhibited poor correlations with water chemistry. While trace element profiles across individual shells showed some synchronous peaks between shells, these patterns were not correlated with time series of water salinity or temperature. Furthermore, the spatial and

**Table 2.** Linear regression statistics for average and ventral margin *A. helmsi* metal/calcium ratios vs. water metal/calcium ratios, temperature and pH. Statistically significant results are presented in bold.

Relationship	Average shell x/Ca		Ventral margin x/Ca	
	r <sup>2</sup>	p	r <sup>2</sup>	p
Sr/Ca <sub>carb</sub> vs Sr/Ca <sub>water</sub>	<0.001	0.94	0.028	0.063
Mg/Ca <sub>carb</sub> vs Mg/Ca <sub>water</sub>	<b>0.075</b>	<b>0.003</b>	0.025	0.077
Ba/Ca <sub>carb</sub> vs Ba/Ca <sub>water</sub>	<b>0.160</b>	<b>&lt;0.001</b>	0.002	0.571
Sr/Ca <sub>carb</sub> vs temperature	<b>0.064</b>	<b>0.006</b>	0.021	0.215
Mg/Ca <sub>carb</sub> vs temperature	0.007	0.345	0.001	0.764
Ba/Ca <sub>carb</sub> vs temperature	<b>0.039</b>	<b>0.035</b>	<b>0.046</b>	<b>0.016</b>
Sr/Ca <sub>carb</sub> vs pH	0.034	0.051	<b>0.041</b>	<b>0.024</b>
Mg/Ca <sub>carb</sub> vs pH	0.008	0.344	0.001	0.744
Ba/Ca <sub>carb</sub> vs pH	0.002	0.642	<b>0.121</b>	<b>&lt;0.001</b>
Sr/Ca <sub>carb</sub> vs salinity	<0.001	0.939	0.005	0.411
Mg/Ca <sub>carb</sub> vs salinity	<b>0.076</b>	<b>0.003</b>	0.023	0.088
Ba/Ca <sub>carb</sub> vs salinity	<b>0.165</b>	<b>&lt;0.001</b>	<b>0.036</b>	<b>0.029</b>
D <sub>Sr</sub> vs temperature	0.004	0.453	0.011	0.254
D <sub>Mg</sub> vs temperature	0.002	0.580	0.004	0.493
D <sub>Ba</sub> vs temperature	<b>0.296</b>	<b>&lt;0.001</b>	<b>0.094</b>	<b>&lt;0.001</b>

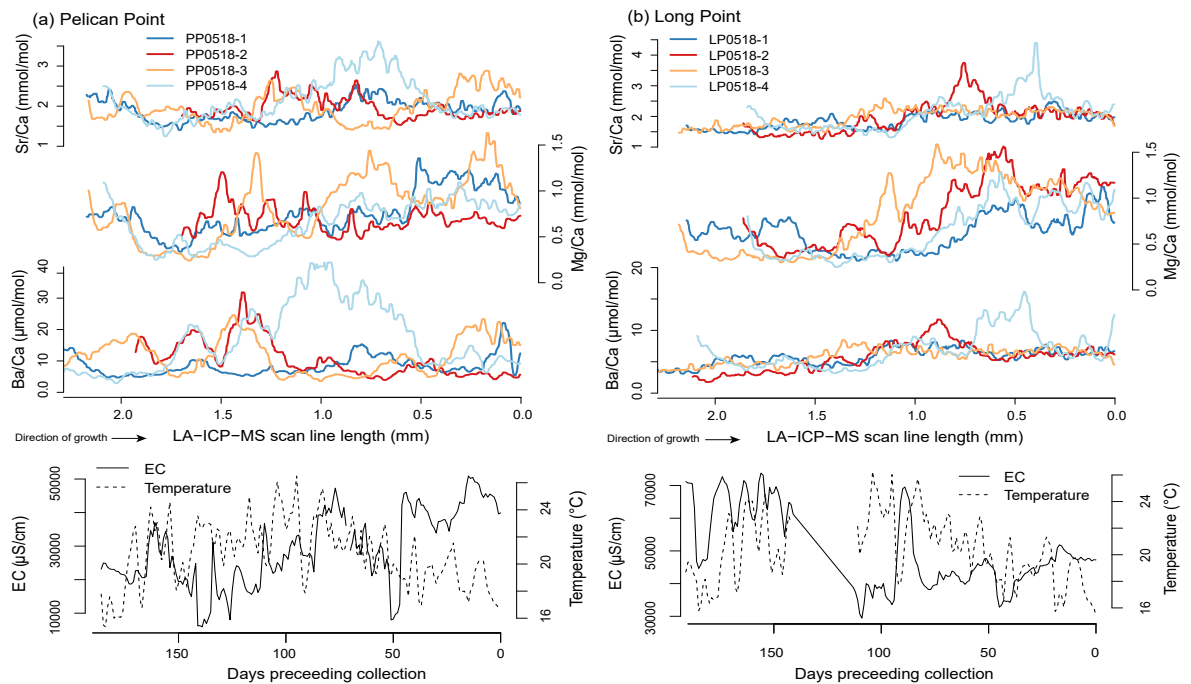


**Figure 6.** Sr/Ca, Mg/Ca and Ba/Ca profiles of four shells of *A. helmsi* collected from (a) Pelican Point and (b) Long Point. Also shown are the temperature and salinity data for each site for the time period possibly corresponding to their lifespan. The ventral margin (0 mm) represents the most recent growth of each shell.

temporal patterns in whole shell geochemistry, or that of the most recent carbonate deposition, exhibited poor correlations with ambient water chemistry and temperature. This absence of environmental controls on the incorporation of Sr/Ca, Mg/Ca and Ba/Ca into *A. helmsi* are in agreement with previous studies of other bivalve taxa (Carré et al., 2006; Lorrain et al., 2005; Poulain et al., 2015; Wanamaker and Gillikin, 2018).

#### 4.1 Environmental controls over the elemental composition of contemporary Coorong waters: Strontium and magnesium

The concentration of Mg, Sr and Ca in the waters of the Coorong Lagoons and Lake Alexandrina responded conservatively to salinity (Figure 2). Previous studies have found similar linear relationships in estuaries globally (Mohan and Walther, 2015; Nelson and Powers, 2020; Surge and Lohmann, 2002), though few studies have investigated these relationships in hypersaline waters (Diouf et al., 2006). The linear response of Mg, Sr and Ca is predicted by the mixing of fresh and marine waters (Walther and Limburg, 2012) and further concentration of elements occurs alongside sodium chloride concentration by evaporation (Gibbs, 1970). Mg/Ca and Sr/Ca displayed logarithmic relationships to salinity (Figure 3). Such non-linear relationships are mathematically predicted for the ratio of two conservative constituents if at least one of the

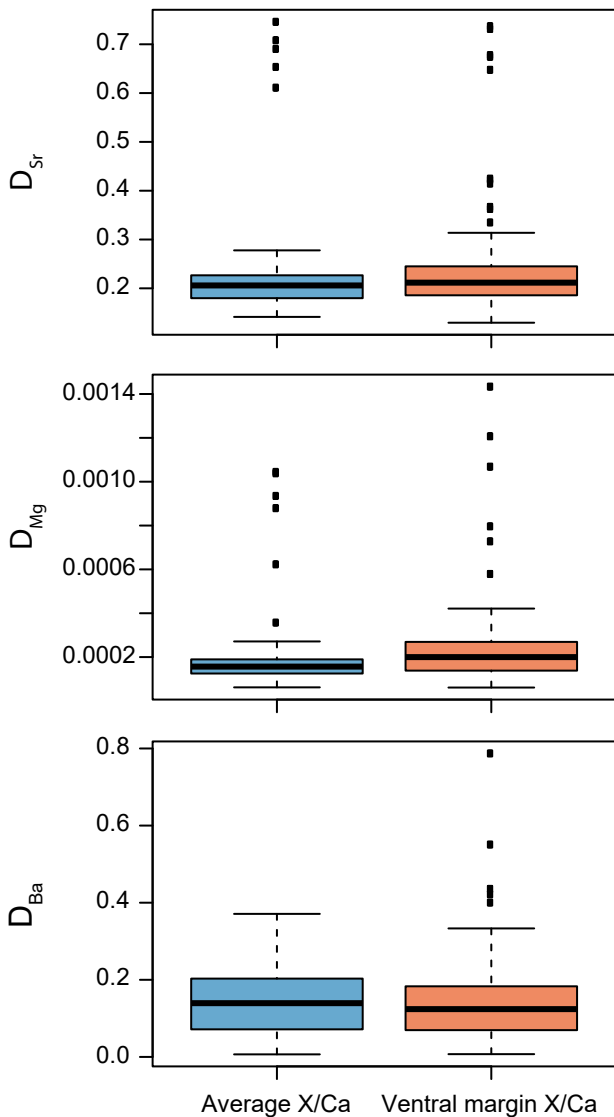


**Figure 7.** Box and whisker plot of partition coefficients of Sr, Mg and Ba for average metal/Ca and ventral margin metal/Ca in *A. helmsi* shells ( $n = 125$ ).

the region experienced widespread rainfall deficit and evaporation (Gillanders and Munro, 2012). The Gillanders and Munro (2012) study allows a direct comparison of relationships during periods of high and low precipitation and/or river discharge (Figure 2; Figure 3). The conservative behaviour of Mg in the Coorong did not differ between the two studies. However, the slope of the linear element-salinity relationship was slightly steeper for Ca and Sr in the current study (Figure 2), compared to Gillanders and Munro (2012).

One possible explanation for the differences in Sr and Ca concentrations at high salinities between the two studies is increased carbonate precipitation facilitating Sr and Ca removal during the Millennium Drought. Gillanders and Munro (2012) proposed aragonite precipitation

constituents has a non-zero endmember (Walther and Limburg, 2012), as observed in the Coorong where, for example, Ca concentrations in fresh waters from Lake Alexandrina (<1 salinity) did not fall below 10 ppm. Similar relationships have been found in previous estuarine studies (Macdonald and Crook, 2010; Nelson and Powers, 2020; Surge and Lohmann, 2002). The relationship between salinity and Mg/Ca or Sr/Ca is steepest at low salinities (<30) and is therefore more likely to be a sensitive tracer for salinity in low salinity waters. It has long been thought that Mg/Ca and Sr/Ca are stable in waters above a salinity of ~10 (Dodd and Crisp, 1982), though recent research has challenged this notion (Lebrato et al., 2020). In this study, it was clear that while the slope of the curve between Mg/Ca and Sr/Ca and salinity decreased at higher salinities, the elemental ratios did not plateau in the salinity range investigated (Figure 3).

A previous study on major and trace element concentrations in the Coorong Lagoons in 2007/2008 was undertaken during the ‘Millennium Drought’ – a period in which



to be the cause of increased scatter in Sr and Ca in hypersaline waters in their study. Water chemistry in the hypersaline southern lagoon is known to be altered by the precipitation of inorganic aragonite rich carbonate crusts and tufa on the sediment surface (Ford, 2007; Shao et al., 2021, 2018) and the fraction of Sr removed from the present day South Lagoon as aragonite has been recently estimated at 35 to 45% (Shao et al., 2021). During 2007-2008, salinity was higher than that observed during the 2016-2018 monitoring period (Figure 2), which leads to an increased concentration of bicarbonate and carbonate mineral precipitation (Haese et al., 2009) and a subsequent decrease in ionic concentration in the residual water. Another possibility is that increased inputs of freshwater provide additional Sr into the lagoons (Beck et al., 2013; Walther and Nims, 2015). Previous studies have suggested Sr inputs from groundwater in the Coorong and Lower Lakes (Shao et al., 2018), and so changes in the relative inputs of freshwater sources (river water and groundwater) could explain the differences in water chemistry during and after drought. Overall, the comparison of water chemistry data between the 2007-2008 and 2016-2018 monitoring periods suggests that Mg concentrations are more likely to be a consistent proxy for lagoonal water salinity, whereas Sr concentrations may vary in time due to changes in freshwater input vs. aragonite export. A combination of trace element and Sr or Ca stable isotope data (e.g. Shao et al. 2018) offer potential to unravel these effects through time.

#### **4.2 Environmental controls over the elemental composition of contemporary Coorong waters: Barium**

Barium concentrations displayed the most dissimilar patterns between the 2007-2008 and 2016-2018 monitoring periods, indicating that the drivers of Ba dynamics in the Coorong estuary have changed over time. Our current study found no relationship between Ba concentration and salinity, in agreement with previous studies in estuarine systems (Moore and Shaw, 2008; Nelson and Powers, 2020; Walther and Nims, 2015). This contrasts to the segmented linear model with a break point around a salinity of 37 found by Gillanders and Munro (2012) in the Coorong waters during the Millennium Drought. However, it is not unusual for Ba behaviour to vary greatly between estuaries and within estuaries due to factors including differences in weathering rates and river flow (Coffey et al., 1997).

There are several possible causes for the differences in Ba patterns between the two time periods, likely due to a change in flow dynamics. Low freshwater flow and associated oxygen depletion, as experienced during the Millennium Drought (Aldridge and Brookes, 2011), can increase the concentration of dissolved iron and influence primary productivity which can both impact Ba removal in estuaries (Coffey et al., 1997; Colbert and McManus, 2005). Low salinity Ba removal can occur due to absorption of Ba to flocculated iron oxyhydroxides (Coffey et al.,

1997; Gillanders and Munro, 2012) which increase in concentration when oxygen levels are low (Aldridge and Brookes, 2011). Barium is then available for desorption at higher salinities (Coffey et al., 1997) and can then be concentrated by evaporation, potentially explaining the break point linear model of Gillanders and Munro (2012). A change in hydrodynamics between 2007-2008 and 2016-2018 could also influence productivity (Lehrter et al., 2009), whereby an increase in productivity is associated with barite precipitation in estuaries (Stecher and Kogut, 1999) which in turn is a mechanism for Ba removal. Productivity in the Coorong and Lake Alexandrina was relatively stable during periods of drought, yet more variable in concert with variable freshwater flows (Murrell et al., 2007). As Ba concentrations are related to river flow, the variable releases from the barrages of the Coorong during the sampling period of the current study and the associated changes in removal/release of Ba could mask the signals observed in other estuaries (Carroll et al., 1993; Edmond et al., 1978; Stecher and Kogut, 1999).

While Ba concentrations showed no significant relationship with salinity, Ba/Ca was found to exhibit a negative power relationship with salinity (Figure 3). Similar patterns have been observed in tank and field studies of Ba/Ca in estuarine waters where Ba and Ca concentrations are non-conservative and conservative with salinity respectively (Macdonald and Crook, 2010; Nelson and Powers, 2020; Walther and Nims, 2015).

### 4.3 Environmental controls on Sr/Ca and Mg/Ca incorporation in *A. helmsi*

The Sr/Ca and Mg/Ca ratios measured in shells of *A. helmsi* in this study are comparable with those measured in a previous geochemical analysis of shells of this species (Chamberlayne et al., 2020). Furthermore, the Sr/Ca and Mg/Ca ratios are within the range of the values reported in other estuarine (e.g. Füllenbach et al., 2015, Poulain et al., 2015), freshwater (e.g. Geeza et al., 2018; Zhao et al., 2017) and marine bivalves (e.g. Carré et al., 2006; Elliot et al., 2009).

Temperature, salinity, pH and water trace element ratios were not strongly correlated to Sr/Ca or Mg/Ca in *A. helmsi* shells (Table 2). Temperature has been hypothesised to control Sr and Mg incorporation into bivalves following the observation of a strong relationship in abiogenic aragonite (Dietzel et al., 2004). Sr/Ca has been found to be temperature controlled in some studies of aragonitic bivalve species (Hart and Blusztajn, 1998; Yan et al., 2013; Zhao et al., 2017), while Mg/Ca has been more successfully related to temperature in calcitic shells (e.g. Freitas et al., 2005; Tynan et al., 2017). A previous study of the trace elemental ratios within *A. helmsi* found significant relationships between both Sr/Ca and Mg/Ca and temperature (Chamberlayne et al., 2020). However, in that previous study water temperature was approximated from air temperature and therefore potentially subject to uncertainties.

Most studies have concluded that Sr/Ca and Mg/Ca in bivalve shells are under physiological control (e.g. Carré et al., 2006; Gillikin et al., 2005; Lorrain et al., 2005; Vander Putten et al., 2000; Wanamaker et al., 2008; Wanamaker and Gillikin, 2018). The incorporation of elements into *A. helmsi* could be influenced by growth rate as observed in several studies of bivalve taxa (e.g. Carré et al., 2006; Freitas et al., 2006; Izumida et al., 2011; Lorrain et al., 2005) and also in inorganic aragonite (Gaetani and Cohen, 2006). A significant relationship between temperature and both Sr/Ca and Mg/Ca was observed in a study by Schöne et al. (2011) after the elimination of vital effects by age detrending Sr/Ca data and growth rate detrending Mg/Ca data. This approach could not be undertaken in *A. helmsi* due to the uncertainties around the growth rate. Staining of sections of *A. helmsi* with Mutvei's solution did not reveal growth lines. A previous study of *A. helmsi* also reported a lack of physical representations of growth on sections examined under both scanning electron microscopy and electron microprobe analysis (Chamberlayne et al., 2020).

Element concentration during reproduction could also contribute to the disequilibrium between elements and waters in *A. helmsi*. Mg enriched organic layers have been found in other bivalve species (Schöne et al., 2010; Takesue and van Geen, 2004) and can form in response to reproduction (Durham et al., 2017). A study on the estuarine bivalve *Ruditapes philippinarum* also found a suite of other elements were concentrated during reproduction (Vieira et al., 2021). Reproduction in *A. helmsi* is reported to be continuous, and young develop in a brood pouch (Wells and Threlfall, 1982c). The effect of their reproductive strategy on the incorporation of elements in *A. helmsi* is unknown and could be a target for future research. Furthermore, as *A. helmsi* inhabit the sediment-water interface, it is possible that the element concentrations in their carbonate shells may reflect the chemistry of the pore water or sediment surface chemistry in addition to the chemistry of the overlying water column (Griscom and Fisher, 2004; Schöne and Krause Jr, 2016). The distribution of elements in pore waters can be heterogeneous compared to the water column (Griscom and Fisher, 2004) and could therefore cause some variance in specimens from the same population. However, *A. helmsi* are suspension feeders (Lautenschlager et al., 2014) and so regularly access the main water column. We did not investigate the chemistry of the pore water in this study, but it could be an interesting avenue for further investigation.

Partition coefficients varied between individuals (Figure 7), and similar to other species imply that the incorporation of Sr and Mg into the carbonate is regulated by physiological processes (Poulain et al., 2015; Schöne et al., 2011). The range of  $D_{Sr}$  and  $D_{Mg}$  found in this study were mostly well below equilibrium and the values were comparable to previous studies for both Sr (eg.  $\sim 0.25$ , Gillikin et al., 2005;  $\sim 0.13$ - $0.28$ , Schöne et al., 2011,  $\sim 0.25$ , Poulain et al., 2015) and Mg (e.g.  $\sim 0.0003$ - $0.0008$ , Geeza et al., 2018;  $\sim 0.0003$ - $0.00042$ , Izumida et al., 2011). Five

---

shells collected in October 2017 from Mundoo Channel had significantly higher  $D_{Sr}$  and  $D_{Mg}$  than the other shells in this study, however this appears to reflect the effects of a short term pulse of freshwater which was not representative of the growth conditions for these organisms. The salinity at Mundoo Channel on the collection day was  $<1$  (Table S1) and accordingly the concentrations of Sr/Ca and Mg/Ca were very low (Figure 3) resulting in the apparently large partition coefficients. Mundoo Channel is located at the mouth of the estuary, near the barrages which control fresh water release from Lake Alexandrina (Figure 1). Only weekly barrage release data are available (Government of South Australia, 2020), however it is likely that the barrages were opened on this day, releasing a pulse of low salinity water which was not recorded in the Sr/Ca or Mg/Ca ratios of the last growth recorded in these shells.

#### 4.4 Environmental controls on Ba/Ca incorporation in *A. helmsi*

The range of Ba/Ca measured in shells in this study ( $\sim 0.002 - 0.03$  mmol/mol) was also consistent with those measured in a previous geochemical analysis of *A. helmsi* (Chamberlayne et al., 2020). Similar values have also been reported in the euryhaline Manila clam, *Ruditapes philippinarum* (Poulain et al., 2015) and estuarine mussel, *Mytilus edulis* (Gillikin et al., 2006). Carbonate Ba/Ca did not strongly or consistently correlate with water Ba/Ca, temperature, pH or salinity in this study (Table 2). Previous studies of estuarine bivalve taxa have found strong relationships between carbonate and water Ba/Ca, suggesting their utility as an estuarine salinity proxy (Gillikin et al., 2006; Poulain et al., 2015). Other studies of marine species have directly correlated shell Ba/Ca and salinity (Izzo et al., 2016; Wanamaker and Gillikin, 2018), though in a culture study of juvenile *Arctica islandica* by Wanamaker and Gillikin (2018) the salinity interaction varied in strength with temperature highlighting the complexity of interactions during biomineralisation. Similarly, Zhao et al. (2017) in a culture study of the salinity tolerant (0-24) *Corbicula fluminea*, found that Ba/Ca in bivalve carbonate was controlled by a combination of factors including temperature, food supply, shell growth rate, and the Ba/Ca ratio of water. The controlled nature of their laboratory study allowed the factors controlling barium concentration in the shell to be identified, most of which would be difficult to disentangle in a highly variable natural environment.

Partition coefficients were variable, though the median values were similar when calculated with both the average Ba/Ca values and the ventral margin Ba/Ca values (Figure 7). There was a weak temperature dependence observed in both average and ventral Ba partition coefficients, a pattern also observed in a previous study on otoliths (Miller, 2009). Apart from some abnormally high values calculated using the ventral margin Ba/Ca values, Ba partition coefficient values

were well below those observed in inorganic aragonite ( $>0.5$ ; Dietzel et al., 2004; Gaetani and Cohen, 2006), suggesting the influence of physiological or biological factors as proposed in previous studies (Geeza et al., 2018; Wanamaker and Gillikin, 2018; Zhao et al., 2017).

Ba/Ca ratios in bivalve shells have previously been characterised by a stable background interrupted by synchronous sharp peaks (e.g. Gillikin et al., 2008; Goodwin et al., 2013; Hatch et al., 2013; Thébault et al., 2009). The cause of these peaks has been attributed to phytoplankton blooms in several studies (Elliot et al., 2009; Thébault et al., 2009; Vander Putten et al., 2000), though several others have been unable to determine the cause (Gillikin et al., 2008; Goodwin et al., 2013; Hatch et al., 2013). Data recording chlorophyll or phytoplankton blooms were not available for this study, but the similarity between some peaks in Ba/Ca transects among specimens (Figure 6) indicates that there may be a common environmental control that could be confounded by other environmental or biological factors as noted above.

## 5. Conclusions and implications for palaeoenvironmental studies

Reliable environmental reconstructions from the geochemistry of biogenic carbonate rely on an understanding of the stability of water chemistry and its correlations to environmental variables (Elsdon and Gillanders, 2006; Mohan and Walther, 2015; Nelson and Powers, 2020; Walther and Limburg, 2012). In this study, significant relationships between water trace elements and salinity were found in the Coorong Lagoons, which we primarily attribute to changes in surface water evaporation. The significant relationships between salinity and the Mg/Ca, Sr/Ca and Ba/Ca ratios in water suggested that these ratios hold potential for reconstructing past hydrological change in the Coorong. Due to the curvilinear relationships of salinity to element ratios, they would be most successfully employed as salinity proxies below marine salinities. The relationship between salinity and Mg/Ca was similar to that found in a previous study on elemental concentration in the Coorong (Gillanders and Munro, 2012). The differences in Sr/Ca and Ba/Ca behaviour alongside salinity in this study compared to the previous study by Gillanders and Munro (2012) were attributed to differences in hydrological regime over time, whereby decreased salinity and increased freshwater inputs in the present study have potentially altered carbonate precipitation dynamics from those experienced during the Millennium Drought. Therefore, Mg/Ca may serve as the most reliable salinity tracer in biogenic carbonates given the stability of these ratios across a range of hydrological states in the Coorong. However, the use of trace elemental geochemistry to reconstruct past environments requires that the geochemical properties of the water are reflected in those of contemporary carbonates, and for the bivalve *A. helmsi*, this appears not to be the case.

Controls over the incorporation of Sr/Ca, Mg/Ca and Ba/Ca into *A. helmsi* could not be constrained in this study. The occurrence of some synchronous peaks in trace elemental transects suggest the possibility of some degree of external control on element incorporation, though this signal is likely confounded by the complex interactions of environmental and biological variables as observed in previous studies (e.g. Zhao et al., 2017). Culture studies where factors such as temperature, salinity, water element chemistry and food amount can be controlled may be necessary to determine the effect of each on the element partitioning into *A. helmsi*. Laboratory or field studies using chemical tracers could also be useful in investigating the influence of physiological variables, such as growth, on element partitioning. The findings from this study indicate that Sr/Ca, Mg/Ca and Ba/Ca in *A. helmsi* are not currently reliable environmental proxies and that additional work would be required before the interpretation of these elemental ratios in (sub)fossil specimens could be made. Furthermore, this study highlights the need for contemporary investigations into the chemical and physical properties of waters prior to the interpretation of proxy data from biogenic carbonates, particularly in highly variable or altered environments.

**Acknowledgements:**

The authors would like to thank Sarah Gilbert from Adelaide Microscopy for her assistance with water and carbonate trace elemental analyses. This research was funded by a Sir Mark Mitchell Foundation Grant, a Lirabenda Endowment Research Grant from the Field Naturalists Society of South Australia and a Conservation Biology Grant from the Nature Conservation Society of South Australia.

**References**

- Aldridge, K.T., Brookes, J.D., 2011. The response of water quality and phytoplankton communities in the Northern Lagoon of the Coorong and Murray Mouth to barrage releases from the Lower Lakes, November 2010 - May 2011. Report to the Department of Environment and Natural Resources and Department for Water, the Government of South Australia. School of Earth & Environmental Sciences, The University of Adelaide, Adelaide.
- Beck, A.J., Charette, M.A., Cochran, J.K., Gonneea, M.E., Peucker-Ehrenbrink, B., 2013. Dissolved strontium in the subterranean estuary - Implications for the marine strontium isotope budget. *Geochim. Cosmochim. Acta* 117, 33–52. <https://doi.org/10.1016/j.gca.2013.03.021>
- Carré, M., Bentaleb, I., Bruguier, O., Ordinola, E., Barrett, N.T., Fontugne, M., 2006. Calcification rate influence on trace element concentrations in aragonitic bivalve shells: Evidences and mechanisms. *Geochim. Cosmochim. Acta* 70, 4906–4920. <https://doi.org/10.1016/j.gca.2006.07.019>
- Carroll, J., Falkner, K.K., Brown, E.T., Moore, W.S., 1993. The role of the Ganges-Brahmaputra mixing zone in supplying barium and  $^{226}\text{Ra}$  to the Bay of Bengal. *Geochim. Cosmochim. Acta* 57, 2981–2990.
- Chamberlayne, B., 2015. Late Holocene seasonal and multicentennial hydroclimate variability in the Coorong Lagoon, South Australia: evidence from stable isotopes and trace element profiles of bivalve molluscs, honours thesis, University of Adelaide, Adelaide.
- Chamberlayne, B.K., Tyler, J.J., Gillanders, B.M., 2020. Environmental Controls on the Geochemistry of a Short-Lived Bivalve in Southeastern Australian Estuaries. *Estuaries and Coasts* 43, 86–101. <https://doi.org/10.1007/s12237-019-00662-7>
- Coffey, M., Dehairs, F., Collette, O., Luther, G., Church, T., Jickells, T., 1997. The Behaviour of Dissolved Barium in Estuaries. *Estuar. Coast. Shelf Sci.* 45, 113–121. <https://doi.org/10.1006/ecss.1996.0157>
- Colbert, D., McManus, J., 2005. Importance of seasonal variability and coastal processes on estuarine manganese and barium cycling in a Pacific Northwest estuary. *Cont. Shelf Res.* 25, 1395–1414. <https://doi.org/10.1016/j.csr.2005.02.003>
- Corrège, T., 2006. Sea surface temperature and salinity reconstruction from coral geochemical tracers. *Palaeogeogr. Palaeoclimatol. Palaeoecol.* 232, 408–428. <https://doi.org/10.1016/j.palaeo.2005.10.014>
- Dietzel, M., Gussone, N., Eisenhauer, A., 2004. Co-precipitation of  $\text{Sr}^{2+}$  and  $\text{Ba}^{2+}$  with aragonite by membrane diffusion of  $\text{CO}_2$  between 10 and 50 °C. *Chem. Geol.* 203, 139–151. <https://doi.org/10.1016/j.chemgeo.2003.09.008>
- Diouf, K., Panfili, J., Labonne, M., Aliaume, C., Tomás, J., Do Chi, T., 2006. Effects of salinity on strontium:calcium ratios in the otoliths of the West African black-chinned tilapia *Sarotherodon melanotheron* in a hypersaline estuary. *Environ. Biol. Fishes* 77, 9–20. <https://doi.org/10.1007/s10641-006-9048-x>

- Dodd, J.R., Crisp, E.L., 1982. Non-linear variation with salinity of Sr/Ca and Mg/Ca ratios in water and aragonitic bivalve shells and implications for paleosalinity studies. *Palaeogeogr. Palaeoclimatol. Palaeoecol.* 38, 45–56.
- Durham, S.R., Gillikin, D.P., Goodwin, D.H., Dietl, G.P., 2017. Rapid determination of oyster lifespans and growth rates using LA-ICP-MS line scans of shell Mg/Ca ratios. *Palaeogeogr. Palaeoclimatol. Palaeoecol.* 485, 201–209. <https://doi.org/10.1016/j.palaeo.2017.06.013>
- Edmond, J.M., Boyle, E.D., Drummond, D., Grant, B., Mislick, T., 1978. Desorption of barium in the plume of the Zaire (Congo) river. *Netherlands J. Sea Res.* 12, 324–328. [https://doi.org/10.1016/0077-7579\(78\)90034-0](https://doi.org/10.1016/0077-7579(78)90034-0)
- Elliot, M., Welsh, K., Chilcott, C., McCulloch, M., Chappell, J., Ayling, B., 2009. Profiles of trace elements and stable isotopes derived from giant long-lived *Tridacna gigas* bivalves: Potential applications in paleoclimate studies. *Palaeogeogr. Palaeoclimatol. Palaeoecol.* 280, 132–142. <https://doi.org/10.1016/j.palaeo.2009.06.007>
- Elsdon, T.S., Gillanders, B.M., 2006. Temporal variability in strontium, calcium, barium, and manganese in estuaries: Implications for reconstructing environmental histories of fish from chemicals in calcified structures. *Estuar. Coast. Shelf Sci.* 66, 147–156. <https://doi.org/10.1016/j.ecss.2005.08.004>
- Falster, G., Delean, S., Tyler, J., 2018. Hydrogen Peroxide Treatment of Natural Lake Sediment Prior to Carbon and Oxygen Stable Isotope Analysis of Calcium Carbonate. *Geochemistry, Geophys. Geosystems* 1–13. <https://doi.org/10.1029/2018GC007575>
- Ford, P.W., 2007. Biogeochemistry of the Coorong. Review and identification of future research requirements. CSIRO Water for a Healthy Country National Research Flagship, Canberra (2007), <https://doi.org/10.4225/08/59aef4ce808ba>
- Freitas, P., Clarke, L.J., Kennedy, H., Richardson, C., Abrantes, F., 2005. Mg/Ca, Sr/Ca, and stable-isotope ( $^{18}\text{O}$  and  $^{13}\text{C}$ ) ratio profiles from the fan mussel *Pinna nobilis*: Seasonal records and temperature relationships. *Geochemistry, Geophys. Geosystems* 6. <https://doi.org/10.1029/2004GC000872>
- Freitas, P.S., Clarke, L.J., Kennedy, H., Richardson, C.A., 2012. The potential of combined Mg/Ca and  $\delta^{18}\text{O}$  measurements within the shell of the bivalve *Pecten maximus* to estimate seawater  $\delta^{18}\text{O}$  composition. *Chem. Geol.* 291, 286–293. <https://doi.org/10.1016/j.chemgeo.2011.10.023>
- Freitas, P.S., Clarke, L.J., Kennedy, H., Richardson, C.A., Abrantes, F., 2006. Environmental and biological controls on elemental (Mg/Ca, Sr/Ca and Mn/Ca) ratios in shells of the king scallop *Pecten maximus*. *Geochim. Cosmochim. Acta* 70, 5119–5133. <https://doi.org/10.1016/j.gca.2006.07.029>
- Füllenbach, C.S., Schöne, B.R., Mertz-Kraus, R., 2015. Strontium/lithium ratio in aragonitic shells of *Cerastoderma edule* (Bivalvia) - A new potential temperature proxy for brackish environments. *Chem. Geol.* 417, 341–355. <https://doi.org/10.1016/j.chemgeo.2015.10.030>
- Gaetani, G.A., Cohen, A.L., 2006. Element partitioning during precipitation of aragonite from seawater: A framework for understanding paleoproxies. *Geochim. Cosmochim. Acta* 70,



- 4617–4634. <https://doi.org/10.1016/j.gca.2006.07.008>
- Geddes, M.C., Butler, A., 1984. Physicochemical and Biological Studies on the Coorong Lagoons, South Australia, and the Effect of Salinity on the Distribution of the Macrobenthos. *Trans. R. Soc. South Aust.* 108, 51–62.
- Geeza, T.J., Gillikin, D.P., Goodwin, D.H., Evans, S.D., Watters, T., Warner, N.R., 2018. Controls on magnesium, manganese, strontium, and barium concentrations recorded in freshwater mussel shells from Ohio. *Chem. Geol.* 1–12. <https://doi.org/10.1016/j.chemgeo.2018.01.001>
- Gibbs, R.J., 1970. Mechanisms Controlling World Water Chemistry. *Science.* 170, 1088–1090.
- Gillanders, B.M., Munro, A.R., 2012. Hypersaline waters pose new challenges for reconstructing environmental histories of fish based on otolith chemistry. *Limnol. Oceanogr.* 57, 1136–1148. <https://doi.org/10.4319/lo.2012.57.4.1136>
- Gillikin, D.P., 2019. Chemical sclerochronology. *Chem. Geol.* 526, 1–6. <https://doi.org/10.1016/j.chemgeo.2019.06.016>
- Gillikin, D.P., De Ridder, F., Ulens, H., Elskens, M., Keppens, E., Baeyens, W., Dehairs, F., 2005a. Assessing the reproducibility and reliability of estuarine bivalve shells (*Saxidomus giganteus*) for sea surface temperature reconstruction: Implications for paleoclimate studies. *Palaeogeogr. Palaeoclimatol. Palaeoecol.* 228, 70–85. <https://doi.org/10.1016/j.palaeo.2005.03.047>
- Gillikin, D.P., Dehairs, F., Lorrain, A., Steenmans, D., Baeyens, W., André, L., 2006. Barium uptake into the shells of the common mussel (*Mytilus edulis*) and the potential for estuarine paleo-chemistry reconstruction. *Geochim. Cosmochim. Acta* 70, 395–407. <https://doi.org/10.1016/j.gca.2005.09.015>
- Gillikin, D.P., Lorrain, A., Navez, J., Taylor, J.W., André, L., Keppens, E., Baeyens, W., Dehairs, F., 2005b. Strong biological controls on Sr/Ca ratios in aragonitic marine bivalve shells. *Geochemistry, Geophys. Geosystems* 6. <https://doi.org/10.1029/2004GC000874>
- Gillikin, D.P., Lorrain, A., Paulet, Y.M., André, L., Dehairs, F., 2008. Synchronous barium peaks in high-resolution profiles of calcite and aragonite marine bivalve shells. *Geo-Marine Lett.* 28, 351–358. <https://doi.org/10.1007/s00367-008-0111-9>
- Goodwin, D.H., Gillikin, D.P., Roopnarine, P.D., 2013. Preliminary evaluation of potential stable isotope and trace element productivity proxies in the oyster *Crassostrea gigas*. *Palaeogeogr. Palaeoclimatol. Palaeoecol.* 373, 88–97. <https://doi.org/10.1016/j.palaeo.2012.03.034>
- Government of South Australia,. 2020. River Murray flow report (Department for Environment and Water, South Australia). Available at: <https://www.waterconnect.sa.gov.au/Pages/Home.aspx>
- Griscom, S.B., Fisher, N.S., 2004. Bioavailability of sediment-bound metals to marine bivalve molluscs: An overview. *Estuaries* 27, 826–838. <https://doi.org/10.1007/BF02912044>
- Haese, R., Murray, E., Wallace, L., 2009. Nutrient sources, water quality, and biogeochemical processes in the Coorong, South Australia. *Geoscience Australia Record* 2009/19,

- Commonwealth Government, Canberra (2009).
- Haese, R.R., Gow, L., Wallace, L., Brodie, R.S., 2008. Identifying groundwater discharge in the Coorong (South Australia). *AusGeo News* 1–6.
- Hart, S.R., Blusztajn, J., 1998. Clams As Recorders of Ocean Ridge Volcanism and Hydrothermal Vent Field Activity. *Science*. 280, 883–886.
- Hatch, M.B.A., Schellenberg, S.A., Carter, M.L., 2013. Ba/Ca variations in the modern intertidal bean clam *Donax gouldi*: An upwelling proxy? *Palaeogeogr. Palaeoclimatol. Palaeoecol.* 373, 98–107. <https://doi.org/10.1016/j.palaeo.2012.03.006>
- Hellstrom, J., Paton, C., Woodhead, J., Hergt, J., 2008. Iolite: software for spatially resolved LA-(quad and MC) ICPMS analysis, in: Sylvester, P. (Ed.), *Laser Ablation ICP-MS in the Earth Sciences: Current Practices and Outstanding Issues*. Mineralogical Association of Canada short course volume 40, p. 343.
- Izumida, H., Yoshimura, T., Suzuki, A., Nakashima, R., Ishimura, T., Yasuhara, M., Inamura, A., Shikazono, N., Kawahata, H., 2011. Biological and water chemistry controls on Sr/Ca, Ba/Ca, Mg/Ca and  $\delta^{18}\text{O}$  profiles in freshwater pearl mussel *Hyriopsis* sp. *Palaeogeogr. Palaeoclimatol. Palaeoecol.* 309, 298–308. <https://doi.org/10.1016/j.palaeo.2011.06.014>
- Izzo, C., Manetti, D., Doubleday, Z.A., Gillanders, B.M., 2016. Calibrating the element composition of *Donax deltoides* shells as a palaeo-salinity proxy. *Palaeogeogr. Palaeoclimatol. Palaeoecol.* 484, 89–96. <https://doi.org/10.1016/j.palaeo.2016.11.038>
- Kanandjembo, A.N., Platell, M.E., Potter, I.C., 2001. The benthic macroinvertebrate community of the upper reaches of an Australian estuary that undergoes marked seasonal changes in hydrology. *Hydrolog. Process.* 15, 2481–2501. <https://doi.org/10.1002/hyp.296>
- Krause-Nehring, J., Brey, T., Thorrold, S.R., 2012. Centennial records of lead contamination in northern Atlantic bivalves (*Arctica islandica*). *Mar. Pollut. Bull.* 64, 233–240. <https://doi.org/10.1016/j.marpolbul.2011.11.028>
- Lautenschlager, A.D., Matthews, T.G., Quinn, G.P., 2014. Utilization of organic matter by invertebrates along an estuarine gradient in an intermittently open estuary. *Estuar. Coast. Shelf Sci.* 149, 232–243. <http://dx.doi.org/10.1016/j.ecss.2014.08.020>
- Lazareth, C.E., Vander Putten, E., André, L., Dehairs, F., 2003. High-resolution trace element profiles in shells of the mangrove bivalve *Isognomon ehippium*: A record of environmental spatio-temporal variations? *Estuar. Coast. Shelf Sci.* 57, 1103–1114. [https://doi.org/10.1016/S0272-7714\(03\)00013-1](https://doi.org/10.1016/S0272-7714(03)00013-1)
- Lebrato, M., Garbe-Schönberg, D., Müller, M.N., Blanco-Ameijeiras, S., Feely, R.A., Lorenzoni, L., Molinero, J.-C., Bremer, K., Jones, D.O.B., Iglesias-Rodriguez, D., Greeley, D., Lamare, M.D., Paulmier, A., Graco, M., Cartes, J., Barcelos e Ramos, J., de Lara, A., Sanchez-Leal, R., Jimenez, P., Paparazzo, F.E., Hartman, S.E., Westernströer, U., Küter, M., Benavides, R., da Silva, A.F., Bell, S., Payne, C., Olafsdottir, S., Robinson, K., Jantunen, L.M., Korablev, A., Webster, R.J., Jones, E.M., Gilg, O., Bailly du Bois, P., Beldowski, J., Ashjian, C., Yahia, N.D., Twining, B., Chen, X.-G., Tseng, L.-C., Hwang, J.-S., Dahms, H.-U., Oschlies, A., 2020. Global variability in seawater Mg:Ca and Sr:Ca

- ratios in the modern ocean. *Proc. Natl. Acad. Sci.* 201918943. <https://doi.org/10.1073/pnas.1918943117>
- Lehrter, J.C., Murrell, M.C., Kurtz, J.C., 2009. Interactions between freshwater input, light, and phytoplankton dynamics on the Louisiana continental shelf. *Cont. Shelf Res.* 29, 1861–1872. <https://doi.org/10.1016/j.csr.2009.07.001>
- Lorrain, A., Gillikin, D.P., Paulet, Y.M., Chauvaud, L., Le Mercier, A., Navez, J., André, L., 2005. Strong kinetic effects on Sr/Ca ratios in the calcitic bivalve *Pecten maximus*. *Geology* 33, 965–968. <https://doi.org/10.1130/G22048.1>
- Macdonald, J.I., Crook, D.A., 2010. Variability in Sr:Ca and Ba:Ca ratios in water and fish otoliths across an estuarine salinity gradient. *Mar. Ecol. Prog. Ser.* 413, 147–161. <https://doi.org/10.3354/meps08703>
- Matthews, T.G., Constable, A.J., 2004. Effect of flooding on estuarine bivalve populations near the mouth of the Hopkins River, Victoria, Australia. *J. Mar. Biol. Assoc. United Kingdom* 84, 633–639.
- Miller, J.A., 2009. The effects of temperature and water concentration on the otolith incorporation of barium and manganese in black rockfish *Sebastes melanops*. *J. Fish Biol.* 75, 39–60. <https://doi.org/10.1111/j.1095-8649.2009.02262.x>
- Mitsuguchi, T., Matsumoto, E., Abe, O., Uchida, T., Isdale, P.J., 1996. Mg/Ca Thermometry in Coral Skeletons. *Science*. 274, 961–963.
- Mohan, J.A., Walther, B.D., 2015. Spatiotemporal Variation of Trace Elements and Stable Isotopes in Subtropical Estuaries: II. Regional, Local, and Seasonal Salinity-Element Relationships. *Estuaries and Coasts* 38, 769–781. <https://doi.org/10.1007/s12237-014-9876-4>
- Moore, W.S., Shaw, T.J., 2008. Fluxes and behavior of radium isotopes, barium, and uranium in seven Southeastern US rivers and estuaries. *Mar. Chem.* 108, 236–254. <https://doi.org/10.1016/j.marchem.2007.03.004>
- Murrell, M.C., Hagy, J.D., Lores, E.M., Greene, R.M., 2007. Phytoplankton production and nutrient distributions in a subtropical estuary: Importance of freshwater flow. *Estuaries and Coasts* 30, 390–402. <https://doi.org/10.1007/BF02819386>
- Nelson, T.R., Powers, S.P., 2020. Elemental Concentrations of Water and Otoliths as Salinity Proxies in a Northern Gulf of Mexico Estuary. *Estuaries and Coasts*. <https://doi.org/10.1007/s12237-019-00686-z>
- O’Neil, D.D., Gillikin, D.P., 2014. Do freshwater mussel shells record road-salt pollution? *Sci. Rep.* 4, 7168. <https://doi.org/10.1038/srep07168>
- Paton, C., Hellstrom, J., Paul, B., Woodhead, J., Hergt, J., 2011. Iolite: Freeware for the visualisation and processing of mass spectrometric data. *J. Anal. At. Spectrom.* 26, 2508. <https://doi.org/10.1039/c1ja10172b>
- Poulain, C., Gillikin, D.P., Thébault, J., Munaron, J.M., Bohn, M., Robert, R., Paulet, Y.M., Lorrain, A., 2015. An evaluation of Mg/Ca, Sr/Ca, and Ba/Ca ratios as environmental

- proxies in aragonite bivalve shells. *Chem. Geol.* 396, 42–50. <https://doi.org/10.1016/j.chemgeo.2014.12.019>
- Schöne, B.R., Dunca, E., Fiebig, J., Pfeiffer, M., 2005. Mutvei's solution: An ideal agent for resolving microgrowth structures of biogenic carbonates. *Palaeogeogr. Palaeoclimatol. Palaeoecol.* 228, 149–166. <https://doi.org/10.1016/j.palaeo.2005.03.054>
- Schöne, B.R., Krause Jr, R.A., 2016. Retrospective environmental biomonitoring – Mussel Watch expanded. *Glob. Planet. Change* 144, 228–251. <https://doi.org/10.1016/j.gloplacha.2016.08.002>
- Schöne, B.R., Radermacher, P., Zhang, Z., Jacob, D.E., 2013. Crystal fabrics and element impurities (Sr/Ca, Mg/Ca, and Ba/Ca) in shells of *Arctica islandica*-Implications for paleoclimate reconstructions. *Palaeogeogr. Palaeoclimatol. Palaeoecol.* 373, 50–59. <https://doi.org/10.1016/j.palaeo.2011.05.013>
- Schöne, B.R., Surge, D., 2014. Bivalve shells: ultra high-resolution paleoclimate archives. *Pages.* 22, 20–21.
- Schöne, B.R., Zhang, Z., Jacob, D., Gillikin, D.P., Tütken, T., Garbe-Schönberg, D., McConnaughey, T., Soldati, A., 2010. Effect of organic matrices on the determination of the trace element chemistry (Mg, Sr, Mg/Ca, Sr/Ca) of aragonitic bivalve shells (*Arctica islandica*) - Comparison of ICP-OES and LA-ICP-MS data. *Geochem. J.* 44, 23–37.
- Schöne, B.R., Zhang, Z., Radermacher, P., Thébault, J., Jacob, D.E., Nunn, E. V., Maurer, A.-F., 2011. Sr/Ca and Mg/Ca ratios of ontogenetically old, long-lived bivalve shells (*Arctica islandica*) and their function as paleotemperature proxies. *Palaeogeogr. Palaeoclimatol. Palaeoecol.* 302, 52–64. <https://doi.org/10.1016/j.palaeo.2010.03.016>
- Semeniuk, V., Wurm, P.A.S., 2000. Mollusc of the Leschenault Inlet estuary: their diversity, distribution, and population dynamics. *J. R. Soc. West. Aust.* 83, 377-418.
- Shao, Y., Farkaš, J., Mosley, L., Tyler, J., Wong, H., Chamberlayne, B., Raven, M., Samanta, M., Holmden, C., Gillanders, B.M., Kolevica, A., Eisenhauer, A., 2020. Impact of salinity and carbonate saturation on stable Sr isotopes ( $\delta^{88/86}\text{Sr}$ ) in a lagoon-estuarine system. *Geochim. Cosmochim. Acta* 293, 461-476. <https://doi.org/10.1016/j.gca.2020.11.014>
- Shao, Y., Farkaš, J., Holmden, C., Mosley, L., Kell-Duivesteyn, I., Izzo, C., Reis-Santos, P., Tyler, J., Törber, P., Frýda, J., Taylor, H., Haynes, D., Tibby, J., Gillanders, B.M., 2018. Calcium and strontium isotope systematics in the lagoon-estuarine environments of South Australia: Implications for water source mixing, carbonate fluxes and fish migration. *Geochim. Cosmochim. Acta* 239, 90–108. <https://doi.org/10.1016/j.gca.2018.07.036>
- Sinclair, D.J., Kinsley, L., McCulloch, M.T., 1998. High resolution analysis of trace elements in corals by laser ablation ICP-MS. *Geochim. Cosmochim. Acta* 62, 1889–1901. [https://doi.org/10.1016/S0016-7037\(98\)00112-4](https://doi.org/10.1016/S0016-7037(98)00112-4)
- Stecher, H.A., Kogut, M.B., 1999. Rapid barium removal in the Delaware estuary. *Geochim. Cosmochim. Acta* 63, 1003–1012. [https://doi.org/10.1016/S0016-7037\(98\)00310-X](https://doi.org/10.1016/S0016-7037(98)00310-X)
- Surge, D.M., Lohmann, K.C., 2002. Temporal and spatial differences in salinity and water

- chemistry in SW Florida estuaries: Effects of human-impacted watersheds. *Estuaries* 25, 393–408. <https://doi.org/10.1007/BF02695982>
- Surge, D.M., Lohmann, K.C., Goodfriend, G.A., 2003. Reconstructing estuarine conditions: Oyster shells as recorders of environmental change, Southwest Florida. *Estuar. Coast. Shelf Sci.* 57, 737–756. [https://doi.org/10.1016/S0272-7714\(02\)00370-0](https://doi.org/10.1016/S0272-7714(02)00370-0)
- Takesue, R.K., van Geen, A., 2004. Mg/Ca, Sr/Ca, and stable isotopes in modern and Holocene *Protothaca staminea* shells from a northern California coastal upwelling region. *Geochim. Cosmochim. Acta* 68, 3845–3861. <https://doi.org/10.1016/j.gca.2004.03.021>
- Thébault, J., Chauvaud, L., L'Helguen, S., Clavier, J., Barats, A., Jacquet, S., Pécheyran, C., Amouroux, D., 2009. Barium and molybdenum records in bivalve shells: Geochemical proxies for phytoplankton dynamics in coastal environments? *Limnol. Oceanogr.* 54, 1002–1014. <https://doi.org/10.4319/lo.2009.54.3.1002>
- Tynan, S., Opdyke, B.N., Walczak, M., Eggins, S., Dutton, A., 2017. Assessment of Mg/Ca in *Saccostrea glomerata* (the Sydney rock oyster) shell as a potential temperature record. *Palaeogeogr. Palaeoclimatol. Palaeoecol.* 484, 79–88. <https://doi.org/10.1016/j.palaeo.2016.08.009>
- Vander Putten, E., Dehairs, F., Keppens, E., Baeyens, W., 2000. High resolution distribution of trace elements in the calcite shell layer of modern *Mytilus edulis*: Environmental and biological controls. *Geochim. Cosmochim. Acta* 64, 997–1011.
- Vieira, S., Barrulas, P., Chainho, P., Dias, C.B., Sroczy, K., Adão, H., 2021. Spatial and Temporal Distribution of the Multi-element Signatures of the Estuarine Non-indigenous Bivalve *Ruditapes philippinarum*. *Biol. Trace Elem. Res.*
- Walther, B.D., Limburg, K.E., 2012. The use of otolith chemistry to characterize diadromous migrations. *J. Fish Biol.* 81, 796–825. <https://doi.org/10.1111/j.1095-8649.2012.03371.x>
- Walther, B.D., Nims, M.K., 2015. Spatiotemporal Variation of Trace Elements and Stable Isotopes in Subtropical Estuaries: I. Freshwater Endmembers and Mixing Curves. *Estuaries and Coasts* 38, 754–768. <https://doi.org/10.1007/s12237-014-9881-7>
- Wanamaker, A.D., Gillikin, D.P., 2018. Strontium, magnesium, and barium incorporation in aragonitic shells of juvenile *Arctica islandica*: Insights from temperature controlled experiments. *Chem. Geol.* 0–1. <https://doi.org/10.1016/j.chemgeo.2018.02.012>
- Wanamaker, A.D., Kreutz, K.J., Wilson, T., Borns, H.W., Introne, D.S., Feindel, S., 2008. Experimentally determined Mg/Ca and Sr/Ca ratios in juvenile bivalve calcite for *Mytilus edulis*: Implications for paleotemperature reconstructions. *Geo-Marine Lett.* 28, 359–368. <https://doi.org/10.1007/s00367-008-0112-8>
- Wells, F.E., Threlfall, T.J., 1982a. Salinity and temperature tolerance of *Hydrococcus brazieri* (T. Woods, 1876) and *Arthritica semen* (Menke, 1843) from the Peel-Harvey estuarine system, Western Australia. *J. Malacol. Soc. Aust.* 5, 151–156.
- Wells, F.E., Threlfall, T.J., 1982b. Density Fluctuations, Growth and Dry Tissue Production of *Hydrococcus Brazieri* (Tenison Woods, 1876) and *Arthritica semen* (Menke, 1843) in Peel

Inlet, Western Australia. *J. Molluscan Stud.* 48, 310–320.

Wells, F.E., Threlfall, T.J., 1982c. Reproductive strategies of *Hydrococcus brazieri* (Tenison Woods, 1876) and *Arthritica semen* (Menke, 1843) in Peel Inlet, Western Australia. *J. Malacol. Soc. Aust.* 5, 157–166.

Yan, H., Shao, D., Wang, Y., Sun, L., 2013. Sr/Ca profile of long-lived *Tridacna gigas* bivalves from South China Sea: A new high-resolution SST proxy. *Geochim. Cosmochim. Acta* 112, 52–65. <https://doi.org/10.1016/j.gca.2013.03.007>

Zhao, L., Schöne, B.R., Mertz-Kraus, R., 2017. Controls on strontium and barium incorporation into freshwater bivalve shells (*Corbicula fluminea*). *Palaeogeogr. Palaeoclimatol. Palaeoecol.* 465, 386–394. <https://doi.org/10.1016/j.palaeo.2015.11.040>

## Supplementary Information

**Table S1.** Location and sampling time for water samples from the Lake Alexandrina and the Coorong Lagoons. Also shown are salinity, pH, water temperature, and element concentrations. Uncertainty in element concentrations is the standard error of triplicate analyses.

Location	Date	Latitude	Longitude	Salinity	pH	Water							
						Temperature (°C)	Mg (ppm)	Ca (ppm)	Sr (ppm)	Ba (ppb)	Mg/Ca (mol/mol)	Sr/Ca (mmol/mol)	Ba/Ca (umol/mol)
Jacks Point	7/02/2017	-36.03	139.57	64.79	8.50	28.08	2529.52	729.28	18.36	64.03±0.75	5.72	11.52	32.02±1.06
Jacks Point	21/03/2017	-36.03	139.57	66.58	8.40	24.28	2857.68	839.97	20.93	68.59±1.69	5.61	11.4	30.95±0.84
Jacks Point	24/04/2017	-36.03	139.57	72.22	8.07	19.13	2775.38	829.85	20.85	109.77	5.51	11.49	26.5
Jacks Point	30/05/2017	-36.03	139.57	62.66	8.21	14.22	2462.12	738.78	18.82	110.65	5.49	11.65	33.48
Jacks Point	7/07/2017	-36.03	139.57	59.59	8.15	12.15	373.03	112.32	2.95	63.9±5.11	5.48	12	35.03±3.44
Jacks Point	27/07/2017	-36.03	139.57	57.64	8.13	11.97	2019.54	649.15	16.16	52.58	5.13	11.39	29.46
Jacks Point	30/08/2017	-36.03	139.56	53.11	8.23	12.39	1818.82	551.62	14.66	55.77	5.44	12.16	31.79
Jacks Point	29/09/2017	-36.03	139.57	52.22	8.32	18.16	1937.23	616.05	15.24	69.09	5.18	11.32	32.42
Jacks Point	25/10/2017	-36.03	139.57	54.55	8.48	16.57	1915.53	568.89	15.74	96.54	5.55	12.66	36.08
Jacks Point	15/11/2017	-36.03	139.57	53.44	8.41	19.69	1906.45	594.09	15.4	57.41	5.29	11.86	35.34
Jacks Point	18/01/2018	-36.03	139.57	69.95	8.31	22.93	2703.59	781.75	21.2	92.23	5.7	12.4	39.79
Jacks Point	28/02/2018	-36.03	139.57	83.60	8.07	21.17	3000.88	825.59	23.67	76.24±2.42	5.99	13.11	39.58±0.46
Jacks Point	30/03/2018	-36.03	139.57	89.82	8.09	23.92	3032.66	894.79	23.64	0	5.59	12.08	0
Jacks Point	3/05/2018	-36.03	139.57	74.20	8.20	15.90	2341.55	672.23	18.26	72.38	5.74	12.42	50.25
Jacks Point	24/05/2018	-36.03	139.57	72.20	8.24	15.62	2498.67	764.38	19.79	85.22	5.39	11.85	48.39
Lake Alexandrina	21/03/2017	-35.51	139.19	0.27	9.05	23.52	17.23	58.41	0.31	62.99±0.50	0.49	2.4	991.21±3.76
Lake Alexandrina	24/04/2017	-35.51	139.19	0.22	7.58	19.50	14.36	43.09	0.27	53.1	0.55	2.87	910.63
Lake Alexandrina	30/05/2017	-35.51	139.19	0.23	8.15	13.63	14.66±0.15	52.15±2.01	0.28±0.005	63.53	0.46±0.01	2.44±0.06	1014.83
Lake Alexandrina	7/07/2017	-35.51	139.19	0.24	8.54	11.50	36.97	45.33	0.26	53.02	1.34	2.64	955.88
Lake Alexandrina	27/07/2017	-35.51	139.19	0.28	7.75	11.77	18.91	67.47	0.32	57.69	0.46	2.19	914.63

Lake Alexandrina	30/08/2017	-35.51	139.19	0.28	9.08	14.43	17.54±0.32	61.31±4.11	0.31±0.003	173	0.48±0.02	2.36±0.16	1793.75
Lake Alexandrina	29/09/2017	-35.51	139.19	0.28	8.78	16.30	19.33	58.47	0.32	62.94	0.54	2.53	1077.11
Lake Alexandrina	25/10/2017	-35.51	139.19	0.28	9.17	20.44	20.54	47.2	0.31	53.44	0.72	3.03	850.12
Lake Alexandrina	15/11/2017	-35.51	139.19	0.29	8.11	20.75	17.56	59.38	0.33	75.25	0.49	2.52	803.69
Lake Alexandrina	18/01/2018	-35.51	139.19	0.31	9.07	32.60	18.76	55.24	0.35	79.82	0.56	2.93	874.36
Lake Alexandrina	28/02/2018	-35.51	139.19	0.34	8.86	21.14	18.71±0.11	60.76±0.45	0.32±0.003	80.92	0.51±0.003	2.41±0.035	1199.29
Lake Alexandrina	30/03/2018	-35.51	139.19	0.40	9.11	20.00	4.55	10.44	0.08	88.03	0.72	3.69	991.18
Lake Alexandrina	3/05/2018	-35.51	139.19	0.35	8.87	16.12	20.09	53.57	0.3	79.8	0.62	2.56	1222.78
Lake Alexandrina	24/05/2018	-35.51	139.19	0.45	8.33	14.12	25.5	55.74	0.38	93.25±2.33	0.75	3.14	1095.77±27.63
Long Point	1/11/2016	-35.70	139.16	7.68	8.35	15.05	251.91±30.15	122.92±3.08	1.77±0.19	38.23	3.36±0.32	6.57±0.562	121.4
Long Point	21/12/2016	-35.70	139.16	9.15	8.35	20.00	356.64	156.25	2.8	41.76	3.76	8.21	104.91
Long Point	7/02/2017	-35.70	139.16	39.00	8.36	22.67	1492.06	489.47	11.3	73.88	5.03	10.56	46.67
Long Point	21/03/2017	-35.70	139.16	22.38	8.15	22.04	172.32±0.23	60.4±1.50	1.3±0.006	67.17	4.71±0.12	9.82±0.202	86.63
Long Point	24/04/2017	-35.70	139.16	22.59	7.95	19.01	838.63	277.62	6.66	66.89	4.98	10.98	82.29
Long Point	30/05/2017	-35.70	139.16	13.04	8.34	13.44	779.75	298.45	5.84	39.66	4.31	8.96	70.66
Long Point	7/07/2017	-35.70	139.16	17.93	8.58	12.56	604.61	218.19	4.58	40.78	4.57	9.61	66.79
Long Point	27/07/2017	-35.67	139.14	15.82	8.55	12.40	568.57±5.49	233.73±9.40	4.41±0.06	34.97	4.03±0.20	8.68±0.45	56.4
Long Point	30/08/2017	-35.70	139.16	31.05	8.21	13.02	1063.08	372.52	8.65	53.01	4.71	10.62	50.15
Long Point	29/09/2017	-35.67	139.16	23.98	8.75	17.27	863.56	297.98	6.66	51.64±7.53	4.78	10.22	60.77±9.74
Long Point	25/10/2017	-35.70	139.16	46.05	8.32	19.98	1589.12±22.64	520.03±6.56	13.07±0.17	105.31	5.04±0.03	11.5±0.12	43.29
Long Point	15/11/2017	-35.70	139.16	20.56	8.43	20.86	1028.67	314.28	8.16	56.84±0.50	5.4	11.88	60.1±1.54
Long Point	18/01/2018	-35.70	139.16	21.71	8.71	29.07	838.61	279.23	6.8	79.57	4.95	11.13	103.44



Long Point	28/02/2018	-35.70	139.16	28.34	8.11	20.49	953.66	337.21	7.6	73.11	4.66	10.31	89.31
Long Point	30/03/2018	-35.70	139.16	30.07	8.23	20.81	1013.1	377.76	7.81	49.43	4.42	9.46	54.17
Long Point	3/05/2018	-35.70	139.16	32.23	8.19	15.71	1061.69	399.39	8.28	48.19	4.38	9.48	59.47
Long Point	24/05/2018	-35.69	139.16	31.37	8.23	14.66	1154.63	1002.59	18.7	40.12	1.9	8.53	45.92
Mark Point	1/11/2016	-35.63	139.08	5.13	8.30	16.80	167.47±36.22	95.17±2.47	1.24±0.23	74.46	2.89±0.55	5.96±0.95	307.62
Mark Point	1/11/2016	-35.62	139.08	5.19	9.37	17.20	215.21	124.59	1.55	70.68	2.85	5.68	268.59
Mark Point	21/12/2016	-35.63	139.08	1.71	8.61	20.53	76.63±0.31	80.72±1.77	0.66±0.004	33.67	1.57±0.03	3.76±0.06	367.88
Mark Point	7/02/2017	-35.63	139.08	21.47	8.57	24.57	784.91±6.54	282.04±14.97	6.3±0.20	113.35	4.6±0.20	10.23±0.20	97.96
Mark Point	21/03/2017	-35.63	139.08	11.30	8.61	22.43	444.29	175.14	3.48	58.52	4.18	9.08	127.7
Mark Point	24/04/2017	-35.63	139.08	16.38	8.22	18.44	597.3	231.02	4.6	49.59	4.26	9.11	82.03
Mark Point	30/05/2017	-35.63	139.08	17.46	8.15	12.45	687.03	268.39	5.01	32.32	4.22	8.54	45.57
Mark Point	7/07/2017	-35.61	139.05				840.39	299.39	6.36	32.76	4.63	9.72	34.07
Mark Point	27/07/2017	-35.63	139.08	8.84	8.32	12.47	367.16	154.73	2.46	34.52	3.91	7.27	107.49
Mark Point	30/08/2017	-35.64	139.10	21.95	8.58	13.88	778.96	299.48	6.49	48.27	4.29	9.91	61.82
Mark Point	29/09/2017	-35.63	139.08	16.57	8.84	18.50	621.4	249.91	4.71	35.91	4.1	8.62	61.4
Mark Point	25/10/2017	-35.63	139.08	36.10	8.49	21.78	1285.31	423.04	10.42	93.38	5.01	11.27	50.26
Mark Point	15/11/2017	-35.63	139.08	20.41	8.31	19.57	775.22	301.44	6.39	61.33	4.24	9.7	76.64
Mark Point	18/01/2018	-35.63	139.08	14.49	8.98	33.17	572.1	205.37	4.53	73.53	4.59	10.09	130.71
Mark Point	28/02/2018	-35.63	139.08	17.58	8.37	21.23	577.85	241.47	4.52	60.73	3.95	8.57	106.16
Mark Point	30/03/2018	-35.63	139.08	33.04	8.29	21.11	1095.83	371.29	8.37	32.46	4.87	10.31	36.91
Mark Point	3/05/2018	-35.63	139.08	31.53	8.38	15.71	1058.67	411.31	7.87	34.9	4.24	8.75	44.88
Mark Point	24/05/2018	-35.60	139.03	26.67	7.84	14.69	929.32±9.76	347.94±3.53	7.11±0.05	37.63	4.4±0.07	9.34±0.12	52.14
Mulbin Yerrok	1/11/2016	-35.67	139.14	3.33	8.07	15.80	292.61	130.88	2.01	26.64±0.84	3.69	7.03	162.19±2.51
Mulbin Yerrok	21/12/2016	-35.67	139.14	6.51	8.20	20.73	261.95	124.99	1.88	37.52	3.46	6.88	138.39
Mulbin Yerrok	7/02/2017	-35.67	139.14	32.36	8.66	24.74	1265.76	402.56	9.69	76.54±1.21	5.18	11.01	60.05±2.02

Mulbin Yerok	21/03/2017	-35.70	139.16	18.35	8.11	21.90	740.27	251.49	5.67	62.74	4.85	10.31	92.4
Mulbin Yerok	24/04/2017	-35.65	139.10	16.73	8.40	18.82	619.82	233.06	4.79	51.95	4.38	9.4	81.88
Mulbin Yerok	30/05/2017	-35.67	139.14	13.24	8.26	13.23	531.35	222.24	3.94	35.21	3.94	8.1	60.37
Mulbin Yerok	7/07/2017	-35.66	139.10	24.33	8.22	12.70	844.15±19.34	307.29±6.70	6.32±0.18	33.54	4.53±0.008	9.4±0.07	37.51
Mulbin Yerok	27/07/2017	-35.67	139.14	11.98	8.56	12.46	411.1	165.11	3.22	37.53	4.11	8.91	80.01
Mulbin Yerok	30/08/2017	-35.66	139.12	27.48	8.32	13.84	947.22	312.11	7.66	49.68	5	11.23	57.29
Mulbin Yerok	29/09/2017	-35.65	139.10	17.53	8.82	18.47	618.83	263.46	4.68	40.01±1.64	3.87	8.12	62.72±0.97
Mulbin Yerok	25/10/2017	-35.65	139.10	40.17	8.55	20.89	1416.8	458.42	11.65	65.11	5.1	11.63	51.01
Mulbin Yerok	15/11/2017	-35.65	139.10	22.55	8.19	19.68	800.89	276.89	6.48	68.56	4.77	10.71	79.93
Mulbin Yerok	18/01/2018	-35.70	139.16	15.01	8.91	32.73	588.66±1.60	239.69±9.20	4.8±0.01	81.81	4.06±0.14	9.19±0.34	133.67
Mulbin Yerok	28/02/2018	-35.65	139.10	25.07	8.54	20.43	824.7	314.63	6.4	58.79	4.32	9.3	80.62
Mulbin Yerok	30/03/2018	-35.70	139.16	34.41	8.42	23.04	1138.87	384.37	8.61	38.5	4.89	10.25	39.06
Mulbin Yerok	3/05/2018	-35.65	139.10	32.58	8.28	15.63	1095.11±33.24	365.52±8.43	8.14±0.29	35.91	4.94±0.16	10.19±0.35	46.16
Mulbin Yerok	24/05/2018	-35.65	139.10	26.49	8.11	14.79	938.37	335.86	7.22	44.46	4.61	9.83	53.49
Mundoo Channel	21/12/2016	-35.54	138.88	0.16	7.78	22.50	18.01	66.24	0.29	53.1	0.45	2.03	867.39
Mundoo Channel	9/02/2017	-35.54	138.88	1.48	7.94	24.35	67.68	81.48	0.58	51.03	1.37	3.23	570.22
Mundoo Channel	12/03/2017	-35.54	138.88	17.45	7.81	23.00	706.07	276.8	5.02	45.52	4.21	8.29	69.61

Mundoo Channel	25/04/2017	-35.54	138.88	23.80	8.27	19.05	958.09	327.84	6.99	28.43	4.82	9.76	24.74
Mundoo Channel	31/05/2017	-35.54	138.88	24.37	8.20	12.17	948.33	339.26	7.05	37.43±1.79	4.61	9.51	35.38±0.37
Mundoo Channel	7/07/2017	-35.54	138.88	24.97	7.82	10.77	825.01	308.53	6.17	45.96	4.41	9.15	53.34
Mundoo Channel	30/08/2017	-35.54	138.88	0.51	8.46	15.23	27.65	55.76	0.34	39.54	0.82	2.8	555.62
Mundoo Channel	29/09/2017	-35.54	138.88	30.69	8.26	15.21	1093.44	393.56	8.2	23.08	4.58	9.53	14.61
Mundoo Channel	25/10/2017	-35.54	138.88	0.48	8.50	21.63	25.41	63.74	0.36	47.91±0.52	0.66	2.59	585±31.88
Mundoo Channel	15/11/2017	-35.54	138.88	19.95	8.29	20.47	720.32	270.37	5.69	67.07	4.39	9.62	83.26
Mundoo Channel	18/01/2018	-35.54	138.88	17.55	8.74	27.57	688.19	275.86	5.27	87.07±0.73	4.11	8.74	121.55±1.28
Mundoo Channel	28/02/2018	-35.54	138.88	24.65	8.46	20.55	829.3	323.74	6.23	51.72	4.22	8.81	73.89
Mundoo Channel	30/03/2018	-35.54	138.88	35.67	8.26	20.68	1194.61	423.07	8.86	28.43±0.18	4.66	9.57	26.68±0.32
Mundoo Channel	3/05/2018	-35.56	138.88	30.12	8.13	16.82	995.36	363.49	7.61	42.23	4.51	9.58	59.07
Mundoo Channel	28/05/2018	-35.54	138.88	25.72	8.18	14.87	917.95	367.35	7.04	45.72	4.12	8.77	55.37
Pamka Point	30/05/2017	-35.90	139.40	30.48	8.31	13.53	1181.69±10.25	389.67±7.14	9.44±0.12	60.65	5±0.10	11.09±0.19	54.52
Pamka Point	30/08/2017	-35.89	139.40	49.08	8.28	11.81	2599.29	857.89	21.23	53.73±2.72	5	11.32	32.29±1.03
Pamka Point	25/10/2017	-35.90	139.40	56.80	8.44	16.93	2610.75	609.17	20.88	67.81	7.07	15.68	38.75
Pamka Point	15/11/2017	-35.90	139.40	66.64	7.91	20.50	2227.91	655.92	17.12	118.35	5.6	11.94	35.15
Pamka Point	18/01/2018	-35.90	139.40	70.80	8.33	25.98	2789.72	832.45	22.19	91.58	5.53	12.19	38.55

Pamka Point	28/02/2018	-35.90	139.40	72.84	8.58	20.09	2421.63	717.87	19.09	95.95	5.56	12.17	51.55
Pamka Point	30/03/2018	-35.90	139.40	44.00	8.33	21.85	1447.99	474.25	11.69	86.72	5.03	11.27	72.54
Pamka Point	3/05/2018	-35.90	139.40	65.28	8.32	15.65	2047.38	661.15	16.48	64.02	5.11	11.4	56.22
Pamka Point	24/05/2018	-35.90	139.40	59.66	8.34	15.86	2127.64	667.48	16.99	64.66±1.38	5.26	11.64	48.08±0.52
Pelican Point	1/11/2016	-35.60	139.03	0.25	8.55	17.76	19.22	56.26	0.26	20.1	0.56	2.15	997.46
Pelican Point	21/12/2016	-35.63	139.08	0.16	8.10	19.40	17.98	60.56	0.27	43.38	0.49	2	933.57
Pelican Point	7/02/2017	-35.60	139.03	15.81	8.67	24.74	601.69	229.74	4.78	79.25	4.32	9.51	133.78
Pelican Point	21/03/2017	-35.60	139.03	4.41	8.67	23.08	203.92	94.59	1.45	75.89	3.55	7.03	317.94
Pelican Point	24/04/2017	-35.60	139.03	14.35	8.54	19.20	536.37±1.44	203.88±5.92	4.05±0.03	41.39	4.34±0.12	9.1±0.20	73.85
Pelican Point	30/05/2017	-35.60	139.03	26.72	8.00	12.51	1065.22	396.41	7.61	21.49	4.43	8.78	20.28
Pelican Point	7/07/2017	-35.60	139.03	1.06	8.07	12.72	70.63	71.27	0.61	47.08±1.07	1.63	3.95	431.55±10.74
Pelican Point	27/07/2017	-35.60	139.03	7.00	7.10	12.40	302.06	127.62	2.07	47.56	3.9	7.43	163.35
Pelican Point	30/08/2017	-35.60	139.03	22.68	8.80	16.06	809.03	291.06	6.37	46.46	4.58	10.01	59.64
Pelican Point	29/09/2017	-35.60	139.03	10.30	9.50	18.75	433.9±12.76	157.69±2.09	2.93±0.03	41.36	4.54±0.18	8.5±0.19	108.51
Pelican Point	25/10/2017	-35.60	139.03	20.67	9.11	23.49	700.17	255.29	5.7	62.42	4.52	10.22	100.58
Pelican Point	15/11/2017	-35.60	139.03	18.94	8.14	19.00	671.16±4.68	265.4±1.65	5.29±0.08	49.65	4.17±0.05	9.12±0.2	64.52
Pelican Point	18/01/2018	-35.60	139.03	13.72	9.52	37.90	514.54	214.57	4.13	78.2	3.95	8.8	141.58

Pelican Point	28/02/2018	-35.60	139.03	3.99	8.89	20.76	159.09	96.11	1.2	68.36	2.73	5.69	401.48
Pelican Point	30/03/2018	-35.60	139.03	23.67	8.77	21.34	795.83±7.07	301.31±4.95	5.95±0.02	60.63	4.36±0.04	9.04±0.12	90.36
Pelican Point	3/05/2018	-35.60	139.03	23.97	8.21	15.69	774.83	303.87	5.77	44.36	4.2	8.68	79.12
Pelican Point	24/05/2018	-35.60	139.03	23.32	7.72	14.40	794.91	319.6	6.14	46.91±1.76	4.1	8.79	68.11±0.64
Rob Point	30/08/2017	-35.79	139.30	43.70	8.36	13.54	1446.9±13.88	438.87±5.51	11.84±0.04	65.31	5.44±0.12	12.34±0.20	38.14
Rob Point	29/09/2017	-35.78	139.30	41.62	8.43	19.01	1483.47	462.06	11.68	62.61±7.35	5.29	11.56	42.19±2.14
Rob Point	25/10/2017	-35.78	139.30	52.39	8.18	17.60	1878.54	624.06	16.21	145.41	4.96	11.88	58.7
Rob Point	15/11/2017	-35.78	139.30	57.45	8.04	20.78	2099.64	647.25	17.29	84.27±9.07	5.35	12.22	38.9±0.78
Rob Point	18/01/2018	-35.78	139.30	55.92	8.64	25.49	2120.75±39.7	644.64±11.23	16.92±0.23	92.24	5.42±0.07	12.01±0.08	49.07
Rob Point	28/02/2018	-35.78	139.30	49.23	8.49	20.22	1603.47	570.87	13.59	70.03	4.63	10.89	70.68
Rob Point	30/03/2018	-35.79	139.30	27.69	8.61	22.76	893.54±5.67	335.66±13.02	7.22±0.02	64.32	4.4±0.16	9.88±0.42	79.86
Rob Point	3/05/2018	-35.78	139.30	41.71	8.33	16.32	1326.06	433.76	10.53	52.25	5.04	11.1	66.83
Rob Point	24/05/2018	-35.78	139.30	42.44	8.28	15.84	1459.86	493.51	11.61	51.92	4.88	10.76	52
Rob Point	7/02/2017	-35.78	139.30	56.00	8.35	25.77	2091.76	634.49	16.14	62.69	5.44	11.64	32.8
Rob Point	21/03/2017	-35.79	139.30	57.20	8.33	24.85	2228.1	743.81	17.35	84.01	4.94	10.67	43.06
Rob Point	24/04/2017	-35.79	139.30	39.20	8.13	20.14	1431.22	470.15	11.41	74.46±3.10	5.02	11.1	57.3±1.96
Rob Point	30/05/2017	-35.79	139.30	24.09	8.30	13.81	958.64	314.73	7.42	51.1	5.02	10.78	58.59
Rob Point	7/07/2017	-36.03	139.57	23.98	8.22	13.21	1110.5	365.38	8.8	54.28±0.83	5.01	11.01	48.08±2.09
Rob Point	27/07/2017	-35.79	139.30	29.39	8.38	12.23	1060.85	343.82	8.44	54.03	5.09	11.23	53.52

**Table S2.** Shell ID, collection site, date of collection, size and average, minimum and maximum Sr/Ca, Mg/Ca and Ba/Ca for all *A. helmsi* specimens. The size was measured using digital callipers along the maximum growth axis.  $\sigma$  = standard deviation.

Shell ID	Site Name	Date	Size (mm)	Whole shell average $\pm 1\sigma$ /minimum/maximum				Ventral margin average $\pm 1\sigma$ /minimum/maximum			
				Sr/Ca (mmol/mol)	Mg/Ca (mmol/mol)	Ba/Ca ( $\mu$ mol/mol)	Ba/Ca ( $\mu$ mol/mol)	Sr/Ca (mmol/mol)	Mg/Ca (mmol/mol)	Ba/Ca ( $\mu$ mol/mol)	Ba/Ca ( $\mu$ mol/mol)
MC0317-1	Mundoo Channel	12/03/2017	1.97	1.42 $\pm$ 0.18/1.03/2.06	0.26 $\pm$ 0.09/0.16/0.65	3.35 $\pm$ 1.01/1.14/7.21	1.62 $\pm$ 0.03/1.59/1.66	0.26 $\pm$ 0.02/0.24/0.28	3.81 $\pm$ 0.51/3.17/4.43		
MC1017-1	Mundoo Channel	25/10/2017	2.26	1.58 $\pm$ 0.35/0.77/2.81	0.68 $\pm$ 0.35/0.21/2	3.88 $\pm$ 1.34/0.85/10.35	1.68 $\pm$ 0.07/1.58/1.74	0.52 $\pm$ 0.04/0.47/0.57	5.53 $\pm$ 0.77/4.84/6.61		
MC1017-2	Mundoo Channel	25/10/2017	2.1	1.69 $\pm$ 0.29/0.97/3.52	0.41 $\pm$ 0.09/0.24/0.77	6.28 $\pm$ 1.86/2.57/19.16	1.76 $\pm$ 0.08/1.7/1.88	0.48 $\pm$ 0.04/0.42/0.5	4.19 $\pm$ 0.27/3.98/4.58		
MC1017-3	Mundoo Channel	25/10/2017	1.98	1.93 $\pm$ 0.45/1.05/4.64	0.58 $\pm$ 0.18/0.2/1.23	7.38 $\pm$ 3.05/2.13/25.63	1.9 $\pm$ 0.17/1.74/2.11	0.7 $\pm$ 0.04/0.64/0.73	6.03 $\pm$ 1.25/4.51/7.52		
MC1017-4	Mundoo Channel	25/10/2017	1.71	1.79 $\pm$ 0.52/0.72/4.17	0.61 $\pm$ 0.31/0.18/1.73	6.31 $\pm$ 2.82/1.96/23.69	1.75 $\pm$ 0.14/1.61/1.88	0.94 $\pm$ 0.23/0.66/1.17	17.63 $\pm$ 4.12/14.64/23.69		
MC1017-5	Mundoo Channel	25/10/2017	2.1	1.84 $\pm$ 0.32/1.2/3.45	0.69 $\pm$ 0.27/0.27/1.66	6.33 $\pm$ 1.74/2.42/13.05	1.91 $\pm$ 0.18/1.69/2.12	0.79 $\pm$ 0.03/0.77/0.83	4.93 $\pm$ 0.79/4.04/5.74		
MC0118-1	Mundoo Channel	18/01/2018	2.08	1.8 $\pm$ 0.39/0.96/4.37	0.32 $\pm$ 0.1/0.14/1.11	7.29 $\pm$ 2.93/1.65/19.02	1.86 $\pm$ 0.25/1.65/2.2	0.85 $\pm$ 0.12/0.73/0.96	8.77 $\pm$ 0.96/7.98/10.1		
MC0518-1	Mundoo Channel	3/05/2018	2	1.72 $\pm$ 0.35/0.96/3.69	0.55 $\pm$ 0.25/0.15/1.52	5.3 $\pm$ 1.69/0.89/11.27	1.67 $\pm$ 0.09/1.55/1.78	0.37 $\pm$ 0.03/0.35/0.41	3.81 $\pm$ 0.51/3.17/4.43		
MC0518-2	Mundoo Channel	3/05/2018	1.92	1.56 $\pm$ 0.28/0.94/2.68	0.49 $\pm$ 0.14/0.2/1	3.98 $\pm$ 1.4/1.19/10.86	1.7 $\pm$ 0.59/1.23/2.56	0.52 $\pm$ 0.02/0.51/0.55	3.91 $\pm$ 0.53/3.32/4.42		
MC0518-3	Mundoo Channel	3/05/2018	1.86	1.57 $\pm$ 0.37/0.88/3.15	0.47 $\pm$ 0.22/0.15/1.38	5.03 $\pm$ 2.09/1.17/15.59	1.74 $\pm$ 0.13/1.61/1.9	0.41 $\pm$ 0.1/0.31/0.54	3.63 $\pm$ 0.74/2.72/4.3		
MC0518-4	Mundoo Channel	3/05/2018	1.67	1.51 $\pm$ 0.24/0.87/2.38	1.61 $\pm$ 0.73/0.53/4.98	4.23 $\pm$ 1.19/1.27/12.4	1.52 $\pm$ 0.15/1.42/1.74	1.13 $\pm$ 0.27/0.74/1.32	2.67 $\pm$ 0.98/1.74/3.9		
MC0518-5	Mundoo Channel	3/05/2018	1.71	1.59 $\pm$ 0.31/0.96/2.94	0.6 $\pm$ 0.17/0.22/1.24	4.55 $\pm$ 1.51/1.23/11.66	2.06 $\pm$ 0.31/1.69/2.34	0.56 $\pm$ 0.04/0.52/0.62	4.47 $\pm$ 0.22/4.18/4.68		
MC0518-6	Mundoo Channel	3/05/2018	1.86	1.57 $\pm$ 0.3/0.98/3.01	0.55 $\pm$ 0.17/0.22/1.47	4.64 $\pm$ 1.78/0.65/10.89	1.87 $\pm$ 0.13/1.72/2.04	0.55 $\pm$ 0.05/0.5/0.62	4.03 $\pm$ 0.93/3.1/5.21		
PP0317-1	Pelican Point	21/03/2017	2.01	1.95 $\pm$ 0.42/0.91/3.65	0.62 $\pm$ 0.36/0.16/1.49	13.16 $\pm$ 7.73/0.36/32.47	1.92 $\pm$ 0.13/1.82/2.1	0.4 $\pm$ 0.05/0.36/0.47	12.81 $\pm$ 1.17/11.76/13.86		
PP0317-2	Pelican Point	21/03/2017	2.18	1.44 $\pm$ 0.33/1.03/2.75	0.31 $\pm$ 0.07/0.2/0.58	3.78 $\pm$ 5.43/0.45/25.19	2.21 $\pm$ 0.03/2.18/2.25	0.51 $\pm$ 0.03/0.48/0.55	20.45 $\pm$ 0.68/19.81/21.36		

PP0817-1	Pelican Point	30/08/2017	1.76	2.18±0.49/1.07/4.48	0.4±0.14/0.17/0.97	22.13±1.69/2.93/76.59	1.94±0.27/1.59/2.25	0.62±0.13/0.43/0.74	7.45±1.58/6.06/9.72
PP0817-2	Pelican Point	30/08/2017	1.61	2.07±0.44/1.01/4.25	0.66±0.28/0.25/1.86	10.34±3.95/3.62/24.59	2.46±0.87/1.84/3.75	0.66±0.04/0.60/0.69	7.53±0.39/7.09/8.04
PP0817-3	Pelican Point	30/08/2017	1.85	2.21±0.53/1.7/5.3	0.82±0.43/0.37/3.65	19.42±14.9/2.91/78.06	2.13±0.06/2.06/2.21	0.82±0.04/0.76/0.87	9.36±1.67/7.57/11.55
PP0817-4	Pelican Point	30/08/2017	1.72	2.18±0.41/1.28/4.4	0.45±0.19/0.18/1.12	16.86±6.71/4.12/36.91	2.54±0.31/2.13/2.88	0.67±0.05/0.62/0.71	9.98±0.63/9.15/10.6
PP1017-1	Pelican Point	25/10/2017	1.78	1.84±0.32/1.01/3.31	0.54±0.19/0.21/1.54	7.05±2.34/2.34/19.54	2.15±0.27/1.75/2.38	0.64±0.15/0.45/0.81	12.47±4.53/7.08/17.45
PP1017-2	Pelican Point	25/10/2017	1.56	2.13±0.53/0.98/4.47	0.58±0.22/0.22/1.35	10.49±4.91/2.02/38.54	2.21±0.13/2.04/2.34	1.11±0.19/0.92/1.32	4.27±1.88/2.6/6.81
PP0118-1	Pelican Point	18/01/2018	1.88	2.12±0.59/0.89/4.36	0.66±0.34/0.19/2.18	8.96±5.16/1.52/27.52	2.58±0.17/2.35/2.72	1.2±0.11/1.05/1.3	23.57±4.27/18.3/27.52
PP0118-2	Pelican Point	18/01/2018	1.69	2.1±0.49/1.19/4.9	0.68±0.29/0.25/2.12	11.68±5.73/3.33/34.75	2.45±0.27/2.18/2.82	1.31±0.21/1.16/1.61	18.13±0.52/17.58/18.68
PP0118-3	Pelican Point	18/01/2018	1.64	1.97±0.38/1.08/4.17	0.96±0.57/0.34/4.39	10.21±3.92/2.72/37.08	2.08±0.44/1.8/2.73	1.15±0.16/1/1.34	13.49±2.31/11.05/16.53
PP0118-4	Pelican Point	18/01/2018	1.72	2.09±0.49/1.06/3.68	0.61±0.23/0.26/1.67	8.77±4.7/1.55/33.47	2.33±0.65/1.56/3.14	0.55±0.07/0.46/0.63	21.57±8.71/14.12/33.47
PP0118-5	Pelican Point	18/01/2018	1.96	2.21±0.56/1.21/4.48	0.48±0.16/0.18/1.19	10.29±5.94/2.23/29.97	2.73±0.39/2.34/3.21	0.7±0.06/0.63/0.76	12.91±2.33/11.13/16.32
PP0118-6	Pelican Point	18/01/2018	1.76	2.21±0.41/1.25/3.79	0.89±0.29/0.39/2.23	12.61±5.26/4.4/37.12	1.77±0.09/1.64/1.86	1.06±0.17/0.85/1.24	6.83±0.58/6.1/7.44
PP0118-7	Pelican Point	18/01/2018	1.82	2.04±0.44/1.12/4.33	0.53±0.16/0.26/1.92	8.61±4.41/1.65/34.8	3.19±0.77/2.69/4.33	0.8±0.09/0.73/0.91	30.01±4/25.16/33.58
PP0518-1	Pelican Point	3/05/2018	1.83	1.89±0.37/1.09/3.57	0.77±0.26/0.25/1.98	9.2±4.52/3.41/32.15	2.15±0.19/1.95/2.36	0.76±0.07/0.70/0.84	21.08±5.96/17.31/29.97
PP0518-2	Pelican Point	3/05/2018	1.78	1.95±0.4/1.24/4.08	0.69±0.18/0.35/1.53	10.62±6.4/2.74/40.55	1.85±0.24/1.58/2.16	0.41±0.04/0.35/0.44	10.15±2.1/8.57/13.14
PP0518-3	Pelican Point	3/05/2018	1.81	1.98±0.49/0.99/4.06	0.83±0.39/0.23/0.4	11.27±6.2/2.55/35.28	3.19±0.42/2.74/3.72	2.43±0.46/1.96/3.04	21.28±6.24/14.5/29.44
PP0518-4	Pelican Point	3/05/2018	1.87	2.16±0.63/1.09/4.73	0.65±0.27/0.17/1.6	17.07±11.39/1.43/74.58	2.91±0.35/2.4/3.18	1.39±0.1/1.31/1.53	20.77±3.29/17.75/25.2
PP0518-5	Pelican Point	3/05/2018	1.88	2.15±0.54/1.07/4.57	0.94±0.39/0.35/4.16	11.32±6.09/1.85/37.9	2.2±0.21/2.02/2.48	1.45±0.09/1.35/1.55	9.26±0.86/8.06/10.07
PP0518-6	Pelican Point	3/05/2018	1.78	2.1±0.59/0.88/4.68	0.88±0.51/0.22/2.99	15.6±8.68/1.7/55.52	1.73±0.14/1.54/1.88	0.73±0.05/0.69/0.79	9.52±2.31/7.56/12.83
PP0518-7	Pelican Point	3/05/2018	1.81	2.01±0.39/1.07/4.27	0.68±0.3/0.24/2.2	14.99±6.89/3.36/58.24	1.65±0.1/1.56/1.79	1.63±0.17/1.42/1.78	7.14±1.71/6.11/9.7
PP0518-8	Pelican Point	3/05/2018	1.88	1.89±0.5/0.9/53.89	0.81±0.4/0.26/1.94	6.45±3.22/0.88/25.26	1.67±0.1/1.62/1.82	0.63±0.05/0.55/0.68	5.48±1.38/4.11/6.7
MP0317-1	Mark Point	21/03/2017	1.89	2.27±0.39/1.41/3.84	0.59±0.26/0.24/1.37	17.45±6.15/7.23/33.66	2±0.07/1.93/2.08	0.58±0.05/0.52/0.64	10.01±0.98/8.86/11.21
MP0317-2	Mark Point	21/03/2017	1.4	1.89±0.22/1.38/2.95	0.62±0.25/0.23/1.46	11.89±3.86/3/25.22	1.91±0.08/1.82/2.01	0.84±0.05/0.79/0.91	12.09±2.64/10.41/16.01
MP0317-3	Mark Point	21/03/2017	2.57	2.27±0.39/1.41/3.84	0.59±0.26/0.24/1.37	17.45±6.15/7.23/33.66	2±0.07/1.93/2.08	0.58±0.05/0.52/0.64	10.01±0.98/8.86/11.21

MP0817-1	Mark Point	30/08/2017	1.38	2.04±0.46/1.24/4.92	0.74±0.29/0.24/2.37	14.43±5.7/4.82/37.25	2.26±0.12/2.12/2.4	1.42±0.06/1.35/1.48	12.85±2.24/11.23/16.17
MP0817-2	Mark Point	30/08/2017	1.51	2.04±0.47/0.92/4.03	0.66±0.32/0.19/1.87	14.72±6.02/3.42/41.32	1.79±0.24/1.44/2	0.3±0.03/0.25/0.33	5.23±1.36/4.18/7.22
MP0817-3	Mark Point	30/08/2017	1.54	2.29±0.54/1.06/5.35	0.65±0.27/0.17/1.77	17.58±6.3/6.39/39.75	2.43±0.38/1.92/2.79	1.22±0.2/1.09/1.52	13.85±1.85/12.1/15.6
MP0817-4	Mark Point	30/08/2017	1.3	2.41±0.53/1.16/5.04	0.99±0.49/0.27/2.73	18.91±7.29/3.89/45.92	1.78±0.3/1.43/2.16	0.46±0.08/0.37/0.54	5.31±1.49/3.89/7.19
MP0817-5	Mark Point	30/08/2017	1.9	1.93±0.44/0.94/4.01	0.64±0.21/0.23/1.59	7.49±3.42/2.55/25.46	2.51±0.14/2.3/2.63	1.04±0.09/0.96/1.15	19.06±1.27/18.06/20.9
MP1017-1	Mark Point	25/10/2017	1.58	2.21±0.51/1.12/4.91	0.93±0.42/0.37/3.29	15.85±7.02/1.37/37.12	1.78±0.12/1.62/1.91	2.03±0.33/1.66/2.38	5.48±0.78/4.62/6.21
MP1017-2	Mark Point	25/10/2017	1.61	1.83±0.42/0.9/3.47	0.45±0.23/0.19/2.81	4.95±1.83/1.74/13.63	2.25±0.48/1.77/2.89	2.11±0.51/1.61/2.81	3.49±0.56/2.68/3.87
MP1017-3	Mark Point	25/10/2017	1.34	2.04±0.64/1.02/5.18	0.77±0.24/0.3/2	12.14±5.56/1.13/34.61	1.75±0.2/1.48/1.92	0.86±0.07/0.79/0.94	3.36±0.85/2.57/4.55
MP1017-4	Mark Point	25/10/2017	1.48	2.56±0.68/1.15/5.45	0.61±0.18/0.31/1.44	11.34±4.25/3.44/31.48	4.79±0.19/4.56/5	0.75±0.14/0.57/0.9	21.2±1.53/19.78/23.36
MP1017-5	Mark Point	25/10/2017	1.75	2.19±0.5/1.19/4.84	0.83±0.3/0.28/1.67	7.07±2.79/1.94/17.82	2.7±0.21/2.47/2.91	1.52±0.07/1.42/1.59	16.75±0.41/6.22/17.19
MP1017-6	Mark Point	25/10/2017	1.86	1.86±0.48/0.92/4.1	0.87±0.44/0.27/2.41	6.57±2.48/1.99/21.25	2.37±0.49/2.1/3.1	0.98±0.09/0.86/1.05	7.8±1.61/6.29/9.75
MP1017-7	Mark Point	25/10/2017	1.91	2.08±0.51/1.14/5.4	0.57±0.33/0.18/1.91	8.38±3.08/1.93/24.76	2.07±0.27/1.8/2.41	1.05±0.14/0.87/1.19	6.92±1.01/5.58/8.02
MP0118-1	Mark Point	18/01/2018	1.99	2.32±0.64/1.13/5.27	0.84±0.34/0.21/1.9	15.72±6.85/3.62/42.58	2.06±0.13/1.95/2.25	1.22±0.27/0.92/1.5	4.83±1.13/3.62/6.05
MP0118-2	Mark Point	18/01/2018	1.74	2.01±0.49/0.84/3.77	0.7±0.28/0.27/2.23	10.08±4.91/1.26/24.93	1.78±0.23/1.51/2	0.47±0.08/0.35/0.53	12.24±2.54/9.63/15.06
MP0118-3	Mark Point	18/01/2018	1.74	1.79±0.39/0.94/4.01	0.76±0.31/0.25/2.51	6.51±3.55/1.98/23.65	2.76±0.28/2.59/3.17	1.73±0.08/1.64/1.8	17.23±4.36/14.08/23.65
MP0118-4	Mark Point	18/01/2018	1.92	2.19±0.57/1.06/4.67	0.6±0.29/0.13/1.58	15.57±7.76/1.37/45.97	2.13±0.18/1.97/2.35	0.72±0.1/0.59/0.83	5.19±1.45/3.72/6.7
MP0118-5	Mark Point	18/01/2018	1.5	2.14±0.43/1.11/3.82	0.74±0.2/0.36/1.8	9.25±4.27/1.89/25.34	2.13±0.2/1.93/2.38	0.86±0.13/0.73/0.97	11.85±1.28/10.29/13.28



MP0118-6	Mark Point	18/01/2018	1.52	1.95±0.38/1.11/4.76	1.09±0.48/0.39/3.09	8.65±3.86/1.99/21.57	2.79±0.21/2.6/3.03	1.05±0.11/0.92/1.15	15.95±1.38/14.36/17.62
MP0518-1	Mark Point	3/05/2018	1.77	2.02±0.35/1.14/3.54	0.6±0.25/0.2/1.41	13.35±4.74/3.91/32.39	1.72±0.16/1.6/1.94	0.88±0.09/0.78/1	6.03±0.79/5.19/7.06
MP0518-2	Mark Point	3/05/2018	1.87	2.26±0.57/0.96/4.15	0.78±0.26/0.34/2.16	12.9±5.91/3.29/44.36	1.95±0.12/1.86/2.13	0.83±0.03/0.81/0.87	7.66±1.35/5.85/9.02
MP0518-3	Mark Point	3/05/2018	1.87	1.98±0.42/1.01/4.02	0.53±0.22/0.17/1.53	15.05±5.86/5.07/47.49	2.02±0.31/1.63/2.32	0.52±0.08/0.45/0.62	9.8±2.59/8.13/13.63
MP0518-4	Mark Point	3/05/2018	1.64	2.01±0.56/1.06/5.59	0.78±0.4/0.2/2.18	12.23±5.53/3.46/40.91	2.22±0.23/1.87/2.38	1.1±0.11/0.97/1.22	6.95±1.65/5.05/8.94
MP0518-5	Mark Point	3/05/2018	1.63	1.95±0.43/1.11/3.82	0.43±0.16/0.17/0.95	6.37±2.18/1.89/15.09	2.03±0.27/1.71/2.26	0.52±0.07/0.43/0.6	7.71±1.32/6.59/9.22
MP0518-6	Mark Point	3/05/2018	1.7	2.19±0.89/1.17/6.65	0.8±0.46/0.16/2.17	10.16±5.95/2.89/41.91	3.63±0.99/2.57/4.92	0.65±0.15/0.46/0.81	24.72±12.43/11.68/38.05
MY0317-1	Mulbin Yerrok	21/03/2017	2.09	1.74±0.29/1.19/3.05	0.37±0.12/0.21/1	6.07±2.6/1.25/12.96	2.19±0.08/2.12/2.27	0.4±0.02/0.38/0.42	10.41±0.8/9.64/11.22
MY0717-1	Mulbin Yerrok	7/07/2017	1.66	1.63±0.36/0.9/3.48	0.69±0.23/0.27/2	6.62±2.82/2.33/22.14	1.9±0.17/1.74/2.1	1.59±0.26/1.4/1.96	7.66±0.58/7.2/8.46
MY0717-2	Mulbin Yerrok	7/07/2017	1.74	1.89±0.35/1.11/4.55	0.42±0.13/0.16/0.87	7.38±1.99/3.32/16.64	1.86±0.07/1.8/1.93	0.74±0.11/0.61/0.87	5.43±0.96/4.42/6.45
MY0717-3	Mulbin Yerrok	7/07/2017	1.79	2.13±0.47/1.14/4.14	0.73±0.4/0.18/1.87	13.91±6.03/3.96/40.7	1.96±0.27/1.76/2.35	0.62±0.08/0.5/0.7	11.42±1.41/10.36/13.5
MY0717-4	Mulbin Yerrok	7/07/2017	1.53	1.85±0.4/0.91/3.4	0.72±0.37/0.18/1.89	5.49±2.07/1.81/13.52	2.01±0.46/1.47/2.6	1.26±0.19/1.04/1.49	4.43±0.41/4.07/5.02
MY0717-5	Mulbin Yerrok	7/07/2017	1.8	1.9±0.38/0.86/3.89	0.48±0.25/0.15/1.65	10.89±4.32/3.26/37.29	1.39±0.11/1.24/1.49	0.62±0.05/0.58/0.69	4.99±0.97/3.81/6.19
MY0717-6	Mulbin Yerrok	7/07/2017	1.88	2.08±0.4/1.11/3.91	0.66±0.2/0.22/1.52	10.11±4.9/2.45/32.72	1.75±0.16/1.58/1.96	1.39±0.13/1.27/1.52	4.79±0.78/4.12/5.9
MY0717-7	Mulbin Yerrok	7/07/2017	1.84	1.92±0.52/0.95/4.04	0.89±0.37/0.34/2.51	11.04±5.94/2/36.63	2.74±0.29/2.38/3.09	1.71±0.19/1.57/1.98	16.34±0.76/15.43/17.25
MY0717-8	Mulbin Yerrok	7/07/2017	1.85	2.15±0.6/0.89/5.36	0.93±0.5/0.27/2.41	12.92±6.58/2.22/47.44	3.97±1.1/2.85/5.36	1.68±0.22/1.52/2.01	29.52±4.83/25.97/36.2
MY0817-1	Mulbin Yerrok	30/08/2017	2.04	1.96±0.32/1.06/3.28	0.58±0.31/0.24/3.73	10.36±3.86/4.21/32.75	1.7±0.48/1.26/2.27	0.49±0.03/0.44/0.51	7.61±1.19/6.55/8.86

MY0817-2	Mulbin Yerrok	30/08/2017	1.79	2.33±0.69/1.1/5.35	1.13±0.69/0.12/3.36	10.76±4.88/2.02/31.27	1.78±0.13/1.69/1.98	0.81±0.09/0.71/0.92	8.44±1.22/7.47/10.13
MY0817-3	Mulbin Yerrok	30/08/2017	1.82	2.32±0.67/1.16/5.1	0.89±0.31/0.33/2.17	9.24±4.54/1.85/27.95	2.57±0.23/2.37/2.9	1.34±0.07/1.26/1.41	15.5±1.97/12.91/17.11
MY0817-4	Mulbin Yerrok	30/08/2017	1.83	2.12±0.55/0.81/3.99	0.6±0.27/0.17/1.43	8.17±3.1/2.27/18.23	3±0.57/2.32/3.61	0.68±0.06/0.63/0.76	10.57±3.03/8.75/15.08
MY0817-5	Mulbin Yerrok	30/08/2017	1.66	1.96±0.43/1/3.65	0.59±0.27/0.15/1.65	8.91±3.2/2.8/21.6	2.64±0.5/2.16/3.29	0.45±0.09/0.36/0.55	12.71±1.33/11.37/14.54
MY0817-6	Mulbin Yerrok	30/08/2017	1.65	2.21±0.59/1.11/5.6	1.03±0.37/0.32/2.72	9.83±4.67/2.17/40.11	1.58±0.22/1.32/1.82	1.16±0.19/1.04/1.45	3.62±0.2/3.34/3.79
MY1017-1	Mulbin Yerrok	25/10/2017	1.69	1.96±0.38/1.04/4.39	0.61±0.23/0.2/1.6	8.76±3.16/2.27/20.34	2.02±0.12/1.88/2.16	0.53±0.11/0.46/0.7	8.15±0.85/7/8.84
MY1017-2	Mulbin Yerrok	25/10/2017	1.6	2.2±0.51/1.23/5.53	0.97±0.32/0.38/2.24	9.01±3.22/2.04/24.75	2.12±0.45/1.71/2.73	1.06±0.09/0.96/1.18	9.49±1.06/8.33/10.48
MY1017-3	Mulbin Yerrok	25/10/2017	1.91	2.13±0.57/1.04/4.13	0.64±0.34/0.18/1.7	12.13±6.16/2.09/31.68	2.62±0.25/2.25/2.81	0.97±0.12/0.82/1.06	20.42±2.37/18.66/23.84
MY1017-4	Mulbin Yerrok	25/10/2017	1.82	2.05±0.51/1.13/5.15	0.57±0.23/0.21/1.5	8.19±3.61/2/25.03	2.2±0.39/1.94/2.79	1.12±0.28/0.84/1.5	8.13±1.21/6.98/9.5
MY1017-5	Mulbin Yerrok	25/10/2017	1.78	2.07±0.45/1.18/4.19	0.61±0.22/0.21/1.48	10.36±4.57/2.53/36.15	2.58±0.28/2.31/2.93	1.06±0.21/0.77/1.26	16.47±4.73/11.32/22.67
MY0118-1	Mulbin Yerrok	18/01/2018	1.33	2.46±0.54/1.31/4.7	0.79±0.22/0.29/1.58	11.93±4.62/57/29.86	2.36±0.32/1.97/2.76	1.14±0.11/1.04/1.25	7.74±0.7/7.15/8.56
MY0118-2	Mulbin Yerrok	18/01/2018	1.89	2.03±0.56/1.1/5.43	0.6±0.21/0.15/1.58	8.24±4.78/1.18/42.88	2.49±0.46/2.11/3.12	1.04±0.11/0.92/1.15	13.01±1.45/11.67/15.07
MY0518-1	Mulbin Yerrok	3/05/2018	2.01	1.57±0.28/0.78/2.56	0.73±0.3/0.19/1.63	4.39±1.66/0.36/10.2	1.4±0.07/1.35/1.5	0.55±0.12/0.42/0.66	4.34±0.51/3.59/4.67
MY0518-2	Mulbin Yerrok	3/05/2018	1.6	2.17±1.03/0.75/5.34	1.34±0.71/0.26/3.14	6.43±5.51/0.13/24.16	1.81±0.28/1.57/2.21	1.03±0.21/0.82/1.31	4.06±0.21/3.81/4.32
MY0518-3	Mulbin Yerrok	3/05/2018	2.04	1.82±0.44/1.07/3.52	0.6±0.34/0.2/1.61	5.56±3.74/0.95/21.31	1.94±0.29/1.61/2.24	1.4±0.17/1.23/1.58	4.25±0.7/3.42/5.06
MY0518-4	Mulbin Yerrok	3/05/2018	1.81	2.05±0.57/0.91/4.97	0.86±0.35/0.22/2.01	7.78±4.07/0.74/23.04	1.95±0.15/1.81/2.09	0.67±0.09/0.57/0.78	7.65±0.59/6.86/8.26
MY0518-5	Mulbin Yerrok	3/05/2018	2.07	2.15±0.54/1.04/3.93	0.96±0.57/0.23/3.14	9.21±4.31/1.35/27	2.37±0.11/2.28/2.54	0.8±0.21/0.55/1	9.78±2.06/7.73/11.91

MY0518-6	Mulbin Yerrok	3/05/2018	1.86	2.44±0.64/1.27/5.3	0.69±0.28/0.21/2.23	10.26±4.53/2.12/27.13	2.22±0.26/2/2.6	0.86±0.09/0.76/0.94	10.46±1.31/8.6/11.66
MY0518-7	Mulbin Yerrok	3/05/2018	1.78	2.07±0.68/1/5.46	0.95±0.54/0.24/3.05	7.78±5.56/0.17/26.37	2.11±0.16/1.99/2.33	0.71±0.02/0.68/0.72	6.9±0.63/6.4/7.79
MY0518-8	Mulbin Yerrok	3/05/2018	1.81	2.22±0.81/0.9/6.31	0.78±0.38/0.29/2.55	10.64±6.57/1.39/34.33	2.5±0.35/1.96/2.69	1.59±0.35/1.23/2.06	11.54±3.49/8.32/16.49
LP0317-1	Long Point	21/03/2017	2.17	1.86±0.53/1.09/3.61	1.04±0.59/0.29/2.46	4.92±2.34/1.63/11.53	1.27±0.07/1.22/1.37	0.37±0.04/0.34/0.42	1.95±0.31/1.63/2.35
LP0317-2	Long Point	21/03/2017	1.87	1.39±0.31/0.93/2.93	0.46±0.17/0.2/1.36	2.79±2.16/0.31/11.15	1.9±0.11/1.7/6/2.03	0.97±0.04/0.92/1.01	5.24±1.623.29/7.24
LP0317-3	Long Point	21/03/2017	1.84	1.66±0.44/1.03/3.15	0.83±0.38/0.35/1.57	3.4±1.72/0.98/10.62	2.15±0.07/2.04/2.22	1.04±0.1/0.89/1.11	10.04±0.46/9.55/10.62
LP0817-1	Long Point	30/08/2017	2.02	2.16±0.5/1/4.15	0.56±0.46/0.14/2.42	12.45±7.08/2.12/41.94	1.95±0.29/1.69/2.37	0.37±0.04/0.33/0.43	7.1±1.1/5.91/8.29
LP0817-2	Long Point	30/08/2017	2.1	1.99±0.5/1.12/4.63	0.68±0.35/0.24/1.85	9.06±3.52/2.96/30.38	2.43±0.37/2.05/2.82	1.38±0.16/1.22/1.58	11.01±0.64/10.22/11.72
LP0817-3	Long Point	30/08/2017	1.72	2±0.55/0.94/4.53	0.79±0.42/0.23/2.27	8.37±3.6/1.63/23.08	2.45±0.36/2.11/2.91	1.29±0.19/1.11/1.54	9.5±1.3/8.09/10.64
LP0817-4	Long Point	30/08/2017	2	1.7±0.37/0.97/3.26	0.48±0.26/0.12/1.54	7.27±2.61/1.74/18.5	2.53±0.54/2.07/3.17	1.05±0.11/0.96/1.15	9.39±0.52/8.87/10.05
LP0817-5	Long Point	30/08/2017	1.97	1.91±0.46/0.89/3.88	0.86±0.5/20.25/3.43	11.79±6.31/1.23/29.75	1.87±0.22/1.7/2.2	1.04±0.05/0.98/1.09	4.88±0.59/4.41/5.73
LP0817-6	Long Point	30/08/2017	1.75	1.91±0.39/0.91/3.57	0.58±0.19/0.22/1.32	7.74±2.66/2.33/19.27	2.54±0.64/2.17/3.49	0.76±0.07/0.71/0.86	10.62±0.93/9.27/11.37
LP0817-7	Long Point	30/08/2017	1.87	2.28±0.53/1.05/5.24	0.84±0.43/0.2/2.06	17.89±6.9/4.12/42.12	2.02±0.46/1.63/2.64	0.5±0.09/0.41/0.63	9.18±2.73/6.64/13.06
LP1017-1	Long Point	25/10/2017	1.86	1.72±0.33/1.12/3.18	0.71±0.5/0.19/2.33	5.54±2.09/1.15/13.5	1.6±0.14/1.4/1.72	0.56±0.05/0.51/0.62	2.94±0.42/2.41/3.29
LP1017-2	Long Point	25/10/2017	1.89	3.06±1.55/1.1/8.7	0.95±0.32/0.48/2.47	13.11±10.79/1.27/47.52	2.8±0.13/2.62/2.89	1.61±0.08/1.49/1.67	9.96±0.77/9.27/10.96
LP1017-3	Long Point	25/10/2017	1.79	2.28±0.84/1.05/6.1	0.99±0.6/0.2/3.12	10.58±6.72/1.68/35.37	2.42±0.35/2.15/2.92	1.35±0.08/1.24/1.41	7.01±2.29/4.11/9.43
LP1017-4	Long Point	25/10/2017	1.93	2.15±0.7/1.09/4.7	0.89±0.56/0.2/2.84	8.48±4.43/1.7/23.53	2.5±0.28/2.24/2.89	1.01±0.13/0.84/1.15	9.84±1.69/8.1/11.81
LP1017-5	Long Point	25/10/2017	1.92	2.19±0.67/0.96/6.9	0.64±0.36/0.17/2.15	9.17±4.77/2.23/33.76	2.47±0.29/2.05/2.66	0.67±0.03/0.64/0.71	7.37±1.18/6.51/9.05
LP1017-6	Long Point	25/10/2017	1.93	2.55±0.52/1.4/4.7	1.1±0.29/0.41/2.27	12.88±3.82/5.42/30.16	1.69±0.24/1.4/1.98	0.49±0.07/0.41/0.56	10.55±2.23/8.51/13.57
LP1017-7	Long Point	25/10/2017	1.7	1.97±0.55/1.06/4.23	0.62±0.24/0.23/1.69	8.35±3.81/1.78/19.93	1.71±0.31/1.28/2.02	1.01±0.08/0.93/1.09	6.36±1.34/4.98/8.01
LP1017-8	Long Point	25/10/2017	1.71	2.26±0.73/1.06/5.83	0.79±0.35/0.26/1.89	7±3.35/1.45/21.54	2.18±0.32/1.88/2.53	1.1±0.14/0.99/1.3	6.52±1.27/5.38/7.88
LP0118-1	Long Point	18/01/2018	1.69	2.45±0.83/1.03/5.37	0.95±0.4/0.37/3.16	7.15±3.29/0.94/16.8	2.24±0.23/2.04/2.56	1.07±0.15/0.93/1.28	7.55±1.11/6.04/8.41
LP0118-2	Long Point	18/01/2018	1.88	1.77±0.46/0.77/3.71	0.66±0.32/0.22/3.17	5.68±2.52/0.56/17.49	1.96±0.2/1.73/2.23	1.01±0.08/0.91/0.8	6.79±1.82/5.41/9.28
LP0118-3	Long Point	18/01/2018	1.36	1.91±0.42/0.99/4.08	1.21±0.77/0.27/3.94	6.04±2.08/1.7/16.32	1.57±0.06/1.52/1.64	0.7±0.03/0.66/0.73	5.1±1.09/4.14/6.05
LP0118-4	Long Point	18/01/2018	1.86	1.8±0.36/0.78/3.73	0.66±0.19/0.26/1.5	4.26±1.76/1.07/16.33	2.28±0.14/2.2/2.49	0.58±0.04/0.54/0.61	7.53±1.45/5.38/8.4

LP0118-5	Long Point	18/01/2018	1.78	1.71±0.34/0.9/3.04	0.71±0.29/0.3/2.25	4.57±1.62/1.55/12.67	2.17±0.15/2.03/2.31	1.12±0.05/1.05/1.16	6.45±0.44/5.85/6.91
LP0118-6	Long Point	18/01/2018	1.76	2.05±0.4/1.23/4.5	0.84±0.34/0.31/2.7	6.45±1.63/2.75/16.13	2.93±0.46/2.6/3.6	2.01±0.5/1.61/2.7	9.56±1.77/8.1/12.06
LP0118-7	Long Point	18/01/2018	1.73	2±0.51/1.01/4.57	0.75±0.29/0.3/2.52	6.32±2.94/1.1/17.35	1.96±0.39/1.49/2.33	0.69±0.11/0.62/0.85	7.46±1.06/6.44/8.77
LP0118-8	Long Point	18/01/2018	1.3	1.98±0.55/1.01/5.79	0.96±0.38/0.31/2.6	6.43±2.57/1.22/18.42	1.68±0.31/1.42/2.13	0.9±0.12/0.79/1.07	2.58±0.61/1.71/3.11
LP0118-9	Long Point	18/01/2018	1.83	2.48±1.28/0.86/8.03	1.05±0.47/0.38/2.75	10.7±9.11/1.24/46.93	2.29±0.14/2.17/2.46	1.19±0.26/0.84/1.41	9.3±1.4/7.62/11.02
LP0518-1	Long Point	3/05/2018	1.92	1.84±0.37/1.02/3.5	0.62±0.22/0.22/1.36	5.67±1.83/1.73/12.7	1.67±0.29/1.25/1.87	0.81±0.04/0.79/0.86	2.99±0.58/2.2/13.54
LP0518-2	Long Point	3/05/2018	1.67	1.98±0.6/0.94/6.03	0.84±0.37/0.23/2.45	5.65±2.57/0.88/16.83	1.88±0.18/1.63/2.04	0.94±0.06/0.87/1	2.06±0.33/1.76/2.51
LP0518-3	Long Point	3/05/2018	1.82	1.96±0.39/0.97/3.66	0.82±0.42/0.22/2.49	5.67±1.86/1.6/15.94	1.51±0.22/1.21/1.68	1.12±0.21/0.93/1.42	3.9±0.27/3.53/4.14
LP0518-4	Long Point	3/05/2018	1.84	1.53±0.32/0.8/2.76	0.7±0.82/0.19/10.27	3.54±1.49/0.35/10.68	1.44±0.1/1.3/1.52	1.07±0.12/0.89/1.14	2.38±1.23/0.58/3.38
LP0518-5	Long Point	3/05/2018	1.72	2.1±0.65/1.02/6.37	0.65±0.32/0.2/1.93	6.89±3.24/2.07/20.48	2.52±0.53/2.05/3.27	1.32±0.14/1.19/1.45	8.15±0.76/7.55/9.25





---

# CHAPTER 4

This chapter is published as:

Chamberlayne, B.K., Tyler, J.J., Gillanders, B.M. (2021). Controls over oxygen isotope fractionation in the waters and bivalves (*Arthritica helmsi*) of an estuarine lagoon system. *Geochemistry, Geophysics, Geosystems*, 22, e2021GC009769. <https://doi.org/10.1029/2021GC009769>

Supplementary information concerning this chapter follows the text.

---





# Statement of Authorship

Title of Paper	Controls over oxygen isotope fractionation in the waters and bivalves ( <i>Arthritica helmsi</i> ) of an estuarine lagoon system
Publication Status	<input checked="" type="checkbox"/> Published <input type="checkbox"/> Accepted for Publication <input type="checkbox"/> Submitted for Publication <input type="checkbox"/> Unpublished and Unsubmitted work written in manuscript style
Publication Details	Chamberlayne, B.K., Tyler, J.J., Gillanders, B.M. (2021). Controls over oxygen isotope fractionation in the waters and bivalves ( <i>Arthritica helmsi</i> ) of an estuarine lagoon system. <i>Geochemistry, Geophysics, Geosystems</i> , 22, e2021GC009769. <a href="https://doi.org/10.1029/2021GC009769">https://doi.org/10.1029/2021GC009769</a>

## Principal Author

Name of Principal Author (Candidate)	Briony Chamberlayne		
Contribution to the Paper	Conceptualisation, procurement and preparation of samples for analysis, statistical analysis, figure production, manuscript preparation and editing.		
Overall percentage (%)	80		
Certification:	This paper reports on original research I conducted during the period of my Higher Degree by Research candidature and is not subject to any obligations or contractual agreements with a third party that would constrain its inclusion in this thesis. I am the primary author of this paper.		
Signature		Date	20/06/2021

## Co-Author Contributions

By signing the Statement of Authorship, each author certifies that:

- i. the candidate's stated contribution to the publication is accurate (as detailed above);
- ii. permission is granted for the candidate to include the publication in the thesis; and
- iii. the sum of all co-author contributions is equal to 100% less the candidate's stated contribution.

Name of Co-Author	Jonathan Tyler		
Contribution to the Paper	Provided guidance and assistance in conceptualisation, data analysis and interpretation. Manuscript editing.		
Signature		Date	21/Jun/2021

Name of Co-Author	Bronwyn Gillanders		
Contribution to the Paper	Provided guidance and assistance in conceptualisation, data analysis and interpretation. Manuscript editing.		
Signature		Date	23 June 2021



## Controls over oxygen isotope fractionation in the waters and bivalves (*Arthritica helmsi*) of an estuarine lagoon system

### Abstract

Oxygen isotope ratios in bivalve shells have long been used as a proxy for environmental change, reflecting both temperature and the oxygen isotope composition of host water. In estuarine systems, the oxygen isotope composition of water is complicated by variable mixing between river and seawater, as well as evaporative enrichment. In addition, due to species-specific variation in temperature-dependent fractionation into bivalve carbonate, modern calibrations are necessary prior to applications in palaeoenvironmental studies. In this study, live specimens of the micromollusc *Arthritica helmsi* were collected from five sites in the Coorong Lagoon, an estuarine system at the mouth of the River Murray, Australia, on six occasions from November 2016 to May 2018. Whole shell oxygen and carbon isotope compositions ( $n = 131$ ) were measured alongside monthly temperature and oxygen and hydrogen isotope analyses of waters from the Coorong and neighbouring Lake Alexandrina ( $n = 137$ ). Oxygen and hydrogen isotope ratios in water were mostly controlled by evaporation of source waters, though a period of high river water discharge was reflected in the isotopic values of the Coorong North Lagoon. A species-specific temperature-dependent oxygen isotope fractionation equation was calibrated for *A. helmsi*:  $T (^{\circ}\text{C}) = (21.39 \pm 0.45) - (4.43 \pm 0.38) * (\delta^{18}\text{O}_{\text{shell}} - \delta^{18}\text{O}_{\text{water}})$ . This equation is similar to other published palaeotemperature equations for biogenic carbonates. These contemporary observations of the isotope hydrology of the Coorong, coupled with our contemporary calibration of oxygen isotope fractionation, lay the foundation for palaeoenvironmental studies using bivalves collected from the sediments of the Coorong.

## 1. Introduction

The use of oxygen isotope ratios in bivalves and other carbonate species as a proxy for past water temperature is a well-established technique in palaeoclimate studies (e.g. Carré et al., 2013; Crippa et al., 2016; Jones et al., 2005; Schöne et al., 2005). Following the initial works of Urey (1947) and Epstein et al. (1951), many studies have successfully reconstructed temperature, most commonly in marine species (e.g. Butler et al., 2012; Carré et al., 2013; Featherstone et al., 2020; Schöne et al., 2004; Surge et al., 2003). A number of studies have also examined isotope ratios in freshwater (e.g. Kelemen et al., 2017; Pfister et al., 2019; Roy et al., 2019; Schöne et al., 2020; Wurster and Patterson, 2001) and estuarine (e.g. Andrus and Rich, 2008; Dettman et al., 2004; Ingram et al., 1996) species, where the interpretation of bivalve oxygen and carbon isotopes can differ from marine species due to the added complexity of variable mixing of marine and river waters, plus evaporation, which lead to variable oxygen and hydrogen isotope compositions in water.

The ability to quantify temperature or salinity changes in palaeoenvironmental studies often relies on the assumption that bivalves fractionate oxygen in accordance with well-established palaeotemperature equations (Böhm et al., 2000; Epstein and Mayeda, 1953; Grossman and Ku, 1986; Kim and O'Neil, 1997). This assumption, however, does not consider the species-specific “vital effects” that are known to cause deviation from expected geochemical relationships (Owen et al., 2002). The variation among published temperature-dependent fractionation factors in bivalve studies highlights the importance of modern calibration studies. From such studies, authors have been able to validate the use of existing palaeotemperature equations (e.g. Huyghe et al., 2020; Lécuyer et al., 2004), or have been able to produce species-specific equations (e.g. Carré et al., 2005; Tynan et al., 2014; Royer et al., 2013). In addition to the potential biological effects, recent research has investigated kinetic effects on the equilibrium oxygen isotope fractionation between organic and inorganic carbonates and water (Daëron et al., 2019; Watkins et al., 2013). The effects of pH, growth rate and salinity on the carbonate-water fractionation factor have been identified in several studies (Dietzel et al., 2009; Kim et al., 2007; Zeebe, 1999) but also excluded by others (Hermoso and Lecasble, 2018; Kim et al., 2006). While there is no general scientific consensus, it is clear that the influence of biological and kinetic factors on oxygen isotope fractionation must be considered.

The oxygen isotope composition of waters are affected by several factors including the mixing of isotopically distinct inputs and subsequent modification by evaporation (Corlis et al., 2003; Epstein and Mayeda, 1953). In estuarine systems, water sources can include a complex mixture of direct precipitation, sea water, groundwater and one or more riverine inputs (e.g. Stalker et al., 2009). As such, although valuable environmental information can be gained from the

oxygen isotope composition of estuarine carbonates, it is first essential to understand the effects of mixing and evaporation on water in the contemporary system. Studies in estuaries in Texas (Laguna Bay, Galveston Bay and Mission Aransas Estuaries; Mohan and Walther, 2015), Western Australia (Shark Bay; Price et al., 2012), California (San Francisco Bay; Ingram et al., 1996) and Florida (Florida Bay; Swart and Price, 2002) have found strong linear relationships between oxygen isotope ratios and salinity despite different mixing and environmental conditions. In addition, water oxygen isotope dynamics have been successfully employed to estimate evaporation (Barrie et al., 2015; Gibson et al., 1993) and to differentiate between the sources of freshwater influxes in estuaries (Price et al., 2012; Stalker et al., 2009; Swart and Price, 2002).

This study explores the oxygen and carbon stable isotope ratios of *Arthritica helmsi* shells from the Coorong Lagoon of South Australia, alongside the oxygen and hydrogen isotope ratios of their host waters. The Coorong, at the mouth of the River Murray, is listed as a Wetland of International Significance under the Ramsar Convention (Department for Environment and Heritage, 2000), primarily for its importance for waterbird populations (Paton et al., 2009). The hydrological management of the Coorong and neighbouring Lake Alexandrina is a subject of considerable debate, with uncertainties surrounding the natural or baseline hydrological state of the estuary (Kingsford et al., 2011; Reeves et al., 2015), and the sources and pathways of polluting waters which contribute to problems of eutrophication and ecosystem damage (Mosley et al., 2014). Research to gain understanding of the past hydrological and ecological conditions of the Coorong using various biomarkers in sediments has been a recent focus (Dick et al., 2011; Gell, 2017; Haynes et al., 2007; Lower et al., 2013; Reeves et al., 2015), including the use of hydrogen isotopes from sediments (McKirby et al., 2010) and trace elemental ratios in otoliths (Disspain et al., 2011).

The sediments of the Coorong Lagoons have an abundance of bivalves, particularly *A. helmsi* (Chamberlayne, 2015), offering potential for reconstruction of past environmental change relevant to contemporary issues. Common in southern Australian estuaries (Matthews and Constable, 2004; Whisson et al., 2004; Lautenschlager et al., 2014), *A. helmsi* is an aragonitic micromollusc (Chamberlayne et al., 2020) that experiences continuous growth over a short lifespan of up to 1 year (Chamberlayne et al., 2020; Wells and Threlfall, 1982b). A monitoring study in a Western Australian estuary reported broad salinity (15 – 55) and temperature tolerances (18 – 32 °C) (Wells and Threlfall, 1982a). In the modern Coorong Lagoons, *A. helmsi* are abundant in the North Lagoon, but are not currently found living in the South Lagoon (Dittmann et al., 2019), likely due to the present hypersaline condition (> 60; Dittmann et al., 2019) falling outside the tolerance of this species (Wells and Threlfall, 1982a). A study of museum specimens has demonstrated that stable isotope analyses of *A. helmsi* shells has

potential to trace past environments, but more research is needed to better constrain the relationship between environmental change and shell chemistry (Chamberlayne et al., 2020).

To further test the reliability of *A. helmsi* as a proxy for past environmental conditions, we analysed the isotopic composition of 135 live collected specimens and their host waters. A species-specific palaeotemperature equation was developed and compared to established palaeotemperature equations. In addition, we explored the principal controls over water oxygen and hydrogen isotope variability in the Coorong Lagoon, thus laying the foundation for interpreting *A. helmsi* oxygen isotope variability as a proxy for past climate and hydrological change in this significant estuarine system.

## 2. Methods

### 2.1 Study site

The Coorong is an inverse estuary at the terminus of Australia's largest river system, the Murray Darling Basin, which drains 14% of the continent and provides water for 50% of Australia's agricultural produce (Commonwealth of Australia (Murray-Darling Basin Authority), 2020). The Coorong estuary is connected to the Murray River via Lake Alexandrina, and is separated into the North and South Lagoons which are narrowly connected at Parnka Point (Figure 1). A north-south salinity gradient, from brackish to hypersaline, has characterised the lagoon over recent decades (Geddes and Butler, 1984; Gillanders and Munro, 2012). A series of barrages erected in the 1940s control freshwater flow from the River Murray, via Lake Alexandrina and Lake Albert, into the North Lagoon which also receives marine water from the Southern Ocean via the Murray Mouth. The connectivity between the Southern Ocean and the Coorong has been maintained via dredging since 2015 (Government of South Australia, 2020). The South Lagoon receives water via the connection to the North Lagoon at Parnka Point; via the South East Drainage Network at Salt Creek; and from groundwater (Haese et al., 2008; Shao et al., 2018).

Rainfall data for the sampling period were sourced from the Australian Bureau of Meteorology's Meningie weather station (station number: 024518; BOM, 2020). Average annual rainfall at Meningie was 468 mm during the sampling period, and the mean of the annual maximum and minimum temperatures during the sampling period were 20.9 °C and 10.3 °C respectively (BOM, 2020). Weekly barrage release data were sourced from the WaterConnect website (Government of South Australia, 2020). Oxygen and hydrogen isotope compositions for local groundwater were sourced from Kell-Duivesteyn (2015) who sampled two groundwater wells adjacent to the North Lagoon.

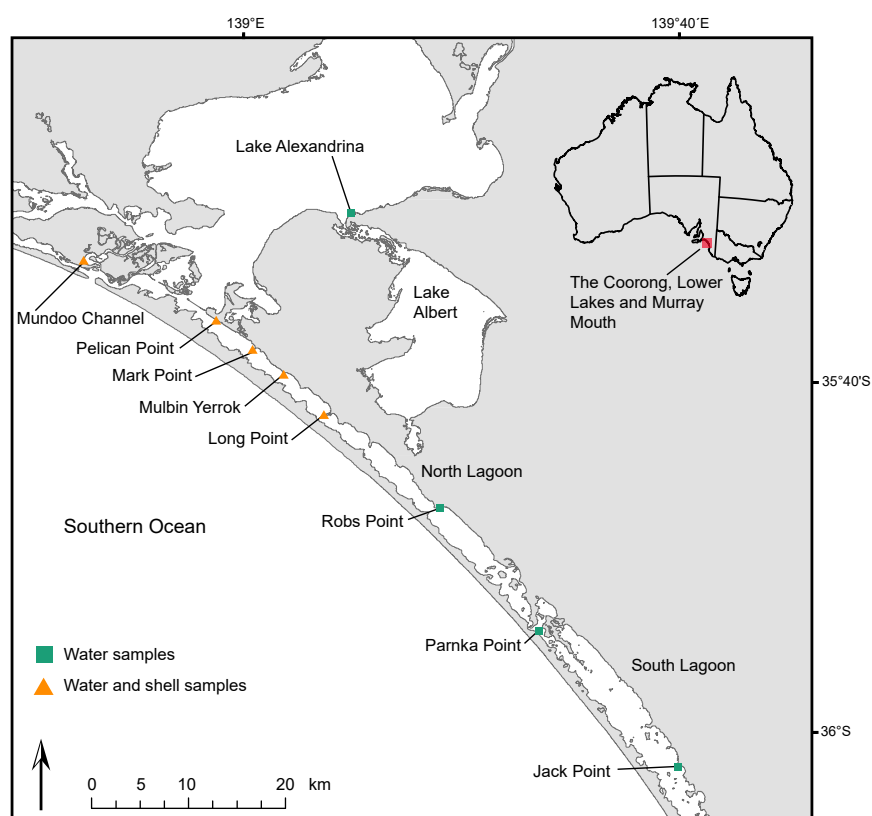


**Figure 1.** Sampling locations in Lake Alexandrina and the Coorong Lagoons at the terminus of the River Murray.

## 2.2 Water sampling and analysis

Surface waters were collected from 9 sites along Lake Alexandrina, the Coorong and Murray Mouth (Figure 1) approximately monthly from November 2016 to May 2018 (see Table S1 for collection times and locations). Water temperature and salinity was measured at each site using a Hanna Instruments HI-98194 multiparameter probe. Water samples were collected in hydrochloric acid washed 250 mL HDPE bottles with zero headspace and refrigerated until isotope analysis.

Hydrogen and oxygen isotopes in waters were determined by cavity ringdown spectroscopy using a Picarro L2130-i isotope analyser at Flinders Analytical, Flinders University. Samples were calibrated against in-house laboratory standards consisting of desalinated water ( $\delta^2\text{H} = 0.95 \text{ ‰}$ ,  $\delta^{18}\text{O} = 7.4 \text{ ‰}$ ) and bottled water ( $\delta^2\text{H} = -73.8 \text{ ‰}$ ,  $\delta^{18}\text{O} = -10.36 \text{ ‰}$ ). An Adelaide rainwater sample ( $\delta^2\text{H} = -52.1 \text{ ‰}$ ,  $\delta^{18}\text{O} = -8.49 \text{ ‰}$ ) was used as an internal laboratory quality control. Oxygen and hydrogen isotope ratios are reported relative to the Vienna Standard Mean Ocean Water (VSMOW) standard using the standard delta ( $\delta$ ) notation in parts per thousand (‰):

$$\delta = \left( \frac{R_{\text{sample}} - R_{\text{standard}}}{R_{\text{standard}}} \right) \times 1000 \quad \delta = \left( \frac{R_{\text{sample}} - R_{\text{standard}}}{R_{\text{standard}}} \right) \times 1000$$

(1)

where R is the isotope ratio ( $^{18}\text{O}/^{16}\text{O}$  or  $^2\text{H}/^1\text{H}$ ).

### 2.3 Shell sampling and analysis

Shells were collected on up to six occasions from five sites along the North Lagoon of the Coorong (Figure 1) from sediments at the sediment water interface using a 2 mm mesh sieve. In total, 135 specimens were collected (see Table S2 for details of specific collection times and locations). Each specimen was measured along its maximum growth axis using digital callipers, the length of each shell is reported in Table S2. The shells ranged from 1.30 mm to 2.77 mm in size and had an average of  $1.80 \pm 0.19$  mm. Shells were treated with an 18%  $\text{H}_2\text{O}_2$  solution, which was buffered to pH 8 using 0.5 M sodium hydroxide, to dissolve any residual organic matter, including the organic matrix within the bivalve, following the method of Falster et al. (2018). Shells were then rinsed in ultra-pure water with a resistivity of 18.2 M $\Omega$  at 25 °C and a pH of 7 and dried for 12 hours at 30 °C. Due to the small size of each shell (1.30 – 2.77 mm), one valve of each specimen was crushed to a fine powder for whole shell isotope analysis.

A sub-sample of approximately 100  $\mu\text{g}$  of crushed whole shell carbonate powder was used for stable isotope analysis. Most (121 of 135) samples were purged with helium for 150 seconds at 20ml/min and then acidified with 104% phosphoric acid and reacted at 70°C for 1 hour using a Nu Instruments GasPrep system with the resultant  $\text{CO}_2$  analysed for  $\delta^{18}\text{O}$  and  $\delta^{13}\text{C}$  with a Nu Instruments Horizon continuous flow isotope ratio mass spectrometer (IRMS). The remaining 14 samples were prepared using a Nu Instruments NuCarb system in-line connected to a Nu Instruments Perspective dual inlet IRMS. In the automated NuCarb system, samples were evacuated to high vacuum, acidified with 105% phosphoric acid at 70°C and the resultant  $\text{CO}_2$  passed through to the IRMS for  $\delta^{18}\text{O}$  and  $\delta^{13}\text{C}$  determination. Data quality for all samples were monitored using laboratory standards ANU-P3 ( $\delta^{18}\text{O} = -0.32$  ‰,  $\delta^{13}\text{C} = +2.24$  ‰), UAC-1 ( $\delta^{18}\text{O} = -18.4$  ‰,  $\delta^{13}\text{C} = -15.0$  ‰) and IAEA CO-8 ( $\delta^{18}\text{O} = -22.7$  ‰,  $\delta^{13}\text{C} = -5.76$  ‰). External reproducibility was  $\pm 0.15$  ‰ ( $1\sigma$ ) and  $\pm 0.1$  ‰ ( $1\sigma$ ) for the Nu Instruments Horizon IRMS and the Nu Instruments Perspective IRMS respectively. Data from four samples (MP0817-1, MY0717-6, MY0817-6, and LP0817-7) were rejected due to technical problems during analysis. Carbon and oxygen isotope values are reported relative to the international standard Vienna Pee Dee Belemnite (VPDB) in parts per thousand (‰) using the delta ( $\delta$ ) notation (Equation 1).

### 2.3 Estimation of shell $\delta^{18}\text{O}$

As shell  $\delta^{18}\text{O}$  and  $\delta^{13}\text{C}$  ratios were measured on the whole valve of an individual specimen of



*A. helmsi*, we interpret this composition to be representative of the integrated signal throughout the lifespan of the individual. A single study has investigated the growth rate and lifespan of *A. helmsi*, which reported a growth rate of 0.3 mm/month and lifespan of ~1 year based on specimens collected in the Peel-Harvey estuary system in Western Australia (Wells and Threlfall, 1982b). Given this uncertainty in the period of time represented by the geochemistry of each shell, we made two comparisons: first, we compared  $\delta^{18}\text{O}$  value of the shells ( $\delta^{18}\text{O}_s$ ) to the temperature and  $\delta^{18}\text{O}$  value of water ( $\delta^{18}\text{O}_w$ ) measured on the date of the collection – a scenario which would assume a short lifespan for *A. helmsi* individuals, with a relatively high population turnover. Second, we estimated the lifespan of each shell based on its size and an assumed growth rate of 0.3 mm/month as estimated by Wells and Threlfall (1982b; Table S2). Average temperature and  $\delta^{18}\text{O}_w$  values for the lifespan of each shell were then calculated to the nearest month based on this age estimation. Observed  $\delta^{18}\text{O}_s$  values were compared to estimates of  $\delta^{18}\text{O}_s$  values calculated from previously published fractionation equations. Both the temperature and  $\delta^{18}\text{O}_w$  composition measured on the date of collection, and the temperature and  $\delta^{18}\text{O}_w$  composition averaged according to the estimated lifespan, were used as parameters in the fractionation equations. Two aragonite-water fractionation equations were used: the equation from Böhm et al. (2000) who added sclerosponge data to improve the equation from Grossman and Ku (1986) which is based on data from foraminifera and gastropods:

$$T(^{\circ}\text{C}) = (20.0 \pm 0.2) - (4.42 \pm 0.10) \times (\delta^{18}\text{O}_{\text{arag./VPDB}} - \delta^{18}\text{O}_{\text{wat./VSMOW}})$$

$$T(^{\circ}\text{C}) = (20.0 \pm 0.2) - (4.42 \pm 0.10) \times (\delta^{18}\text{O}_{\text{arag./VPDB}} - \delta^{18}\text{O}_{\text{wat./VSMOW}}) \quad (2)$$

and the equation from Carré et al. (2005) which was calculated from measurements on the bivalve *Mesodesma donacium*:

$$T(^{\circ}\text{C}) = (17.41 \pm 1.15) - (3.66 \pm 0.16) \times (\delta^{18}\text{O}_{\text{arag./VPDB}} - \delta^{18}\text{O}_{\text{wat./VSMOW}})$$

$$T(^{\circ}\text{C}) = (17.41 \pm 1.15) - (3.66 \pm 0.16) \times (\delta^{18}\text{O}_{\text{arag./VPDB}} - \delta^{18}\text{O}_{\text{wat./VSMOW}}) \quad (3)$$

### 3. Results:

#### 3.1 Environmental conditions

Water temperature across the Coorong Lagoon varied seasonally (Figure 2a) with a maximum temperature of 37.9 °C measured at Pelican Point in January 2018 and a minimum temperature of 10.7 °C at Mundoo Channel in July 2017. Spatial variation in temperature across the lagoons was low as indicated by low between-site variance about the mean of all sites for each sampling date (standard error <0.8), with the exception of January 2018 where

the between-site standard error was 1.5. The volume of water released from Lake Alexandrina into the Coorong via barrage opening varied greatly over the sampling period (Figure 2b). Significant releases (>3300 GL) through the summer of 2016 were followed by a prolonged period of limited releases totalling <1100 GL for the remainder of the sampling period. The greatest monthly release was 1421 GL in November 2016, while the releases in May 2018 totalled only 8 GL. Rainfall was less seasonal than water temperature during the sampling period (Figure 2c). The lowest monthly total rainfall of 2.8 mm was recorded in March 2018,

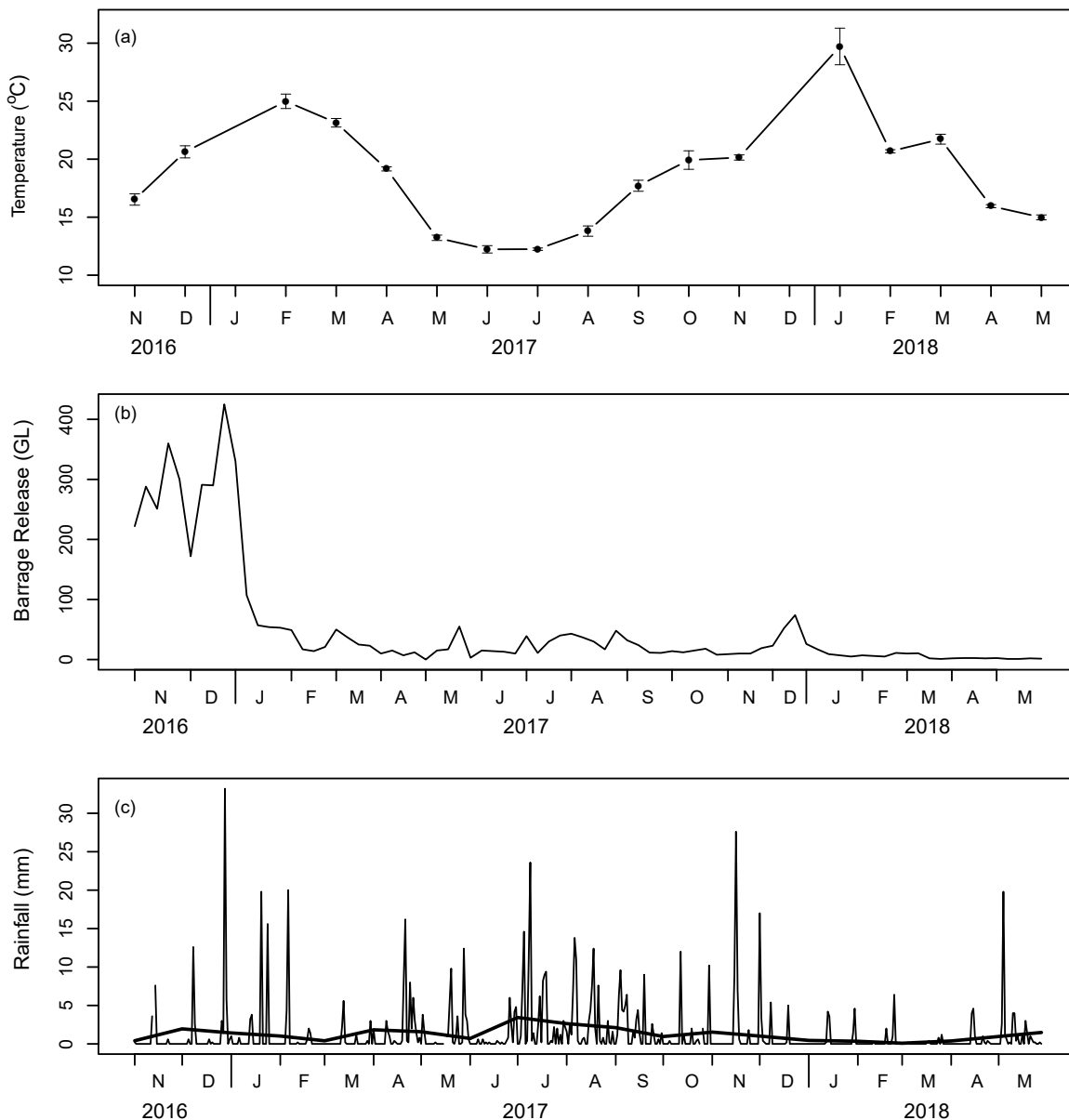


**Figure 2.** Summary of environmental data from November 2016 to May 2018. (a) Water temperature for the sampling period. The replicates were each of the 9 sampling sites. Error bars indicate  $\pm 1$  SE. (b) Weekly barrage release volumes for the sampling period. (c) Daily rainfall and average monthly rainfall for the sampling period.

while the highest monthly total was 106 mm in July 2017.

## 3.2 Water chemistry

### 3.2.1 Salinity

Salinity ranged from 0.16 in December 2016 at Mundoo Channel and Pelican Point to 89.8 in March 2018 at Jack Point (Figure 3a). Lake Alexandrina was consistently fresh ( $<0.5$ ) during the sampling period. Salinity in the North Lagoon was more variable both temporally and spatially, ranging from 0.16 – 26.7 at Pelican Point to 24 – 57.5 at Robs Point. There was no clear seasonal pattern to salinity in the North Lagoon. During November and December 2016, consistently low salinity (0.16 – 9.15) in the North Lagoon corresponded with a high discharge of freshwater from Lake Alexandrina (Figure 2b). In contrast, the South Lagoon, as indicated by data from Jack Point, experienced a seasonal range of salinity with highest values between January and May and lowest values between June and November (Figure 3a).

### 3.2.2 Oxygen and hydrogen isotopes in water

The results of isotopic analyses of waters and associated uncertainties are summarised in Table S1. In summary,  $\delta^{18}\text{O}_w$  values in the Coorong Lagoons ranged from  $-2.81$  ‰ at Pelican Point in November 2016 to  $+5.78$  ‰ at Parnka Point in January 2018 (Figure 3b).  $\delta^{18}\text{O}_w$  values in Lake Alexandrina ranged from  $-0.06$  ‰ in April 2017 to  $+2.28$  ‰ measured in March of 2018. This seasonal pattern of higher  $\delta^{18}\text{O}_w$  values during the summer months was also observed in the South Lagoon including at Jack Point where the maximum value of  $+5.54$  ‰ was recorded in February 2018 and the minimum value of  $+1.36$  ‰ was recorded in August 2017. The North Lagoon also showed a similar seasonal pattern; with the exception of November and December 2016 where values ranged between  $-2.81$  ‰ and  $+0.02$  ‰ at all sites in the North Lagoon.  $\delta^{18}\text{O}_w$  values increased with distance from the Murray River mouth and Lake Alexandrina barrages. For example, in February of 2017 water samples from Pelican Point at the northern end of the North Lagoon had a  $\delta^{18}\text{O}_w$  value of  $+1.36$  ‰ while the waters at Robs Point at the southern end of the North Lagoon were  $+5.54$  ‰ (Figure 3b).

The  $\delta^{18}\text{O}_w$  values from all Coorong Lagoon sites (excluding Lake Alexandrina) showed a linear relationship to salinity where  $\delta^{18}\text{O}_w = 0.065 \times \text{salinity} - 2.55$  ( $R^2 = 0.629$ ,  $p < 0.0001$ ; Figure 4). However the slope, intercept and coefficient of determination differed between sites, with the  $R^2$  of the regression varying between 0.20 at Pelican Point and 0.68 at Jack Point (Figure S1; Table S3). Low salinity waters from the North Lagoon collected in November and December 2016 have  $\delta^{18}\text{O}_w$  values lower than would be predicted by linear regression ( $< -1$  ‰). Water  $\delta^{18}\text{O}$  values displayed a linear relationship with water  $\delta^2\text{H}$  values, described by the relationship  $\delta^2\text{H} = 5.65 \times \delta^{18}\text{O} + 0.97$  ( $R^2 = 0.978$ ,  $p < 0.0001$ ; Figure 5). The slope of this line (5.65) differs

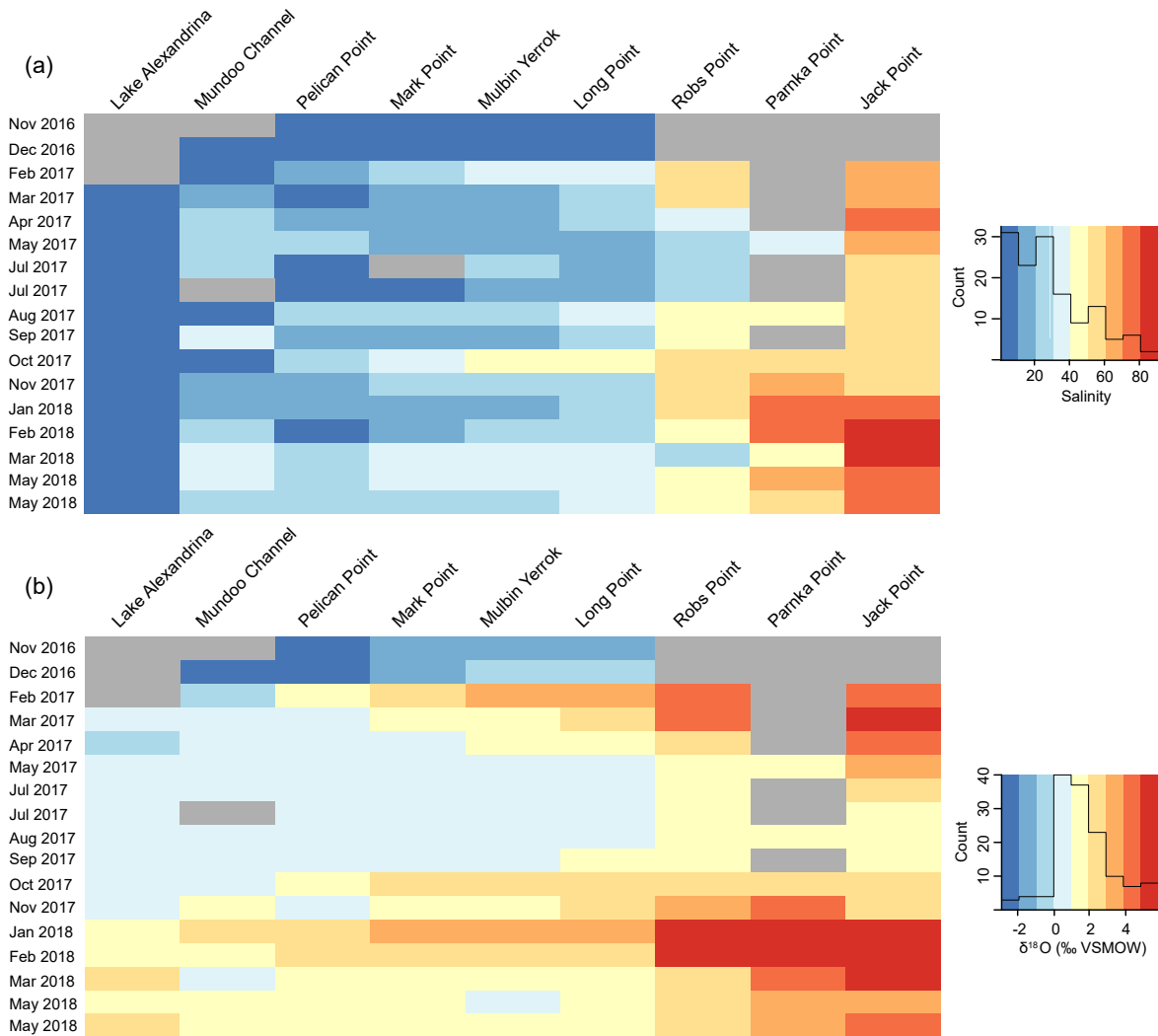


**Figure 3.** Heat maps showing water (a) salinity and (b) oxygen isotope composition of each sampling location for each sampling time. The colour key is fitted with a histogram to show the distribution of values. Grey shading indicates missing data.

from that of the Adelaide Meteoric Water Line (Adelaide MWL; slope =7.25) as defined by the isotopic composition of Adelaide rainfall sourced from the Global Network for Isotopes in Precipitation (GNIP; IAEA/WMO, 2020b). Our data are therefore consistent with a Local Evaporation Line (LEL; Gibson et al., 2016), where the LEL and Adelaide MWL intersect at  $\delta^{18}\text{O} = -4.31$  ‰,  $\delta^2\text{H} = -23.40$  ‰. The slope of the relationship between water  $\delta^{18}\text{O}$  and  $\delta^2\text{H}$  differs slightly between sampling locations varying from 4.93 at Jack Point to 6.88 at Lake Alexandrina (Table S4). A slight difference was also observed between sampling times where slopes ranged from 5.12 in May 2018 to 7.59 in September 2017 (Table S5).

The  $\delta^{18}\text{O}_w$  and  $\delta^2\text{H}_w$  value at the intercept with zero salinity varied spatially (Figure 5; Table S3). The zero-salinity  $\delta^{18}\text{O}_w$  intercept at sites from the North Lagoon ranged from  $-0.06$  to  $-0.83$  ‰

while Lake Alexandrina and Jack Point had zero-salinity intercept  $\delta^{18}\text{O}_w$  values of  $-2.86\text{‰}$  and  $-3.88\text{‰}$  respectively (Figure 5; Figure S1; Table S3). The  $\delta^2\text{H}_w$  values at the zero intercept with salinity were also markedly different at Lake Alexandrina ( $-24\text{‰}$ ) and Jack Point ( $-17.75\text{‰}$ ) than for the other sampling locations which ranged from  $-0.91$  to  $-6.9\text{‰}$  (Figure 5; Figure S2; Table S3). Combined, the  $\delta^{18}\text{O}_w$  and  $\delta^2\text{H}_w$  values of the zero intercept with salinity plot closely to the LEL, with the exception of Lake Alexandrina which instead was closely aligned with a linear regression model fitted to the Murray River data from the Global Network of Isotopes in Rivers (GNIR; IAEA/WMO, 2020a), and Jack Point which plotted closer to the Adelaide MWL (Figure 5).

### 3.3 Oxygen and carbon isotopes in shells

The  $\delta^{18}\text{O}_s$  values of all analysed whole shell samples ( $n = 131$ ) ranged from  $-0.36\text{‰}$  in shell MP0817-1 collected from Mark Point in August 2017 to  $+3.74\text{‰}$  in shell MP0518-6 collected from Mark Point in May 2018 (Table S2). The  $\delta^{13}\text{C}_s$  values of whole shell analyses ranged from  $-4.36\text{‰}$  in shell PP0817-4 collected from Pelican Point in August 2017 to  $+0.19\text{‰}$  in shell PP0518-5 collected from Pelican Point in May 2018. The correlation between  $\delta^{18}\text{O}$

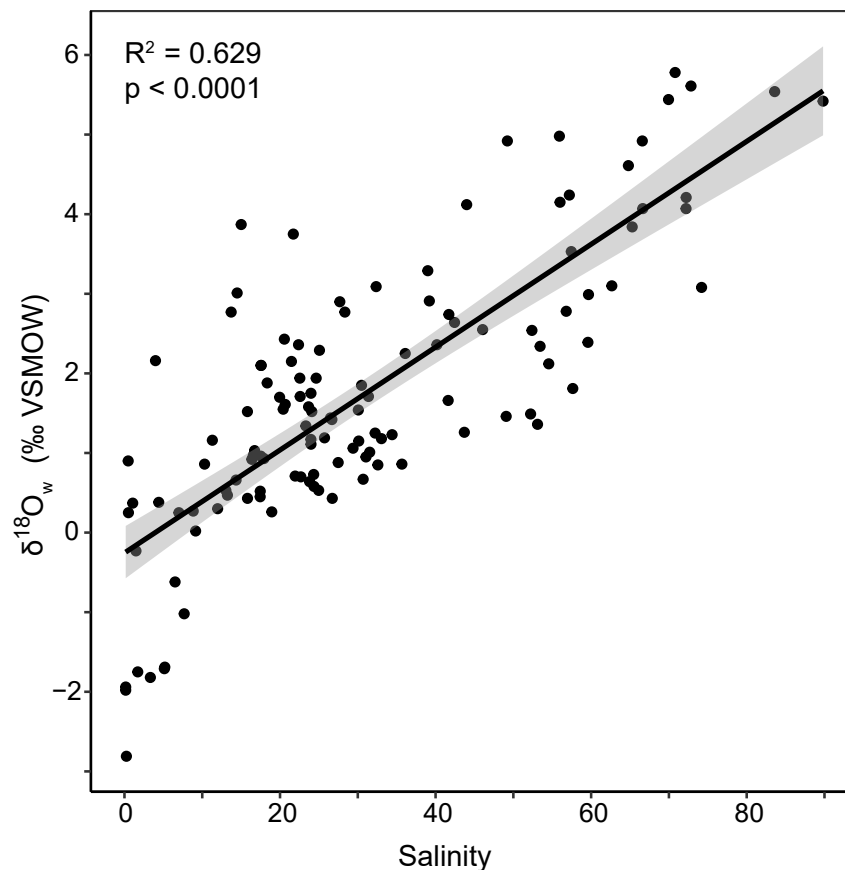


**Figure 4.**  $\delta^{18}\text{O}$  – salinity relationship for all Coorong Lagoon water samples collected between November 2016 and May 2018 with the line of best fit. The grey shaded area indicates the 95% confidence interval.

and  $\delta^{13}\text{C}$  values in shells was weak ( $R^2 = 0.293$ ,  $p < 0.0001$ ; Figure S3). One factor ANOVA determined that  $\delta^{18}\text{O}_s$  and  $\delta^{13}\text{C}_s$  values did not differ by collection season ( $F_{3,127} = 1.55$ ,  $p = 0.21$ ;  $F_{3,127} = 1.04$ ,  $p = 0.38$  respectively). However, when site was considered an additional variable in a two-factor ANOVA, the interaction between season and site had a significant effect on carbon isotope values ( $F_{11,112} = 5.57$ ,  $p < 0.001$ ). Shells from Pelican Point collected in winter and spring were found to have significantly different  $\delta^{13}\text{C}_s$  values than shells collected during summer and autumn (Figure S4).

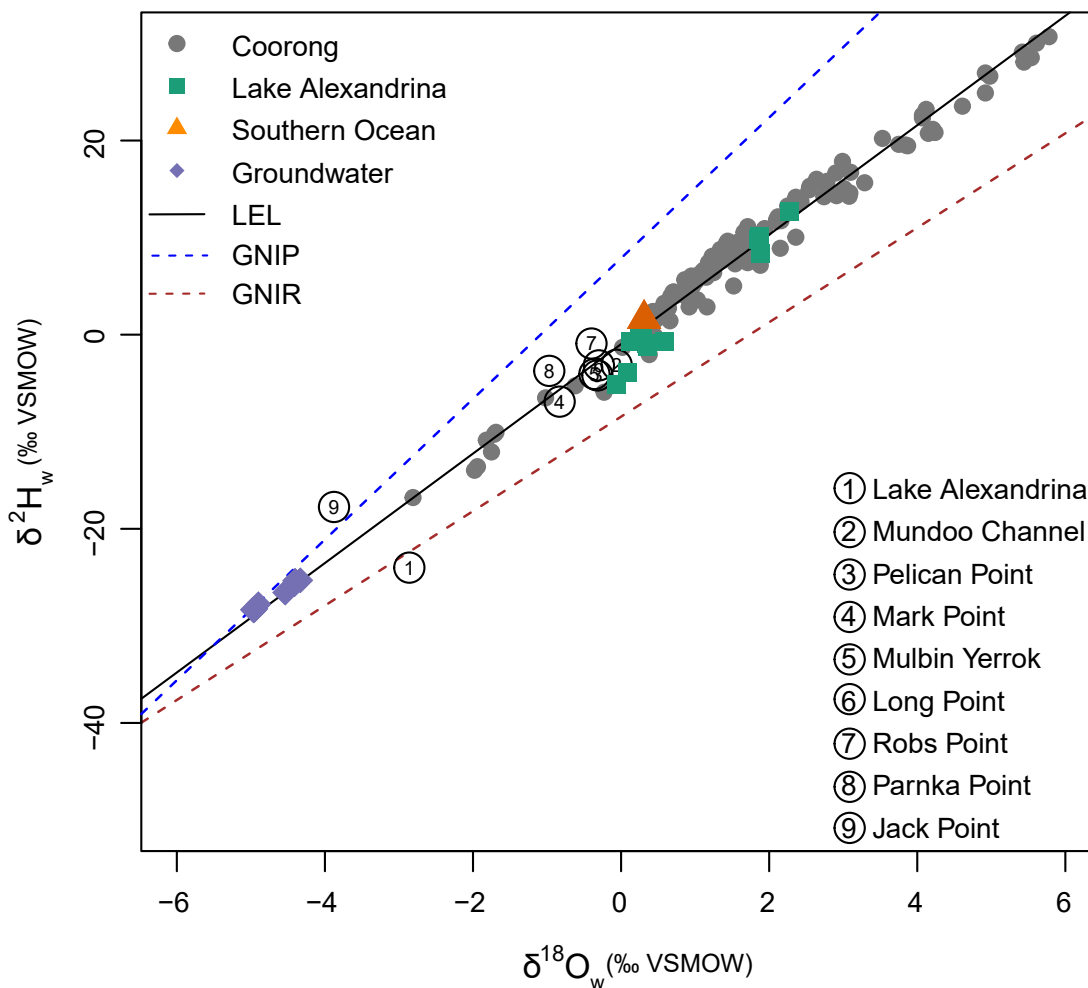


**Figure 5.** Stable isotope composition ( $\delta^{18}\text{O}$  and  $\delta^2\text{H}$ ) of waters from sampling sites in the Coorong Lagoons (grey circles) and Lake Alexandrina (green squares). Also depicted are  $\delta^{18}\text{O}$  and  $\delta^2\text{H}$  compositions for local groundwater (purple diamonds) and the Southern Ocean (orange triangle) from Kell-Duivesteyn (2015). The line of best fit through all samples from the Coorong Lagoons and Lake Alexandrina is shown (local evaporation line). The bold black line is the global meteoric water line (GMWL). Best fit lines through the  $\delta^{18}\text{O}$  and  $\delta^2\text{H}$  values of Adelaide rainfall and the Murray River are sourced from the Global Network for Isotopes in Precipitation (GNIP) and the Global Network for Isotopes in Rivers (GNIR) respectively. Also plotted are the  $\delta^{18}\text{O}$  and  $\delta^2\text{H}$  values for the intercept with zero salinity for each sampling location (numbered circles).

### 3.4 Carbonate-water fractionation factor

The carbonate-water fractionation factor ( $\delta^{18}\text{O}_{\text{s (VPDB)}} - \delta^{18}\text{O}_{\text{w (VSMOW)}}$ ;  $\sim$  epsilon) ranged from  $-2.72$  to  $+2.73$  when using the  $\delta^{18}\text{O}_{\text{w}}$  values from the day of collection and from  $-1.22$  to  $+2.80$  when using the  $\delta^{18}\text{O}_{\text{w}}$  values averaged over the estimated lifetime of each shell (Figure 6). The carbonate-water fractionation factor was linearly correlated with water temperature on the date of collection ( $R^2 = 0.509$ ,  $p < 0.0001$ ; Figure 6a) producing the following equation:  $T$  ( $^{\circ}\text{C}$ ) =  $(21.39 \pm 0.45) - (4.43 \pm 0.38) * (\delta^{18}\text{O}_{\text{shell}} - \delta^{18}\text{O}_{\text{water}})$ . The slope ( $-4.43 \pm 0.38$ ) of this linear regression was within the error of that estimated by Bohm et al. (2000; Equation 2), while the intercept ( $21.39 \pm 0.45$ ) differed slightly. The standard error for a predicted temperature value is  $\pm 5.1$   $^{\circ}\text{C}$ . In contrast, there was no relationship found between epsilon and temperature when averaged over the estimated growth period (Figure 6b).

When salinity was considered as an additional variable to temperature as determinants of the carbonate-water fractionation factor, an additional 7% of variance was explained by multiple linear regression. A significant regression equation was found ( $F=90.36$ ,  $p < 0.0001$ ) with an  $R^2$  of 0.579 and both temperature ( $p < 0.0001$ ) and salinity ( $p < 0.0001$ ) were significant predictors of fractionation. An ANOVA test demonstrated that the two part multiple linear regression model was a significant improvement upon the single variable (temperature only) model ( $F_{1,128} = 22.41$ ,  $p < 0.001$ ). Furthermore, a variance inflation factor of 1.25 for temperature and salinity indicate that the multiple linear regression model was not adversely affected by collinearity

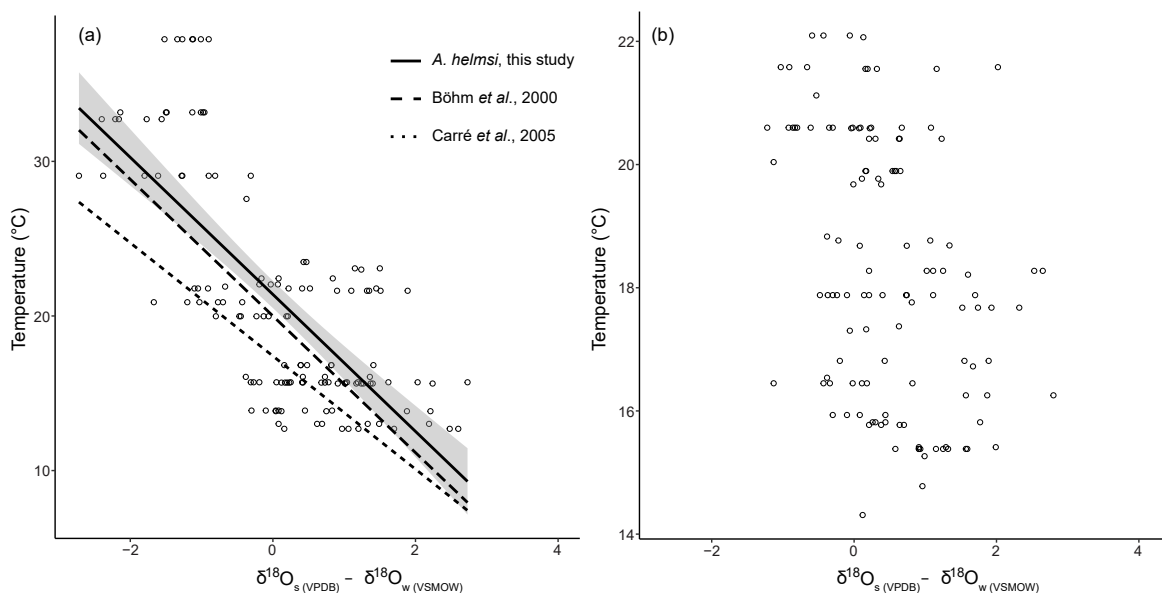


**Figure 6.** Oxygen isotope fractionation vs temperature for both (a) collection temperature and  $\delta^{18}\text{O}_{\text{w}}$  values and (b) averaged temperature and  $\delta^{18}\text{O}_{\text{w}}$  values. Included in (a) are comparisons to previous studies. The grey shaded area in (a) illustrates the 95% confidence interval for *A. helmsi*.

between predictors. The predicted carbonate-water fractionation factor from the multiple linear regression was linearly correlated to the observed carbonate-water fractionation factor ( $R^2 = 0.582$ ,  $p < 0.0001$ ; Figure 7) with a slope of 1 and importantly no obvious bias with respect to the model residuals. A multiple linear regression with pH as an additional variable to temperature found that pH was not a significant predictor ( $p = 0.74$ ) of carbonate-water fractionation.

### 3.5 Comparison of measured oxygen isotope ratios with predicted values

The measured  $\delta^{18}\text{O}_s$  values of *A. helmsi* were plotted against the  $\delta^{18}\text{O}_s$  values predicted by the equation developed in this study, as well as equations from Böhm et al. (2000; Equation 2) and Carré et al. (2005; Equation 3) in Figure 8. The predicted  $\delta^{18}\text{O}_s$  values were calculated using both the  $\delta^{18}\text{O}_w$  composition and temperature of water from the collection day and also the average values predicted over the lifetime of the shell. Figure 8 shows that there was generally overlap between measured and predicted  $\delta^{18}\text{O}_s$  values, though this pattern was inconsistent.  $\delta^{18}\text{O}$  compositions in shells from Mundoo Channel were not well reflected by the predicted  $\delta^{18}\text{O}_s$  values, while predicted and measured  $\delta^{18}\text{O}_s$  values in shells from Pelican Point showed good agreement. Predicted  $\delta^{18}\text{O}_s$  values at Pelican Point best reflected measured values when the average temperature and  $\delta^{18}\text{O}_w$  compositions were used. At Mulbin Yerrok and Long Point, there was more overlap in the predicted values calculated from collection day and averaged water parameters. An offset of 0.31 ‰ ( $\pm 0.002$  ‰) existed between  $\delta^{18}\text{O}_s$  predicted using the equation developed in this study and the equation from Böhm et al. (2000).

## 4. Discussion:

Quantifying the isotope fractionation between living bivalve shells and their surrounding water is essential for the use of carbonate oxygen isotopes in palaeoenvironmental studies. In this study, we examined oxygen isotope ratios in live specimens of the estuarine bivalve *A. helmsi* alongside the oxygen and hydrogen isotope compositions of ambient waters. Variability in the  $\delta^{18}\text{O}_w$  and  $\delta^2\text{H}_w$  values of Coorong and Lake Alexandrina waters was primarily linked to the evaporation of mixed waters, in addition to occasional large freshwater releases from the River Murray and Lake Alexandrina into the North Lagoon. A new temperature dependent fractionation equation was developed for *A. helmsi*, which was found to have a similar slope to the relationship published by Böhm et al. (2000). A relatively high amount of scatter in this relationship could be explained by uncertainties surrounding the age of the shells, or some level of disequilibrium caused by kinetic growth rate effects. Despite these uncertainties, the development of a temperature dependent of aragonite – water fractionation equation for *A. helmsi* lays the foundation for subsequent interpretation of  $\delta^{18}\text{O}_s$  values from (sub)fossil



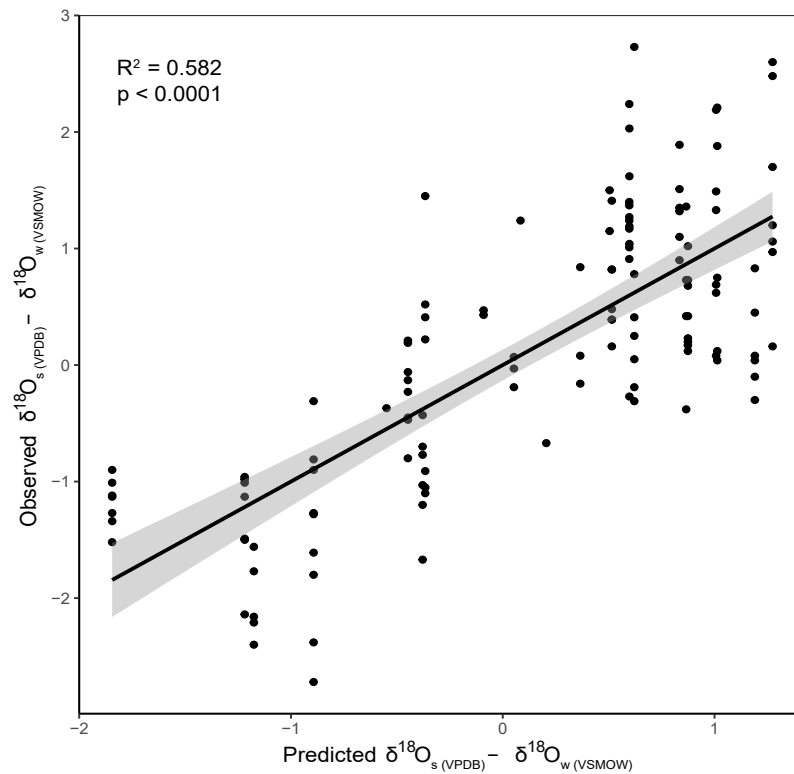


**Figure 7.** Predicted vs observed oxygen isotope fractionation in shells of *A. helmsi* collected from the Coorong Lagoon between March 2017 and May 2018. The predicted values are calculated via a multiple linear regression with temperature and salinity of the water at the time of shell collection as variables. The 1:1 line and 95% confidence interval are also illustrated.

specimens.

#### 4.1 Controls on the oxygen and hydrogen isotopes of Coorong waters

The processes that control the oxygen and hydrogen isotope composition of surface waters are well understood, with isotope ratios primarily varying as a function of evaporation and replenishment by precipitation (for comprehensive reviews see Gat, 2002; Gibson et al., 2016). However, in estuarine systems, additional complexities make interpretation of water isotope ratios more challenging, largely due to uncertainties arising from water inputs from several different sources, in addition to dynamic geomorphological variability (Cooper et al., 1997; Price et al., 2012). The Coorong and Lower Lakes system is additionally complex due to the management of river water flow through barrage structures into the Coorong. In the modern system, significant freshwater flows are only released through the barrages when Lake Alexandrina levels are high due to high River Murray discharge. During these times the  $\delta^{18}\text{O}_w$  value is expected to be lower due to the high proportion of local and headwater rainwater in the river, and due to a reduction in the water residence time, and thus evaporation, in both the river

basin and Lake Alexandrina. In contrast, during dry periods, the barrages act to accentuate the effects of evaporation by restricting the flow of freshwater into the Coorong, and waters that are released will have a higher  $\delta^{18}\text{O}_w$  value due to the reduced discharge of the river and increased evaporation. The isotopic composition of Murray River waters was not measured in this study, but Simpson and Herczeg (1991) in their study of River Murray oxygen and hydrogen ratios suggest extensive evaporative enrichment of surface waters throughout the Murray Basin. They found Lake Alexandrina to have  $\delta^{18}\text{O}_w$  values 0.6 to 4.67 ‰ higher than those measured in the Murray River at Tailem Bend in the same time period (Simpson and Herczeg 1991).

A positive linear relationship between  $\delta^{18}\text{O}_w$  values and salinity was observed in this study in agreement with previous studies in estuaries (Figure 4; Ingram et al., 1996; Price et al., 2012; Surge and Lohmann, 2002). As salinity and  $\delta^{18}\text{O}_w$  values both increase during evaporation, this relationship would be expected in estuaries which receive relatively little, or invariable influence from fluvial sources. However, the  $\delta^{18}\text{O}_w$  – salinity relationship may depart from linearity if there are variations in the composition of the freshwater endmember (Mohan and Walther, 2015; Walther and Nims, 2015). In particular, this phenomenon could explain variable  $\delta^{18}\text{O}_w$  values in the northern reaches of the Coorong (e.g. Mundoo Channel, Pelican Point), where the barrage system accentuates evaporation of low salinity waters in Lake Alexandrina, leading to a wide range of  $\delta^{18}\text{O}_w$  values at low (<5) salinity (Figure 3; Figure S1; Table S3). The  $\delta^{18}\text{O}_w$  and  $\delta^2\text{H}_w$  analyses of Coorong and Lake Alexandrina waters exhibited a LEL typical of evaporative systems (Figure 5; Gibson et al., 1993). Previous studies of estuaries in similar climates have also found that the replenishment from either fresh or marine waters is small relative to evaporation leading to consistently enriched  $\delta^{18}\text{O}_w$  values (Stalker et al., 2009; Surge and Lohmann, 2002; Walther and Nims, 2015). During the period of high barrage release in November and December 2016, the  $\delta^{18}\text{O}_w$  values in the North Lagoon from Pelican Point to Long Point ranged from  $-2.81$  to  $+0.02$  ‰, i.e. lower than average sea water (Figure 3b). The  $\delta^{18}\text{O}_w$  and  $\delta^2\text{H}_w$  of the samples from late 2016 fall between groundwater/rainwater and Lake Alexandrina waters on the LEL (Figure 5), suggesting a higher proportion of rainwater, either from the Murray River headwaters or by groundwater. Outside of this period,  $\delta^{18}\text{O}_w$  values were found to be higher than those of seawater (Figure 3b), indicating that evaporation is the primary control over water  $\delta^{18}\text{O}_w$  in the Coorong with water mixing from large freshwater releases also having an effect in the North Lagoon.

The positive linear correlations between  $\delta^{18}\text{O}_w$  values and salinity observed in this study allow the interpretation of the freshwater sources for each of the sampling locations (Price et al., 2012; Stalker et al., 2009; Swart and Price, 2002). As changes in oxygen isotope composition and salinity are both driven by evaporation, the  $\delta^{18}\text{O}_w$  value of the intercept at zero salinity can be interpreted as the  $\delta^{18}\text{O}_w$  value of the freshwater which is primarily responsible for diluting

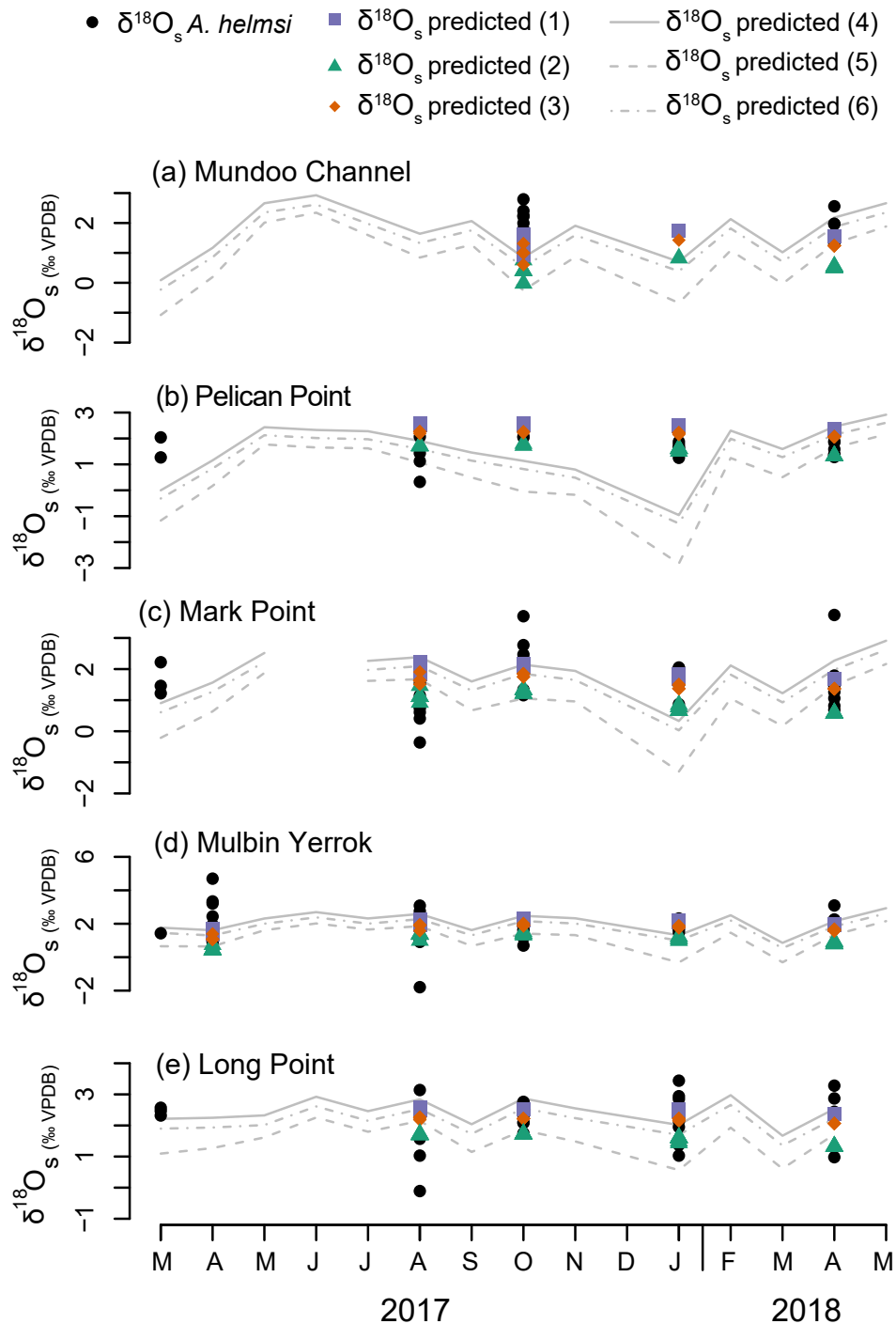


**Figure 8.** Measured  $\delta^{18}\text{O}_s$  values in *A. helmsi* and predicted  $\delta^{18}\text{O}_s$  values in aragonitic shells from each sampling location.  $\delta^{18}\text{O}_s$  values are predicted from the equations derived in this study (1 and 4), of Carré et al. (2005) (2 and 5) and Böhm et al. (2000) (3 and 6). Predicted values for 1, 2 and 3 (purple squares, orange diamonds and green triangles) were calculated using average temperature and  $\delta^{18}\text{O}_w$  values, while the predicted values for 4, 5 and 6 (solid, dashed and dot-dashed lines) were calculated using the temperature and  $\delta^{18}\text{O}_w$  values measured on the day of shell collection. Measured values are shown by solid black circles.

salinity (Swart and Price, 2002). In this study, the zero intercept values of  $\delta^{18}\text{O}_w$  and  $\delta^2\text{H}_w$  confirm that the Coorong North Lagoon is primarily diluted by Lake Alexandrina water, which in turn is sourced from Murray River water. Jack Point in the South Lagoon, however, appears to be primarily replenished by rain water, either direct upon the lagoon or transported via local runoff or groundwater (Figure 5). Groundwater seeps in the South Lagoon have previously been identified as an important source of fresh water both currently and historically (Haese et al., 2008; Kell-Duivestein 2015). These interpretations are consistent with radiogenic strontium isotope data, which suggested that North Lagoon waters represent a mixing of seawater and freshwater from Lake Alexandrina while the South Lagoon waters are sourced primarily from continental waters, consistent with local groundwater, yet extensively salinised by evaporation (Shao et al., 2018). These results also indicate that the large barrage release in late 2016 was not substantial or sustained enough to lower the salinity in the South Lagoon, in contrast to releases described in the 1980s (Geddes and Butler, 1984).

#### 4.2 Aragonite-water oxygen isotope fractionation in *A. helmsi* shells

Monitoring of  $\delta^{18}\text{O}_w$  composition and water temperature alongside shell collection allowed the development of a new species-specific temperature dependent oxygen isotope fractionation equation for *A. helmsi* for use in palaeoclimate studies. The slope of the *A. helmsi* calibration was within error of the equation produced by Böhm et al. (2000), which is largely based upon the palaeotemperature equation of Grossman and Ku (1986; Figure 6). Calibration studies of several other aragonitic bivalve species from brackish environments have also found fractionation relationships similar to that of Böhm et al. (2000; Hallmann et al., 2009; Simstich et al., 2005; Torres et al., 2011) and Grossman and Ku (1986) (Andrus and Rich, 2008; Lécuyer et al., 2004).

The inclusion of salinity in addition to temperature as a determinant of carbonate-water fractionation in *A. helmsi* explained a further 7% of variance compared to temperature alone (Figure 7). Previous studies investigating the effect of salinity on the oxygen isotope fractionation into aragonite have found no significant effect of salinity at marine salinity ranges (Kim et al., 2007). However, other authors have found a combination of temperature, salinity, precipitation rate and pH determine fractionation between aragonite and water (Wang et al., 2013). The pH of surrounding waters was not found to be a significant determinant of the carbonate-water fractionation factor in *A. helmsi*. Precipitation experiments of inorganic aragonite also found the aragonite – water fractionation factor was independent of the pH of the parent solution (Kim et al., 2006). In contrast, pH has been demonstrated to influence oxygen isotope fractionation in both inorganic (Dietzel et al., 2009; Watkins et al., 2014) and organic calcite (Zeebe, 1999). Furthermore, deviations from oxygen isotope equilibrium in

the calcitic bivalve *Pecten maximus* have been hypothesised as reflecting a difference in pH between surrounding waters and the extrapallial fluid (EPF) at the site of mineralisation (Owen et al., 2002). The chemistry of the EPF was not investigated in our study, but presents another possible explanation for deviation from equilibrium.

Uncertainties surrounding the growth rate and age of the *A. helmsi* specimens in this study could also be responsible for increased error in predicted temperatures and high scatter in the relationship between temperature and the fractionation factor. In a recent study, the oyster *Magallana gigas* was found to precipitate calcite in disequilibrium in the early stages of life, before a slowing in the growth rate in the adult phase resulted in equilibrium fractionation (Huyghe et al., 2020). These results were in agreement with the suggestion by Coplen (2007) and Daëron et al. (2019) that precipitation at isotopic equilibrium is possible only at very slow growth rates. As sections of juvenile and adult growth in *A. helmsi* could not be determined, the whole shell sampling of *A. helmsi* includes the juvenile portions and could therefore include periods of fast and variable growth which could result in isotopic disequilibrium. Furthermore, a study investigating fractionation between water and larval aragonite of the scallop, *Placopecten magellanicus*, demonstrated that those reared under “stressful” conditions (low salinity and temperature) exhibited a departure from oxygen isotope equilibrium (Owen et al., 2008). In our study, *A. helmsi* were at times exposed to conditions outside of their salinity and temperature tolerance (Wells and Threlfall, 1982a; Figure 2a; Figure 3a). Temperature extremes in particular do not appear to be well recorded in *A. helmsi* (Figure 6) in agreement with findings for other bivalve species (Schöne et al., 2006). Though a range of kinetic effects could be responsible for *A. helmsi* not reaching exact equilibrium, the similarity to the palaeotemperature equation from Böhm et al. (2000) suggests that the oxygen isotope ratios in *A. helmsi* shell aragonite can be useful as a tracer of past environmental change.

While water temperature was found to produce a significant correlation with  $\delta^{18}\text{O}_s - \delta^{18}\text{O}_w$  when applying the temperature and  $\delta^{18}\text{O}_w$  values measured on the day of shell collection, average temperature and  $\delta^{18}\text{O}_w$  values based on the estimated lifespan of the shells did not exhibit any correlation (Figure 6). *A. helmsi* do not show annual growth banding (Chamberlayne et al., 2020; Wells and Threlfall, 1982b) and were found to grow at a constant rate of 0.3 mm/month during a long term field study by Wells and Threlfall (1982b). As conditions on the date of collection produced a significant temperature relationship, the estimation of the shell lifespan may not have been robust. One potential explanation is that the shells in the Coorong population experienced a shorter lifespan and faster growth than those in the study by Wells and Threlfall (1982b), and therefore reflected the temperature and  $\delta^{18}\text{O}_w$  composition close to their collection day in their carbonate. Growth rate been shown experimentally to be affected by temperature and food availability in bivalve shells (Zhao et al., 2017). While the temperatures

recorded in the study by Wells and Threlfall (1982a; 18 - 32 °C) were similar to those recorded in this study (Figure 2a), it is possible that the nutrient rich Coorong waters (Grigg et al., 2009) contributed to higher aquatic primary productivity and thus faster bivalve growth in the Coorong population. Another potential explanation for the lack of correlation with averaged data are high variability in temperature and/or  $\delta^{18}\text{O}_w$  that was not captured by the monthly frequency of our sampling.

### 4.3 Carbon isotopes in *A. helmsi*

Changes in the carbon isotope composition of *A. helmsi* were not a major focus of this study. The processes that are thought to affect  $\delta^{13}\text{C}_s$  values include the carbon isotope composition of dissolved inorganic carbon (DIC) of water (Gillikin et al., 2006; McConnaughey and Gillikin, 2008; Owen et al., 2008; Poulain et al., 2010) and metabolic carbon incorporated through the diet of the bivalve (Gillikin et al., 2007, 2006; Lorrain et al., 2004; Poulain et al., 2010). Some authors have proposed the use of  $\delta^{13}\text{C}_s$  values as a salinity proxy in estuaries due to the relationship between salinity and the carbon isotope composition of DIC (Gillikin et al., 2006; Poulain et al., 2010). However, the  $\delta^{13}\text{C}$  values of DIC in the Coorong were not measured in this study and there was no correlation between  $\delta^{13}\text{C}_s$  values and salinity. Metabolic carbon has been estimated to contribute less than 10% to  $\delta^{13}\text{C}_s$  in deep sea molluscs (Gillikin et al., 2006; Lorrain et al., 2004; McConnaughey et al., 1997) and up to 35% in a freshwater species (Gillikin et al., 2009). In the Coorong, variability in  $\delta^{13}\text{C}$  values of particulate organic matter, which predominantly reflects phytoplankton, exhibited a strong north-south gradient, possibly in response to the mixing of marine and terrestrial carbon sources (Priestley pers. comm). This gradient, along with the north- south salinity gradient, was not reflected in the  $\delta^{13}\text{C}$  values of *A. helmsi* shells (Figure S4). Therefore, it is possible that  $\delta^{13}\text{C}$  values of *A. helmsi* shells reflect a complex interaction behind the bivalve diet and water DIC. A more detailed investigation into these processes would be an interesting avenue for future research.

## 5. Conclusions and implications for palaeoclimate studies

This study evaluated the environmental controls over oxygen and hydrogen isotope compositions of water, and oxygen isotope compositions of bivalve carbonate, in the Coorong Lagoon – an inverse estuary at the mouth of the River Murray, Australia. Variability in the oxygen and hydrogen isotope ratios of water in the Coorong is primarily affected by evaporative enrichment of  $^{18}\text{O}$  across a North-South gradient, with the majority of measured  $\delta^{18}\text{O}_w$  observations being higher than sea water. By combining  $\delta^{18}\text{O}_w$  and salinity measurements, our data suggest that

waters in the North Lagoon are primarily fed by the River Murray, whereas those in the South Lagoon exhibit a closer similarity to rainfall, presumably via direct precipitation, local runoff and groundwater. With respect to the oxygen isotope composition of the aragonitic bivalve *A. helmsi*, the similarity between the species-specific palaeotemperature equation developed in this study and the palaeotemperature equation from Böhm et al. (2000) indicate that our equation can be applied to (sub)fossil bivalve shells to infer past hydroclimate.

From the *A. helmsi* temperature dependent fractionation equation developed in this study, an increase in  $\delta^{18}\text{O}_s$  by 1 ‰ could be caused by a decrease in temperature by  $\sim 4.3$  °C or an increase in  $\delta^{18}\text{O}_w$  by 1 ‰ which is equivalent to an increase in salinity by  $\sim 15$  (Figure 4). The Coorong Lagoons have highly variable salinity and temperature annually (Figure 2a; Figure 3a) and so studies investigating  $\delta^{18}\text{O}_s$  values in the past will need to consider both changes in temperature and the isotopic composition of water as causes for carbonate isotopic shifts. Due to the short lifespan of *A. helmsi*, analysis of individual shells will likely have a seasonal bias and will only provide a limited window of temperature or water isotope variability. An approach taken to mitigate such biases in other short lived biogenic carbonates, such as ostracods, is to average several individuals from the same stratigraphic layer (e.g. Pérez et al., 2013). In addition to averaged bulk measurements providing information on long term climate trends, studies have measured the  $\delta^{18}\text{O}$  values of many individual foraminifera and ostracods to investigate the seasonal amplitude of past temperature and/or hydroclimatic change (Dixit et al., 2015; Koutavas et al., 2006). Similar approaches to the interpretation of *A. helmsi*  $\delta^{18}\text{O}$  values in palaeoenvironmental studies are recommended due to the small size and short lifespan of this species.

#### **Acknowledgements:**

The authors would like to thank Mark Rollog, Kristine Neilson and Robert Klaebe for assistance with carbonate isotopic analyses; and Daniel Jardine and Jason Young from Flinders Analytical, Flinders University, for assistance with water isotope analyses.

#### **Funding:**

This research was supported by a Sir Mark Mitchell Foundation Grant, a Lirabenda Endowment Research Grant from the Field Naturalists Society of South Australia and a Conservation Biology Grant from the Nature Conservation Society of South Australia. Funding for equipment was through an ARC LIEF grant (LE120100054).

**Data Availability Statement:**

The original data from this research is archived in the Mendeley Data repository (<http://dx.doi.org/10.17632/3fg277j4vz.1>).

**References:**

- Andrus, C.F.T., Rich, K.W., 2008. A preliminary assessment of oxygen isotope fractionation and growth increment periodicity in the estuarine clam *Rangia cuneata*. *Geo-Marine Lett.* 28, 301–308. <https://doi.org/10.1007/s00367-008-0109-3>
- Barrie, G.M., Worden, R.H., Barrie, C.D., Boyce, A.J., 2015. Extensive evaporation in a modern temperate estuary: Stable isotopic and compositional evidence. *Limnol. Oceanogr.* 60, 1241–1250. <https://doi.org/10.1002/lno.10091>
- Böhm, F., Joachimski, M.M., Dullo, W.C., Eisenhauer, A., Lehnert, H., Reitner, J., Wörheide, G., 2000. Oxygen isotope fractionation in marine aragonite of coralline sponges. *Geochim. Cosmochim. Acta* 64, 1695–1703. [https://doi.org/10.1016/S0016-7037\(99\)00408-1](https://doi.org/10.1016/S0016-7037(99)00408-1)
- BOM (Australian Bureau of Meteorology). 2020. Climate Data Online [Online]. Available at: <http://www.bom.gov.au/climate/data/>
- Butler, P.G., Wanamaker, A.D., Scourse, J.D., Richardson, C.A., Reynolds, D.J., 2012. Variability of marine climate on the North Icelandic Shelf in a 1357-year proxy archive based on growth increments in the bivalve *Arctica islandica*. *Palaeogeogr. Palaeoclimatol. Palaeoecol.* 373, 141–151. <https://doi.org/10.1016/j.palaeo.2012.01.016>
- Carré, M., Bentaleb, I., Blamart, D., Ogle, N., Cardenas, F., Zevallos, S., Kalin, R.M., Ortlieb, L., Fontugne, M., 2005. Stable isotopes and sclerochronology of the bivalve *Mesodesma donacium*: Potential application to Peruvian paleoceanographic reconstructions. *Palaeogeogr. Palaeoclimatol. Palaeoecol.* 228, 4–25. <https://doi.org/10.1016/j.palaeo.2005.03.045>
- Carré, M., Sachs, J.P., Schauer, A.J., Rodríguez, W.E., Ramos, F.C., 2013. Reconstructing El Niño-Southern Oscillation activity and ocean temperature seasonality from short-lived marine mollusk shells from Peru. *Palaeogeogr. Palaeoclimatol. Palaeoecol.* 371, 45–53. <https://doi.org/10.1016/j.palaeo.2012.12.014>
- Chamberlayne, B., 2015. Late Holocene seasonal and multicentennial hydroclimate variability in the Coorong Lagoon, South Australia: evidence from stable isotopes and trace element profiles of bivalve molluscs, honours thesis, University of Adelaide, Adelaide.
- Chamberlayne, B.K., Tyler, J.J., Gillanders, B.M., 2020. Environmental controls on the geochemistry of a short-lived bivalve in southeastern Australian estuaries. *Estuaries and Coasts* 43, 86–101. <https://doi.org/10.1007/s12237-019-00662-7>
- Commonwealth of Australia (Murray-Darling Basin Authority), 2020. About the Basin.



Available at: <https://www.mdba.gov.au/>

- Cooper, L.W., Whitley, T.E., Grebe, J.M., Weingartner, T., 1997. The nutrient, salinity, and stable oxygen isotope composition of Bering and Chukchi Seas waters in and near the Bering Strait. *J. Geophys. Res. Ocean.* 102, 12563–12573. <https://doi.org/10.1029/97JC00015>
- Coplen, T.B., 2007. Calibration of the calcite-water oxygen-isotope geothermometer at Devils Hole, Nevada, a natural laboratory. *Geochim. Cosmochim. Acta* 71, 3948–3957. <https://doi.org/10.1016/j.gca.2007.05.028>
- Corlis, N.J., Veeh, H.H., Dighton, J.C., Herczeg, A.L., 2003. Mixing and evaporation processes in an inverse estuary inferred from  $\delta^2\text{H}$  and  $\delta^{18}\text{O}$ . *Cont. Shelf Res.* 23, 835–846. [https://doi.org/10.1016/S0278-4343\(03\)00029-3](https://doi.org/10.1016/S0278-4343(03)00029-3)
- Crippa, G., Angiolini, L., Bottini, C., Erba, E., Felletti, F., Frigerio, C., Hennissen, J.A.I., Leng, M.J., Petrizzo, M.R., Raffi, I., Raineri, G., Stephenson, M.H., 2016. Seasonality fluctuations recorded in fossil bivalves during the early Pleistocene: Implications for climate change. *Palaeogeogr. Palaeoclimatol. Palaeoecol.* 446, 234–251. <https://doi.org/10.1016/j.palaeo.2016.01.029>
- Daëron, M., Drysdale, R.N., Peral, M., Huyghe, D., Blamart, D., Coplen, T.B., Lartaud, F., Zanchetta, G., 2019. Most Earth-surface calcites precipitate out of isotopic equilibrium. *Nat. Commun.* 10, 1–7. <https://doi.org/10.1038/s41467-019-08336-5>
- Department for Environment and Heritage, 2000. Coorong, and Lakes Alexandrina and Albert Ramsar Management Plan. Adelaide: South Australian Department for Environment and Heritage.
- Dettman, D.L., Flessa, K.W., Roopnarine, P.D., Schöne, B.R., Goodwin, D.H., 2004. The use of oxygen isotope variation in shells of estuarine mollusks as a quantitative record of seasonal and annual Colorado River discharge. *Geochim. Cosmochim. Acta* 68, 1253–1263. <https://doi.org/10.1016/j.gca.2003.09.008>
- Dick, J., Haynes, D., Tibby, J., Garcia, A., Gell, P., 2011. A history of aquatic plants in the Coorong, a Ramsar-listed coastal wetland, South Australia. *J. Paleolimnol.* 46, 623–635. <https://doi.org/10.1007/s10933-011-9510-4>
- Dietzel, M., Tang, J., Leis, A., Köhler, S.J., 2009. Oxygen isotopic fractionation during inorganic calcite precipitation - Effects of temperature, precipitation rate and pH. *Chem. Geol.* 268, 107–115. <https://doi.org/10.1016/j.chemgeo.2009.07.015>
- Disspain, M., Wallis, L.A., Gillanders, B.M., 2011. Developing baseline data to understand environmental change: a geochemical study of archaeological otoliths from the Coorong, South Australia. *J. Archaeol. Sci.* 38, 1842–1857. <https://doi.org/10.1016/j.jas.2011.03.027>
- Dittmann, S., Lam Gordillo, O. & Baring R. 2019. Benthic macroinvertebrate survey 2018-2019 report. Coorong, Lower Lakes and Murray Mouth Icon Site. Report for the Department for Environment and Water and the Murray-Darling Basin Authority. Flinders University, Adelaide.

- Dixit, Y., Hodell, D.A., Sinha, R., 2015. Oxygen isotope analysis of multiple, single ostracod valves as a proxy for combined variability in seasonal temperature and lake water oxygen isotopes. *J. Paleolimnol.* 53, 35–45.
- Epstein, S., Buchsbaum, R., Lownstam, H., Urey, H.C., 1951. Carbonate-water isotopic temperature scale. *Bull. Geol. Soc. Am.* 62, 417–426.
- Epstein, S., Mayeda, T., 1953. Variation of O<sup>18</sup> content of waters from natural sources. *Geochim. Cosmochim. Acta* 4, 213–224.
- Falster, G., Delean, S., Tyler, J., 2018. Hydrogen peroxide treatment of natural lake sediment prior to carbon and oxygen stable isotope analysis of calcium carbonate. *Geochemistry, Geophys. Geosystems* 1–13. <https://doi.org/10.1029/2018GC007575>
- Featherstone, A.M., Butler, P.G., Schöne, B.R., Peharda, M., Thébault, J., 2020. A 45-year sub-annual reconstruction of seawater temperature in the Bay of Brest, France, using the shell oxygen isotope composition of the bivalve *Glycymeris glycymeris*. *The Holocene* 30, 3–12. <https://doi.org/10.1177/0959683619865592>
- Gat, J.R., 2002. Oxygen and Hydrogen Isotopes in the Hydrologic Cycle. *Annu. Rev. Earth Planet. Sci.* 24, 225–262. <https://doi.org/10.1146/annurev.earth.24.1.225>
- Geddes, M.C., Butler, A., 1984. Physicochemical and biological studies on the Coorong Lagoons, South Australia, and the effect of salinity on the distribution of the macrobenthos. *Trans. R. Soc. South Aust.* 108, 51–62.
- Gell, P.A., 2017. Paleolimnological History of the Coorong: Identifying the natural ecological character of a Ramsar wetland in crisis, in: Weckström, K., Saunders, K.M., Gell, P.A., Skilbeck, C.G., *Applications of Paleoenvironmental Techniques in Estuarine Studies*. Springer Netherlands, Dordrecht, pp. 587–613. [https://doi.org/10.1007/978-94-024-0990-1\\_23](https://doi.org/10.1007/978-94-024-0990-1_23)
- Gibson, J.J., Birks, S.J., Yi, Y., 2016. Stable isotope mass balance of lakes: A contemporary perspective. *Quat. Sci. Rev.* 131, 316–328. <https://doi.org/10.1016/j.quascirev.2015.04.013>
- Gibson, J.J., Edwards, T.W.D., Bursley, G.G., Prowse, T.D., 1993. Estimating evaporation using stable isotopes: quantitative results and sensitivity analysis for two catchments in northern Canada. *Nord. Hydrol.* 24, 79–94. <https://doi.org/10.2166/nh.1993.0015>
- Gillanders, B.M., Munro, A.R., 2012. Hypersaline waters pose new challenges for reconstructing environmental histories of fish based on otolith chemistry. *Limnol. Oceanogr.* 57, 1136–1148. <https://doi.org/10.4319/lo.2012.57.4.1136>
- Gillikin, D.P., Hutchinson, K.A., Kumai, Y., 2009. Ontogenic increase of metabolic carbon in freshwater mussel shells (*Pyganodon cataracta*). *J. Geophys. Res. Biogeosciences* 114, 1–6. <https://doi.org/10.1029/2008JG000829>
- Gillikin, D.P., Lorrain, A., Bouillon, S., Willenz, P., Dehairs, F., 2006. Stable carbon isotopic composition of *Mytilus edulis* shells: relation to metabolism, salinity,  $\delta^{13}\text{C}_{\text{DIC}}$  and phytoplankton. *Org. Geochem.* 37, 1371–1382. <https://doi.org/10.1016/j.orggeochem.2006.03.008>

- Gillikin, D.P., Lorrain, A., Meng, L., Dehairs, F., 2007. A large metabolic carbon contribution to the  $\delta^{13}\text{C}$  record in marine aragonitic bivalve shells. *Geochim. Cosmochim. Acta* 71, 2936–2946. <https://doi.org/10.1016/j.gca.2007.04.003>
- Government of South Australia,. 2020. River Murray flow report (Department for Environment and Water, South Australia). Available at: <https://www.waterconnect.sa.gov.au/Pages/Home.aspx>
- Grigg, N.J., Robson, B.J., Webster, I.T., Ford, P.W., 2009. Water for a healthy country nutrient budgets and biogeochemical modelling of the Coorong. CSIRO: Water for a Healthy Country National Research Flagship
- Grossman, E.L., Ku, T.L., 1986. Oxygen and carbon isotope fractionation in biogenic aragonite: Temperature effects. *Chem. Geol.* 59, 59–74. [https://doi.org/10.1016/0168-9622\(86\)90057-6](https://doi.org/10.1016/0168-9622(86)90057-6)
- Haese, R.R., Gow, L., Wallace, L., Brodie, R.S., 2008. Identifying groundwater discharge in the Coorong (South Australia). *AusGeo News* 1–6.
- Hallmann, N., Burchell, M., Schöne, B.R., Irvine, G. V., Maxwell, D., 2009. High-resolution sclerochronological analysis of the bivalve mollusk *Saxidomus gigantea* from Alaska and British Columbia: techniques for revealing environmental archives and archaeological seasonality. *J. Archaeol. Sci.* 36, 2353–2364. <https://doi.org/10.1016/j.jas.2009.06.018>
- Haynes, D., Gell, P., Tibby, J., Hancock, G., Goonan, P., 2007. Against the tide: The freshening of naturally saline coastal lakes, southeastern South Australia. *Hydrobiologia* 591, 165–183. <https://doi.org/10.1007/s10750-007-0802-7>
- Hermoso, M., Lecasble, M., 2018. The effect of salinity on the biogeochemistry of the coccolithophores with implications for coccolith-based isotopic proxies. *Biogeosciences* 15, 6761–6772.
- Huyghe, D., Emmanuel, L., de Rafelis, M., Renard, M., Ropert, M., Labourdette, N., Lartaud, F., 2020. Oxygen isotope disequilibrium in the juvenile portion of oyster shells biases seawater temperature reconstructions. *Estuar. Coast. Shelf Sci.* 240, 106777. <https://doi.org/10.1016/j.ecss.2020.106777>
- IAEA/WMO (2020a). Global Network of Isotopes in Precipitation. The GNIP Database. Accessible at: <https://nucleus.iaea.org/wiser>
- IAEA (2020b). Global Network of Isotopes in Rivers. The GNIR Database. Accessible at: <https://nucleus.iaea.org/wiser>
- Ingram, B.L., Conrad, M.E., Ingle, J.C., 1996. Stable isotope and salinity systematics in estuarine waters and carbonates: San Francisco Bay. *Geochim. Cosmochim. Acta* 60, 455–467. [https://doi.org/10.1016/0016-7037\(95\)00398-3](https://doi.org/10.1016/0016-7037(95)00398-3)
- Jones, D.S., Quitmyer, I.R., Andrus, C.F.T., 2005. Oxygen isotopic evidence for greater seasonality in Holocene shells of *Donax variabilis* from Florida. *Palaeogeogr. Palaeoclimatol. Palaeoecol.* 228, 96–108. <https://doi.org/10.1016/j.palaeo.2005.03.046>
- Kelemen, Z., Gillikin, D.P., Graniero, L.E., Havel, H., Darchambeau, F., Borges, A. V., Yambélé,

- A., Bassirou, A., Bouillon, S., 2017. Calibration of hydroclimate proxies in freshwater bivalve shells from Central and West Africa. *Geochim. Cosmochim. Acta* 208, 41–62. <https://doi.org/10.1016/j.gca.2017.03.025>
- Kell-Duivesteyn, I., 2015. Tracing the groundwater inputs and water-mass mixing in the Coorong lagoons (South Australia) using strontium isotopes, honours thesis, University of Adelaide, Adelaide.
- Kim, S.-T., Hillaire-Marcel, C., Mucci, A., 2006. Mechanisms of equilibrium and kinetic oxygen isotope effects in synthetic aragonite at 25°C. *Geochim. Cosmochim. Acta* 70, A318. <https://doi.org/10.1016/j.gca.2006.06.643>
- Kim, S.-T., O’Neil, J.R., 1997. Equilibrium and nonequilibrium oxygen isotope effects in synthetic carbonates. *Geochim. Cosmochim. Acta* 61, 3461–3475. [https://doi.org/10.1016/S0016-7037\(97\)00169-5](https://doi.org/10.1016/S0016-7037(97)00169-5)
- Kim, S.T., O’Neil, J.R., Hillaire-Marcel, C., Mucci, A., 2007. Oxygen isotope fractionation between synthetic aragonite and water: Influence of temperature and Mg<sup>2+</sup> concentration. *Geochim. Cosmochim. Acta* 71, 4704–4715. <https://doi.org/10.1016/j.gca.2007.04.019>
- Kingsford, R.T., Walker, K.F., Lester, R.E., Young, W.J., Fairweather, P.G., Sammut, J., Geddes, M.C., 2011. A Ramsar wetland in crisis the Coorong, lower lakes and Murray mouth, Australia. *Mar. Freshw. Res.* 62, 255–265. <https://doi.org/10.1071/MF09315>
- Koutavas, A., DeMenocal, P.B., Olive, G.C., Lynch-Stieglitz, J., 2006. Mid-Holocene El Niño–Southern Oscillation (ENSO) attenuation revealed by individual foraminifera in eastern tropical Pacific sediments. *Geology* 34, 993–996. <https://doi.org/10.1130/G22810A.1>
- Lautenschlager, A. D., Matthews, T. G., & Quinn, G. P. (2014). Utilization of organic matter by invertebrates along an estuarine gradient in an intermittently open estuary. *Estuarine, Coastal and Shelf Science*, 149, 232–243. <https://doi.org/10.1016/j.ecss.2014.08.020>
- Lécuyer, C., Reynard, B., Martineau, F., 2004. Stable isotope fractionation between mollusc shells and marine waters from Martinique Island. *Chem. Geol.* 213, 293–305. <https://doi.org/10.1016/j.chemgeo.2004.02.001>
- Lorrain, A., Paulet, Y.M., Chauvaud, L., Dunbar, R., Mucciarone, D., Fontugne, M., 2004. δ<sup>13</sup>C variation in scallop shells: Increasing metabolic carbon contribution with body size? *Geochim. Cosmochim. Acta* 68, 3509–3519. <https://doi.org/10.1016/j.gca.2004.01.025>
- Lower, C.S., Cann, J.H., Haynes, D., 2013. Microfossil evidence for salinity events in the Holocene Coorong Lagoon, South Australia. *Aust. J. Earth Sci.* 60, 573–587. <https://doi.org/10.1080/08120099.2013.823112>
- Matthews, T. G., & Constable, A. J. (2004). Effect of flooding on estuarine bivalve populations near the mouth of the Hopkins River, Victoria, Australia. *Journal of the Marine Biological Association of the United Kingdom*, 84, 633–639.
- McConnaughey, T.A., Burdett, J., Whelan, J.F., Paull, C.K., 1997. Carbon isotopes in biological carbonates: Respiration and photosynthesis. *Geochim. Cosmochim. Acta* 61, 611–622. [https://doi.org/10.1016/S0016-7037\(96\)00361-4](https://doi.org/10.1016/S0016-7037(96)00361-4)

- McConnaughey, T.A., Gillikin, D.P., 2008. Carbon isotopes in mollusk shell carbonates. *Geo-Marine Lett.* 28, 287–299. <https://doi.org/10.1007/s00367-008-0116-4>
- McKirdy, D.M., Thorpe, C.S., Haynes, D.E., Grice, K., Krull, E., Halverson, G.P., Webster, L.J., 2010. The biogeochemical evolution of the Coorong during the mid- to late Holocene: An elemental, isotopic and biomarker perspective. *Org. Geochem.* 41, 96–110.
- Mohan, J.A., Walther, B.D., 2015. Spatiotemporal variation of trace elements and stable isotopes in subtropical estuaries: II. Regional, local, and seasonal salinity-element relationships. *Estuaries and Coasts* 38, 769–781. <https://doi.org/10.1007/s12237-014-9876-4>
- Mosley, L.M., Fitzpatrick, R.W., Palmer, D., Leyden, E., Shand, P., 2014. Changes in acidity and metal geochemistry in soils, groundwater, drain and river water in the Lower Murray River after a severe drought. *Sci. Total Environ.* 485–486, 281–291. <https://doi.org/10.1016/j.scitotenv.2014.03.063>
- Owen, E.F., Wanamaker, A.D., Feindel, S.C., Schöne, B.R., Rawson, P.D., 2008. Stable carbon and oxygen isotope fractionation in bivalve (*Placocopecten magellanicus*) larval aragonite. *Geochim. Cosmochim. Acta* 72, 4687–4698. <https://doi.org/10.1016/j.gca.2008.06.029>
- Owen, R., Kennedy, H., Richardson, C., 2002. Experimental investigation into partitioning of stable isotopes between scallop (*Pecten maximus*) shell calcite and sea water. *Palaeogeogr. Palaeoclimatol. Palaeoecol.* 185, 163–174. [https://doi.org/10.1016/S0031-0182\(02\)00297-3](https://doi.org/10.1016/S0031-0182(02)00297-3)
- Paton, D.C., Rogers, D.J., Hill, B.M., Bailey, C.P., Ziembicki, M., 2009. Temporal changes to spatially stratified waterbird communities of the Coorong, South Australia: Implications for the management of heterogenous wetlands. *Anim. Conserv.* 12, 408–417. <https://doi.org/10.1111/j.1469-1795.2009.00264.x>
- Pérez, L., Curtis, J., Brenner, M., Hodell, D., Escobar, J., Lozano, S., Schwal, A., 2013. Stable isotope values ( $\delta^{18}\text{O}$  &  $\delta^{13}\text{C}$ ) of multiple ostracode species in a large neotropical lake as indicators of past changes in hydrology. *Quat. Sci. Rev.* 66, 96–111. <https://doi.org/10.1016/j.quascirev.2012.10.044>
- Pfister, L., Grave, C., Beisel, J.N., McDonnell, J.J., 2019. A global assessment of freshwater mollusk shell oxygen isotope signatures and their relation to precipitation and stream water. *Sci. Rep.* 9, 1–6. <https://doi.org/10.1038/s41598-019-40369-0>
- Poulain, C., Lorrain, A., Mas, R., Gillikin, D.P., Dehairs, F., Robert, R., Paulet, Y.M., 2010. Experimental shift of diet and DIC stable carbon isotopes: Influence on shell  $\delta^{13}\text{C}$  values in the Manila clam *Ruditapes philippinarum*. *Chem. Geol.* 272, 75–82. <https://doi.org/10.1016/j.chemgeo.2010.02.006>
- Price, R.M., Skrzypek, G., Grierson, P.F., Swart, P.K., Fourqurean, J.W., 2012. The use of stable isotopes of oxygen and hydrogen to identify water sources in two hypersaline estuaries with different hydrologic regimes. *Mar. Freshw. Res.* 63, 952–966. <https://doi.org/10.1071/MF12042>
- Reeves, J.M., Haynes, D., García, A., Gell, P.A., 2015. Hydrological change in the Coorong estuary, Australia, past and present: Evidence from fossil invertebrate and algal assemblages.

- Estuaries and Coasts 38, 2101–2116. <https://doi.org/10.1007/s12237-014-9920-4>
- Roy, R., Wang, Y., Jiang, S., 2019. Growth pattern and oxygen isotopic systematics of modern freshwater mollusks along an elevation transect: Implications for paleoclimate reconstruction. *Palaeogeogr. Palaeoclimatol. Palaeoecol.* 532, 109243. <https://doi.org/10.1016/j.palaeo.2019.109243>
- Royer, C., Thébault, J., Chauvaud, L., Olivier, F., 2013. Structural analysis and paleoenvironmental potential of dog cockle shells (*Glycymeris glycymeris*) in Brittany, northwest France. *Palaeogeogr. Palaeoclimatol. Palaeoecol.* 373, 123–132. <https://doi.org/10.1016/j.palaeo.2012.01.033>
- Schöne, B.R., Freyre Castro, A.D., Fiebig, J., Houk, S.D., Oschmann, W., Kröncke, I., 2004. Sea surface water temperatures over the period 1884–1983 reconstructed from oxygen isotope ratios of a bivalve mollusk shell (*Arctica islandica*, southern North Sea). *Palaeogeogr. Palaeoclimatol. Palaeoecol.* 212, 215–232. <https://doi.org/10.1016/j.palaeo.2004.05.024>
- Schöne, B.R., Meret, A.E., Baier, S.M., Fiebig, J., Esper, J., McDonnell, J., Pfister, L., 2020. Freshwater pearl mussels from northern Sweden serve as long-term, high-resolution stream water isotope recorders. *Hydrol. Earth Syst. Sci.* 24, 673–696. <https://doi.org/10.5194/hess-24-673-2020>
- Schöne, B.R., Pfeiffer, M., Pohlmann, T., Siegismund, F., 2005. A seasonally resolved bottom-water temperature record for the period AD 1866–2002 based on shells of *Arctica islandica* (Mollusca, North Sea). *Int. J. Climatol.* 25, 947–962. <https://doi.org/10.1002/joc.1174>
- Schöne, B.R., Rodland, D.L., Fiebig, J., Oschmann, W., Goodwin, D., Flessa, K.W., Dettman, D., 2006. reliability of multitaxon, multiproxy reconstructions of environmental conditions from accretionary biogenic skeletons. *J. Geol.* 114, 267–285. <https://doi.org/10.1086/501219>
- Shao, Y., Farkaš, J., Holmden, C., Mosley, L., Kell-Duivesteyn, I., Izzo, C., Reis-Santos, P., Tyler, J., Törber, P., Frýda, J., Taylor, H., Haynes, D., Tibby, J., Gillanders, B.M., 2018. Calcium and strontium isotope systematics in the lagoon-estuarine environments of South Australia: Implications for water source mixing, carbonate fluxes and fish migration. *Geochim. Cosmochim. Acta* 239, 90–108. <https://doi.org/10.1016/j.gca.2018.07.036>
- Simpson, H.J., Herczeg, A.L., 1991. Stable Isotopes as an Indicator of Evaporation in the River Murray, Australia. *Water Resour. Res.* 27, 1925–1935.
- Simstich, J., Harms, I., Karcher, M.J., Erlenkeuser, H., Stanovoy, V., Kodina, L., Bauch, D., Spielhagen, R.F., 2005. Recent freshening in the Kara Sea (Siberia) recorded by stable isotopes in Arctic bivalve shells. *J. Geophys. Res. C Ocean.* 110, 1–11. <https://doi.org/10.1029/2004JC002722>
- Stalker, J.C., Price, R.M., Swart, P.K., 2009. Determining spatial and temporal inputs of freshwater, including submarine groundwater discharge, to a subtropical estuary using geochemical tracers, Biscayne Bay, South Florida. *Estuaries and Coasts* 32, 694–708. <https://doi.org/10.1007/s12237-009-9155-y>
- Surge, D.M., Lohmann, K.C., 2002. Temporal and spatial differences in salinity and water

- chemistry in SW Florida estuaries: Effects of human-impacted watersheds. *Estuaries* 25, 393–408. <https://doi.org/10.1007/BF02695982>
- Surge, D.M., Lohmann, K.C., Goodfriend, G.A., 2003. Reconstructing estuarine conditions: Oyster shells as recorders of environmental change, Southwest Florida. *Estuar. Coast. Shelf Sci.* 57, 737–756. [https://doi.org/10.1016/S0272-7714\(02\)00370-0](https://doi.org/10.1016/S0272-7714(02)00370-0)
- Swart, P.K., Price, R., 2002. Origin of salinity variations in Florida Bay. *Limnol. Oceanogr.* 47, 1234–1241. <https://doi.org/10.4319/lo.2002.47.4.1234>
- Torres, M.E., Zima, D., Falkner, K.K., McDonald, R.W., O'Brien, M., Schöne, B.R., Siferd, T., 2011. Hydrographic Changes in Nares Strait (Canadian Arctic Archipelago) in Recent Decades Based on  $\delta^{18}\text{O}$  Profiles of Bivalve Shells. *Arctic*, 64, 45–58.
- Tynan, S., Dutton, A., Eggins, S., Opdyke, B., 2014. Oxygen isotope records of the Australian flat oyster (*Ostrea angasi*) as a potential temperature archive. *Marine Geology*, 357, 195–209. <https://doi.org/10.1016/j.margeo.2014.07.009>
- Urey, H.C., 1947. The thermodynamic properties of isotopic substances. *J. Chem. Soc.* 562–581.
- Walther, B.D., Nims, M.K., 2015. Spatiotemporal variation of trace elements and stable isotopes in subtropical estuaries: I. Freshwater endmembers and mixing curves. *Estuaries and Coasts* 38, 754–768. <https://doi.org/10.1007/s12237-014-9881-7>
- Wang, Z., Gaetani, G., Liu, C., Cohen, A., 2013. Oxygen isotope fractionation between aragonite and seawater: Developing a novel kinetic oxygen isotope fractionation model. *Geochim. Cosmochim. Acta* 117, 232–251. <https://doi.org/10.1016/j.gca.2013.04.025>
- Watkins, J.M., Hunt, J.D., Ryerson, F.J., DePaolo, D.J., 2014. The influence of temperature, pH, and growth rate on the  $\delta^{18}\text{O}$  composition of inorganically precipitated calcite. *Earth Planet. Sci. Lett.* 404, 332–343. <https://doi.org/10.1016/j.epsl.2014.07.036>
- Watkins, J.M., Nielsen, L.C., Ryerson, F.J., Depaolo, D.J., 2013. The influence of kinetics on the oxygen isotope composition of calcium carbonate. *Earth Planet. Sci. Lett.* 375, 349–360. <https://doi.org/10.1016/j.epsl.2013.05.054>
- Wells, F.E., Threlfall, T.J., 1982a. Salinity and temperature tolerance of *Hydrococcus brazieri* (T. Woods, 1876) and *Arthritica semen* (Menke, 1843) from the Peel-Harvey estuarine system, Western Australia. *J. Malacol. Soc. Aust.* 5, 151–156.
- Wells, F.E., Threlfall, T.J., 1982b. Density fluctuations, growth and dry tissue production of *Hydrococcus Brazieri* (Tenison Woods, 1876) and *Arthritica semen* (Menke, 1843) in Peel Inlet, Western Australia. *J. Molluscan Stud.* 48, 310–320.
- Whisson, C. S., Wells, F. E., & Rose, T. (2004). The benthic invertebrate fauna of the Peel-Harvey Estuary of south-western Australia after completion of the Dawesville Channel. *Records of the Western Australian Museum*, 22, 81–90.
- Wurster, C.M., Patterson, W.P., 2001. Seasonal variation in stable oxygen and carbon isotope values recovered from modern lacustrine freshwater molluscs: Paleoclimatological

implications for sub-weekly temperature records. *J. Paleolimnol.* 26, 205–218. <https://doi.org/10.1023/A:1011194011250>

Zeebe, R., 1999. An explanation of the effect of seawater carbonate concentration on foraminiferal oxygen isotopes. *Geochim. Cosmochim. Acta* 63, 2001–2007.

Zhao, L., Schöne, B.R., Mertz-Kraus, R., 2017. Controls on strontium and barium incorporation into freshwater bivalve shells (*Corbicula fluminea*). *Palaeogeogr. Palaeoclimatol. Palaeoecol.* 465, 386–394. <https://doi.org/10.1016/j.palaeo.2015.11.040>



## Supplementary Information

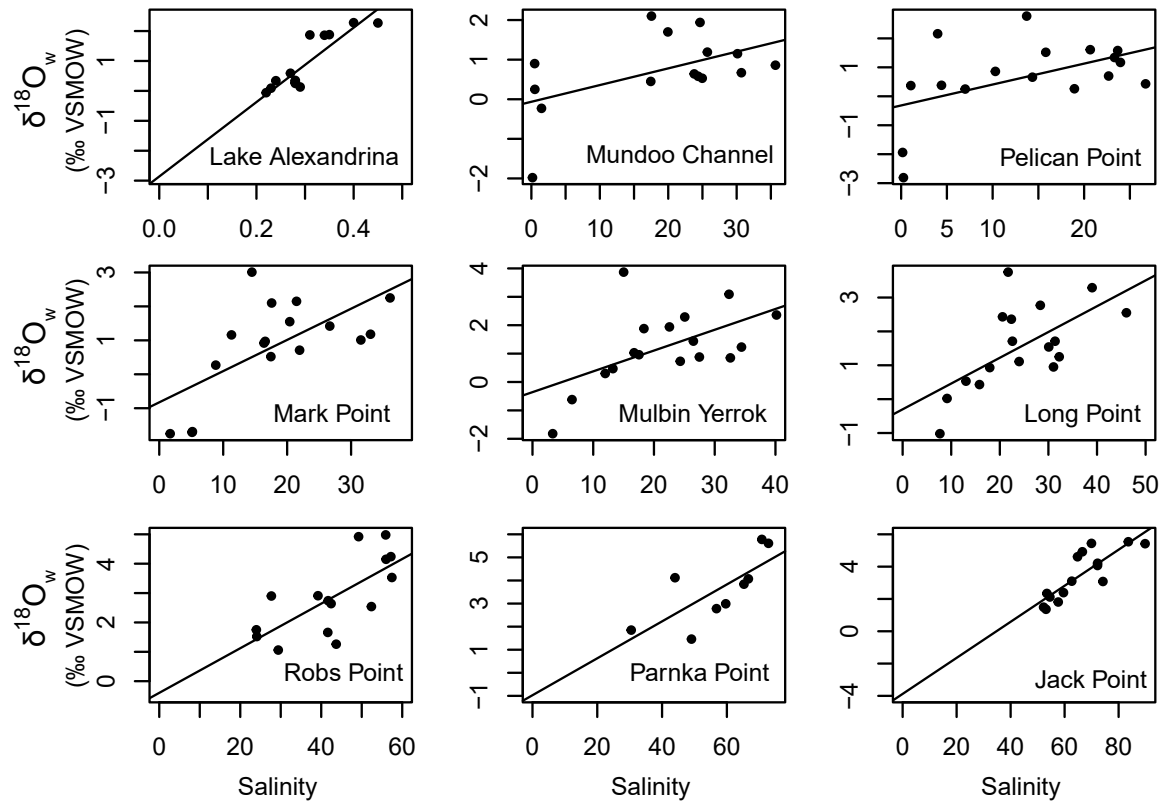


**Figure S1.**  $\delta^{18}\text{O}_w$  – salinity relationship for each sample location. See Table S3 for intercept and coefficient of determination.

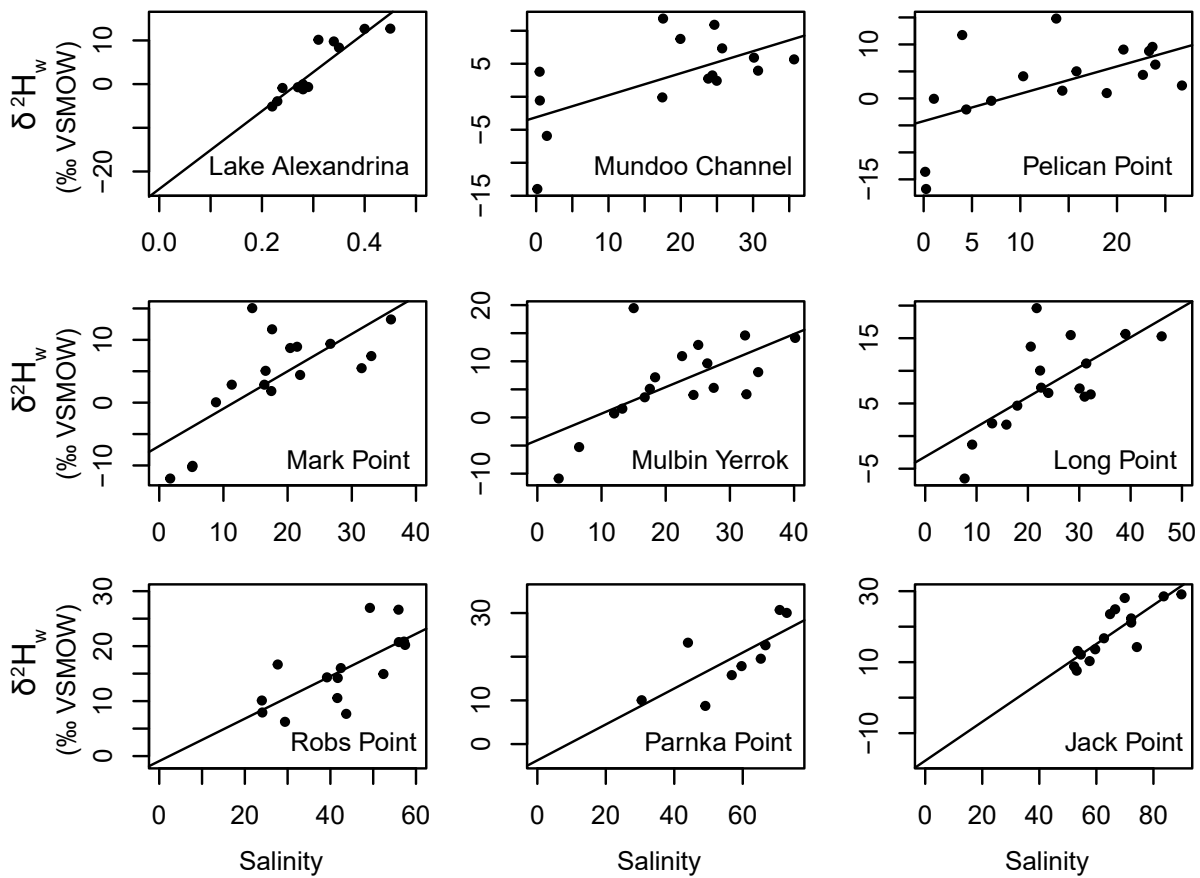


**Figure S2.**  $\delta^2\text{H}_w$  – salinity relationship for each sample location with lines of best fit. See Table S3 for intercept and coefficient of determination.

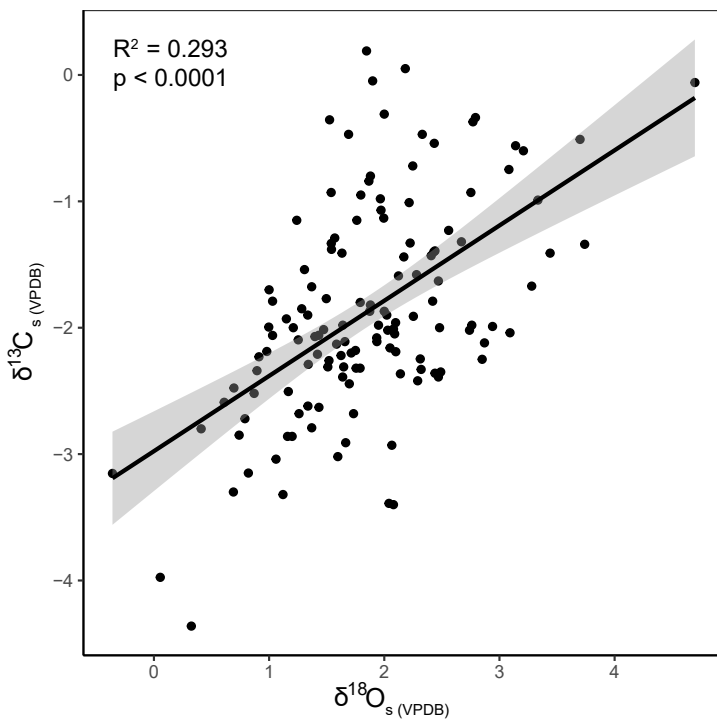


**Figure S3.**  $\delta^{18}\text{O}$  –  $\delta^{13}\text{C}$  relationship for all *A. helmsi* samples collected between March 2017 and May 2018 with the line of best fit. The grey shaded area indicates the 95% confidence interval.

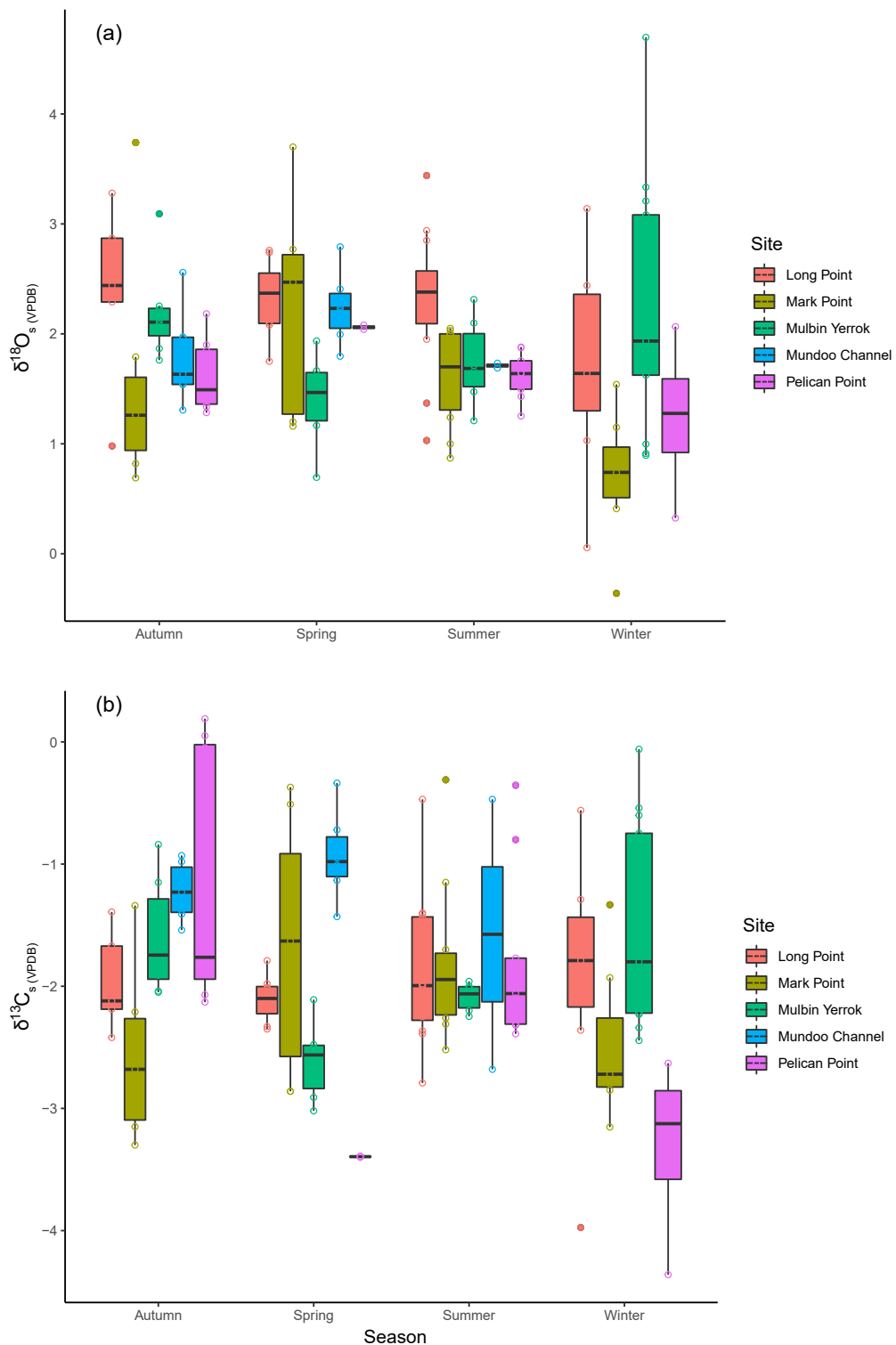


**Figure S4.** Boxplot of (a)  $\delta^{18}\text{O}$  and (b)  $\delta^{13}\text{C}$  for all *A. helmsi* specimens grouped by collection season and site of collection. Whiskers show the upper and lower values, interquartile range is indicated by the box and the horizontal line inside the box indicates the median value. Outliers are indicated by the solid circles.

**Table S1.** Location and sampling time for water samples from Lake Alexandrina and the Coorong Lagoons. Also shown are salinity, temperature, oxygen and hydrogen isotope values for waters.  $\sigma$  = standard deviation.

Location	Date	Latitude	Longitude	Salinity	Temperature (°C)	$\delta^{18}\text{O} \pm \sigma$ (‰ VSMOW)	$\delta^2\text{H} \pm \sigma$ (‰ VSMOW)
Jacks Point	07/02/2017	-36.03	139.57	64.79	28.08	4.61±0.041	23.54±0.113
Jacks Point	21/03/2017	-36.03	139.57	66.58	24.28	4.92±0.083	24.90±0.272
Jacks Point	24/04/2017	-36.03	139.57	72.22	19.13	4.21±0.056	21.15±0.193
Jacks Point	30/05/2017	-36.03	139.57	62.66	14.22	3.10±0.041	16.73±0.163
Jacks Point	07/07/2017	-36.03	139.57	59.59	12.15	2.39±0.073	13.63±0.116
Jacks Point	27/07/2017	-36.03	139.57	57.64	11.97	1.81±0.032	10.31±0.05
Jacks Point	30/08/2017	-36.03	139.06	53.11	12.39	1.36±0.054	7.60±0.364
Jacks Point	29/09/2017	-36.03	139.57	52.22	18.16	1.49±0.077	8.81±0.211
Jacks Point	25/10/2017	-36.03	139.57	54.55	16.57	2.12±0.008	12.14±0.442
Jacks Point	15/11/2017	-36.03	139.57	53.44	19.69	2.34±0.066	13.16±0.45
Jacks Point	18/01/2018	-36.03	139.57	69.95	22.93	5.44±0.029	28.08±0.33
Jacks Point	28/02/2018	-36.03	139.57	83.60	21.17	5.54±0.101	28.54±1.025
Jacks Point	30/03/2018	-36.03	139.57	89.82	23.92	5.42±0.037	29.11±0.24
Jacks Point	03/05/2018	-36.03	139.57	74.20	15.90	3.08±0.035	14.26±0.066
Jacks Point	24/05/2018	-36.03	139.57	72.20	15.62	4.07±0.027	22.33±0.21
Lake Alexandrina	21/03/2017	-35.51	139.19	0.27	23.52	0.59±0.023	-0.71±0.12
Lake Alexandrina	24/04/2017	-35.51	139.19	0.22	19.50	-0.06±0.025	-5.12±0.146
Lake Alexandrina	30/05/2017	-35.51	139.19	0.23	13.63	0.09±0.065	-3.92±0.339
Lake Alexandrina	07/07/2017	-35.51	139.19	0.24	11.50	0.34±0.052	-0.88±0.147
Lake Alexandrina	27/07/2017	-35.51	139.19	0.28	11.77	0.35±0.025	-1.19±0.435
Lake Alexandrina	30/08/2017	-35.51	139.19	0.28	14.43	0.29±0.013	-0.39±0.087
Lake Alexandrina	29/09/2017	-35.51	139.19	0.28	16.30	0.28±0.06	-0.51±0.315
Lake Alexandrina	25/10/2017	-35.51	139.19	0.28	20.44	0.25±0.024	-0.04±0.143
Lake Alexandrina	15/11/2017	-35.51	139.19	0.29	20.75	0.13±0.01	-0.66±0.119
Lake Alexandrina	18/01/2018	-35.51	139.19	0.31	32.60	1.87±0.041	10.15±0.277

Lake Alexandrina	28/02/2018	-35.51	139.19	0.34	21.14	1.86±0.036	9.77±0.354
Lake Alexandrina	30/03/2018	-35.51	139.19	0.40	20.00	2.28±0.029	12.66±0.33
Lake Alexandrina	03/05/2018	-35.51	139.19	0.35	16.12	1.88±0.034	8.36±0.156
Lake Alexandrina	24/05/2018	-35.51	139.19	0.45	14.12	2.27±0.022	12.7±0.048
Long Point	01/11/2016	-35.70	139.16	7.68	15.05	-1.02±0.025	-6.51±0.199
Long Point	21/12/2016	-35.70	139.16	9.15	20.00	0.02±0.038	-1.31±0.267
Long Point	07/02/2017	-35.70	139.16	39.00	22.67	3.29±0.057	15.65±0.348
Long Point	21/03/2017	-35.70	139.16	22.38	22.04	2.36±0.065	10.04±0.111
Long Point	24/04/2017	-35.70	139.16	22.59	19.01	1.71±0.014	7.42±0.127
Long Point	30/05/2017	-35.70	139.16	13.04	13.44	0.53±0.027	1.94±0.095
Long Point	07/07/2017	-35.70	139.16	17.93	12.56	0.93±0.038	4.66±0.132
Long Point	27/07/2017	-35.67	139.14	15.82	12.40	0.43±0.036	1.75±0.161
Long Point	30/08/2017	-35.70	139.16	31.05	13.02	0.95±0.017	6.04±0.09
Long Point	29/09/2017	-35.67	139.16	23.98	17.27	1.11±0.057	6.61±0.283
Long Point	25/10/2017	-35.70	139.16	46.05	19.98	2.55±0.056	15.29±0.236
Long Point	15/11/2017	-35.70	139.16	20.56	20.86	2.43±0.045	13.71±0.107
Long Point	18/01/2018	-35.70	139.16	21.71	29.07	3.75±0.028	19.61±0.094
Long Point	28/02/2018	-35.70	139.16	28.34	20.49	2.77±0.022	15.48±0.089
Long Point	30/03/2018	-35.70	139.16	30.07	20.81	1.54±0.028	7.30±0.204
Long Point	03/05/2018	-35.70	139.16	32.23	15.71	1.25±0.029	6.39±0.148
Long Point	24/05/2018	-35.69	139.16	31.37	14.66	1.71±0.038	11.13±0.118
Mark Point	01/11/2016	-35.63	139.08	5.13	16.80	-1.71±0.011	-10.25±0.077
Mark Point	01/11/2016	-35.62	139.08	5.19	17.20	-1.69±0.01	-10.06±0.095
Mark Point	21/12/2016	-35.63	139.08	1.71	20.53	-1.75±0.027	-12.08±0.184
Mark Point	07/02/2017	-35.63	139.08	21.47	24.57	2.15±0.02	8.90±0.113
Mark Point	21/03/2017	-35.63	139.08	11.30	22.43	1.16±0.028	2.86±0.093
Mark Point	24/04/2017	-35.63	139.08	16.38	18.44	0.92±0.017	2.86±0.158

Mark Point	30/05/2017	-35.63	139.08	17.46	12.45	0.52±0.04	1.85±0.12
Mark Point	07/07/2017	-35.61	139.05			0.68±0.053	3.80±0.073
Mark Point	27/07/2017	-35.63	139.08	8.84	12.47	0.27±0.044	0.06±0.131
Mark Point	30/08/2017	-35.64	139.10	21.95	13.88	0.71±0.045	4.41±0.08
Mark Point	29/09/2017	-35.63	139.08	16.57	18.50	0.97±0.045	5.07±0.118
Mark Point	25/10/2017	-35.63	139.08	36.10	21.78	2.25±0.039	13.25±0.152
Mark Point	15/11/2017	-35.63	139.08	20.41	19.57	1.55±0.031	8.70±0.11
Mark Point	18/01/2018	-35.63	139.08	14.49	33.17	3.01±0.024	15.05±0.099
Mark Point	28/02/2018	-35.63	139.08	17.58	21.23	2.10±0.017	11.68±0.196
Mark Point	30/03/2018	-35.63	139.08	33.04	21.11	1.18±0.043	7.42±0.145
Mark Point	03/05/2018	-35.63	139.08	31.53	15.71	1.01±0.054	5.49±0.153
Mark Point	24/05/2018	-35.60	139.03	26.67	14.69	1.42±0.016	9.37±0.054
Mulbin Yerrok	01/11/2016	-35.67	139.14	3.33	15.80	-1.82±0.025	-10.87±0.07
Mulbin Yerrok	21/12/2016	-35.67	139.14	6.51	20.73	-0.62±0.028	-5.27±0.126
Mulbin Yerrok	07/02/2017	-35.67	139.14	32.36	24.74	3.09±0.072	14.6±0.113
Mulbin Yerrok	21/03/2017	-35.70	139.16	18.35	21.90	1.88±0.042	7.15±0.114
Mulbin Yerrok	24/04/2017	-35.65	139.10	16.73	18.82	1.03±0.084	3.59±0.424
Mulbin Yerrok	30/05/2017	-35.67	139.14	13.24	13.23	0.47±0.049	1.56±0.102
Mulbin Yerrok	07/07/2017	-35.66	139.10	24.33	12.70	0.73±0.05	4.01±0.169
Mulbin Yerrok	27/07/2017	-35.67	139.14	11.98	12.46	0.30±0.041	0.71±0.135
Mulbin Yerrok	30/08/2017	-35.66	139.12	27.48	13.84	0.88±0.037	5.27±0.148
Mulbin Yerrok	29/09/2017	-35.65	139.10	17.53	18.47	0.96±0.019	5.10±0.105
Mulbin Yerrok	25/10/2017	-35.65	139.10	40.17	20.89	2.36±0.007	14.16±0.094
Mulbin Yerrok	15/11/2017	-35.65	139.10	22.55	19.68	1.94±0.101	10.92±0.249
Mulbin Yerrok	18/01/2018	-35.70	139.16	15.01	32.73	3.87±0.037	19.46±0.109
Mulbin Yerrok	28/02/2018	-35.65	139.10	25.07	20.43	2.29±0.006	12.91±0.133
Mulbin Yerrok	30/03/2018	-35.70	139.16	34.41	23.04	1.23±0.039	8.07±0.027

Mulbin Yerrok	03/05/2018	-35.65	139.10	32.58	15.63	0.85±0.025	4.13±0.175
Mulbin Yerrok	24/05/2018	-35.65	139.10	26.49	14.79	1.44±0.056	9.63±0.109
Mundoo Channel	21/12/2016	-35.54	138.88	0.16	22.50	-1.98±0.018	-13.97±0.075
Mundoo Channel	09/02/2017	-35.54	138.88	1.48	24.35	-0.23±0.054	-5.93±0.354
Mundoo Channel	12/03/2017	-35.54	138.88	17.45	23.00	0.45±0.03	-0.10±0.246
Mundoo Channel	25/04/2017	-35.54	138.88	23.80	19.05	0.64±0.033	2.74±0.18
Mundoo Channel	31/05/2017	-35.54	138.88	24.37	12.17	0.58±0.03	3.23±0.118
Mundoo Channel	07/07/2017	-35.54	138.88	24.97	10.77	0.53±0.11	2.42±0.233
Mundoo Channel	30/08/2017	-35.54	138.88	0.51	15.23	0.25±0.015	-0.57±0.104
Mundoo Channel	29/09/2017	-35.54	138.88	30.69	15.21	0.67±0.06	3.95±0.354
Mundoo Channel	25/10/2017	-35.54	138.88	0.48	21.63	0.90±0.023	3.79±0.128
Mundoo Channel	15/11/2017	-35.54	138.88	19.95	20.47	1.70±0.043	8.76±0.256
Mundoo Channel	18/01/2018	-35.54	138.88	17.55	27.57	2.10±0.022	11.84±0.162
Mundoo Channel	28/02/2018	-35.54	138.88	24.65	20.55	1.94±0.052	10.9±0.327
Mundoo Channel	30/03/2018	-35.54	138.88	35.67	20.68	0.86±0.05	5.66±0.259
Mundoo Channel	03/05/2018	-35.56	138.88	30.12	16.82	1.15±0.03	5.92±0.163
Mundoo Channel	28/05/2018	-35.54	138.88	25.72	14.87	1.19±0.033	7.33±0.155
Parnka Point	30/05/2017	-35.90	139.40	30.48	13.53	1.85±0.016	10.04±0.18
Parnka Point	30/08/2017	-35.89	139.40	49.08	11.81	1.46±0.085	8.74±0.294
Parnka Point	25/10/2017	-35.90	139.40	56.80	16.93	2.78±0.048	15.79±0.166
Parnka Point	15/11/2017	-35.90	139.40	66.64	20.50	4.07±0.081	22.62±0.326
Parnka Point	18/01/2018	-35.90	139.40	70.80	25.98	5.78±0.064	30.70±0.469
Parnka Point	28/02/2018	-35.90	139.40	72.84	20.09	5.61±0.07	30.03±0.093
Parnka Point	30/03/2018	-35.90	139.40	44.00	21.85	4.12±0.026	23.21±0.154
Parnka Point	03/05/2018	-35.90	139.40	65.28	15.65	3.84±0.029	19.54±0.166
Parnka Point	24/05/2018	-35.90	139.40	59.66	15.86	2.99±0.056	17.85±0.121
Pelican Point	01/11/2016	-35.60	139.03	0.25	17.76	-2.81±0.062	-16.78±0.094

Pelican Point	21/12/2016	-35.63	139.08	0.16	19.40	-1.94±0.022	-13.60±0.092
Pelican Point	07/02/2017	-35.60	139.03	15.81	24.74	1.52±0.024	5.02±0.033
Pelican Point	21/03/2017	-35.60	139.03	4.41	23.08	0.38±0.016	-2.05±0.14
Pelican Point	24/04/2017	-35.60	139.03	14.35	19.20	0.66±0.032	1.43±0.173
Pelican Point	30/05/2017	-35.60	139.03	26.72	12.51	0.43±0.059	2.39±0.105
Pelican Point	07/07/2017	-35.60	139.03	1.06	12.72	0.37±0.029	-0.07±0.142
Pelican Point	27/07/2017	-35.60	139.03	7.00	12.40	0.25±0.019	-0.44±0.191
Pelican Point	30/08/2017	-35.60	139.03	22.68	16.06	0.70±0.014	4.36±0.075
Pelican Point	29/09/2017	-35.60	139.03	10.30	18.75	0.86±0.025	4.10±0.113
Pelican Point	25/10/2017	-35.60	139.03	20.67	23.49	1.61±0.013	9.05±0.05
Pelican Point	15/11/2017	-35.60	139.03	18.94	19.00	0.26±0.025	0.99±0.205
Pelican Point	18/01/2018	-35.60	139.03	13.72	37.90	2.77±0.024	14.79±0.162
Pelican Point	28/02/2018	-35.60	139.03	3.99	20.76	2.16±0.04	11.74±0.292
Pelican Point	30/03/2018	-35.60	139.03	23.67	21.34	1.58±0.055	9.55±0.061
Pelican Point	03/05/2018	-35.60	139.03	23.97	15.69	1.17±0.033	6.26±0.201
Pelican Point	24/05/2018	-35.60	139.03	23.32	14.40	1.34±0.046	8.77±0.071
Robb Point	30/08/2017	-35.79	139.30	43.70	13.54	1.26±0.079	7.68±0.158
Robb Point	29/09/2017	-35.78	139.30	41.62	19.01	1.66±0.093	10.56±0.258
Robb Point	25/10/2017	-35.78	139.30	52.39	17.60	2.54±0.08	14.93±0.242
Robb Point	15/11/2017	-35.78	139.30	57.45	20.78	3.53±0.04	20.22±0.115
Robb Point	18/01/2018	-35.78	139.30	55.92	25.49	4.98±0.046	26.63±0.133
Robb Point	28/02/2018	-35.78	139.30	49.23	20.22	4.92±0.023	26.96±0.263
Robb Point	30/03/2018	-35.79	139.30	27.69	22.76	2.90±0.05	16.66±0.322
Robb Point	03/05/2018	-35.78	139.30	41.71	16.32	2.74±0.013	14.21±0.105
Robb Point	24/05/2018	-35.78	139.30	42.44	15.84	2.64±0.031	16.01±0.224
Robb Point	07/02/2017	-35.78	139.30	56.00	25.77	4.15±0.021	20.74±0.265
Robb Point	21/03/2017	-35.79	139.30	57.20	24.85	4.24±0.026	20.83±0.109



Robs Point	24/04/2017	-35.79	139.30	39.20	20.14	2.91±0.059	14.32±0.141
Robs Point	30/05/2017	-35.79	139.30	24.09	13.81	1.52±0.033	7.93±0.056
Robs Point	07/07/2017	-36.03	139.57	23.98	13.21	1.75±0.023	10.11±0.111

**Table S2.** Shell ID, sampling location and sampling time for *A. helmsi* samples from the North Coorong Lagoon. Also shown are the size and oxygen and carbon isotope values for each shell.  $\sigma$  = standard deviation. Date is shown as day, month and year.

Shell ID	Location	Date	Size (mm)	$\delta^{18}\text{O} \pm \sigma$ (‰) VPDB	$\delta^{13}\text{C} \pm \sigma$ (‰) VPDB
LP0317-1	Long Point	21/03/2017	2.17	2.32±0.11	-1.30±0.08
LP0317-2	Long Point	21/03/2017	1.87	2.47±0.11	-0.31±0.08
LP0317-3	Long Point	21/03/2017	1.84	2.57±0.11	-1.26±0.08
LP0817-1	Long Point	30/08/2017	2.02	1.03±0.05	-1.79±0.06
LP0817-2	Long Point	30/08/2017	2.10	1.57±0.06	-1.29±0.04
LP0817-3	Long Point	30/08/2017	1.72	2.44±0.12	-2.36±0.05
LP0817-4	Long Point	30/08/2017	2.00	2.28±0.12	-1.58±0.25
LP0817-5	Long Point	30/08/2017	1.97	1.64±0.10	-1.98±0.19
LP0817-6	Long Point	30/08/2017	1.75	3.14±0.15	-0.56±0.08
LP0817-7	Long Point	30/08/2017	1.87	-0.13±0.11	0.11±0.04
LP1017-1	Long Point	25/10/2017	1.86	2.08±0.05	-2.01±0.04
LP1017-2	Long Point	25/10/2017	1.89	2.42±0.05	-1.79±0.06
LP1017-3	Long Point	25/10/2017	1.79	1.75±0.06	-2.18±0.06
LP1017-4	Long Point	25/10/2017	1.93	2.49±0.08	-2.35±0.14
LP1017-5	Long Point	25/10/2017	1.92	2.32±0.16	-2.33±0.08
LP1017-6	Long Point	25/10/2017	1.93	2.76±0.08	-1.98±0.25
LP1017-7	Long Point	25/10/2017	1.70	2.74±0.18	-2.02±0.05
LP1017-8	Long Point	25/10/2017	1.71	2.10±0.09	-2.19±0.25
LP0118-1	Long Point	18/01/2018	1.69	2.48±0.06	-2.00±0.01
LP0118-2	Long Point	18/01/2018	1.88	2.47±0.07	-2.39±0.05
LP0118-3	Long Point	18/01/2018	1.36	2.94±0.10	-1.99±0.03
LP0118-4	Long Point	18/01/2018	1.86	2.85±0.07	-2.25±0.03
LP0118-5	Long Point	18/01/2018	1.78	3.44±0.06	-1.41±0.04
LP0118-6	Long Point	18/01/2018	1.76	2.14±0.09	-2.37±0.10
LP0118-7	Long Point	18/01/2018	1.73	1.95±0.10	-1.98±0.08
LP0118-8	Long Point	18/01/2018	1.30	1.03±0.36	-2.06±0.03
LP0118-9	Long Point	18/01/2018	1.83	1.37±0.28	-2.79±0.16
LP0518-1	Long Point	03/05/2018	1.92	2.29±0.07	-2.42±0.05

LP0518-2	Long Point	03/05/2018	1.67	0.98±0.20	-2.19±0.11
LP0518-3	Long Point	03/05/2018	1.82	3.28±0.13	-1.67±0.08
LP0518-4	Long Point	03/05/2018	1.84	2.87±0.07	-2.12±0.20
LP0518-5	Long Point	03/05/2018	1.72	2.44±0.18	-1.39±0.06
MP0317-1	Mark Point	21/03/2017	1.89	1.22±0.11	-1.66±0.08
MP0317-2	Mark Point	21/03/2017	1.40	1.46±0.11	-1.11±0.08
MP0317-3	Mark Point	21/03/2017	2.57	2.22±0.11	-0.27±0.08
MP0817-1	Mark Point	30/08/2017	1.38	-0.36±0.41	-3.15±0.17
MP0817-2	Mark Point	30/08/2017	1.51	0.41±0.11	-2.80±0.04
MP0817-3	Mark Point	30/08/2017	1.54	0.61±0.16	-2.59±0.08
MP0817-4	Mark Point	30/08/2017	1.30	0.74±0.08	-2.85±0.02
MP0817-5	Mark Point	30/08/2017	1.90	1.54±0.18	-1.33±0.31
MP1017-1	Mark Point	25/10/2017	1.58	1.16±0.06	-2.86±0.03
MP1017-2	Mark Point	25/10/2017	1.61	1.20±0.07	-2.86±0.08
MP1017-3	Mark Point	25/10/2017	1.34	1.34±0.03	-2.29±0.02
MP1017-4	Mark Point	25/10/2017	1.48	2.33±0.11	-1.31±0.04
MP1017-5	Mark Point	25/10/2017	1.75	2.47±0.05	-1.63±0.04
MP1017-6	Mark Point	25/10/2017	1.86	2.77±0.24	-0.37±0.09
MP1017-7	Mark Point	25/10/2017	1.91	3.70±0.20	-0.51±0.23
MP0118-1	Mark Point	18/01/2018	1.99	0.87±0.07	-2.52±0.06
MP0118-2	Mark Point	18/01/2018	1.74	1.51±0.08	-2.31±0.05
MP0118-3	Mark Point	18/01/2018	1.74	1.88±0.10	-1.82±0.03
MP0118-4	Mark Point	18/01/2018	1.92	2.00±0.05	-1.87±0.22
MP0118-5	Mark Point	18/01/2018	1.50	2.03±0.06	-2.02±0.04
MP0118-6	Mark Point	18/01/2018	1.52	2.05±0.08	-2.16±0.03
MP0518-1	Mark Point	03/05/2018	1.77	0.69±0.05	-3.30±0.05
MP0518-2	Mark Point	03/05/2018	1.87	0.82±0.06	-3.15±0.07
MP0518-3	Mark Point	03/05/2018	1.87	1.06±0.16	-3.04±0.08
MP0518-4	Mark Point	03/05/2018	1.64	1.26±0.25	-2.68±0.12
MP0518-5	Mark Point	03/05/2018	1.63	1.79±0.18	-2.32±0.07

MP0518-6	Mark Point	03/05/2018	1.70	3.74±0.12	-1.34±0.12
MY0317-1	Mulbin Yerrok	21/03/2017	2.09	1.43±0.11	-1.96±0.08
MY0717-1	Mulbin Yerrok	07/07/2017	1.66	3.21±0.08	-0.60±0.02
MY0717-2	Mulbin Yerrok	07/07/2017	1.74	3.33±0.07	-0.99±0.03
MY0717-3	Mulbin Yerrok	07/07/2017	1.79	1.70±0.17	-2.44±0.11
MY0717-4	Mulbin Yerrok	07/07/2017	1.53	2.43±0.20	-0.54±0.09
MY0717-5	Mulbin Yerrok	07/07/2017	1.80	0.89±0.09	-2.34±0.23
MY0717-6	Mulbin Yerrok	07/07/2017	1.88	4.70±0.14	-0.06±0.18
MY0717-7	Mulbin Yerrok	07/07/2017	1.84	1.93±0.10	-2.08±0.22
MY0717-8	Mulbin Yerrok	07/07/2017	1.85	1.79±0.11	-1.80±0.27
MY0817-1	Mulbin Yerrok	30/08/2017	2.04	0.91±0.05	-2.23±0.02
MY0817-2	Mulbin Yerrok	30/08/2017	1.79	1.62±0.06	-2.22±0.03
MY0817-3	Mulbin Yerrok	30/08/2017	1.82	2.75±0.04	-0.93±0.05
MY0817-4	Mulbin Yerrok	30/08/2017	1.83	3.08±0.14	-0.75±0.04
MY0817-5	Mulbin Yerrok	30/08/2017	1.66	1.00±0.26	-2.00±0.04
MY0817-6	Mulbin Yerrok	30/08/2017	1.65	-1.80±0.11	-1.44±0.04
MY1017-1	Mulbin Yerrok	25/10/2017	1.69	1.60±0.05	-3.02±0.05
MY1017-2	Mulbin Yerrok	25/10/2017	1.60	1.94±0.06	-2.11±0.04
MY1017-3	Mulbin Yerrok	25/10/2017	1.91	1.34±0.04	-2.62±0.04
MY1017-4	Mulbin Yerrok	25/10/2017	1.82	1.66±0.15	-2.91±0.09
MY1017-5	Mulbin Yerrok	25/10/2017	1.78	1.17±0.18	-2.51±0.07
MY0118-1	Mulbin Yerrok	18/01/2018	1.33	1.47±0.17	-2.02±0.10
MY0118-2	Mulbin Yerrok	18/01/2018	1.89	2.31±0.14	-2.25±0.30
MY0518-1	Mulbin Yerrok	03/05/2018	2.01	1.87±0.08	-0.84±0.02
MY0518-2	Mulbin Yerrok	03/05/2018	1.60	2.22±0.05	-1.33±0.02
MY0518-3	Mulbin Yerrok	03/05/2018	2.04	1.76±0.04	-1.15±0.03
MY0518-4	Mulbin Yerrok	03/05/2018	1.81	2.12±0.05	-1.59±0.07
MY0518-5	Mulbin Yerrok	03/05/2018	2.07	2.02±0.04	-1.90±0.08
MY0518-6	Mulbin Yerrok	03/05/2018	1.86	3.09±0.15	-2.04±0.21
MY0518-7	Mulbin Yerrok	03/05/2018	1.78	2.25±0.20	-1.91±0.11

MY0518-8	Mulbin Yerrok	03/05/2018	1.81	2.09±0.14	-2.05±0.36
MC0317-1	Mundoo Channel	12/03/2017	1.97	1.91±0.11	-0.43±0.08
MC1017-1	Mundoo Channel	25/10/2017	2.26	1.80±0.07	-0.95±0.06
MC1017-2	Mundoo Channel	25/10/2017	2.10	2.00±0.15	-1.13±0.10
MC1017-3	Mundoo Channel	25/10/2017	1.98	2.22±0.21	-1.01±0.15
MC1017-4	Mundoo Channel	25/10/2017	1.71	2.25±0.23	-0.72±0.08
MC1017-5	Mundoo Channel	25/10/2017	2.10	2.79±0.07	-0.34±0.40
MC0118-1	Mundoo Channel	18/01/2018	2.08	1.73±0.09	-2.68±0.06
MC0518-1	Mundoo Channel	03/05/2018	2.00	1.54±0.09	-0.93±0.24
Mc0518-2	Mundoo Channel	03/05/2018	1.92	1.54±0.03	-1.38±0.05
MC0518-3	Mundoo Channel	03/05/2018	1.86	1.63±0.05	-1.41±0.02
MC0518-4	Mundoo Channel	03/05/2018	1.67	1.97±0.10	-0.98±0.02
MC0518-5	Mundoo Channel	03/05/2018	1.71	1.97±0.25	-1.07±0.10
MC0518-6	Mundoo Channel	03/05/2018	1.86	2.56±0.11	-1.23±0.23
PP0317-1	Pelican Point	21/03/2017	2.01	2.04±0.11	-0.65±0.08
PP0317-2	Pelican Point	21/03/2017	2.18	1.27±0.11	-0.22±0.04
PP0817-1	Pelican Point	30/08/2017	1.76	1.12±0.04	-3.32±0.04
PP0817-2	Pelican Point	30/08/2017	1.61	2.07±0.07	-2.93±0.02
PP0817-3	Pelican Point	30/08/2017	1.85	1.43±0.04	-2.63±0.04
PP0817-4	Pelican Point	30/08/2017	1.72	0.32±0.21	-4.36±0.08
PP1017-1	Pelican Point	25/10/2017	1.78	2.08±0.16	-3.40±0.08
PP1017-2	Pelican Point	25/10/2017	1.56	2.04±0.09	-3.39±0.08
PP0118-1	Pelican Point	18/01/2018	1.88	1.43±0.09	-2.06±0.03
PP0118-2	Pelican Point	18/01/2018	1.69	1.64±0.07	-2.39±0.04
PP0118-3	Pelican Point	18/01/2018	1.64	1.65±0.07	-2.31±0.03
PP0118-4	Pelican Point	18/01/2018	1.72	1.50±0.08	-1.77±0.02
PP0118-5	Pelican Point	18/01/2018	1.96	1.76±0.07	-2.32±0.06
PP0118-6	Pelican Point	18/01/2018	1.76	1.87±0.09	-1.87±0.02
PP0118-7	Pelican Point	18/01/2018	1.82	1.25±0.05	-2.10±0.03
PP0518-1	Pelican Point	03/05/2018	1.83	1.59±0.08	-2.13±0.02

---

PP0518-2	Pelican Point	03/05/2018	1.78	1.34±0.04	-1.90±0.04
PP0518-3	Pelican Point	03/05/2018	1.81	1.28±0.05	-1.85±0.01
PP0518-4	Pelican Point	03/05/2018	1.87	1.40±0.06	-2.07±0.02
PP0518-5	Pelican Point	03/05/2018	1.88	1.85±0.05	0.19±0.04
PP0518-6	Pelican Point	03/05/2018	1.78	1.90±0.14	-0.05±0.13
PP0518-7	Pelican Point	03/05/2018	1.81	1.37±0.12	-1.68±0.46
PP0518-8	Pelican Point	03/05/2018	1.88	2.18±0.24	0.05±0.16

---

**Table S3.**  $\delta^{18}\text{O}_w$  and  $\delta^2\text{H}_w$  relationship to salinity for each sampling location and the corresponding intercept and  $R^2$  values.  $R^2$  values are statistically significant at the 95% confidence limits for all sampling locations.

Site	$\delta^{18}\text{O}$ intercept	$R^2$	$\delta^2\text{H}$ intercept	$R^2$
Lake Alexandrina	-2.86	0.77	-24	0.82
Mundoo Channel	-0.06	0.22	-3.1	0.33
Pelican Point	-0.32	0.2	-4.2	0.29
Mark Point	-0.83	0.39	-6.9	0.51
Mulbin Yerrok	-0.36	0.26	-4.05	0.37
Long Point	-0.3	0.36	-3.16	0.44
Rob's Point	-0.4	0.47	-0.91	0.47
Parnka Point	-0.97	0.48	-3.73	0.48
Jack Point	-3.88	0.68	-17.75	0.67

**Table S4.** Slope and intercept for the linear regression between  $\delta^{18}\text{O}_w$  and  $\delta^2\text{H}_w$  for each sampling site.  $R^2$  values are statistically significant at the 95% confidence limits for all sampling locations.

Site	Slope	Intercept	$R^2$
Lake Alexandrina	6.88	-3.23	0.97
Mundoo Channel	6.60	-1.66	0.97
Pelican Point	5.93	-1.27	0.97
Mark Point	5.68	-0.85	0.97
Mulbin Yerrok	5.46	-0.53	0.96
Long Point	5.45	-0.48	0.96
Rob's Point	5.00	1.33	0.97
Parnka Point	5.14	1.29	0.99
Jack Point	4.93	1.23	0.99
All sites	5.65	0.97	0.98

**Table S5.** Slope and intercept for the linear regression between  $\delta^{18}\text{O}_w$  and  $\delta^2\text{H}_w$  for each sampling time.  $R^2$  values are statistically significant at the 95% confidence limits for all sampling times.

<b>Date</b>	<b>Slope</b>	<b>Intercept</b>	<b>R<sup>2</sup></b>
1/11/2016	5.77	-0.44	0.99
21/12/2016	6.26	-1.40	0.99
7/02/2017	5.97	-3.97	0.99
21/03/2017	5.81	-3.73	0.99
24/04/2017	5.79	-2.66	0.98
30/05/2017	6.11	-1.53	0.96
7/07/2017	6.65	-1.70	0.97
27/07/2017	7.02	-2.00	0.96
30/08/2017	7.49	-1.75	0.95
29/09/2017	7.59	-2.13	0.98
25/10/2017	6.57	-1.74	0.99
15/11/2017	5.89	-0.82	0.99
18/01/2018	5.17	0.29	0.99
28/02/2018	5.18	0.75	0.99
30/03/2018	5.27	0.94	0.99
3/05/2018	4.89	0.18	0.99
24/05/2018	5.12	1.95	0.99
All dates	5.65	0.97	0.98







---

# CHAPTER 5

Chamberlayne, B.K., Tyler, J.J., Gillanders, B.M., Tibby, J., Haynes, D., 2021. Palaeohydrology of the southern Coorong Lagoon, South Australia, inferred from the oxygen isotope ratios of fossil bivalves

Supplementary information concerning this chapter follows the text.

---

## Statement of Authorship

Title of Paper	Palaeohydrology of the southern Coorong Lagoon, South Australia, inferred from the oxygen isotope ratios of fossil bivalves
Publication Status	<input type="checkbox"/> Published <input type="checkbox"/> Accepted for Publication <input type="checkbox"/> Submitted for Publication <input checked="" type="checkbox"/> Unpublished and Unsubmitted work written in manuscript style
Publication Details	

### Principal Author

Name of Principal Author (Candidate)	Briony Chamberlayne			
Contribution to the Paper	Preparation and analysis of samples for isotope analysis, statistical analysis, figure production, manuscript preparation and editing.			
Overall percentage (%)	80			
Certification:	This paper reports on original research I conducted during the period of my Higher Degree by Research candidature and is not subject to any obligations or contractual agreements with a third party that would constrain its inclusion in this thesis. I am the primary author of this paper.			
Signature	<table border="1" style="width: 100%;"> <tr> <td style="width: 80%;"></td> <td style="width: 20%;">Date</td> <td>14/06/2021</td> </tr> </table>		Date	14/06/2021
	Date	14/06/2021		

### Co-Author Contributions

By signing the Statement of Authorship, each author certifies that:

- i. the candidate's stated contribution to the publication is accurate (as detailed above);
- ii. permission is granted for the candidate to include the publication in the thesis; and
- iii. the sum of all co-author contributions is equal to 100% less the candidate's stated contribution.

Name of Co-Author	Jonathan Tyler			
Contribution to the Paper	Provided guidance and assistance in data analysis, interpretation and manuscript editing.			
Signature	<table border="1" style="width: 100%;"> <tr> <td style="width: 80%;"></td> <td style="width: 20%;">Date</td> <td>28/06/2021</td> </tr> </table>		Date	28/06/2021
	Date	28/06/2021		

Name of Co-Author	Bronwyn Gillanders			
Contribution to the Paper	Provided guidance and assistance in data analysis, interpretation and manuscript editing.			
Signature	<table border="1" style="width: 100%;"> <tr> <td style="width: 80%;"></td> <td style="width: 20%;">Date</td> <td>27 June 2021</td> </tr> </table>		Date	27 June 2021
	Date	27 June 2021		

Name of Co-Author	John Tibby		
Contribution to the Paper	Provided sediment core for sampling, assistance in interpretation of data and manuscript editing.		
Signature		Date	18/6/2021

Name of Co-Author	Deborah Haynes		
Contribution to the Paper	Provided sediment core for sampling, manuscript editing.		
Signature		Date	27/06/2021



## Palaeohydrology of the southern Coorong Lagoon, South Australia, inferred from the oxygen isotope ratios of fossil bivalves

### Abstract

Multi-centennial records of past hydroclimate change are essential to understanding the baseline state and resilience of aquatic ecosystems to climatic events, in addition to guiding conservation and restoration efforts. Here, we present a 1750-year record of hydroclimate variability in the South Lagoon of the Coorong, part of the estuarine wetland system at the mouth of the Murray River, South Australia. Oxygen and carbon isotope ratios were measured on shells of *Arthritica helmsi* preserved in sediments, where each sample (n=123) was comprised of five individual shells. The range of oxygen isotope values in the sedimentary shells does not differ significantly from that range predicted for the present day South Lagoon, suggesting that the restricted and highly evaporated modern day conditions are not markedly different to the pre-European state over the last 1750 years, although the absence of *A. helmsi* in the contemporary lagoon is likely a response to increased salinity during the last century. The oxygen isotope record shows two periods of persistent low and high moisture balance from ~500–1000 years and ~1300–1800 respectively. Similarity to other regional records suggest a common driver for southeast Australian hydroclimate, where the timing and variability in ocean-atmosphere interactions appear influential. This study presents the most comprehensively dated record of hydrological change in the Coorong Lagoons. The insights provided by this study into the natural variability of the Coorong South Lagoon are potentially useful in guiding management efforts in the currently degraded system.

## 1. Introduction

Records of hydroclimate variability in Australia for the recent millennia are rare, mostly due to a scarcity of traditional archives such as tree ring chronologies and ice cores on mainland Australia (Dixon et al., 2017; Neukom and Gergis, 2011, Jansen et al., 2007). A recent review of hydroclimate records for the past 2000 years in Australasia found only nine high-quality records from Australia (Dixon et al., 2017). The relatively low number of high-quality records in comparison with other geographic regions limits our understanding of the influence of the remote drivers of rainfall across Australia including the El Niño Southern Oscillation (ENSO), Interdecadal Pacific Oscillation (IPO), Indian Ocean Dipole (IOD) and Southern Annular Mode (SAM) (Gallant et al., 2012; Risbey et al., 2009). A better understanding of natural, low frequency climate variability associated with these climate drivers, along with the reconstruction of decadal to multi-decadal climate extremes such as drought or flood, could assist in placing recent events into context and aid in assessing the risk of future events (e.g. O'Donnell et al., 2021). This is especially relevant for estuarine ecosystems which are highly sensitive to climatic extremes (e.g. Scanes et al., 2020).

The Coorong Lagoons of South Australia are no exception. The Coorong's baseline ecological state and the resilience of the system to major climatic events is relatively unknown (Kingsford et al., 2011; Reeves et al., 2015). The Coorong, along with Lakes Alexandrina and Albert (the Lower Lakes) form a large wetland at the mouth of the Murray River, which along with the Darling River drains the > 1,000,000 km<sup>2</sup> Murray-Darling Basin (MDB). The MDB is Australia's most important agricultural region, providing around 40% of Australia's produce, while the region generally is of great economic, cultural and environmental importance to Australia (MDBA, 2021). The Coorong, along with 15 other wetlands in the MDB, has been recognised as a wetland of global significance by inclusion into the Ramsar Convention for Globally Significant Wetlands (Department of Agriculture, Water and the Environment, 2021) primarily due to its biodiversity, especially for waterbird species (Paton et al., 2009). In recent years the condition of the Coorong Lagoons has been in decline, with rising salinity, eutrophication and declining biodiversity all linked to declining river discharge due to agricultural water extraction (Dittmann et al., 2019; Kingsford et al., 2011; Mosley et al., 2020). Current management efforts are focussed on increasing system flushing and reversing eutrophication (Mosley et al., 2020) including consideration of proposals to open up the Coorong to the Southern Ocean. However, as an inverse estuary, the Coorong is a unique environmental system and despite its proximity to the ocean, its natural (pre-impacted) hydrological state is highly uncertain (Reeves et al., 2015). In this respect, palaeo-environmental studies can provide context regarding long term state of the Coorong, including the range of and resilience to natural hydroclimate variability (Saunders and Taffs, 2009).



A number of studies have been undertaken to understand the palaeo-environment of the Coorong Lagoons. Many of these investigated fossil invertebrate and algal assemblages (Dick et al., 2011; Krull et al., 2009; Lower et al., 2013; Reeves et al., 2015) and have concluded that the current state of the wetland is unusual in its history. However, many of the dominant species found within the assemblages have broad environmental tolerances and hence gave rise to ambiguity in the interpretations. Other studies have included investigations of the carbon, nitrogen and hydrogen isotope composition of organic matter as well as lipid biomarkers as proxies for variations in the source of organic matter and salinity (McKirdy et al., 2010; Tulipani et al., 2014). These methods have found that the two lagoons have been separate chemical systems for millennia (McKirdy et al., 2010) although both lagoons have experienced recent salinization (McKirdy et al., 2010; Tulipani et al., 2014). Recent sediments have been well dated using lead 210 ( $^{210}\text{Pb}$ ), fallout product caesium ( $^{137}\text{Cs}$ ), plutonium ( $^{238/239/240}\text{Pu}$ ) and the first arrival of exotic *Pinus radiata* pollen (Krull et al., 2009). However, several previous studies have encountered challenges related to dating uncertainty, largely down to a relatively small number of radiocarbon dates, which make it difficult to place long term changes into a regional context (e.g McKirdy et al., 2010).

Here, we use the geochemistry of the bivalve *Arthritica helmsi*, which are readily preserved in Coorong sediments, to add to the growing body of research investigating the palaeoenvironmental history of this significant wetland. A modern study of oxygen isotope fractionation in *A. helmsi* has demonstrated the ability of this species to record environmental variation (Chamberlayne et al., 2021) highlighting the potential for use in palaeoenvironmental studies. In this study we analyse oxygen and carbon isotopes from shells preserved in a sediment core from the South Lagoon in order to (i) understand hydrological change throughout the history of the Coorong's South Lagoon; and (ii) assess the drivers of hydrological change in the context of regional climate variability.

## 2. Methods

### 2.1 Site description

The Coorong Lagoons and Lower Lakes comprise the River Murray estuary (Figure 1). The lagoons are separated from the Southern Ocean by a series of Holocene dunes (Murray-Wallace, 2018) except at the Murray Mouth, which is the drainage point for the Murray Darling Basin - Australia's largest river system. The Coorong Lagoons are divided by a narrow channel at Parnka Point where the lagoons are separated into the northern and southern sections referred to as the North Lagoon and the South Lagoon (Figure 1). A reverse estuary, the lagoons are characterised

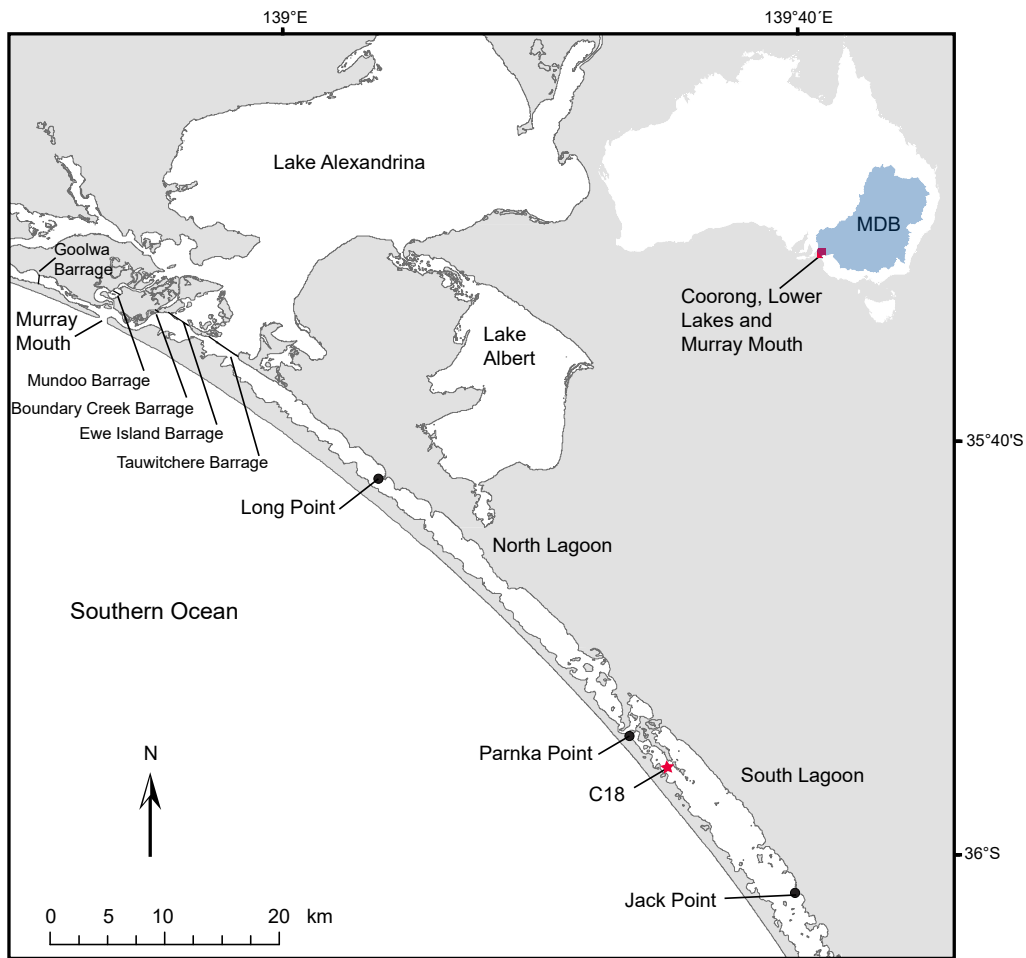


**Figure 1.** Map of the Coorong, Lower Lakes and Murray Mouth – the wetland system at the terminus of the Murray Darling Basin (MDB). The sampling location for core C18 is highlighted with a red star.

by a north-south salinity gradient of fresh to hypersaline (Gillanders and Munro, 2012; Shao et al., 2021). A series of barrages constructed in the 1940s to restrict marine incursions into Lake Alexandrina now regulate freshwater releases from Lake Alexandrina into the Coorong and Murray Mouth (Maheshwari et al., 1995). Currently, water in the North Lagoon is recharged by outflow from Lake Alexandrina and the Murray River, while the South Lagoon is primarily recharged by direct rainfall and continental run-off (Chamberlayne et al., 2021; Shao et al., 2018). The Coorong and Lower Lakes are a culturally important site for the Ngarrindjeri people (Ngarrindjeri Nation & Hemming, 2019). Furthermore, the wetland has been recognised under the Ramsar Convention on Wetlands of International Importance (Phillips and Muller 2006) largely due to the importance for waterbird communities (Paton et al., 2009).

## 2.2 Sample collection and preparation

Core C18 was extracted from the South Lagoon (Figure 1) in 2005 using a Livingstone piston corer and 50mm PVC pipe (Chambers and Cameron, 2001) and stored at 4 °C in refrigerated facilities at The University of Adelaide. The 130 cm core was sliced longitudinally and one half was sampled for diatom and preliminary radiocarbon analyses (Krull et al., 2009). The core was then cut into 1 cm intervals and freeze dried. Shells for analysis were picked from the dried sediment and cleaned using a brush and distilled water and oven dried at 40 °C for 12 hours.

## 2.3 Chronology

The chronology of core C18 was established via a combination of accelerator mass spectrometry (AMS  $^{14}\text{C}$ ) radiocarbon dating and the first appearance of the *Pinus radiata* pollen. Seventeen  $^{14}\text{C}$  dates were obtained from bivalve shells sampled throughout the core (Table S1). The exotic *Pinus* pollen was first introduced to Australia by Europeans and so its detection in sediments can be used as a chronostratigraphic marker for the first European colonisation in the region (Tibby, 2003).  $^{210}\text{Pb}$  and  $^{137}\text{Cs}$  dating of adjacent cores in the Coorong Lagoons indicates that the first detection of *Pinus* is representative of ~1955 CE (Gell and Haynes, 2005; Krull et al., 2009). In core C18, *Pinus* first appears at 9 cm depth (Krull et al., 2009).

To assess the presence of ‘old carbon’ from groundwater which has affected radiocarbon dating in other southeast Australian lakes (Barr et al., 2014; Gouramanis et al., 2010; Wilkins et al., 2012), the  $^{14}\text{C}$  age for the depth corresponding to *Pinus* arrival was compared to the age determined by  $^{210}\text{Pb}$  dating following the method of Barr et al. (2014). To compare the two ages, the  $^{210}\text{Pb}$  derived age of *Pinus* arrival determined from adjacent cores must first be expressed in equivalent  $^{14}\text{C}$  years ( $^{14}\text{C}_{210\text{Pb}}$ ). This was achieved by projecting a probability density curve based upon the mean  $^{210}\text{Pb}$  age and standard deviations against the Southern Hemisphere  $^{14}\text{C}$  calibration curve (Hogg et al., 2020). The mean  $^{14}\text{C}$  age within the error bracket was used to estimate  $^{14}\text{C}_{210\text{Pb}}$ , weighted by its probability. The reservoir age was then estimated by subtracting  $^{14}\text{C}_{210\text{Pb}}$  from measured  $^{14}\text{C}$ , and the error was calculated as the sum of the measured  $^{14}\text{C}$  and the one-sigma error associated with  $^{14}\text{C}_{210\text{Pb}}$ . This old carbon effect was then subtracted from all  $^{14}\text{C}$  measurements from core C18 prior to calibration with the Southern Hemisphere calibration curve (Hogg et al., 2020) using the program Bacon (Blaauw and Christen, 2011) in RStudio (R Core Team, 2018).

## 2.4 Stable isotope analysis

Five pre-cleaned shells, collected at 1 cm intervals throughout core C18 were crushed to a fine powder using an agate mortar and pestle. A sub-sample of approximately 100  $\mu\text{g}$  from this carbonate powder was used for stable isotope analysis. In addition, to assess the degree of

intra-sample variability, multiple individual shells of *A. helmsi* were also analysed from five samples taken at depths of 11 cm (n=30), 26 cm (n=29), 57 cm (n=27), 92 cm (n=30) and 119 cm (n=27). Data from these intervals were integrated into the isotope curve by calculating the weighted mean of the bulk sample and replicate samples from particular depths. Samples were flushed with helium and then acidified with 105% phosphoric acid at 70°C before isotope analysis of the resulting CO<sub>2</sub> using a Nu Instruments GasPrep in-line with a Nu Instruments Nu Horizon Isotope Ratio Mass Spectrometer in continuous flow mode. Laboratory standards ANU-P3 ( $\delta^{13}\text{C} = 2.2\text{‰}$ ,  $\delta^{18}\text{O} = -0.3\text{‰}$ ) and UAC-1 ( $\delta^{13}\text{C} = -15.0\text{‰}$ ,  $\delta^{18}\text{O} = -18.4\text{‰}$ ) accounted for 27 of each 100 analyses, the precision is better than 0.12 ‰ for  $\delta^{18}\text{O}$  and 0.07 ‰ for  $\delta^{13}\text{C}$  based on replicate analyses of these standards. Oxygen and carbon isotope data are reported as  $\delta^{18}\text{O}_s$  and  $\delta^{13}\text{C}_s$  respectively, relative to Vienna Pee Dee Belemnite (VPDB) standard using the standard delta ( $\delta$ ) notation in parts per thousand (‰):

$$\delta = \left( \frac{R_{\text{sample}} - R_{\text{standard}}}{R_{\text{standard}}} \right) \times 1000 \quad (1)$$

where R is the isotope ratio ( $^{18}\text{O}/^{16}\text{O}$  or  $^{13}\text{C}/^{12}\text{C}$ ).

## 2.5 Comparison of oxygen isotope ratios in core and modern *A. helmsi*

The oxygen isotope ratios measured on shells of *A. helmsi* extracted from sediment core C18 are compared to the ratios measured and predicted for modern populations in the North and South Coorong Lagoons. Oxygen isotope ratios for live collected individuals of *A. helmsi* from the North Coorong Lagoon are sourced from Chamberlayne et al. (2021) who measured  $\delta^{18}\text{O}$  on shells from five locations throughout the North Lagoon from 2016-2018. As there are currently no living populations of *A. helmsi* in the South Lagoon (Dittmann et al., 2019), the oxygen isotope ratios of shells predicted by current conditions were calculated from measurements of temperature and oxygen isotope composition of waters sourced from Chamberlayne et al. (2021). The  $\delta^{18}\text{O}_s$  predicted for populations for Parnka Point and Jacks Point were calculated from the temperature-dependent oxygen isotope fractionation equation developed for *A. helmsi* by Chamberlayne et al. (2021):

$$T (\text{°C}) = (21.39 \pm 0.45) - (4.43 \pm 0.38) * (\delta^{18}\text{O}_{\text{shell}} - \delta^{18}\text{O}_{\text{water}}) \quad (2)$$

To determine whether the oxygen isotope compositions varied between sites, we first tested if the data sets were normally distributed using a Shapiro-Wilk test. As the data from core C18 were not normally distributed ( $w = 0.977$ ,  $p = 0.037$ ), Wilcoxon  $\mu$ -tests were used to compare groups.

### 3. Results

#### 3.1 Chronology

The age offset due to ‘old carbon’ in the Coorong South Lagoon was calculated by comparing the  $^{14}\text{C}$  age of bivalves from the depth corresponding with the first occurrence of *Pinus* pollen in core C18. In other South Lagoon cores, gamma spectrometry-based  $^{210}\text{Pb}$  analyses indicate that the first occurrence of *Pinus* in the sediments denotes  $1955 \pm 5$  CE ( $-5 \pm 5$  years BP; Krull et al., 2009). This  $^{210}\text{Pb}$  derived age was estimated to equate to  $169 \pm 10$   $^{14}\text{C}$  years BP which was subtracted from the equivalent measured radiocarbon age ( $985 \pm 30$   $^{14}\text{C}$  years BP) to produce an age offset of  $816 \pm 40$   $^{14}\text{C}$  years BP. The results of AMS radiocarbon dating are summarised in Table S1 (supplementary information). The age-depth model produced following the application of this offset to measured radiocarbon ages is shown in Figure 2. Three samples were found to be more than 500 years older than the above or below samples and were therefore deemed to be outliers and excluded from the age-depth model (Table S1). The mean basal age for core C18 is 1755 cal yr BP (195 CE).

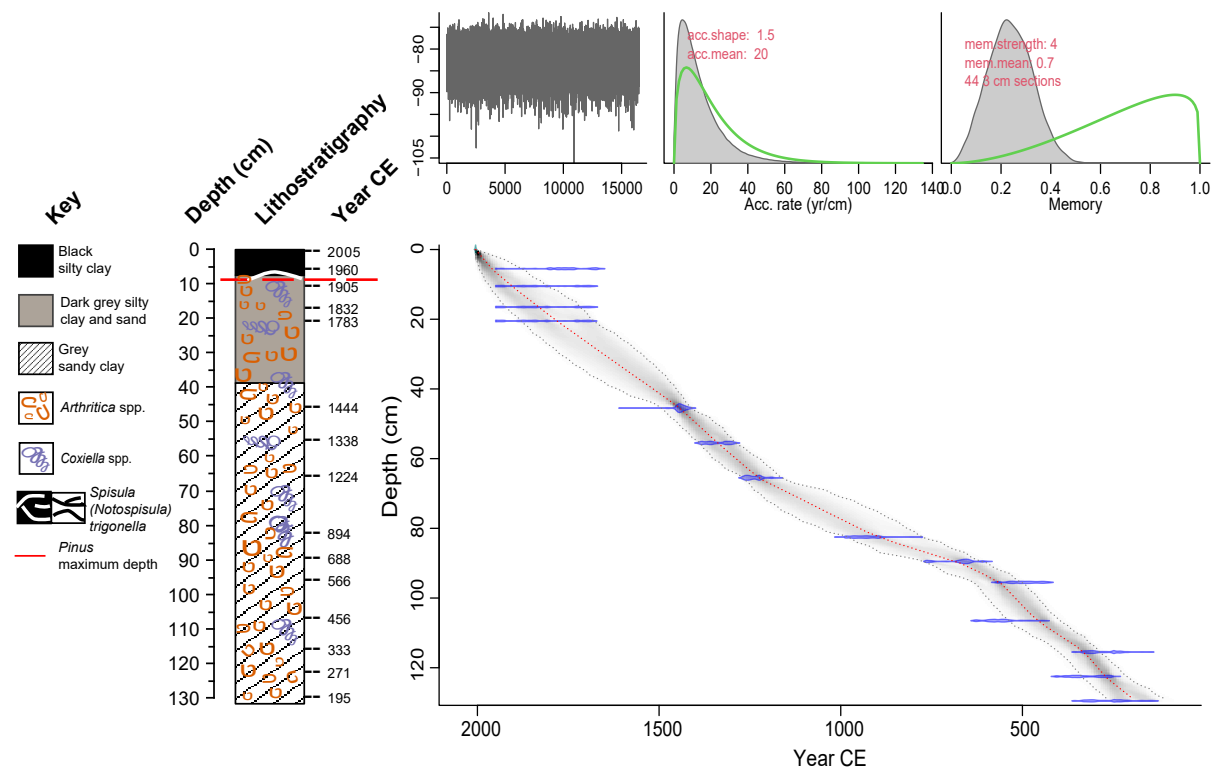


**Figure 2.** Age-depth model and lithostratigraphy for core C18. Blue markers show the probability distributions for each dated sample. The grey dotted lines indicate the modelled 95% confidence intervals, where darker shading indicate more likely ages. The modelled weighted mean age is shown by the red dotted line. Upper panels indicate the iterations performed, accumulation rate and memory used to construct the model.

### 3.2 Oxygen isotope ratios

The  $\delta^{18}\text{O}_s$  values measured from each centimetre of core C18 ( $n=123$ ) ranged from 2.86 ‰ at 104 cm to 5.20 ‰ at 61 cm (Table S2) with a mean of 3.95 ‰ (Figure 3).  $\delta^{18}\text{O}_s$  values were above average from ~269–439, 529–1065, 1218–1321 and 1789–2005 CE and below average for the time periods ~195–275, 439–529, 1065–1218 and 1299–1789 CE (Figure 3). The oxygen isotope compositions of multiple individual *A. helmsi* shells from five intervals showed high variability (Figure 4a). The median  $\delta^{18}\text{O}_s$  ranged from  $4.61 \pm 0.69$  ‰ at 119 cm (300 CE) to  $3.84 \pm 0.64$  ‰ at 57 cm (1321 CE; Figure 4a). Excluding outliers, the range of values measured was highest at 119 cm (2.66 ‰; 300 CE) and lowest at 92 cm (0.99 ‰; 631 CE).

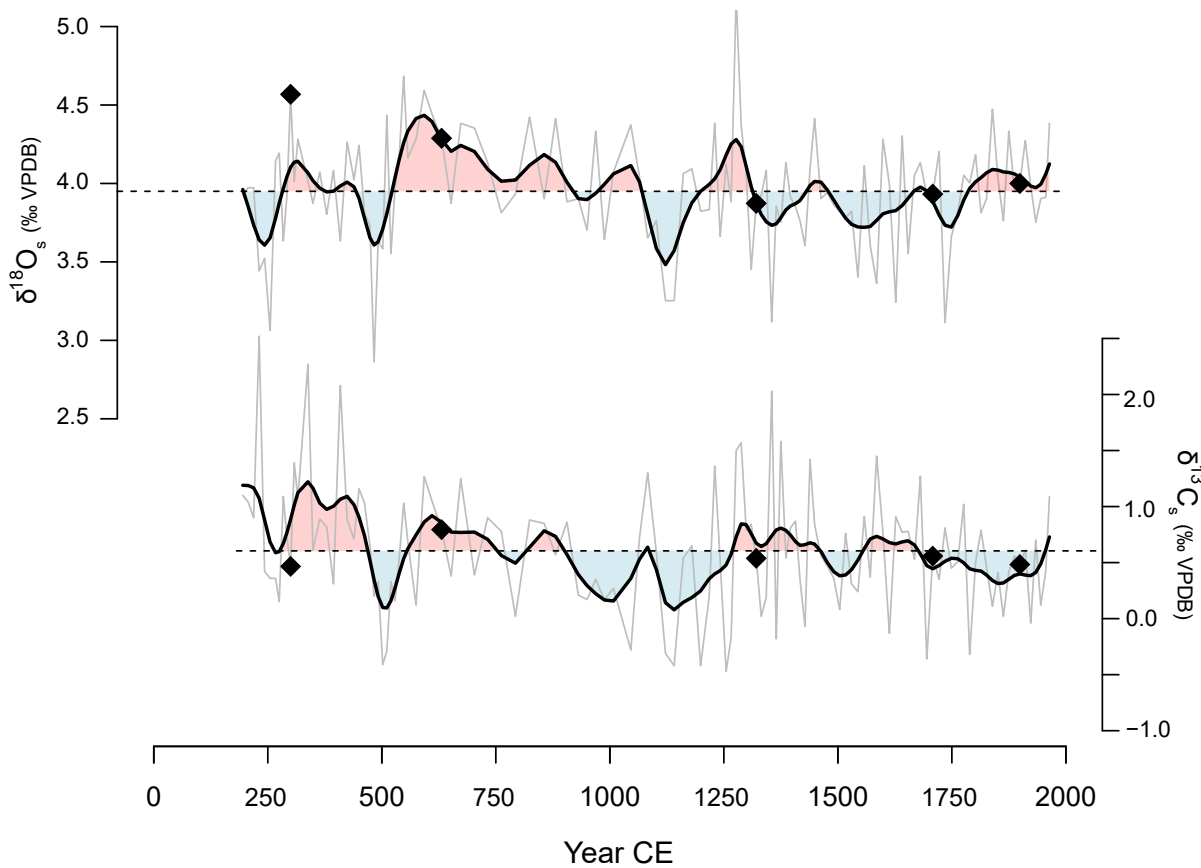


**Figure 3.** *Arthritica helmsi* oxygen and carbon isotope ratios from core C18 plotted against time. The grey line represents a bulk measurement ( $n=5$ ) from each centimetre of C18. The dashed line indicates mean values and the bold line is a smooth spline ( $\text{spar}=0.4$ ) through measured data. Blue shading indicates periods of below average isotope ratios, while the red shading indicates periods of above average isotope ratios. Black diamonds indicate where data from multiple individuals ( $n \geq 27$ ) are incorporated into the bulk curve, as displayed in Figure 4.

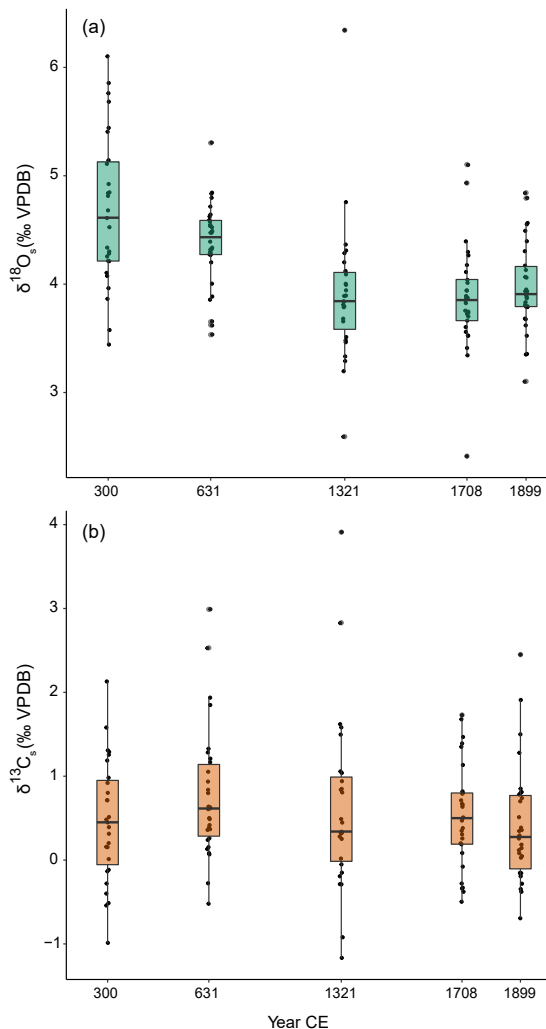


**Figure 4.** Boxplots of oxygen and carbon isotope ratios of *A. helmsi* shells. Data are obtained from analyses of multiple individual shells from depths corresponding to age 311 ( $n = 30$ ), 629 ( $n = 29$ ), 1305 ( $n = 27$ ), 1621 ( $n = 30$ ) and 1884 CE ( $n = 27$ ).

The Wilcoxon test indicated that the distribution of oxygen isotope values for shells of *A. helmsi* extracted from core C18 were not significantly different from the  $\delta^{18}\text{O}_s$  values predicted by the modern water  $\delta^{18}\text{O}$  and temperature at Jacks Point ( $p = 0.15$ ) and Parnka Point ( $p = 0.18$ ) in the Coorong South Lagoon (Figure 5a). The range of  $\delta^{18}\text{O}_s$  values measured from core C18 was, however, smaller than that predicted for modern carbonates. When the range of measured  $\delta^{18}\text{O}_s$  values from the North Lagoon was compared to the values from core C18, the two populations were significantly different ( $p < 0.001$ ; Figure 5b).

### 3.3 Carbon isotope ratios

The bulk  $\delta^{13}\text{C}_s$  values measured from each centimetre of core C18 ( $n = 123$ ) ranged from  $-0.47$  ‰ at 63 cm to  $2.52$  ‰ at 126 cm (Table S2) with a mean of  $0.60$  ‰ (Figure 3).  $\delta^{13}\text{C}_s$  values were above average from  $\sim 267$ – $474$ ,  $538$ – $906$  and  $1255$ – $1463$  CE and below average for the time periods  $195$ – $275$ ,  $439$ – $529$ ,  $1065$ – $1218$  and  $1299$ – $1789$  CE (Figure 3). The carbon isotope compositions of individual *A. helmsi* from five intervals showed high variability, though the range of variability was reasonably consistent between depths (Figure 4b). The median  $\delta^{13}\text{C}_s$  ranged from  $0.28$  ‰ at 11 cm (1899 CE) to  $0.45$  ‰ at 119 cm (300 CE; Figure 4b). The range of values measured was the highest at 119 cm ( $3.12$  ‰; 300 CE) and was the lowest at 26 cm ( $2.23$  ‰; 1708 CE).

## 4. Discussion

Proxy records of hydroclimate are required to understand variability extending past Australia's short instrumental climate record. This study presents variation in the oxygen and carbon isotope ratios of shells of *A. helmsi* spanning the last ~1750 years in the South Lagoon of the Coorong estuary system. This record is constrained by 17 radiocarbon dates allowing accurate identification of the timing of hydrological change. Here, we interpret the record in context of previous studies of Coorong palaeohydrology, in addition to regional hydroclimate reconstructions. Furthermore, the possible drivers of hydrological change in the Coorong's South Lagoon are considered.

### 4.1 Palaeohydrology of the Coorong South Lagoon

#### 4.1.1 Evidence from the oxygen isotope composition of *A. helmsi*

The processes that control the fractionation of oxygen into the carbonate of *A. helmsi* were examined in a previous study of modern populations in the Coorong Lagoons by Chamberlayne et al. (2021). A temperature dependent fractionation equation was developed in that study which determined that an increase in  $\delta^{18}\text{O}_s$  by 1 ‰ corresponds to a decrease in temperature by ~4.43 °C or an increase in the  $\delta^{18}\text{O}$  of water by 1 ‰ (Chamberlayne et al., 2021). Similarly, a change in water temperature by 1 °C is expressed as a ~0.23 ‰ change in the oxygen isotope value of *A. helmsi*. As this study sampled multiple shells per sample to reduce seasonal and inter-annual bias in the signal captured by the oxygen isotope composition of shells, we interpret this record to be more heavily influenced by the isotopic composition of water rather than temperature, given the relatively low variance in estimated average temperatures across the last 2000 years (Tardif et al., 2019). The oxygen isotopic composition of modern Coorong waters have a positive linear relationship to salinity, though the slope and strength of this relationship varies spatially (Chamberlayne et al., 2021). As such, the oxygen isotope record developed in this study is interpreted as reflecting the precipitation/evaporation (P/E) balance of the lagoon.

The oxygen isotope record from *A. helmsi* for the past ~1750 years shows periods of enhanced and reduced P/E (Figure 3), however overall the data express relatively low variance in  $\delta^{18}\text{O}_s$  values around the mean, and a lack of any distinct trend throughout the time period. In agreement with this finding, previous studies of foraminifera (Dick et al., 2011) and diatom assemblages (McKirdy et al., 2010) in sediments of the Coorong South Lagoon suggest that water quality was relatively stable for at least the 3000 years prior to the 1950s. Estimates of the pre-European salinity of the South Lagoon from microfossil and geochemical evidence range from estuarine (Dick et al., 2011) to slightly above that of seawater (Reeves et al., 2015) based



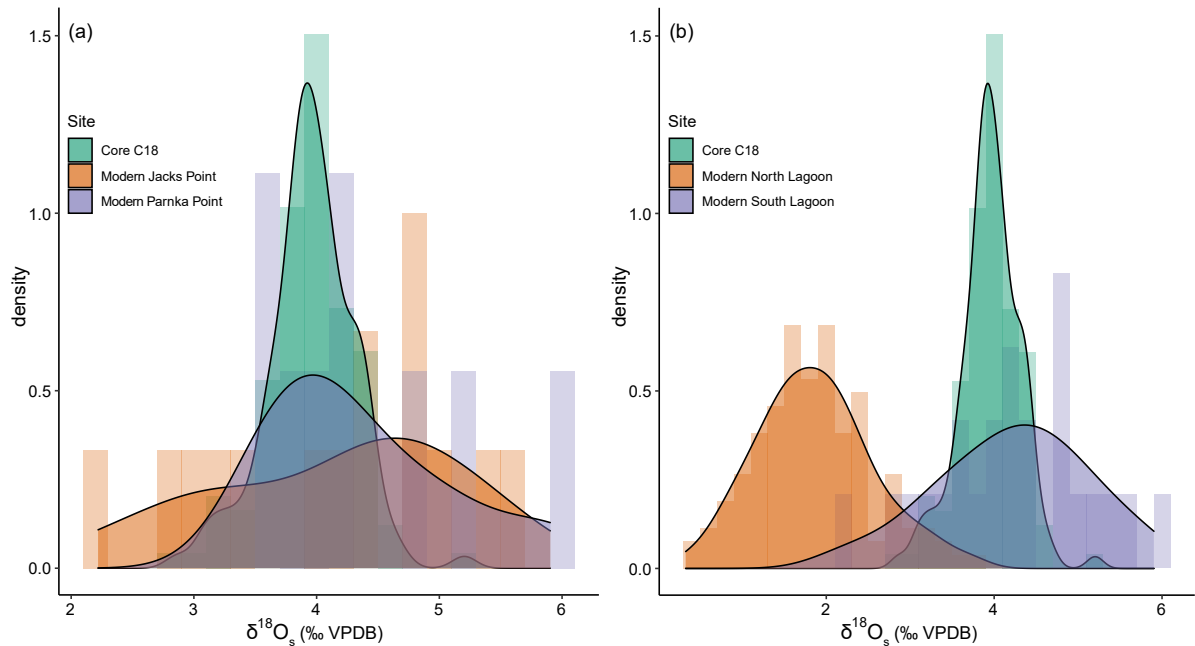


**Figure 5.** Probability density functions and histograms of *A. helmsi*  $\delta^{18}\text{O}_s$  comparing values from core C18 with (a) modern  $\delta^{18}\text{O}_s$  values estimated for two locations in the South Lagoon and (b) a comparison between the North and South Lagoon. Modern  $\delta^{18}\text{O}_s$  values for the North Lagoon are actual observations made by Chamberlayne et al. (2021).  $\delta^{18}\text{O}_s$  values for the modern South Lagoon sites Jacks Point and Parnka Point are estimates calculated using temperature and  $\delta^{18}\text{O}_w$  data from Chamberlayne et al. (2021) using the oxygen isotope fractionation equation developed in that study.

on microfauna and microflora assemblages. Excursions in hydrogen isotope ratios of *n*-alkanes and concurrent diatom-inferred reductions in salinity have highlighted two major freshening events in the last 2000 years attributed to increased surface runoff and input of groundwater (McKirdy et al., 2010). The timing of these events (~1100 and 1410 CE; McKirdy et al., 2010) possibly correspond to periods of decreased  $\delta^{18}\text{O}_s$  values in shells of *A. helmsi* (Figure 3) and hence periods of high P/E.

The presence of *A. helmsi* in the South Lagoon sediments suggests favourable conditions for this species (salinity <55; Wells and Threlfall, 1982). This finding is in agreement with the evidence that the aquatic plant *Ruppia megacarpa*, which has a salinity tolerance of 2 to 50, was the dominant species of *Ruppia* in the South Lagoon for the 3000 years prior to European arrival (Dick et al., 2011). Furthermore, a study of the past hydrology of the Coorong Lagoons focussed on the change occurring in the 20<sup>th</sup> century as a result of the construction of regulatory structures and increased land clearance and water abstraction throughout the MDB (Krull et al., 2009). It is during this period that *A. helmsi* disappear from core C18 (~1965) and a black, silty clay appears, characterised by anoxia and highly reducing conditions (Figure 2; Krull et al., 2009). The combination of high salinity and anoxia in the South Coorong Lagoon is not suitable for *A. helmsi* (Dittmann et al., 2019) and this, along with other environmental

indicators, suggests a departure from the conditions that prevailed prior to this time (Kingsford et al., 2011). However, the oxygen isotope values measured from sedimentary shells are not significantly different from the values estimated for modern populations calculated from measured water temperature and oxygen isotope composition in the South Lagoon (Figure 5a). While the range of the predicted modern values is broader for both Parnka Point and Jacks Point than those observed in core C18, the overlap in values suggests that the Coorong South Lagoon has for the past ~1750 years been an isolated, highly evaporated system.

In addition to falling within the range of predicted South Lagoon populations, the  $\delta^{18}\text{O}_s$  values from core C18 are statistically different from the  $\delta^{18}\text{O}_s$  values measured from modern populations in the Coorong North Lagoon (Figure 5b). The waters in which the shells from the North Lagoon were collected range in salinity from 0 to 46 and in  $\delta^{18}\text{O}$  from -2.81 ‰ to 3.87 ‰ (Chamberlayne et al., 2021). The higher  $\delta^{18}\text{O}_s$  values from core C18 compared to those from the modern North Lagoon suggest the South Lagoon has for the past 1750 years been a more evaporated, and therefore likely more saline, system than the contemporary North Lagoon. Evidence of the North and South Lagoons being separate geochemical systems through time has also been inferred through the analysis of carbon and nitrogen isotope ratios from sediment cores from the two lagoons (McKirdy et al., 2010). Furthermore, microfauna assemblages point to the South Lagoon being more saline than the North Lagoon for at least the last millennium (Reeves et al., 2015). As a consequence, while it is reasonable to infer that the Coorong South Lagoon has undergone a degree of salinity increase over the last century, a consequence of both climate change and the construction of the barrages, it appears that the increase in salinity was not large and that additional stressors – namely eutrophication and anoxia – almost certainly have played a significant role in the loss of biodiversity in the system. This study did not analyse  $\delta^{18}\text{O}$  in *A. helmsi* shells in sediments of the North Lagoon, though this would allow a comparison of the hydrology of each lagoon through time and therefore be an interesting avenue for future research.

#### 4.1.2 Evidence from the carbon isotope composition of *A. helmsi*

Carbon isotope ratios in *A. helmsi* shells from core C18 show periods of higher and lower values around a mean of 0.60 ‰ (Figure 3). The range of  $\delta^{13}\text{C}$  values measured in shells from the South Lagoon sediments (-0.47–2.52 ‰) are comparable to the range measured in *A. helmsi* shells from estuarine and marine environments in south-eastern Australia (-0.91–2.85 ‰; Chamberlayne et al., 2020), though are higher than the range from modern populations from the Coorong North Lagoon (-4.36–0.19 ‰; Chamberlayne et al., 2021). The relatively small and consistent range of  $\delta^{13}\text{C}$  values in C18 (Figure 4b) indicates that there have not been any large-scale persistent shifts in environmental conditions in the past 1750 years in the

South Lagoon. By comparison, in a study by Gillikin et al. (2006)  $\delta^{13}\text{C}$  values of the mussel *Mytilus edulis* exhibited a marked shift of  $> 3 \text{ ‰}$  between a marine to an estuarine site, but no comparable change is observed in our data. Comparison to modern populations from the South Lagoon are not possible due to the lack of living *A. helmsi* due to unsuitable contemporary conditions (Dittmann et al., 2019).

The controls on the fractionation of carbon isotopes into *A. helmsi* are not well understood (Chamberlayne et al., 2021). Previous studies have suggested that ambient dissolved inorganic carbon ( $\text{DIC}_{\text{water}}$ ) and diet can be controlling factors, and as such  $\delta^{13}\text{C}$  in bivalve shells can record processes such as estuarine mixing and ecosystem metabolism (McConnaughey and Gillikin, 2008; Poulain et al., 2010). *A. helmsi* are filter feeders (Ponder, 1998) and have a substantial input of terrestrial and freshwater material in their diet (Lautenschlager et al., 2014). Changes in water sources and relative inputs may therefore alter the diet of *A. helmsi* as well as affecting  $\text{DIC}_{\text{water}}$ . Fluvially transported  $\text{DIC}_{\text{water}}$  typically has a lower  $\delta^{13}\text{C}$  than marine waters (McConnaughey and Gillikin, 2008), which could be a contributing factor to the modern population from the North Lagoon recording lower  $\delta^{13}\text{C}$  values than the shells from core C18 in the South Lagoon. Oxygen and hydrogen isotope compositions of waters from the modern North and South Lagoons showed that the North Lagoon is primarily recharged by River Murray waters while the South Lagoon receives freshwater from rainfall via precipitation, groundwater and run-off (Chamberlayne et al., 2021). The difference in carbon isotope values in *A. helmsi* from core C18 and living shells in the North Lagoon are consistent with this finding, although studies exploring the relationship between shell  $\delta^{13}\text{C}$  and  $\text{DIC}_{\text{water}}$  are required further validate this interpretation.

## 4.2 Regional coherence of hydroclimate variability

### 4.2.1 500–1000 CE

The *A. helmsi* oxygen isotope record (Figure 3) suggests multi-decadal to centennial scale variability in moisture balance throughout the past  $\sim 1800$  years in the Coorong South Lagoon. A significant period of drier than average conditions occurred from  $\sim 500$  to 1000 CE. This period of aridity is also recorded in a diatom-inferred lake-water conductivity (salinity) record from Lake Surprise, western Victoria (Figure 6; Barr et al., 2014). From  $\sim 650$ –850 CE, conductivity was high in Lake Surprise and combined with a corresponding increase in the proportion of littoral diatom species suggests a reduction in lake depth during this time period (Barr et al., 2014). Warmer temperatures and lower lake-levels are also inferred by the increased frequency of aragonite laminae in the sediments of Lake Keilambete and Lake Gnotuk, also in western Victoria (Figure 6; Wilkins et al., 2013). Furthermore, alkenone-derived sea surface temperatures (SST) in the Great Australian Bight offshore South Australia show a warm anomaly

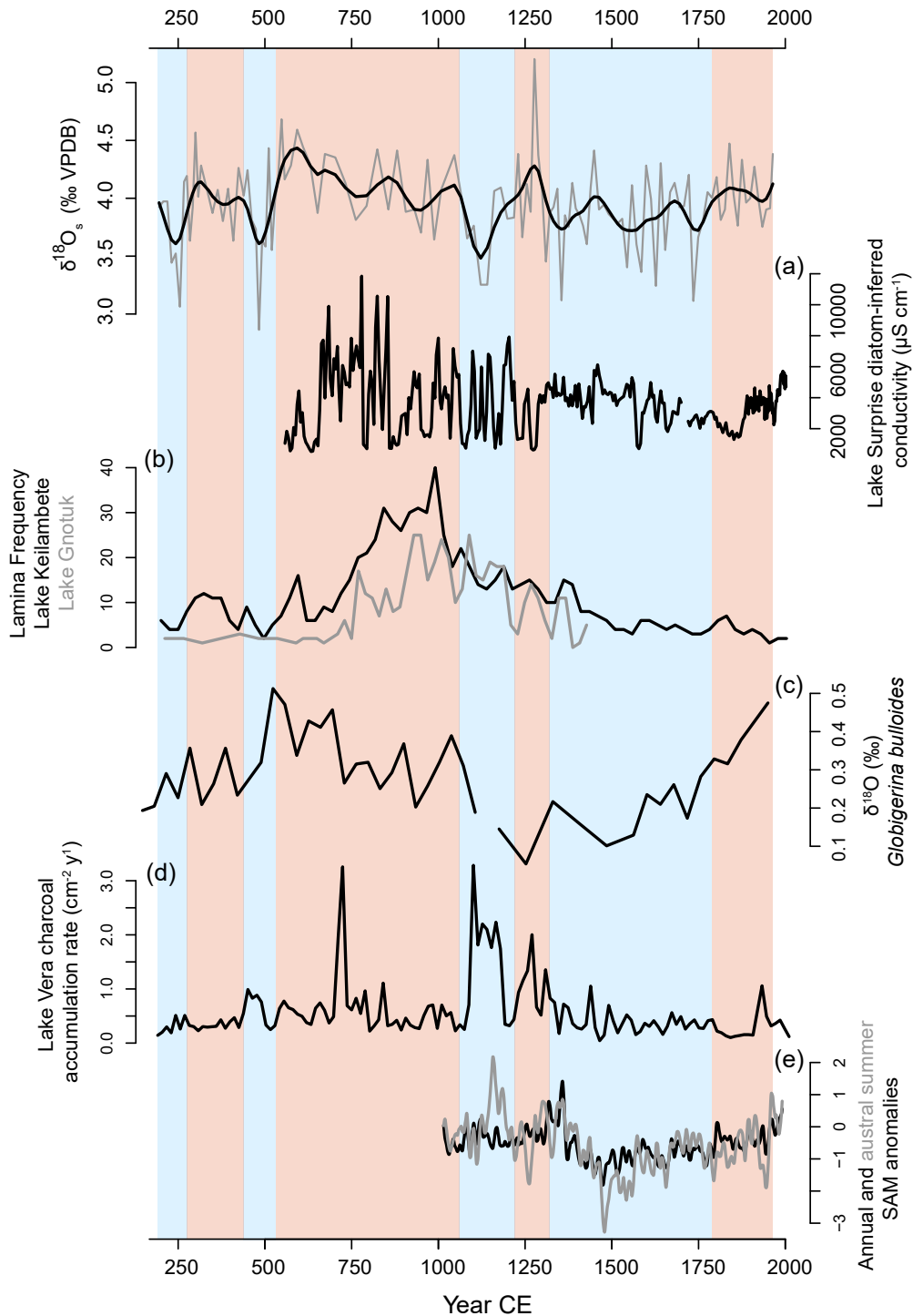


**Figure 6.**  $\delta^{18}\text{O}_s$  from core C18 *A. helmsi* shells compared against: (a) Diatom-inferred lake conductivity from Lake Surprise, Victoria, Australia (Barr et al., 2014); (b) carbonate lamina frequency in the sediments of Lake Keilambete and Lake Gnotuk, Victoria, Australia (Wilkins et al., 2013); (c)  $\delta^{18}\text{O}$  of *Globigerina bulloides* from Murray Canyon core MD03-2611 (Moros et al., 2009); (d) Charcoal accumulation rate in the sediments of Lake Vera, Tasmania, Australia (Fletcher et al., 2018); (e) Austral summer and annual mean Southern Annular Mode index reconstructions (Dätwyler et al., 2018). Red and blue shading represents periods of higher and lower than average *A. helmsi*  $\delta^{18}\text{O}_s$  respectively.

from 650 to 950 CE despite an overall cooling trend in the late Holocene (Perner et al., 2018). Agreement between these records from western Victoria and offshore South Australia show that the period of aridity from ~ 500 to 1000 CE appears to be captured among the relatively few high-resolution records of south-eastern Australian hydroclimate variability covering this time period. However not all records from the region have found this time period to be warm or dry. Fletcher et al. (2018) concluded that the phase from 1400 to 1000 years BP was relatively wet in Tasmania from their analysis of pollen and charcoal in lake sediments (Figure 6), though vegetation based records can be less sensitive to hydroclimate at decadal to centennial scales.

#### 4.2.2 1300–1800 years CE

A significant period of high moisture balance from ~ 1300 to 1800 CE was evident in the  $\delta^{18}\text{O}_s$  record from the Coorong (Figure 3). The timing of this event corresponds with the period known as the Little Ice Age (LIA), a period of significant global climate change including cooling over the Northern Hemisphere continents (Gebbie and Huybers, 2019). Several other sites in south-eastern Australia have also recorded climates with high effective moisture during this time period suggesting a degree of regional coherence. Lakes in western Victoria showed low variability with reconstructions indicating high P/E ratios prior to 1840 CE (Jones et al., 2001), low conductivity at Lake Surprise from ~1400 to 1880 CE (Figure 6; Barr et al., 2014) and increasing lake levels in Lake Keilambete after 1500 CE (Wilkins et al., 2013). Furthermore, oxygen isotope ratios in the planktonic foraminifer species *Globigerina bulloides* from marine sediments offshore South Australia indicate that the LIA was possibly a prominent cold phase (Figure 6; Moros et al., 2009).

A recent study examining coherent variability in proxy records of south-eastern Australia hydroclimate during the last 1200 years has identified two vectors interpreted to reflect hydroclimate changes (Dixon et al., 2019). The statistical analysis included eight proxy records which met stringent criteria for suitability in the analysis as outlined in Dixon et al. (2017). The analysis suggests an increase in effective moisture between 900 and 1750 CE and generally wetter conditions between 1400 and 1750 CE (Dixon et al., 2019). The agreement of the results of this regional synthesis with the interpretation of the Coorong oxygen isotope record suggests that hydroclimate variability in the Coorong may have been consistent with broader, regional scale variability and climate forcing. This outcome is not necessarily surprising, given the size and geographic range of the Murray Darling Basin across south-eastern Australia.

### 4.3 Drivers of hydroclimate in the Coorong South Lagoon

Rainfall in south-eastern Australia is driven by multiple large-scale ocean-atmosphere interactions including ENSO, IOD and SAM which can effect autumn, summer and spring

rainfall on different timescales (Gallant et al., 2012; Risbey et al., 2009). As such, the moisture balance in the Coorong is controlled by multiple and co-varying drivers and so is difficult to attribute to a single climate process. Of those drivers, the effect of ENSO on hydroclimate in south-eastern Australia during the last two millennia presents a conundrum, since the transition from the Medieval Climate Anomaly (MCA) to LIA in the Northern Hemisphere (e.g. Wanamaker et al., 2012) is often inferred to have coincided with a shift from a more La Niña-like climate towards El Niño dominance (Mann et al., 2009; Perner et al., 2018). In south-eastern Australia, however, this shift is one towards wetter climate during the LIA, thus contrasting with the expected relationship between El Niño-like climates and drought (Wang and Hendon, 2007).

In a recent review of palaeoclimate informed IOD trends, variability and interactions, Abram et al. (2020) propose that changes in mean hydroclimate from prolonged periods of drier or wetter than average conditions could be explained by changes in the strength of interannual IOD and ENSO variability rather than changes in the mean state of either forcing. Furthermore, studies of recent droughts in Australia have concluded that the lack of La Niña and negative IOD events, hence reduced interannual variability, is responsible for prolonged drought conditions (King et al., 2020; Ummenhofer et al., 2009). The shift from dry to wet conditions observed in the Coorong and other south-eastern Australian records around 1300 CE broadly coincides with mid-millennium increase in the variability of IOD and ENSO in the eastern equatorial Indian Ocean (Abram et al., 2020b), and amplified ENSO variability in the tropical Pacific (Rustic et al., 2015). Furthermore, low ENSO variability from 0–1000 CE (Tardif et al., 2019) corresponds with mostly dry conditions in the South Lagoon and south-eastern Australia.

The southern westerly winds (SWW), which are largely described by the SAM index, are also known to impact hydroclimate in south-eastern Australia (Marshall, 2003; Risbey et al., 2009), particularly the generation of frontal rainfall during the winter, albeit over shorter timescales than ENSO and the IOD (King et al., 2020). Positive phases of SAM, in association with a southerly shift of the SWW, have been related to reduced rainfall in south-eastern Australia in several studies (Cai and Cowan, 2006; Hendon et al., 2007; Risbey et al., 2009). Proxy data based reconstructions of SAM show a negative trend from ~1300 CE (Abram et al., 2014; Dätwyler et al., 2018) coinciding with the shift from dry to wet hydroclimate in the South Lagoon (Figure 6). However, this observation contrasts with inferred period of dry conditions recorded by pollen and charcoal data from lake sediments in Tasmania, which are interpreted to reflect a positive SAM anomaly between 950–1450 CE (Fletcher et al., 2018). This period is inferred to have been a period of both wet (~1000–1200 CE) and dry (1200–1300) conditions in the Coorong (Figure 6). It is possible that the timing of positive SAM events could cause this variation. A high index polarity of SAM during winter has been found to result in decreased

daily rainfall over southeast and southwest Australia, whereas during summer it is associated with decreased rainfall in western Tasmania but increased rainfall in the south-eastern region of mainland Australia (Hendon et al., 2007). As a consequence, differences in the seasonal effects of SAM on the climate of mainland Australia and Tasmania may explain the apparent differences in timing of wet and dry periods between the two regions. Reconstructions of SAM during the last millennium suggest increased Austral summer anomalies at ~1150 CE, which were not evident in annual SAM anomalies which instead peak at ~1300 CE (Figure 6; Dätwyler et al., 2018). The temporal similarities in summer and annual positive SAM events and the wet and dry phases in the Coorong suggest that the season of SAM anomalies may therefore be an influential driver of multi-decadal to centennial scale hydroclimate variability in the Coorong, and possibly over regional south-eastern Australia.

## 5. Conclusions

This study aimed to examine hydrological change over the last 1750 years in the Coorong South Lagoon, South Australia, through the analysis of oxygen and carbon isotopes of bivalve shells preserved in lagoonal sediments. Variability in  $\delta^{18}\text{O}_s$  was interpreted as an inverse function of the balance of precipitation over evaporation in the Coorong's catchment. The overall range of  $\delta^{18}\text{O}_s$  values measured from shells of *A. helmsi* suggest that the modern day amount of evaporative enrichment of water in the Coorong South Lagoon has not shifted markedly compared to the baseline set over the last 1750 years, during which time the South Lagoon has always been a highly evaporated water body. Furthermore, the sedimentary  $\delta^{18}\text{O}_s$  values differ significantly from those in the modern day North Lagoon, reinforcing previous suggestions that the two lagoons have evolved as separate systems and that the modern North Lagoon is not an analogue for the pre-impacted South Lagoon. Two extended periods of low and high P/E were inferred from ~530 to 1050 and ~1300 to 1790 respectively, consistent with other hydroclimate records in the region, in turn suggesting a common driver for multi-decadal to centennial scale hydroclimate variability in south-eastern Australia. Comparison with reconstructed indices for major ocean-atmosphere interactions suggest an importance of the timing of SAM anomalies on hydroclimate in the Coorong, while variability in IOD and ENSO may have contributed to changes in mean state. This study contributes to our understanding of the mechanisms of natural hydrological variability in the Coorong South Lagoon. By refining knowledge of the influence of large-scale climate drivers over hydroclimate at the Coorong and across south-eastern Australia, such data can assist in understanding the resilience of these hydrological systems to long term trajectories of climatic change.

## Acknowledgements

We would like to thank Mark Rollog for his assistance with stable isotope analyses. This project was undertaken while BC was the recipient of an Australian Postgraduate Award and an Australian Institute of Nuclear Science and Engineering (AINSE) Honours Scholarship. We acknowledge the Coorong, Lower Lakes and Murray Mouth region and surrounding areas as Ngarrindjeri Country and thank the Ngarrindjeri Regional Authority for permission to undertake the coring. Coring, and radiocarbon dating obtained by DH, was funded by Australian Research Project LP0667819.

## References

- Abram, N.J., Hargreaves, J.A., Wright, N.M., Thirumalai, K., Ummenhofer, C.C., England, M.H., 2020a. Palaeoclimate perspectives on the Indian Ocean Dipole. *Quat. Sci. Rev.* 237, 106302. <https://doi.org/10.1016/j.quascirev.2020.106302>
- Abram, N.J., Mulvaney, R., Vimeux, F., Phipps, S.J., Turner, J., England, M.H., 2014. Evolution of the Southern Annular Mode during the past millennium. *Nat. Clim. Chang.* 4, 564–569. <https://doi.org/10.1038/nclimate2235>
- Abram, N.J., Wright, N.M., Ellis, B., Dixon, B.C., Wurtzel, J.B., England, M.H., Ummenhofer, C.C., Philiposian, B., Cahyarini, S.Y., Yu, T.L., Shen, C.C., Cheng, H., Edwards, R.L., Heslop, D., 2020b. Coupling of Indo-Pacific climate variability over the last millennium. *Nature* 579, 385–392. <https://doi.org/10.1038/s41586-020-2084-4>
- Barr, C., Tibby, J., Gell, P., Tyler, J., Zawadzki, A., Jacobsen, G.E., 2014. Climate variability in south-eastern Australia over the last 1500 years inferred from the high-resolution diatom records of two crater lakes. *Quat. Sci. Rev.* 95, 115–131. <https://doi.org/10.1016/j.quascirev.2014.05.001>
- Blaauw, M., Christen, J.A., 2011. Flexible Paleoclimate Age-Depth Models Using an Autoregressive Gamma Process. *Bayesian Anal.* 6, 457–474. <https://doi.org/10.1214/11-BA618>
- Cai, W., Cowan, T., 2006. SAM and regional rainfall in IPCC AR4 models: Can anthropogenic forcing account for southwest Western Australian winter rainfall reduction? *Geophys. Res. Lett.* 33, 1–5. <https://doi.org/10.1029/2006GL028037>
- Chamberlayne, B.K., Tyler, J.J., Gillanders, B.M., 2021. Controls Over Oxygen Isotope Fractionation in the Waters and Bivalves (*Arthritica helmsi*) of an Estuarine Lagoon System. *Geochemistry, Geophys. Geosystems* 22, 1–18. <https://doi.org/10.1029/2021gc009769>
- Chamberlayne, B.K., Tyler, J.J., Gillanders, B.M., 2020. Environmental Controls on the Geochemistry of a Short-Lived Bivalve in Southeastern Australian Estuaries. *Estuaries and Coasts* 43, 86–101. <https://doi.org/10.1007/s12237-019-00662-7>
- Chambers J.W. & Cameron N.G., 2001. A rod-less piston corer for lake sediments: an improved,



- rope-operated percussion corer. *J. Paleolimnol.* 25, 117-122.
- Dätwyler, C., Neukom, R., Abram, N.J., Gallant, A.J.E., Grosjean, M., Jacques-Coper, M., Karoly, D.J., Villalba, R., 2018. Teleconnection stationarity, variability and trends of the Southern Annular Mode (SAM) during the last millennium. *Clim. Dyn.* 51, 2321–2339. <https://doi.org/10.1007/s00382-017-4015-0>
- Department of Agriculture, Water and the Environment, 2021. The Ramsar Convention on Wetlands. <http://www.environment.gov.au/water/wetlands/ramsar> (accessed 17 May 2021).
- Dick, J., Haynes, D., Tibby, J., Garcia, A., Gell, P., 2011. A history of aquatic plants in the Coorong, a Ramsar-listed coastal wetland, South Australia. *J. Paleolimnol.* 46, 623–635. <https://doi.org/10.1007/s10933-011-9510-4>
- Dittmann, S., Gordillo, O.L., Baring, R., 2019. Benthic Macroinvertebrate survey 2018-2019 report Coorong, Lower Lakes and Murray Mouth Icon Site. Report for the Department of Environment and Water and the Murray-Darling Basin Authority. Flinders University, Adelaide.
- Dixon, B., Tyler, J., Henley, B.J., Drysdale, R., 2019. Regional patterns of hydroclimate variability in southeastern Australia over the past 1200 years. *Earth Sp. Sci. Open Arch.* <https://doi.org/10.1002/essoar.10501482.1>
- Dixon, B.C., Tyler, J.J., Lorrey, A.M., Goodwin, I.D., Gergis, J., Drysdale, R.N., 2017. Low-resolution Australasian palaeoclimate records of the last 2000 years. *Clim. Past* 13, 1403–1433. <https://doi.org/10.5194/cp-13-1403-2017>
- Fletcher, M.S., Benson, A., Bowman, D.M.J.S., Gadd, P.S., Heijnis, H., Mariani, M., Saunders, K.M., Wolfe, B.B., Zawadzki, A., 2018. Centennial-scale trends in the Southern Annular Mode revealed by hemisphere-wide fire and hydroclimatic trends over the past 2400 years. *Geology* 46, 363–366. <https://doi.org/10.1130/G39661.1>
- Gallant, A.J.E., Kiem, A.S., Verdon-Kidd, D.C., Stone, R.C., Karoly, D.J., 2012. Understanding hydroclimate processes in the Murray-Darling Basin for natural resources management. *Hydrol. Earth Syst. Sci.* 16, 2049–2068. <https://doi.org/10.5194/hess-16-2049-2012>
- Gebbie, G., Huybers, P., 2019. The little ice age and 20th-century deep pacific cooling. *Science*. 363, 70–74. <https://doi.org/10.1126/science.aar8413>
- Gell, P., Haynes, D., 2005. A Palaeoecological Assessment of Water Quality Change in the Coorong, South Australia. Report for the Department of Water, Land and Biodiversity Conservation, South Australia, University of Adelaide, Adelaide.
- Gillanders, B.M., Munro, A.R., 2012. Hypersaline waters pose new challenges for reconstructing environmental histories of fish based on otolith chemistry. *Limnol. Oceanogr.* 57, 1136–1148. <https://doi.org/10.4319/lo.2012.57.4.1136>
- Gillikin, D.P., Lorrain, A., Bouillon, S., Willenz, P., Dehairs, F., 2006. Stable carbon isotopic composition of *Mytilus edulis* shells: relation to metabolism, salinity,  $\delta^{13}\text{C}_{\text{DIC}}$  and phytoplankton. *Org. Geochem.* 37, 1371–1382. <https://doi.org/10.1016/j.orggeochem.2006.05.001>

orggeochem.2006.03.008

- Gouramanis, C., Wilkins, D., De Deckker, P., 2010. 6000 years of environmental changes recorded in Blue Lake, South Australia, based on ostracod ecology and valve chemistry. *Palaeogeogr. Palaeoclimatol. Palaeoecol.* 297, 223–237. <https://doi.org/10.1016/j.palaeo.2010.08.005>
- Hendon, H.H., Thompson, D.W.J., Wheeler, M.C., 2007. Australian rainfall and surface temperature variations associated with the Southern Hemisphere annular mode. *J. Clim.* 20, 2452–2467. <https://doi.org/10.1175/JCLI4134.1>
- Hogg, A.G., Heaton, T.J., Hua, Q., Palmer, J.G., Turney, C.S., Southon, J., Bayliss, A., Blackwell, P.G., Boswijk, G., Bronk Ramsey, C., Pearson, C., Petchey, F., Reimer, P., Reimer, R., Wacker, L., 2020. SHCal20 SOUTHERN HEMISPHERE CALIBRATION, 0–55,000 YEARS CAL BP. *Radiocarbon* 00, 1–20. <https://doi.org/10.1017/rdc.2020.59>
- Jones, R.N., McMahon, T.A., Bowler, J.M., 2001. Modelling historical lake levels and recent climate change at three closed lakes, Western Victoria, Australia (c.1840-1990). *J. Hydrol.* 246, 159–180. [https://doi.org/10.1016/S0022-1694\(01\)00369-9](https://doi.org/10.1016/S0022-1694(01)00369-9)
- King, A.D., Pitman, A.J., Henley, B.J., Ukkola, A.M., Brown, J.R., 2020. The role of climate variability in Australian drought. *Nat. Clim. Chang.* 10, 173–183. <https://doi.org/10.1038/s41558-020-0712-5>
- Kingsford, R.T., Walker, K.F., Lester, R.E., Young, W.J., Fairweather, P.G., Sammut, J., Geddes, M.C., 2011. A Ramsar wetland in crisis the Coorong, Lower Lakes and Murray Mouth, Australia. *Mar. Freshw. Res.* 62, 255–265. <https://doi.org/10.1071/MF09315>
- Krull, E., Haynes, D., Lamontagne, S., Gell, P., McKirdy, D., Hancock, G., McGowan, J., Smernik, R., 2009. Changes in the chemistry of sedimentary organic matter within the Coorong over space and time. *Biogeochemistry* 92, 9–25. <https://doi.org/10.1007/s10533-008-9236-1>
- Lautenschlager, A.D., Matthews, T.G., Quinn, G.P., 2014. Utilization of organic matter by invertebrates along an estuarine gradient in an intermittently open estuary. *Estuar. Coast. Shelf Sci.* 149, 232–243. <https://doi.org/10.1016/j.ecss.2014.08.020>
- Lower, C.S., Cann, J.H., Haynes, D., 2013. Microfossil evidence for salinity events in the Holocene Coorong Lagoon, South Australia. *Aust. J. Earth Sci.* 60, 573–587. <https://doi.org/10.1080/08120099.2013.823112>
- Maheshwari, B.L., Walker, K.F., McMahon, T.A., 1995. Effects of regulation on the flow regime of the river Murray, Australia. *Regul. Rivers Res. Manag.* 10, 15–38. <https://doi.org/10.1002/rrr.3450100103>
- Mann, M.E., Zhang, Z., Rutherford, S., Bradley, R.S., Hughes, M.K., Shindell, D., Ammann, C., Faluvegi, G., Fenbiao, N., 2009. Global Signatures and Dynamical Origins of the Little Ice Age and Medieval Climate Anomaly. *Science.* 326, 1256–1260.
- Marshall, G.J., 2003. Trends in the Southern Annular Mode from observations and reanalyses. *J. Clim.* 16, 4134–4143. [https://doi.org/10.1175/1520-0442\(2003\)016<4134:TITSAM>2](https://doi.org/10.1175/1520-0442(2003)016<4134:TITSAM>2)

.0.CO;2

- McConnaughey, T.A., Gillikin, D.P., 2008. Carbon isotopes in mollusk shell carbonates. *Geo-Marine Lett.* 28, 287–299. <https://doi.org/10.1007/s00367-008-0116-4>
- McKirdy, D.M., Thorpe, C.S., Haynes, D.E., Grice, K., Krull, E., Halverson, G.P., Webster, L.J., 2010. The biogeochemical evolution of the Coorong during the mid- to late Holocene: An elemental, isotopic and biomarker perspective. *Org. Geochem.* 41, 96–110.
- MDBA (Murray-Darling Basin Authority), 2021, The Murray-Darling Basin and why it's important. <https://www.mdba.gov.au/importance-murray-darling-basin> (accessed 17 May 2021).
- Moros, M., De Deckker, P., Jansen, E., Perner, K., Telford, R.J., 2009. Holocene climate variability in the Southern Ocean recorded in a deep-sea sediment core off South Australia. *Quat. Sci. Rev.* 28, 1932–1940. <https://doi.org/10.1016/j.quascirev.2009.04.007>
- Mosley LM, Priestley S, Brookes J, Dittmann S, Farkaš J, Farrell M, Ferguson AJ, Gibbs M, Hipsey M, Huang J, Lam-Gordillo O, Simpson SL, Teasdale PR, Tyler JJ, Waycott M, Welsh DT (2020) Coorong water quality synthesis with a focus on the drivers of eutrophication. Goyder Institute for Water Research Technical Report Series No. 20/10.
- Murray-Wallace, C. V., 2018. Quaternary History of the Coorong Coastal Plain, Southern Australia, Quaternary History of the Coorong Coastal Plain, Southern Australia. <https://doi.org/10.1007/978-3-319-89342-6>
- Neukom, R., Gergis, J., 2011. Southern Hemisphere high-resolution palaeoclimate records of the last 2000 years. *The Holocene* 22, 501–524. <https://doi.org/10.1177/0959683611427335>
- Ngarrindjeri Nation, Hemming, S., 2019. Ngarrindjeri Nation Yarrluwar-Ruwe Plan: Caring for Ngarrindjeri Country and Culture: Kungun Ngarrindjeri Yunnan (Listen to Ngarrindjeri People Talking, in: Mosley, L., Ye, Q., Shepherd, S., Hemming, S., Fitzpatrick, R. (Eds.), Natural History of the Coorong, Lower Lakes and Murray Mouth Region (Yarrluwar-Ruwe). University of Adelaide Press, Adelaide, pp. 3–21.
- O'Donnell, A.J., Mccaw, W.L., Cook, E.R., Grierson, P.F., 2021. Megadroughts and pluvials in southwest Australia : 1350 – 2017 CE. *Clim. Dyn.* <https://doi.org/10.1007/s00382-021-05782-0>
- Paton, D.C., Rogers, D.J., Hill, B.M., Bailey, C.P., Ziembicki, M., 2009. Temporal changes to spatially stratified waterbird communities of the Coorong, South Australia: Implications for the management of heterogenous wetlands. *Anim. Conserv.* 12, 408–417. <https://doi.org/10.1111/j.1469-1795.2009.00264.x>
- Perner, K., Moros, M., De Deckker, P., Blanz, T., Wacker, L., Telford, R., Siegel, H., Schneider, R., Jansen, E., 2018. Heat export from the tropics drives mid to late Holocene palaeoceanographic changes offshore southern Australia. *Quat. Sci. Rev.* 180, 96–110. <https://doi.org/10.1016/j.quascirev.2017.11.033>
- Ponder, W.F., 1998. Superfamily Galeommatoidea, Mollusca, Part A : The Southern Synthesis. Fauna of Australia. CSIRO Publishing, Melbourne.

- Poulain, C., Lorrain, A., Mas, R., Gillikin, D.P., Dehairs, F., Robert, R., Paulet, Y.M., 2010. Experimental shift of diet and DIC stable carbon isotopes: Influence on shell  $\delta^{13}\text{C}$  values in the Manila clam *Ruditapes philippinarum*. *Chem. Geol.* 272, 75–82. <https://doi.org/10.1016/j.chemgeo.2010.02.006>
- Reeves, J.M., Haynes, D., García, A., Gell, P.A., 2015. Hydrological Change in the Coorong Estuary, Australia, Past and Present: Evidence from Fossil Invertebrate and Algal Assemblages. *Estuaries and Coasts* 38, 2101–2116. <https://doi.org/10.1007/s12237-014-9920-4>
- Risbey, J.S., Pook, M.J., McIntosh, P.C., Wheeler, M.C., Hendon, H.H., 2009. On the remote drivers of rainfall variability in Australia. *Mon. Weather Rev.* 137, 3233–3253. <https://doi.org/10.1175/2009MWR2861.1>
- Rustic, G.T., Koutavas, A., Marchitto, T.M., Linsley, B.K., 2015. Dynamical excitation of the tropical Pacific Ocean and ENSO variability by Little Ice Age cooling. *Science.* 350, 1537–1541. <https://doi.org/10.1126/science.aac9937>
- Saunders, K.M., Taffs, K.H., 2009. Palaeoecology: A tool to improve the management of Australian estuaries. *J. Environ. Manage.* 90, 2730–2736. <https://doi.org/10.1016/j.jenvman.2009.03.001>
- Scanes, E., Scanes, P.R., Ross, P.M., 2020. Climate change rapidly warms and acidifies Australian estuaries. *Nat. Commun.* 11, 1–11. <https://doi.org/10.1038/s41467-020-15550-z>
- Shao, Y., Farkaš, J., Holmden, C., Mosley, L., Kell-Duivesteyn, I., Izzo, C., Reis-Santos, P., Tyler, J., Törber, P., Frýda, J., Taylor, H., Haynes, D., Tibby, J., Gillanders, B.M., 2018. Calcium and strontium isotope systematics in the lagoon-estuarine environments of South Australia: Implications for water source mixing, carbonate fluxes and fish migration. *Geochim. Cosmochim. Acta* 239, 90–108. <https://doi.org/10.1016/j.gca.2018.07.036>
- Shao, Y., Farkaš, J., Mosley, L., Tyler, J., Wong, H., Chamberlayne, B.K., Raven, M., Samanta, M., Holmden, C., Gillanders, B.M., Kolevica, A., Eisenhauer, A., 2021. Impact of salinity and carbonate saturation on stable Sr isotopes ( $d_{88/86}\text{Sr}$ ) in a lagoon-estuarine system. *Geochim. Cosmochim. Acta* 293, 461–476. <https://doi.org/10.1016/j.gca.2020.11.014>
- Tardif, R., Hakim, G.J., Perkins, W.A., Horlick, K.A., Erb, M.P., Emile-Geay, J., Anderson, D.M., Steig, E.J., Noone, D., 2019. Last Millennium Reanalysis with an expanded proxy database and seasonal proxy modeling. *Clim. Past* 15, 1251–1273. <https://doi.org/10.5194/cp-15-1251-2019>
- Tibby, J., 2003. Explaining lake and catchment change using sediment derived and written histories: An Australian perspective. *Sci. Total Environ.* 310, 61–71. [https://doi.org/10.1016/S0048-9697\(02\)00623-X](https://doi.org/10.1016/S0048-9697(02)00623-X)
- Tulipani, S., Grice, K., Krull, E., Greenwood, P., Revill, A.T., 2014. Salinity variations in the northern Coorong Lagoon, South Australia: Significant changes in the ecosystem following human alteration to the natural water regime. *Org. Geochem.* 75, 74–86. <https://doi.org/10.1016/j.orggeochem.2014.04.013>
- Ummenhofer, C.C., England, M.H., McIntosh, P.C., Meyers, G.A., Pook, M.J., Risbey, J.S.,

- Gupta, A. Sen, Taschetto, A.S., 2009. What causes southeast Australia's worst droughts? *Geophys. Res. Lett.* 36, 1–5. <https://doi.org/10.1029/2008GL036801>
- Wanamaker, A.D., Butler, P.G., Scourse, J.D., Heinemeier, J., Eiríksson, J., Knudsen, K.L., Richardson, C.A., 2012. Surface changes in the North Atlantic meridional overturning circulation during the last millennium. *Nat. Commun.* 3. <https://doi.org/10.1038/ncomms1901>
- Wang, G., Hendon, H.H., 2007. Sensitivity of Australian rainfall to inter-El Niño variations. *J. Clim.* 20, 4211–4226. <https://doi.org/10.1175/JCLI4228.1>
- Wells, F.E., Threlfall, T.J., 1982. Salinity and temperature tolerance of *Hydrococcus brazieri* (T. Woods, 1876) and *Arthritica semen* (Menke, 1843) from the Peel-Harvey estuarine system, Western Australia. *J. Malacol. Soc. Aust.* 5, 151–156.
- Wilkins, D., De Deckker, P., Fifield, L.K., Gouramanis, C., Olley, J., 2012. Comparative optical and radiocarbon dating of laminated Holocene sediments in two maar lakes: Lake Keilambete and Lake Gnotuk, south-western Victoria, Australia. *Quat. Geochronol.* 9, 3–15. <https://doi.org/10.1016/j.quageo.2012.01.008>
- Wilkins, D., Gouramanis, C., De Deckker, P., Fifield, L.K., Olley, J., 2013. Holocene lake-level fluctuations in Lakes Keilambete and Gnotuk, southwestern Victoria, Australia. *The Holocene* 23, 784–795. <https://doi.org/10.1177/0959683612471983>

## Supplementary Information

**Table S1.** Results from the AMS  $^{14}\text{C}$  analyses used to construct the age model in Bacon (Blaauw and Christen, 2011). Italicised samples were identified as outliers and excluded from the age model. Calibrated years BP (Cal yr BP) represents the ‘best’ estimation of calibrated age calculated in the age model where present is 1950 CE. Samples with prefix ‘-Wk’ were dated at Waikato University, those with the prefix ‘OZ’ and ‘C18’ were dated at the Australian Nuclear Science and Technology Organisation (ANSTO) AMS facility (Fink et al. 2004). Core C18 was collected in 2005 and so the surface has been assigned an age of -55 years BP.

Laboratory ID	Sample type	Depth (cm)	$^{14}\text{C}$ age	$1\sigma$ error	$^{14}\text{C}$ age with offset applied	Cal yr BP	Collected and prepared by
surface		0	-55	1	-55	-55	
OZZ021	<i>A. helmsi</i> shell	5.5	1030	30	214	-10	Y. Shao
<i>OZS803</i>	<i>A. helmsi</i> shell	9.5	<i>1720</i>	25	<i>904</i>	33	<i>B. Chamberlayne</i>
OZZ022	<i>A. helmsi</i> shell	10.5	985	30	169	45	Y. Shao
OZZ023	<i>A. helmsi</i> shell	16.5	985	30	169	117.5	Y. Shao
OZS804	<i>A. helmsi</i> shell	20.5	985	25	169	167.5	Y. Shao
<i>Wk-24750</i>	<i>A. helmsi</i> shell	<i>30.5</i>	<i>1584</i>	<i>30</i>	<i>768</i>	<i>302.5</i>	<i>D. Haynes</i>
<i>OZZ024</i>	<i>A. helmsi</i> shell	<i>30.5</i>	<i>1575</i>	<i>35</i>	<i>759</i>	<i>302.5</i>	<i>Y. Shao</i>
OZS805	<i>A. helmsi</i> shell	45.5	1320	25	504	506	B. Chamberlayne
OZZ025	<i>A. helmsi</i> shell	55.5	1505	30	689	612.5	Y. Shao
OZS806	<i>A. helmsi</i> shell	65.5	1665	20	849	726	B. Chamberlayne
Wk-24751	<i>A. helmsi</i> shell	82.5	1987	30	1171	1056.5	D. Haynes
OZZ026	<i>A. helmsi</i> shell	89.5	2235	35	1419	1262	Y. Shao
OZS807	<i>A. helmsi</i> shell	95.5	2420	25	1604	1384	B. Chamberlayne
OZZ027	<i>A. helmsi</i> shell	106.5	2365	30	1549	1494	Y. Shao
OZS808	<i>A. helmsi</i> shell	115.5	2630	25	1814	1617.5	B. Chamberlayne
OZZ028	<i>A. helmsi</i> shell	122.5	2565	35	1749	1679	Y. Shao
Wk-24752	<i>A. helmsi</i> shell	129.5	2638	30	1822	1755	D. Haynes

**Table S2.** Oxygen and carbon isotope ratios from *Arthritica helmsi* samples from each centimetre of sediment from core C18 from the Coorong South Lagoon. Each sample is comprised of five shells of *A. helmsi*. Also shown is the age in years BP and year CE for each sample as determined by radiocarbon dating and age modelling (see section 2.3).

Depth interval upper (cm)	Depth interval lower (cm)	Age years BP	Age year CE	$\delta^{13}\text{C}_s$ (‰ VPDB)	$\delta^{18}\text{O}_s$ (‰ VPDB)
5	6	-14	1964	1.09	4.38
6	7	-6	1956	0.43	3.91
7	8	5	1945	0.12	3.90
8	9	16	1934	0.70	3.75
9	10	27	1923	-0.04	3.98
10	11	39	1911	0.61	4.27
11	12	51	1899	0.48	4.00
12	13	63	1887	0.56	3.96
13	14	75	1875	0.42	4.33
14	15	87	1863	0.02	3.76
15	16	99	1851	0.41	4.03
16	17	111	1839	0.11	4.47
17	18	124	1826	0.46	3.90
18	19	136	1814	0.79	3.81
19	20	148	1802	0.50	4.18
20	21	161	1789	-0.32	4.00
21	22	174	1776	1.02	4.05
22	23	187	1763	0.51	3.81
23	24	201	1749	0.45	3.66
24	25	215	1735	0.81	3.11
25	26	228	1722	0.35	4.20
26	27	242	1708	0.56	3.93
27	28	255	1695	-0.36	3.92
28	29	269	1681	1.27	4.13
29	30	282	1668	0.53	4.05
30	31	296	1654	0.78	3.55
31	32	309	1641	0.77	4.30
32	33	323	1627	0.91	3.24
33	34	337	1613	-0.13	3.99
34	35	351	1599	0.76	4.28
35	36	365	1585	1.45	3.36
36	37	379	1571	0.37	3.60
37	38	392	1558	0.91	4.11
38	39	406	1544	0.24	3.40
39	40	420	1530	0.31	3.82
40	41	433	1517	0.76	3.78
41	42	446	1504	0.08	3.82
42	43	459	1491	0.36	3.86
43	44	473	1477	0.47	3.94
44	45	487	1463	0.56	3.90
45	46	501	1449	0.84	4.41
46	47	511	1439	1.42	4.09
47	48	522	1428	-0.07	3.60

---

48	49	533	1417	0.35	3.76
49	50	543	1407	0.87	3.85
50	51	554	1396	0.81	3.91
51	52	564	1386	0.54	4.13
52	53	575	1375	1.58	3.75
53	54	585	1365	-0.18	3.85
54	55	595	1355	2.03	3.12
55	56	607	1343	0.19	4.08
56	57	618	1332	0.02	3.92
57	58	629	1321	0.54	3.87
58	59	640	1310	0.84	3.45
59	60	651	1299	0.79	4.06
60	61	662	1288	1.57	4.37
61	62	673	1277	1.50	5.20
62	63	684	1266	-0.17	3.88
63	64	695	1255	-0.47	4.12
64	65	708	1242	0.51	3.66
65	66	720	1230	1.36	4.38
66	67	732	1218	0.20	3.83
67	68	751	1199	-0.42	3.82
68	69	770	1180	0.65	4.09
69	70	789	1161	0.54	4.06
70	71	809	1141	-0.42	3.25
71	72	828	1122	-0.31	3.25
72	73	848	1102	0.59	3.76
73	74	867	1083	1.30	3.65
74	75	885	1065	0.72	4.04
75	76	904	1046	-0.28	4.37
77	78	942	1008	0.27	4.07
78	79	962	988	0.17	3.64
79	80	981	969	0.35	4.33
80	81	1000	950	0.17	3.70
81	82	1019	931	0.21	3.90
82	83	1044	906	0.86	3.88
83	84	1069	881	0.57	4.41
84	85	1094	856	0.85	3.90
85	86	1126	824	0.88	4.42
86	87	1157	793	0.02	3.93
87	88	1188	762	0.78	3.81
88	89	1218	732	0.90	4.13
89	90	1247	703	0.39	4.35
90	91	1277	673	1.25	4.38
91	92	1298	652	0.38	3.87
92	93	1319	631	0.79	4.29
93	94	1340	610	1.05	4.44
94	95	1357	593	1.27	4.59

---



---

95	96	1375	575	0.12	4.28
96	97	1393	557	0.69	4.16
97	98	1402	548	1.03	4.68
98	99	1412	538	0.53	4.16
99	100	1421	529	0.16	3.97
100	101	1430	520	0.33	3.55
101	102	1439	511	-0.29	4.43
102	103	1448	502	-0.41	3.58
103	104	1458	492	0.33	3.63
104	105	1467	483	0.20	2.86
105	106	1476	474	0.65	3.73
106	107	1488	462	1.03	3.81
107	108	1500	450	1.16	4.24
108	109	1511	439	0.71	4.02
109	110	1526	424	0.88	4.26
110	111	1541	409	2.08	3.63
111	112	1556	394	0.31	4.08
112	113	1571	379	0.82	3.80
113	114	1586	364	0.89	4.07
114	115	1601	349	0.61	3.87
115	116	1612	338	2.27	4.01
117	118	1634	316	1.07	4.28
118	119	1642	308	1.39	4.01
119	120	1650	300	0.47	4.57
120	121	1658	292	0.72	3.92
121	122	1666	284	1.09	3.63
122	123	1675	275	0.15	4.19
123	124	1683	267	0.36	4.14
124	125	1695	255	0.36	3.06
125	126	1707	243	0.42	3.52
126	127	1719	231	2.52	3.44
127	128	1731	219	0.90	3.97
128	129	1743	207	1.04	3.97
129	130	1755	195	1.10	3.92

---



---

# CHAPTER 6

Key outcomes and suggestions for future research

---



## **1. Key outcomes**

The overarching goal of this thesis was to contribute to the knowledge of hydrological variability in the Coorong Lagoons during the past 2000 years by developing a new palaeoenvironmental record using bivalve geochemistry. In the following discussion, the key outcomes of this thesis will be outlined in the context of the three specific aims. Suggestions for future research informed by the outcomes of this thesis are also discussed.

### **1.1 Understand the modern elemental and stable isotope composition of the waters in the Coorong Lagoons**

The elemental composition of the waters of the modern Coorong Lagoons and Lake Alexandrina were investigated in Chapter 3. The analysis of water samples from nine sites found that Mg, Sr and Ca respond conservatively to salinity while no relationship was found between Ba and salinity. Curvilinear relationships between Mg/Ca, Sr/Ca and Ba/Ca and salinity were consistent with previous studies. However, while the slope of the Mg/Ca and Sr/Ca curves decreased at higher salinities, the suggestion that Mg/Ca and Sr/Ca were stable in waters with a salinity higher than 10 (Dodd and Crisp, 1982) was not supported by the findings of this chapter. A previous study investigated the Mg, Sr, Ba and Ca concentrations in the Coorong Lagoons during a period of drought (Gillanders and Munro, 2012). Comparison with this study revealed that the relationship between Mg/Ca and salinity was consistent between the two different environmental scenarios, while differences in Sr/Ca and Ba/Ca behaviour was attributed to altered carbonate precipitation dynamics due to changes in the hydrological regime. Proxies that record the Mg/Ca of water may therefore serve as robust tracers for salinity in the Coorong Lagoons given the stability of the relationship through different hydrological conditions.

The environmental controls over the oxygen and hydrogen composition of Coorong and Lake Alexandrina waters were determined in Chapter 4. A number of isotope analyses on waters (n=137) facilitated the determination of a local evaporative line which was typical of an evaporative system. Therefore, the primary influence on the oxygen and hydrogen isotope values of waters was found to be evaporative enrichment, though large freshwater inputs were also reflected in the oxygen and hydrogen isotope ratios of waters in the North Lagoon. Importantly, by combining salinity and oxygen and hydrogen isotope ratios, this Chapter determined that the North Lagoon of the Coorong was primarily recharged by Murray River waters via Lake Alexandrina while the South Lagoon was primarily recharged by precipitation, either direct or via surface runoff and groundwater. The understanding gained in Chapters 3 and 4 on the drivers of stable isotope and elemental cycling in modern estuarine waters is critical

for the interpretation of the elemental and stable isotope composition of carbonate and organic materials in estuarine sediments.

## 1.2 Calibrate trace elemental and stable isotope geochemical signals in modern specimens of the bivalve *Arthritica helmsi* against modern hydrological and hydrochemical gradients

Calibration studies to identify the geochemical response in biogenic carbonate to changes in environment are required to achieve reliable interpretations of geochemical data in palaeoenvironmental studies. The controls on the geochemistry of the micro bivalve *Arthritica helmsi* were explored in Chapters 2, 3 and 4 of this thesis. In Chapter 2, specimens were sourced from museum collections over a broad spatial area to assess the geochemical response in the shells to differences in environment. The trace elemental ratios Sr/Ca, Mg/Ca and Sr/Li were significantly correlated to air temperature, while oxygen and carbon isotopes reflected broad scale environmental differences, namely differences between marine, estuarine and freshwater environments. However, uncertainties remained due to the poorly constrained environmental data available for comparison to shell carbonate geochemistry. Furthermore, *A. helmsi* were confirmed to be composed entirely of aragonite and the absence of growth rings was confirmed via microscopy and electron microprobe methods.

In Chapters 3 and 4, field studies were undertaken to further investigate and constrain the relationships observed in Chapter 2. Chapter 3 investigated the controls on the incorporation of Mg, Sr and Ba into *A. helmsi* carbonate. The Mg/Ca, Sr/Ca and Ba/Ca values measured in live collected *A. helmsi* shells from the North Coorong Lagoon (n=125) were similar to previous studies, in addition to having similar partition coefficients. However, the shell elemental ratios did not correlate to temperature, salinity, pH or elemental ratios of water, indicating that element incorporation in *A. helmsi* may be strongly influenced by biological factors. As such, the interpretation of trace elemental chemistry in *A. helmsi* currently remains unresolved and so the trace elemental chemistry of this species is not suitable for use as a proxy for past environments. In contrast, the oxygen isotope composition ( $\delta^{18}\text{O}_s$ ) of *A. helmsi* was shown in Chapter 4 to be a reliable proxy for past hydroclimate. A temperature-dependent oxygen isotope fractionation equation was developed in Chapter 4 by comparing the  $\delta^{18}\text{O}_s$  of live collected bivalves from the Coorong North Lagoon (n=131) to ambient temperature and  $\delta^{18}\text{O}$  of water. Furthermore, the results of this chapter suggest that the time to reach maximum size may be shorter for *A. helmsi* than previously proposed (approximately 9 months; Wells and Threlfall, 1982). The species-specific fractionation equation developed in Chapter 4, along with the understanding of water isotope hydrology, lay the foundations for the interpretation of oxygen isotope ratios measured on *A. helmsi* collected from the sediments of the Coorong Lagoons.

### **1.3 Contribute to the knowledge of hydrological variability in the Coorong Lagoons during the past 2000 years through the application of stable isotope and trace element calibrations to sub-fossil specimens**

The successful modern calibration of oxygen isotope ratios  $\delta^{18}\text{O}_s$  in *A. helmsi* shells in Chapter 4 was followed in Chapter 5 by an application of this relationship to shells from sediments of the Coorong South Lagoon. The outcome of Chapter 5 is the most comprehensively dated record of hydroclimate change in the Coorong South Lagoon to date. The range of  $\delta^{18}\text{O}_s$  measured in shells from sediments indicate that the South Lagoon has for the past 1750 years been a highly evaporated water body which has not shifted significantly through the duration of this record. In addition, the  $\delta^{18}\text{O}_s$  values measured on shells from the sediments of the South Lagoon were significantly different from the  $\delta^{18}\text{O}_s$  values measured in shells collected from the modern North Lagoon in Chapter 4, highlighting that the marine dominated modern North Lagoon is not a modern analogue for the pre-European South Lagoon. The precipitation/evaporation balance from the Coorong's South Lagoon was found to be relatively low between ~530 and 1050 CE and relatively high between ~1300 and 1790 which is consistent with reconstructions of hydroclimate in the wider southeastern Australian region suggesting a common driver for hydroclimate variability on multi-decadal to centennial scales. There are relatively few well dated high-resolution records of hydroclimate from southeastern Australia and so this record is a valuable contribution to understanding long term climate variability in the region. The oxygen isotope inferred hydroclimate reconstruction for the Coorong's South Lagoon presented in Chapter 5 is a significant contribution to the knowledge of hydroclimate variability in this globally important wetland. Importantly, increased knowledge of the natural range of variability can guide management efforts towards the preservation or restoration of pre-impact conditions.

## **2. Suggestions for future research**

This thesis explored the controls of the geochemistry of modern populations of *A. helmsi* with variable success. While trace element ratios could not be linked to environmental variables, oxygen isotope ratios were successfully related to temperature and the oxygen isotope ratio of ambient waters. One limitation throughout Chapters 3 and 4 was an inability to constrain the growth rate and age of individual shells of *A. helmsi*. Chemical tagging of specimens in field studies, or laboratory culture studies are required to determine the growth of this species and any growth related kinetic vital effects. In addition, higher resolution scanning electron microscopy on fractured rather than polished shells may further examine microgrowth structures. Furthermore, culture studies may be able to disentangle the various possible factors potentially contributing to elemental incorporation in bivalves.

Higher resolution methods of oxygen isotope analysis may also contribute to the understanding of growth in *A. helmsi*. In Chapters 2 and 4, the oxygen isotope ratio data obtained was measured on whole shells of *A. helmsi* due to their small size not being suitable for micro-milling and subsequent analysis. Sensitive High Resolution Ion Micro Probe (SHRIMP) mass spectrometers allow *in situ* isotopic micro-analysis with a spatial resolution of 5–20 microns and could be used in future studies to test whether *A. helmsi* precipitate carbonate in layers.

*Arthritica helmsi* based oxygen isotope records should be extended to other sites in the North and South Lagoons of the Coorong to gain a spatial understanding of evaporative effects in the system through time. In particular, a comparison of the record developed in this thesis to a record from the North Lagoon would allow the current salinity gradient to be placed into the context of the past 2000 years. Furthermore, extensive radiocarbon dating of sediment cores from other sites in the lagoons would further constrain the reservoir effect calculated in Chapter 5.

In addition to further studies investigating  $\delta^{18}\text{O}_s$  from other locations, future studies could employ further novel isotope tracers. Radiogenic strontium isotope ratios have been shown to trace source waters in the Coorong Lagoons (Shao et al., 2018) and can therefore act a water provenance tool when reconstructed through the analysis of bivalve carbonate (Holmden et al., 1997). Another potential tool to provenance water sources in the Coorong is hydrogen isotope analysis of bivalves. Chapter 4 showed that when combined, oxygen and hydrogen isotope ratios of waters reflect differing sources of fresh water input. As bivalves can record the relative distribution of hydrogen isotope values from the waters in which they have inhabited (Carroll et al., 2006), these data in addition to oxygen isotope analyses could trace changes in source water input through time. However, modern calibration studies should be undertaken for both strontium and hydrogen isotope tracers before their application in palaeoenvironmental studies.

Neither the temperature nor  $\delta^{18}\text{O}$  of water were able to be quantitatively reconstructed from the  $\delta^{18}\text{O}$  of *A. helmsi* due to the influence of both unknowns on the isotopic values of the shells. One potential avenue for quantitative temperature reconstructions from *A. helmsi* shells is the application of clumped isotope thermometry, the analysis of the frequency of bonding between heavy  $^{18}\text{O}$  and  $^{13}\text{C}$  atoms within the carbonate matrix (see Eiler, 2011 for review). A relatively recent technique, clumped isotope analyses allow the inference of temperature independent of variations in the isotope composition of source water (Ghosh et al., 2006). This technique has recently been applied to bivalve shells to reconstruct sea surface temperature (de Winter et al., 2021), however the relatively coarse precision ( $\sim \pm 2^\circ\text{C}$ ) attainable by state of the art techniques may undermine the value of this technique to infer late Holocene scale variability.



### 3. Summary

This thesis has successfully contributed to the understanding of the controls of element concentrations and isotope compositions of waters in the Coorong Lagoons. In addition, a successful calibration of oxygen isotope ratios as an environmental proxy in *A. helmsi* shells highlighted the potential of the geochemistry of this species as a proxy for past environments. The application of this calibration to shells preserved in the sediments of the Coorong South Lagoon has resulted in the development of a 1750 year record of hydrological change in this globally important wetland. Future studies aimed at further refining growth rates of *A. helmsi*, wider applications of oxygen isotope based reconstructions in *A. helmsi*, and additional investigations of novel isotope proxies are recommended. The outcomes of this thesis are a significant contribution to the knowledge of bivalve geochemistry as a proxy in palaeoenvironmental studies. Few studies investigate short-lived species such as *A. helmsi*; this thesis demonstrates the potential for applications of bivalve geochemistry based palaeoenvironmental studies in coastal wetlands in arid to semi-arid environments where traditional archives such as tree rings and ice cores are absent, and small short-lived molluscs are common. This thesis provides a significant contribution to the understanding of past hydroclimate in the Coorong South Lagoon, and has potential implications for modern hydrological management. Salinity targets and freshwater flow requirements are some management decisions which could be guided by these findings. Furthermore, this thesis contributes to the knowledge of hydroclimate in the southeast Australia region over the past 2000 years, and highlights the potential for similar techniques using bivalve geochemistry to be applied in other wetlands.

#### 4. References

- Carroll, M., Romanek, C., Paddock, L., 2006. The relationship between the hydrogen and oxygen isotopes of freshwater bivalve shells and their home streams. *Chem. Geol.* 234, 211–222. <https://doi.org/10.1016/j.chemgeo.2006.04.012>
- de Winter, N.J., Müller, I.A., Kocken, I.J., Thibault, N., Ullmann, C. V., Farnsworth, A., Lunt, D.J., Claeys, P., Ziegler, M., 2021. Absolute seasonal temperature estimates from clumped isotopes in bivalve shells suggest warm and variable greenhouse climate. *Commun. Earth Environ.* 2, 1–8. <https://doi.org/10.1038/s43247-021-00193-9>
- Dodd, J.R., Crisp, E.L., 1982. Non-linear variation with salinity of Sr/Ca and Mg/Ca ratios in water and aragonitic bivalve shells and implications for paleosalinity studies. *Palaeogeogr. Palaeoclimatol. Palaeoecol.* 38, 45–56.
- Eiler, J.M., 2011. Paleoclimate reconstruction using carbonate clumped isotope thermometry. *Quat. Sci. Rev.* 30, 3575–3588. <https://doi.org/10.1016/j.quascirev.2011.09.001>
- Ghosh, P., Adkins, J., Affek, H., Balta, B., Guo, W., Schauble, E.A., Schrag, D., Eiler, J.M., 2006.  $^{13}\text{C}$ - $^{18}\text{O}$  bonds in carbonate minerals: A new kind of paleothermometer. *Geochim. Cosmochim. Acta* 70, 1439–1456. <https://doi.org/10.1016/j.gca.2005.11.014>
- Gillanders, B.M., Munro, A.R., 2012. Hypersaline waters pose new challenges for reconstructing environmental histories of fish based on otolith chemistry. *Limnol. Oceanogr.* 57, 1136–1148. <https://doi.org/10.4319/lo.2012.57.4.1136>
- Holmden, C., Creaser, R.A., Muehlenbachs, K., 1997. Palaeosalinities in ancient brackish water systems determined by  $^{87}\text{Sr}/^{86}\text{Sr}$  ratios in carbonate fossils: A case study from the Western Canada Sedimentary Basin. *Geochim. Cosmochim. Acta* 61, 2105–2118.
- Shao, Y., Farkaš, J., Holmden, C., Mosley, L., Kell-Duivesteyn, I., Izzo, C., Reis-Santos, P., Tyler, J., Törber, P., Frýda, J., Taylor, H., Haynes, D., Tibby, J., Gillanders, B.M., 2018. Calcium and strontium isotope systematics in the lagoon-estuarine environments of South Australia: Implications for water source mixing, carbonate fluxes and fish migration. *Geochim. Cosmochim. Acta* 239, 90–108. <https://doi.org/10.1016/j.gca.2018.07.036>
- Wells, F.E., Threlfall, T.J., 1982. Density Fluctuations , Growth and Dry Tissue Production of *Hydrococcus Brazieri* (Tenison Woods, 1876) and *Arthritica semen* (Menke, 1843) in Peel Inlet, Western Australia. *J. Molluscan Stud.* 48, 310–320.





---

# Appendix 1

Published forms of journal articles arising from Chapter 2, Chapter 3 and Chapter 4.

---





# Environmental Controls on the Geochemistry of a Short-Lived Bivalve in Southeastern Australian Estuaries

Briony K. Chamberlayne<sup>1</sup> · Jonathan J. Tyler<sup>1</sup> · Bronwyn M. Gillanders<sup>2</sup>Received: 22 March 2019 / Revised: 23 September 2019 / Accepted: 16 October 2019 / Published online: 26 November 2019  
© Coastal and Estuarine Research Federation 2019

## Abstract

Geochemical signals in bivalve carbonate hold the potential to record environmental change over timescales from months to centuries; however, not all bivalves provide reliable proxy records, and modern studies are essential to calibrate these relationships prior to use in palaeo-environmental reconstruction. In this study, 19 shells of the estuarine bivalve *Arthritica helmsi*, from 14 sites in Southeastern Australia, were obtained from museum collections and analysed for trace elemental (Sr/Ca, Mg/Ca, Sr/Li and Ba/Ca) and stable isotopic ratios ( $^{18}\text{O}/^{16}\text{O}$  and  $^{13}\text{C}/^{12}\text{C}$ ). Mean Sr/Ca and Mg/Ca exhibited significant negative correlations to temperature ( $R^2 = 0.49$ ,  $p = 0.001$ ;  $R^2 = 0.25$ ,  $p = 0.02$ ) in agreement with previously published models for trace element partitioning into inorganic aragonite. In addition, the within-shell range of Sr/Ca and Mg/Ca, as measured by laser ablation ICP-MS, correlated to the temperature range ( $R^2 = 0.22$ ,  $p = 0.03$ ;  $R^2 = 0.46$ ,  $p = 0.002$ , respectively). Sr/Li ratios were also negatively correlated to temperature ( $R^2 = 0.34$ ,  $p = 0.008$ ); however, a significant difference in the model coefficients with previous studies indicates this proxy should be applied with caution. Both oxygen and carbon isotope values exhibited large differences between shells from terrestrial, estuarine and marine waters, suggesting that these stable isotopes hold a potential to record large environmental changes such as sea-level changes or freshening/salinisation in estuarine environments. This study presents the first geochemical study of *Arthritica helmsi*, highlighting its potential as an environmental tracer.

**Keywords** *Arthritica helmsi* · Trace elements · Stable isotopes · Laser ablation ICP-MS · Museum specimens

## Introduction

The shell chemistry of living and fossil bivalves has emerged as a useful tool for reconstructing various palaeo-hydrological variables including temperature (e.g. Hart and Blusztajn 1998; Schöne et al. 2004), salinity (e.g. Gillikin et al. 2005; Izzo et al. 2016), aquatic productivity (e.g. Wanamaker et al. 2009; Goodwin et al. 2013) and anthropogenic pollution

(e.g. Krause-Nehring et al. 2012; O’Neil and Gillikin 2014). Bivalves are particularly useful for such reconstructions as they periodically accrete carbonate, are widely dispersed and are abundant in archaeological and sedimentary deposits (Schöne and Gillikin 2013). Depending on the lifespan of the species, reconstructions can represent seasonal to centennial timescales. As such, multiple specimens of one species can provide material for reconstructions spanning millennia (Butler et al. 2009), allowing a unique perspective not only on long-term climate variability but also on how patterns of seasonal climate variability evolve alongside long-term climate on multi-centennial timescales (Schöne and Fiebig 2009; Carré et al. 2013). To date, many of these studies have focussed on marine taxa; however, an increasing number of studies have addressed freshwater, brackish and estuarine environments (Surge and Lohmann 2008; Kelemen et al. 2017; Geeza et al. 2018).

Several geochemical tracers have been employed to reconstruct climate and environmental variables in bivalves with perhaps the most successful being oxygen isotope ratios as a water temperature proxy, particularly in marine environments (Urey et al. 1951; Mook 1971; Grossman and Ku 1986; Carré

---

Communicated by Zhanfei Liu

**Electronic supplementary material** The online version of this article (<https://doi.org/10.1007/s12237-019-00662-7>) contains supplementary material, which is available to authorized users.

✉ Briony K. Chamberlayne  
briony.chamberlayne@adelaide.edu.au

<sup>1</sup> Department of Earth Sciences and Sprigg Geobiology Centre, The University of Adelaide, Adelaide 5005, SA, Australia

<sup>2</sup> Southern Seas Ecology Laboratories and the Environment Institute, School of Biological Sciences, The University of Adelaide, Adelaide 5005, SA, Australia

et al. 2014). However, this proxy can be difficult in freshwater or estuarine environments due to the need to constrain the oxygen isotope composition of water (Epstein and Mayeda 1953). When the oxygen isotope composition of water cannot be measured, it is often estimated from its relationship with salinity (e.g. Schöne et al. 2004; Carré et al. 2013) or is assumed to be constant over the lifetime of the shell (e.g. Andrus and Rich 2008). Alternatively, it can also be estimated from climate models in marine environments (Tindall et al. 2010; Bougeois et al. 2014). These approaches present challenges for calibration studies and environmental reconstructions in non-marine aquatic ecosystems, such as estuaries, where isotopically distinct water end members mix to an unknown proportion and monitoring data are scarce.

To overcome these challenges, a search for independent temperature and salinity proxies has been a focus of recent studies. Element to calcium ratios for Mg/Ca and Sr/Ca remains relatively constant in waters with a salinity above 10 (Dodd and Crisp 1982) and so the incorporation of these elements into biogenic carbonates is thought to be temperature controlled. These elements have been successfully used in corals to reconstruct temperature (e.g. McCulloch et al. 1996; Mitsuguchi et al. 1996), where partition coefficients are generally close to 1 (Weber 1973). However, lower partition coefficients observed in bivalves (Gillikin et al. 2006a, Izumida et al. 2011; Zhao et al. 2017; Geeza et al. 2018) support the conclusions of many studies that incorporation of trace elements into bivalve carbonate is strongly affected by vital and kinetic effects (Urey et al. 1951; Elliot et al. 2009; Wanamaker and Gillikin 2018; see Schöne 2008 for review). Despite this, many studies have successfully calibrated shell Sr/Ca or Mg/Ca against temperature (Surge and Walker 2006; Freitas et al. 2012; Mouchi et al. 2013; Tynan et al. 2016), although these relationships can differ greatly between species or even specimens within the same species (Hart and Blusztajn 1998; Lorrain et al. 2005; Schöne et al. 2011). In addition to temperature proxies, bivalve Ba/Ca has been explored as a potential salinity proxy (Gillikin et al. 2006a, 2008; Poulain et al. 2015). The Ba/Ca ratio of bivalves is closely related to the Ba/Ca ratio of water which shares a relationship to salinity in estuarine and near-shore environments (Gillikin et al. 2006a; Izzo et al. 2016). Furthermore, the carbon isotope ratio of bivalve carbonate is in part dependent on the dissolved inorganic carbonate of ambient water and as such has been investigated as a proxy for carbon processes such as upwelling (Ferguson et al. 2013) and productivity (Goodwin et al. 2013). However, both Ba/Ca and carbon isotopes are prone to metabolic and kinetic effects which make interpretation complex (McConnaughey and Gillikin 2008). Recently, there has been some success in overcoming the challenge of biological effects with the development of alternative proxies such as Sr/Li where Sr/Ca and Li/Ca are normalised to lessen the influence of vital effects (Füllenbach et al. 2015).

As the reliability of the relationship between geochemical proxies and carbonate chemistry can vary between species, it is important to validate the technique through modern calibration prior to application in palaeo-environmental studies. In these calibration studies, the carbonate chemistry of modern populations can be compared with known hydrological conditions assisting with validation of the technique and identification of species-specific relationships. Modern field-based calibration studies, however, can be both time consuming and costly, requiring frequent travel and the deployment of monitoring equipment. In addition, the seasonal and inter-annual range of variability at an individual location can often be relatively small, compared with the range of variability often measured in palaeo-environmental studies. To supplement temporal calibration studies, space-for-time substitution is a viable alternative (Tyler et al. 2008). In this respect, museum bivalve collections are a potentially valuable resource with which to preliminarily explore modern climate-geochemistry relationships. Museum archives present a wealth of readily available specimens, often collected across a wide geographical/environmental gradient. However, a lack of information upon collection, varying storage methods and obtaining reliable instrumental environmental information also mean that museum-archived specimens are not without their challenges.

The aim of this study was to investigate the utility of the short-lived micromollusc *Arthritica helmsi* (Galeommatoidea: Leptonidae) shells as a proxy for environmental geochemical processes. *A. helmsi* is widely abundant in southern Australian estuarine environments and has been found in great quantities in some sedimentary profiles, e.g. in the Coorong Lagoon, South Australia (Chamberlayne 2015). Although the mollusc is short lived, the abundance of the fossils in such environments presents the opportunity to develop sub-annual records of hydrological change in the context of multi-centennial records based on multiple individuals. Museum samples collected across a range of locations in southeastern Australia were used for calibration against environmental data covering the tolerances of this species. Specifically, the aims of this research were to: (1) examine intra-shell and intra-population geochemical variation in specimens across a temporal and environmental gradient and (2) determine relationships between shell geochemical composition and environmental parameters.

## Materials and Methods

### Specimens

*Arthritica helmsi* (Fig. 1) are endemic to southern Australian estuaries and are well adapted to these dynamic environments. Field based studies found that *A. helmsi* are active in salinities



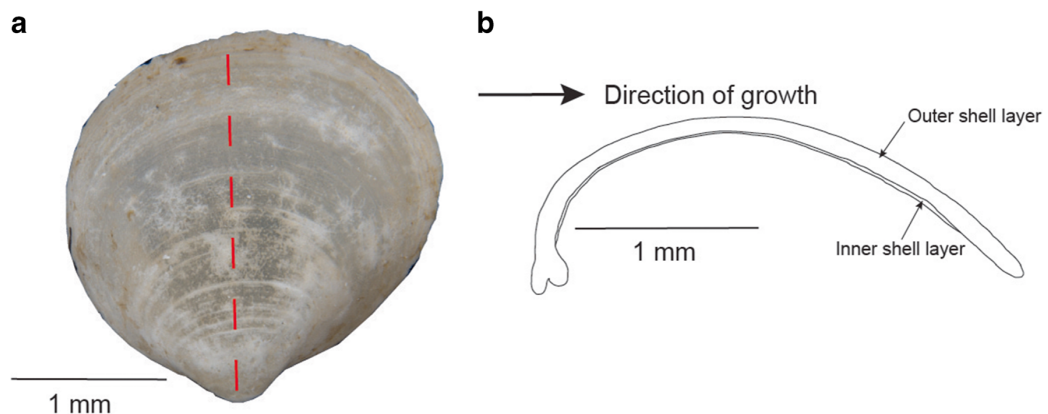


**Fig. 1** **a** *A. helmsi* shell showing the maximum growth axis (red dashed line). **b** Cross section of *A. helmsi* showing the inner and outer aragonite layers and the direction of growth. Scale bars are 1 mm

ranging from 15 to 55 with a temperature tolerance of 18–32 °C and can survive for short periods of time outside of these optimal conditions (Wells and Threlfall 1982a). The absence of discrete breeding periods can lead to population densities exceeding 8000 individuals/m<sup>2</sup> in favourable conditions (Wells and Threlfall 1982b, c). Growth is continuous at approximately 0.3 mm/month occurring over their lifetime of ~1 year, and there is an absence of visible growth rings (Wells and Threlfall 1982b).

The specimens used in this study were obtained from collections at The Australian Museum (AM; Sydney), Museum Victoria (VM; Melbourne) and Tasmanian Museum and Art Gallery (TM; Hobart). To be included in the analyses, the location and timing of collection must have been recorded; 19 shells from 14 sites along the temperate coast of southern Australia met these criteria (Table 1; Fig. 2). Samples from the Australian Museum were specified as being collected live, but specimens from Museum Victoria and Tasmanian Museum and Art Gallery did not specify whether the organisms were live upon collection. Consequently, shells which were not preserved well or showed signs of transport were not included for analysis. For subsequent analyses, we assumed that all samples were live at collection. Each shell was classified as growing in either terrestrial, marine, or estuarine waters based on the collection location (Table 1).

## Geochemical Analyses

### Sample Preparation

Shells had been stored either dry or in ethanol following collection, although the exact pre-treatment procedures of each collection were unknown (Table 1). Shells were mechanically cleaned in ultra-pure water with a resistivity of 18.2 MΩ at 25 °C and a pH of 7 before being placed in a drying oven overnight at 30 °C. In order to estimate the age of each shell, the

length of the maximum growing axis was measured with digital callipers. Due to the small size of the shell, one whole valve from each shell was crushed for whole shell stable isotope analysis. The other valve was embedded in epoxy resin spiked with 40 ppm indium to enable distinction between the shell carbonate and resin. Shells were then sectioned to approximately 0.8 mm along the growth axis using a Buehler Isomet Low-Speed Saw with diamond edge blades. Sections were polished on fine lapping paper to a thickness of 0.5 mm before being adhered to slides with indium-spiked thermoplastic glue.

### Shell Microstructure and Mineralogy

Polished thin sections were quantitatively mapped using a Cameca SXFive Electron Microprobe running the PeakSite software and equipped with 5 WDS X-ray detectors. Beam conditions were set at an accelerating voltage of 15 kV and 100 nA, utilising a focussed beam. Mapped area dimensions ranged from 0.8 to 2 mm in both *x*- and *y*-axes, at a pixel resolution of 2 μm. Pixel dwell time in all maps was set to 100 ms. Calibration and quantitative data reduction of maps was carried out in Probe for EPMA, distributed by Probe Software Inc. Colour images of the maps were processed in Surfer 10 distributed by Golden Software. Calibration was performed on certified natural standards of calcite, dolomite and Celestine from Astimex.

Each sample was mapped for three elements (Mg, Ca and Sr). Mg was mapped on three separate TAP crystals and aggregated for enhanced detection limits. Map quantification was conducted in CalcImage, a module of Probe for EPMA. Stoichiometric C was entered into the map quantification calculations for accurate matrix corrections. Background subtraction on the maps was performed via the mean atomic number (MAN) background correction (Donovan and Tingle 1996; Donovan and Armstrong 2014), omitting the need for a

**Table 1** Shown are collection location, latitude and longitude, date of collection, how samples were preserved, size of shells, whether shells were alive at the time of collection and the water source

Shell ID	Location	Latitude	Longitude	Date of collection	Preservation	Size (mm)	Live collection	Water source
AM1	Merricks Creek	− 38.40	145.15	19 Feb 1990	Dry	1.80	Yes	Terrestrial
AM2	Simpsons Bay	− 34.08	151.13	10 Aug 1975	Dry	1.68	Yes	Marine
AM3	Trunketabella Creek	− 36.05	150.05	28 Nov 1989	Dry	2.10	Yes	Terrestrial
AM4	Simpsons Bay	− 34.08	151.14	22 Sep 1972	Dry	1.70	Yes	Marine
AM5	Yowaka River	− 36.96	149.87	28 Nov 1989	Dry	1.90	Yes	Terrestrial
AM6	Tuross Inlet	− 36.08	150.13	8 Aug 1974	Dry	2.00	Yes	Estuarine
AM7	Clyde River	− 35.67	150.15	12 Oct 1974	Dry	2.30	Yes	Terrestrial
AM8	Wagonga Inlet	− 36.22	150.12	17 Sep 1974	Dry	2.00	Yes	Estuarine
AM9	Lake Macquarie	− 32.97	151.63	18 Sep 1953	Dry	2.16	Yes	Marine
AM10	Swan Bay	− 38.26	144.63	18 Sep 1973	Dry	2.00	Yes	Marine
TM1	North Oyster Bay	− 42.67	148.05	10 Jan 1967	Dry	1.10	Unspecified	Marine
TM2	North Oyster Bay	− 42.67	148.05	10 Jan 1967	Dry	0.90	Unspecified	Marine
TM3	North Oyster Bay	− 42.67	148.05	10 Jan 1967	Dry	1.40	Unspecified	Marine
VM1	Corner Inlet	− 38.90	146.32	21 Nov 1983	Ethanol 70%	2.40	Unspecified	Marine
VM2	Port Welshpool	− 38.70	146.45	20 Nov 1983	Ethanol 70%	1.50	Unspecified	Marine
VM3	Port Welshpool	− 38.70	146.45	22 Nov 1983	Ethanol 70%	2.40	Unspecified	Marine
VM4	Sea Elephant Lagoon	− 39.82	144.12	08 Mar 1980	Ethanol 70%	2.20	Unspecified	Estuarine
VM5	Sea Elephant Lagoon	− 39.82	144.12	08 mar 1980	Ethanol 70%	2.50	Unspecified	Estuarine
VM6	Painkalac Creek	− 38.47	144.10	23 Nov 1957	Dry	2.00	Unspecified	Terrestrial

second pass ‘off-peak’ map acquisition. Following this, each pixel goes through full ZAF-corrected quantification identical to traditional spot analysis. The average minimum detection limits (99% CI) in weight per cent for the quantitative maps were: Mg (0.02), Ca (0.05) and Sr (0.16).

Polished thin sections of *A. helmsi* were examined using a FEI Quanta 450 FEG Scanning Electron Microscope (SEM) at Adelaide Microscopy, The University of Adelaide. Thin sections were carbon coated prior to analysis. Images captured are backscattered electron images taken using a 15-kV beam voltage and a spot size of 4.

The carbonate mineralogy of *A. helmsi* was determined using a Bruker D8 Advance X-ray diffractometer located at the Mawson Laboratories, The University of Adelaide. Approximately 1 g of powdered sample (> 100 valves) was loaded into a sample holder with vibration to minimise orientation. Sample rotation was 30 rotations/min, scanning 2 theta from 5° to 65° with a Cu source operating at 40 kV and 40 amps.

#### Trace Element Ratio Analysis

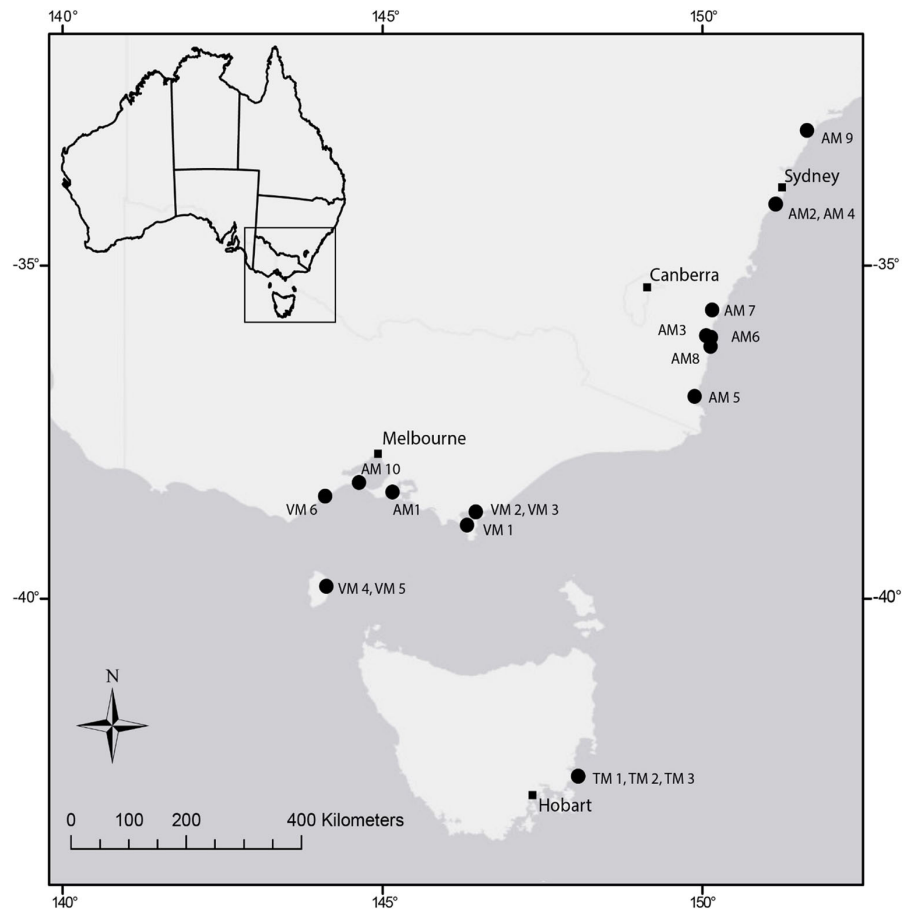
The elemental concentrations of specimens were determined using a New Wave Q-Switched Nd YAG 213 nm UV laser coupled with an Agilent 7500cs ICP-MS at Adelaide Microscopy, The University of Adelaide. Concentrations of <sup>7</sup>Li, <sup>24</sup>Mg, <sup>88</sup>Sr, <sup>138</sup>Ba and <sup>43</sup>Ca were measured in addition to <sup>44</sup>Ca as an internal standard and

<sup>115</sup>In as an indicator of resin contamination. To measure instrument drift, external standards NIST SRM 612 and the USGS carbonate standard MACS-3 were analysed periodically resulting in a mean coefficient of variation of < 4% for all elements analysed. Trace element time series were produced through continuous ablation of transects along the outer margin of the shell. Samples were pre-ablated with a 40-µm diameter spot size prior to ablation with a 30-µm spot size at 10 µm/s scan speed with a repetition rate of 10 Hz. Data reduction was performed in Iolite (Hellstrom et al. 2008; Paton et al. 2011), and elements are expressed as ratios to Ca. To reduce the effect of instrumental noise, elemental profiles were smoothed with a 7-point running mean and 7-point running median (Sinclair et al. 1998).

#### Stable Oxygen and Carbon Isotopes

A sub-sample of approximately 100 µg crushed whole shell carbonate powder was used for stable isotope analysis. Samples were flushed with helium and then acidified with 105% phosphoric acid at 70°C using a Nu Instruments GasPrep, with resultant CO<sub>2</sub> analysed for <sup>18</sup>O/<sup>16</sup>O and <sup>13</sup>C/<sup>12</sup>C with a Nu Instruments Horizon continuous flow isotope ratio mass spectrometer. Repeat measurements of laboratory standards ANU-P3 (δ<sup>18</sup>O = − 0.32‰, δ<sup>13</sup>C = + 2.2‰), UAC-1 (δ<sup>18</sup>O = − 18.4‰, δ<sup>13</sup>C = − 15.0‰) and IAEA CO-8 (δ<sup>18</sup>O = − 22.7‰, δ<sup>13</sup>C = − 5.76‰) had an analytical

**Fig. 2** Map of Southeastern Australia showing the location of *A. helmsi* collection sites outlined in Table 1



precision of  $\pm 0.1\%$ . Isotope results are reported relative to the Vienna Pee Dee Belemnite (VPDB) international standard using the standard delta ( $\delta$ ) notation in parts per thousand ( $\text{‰}$ ):

$$\delta = \left( \frac{R_{\text{sample}} - R_{\text{standard}}}{R_{\text{standard}}} \right) \times 1000 \quad (1)$$

where  $R$  is the isotope ratio ( $^{18}\text{O}/^{16}\text{O}$  or  $^{13}\text{C}/^{12}\text{C}$ ). The oxygen isotope ratio of source water was estimated for each sample from their relationship with temperature and the  $\delta^{18}\text{O}$  of carbonate using the equation of Böhm et al. (2000):

$$\delta^{18}\text{O}_w = \frac{T - (20.0 \pm 0.2)}{(4.42 \pm 0.1)} + \delta^{18}\text{O}_s \text{ for } 3^\circ\text{C} < T < 28^\circ\text{C} \quad (2)$$

where  $\delta^{18}\text{O}_w$  is the oxygen isotope value of water,  $\delta^{18}\text{O}_s$  is the oxygen isotope value of shell aragonite and  $T$  is the temperature in degrees Celsius.

### Climate Data

Elemental and isotopic compositions of the shells were regressed against local environmental data sourced from the

Scientific Information for Land Owners (SILO) data base (Jeffrey et al. 2001) as instrumental climate and environmental data from the sites at the time of collection was not available. The SILO data base provides ‘Patched Point’ daily estimates for a range of climate variables interpolated from observational climate records from the Australian Bureau of Meteorology. The number of days of climate data used in the regression for each shell was determined through an estimate of the number of days the shell had lived based on shell length and a growth rate of 0.3 mm/month, based on previous research (Wells and Threlfall 1982a).

## Results

### Climate Data

SILO data from the collection sites exhibited a 4.8 °C range in average air temperature and a 1342.5-mm range in total precipitation during the time periods defined by the age of the shell (Table 2). As air temperatures are usually correlated to water temperatures over time (McCombie 1959; Livingstone and Lotter 1998; Wurster and Patterson 2001), the SILO air

**Table 2** Temperature and precipitation information for the lifespan of each shell sourced from the SILO database

Shell ID	Age (days)	Average temperature (°C)	Temperature range (°C)	Total precipitation (mm)
AM1	180	15.77	9.81	356.60
AM2	168	15.80	8.89	929.80
AM3	210	13.65	9.14	523.40
AM4	170	15.77	9.81	356.60
AM5	190	12.42	9.52	452.60
AM6	200	16.02	8.00	1168.30
AM7	230	14.61	9.09	1495.10
AM8	200	13.85	8.10	1195.80
AM9	216	16.24	10.37	703.90
AM10	200	12.39	7.95	302.90
TM1	110	12.37	8.75	191.30
TM2	90	12.82	8.99	152.50
TM3	140	11.76	8.41	294.00
VM1	240	11.81	6.33	801.20
VM2	140	11.42	7.44	392.60
VM3	230	11.63	7.09	719.70
VM4	220	13.68	6.03	644.10
VM5	250	13.32	5.88	699.40
VM6	200	11.46	8.56	332.30

temperature was used as an approximation of water temperatures in these locations. The salinity and oxygen isotope composition of water was not measured at the time of bivalve sampling, therefore the total rainfall amount from SILO was used as a proxy for the degree of freshwater—marine mixing, which in turn is often manifest in the salinity and  $\delta^{18}\text{O}$  of estuarine waters (Bar-Matthews et al. 2003). Temperature and precipitation both varied in response to latitude with the sites at higher latitudes experiencing higher temperatures and rainfall than those at lower latitudes (Fig. S1 (Electronic Supplementary Material (ESM))).

## Geochemical Data

### Shell Microstructure and Minerology

Element maps show MgO to have varied from ~ 0.01 to 0.20 wt% and SrO to have varied from ~ 0.05 to 0.60 wt % (Fig. 3a,b). SrO is more variable in the specimen than MgO, and both elements show sections of higher concentration along the inner margin. CaO values for majority of the shell ranged from ~ 50 to 53 wt%, but there are portions which exhibit much lower (~ 47 wt%) concentration. These sections appear to occur alongside cracks in the shell. There does not appear to be any evidence of banding in any element map.

SEM images display a massive ultra-structure with a lack of banding (Fig. 3d–f). Both the umbo region (Fig. 3e) and the ventral margin (Fig. 3f) show a uniform composition with some cracking. These cracks correspond to regions of

increased magnesium and strontium and lower calcium observed in Fig. 3a–c.

The XRD pattern from a bulk sample of several individuals of *A. helmsi* corresponds with the intensity and spacing of aragonite (Fig. S2 (ESM)). Trace amounts (< 0.5%) of calcite were also present in the sample but were so minor that *A. helmsi* can be considered aragonitic.

### Shell Trace Elemental Ratios

Trace elemental data showed variation both within and between shells (Table 3; Figs. S3, S4, S5, S6, S7, S8, S9 and S10 (ESM)). Mean Mg/Ca ratios varied from 0.287 mmol/mol in shell AM9 (Lake Macquarie) to 0.754 mmol/mol in shell AM10 (Swan Bay). The largest intra-shell range was 1.15 mmol/mol in shell VM4 from Sea Elephant Lagoon which also had the highest maximum value of 1.39 mmol/mol. Mean shell Sr/Ca ratios ranged from 1.24 to 2.22 mmol/mol in shells VM1 (Corner Inlet) and VM6 (Painkalac Creek) respectively. Shell VM6 also had the highest recorded value of Sr/Ca at 2.81 mmol/mol, while shell VM3 (Port Welshpool) had the lowest maximum value (1.50 mmol/mol) and also the lowest intra-shell range (0.369 mmol/mol) of all shells. Shells VM2 and VM6 had considerably higher mean Sr/Li values (1226 and 1283 mmol/mol, respectively). The intra-shell range of Sr/Li values was highly variable with the largest being 2365 mmol/mol in AM5 (Yowaka River) and the smallest being 339.8 mmol/mol in AM2 from Simpsons Bay. Intra-shell ranges were also variable in Ba/Ca ratios

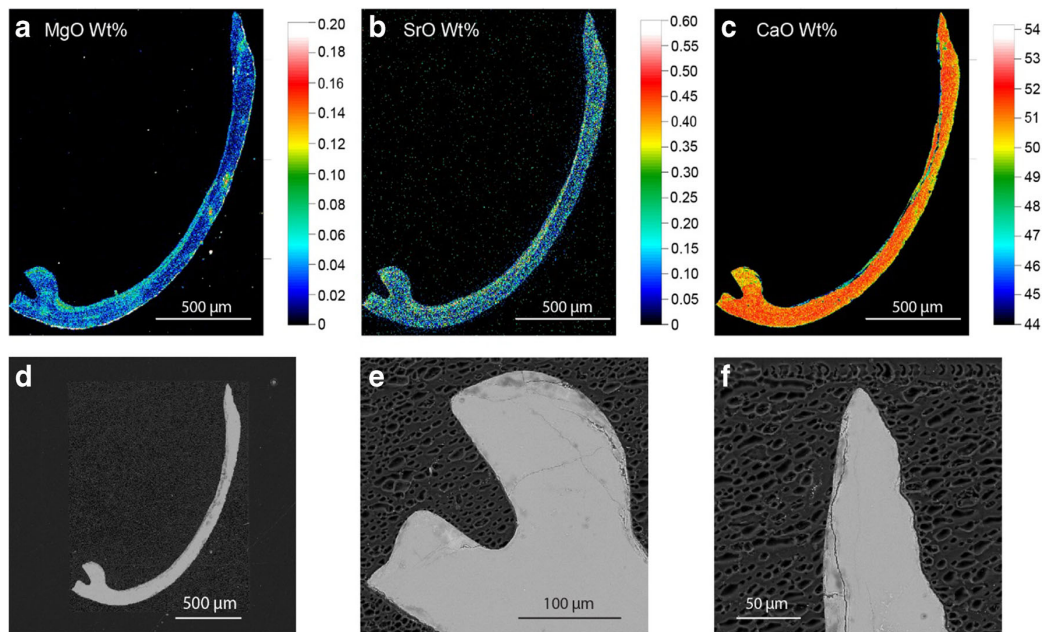


**Fig. 3** Trace element concentrations and microstructures in a thin section of *A. helmsi*; **a** MgO wt%, **b** SrO wt%, and **c** CaO wt%. **d–f** SEM images showing a massive ultra-structure in the whole shell (**d**), umbo region (**e**) and ventral margin (**f**)

which ranged from 0.797  $\mu\text{mol/mol}$  in TM3 (North Oyster Bay) to 33.3  $\mu\text{mol/mol}$  in AM8 (Wagonga Inlet). Mean values were also highly variable and the shells with the highest and lowest means also had the highest and lowest minimum values of Ba/Ca (shells AM1 and VM5). Maximum values are more variable than minimum values in all trace elemental ratios. All continuous transects had peaks that were randomly distributed throughout the shells (Figs. S3, S4, S5 and S6 (ESM)). In some specimens these peaks appear cyclical, particularly for Sr/Ca and Mg/Ca elemental ratios.

There were two collection dates where multiple shells were analysed. Shells TM1, TM2 and TM3 from North Oyster Bay, and shells VM4 and VM5 from Sea Elephant Lagoon, allowing intra-population comparison. Within-shell trace element patterns from the same location show similar trends but were not correlated in time (Fig. 4). All shells show similar ranges of trace element ratios with the exception of Ba/Ca in TM1 where the values were significantly higher than those of TM2 and TM3 (Fig. 4).

#### Shell and Water Isotopes

Whole shell  $\delta^{18}\text{O}$  values varied between shells with values ranging from  $-1.40\text{‰}$  in shell AM5 from Yowaka River to  $2.31\text{‰}$  in shell VM3 from Port Welshpool with an average of  $0.84 \pm 0.08\text{‰}$  (Table 3). The average  $\delta^{13}\text{C}$  value was  $-1.21 \pm 0.07\text{‰}$ ; values ranged from  $-10.81$  to  $2.85\text{‰}$  in shells AM3 from Trunketabella Creek and TM3 from North Oyster Bay, respectively (Table 3).  $\delta^{18}\text{O}$  and  $\delta^{13}\text{C}$  of shells showed a

positive co-variation ( $R^2 = 0.32$ ,  $p = 0.011$ ; Fig. S11 (ESM)). Calculated source water  $\delta^{18}\text{O}$  ranged from  $-3.11\text{‰}$  at Yowaka River to  $1.09\text{‰}$  at Clyde River which are realistic values for estuarine waters (Table 3).

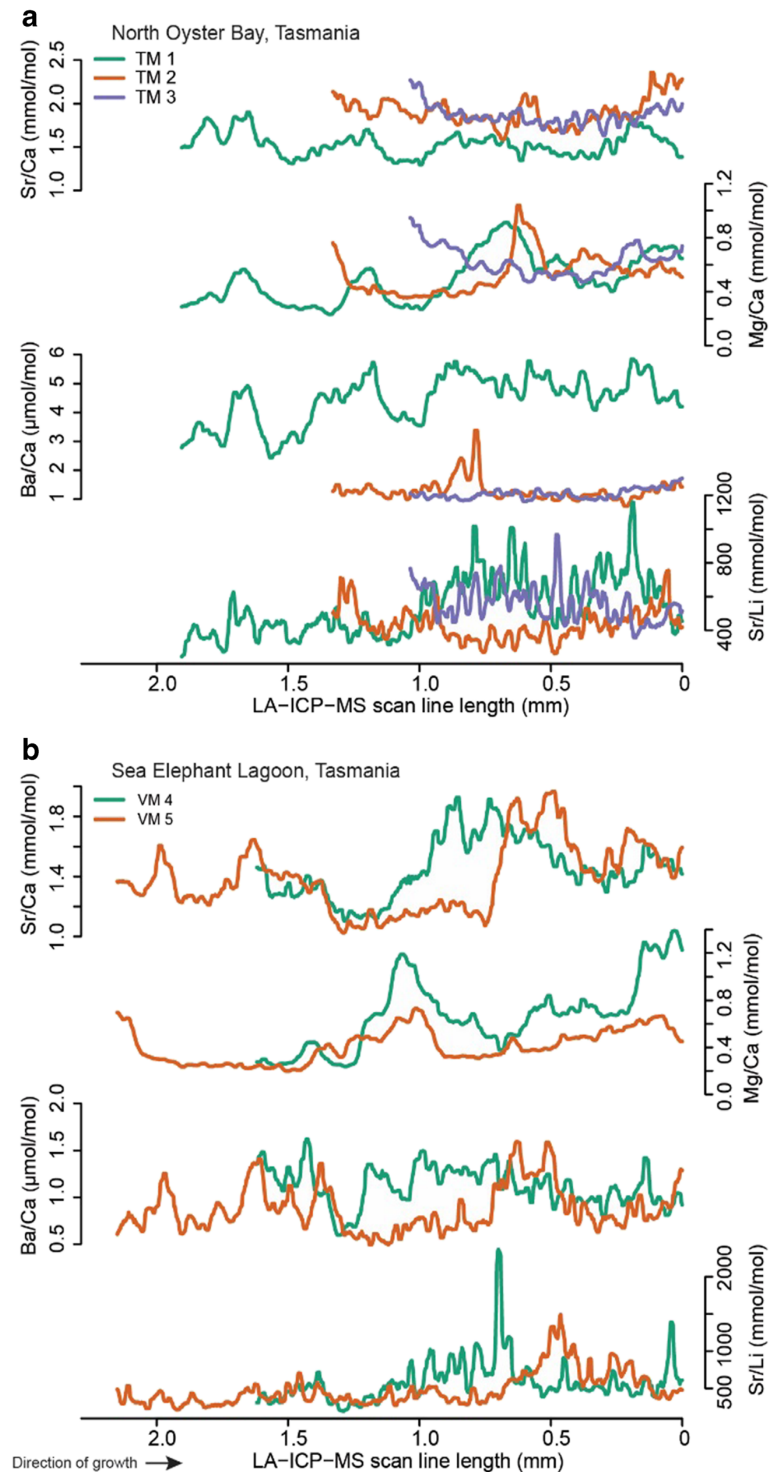
#### Geochemical–Environmental Data Relationships

Initial comparisons between shell geochemistry and environmental data indicated no correlations, however the analyses were consistently skewed by two samples, VM1 and VM3 which exhibited markedly lower Sr/Ca, Mg/Ca and Sr/Li data (Fig. 5). These samples are two of six samples that were stored in ethanol, which may offer one explanation for their anomalous values; these samples may also not have been living upon collection (Table 1). When the samples were removed from the analyses, significant relationships emerge between temperature and trace element ratios. These relationships are summarised in Table 4. Temperature was significantly negatively correlated with Sr/Ca ( $R^2 = 0.49$ ,  $p = 0.001$ ), Mg/Ca ( $R^2 = 0.25$ ,  $p = 0.023$ ) and Sr/Li ( $R^2 = 0.34$ ,  $p = 0.009$ ; Fig. 5). The predicted temperature range based on lifespan was also negatively correlated to the range of intra-shell Sr/Ca ( $R^2 = 0.22$ ,  $p = 0.003$ ) and Mg/Ca ( $R^2 = 0.45$ ,  $p = 0.002$ ; Fig. 6). The effect of including/excluding ethanol stored shells in the analysis was mixed. For Mg/Ca, the correlation with temperature increased from  $R^2 = 0.25$  to  $0.31$ ; however, for all other geochemical data, the correlation decreased when all ethanol stored shells were excluded. Similarly, there were mixed results when removing shells which were not specified as live

**Table 3** Average, minimum, and maximum Sr/Ca, Mg/Ca, Sr/Li, and Ba/Ca for *A. helmsi* specimens as well as  $\delta^{18}\text{O}$  and  $\delta^{13}\text{C}$  and predicted water  $\delta^{18}\text{O}$  for each specimen.  $\sigma$  = standard deviation

Shell ID	Average $\pm 1\sigma$ /minimum/maximum									
	Sr/Ca (mmol/mol)	Mg/Ca (mmol/mol)	Sr/Li (mmol/mol)	Ba/Ca ( $\mu\text{mol/mol}$ )	$\delta^{18}\text{O}_{\text{shell}}$	$\delta^{13}\text{C}_{\text{shell}}$	$\delta^{18}\text{O}_{\text{water}}$			
AM1	1.39 $\pm$ 0.14/1.13/1.71	0.35 $\pm$ 0.06/0.25/0.50	550.4 $\pm$ 191.0/277.8/1602.6	11.70 $\pm$ 2.60/8.19/17.79	-0.55 $\pm$ 0.03	-0.28 $\pm$ 0.04	-1.14 $\pm$ 0.07			
AM2	1.28 $\pm$ 0.13/1.08/1.63	0.43 $\pm$ 0.09/0.29/0.65	284.8 $\pm$ 52.6/132.5/472.3	1.65 $\pm$ 0.62/0.83/3.09	0.67 $\pm$ 0.04	-10.81 $\pm$ 0.03	0.09 $\pm$ 0.07			
AM3	1.71 $\pm$ 0.15/1.36/1.97	0.44 $\pm$ 0.07/0.27/0.54	650.8 $\pm$ 181.9/311.9/1364.1	2.77 $\pm$ 0.82/1.49/5.28	-1.34 $\pm$ 0.02	-9.75 $\pm$ 0.05	-2.41 $\pm$ 0.08			
AM4	1.40 $\pm$ 0.08/1.24/1.64	0.51 $\pm$ 0.10/0.36/0.83	321.4 $\pm$ 99.0/136.5/627.6	2.96 $\pm$ 0.62/1.65/4.15	0.50 $\pm$ 0.10	0.09 $\pm$ 0.04	-0.09 $\pm$ 0.07			
AM5	1.79 $\pm$ 0.17/1.52/2.24	0.40 $\pm$ 0.07/0.25/0.58	721.7 $\pm$ 361.0/194.3/2560.1	6.87 $\pm$ 3.29/1.96/15.21	-1.40 $\pm$ 0.26	-2.71 $\pm$ 0.42	-2.74 $\pm$ 0.09			
AM6	1.37 $\pm$ 0.16/1.02/1.94	0.44 $\pm$ 0.22/0.21/1.26	391.1 $\pm$ 152.5/203.6/1132.3	2.20 $\pm$ 1.00/0.65/5.28	0.61 $\pm$ 0.09	1.20 $\pm$ 0.05	0.08 $\pm$ 0.07			
AM7	1.73 $\pm$ 0.17/1.40/2.08	0.59 $\pm$ 0.10/0.39/0.80	426.1 $\pm$ 128.9/211.3/907.7	5.72 $\pm$ 2.95/2.09/20.86	2.31 $\pm$ 0.07	-4.32 $\pm$ 0.04	1.46 $\pm$ 0.07			
AM8	1.32 $\pm$ 0.24/0.97/2.10	0.55 $\pm$ 0.09/0.42/1.06	231.80 $\pm$ 116.7/82.4/522.6	9.00 $\pm$ 4.19/2.66/33.35	0.32 $\pm$ 0.05	1.75 $\pm$ 0.03	-0.70 $\pm$ 0.08			
AM9	1.49 $\pm$ 0.18/1.25/1.92	0.29 $\pm$ 0.04/0.21/0.38	348.5 $\pm$ 90.2/67.9/739.5	2.21 $\pm$ 0.39/1.51/3.11	1.42 $\pm$ 0.05	1.66 $\pm$ 0.06	0.94 $\pm$ 0.07			
AM10	1.45 $\pm$ 0.25/1.16/2.42	0.75 $\pm$ 0.23/0.37/1.23	266.5 $\pm$ 131.4/149.5/725.4	2.02 $\pm$ 0.54/1.10/3.34	1.73 $\pm$ 0.05	0.02 $\pm$ 0.05	0.38 $\pm$ 0.09			
TM1	1.57 $\pm$ 0.14/1.33/1.94	0.49 $\pm$ 0.18/0.23/0.91	538.9 $\pm$ 174.2/244.0/1158.8	4.45 $\pm$ 0.84/2.44/5.83	0.93 $\pm$ 0.09	2.10 $\pm$ 0.05	-0.43 $\pm$ 0.09			
TM2	1.91 $\pm$ 0.16/1.59/2.35	0.53 $\pm$ 0.15/0.35/1.04	433.0 $\pm$ 93.2/261.5/754.7	1.30 $\pm$ 0.36/0.75/3.37	1.39 $\pm$ 0.26	1.78 $\pm$ 0.23	0.14 $\pm$ 0.08			
TM3	1.87 $\pm$ 0.11/1.64/2.27	0.63 $\pm$ 0.11/0.47/0.95	562.3 $\pm$ 106.6/357.3/966.8	1.18 $\pm$ 0.17/0.92/1.72	1.71 $\pm$ 0.11	2.85 $\pm$ 0.01	0.22 $\pm$ 0.09			
VM1	1.24 $\pm$ 0.15/1.00/1.77	0.34 $\pm$ 0.11/0.20/0.62	298.5 $\pm$ 79.2/171.5/530.1	0.95 $\pm$ 0.17/0.63/1.51	0.67 $\pm$ 0.05	0.85 $\pm$ 0.05	-0.81 $\pm$ 0.09			
VM2	2.06 $\pm$ 0.26/1.64/2.64	0.53 $\pm$ 0.21/0.27/1.02	1226.4 $\pm$ 345.3/802.3/2563.5	1.83 $\pm$ 0.36/1.31/2.73	1.91 $\pm$ 0.06	1.06 $\pm$ 0.05	0.34 $\pm$ 0.09			
VM3	1.31 $\pm$ 0.09/1.13/1.50	0.35 $\pm$ 0.09/0.22/0.52	370.5 $\pm$ 155.6/173.9/868.9	1.75 $\pm$ 0.28/1.21/2.64	2.31 $\pm$ 0.04	-0.29 $\pm$ 0.04	0.79 $\pm$ 0.09			
VM4	1.45 $\pm$ 0.20/1.10/1.93	0.67 $\pm$ 0.30/0.24/1.39	588.7 $\pm$ 288.3/196.7/2362.3	1.12 $\pm$ 0.21/0.60/1.62	1.01 $\pm$ 0.07	-0.91 $\pm$ 0.01	-0.05 $\pm$ 0.08			
VM5	1.39 $\pm$ 0.23/1.03/1.97	0.41 $\pm$ 0.14/0.20/0.73	487.2 $\pm$ 225.6/219.3/1490.3	0.88 $\pm$ 0.25/0.49/1.59	1.43 $\pm$ 0.06	-0.81 $\pm$ 0.07	0.29 $\pm$ 0.08			
VM6	2.22 $\pm$ 0.20/1.58/2.81	0.62 $\pm$ 0.14/0.39/0.91	1283.7 $\pm$ 344.5/622.3/2231.8	6.60 $\pm$ 1.44/3.25/10.91	0.35 $\pm$ 0.03	-6.38 $\pm$ 0.09	-1.21 $\pm$ 0.09			

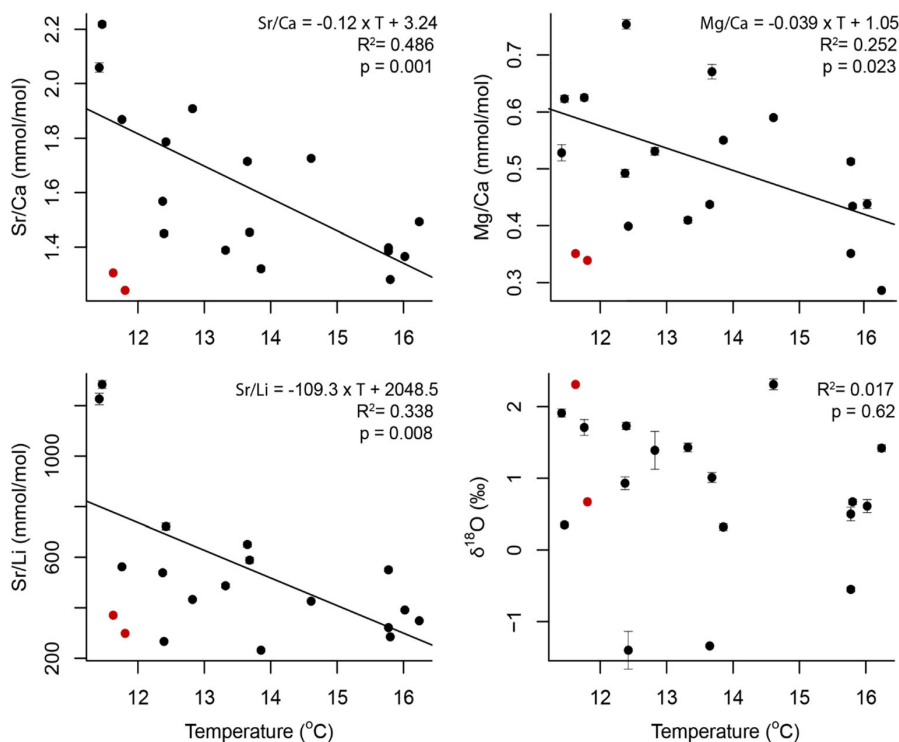
**Fig. 4** Sr/Ca, Mg/Ca, Ba/Ca and Sr/Li profiles across outer layer of shells of the same collection from **a** North Oyster Bay and **b** Sea Elephant Lagoon. The ventral margin of each shell (0 mm) represents the most recent growth before collection



collected. The only relationship to improve when these shells were excluded was Sr/Ca range and temperature range which improved from  $R^2 = 0.22$  to 0.53. Ba/Ca ratios did not correlate with any trace element or environmental data.

Shell  $\delta^{18}\text{O}$  and  $\delta^{13}\text{C}$  values did not exhibit any correlation with either temperature or rainfall, but values could be grouped based on the classification of water source for the site from which they were collected (Fig. 7). Higher values for both  $\delta^{18}\text{O}$  and  $\delta^{13}\text{C}$  were measured from sites for which

**Fig. 5** Mean Sr/Ca, Mg/Ca and Sr/Li concentrations from shell transects and whole shell  $\delta^{18}\text{O}$  versus temperature in individual *A. helmsi* shells. Samples in red (VM1 and VM3) are excluded from all linear models. Error bars are  $\pm$  SE



waters were terrestrially derived to those which had marine waters. Terrestrially sourced sites showed a greater range in both  $\delta^{18}\text{O}$  and  $\delta^{13}\text{C}$  (3.71‰, 8.1‰) compared with estuarine (1.11‰, 2.66‰) and marine waters (1.41‰, 3.13‰). Mean  $\delta^{13}\text{C}$  values of -6.8, 0.31 and 1.16‰ for terrestrial, estuarine and marine waters respectively indicated terrestrial waters were isotopically distinct from the estuarine and marine waters. Mean  $\delta^{18}\text{O}$  shell values also showed an increase from terrestrial (-0.126‰) to estuarine (0.843‰) to marine waters (1.28‰). However, the range of shell  $\delta^{18}\text{O}$  values in each category indicated that terrestrial waters were not distinct from estuarine and marine waters (Fig. 7). This trend was mirrored in the inferred source water  $\delta^{18}\text{O}$  where mean values also

increased from terrestrial (-1.58‰) to estuarine (-0.47‰) to marine (-0.17‰) waters, although a large range of

**Table 4** Relationship between geochemical analyses and temperature variables. Shown are the equations for the models of best-fit and the R-squared values.

Analysis	Variable	Relationship	R <sup>2</sup>
Sr/Ca mean	Temperature mean	$\text{Sr/Ca} = -0.12 \times T + 3.24$	0.486
Sr/Ca range	Temperature range	$\text{Sr/Ca} = -0.11 \times T + 1.70$	0.222
Mg/Ca mean	Temperature mean	$\text{Mg/Ca} = -0.039 \times T + 1.05$	0.252
Mg/Ca range	Temperature range	$\text{Mg/Ca} = -0.158 \times T + 1.91$	0.455
Sr/Li mean	Temperature mean	$\text{Sr/Li} = -109.3 \times T + 2048.5$	0.338
Sr/Li range	Temperature range	No relationship	0.047
Ba/Ca mean	Temperature mean	No relationship	0.012
Ba/Ca range	Temperature range	No relationship	0.026
$\delta^{18}\text{O}_{\text{shell}}$	Temperature mean	No relationship	0.017

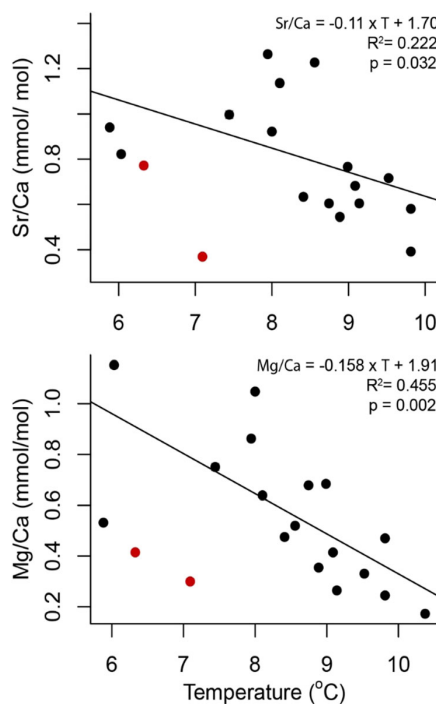


**Fig. 6** Range of Sr/Ca and Mg/Ca concentrations versus range of temperature experienced by individual *A. helmsi* shells. Samples in red (VM1 and VM3) are excluded from all linear models



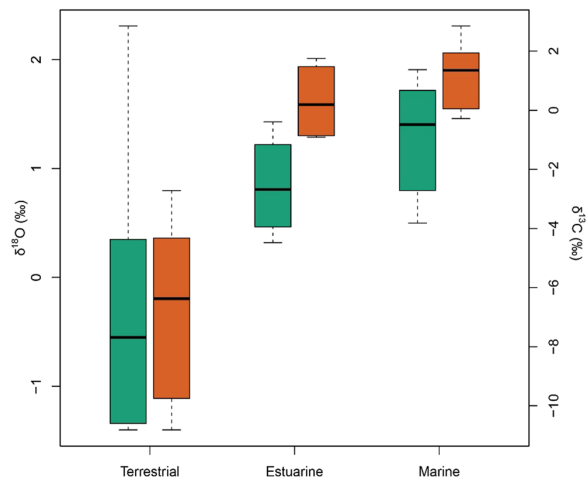


**Fig. 7** Oxygen (green) and carbon (orange) isotopes of *A. helmsi* shells grouped per the source waters of their environment. Whiskers show the upper and lower values, interquartile range is indicated by the box and the horizontal line inside the box indicates the median value. Terrestrial  $n = 5$ , estuarine  $n = 4$  and marine  $n = 8$ . Values from shells VM1 and VM3 are excluded

terrestrial values ( $-3.11$ – $4.20‰$ ) meant that terrestrial waters were not distinct from estuarine and marine waters.

## Discussion

Museum bivalve collections offer great potential for calibrating shell geochemistry-environment relationships, facilitating access to specimens collected across a wide geographic and temporal gradient with a relatively minimal cost and time expense. This is particularly beneficial when exploring the geochemical signatures in hitherto unstudied bivalve species, such as *Arthritica helmsi*, which is an abundant and cosmopolitan species in southern Australia. However, museum specimen collection and storage methods can add complications for geochemical analyses. For example, storage in ethanol and several pre-treatment options have been shown to alter both isotopic ratios and trace elemental ratios in biogenic carbonates (Milton and Chenery 1998; Krause-Nehring et al. 2011; Schöne et al. 2017). Furthermore, a lack of detailed records on the conditions of specimens at the time of collection, as well as a lack of environmental variable data for the specific habitat and lifespan of the individual specimen, mean that museum collections are, at best, a useful source of preliminary information. In the present study, it was difficult to constrain the influence of the sample treatment and storage, providing a potential source of error. Nevertheless, three of the four trace element ratios investigated (Sr/Ca, Mg/Ca and Sr/Li) were exhibited significant correlations with air temperature, conforming to expected relationships based on other bivalve taxa (Füllenbach et al. 2015; Zhao et al. 2017). In addition,

both oxygen and carbon isotope ratios broadly varied with water source, demonstrating that the geochemistry of *A. helmsi* has potential as an environmental tracer, albeit subject to further refinement of these relationships.

## Trace Elemental Ratios

Temperature was found to be most strongly correlated with Sr/Ca in *A. helmsi*, particularly when samples stored in ethanol were excluded, whereby shells from colder waters were found to have higher strontium concentrations than those from warmer waters. This negative relationship is consistent with both inorganic precipitation experiments (Dietzel et al. 2004; Gaetani and Cohen 2006) and some other bivalve species (Dodd 1965; Schöne et al. 2011; Yan et al. 2013; Füllenbach et al. 2015; Zhao et al. 2017). However, the slope of the relationship between temperature and Sr/Ca in *A. helmsi* is significantly greater ( $-0.12$ ) than that of other bivalves ( $-0.06$ , Yan et al. 2013;  $-0.02$ , Füllenbach et al. 2015;  $-0.02$ , Zhao et al. 2017) and synthetic aragonite ( $-0.04$ , Dietzel et al. 2004). Temperature was also found to be negatively correlated to Mg/Ca in *A. helmsi* shells in agreement with inorganic aragonite (Gaetani and Cohen 2006). There are few studies which find a temperature control of Mg/Ca in aragonitic bivalves, with the majority concluding that Mg/Ca ratios primarily reflect a physiological control (e.g. Elliot et al. 2009; Poulain et al. 2015; Wanamaker and Gillikin 2018). Mg/Ca has more successfully been applied as a temperature tracer in calcitic shells, however in these studies the regressions have positive slopes (e.g. Vander Putten et al. 2000; Wanamaker et al. 2008; Freitas et al. 2012; Tynan et al. 2016). It is possible that the correlation here is in fact an indirect link between temperature and metabolism or growth rate. To resolve these questions, further culture or field based studies are required.

Temperature reconstructions from shell Sr/Ca and Mg/Ca are reliant on the notion that water Sr/Ca and Mg/Ca are stable above salinities of  $\sim 10$  PSU (Dodd and Crisp 1982). Water Sr/Ca in particular has been shown to be strongly reflected in bivalve Sr/Ca in both marine (Lorens and Bender 1980) and freshwater bivalves (Zhao et al. 2017; Geeza et al. 2018). The range of Sr/Ca in *A. helmsi* ( $\sim 1$ – $3$  mmol/mol) compares well with other studies ( $\sim 0.5$ – $3$  mmol/mol, Lorens and Bender 1980;  $\sim 1$ – $6$  mmol/mol, Geeza et al. 2018;  $\sim 1$ – $4$  mmol/mol, Zhao et al. 2017), and so we would expect the distribution coefficient ( $K_D^{Sr/Ca}$ ) to compare well given that Sr/Ca of water should be relatively stable. This would result in  $K_D^{Sr/Ca}$  values in the range of 0.16 (Geeza et al. 2018) to 0.23 (Lorens and Bender 1980; Zhao et al. 2017) which are well below that of abiogenic aragonite (Gaetani and Cohen 2006). However, due to a lack of instrumental salinity or water chemistry measurements in this study, we cannot be sure of past salinity variations in these estuarine sites. It is reasonable to expect that most sites have seasonally variable water chemistry, in

addition to periods of low salinity which could cause imprecise estimates of distribution coefficients and temperature reconstructions, particularly at those sites with large terrestrial influences (AM1, AM3, AM5, AM7 and VM6). A further complication is the low tolerance of *A. helmsi* to salinities < 10 PSU (Wells and Threlfall 1982a), meaning that bivalves in these environments may have been more seasonal in their growth habits than at other sites.

Recently, the Sr/Li ratio of biogenic carbonate has been investigated as a temperature proxy in brackish environments due to its potential to reduce the influence of vital effects (Füllenbach et al. 2015). By normalising Sr/Ca to Li/Ca, Füllenbach et al. (2015) observed a reduction in scatter and an increase in the sensitivity to temperature. Similar methods have been successfully applied in foraminifera and corals (Bryan and Marchitto 2008; Case et al. 2010; Montagna et al. 2014); however, not all studies with molluscs have demonstrated significant correlations between Li/Ca and water temperature (Graniero et al. 2017). The exact mechanism of lithium incorporation into aragonite is not well understood, though it is likely that this occurs via the substitution of  $\text{Li}^+$  for  $\text{Ca}^{2+}$  to form lithium carbonate  $\text{Li}_2\text{CO}_3$  (Thébault et al. 2009b; Hathorne et al. 2013). Here, we find a statistically significant relationship between average temperature and Sr/Li; however, the equation of this relationship ( $\text{Sr/Li} = -109.3 * T + 2048.5$ ,  $R^2 = 0.34$ ) differs significantly from that of Füllenbach et al. (2015;  $\text{Sr/Li} = -12.3 * T + 319$ ,  $R^2 = 0.81$ ). There was also no relationship between the range of air temperature at each site and the range of Sr/Li values. Although the difference between our observed relationship and that of Füllenbach et al. (2015) could be explained by differences in the Li and Sr concentrations of the host waters, Sr/Li also explained less variance than Sr/Ca suggesting that other factors, for example the poor constraint on water temperatures at the time of growth, represent larger sources of uncertainty than vital effects in this study. Therefore, while a significant relationship between Sr/Li and temperature was found in *A. helmsi*, caution should be used with this proxy, particularly given the large differences in slope to that of previous studies.

Shell Ba/Ca has been proposed as a salinity or productivity proxy in many bivalve species as it has been strongly correlated to the Ba/Ca of waters (Gillikin et al. 2006a, Elliot et al. 2009; Poulain et al. 2015; Izzo et al. 2016). In agreement to empirical studies with inorganic aragonite (Dietzel et al. 2004; Gaetani and Cohen 2006), previous studies have also found a strong correlation between Ba/Ca and temperature (Geeza et al. 2018; Wanamaker and Gillikin 2018); however, these correlations have been attributed to co-variance with growth rates and thus discounted as a pure temperature effect. Our results showed no response of Ba/Ca to temperature or precipitation, but instead shell Ba/Ca was highly variable among specimens from the same collection location. Many studies have found that within-shell Ba/Ca transects are

characterised by a relatively flat background signal with sharp peaks (Gillikin et al. 2008; Thébault et al. 2009a; Hatch et al. 2013); this pattern was not found consistently in this study. This evidence does not support the use of Ba/Ca as an environmental proxy in *A. helmsi*.

**Investigation of Element Ca** profiles of shells from the same collections illustrated similar patterns in Sr/Ca and Mg/Ca between shells, however these patterns appear to have a phase offset between samples. The similar patterns and values (particularly in shells VM4 and VM5) suggest that individual shells are responding to the same forcing, while the offset indicates that either shells were not living when collected or that there is a difference in growth rate between the two shells. As these shells are different sizes and therefore have different inferred ages, it is possible that as in other species, individuals experience varying growth rates and vital effects through ontogeny (Schöne et al. 2011). If this were the case, a faster growing individual would deposit more carbonate which could explain the phase offset. However, field based studies on *A. helmsi* suggesting a constant growth rate (Wells and Threlfall 1982c) are supported in this study by a lack of imaging evidence for growth lines. The impact of growth rate on elemental ratios in bivalves is unclear as many studies report it as being both significant (e.g. Takesue and van Geen 2004; Lorrain et al. 2005; Izumida et al. 2011; Wanamaker and Gillikin 2018) and insignificant (e.g. Stecher et al. 1996; Füllenbach et al. 2015; Geeza et al. 2018). The conditions of the current study do not allow conclusions on the role of growth rate on element incorporation. As such, we cannot be sure of the cause of this phase offset, particularly given we cannot guarantee the age of each specimen or whether the specimens were live collected. Shell microstructure has also been linked to trace element ratios with higher Sr/Ca values occurring at circatidal (Füllenbach et al. 2017) and diurnal (Sano et al. 2012) growth lines. However, the homogeneous shell architecture in this species indicates that it is possible that the potentially seasonal patterns observed in some individuals are driven by environmental variation rather than microstructure.

### Stable Isotopes

Deciphering the relationship between stable isotopes and the environment was hindered in this study due to our lack of control over the source water  $\delta^{18}\text{O}$ ,  $\delta^{13}\text{C}$ , DIC and salinity. Nevertheless, when bivalve stable isotope ratios are grouped by environmental water source, distinct isotopic differences were revealed. Both  $\delta^{18}\text{O}$  and  $\delta^{13}\text{C}$  exhibited higher values in marine environments and the range of values decreased moving from terrestrial (freshwater) through to marine influenced environments. This suggests that both ratios reflect a common environmental forcing, most likely the mixing of

isotopically distinct marine and fresh waters in coastal environments. The  $\delta^{18}\text{O}$  of bivalves reflects the temperature and isotopic composition of the water in which they grew (Epstein et al. 1953); as there is no correlation between temperature or any trace elemental ratios and shell  $\delta^{18}\text{O}$  it is clear that  $\delta^{18}\text{O}$  of waters is the dominant control, as in other estuarine studies (Dettman et al. 2004; Andrus and Rich 2008). Water oxygen isotopic values often correlate with salinity (Fry 2002) and so the variation observed in this study likely records a combination of water mixing and evaporation, accounting for the large variation, particularly in terrestrial influenced sites.

Shell  $\delta^{13}\text{C}$  is also related to salinity through the strong relationship between salinity and dissolved inorganic carbon (DIC) (Fry 2002; Gillikin et al. 2006b; Poulain et al. 2010). It has been experimentally confirmed that the carbon incorporated into bivalve carbonate is sourced from both water DIC and metabolic DIC from food (Poulain et al. 2010). However, the same study found a strong relationship between bivalve  $\delta^{13}\text{C}$  and the  $\delta^{13}\text{C}$  of DIC ( $R^2 = 0.77$ ), supporting the conclusions of previous studies that aquatic molluscs derive the majority of their carbon from ambient DIC (McConnaughey and Gillikin 2008; Owen et al. 2008; Poulain et al. 2010). In addition to salinity, DIC is influenced by water source as fluvially transported DIC typically has a lower  $\delta^{13}\text{C}$  than marine DIC due to the presence of  $\text{CO}_2$  derived from the decomposition of terrestrial plants (McConnaughey and Gillikin 2008). This isotopic offset between water sources is observed in this study where bivalves from terrestrial waters (rivers and creeks) exhibit lower  $\delta^{13}\text{C}$  compared with bivalves from estuarine and marine environments. Similar results are reported by previous studies which found distinct differences in  $\delta^{13}\text{C}$  in bivalves from riverine and deltaic environments (Vanhof et al. 2013) and within shells transplanted from a marine to an estuarine environment (Gillikin et al. 2006b). While  $\delta^{13}\text{C}$  appears to respond to environmental changes, age related trends and uncertainties regarding the influence of metabolic DIC make quantitative salinity or DIC reconstruction from  $\delta^{13}\text{C}_{\text{shell}}$  difficult (Gillikin et al. 2006b, 2007; Poulain et al. 2010; Butler et al. 2011). Our results support those of previous studies that large changes in bivalve  $\delta^{13}\text{C}$  can reflect large changes in the  $\delta^{13}\text{C}$  of DIC and therefore differences in environment with respect to salinity and the mixing of fresh/marine water source (Gillikin et al. 2006b; Vanhof et al. 2013; Lacey et al. 2018). As a consequence, stable isotope ratios  $\delta^{18}\text{O}$  and  $\delta^{13}\text{C}$  of *A. helmsi* offer potential to determine large scale changes in environment which could be potentially useful for inferring the marine–freshwater mixing regime in palaeo-estuarine settings, or for studies of sea level change.

## Conclusions

This study presents the first geochemical analysis of aragonitic shells of the bivalve *Arthritica helmsi*, a short lived micromollusc common to southern Australian estuaries. Several trace elemental ratios were significantly correlated to temperature—namely average Sr/Ca, Mg/Ca and Sr/Li ratios—and stable isotope tracers  $\delta^{18}\text{O}$  and  $\delta^{13}\text{C}$  broadly recorded large environmental differences. Trace element transects through individual shells from the same collection revealed similar patterns in Sr/Ca and Mg/Ca but timing of peaks did not correspond suggesting a phase offset or that one individual was not living when collected. In part, the uncertainties exhibited by this study are due to poorly constrained environmental data, including the water chemistry, temperature, salinity and isotopic composition of the water at the time of shell growth. Further uncertainty arises from a lack of detailed knowledge of when the shells were growing and whether some shells may have been dead at time of collection. As a consequence, although analysis of museum specimens provides a valuable first look at the geographical trends in the geochemistry of bivalve shells, further research under more controlled conditions is required. Nevertheless, this study demonstrates interesting patterns in the geochemistry of *A. helmsi* shells, suggesting that geochemical analysis of fossil shells of this species has potential as a tracer of past climates, hydrology and ecology.

**Acknowledgements** The authors would like to acknowledge Kirrily Moore from the Tasmanian Museum and Art Gallery, Chris Rowley from Museum Victoria and Mandy Reid from The Australian Museum for providing samples for this study. Sarah Gilbert, Mark Rollog, Ben Wade, Tony Hall and Ken Neubauer are thanked for their assistance with trace elemental analyses, stable isotope analyses, electron microprobe analyses, XRD analysis and SEM imaging, respectively.

**Funding Information** This research was supported by a grant from the Sir Mark Mitchell Foundation, South Australia.

## References

- Andrus, C.F.T., and K.W. Rich. 2008. A preliminary assessment of oxygen isotope fractionation and growth increment periodicity in the estuarine clam *Rangia cuneata*. *Geo-Marine Letters* 28: 301–308. <https://doi.org/10.1007/s00367-008-0109-3>.
- Bar-Matthews, M., A. Ayalon, M. Gilmour, A. Matthews, and C.J. Hawkesworth. 2003. Sea–land oxygen isotopic relationships from planktonic foraminifera and speleothems in the Eastern Mediterranean region and their implication for paleorainfall during interglacial intervals. *Geochimica et Cosmochimica Acta* 67: 3181–3199.
- Böhm, F., M.M. Joachimski, W.C. Dullo, A. Eisenhauer, H. Lehnert, J. Reitner, and G. Wörheide. 2000. Oxygen isotope fractionation in marine aragonite of coralline sponges. *Geochimica et*

- Cosmochimica Acta* 64: 1695–1703. [https://doi.org/10.1016/S0016-7037\(99\)00408-1](https://doi.org/10.1016/S0016-7037(99)00408-1).
- Bougeois, L., M. de Rafélis, G.J. Reichart, L.J. de Nooijer, F. Nicollin, and G. Dupont-Nivet. 2014. A high resolution study of trace elements and stable isotopes in oyster shells to estimate central asian middle eocene seasonality. *Chemical Geology* 363: 200–212. <https://doi.org/10.1016/j.chemgeo.2013.10.037>.
- Bryan, S.P., and T.M. Marchitto. 2008. Mg/Ca-temperature proxy in benthic foraminifera: New calibrations from the Florida Straits and a hypothesis regarding Mg/Li. *Paleoceanography* 23: 1–17. <https://doi.org/10.1029/2007PA001553>.
- Butler, P.G., C.A. Richardson, J.D. Scourse, R. Witbaard, B.R. Schöne, N.M. Fraser, A.D. Wanamaker, C.L. Bryant, I. Harris, and I. Robertson. 2009. Accurate increment identification and the spatial extent of the common signal in five *Arctica islandica* chronologies from the Fladen Ground, northern North Sea. *Paleoceanography* 24: 1–18. <https://doi.org/10.1029/2008PA001715>.
- Butler, P.G., A.D. Wanamaker, J.D. Scourse, C.A. Richardson, and D.J. Reynolds. 2011. Long-term stability of  $\delta^{13}\text{C}$  with respect to biological age in the aragonite shell of mature specimens of the bivalve mollusk *Arctica islandica*. *Palaeogeography, Palaeoclimatology, Palaeoecology* 302: 21–30. <https://doi.org/10.1016/j.palaeo.2010.03.038>.
- Carré, M., J.P. Sachs, A.J. Schauer, W.E. Rodríguez, and F.C. Ramos. 2013. Reconstructing El Niño-Southern Oscillation activity and ocean temperature seasonality from short-lived marine mollusk shells from Peru. *Palaeogeography, Palaeoclimatology, Palaeoecology* 371: 45–53. <https://doi.org/10.1016/j.palaeo.2012.12.014>.
- Carré, M., J.P. Sachs, S. Purca, A.J. Schauer, P. Braconnot, R.A. Falcón, M. Julien, and D. Lavallée. 2014. Holocene history of ENSO variance and asymmetry in the eastern tropical Pacific. *Science* 345 (6200): 1045–1048.
- Case, D.H., L.F. Robinson, M.E. Auro, and A.C. Gagnon. 2010. Environmental and biological controls on Mg and Li in deep-sea scleractinian corals. *Earth and Planetary Science Letters* 300: 215–225. <https://doi.org/10.1016/j.epsl.2010.09.029>.
- Chamberlayne, B.K. 2015. Late Holocene seasonal and multicentennial hydroclimate variability in the Coorong Lagoon, South Australia: evidence from stable isotopes and trace element profiles of bivalve molluscs (unpublished honours thesis), The University of Adelaide, Adelaide, Australia.
- Dettman, D.L., K.W. Flessa, P.D. Roopnarine, B.R. Schöne, and D.H. Goodwin. 2004. The use of oxygen isotope variation in shells of estuarine mollusks as a quantitative record of seasonal and annual Colorado River discharge. *Geochimica et Cosmochimica Acta* 68: 1253–1263. <https://doi.org/10.1016/j.gca.2003.09.008>.
- Dietzel, M., N. Gussone, and A. Eisenhauer. 2004. Co-precipitation of  $\text{Sr}^{2+}$  and  $\text{Ba}^{2+}$  with aragonite by membrane diffusion of  $\text{CO}_2$  between 10 and 50 °C. *Chemical Geology* 203: 139–151. <https://doi.org/10.1016/j.chemgeo.2003.09.008>.
- Dodd, J. Robert. 1965. Environmental control of strontium and magnesium in *Mytilus*. *Geochimica et Cosmochimica Acta* 29: 385–398. [https://doi.org/10.1016/0016-7037\(65\)90035-9](https://doi.org/10.1016/0016-7037(65)90035-9).
- Dodd, J.R., and E.L. Crisp. 1982. Non-linear variation with salinity of Sr/Ca and Mg/Ca ratios in water and aragonitic bivalve shells and implications for paleosalinity studies. *Palaeogeography, Palaeoclimatology, Palaeoecology* 38: 45–56.
- Donovan, J.J., and J.T. Armstrong. 2014. A new EPMA method for fast trace element analysis in simple matrices. *Microscopy and Microanalysis* 20: 724–725. <https://doi.org/10.1017/S1431927614005340>.
- Donovan, J.J., and T.N. Tingle. 1996. An improved mean atomic number background correction for quantitative microanalysis. *Microscopy and Microanalysis*. <https://doi.org/10.1017/S1431927696210013>.
- Elliot, M., K. Welsh, C. Chilcott, M. McCulloch, J. Chappell, and B. Ayling. 2009. Profiles of trace elements and stable isotopes derived from giant long-lived *Tridacna gigas* bivalves: Potential applications in paleoclimate studies. *Palaeogeography, Palaeoclimatology, Palaeoecology* 280: 132–142. <https://doi.org/10.1016/j.palaeo.2009.06.007>.
- Epstein, S., and T. Mayeda. 1953. Variation of  $\text{O}^{18}$  content of waters from natural sources. *Geochimica et Cosmochimica Acta* 4: 213–224.
- Epstein, S., R. Buchsbaum, H.A. Lowenstam, and H.C. Urey. 1953. Revised carbonate-water isotopic temperature scale. *Geological Society of America Bulletin* 64: 1315–1325. [https://doi.org/10.1130/0016-7606\(1953\)64](https://doi.org/10.1130/0016-7606(1953)64).
- Ferguson, J.E., K.R. Johnson, G. Santos, L. Meyer, and A. Tripathi. 2013. Investigating  $\delta^{13}\text{C}$  and  $\Delta^{14}\text{C}$  within *Mytilus californianus* shells as proxies of upwelling intensity. *Geochemistry, Geophysics, Geosystems* 14: 1856–1865. <https://doi.org/10.1002/ggge.20090>.
- Freitas, P.S., L.J. Clarke, H. Kennedy, and C.A. Richardson. 2012. The potential of combined Mg/Ca and  $\delta^{18}\text{O}$  measurements within the shell of the bivalve *Pecten maximus* to estimate seawater  $\delta^{18}\text{O}$  composition. *Chemical Geology* 291: 286–293. <https://doi.org/10.1016/j.chemgeo.2011.10.023>.
- Fry, B. 2002. Conservative mixing of stable isotopes across estuarine salinity gradients: A conceptual framework for monitoring watershed influences on downstream fisheries production. *Estuaries* 25: 264–271. <https://doi.org/10.1007/BF02691313>.
- Füllenbach, C.S., B.R. Schöne, and R. Mertz-Kraus. 2015. Strontium/lithium ratio in aragonitic shells of *Cerastoderma edule* (Bivalvia)—A new potential temperature proxy for brackish environments. *Chemical Geology* 417: 341–355. <https://doi.org/10.1016/j.chemgeo.2015.10.030>.
- Füllenbach, C.S., B.R. Schöne, K. Shirai, N. Takahata, A. Ishida, and Y. Sano. 2017. Minute co-variations of Sr/Ca ratios and microstructures in the aragonitic shell of *Cerastoderma edule* (Bivalvia)—are geochemical variations at the ultra-scale masking potential environmental signals? *Geochimica et Cosmochimica Acta* 205: 256–271. <https://doi.org/10.1016/j.gca.2017.02.019>.
- Gaetani, G.A., and A.L. Cohen. 2006. Element partitioning during precipitation of aragonite from seawater: A framework for understanding paleoproxies. *Geochimica et Cosmochimica Acta* 70: 4617–4634. <https://doi.org/10.1016/j.gca.2006.07.008>.
- Geeza, T.J., D.P. Gillikin, D.H. Goodwin, S.D. Evans, T. Watters, and N.R. Warner. 2018. Controls on magnesium, manganese, strontium, and barium concentrations recorded in freshwater mussel shells from Ohio. *Chemical Geology*: 1–12. <https://doi.org/10.1016/j.chemgeo.2018.01.001>.
- Gillikin, David Paul, F. De Ridder, H. Ulens, M. Elskens, E. Keppens, W. Baeyens, and F. Dehairs. 2005. Assessing the reproducibility and reliability of estuarine bivalve shells (*Saxidomus giganteus*) for sea surface temperature reconstruction: Implications for paleoclimate studies. *Palaeogeography, Palaeoclimatology, Palaeoecology* 228: 70–85. <https://doi.org/10.1016/j.palaeo.2005.03.047>.
- Gillikin, D.P., F. Dehairs, A. Lorrain, D. Steenmans, W. Baeyens, and L. André. 2006a. Barium uptake into the shells of the common mussel (*Mytilus edulis*) and the potential for estuarine paleo-chemistry reconstruction. *Geochimica et Cosmochimica Acta* 70: 395–407. <https://doi.org/10.1016/j.gca.2005.09.015>.
- Gillikin, D.P., A. Lorrain, S. Bouillon, P. Willenz, and F. Dehairs. 2006b. Stable carbon isotopic composition of *Mytilus edulis* shells: Relation to metabolism, salinity,  $\delta^{13}\text{C}_{\text{DIC}}$  and phytoplankton. *Organic Geochemistry* 37: 1371–1382. <https://doi.org/10.1016/j.orggeochem.2006.03.008>.
- Gillikin, D.P., A. Lorrain, L. Meng, and F. Dehairs. 2007. A large metabolic carbon contribution to the  $\delta^{13}\text{C}$  record in marine aragonitic bivalve shells. *Geochimica et Cosmochimica Acta* 71: 2936–2946. <https://doi.org/10.1016/j.gca.2007.04.003>.

- Gillikin, David Paul, A. Lorrain, Y.M. Paulet, L. André, and F. Dehairs. 2008. Synchronous barium peaks in high-resolution profiles of calcite and aragonite marine bivalve shells. *Geo-Marine Letters* 28 (5–6): 351–358. <https://doi.org/10.1007/s00367-008-0111-9>.
- Goodwin, D.H., D.P. Gillikin, and P.D. Roopnarine. 2013. Preliminary evaluation of potential stable isotope and trace element productivity proxies in the oyster *Crassostrea gigas*. *Palaeogeography, Palaeoclimatology, Palaeoecology* 373: 88–97. <https://doi.org/10.1016/j.palaeo.2012.03.034>.
- Graniero, L.E., D. Surge, D.P. Gillikin, I. Briz, and M. Álvarez. 2017. Assessing elemental ratios as a paleotemperature proxy in the calcite shells of patelloid limpets. *Palaeogeography, Palaeoclimatology, Palaeoecology* 465: 376–385. <https://doi.org/10.1016/j.palaeo.2016.10.021>.
- Grossman, E.L., and T.-L. Ku. 1986. Oxygen and carbon isotope fractionation in biogenic aragonite: Temperature effects. *Chemical Geology: Isotope Geoscience Section* 59: 59–74. [https://doi.org/10.1016/0168-9622\(86\)90057-6](https://doi.org/10.1016/0168-9622(86)90057-6).
- Hart, S.R., and J. Blusztajn. 1998. Clams as recorders of ocean ridge volcanism and hydrothermal vent field activity. *Science* 280 (5365): 883–886.
- Hatch, M.B.A., S.A. Schellenberg, and M.L. Carter. 2013. Ba/Ca variations in the modern intertidal bean clam *Donax gouldii*: An upwelling proxy? *Palaeogeography, Palaeoclimatology, Palaeoecology* 373: 98–107. <https://doi.org/10.1016/j.palaeo.2012.03.006>.
- Hathome, E.C., T. Felis, A. Suzuki, H. Kawahata, and G. Cabioch. 2013. Lithium in the aragonite skeletons of massive *Porites* corals: A new tool to reconstruct tropical sea surface temperatures. *Paleoceanography* 28: 143–152. <https://doi.org/10.1029/2012PA002311>.
- Hellstrom, J., C. Paton, J. Woodhead, and Hergt, J. 2008. Iolite: Software for spatially resolved LA-(quad and MC) ICPMS analysis. In: Laser ablation ICP-MS in the Earth sciences: Current practices and outstanding issues, ed. Sylvester, P., 343. Mineralogical Association of Canada short course vol 40.
- Izumida, H., T. Yoshimura, A. Suzuki, R. Nakashima, T. Ishimura, M. Yasuhara, A. Inamura, N. Shikazono, and H. Kawahata. 2011. Biological and water chemistry controls on Sr/Ca, Ba/Ca, Mg/Ca and  $\delta^{18}\text{O}$  profiles in freshwater pearl mussel *Hyriopsis* sp. *Palaeogeography, Palaeoclimatology, Palaeoecology* 309: 298–308. <https://doi.org/10.1016/j.palaeo.2011.06.014>.
- Izzo, C., D. Manetti, Z.A. Doubleday, and B.M. Gillanders. 2016. Calibrating the element composition of *Donax deltooides* shells as a palaeo-salinity proxy. *Palaeogeography, Palaeoclimatology, Palaeoecology* 484: 89–96. <https://doi.org/10.1016/j.palaeo.2016.11.038>.
- Jeffrey, S.J., J.O. Carter, K.B. Moodie, and A.R. Beswick. 2001. Using spatial interpolation to construct a comprehensive archive of Australian climate data. *Environmental Modelling and Software* 16: 309–330. [https://doi.org/10.1016/S1364-8152\(01\)00008-1](https://doi.org/10.1016/S1364-8152(01)00008-1).
- Kelemen, Z., D.P. Gillikin, L.E. Graniero, H. Havel, F. Darchambeau, A.V. Borges, A. Yambélé, A. Bassirou, and S. Bouillon. 2017. Calibration of hydroclimate proxies in freshwater bivalve shells from Central and West Africa. *Geochimica et Cosmochimica Acta* 208: 41–62. <https://doi.org/10.1016/j.gca.2017.03.025>.
- Krause-Nehring, J., A. Klgel, G. Nehrke, B. Brellochs, and T. Brey. 2011. Impact of sample pretreatment on the measured element concentrations in the bivalve *Arctica islandica*. *Geochemistry, Geophysics, Geosystems* 12. <https://doi.org/10.1029/2011GC003630>.
- Krause-Nehring, J., T. Brey, and S.R. Thorrold. 2012. Centennial records of lead contamination in northern Atlantic bivalves (*Arctica islandica*). *Marine Pollution Bulletin* 64 (2): 233–240. <https://doi.org/10.1016/j.marpolbul.2011.11.028>.
- Lacey, J.H., M.J. Leng, E.N. Peckover, J.R. Dean, T. Wilke, A. Francke, X. Zhang, A. Masi, and B. Wagner. 2018. Investigating the environmental interpretation of oxygen and carbon isotope data from whole and fragmented bivalve shells. *Quaternary Science Reviews* 194: 55–61. <https://doi.org/10.1016/j.quascirev.2018.06.025>.
- Livingstone, D.M., and A.F. Lotter. 1998. The relationship between air and water temperatures in lakes of the Swiss Plateau: A case study with palaeolimnological implication. *Journal of Paleolimnology* 19: 181–198. <https://doi.org/10.1023/a:1007904817619>.
- Lorens, R.B., and M.L. Bender. 1980. The impact of solution chemistry on *Mytilus edulis* calcite and aragonite. *Geochimica et Cosmochimica Acta* 44: 1265–1278. [https://doi.org/10.1016/0016-7037\(80\)90087-3](https://doi.org/10.1016/0016-7037(80)90087-3).
- Lorrain, A., D.P. Gillikin, Y.M. Paulet, L. Chauvaud, A. Le Mercier, J. Navez, and L. André. 2005. Strong kinetic effects on Sr/Ca ratios in the calcitic bivalve *Pecten maximus*. *Geology* 33: 965–968. <https://doi.org/10.1130/G22048.1>.
- McCombie, A.M. 1959. Some relations between air temperatures and the surface water temperatures of lakes. *Limnology and Oceanography* 4: 252–258. <https://doi.org/10.4319/lo.1959.4.3.0252>.
- McConnaughey, T.A., and D.P. Gillikin. 2008. Carbon isotopes in mollusk shell carbonates. *Geo-Marine Letters* 28: 287–299. <https://doi.org/10.1007/s00367-008-0116-4>.
- McCulloch, M., G. Mortimer, T. Esat, L. Xianhua, B. Pillans, and J. Chappell. 1996. High resolution windows into early Holocene climate: Sr/Ca coral records from the Huon Peninsula. *Earth and Planetary Science Letters* 138: 169–178. [https://doi.org/10.1016/0012-821X\(95\)00230-A](https://doi.org/10.1016/0012-821X(95)00230-A).
- Milton, D.A., and S.R. Chenery. 1998. The effect of otolith storage methods on the concentrations of elements detected by laser-ablation ICPMS. *Journal of Fish Biology* 53: 785–794. <https://doi.org/10.1006/jfbi.1998.0745>.
- Mitsuguchi, T., E. Matsumoto, O. Abe, T. Uchida, and P.J. Isdale. 1996. Mg/Ca Thermometry in Coral Skeletons. *Science* 274 (5289): 961–963.
- Montagna, P., M. McCulloch, E. Douville, M. López Correa, J. Trotter, R. Rodolfo-Metalpa, D. Dissard, et al. 2014. Li/Mg systematics in scleractinian corals: Calibration of the thermometer. *Geochimica et Cosmochimica Acta* 132: 288–310. <https://doi.org/10.1016/j.gca.2014.02.005>.
- Mook, W.G. 1971. Paleotemperatures and chlorinities from stable carbon and oxygen isotopes in shell carbonate. *Palaeogeography, Palaeoclimatology, Palaeoecology* 9: 245–263. [https://doi.org/10.1016/0031-0182\(71\)90002-2](https://doi.org/10.1016/0031-0182(71)90002-2).
- Mouchi, V., M. de Raféllis, F. Lartaud, M. Fialin, and E. Verrecchia. 2013. Chemical labelling of oyster shells used for time-calibrated high-resolution Mg/Ca ratios: A tool for estimation of past seasonal temperature variations. *Palaeogeography, Palaeoclimatology, Palaeoecology* 373: 66–74. <https://doi.org/10.1016/j.palaeo.2012.05.023>.
- O’Neil, D.D., and D.P. Gillikin. 2014. Do freshwater mussel shells record road-salt pollution? *Scientific Reports* 4: 7168. <https://doi.org/10.1038/srep07168>.
- Owen, E.F., A.D. Wanamaker, S.C. Feindel, B.R. Schöne, and P.D. Rawson. 2008. Stable carbon and oxygen isotope fractionation in bivalve (*Placopecten magellanicus*) larval aragonite. *Geochimica et Cosmochimica Acta* 72: 4687–4698. <https://doi.org/10.1016/j.gca.2008.06.029>.
- Paton, C., J. Hellstrom, B. Paul, J. Woodhead, and J. Hergt. 2011. Iolite: FreeWare for the visualisation and processing of mass spectrometric data. *Journal of Analytical Atomic Spectrometry* 26: 2508. <https://doi.org/10.1039/c1ja10172b>.
- Poulain, C., A. Lorrain, R. Mas, D.P. Gillikin, F. Dehairs, R. Robert, and Y.M. Paulet. 2010. Experimental shift of diet and DIC stable carbon isotopes: Influence on shell  $\delta^{13}\text{C}$  values in the Manila clam *Ruditapes philippinarum*. *Chemical Geology* 272: 75–82. <https://doi.org/10.1016/j.chemgeo.2010.02.006>.

- Poulain, C., D.P. Gillikin, J. Thébault, J.M. Munaron, M. Bohn, R. Robert, Y.M. Paulet, and A. Lorrain. 2015. An evaluation of Mg/Ca, Sr/Ca, and Ba/Ca ratios as environmental proxies in aragonite bivalve shells. *Chemical Geology* 396: 42–50. <https://doi.org/10.1016/j.chemgeo.2014.12.019>.
- Sano, Y., S. Kobayashi, K. Shirai, N. Takahata, K. Matsumoto, T. Watanabe, K. Sowa, and K. Iwai. 2012. Past daily light cycle recorded in the strontium/calcium ratios of giant clam shells. *Nature Communications* 3: 761. <https://doi.org/10.1038/ncomms1763>.
- Schöne, B.R. 2008. The curse of physiology—Challenges and opportunities in the interpretation of geochemical data from mollusk shells. *Geo-Marine Letters* 28: 269–285. <https://doi.org/10.1007/s00367-008-0114-6>.
- Schöne, B.R., and J. Fiebig. 2009. Seasonality in the North Sea during the Allerød and Late Medieval Climate Optimum using bivalve sclerochronology. *International Journal of Earth Sciences* 98: 83–98.
- Schöne, B.R., and D.P. Gillikin. 2013. Unraveling environmental histories from skeletal diaries—Advances in sclerochronology. *Palaeogeography, Palaeoclimatology, Palaeoecology* 373: 1–5. <https://doi.org/10.1016/j.palaeo.2012.11.026>.
- Schöne, B.R., A.D. Freyre Castro, J. Fiebig, S.D. Houk, W. Oschmann, and I. Kröncke. 2004. Sea surface water temperatures over the period 1884–1983 reconstructed from oxygen isotope ratios of a bivalve mollusk shell (*Arctica islandica*, southern North Sea). *Palaeogeography, Palaeoclimatology, Palaeoecology* 212: 215–232. <https://doi.org/10.1016/j.palaeo.2004.05.024>.
- Schöne, B.R., Z. Zhang, P. Radermacher, J. Thébault, D.E. Jacob, E.V. Nunn, and A.-F. Maurer. 2011. Sr/Ca and Mg/Ca ratios of ontogenetically old, long-lived bivalve shells (*Arctica islandica*) and their function as paleotemperature proxies. *Palaeogeography, Palaeoclimatology, Palaeoecology* 302: 52–64. <https://doi.org/10.1016/j.palaeo.2010.03.016>.
- Schöne, B.R., K. Schmitt, and M. Maus. 2017. Effects of sample pretreatment and external contamination on bivalve shell and Carrara marble  $\delta^{18}\text{O}$  and  $\delta^{13}\text{C}$  signatures. *Palaeogeography, Palaeoclimatology, Palaeoecology* 484: 22–32. <https://doi.org/10.1016/j.palaeo.2016.10.026>.
- Sinclair, D.J., L. Kinsley, and M.T. McCulloch. 1998. High resolution analysis of trace elements in corals by laser ablation ICP-MS. *Geochimica et Cosmochimica Acta* 62: 1889–1901. [https://doi.org/10.1016/S0016-7037\(98\)00112-4](https://doi.org/10.1016/S0016-7037(98)00112-4).
- Stecher, H.A., D.E. Krantz, C.J. Lord, G.W. Luther, and K.W. Bock. 1996. Profiles of strontium and barium in *Mercenaria mercenaria* and *Spisula solidissima* shells. *Geochimica et Cosmochimica Acta* 60: 3445–3456. [https://doi.org/10.1016/0016-7037\(96\)00179-2](https://doi.org/10.1016/0016-7037(96)00179-2).
- Surge, D., and K.C. Lohmann. 2008. Evaluating Mg/Ca ratios as a temperature proxy in the estuarine oyster, *Crassostrea virginica*. *Journal of Geophysical Research* 113: 1–9.
- Surge, D., and K.J. Walker. 2006. Geochemical variation in microstructural shell layers of the southern quahog (*Mercenaria campechiensis*): Implications for reconstructing seasonality. *Palaeogeography, Palaeoclimatology, Palaeoecology* 237: 182–190. <https://doi.org/10.1016/j.palaeo.2005.11.016>.
- Takesue, R.K., and A. van Geen. 2004. Mg/Ca, Sr/Ca, and stable isotopes in modern and Holocene *Protothaca staminea* shells from a northern California coastal upwelling region. *Geochimica et Cosmochimica Acta* 68: 3845–3861. <https://doi.org/10.1016/j.gca.2004.03.021>.
- Thébault, J., L. Chauvaud, S. L'Helgouen, J. Clavier, A. Barats, S. Jacquet, C. Pécuyer, and D. Amouroux. 2009a. Barium and molybdenum records in bivalve shells: Geochemical proxies for phytoplankton dynamics in coastal environments? *Limnology and Oceanography* 54: 1002–1014. <https://doi.org/10.4319/lo.2009.54.3.1002>.
- Thébault, J., B.R. Schöne, N. Hallmann, M. Barth, and E.V. Nunn. 2009b. Investigation of Li/Ca variations in aragonitic shells of the ocean quahog *Arctica islandica*, northeast Iceland. *Geochemistry, Geophysics, Geosystems* 10. <https://doi.org/10.1029/2009GC002789>.
- Tindall, J., R. Flecker, P. Valdes, D.N. Schmidt, P. Markwick, and J. Harris. 2010. Modelling the oxygen isotope distribution of ancient seawater using a coupled ocean-atmosphere GCM: Implications for reconstructing early Eocene climate. *Earth and Planetary Science Letters* 292: 265–273. <https://doi.org/10.1016/j.epsl.2009.12.049>.
- Tyler, J.J., M.J. Leng, H.J. Sloane, D. Sachse, and G. Gleixner. 2008. Oxygen isotope ratios of sedimentary biogenic silica reflect the European transcontinental climate gradient. *Journal of Quaternary Science* 23: 341–350. <https://doi.org/10.1002/jqs>.
- Tynan, S., B.N. Opdyke, M. Walczak, S. Eggins, and A. Dutton. 2016. Assessment of Mg/Ca in *Saccostrea glomerata* (the Sydney rock oyster) shell as a potential temperature record. *Palaeogeography, Palaeoclimatology, Palaeoecology* 484: 79–88. <https://doi.org/10.1016/j.palaeo.2016.08.009>.
- Urey, H.C., H.A. Lowenstam, S. Epstein, and C.R. McKinney. 1951. Measurement of paleotemperatures and temperatures of the Upper Cretaceous of England, Denmark and the Southeastern United States. *Bulletin of the Geological Society of America* 62: 399–416.
- Vander Putten, E., F. Dehairs, E. Keppens, and W. Baeyens. 2000. High resolution distribution of trace elements in the calcite shell layer of modern *Mytilus edulis*: Environmental and biological controls. *Geochimica et Cosmochimica Acta* 64: 997–1011.
- Vonhof, H.B., J.C.A. Joordens, M.L. Noback, J.H.J.L. van der Lubbe, C.S. Feibel, and D. Kroon. 2013. Environmental and climatic control on seasonal stable isotope variation of freshwater molluscan bivalves in the Turkana Basin (Kenya). *Palaeogeography, Palaeoclimatology, Palaeoecology* 383–384: 16–26. <https://doi.org/10.1016/j.palaeo.2013.04.022>.
- Wanamaker, A.D., and D.P. Gillikin. 2018. Strontium, magnesium, and barium incorporation in aragonitic shells of juvenile *Arctica islandica*: Insights from temperature controlled experiments. *Chemical Geology*. <https://doi.org/10.1016/j.chemgeo.2018.02.012>.
- Wanamaker, A.D., K.J. Kreutz, T. Wilson, H.W. Borns, D.S. Introne, and S. Feindel. 2008. Experimentally determined Mg/Ca and Sr/Ca ratios in juvenile bivalve calcite for *Mytilus edulis*: Implications for paleotemperature reconstructions. *Geo-Marine Letters* 28 (5–6): 359–368. <https://doi.org/10.1007/s00367-008-0112-8>.
- Wanamaker, A.D., K.J. Kreutz, B.R. Schöne, K.A. Maasch, A.J. Pershing, H.W. Borns, D.S. Introne, and S. Feindel. 2009. A Late Holocene paleo-productivity record in the western Gulf of Maine, USA, inferred from growth histories of the long-lived ocean quahog (*Arctica islandica*). *International Journal of Earth Sciences* 98: 19–29.
- Weber, J.N. 1973. Incorporation of strontium into reef coral skeletal carbonate. *Geochimica et Cosmochimica Acta* 37: 2173–2190. [https://doi.org/10.1016/0016-7037\(73\)90015-X](https://doi.org/10.1016/0016-7037(73)90015-X).
- Wells, F.E., and T.J. Threlfall. 1982a. Salinity and temperature tolerance of *Hydrococcus brazieri* (T. Woods, 1876) and *Arthritica semen* (Menke, 1843) from the Peel-Harvey estuarine system, Western Australia. *Journal of the Malacological Society of Australia* 5: 151–156.
- Wells, F.E., and T.J. Threlfall. 1982b. Reproductive strategies of *Hydrococcus brazieri* (Tenison Woods, 1876) and *Arthritica semen* (Menke, 1843) in Peel Inlet, Western Australia. *Journal of the Malacological Society of Australia* 5: 157–166.
- Wells, F.E., and T.J. Threlfall. 1982c. Density fluctuations, growth and dry tissue production of *Hydrococcus brazieri* (Tenison Woods, 1876) and *Arthritica semen* (Menke, 1843) in peel inlet, Western Australia. *Journal of Molluscan Studies* 48: 310–320.
- Wurster, C.M., and W.P. Patterson. 2001. Seasonal variation in stable oxygen and carbon isotope values recovered from modern lacustrine freshwater molluscs: Paleoclimatological implications for sub-weekly temperature records. *Journal of Paleolimnology* 26: 205–218. <https://doi.org/10.1023/A:1011194011250>.



Contents lists available at ScienceDirect

Estuarine, Coastal and Shelf Science

journal homepage: <http://www.elsevier.com/locate/ecss>

## Elemental concentrations of waters and bivalves in the fresh to hypersaline Coorong Lagoons, South Australia: Implications for palaeoenvironmental studies

Briony K. Chamberlayne<sup>a,\*</sup>, Jonathan J. Tyler<sup>a</sup>, Bronwyn M. Gillanders<sup>b</sup><sup>a</sup> Department of Earth Sciences and Sprigg Geobiology Centre, The University of Adelaide, North Terrace, Adelaide, South Australia, 5005, Australia<sup>b</sup> Southern Seas Ecology Laboratories and the Environment Institute, School of Biological Sciences, The University of Adelaide, Adelaide, SA, Australia

### ARTICLE INFO

#### Keywords:

*Arthritica helmsi*  
Bivalve  
Trace element  
Proxy  
Coorong lagoon

### ABSTRACT

Element-to-calcium ratios of bivalve shells are potentially useful proxies for environmental change, provided the relationship between the environmental variable and element ratio are calibrated using modern specimens. In this study we investigate the utility of trace elemental ratios in the estuarine micromollusc *Arthritica helmsi* as (palaeo)environmental proxies. Sr/Ca, Mg/Ca and Ba/Ca ratios were measured in waters ( $n = 137$ ) and live bivalves ( $n = 125$ ) were collected along a salinity gradient from fresh to hypersaline in the Coorong Lagoon and Lake Alexandrina, at the terminus of the Murray River, South Australia. Water Mg, Sr and Ca exhibited linear relationships with salinity, while Ba showed no relationship. Mg/Ca and Sr/Ca in water both showed positive logarithmic responses to increasing salinity, while the response of Ba/Ca was best explained by a negative power function. The Sr concentration and Sr/Ca of water collected between 2016 and 2018 were elevated compared to a previous study conducted between 2007 and 2008, possibly due to a higher river flow regime in the more recent period. The range of Sr/Ca, Mg/Ca and Ba/Ca measured in *A. helmsi* were in agreement with previous studies, as were the range of partition coefficients. However, the incorporation of Sr/Ca, Mg/Ca and Ba/Ca did not correlate with water elemental ratios, temperature, salinity or pH and are therefore likely to be more heavily influenced by biological processes. As a consequence, while the elemental composition of other carbonate fossils within the Coorong system may hold potential to reconstruct past climate and environmental change, the trace element geochemistry of *A. helmsi* aragonite shells, and possibly other similar micro-bivalve molluscs, should be treated with caution as a palaeoenvironmental tracer.

### 1. Introduction

The geochemical signals preserved in bivalve shell carbonate provide a potential archive of climate variability spanning months to millennia depending on the species (Schone and Surge, 2014). Following the success of trace elemental ratios, notably Mg/Ca and Sr/Ca, as palaeothermometers in corals and other carbonate biominerals (e.g. Corrège, 2006; Mitsuguchi et al., 1996; Sinclair et al., 1998), the usefulness of these ratios as environmental recorders in bivalve species has been extensively studied in recent years (see Gillikin, 2019). Much of this growing body of research focusses on marine taxa (e.g. Carré et al., 2006; Elliot et al., 2009; Schöne et al., 2011), while a smaller body of work explores bivalve carbonate proxies in freshwater (e.g. Geeza et al., 2018; Izumida et al., 2011; Zhao et al., 2017) and estuarine species (e.g.

Gillikin et al., 2006; Lazareth et al., 2003; Surge et al., 2003). Continuous profiles of chemical change in shell carbonate are possible due to the sequential nature of growth, which can be analysed using high resolution techniques such as laser ablation – inductively coupled plasma – mass spectrometry (LA-ICP-MS). Such techniques record seasonal (Durham et al., 2017) and even daily (Poulain et al., 2015) cycles in bivalve carbonate geochemistry which can be used to provide baselines for natural seasonal variability, or record sudden events such as discharges or pollution to waterways (e.g. Krause-Nehring et al., 2012; O’Neil and Gillikin, 2014).

Strontium, magnesium and barium are three commonly examined metals in bivalve shells and have been employed as proxies for environmental conditions with mixed success. Mg/Ca and Sr/Ca have been extensively tested as temperature proxies (e.g. Freitas et al., 2005;

\* Corresponding author.

E-mail address: [briony.chamberlayne@adelaide.edu.au](mailto:briony.chamberlayne@adelaide.edu.au) (B.K. Chamberlayne).

<https://doi.org/10.1016/j.ecss.2021.107354>

Received 1 January 2021; Received in revised form 19 March 2021; Accepted 24 March 2021

Available online 2 April 2021

0272-7714/© 2021 Elsevier Ltd. All rights reserved.

Poulain et al., 2015; Schöne et al., 2011; Wanamaker and Gillikin, 2018), though many studies have found that these ratios are controlled by biological effects such as metabolism and growth rate (e.g. Gillikin et al., 2005; Lorrain et al., 2005; Vander Putten et al., 2000). However, some species have been shown to reliably record temperature variation in their Mg/Ca (Freitas et al., 2012; Tynan et al., 2017) and Sr/Ca ratios (Yan et al., 2013; Zhao et al., 2017). Ba/Ca ratios display a relatively invariable background interrupted by sharp peaks (Gillikin et al., 2008), which have been related to phytoplankton blooms in several studies (e.g. Elliot et al., 2009; Thébaud et al., 2009). Ba/Ca in bivalves also correlates with Ba/Ca of the ambient waters that the bivalve grew in (Izzo et al., 2016; Poulain et al., 2015), which often co-vary with salinity (Walther and Nims, 2015). Though many studies have had success reconstructing various environmental variables from elemental ratios in bivalves, other studies have uncovered intra-population heterogeneity at the micro-metre scale (Schöne et al., 2013). In addition, uncertainties around element partitioning in juveniles and fast growing species have also hindered the interpretation of elemental patterns in bivalve carbonate (Wanamaker and Gillikin, 2018). The conflicting results of previous studies of bivalve taxa highlight the need for species specific calibrations. This is especially important in estuarine environments where water chemistries are dynamic and determined by mixing from various distinct water sources as well as processes such as evaporation, in contrast to relatively stable marine waters (Walther and Nims, 2015). It is therefore essential to understand the drivers of water chemistry in such systems to rigorously interpret the signals in biogenic carbonates (Elsdon and Gillanders, 2006).

In this study, we examine the Sr/Ca, Mg/Ca and Ba/Ca patterns in the micro-mollusc *Arthritica helmsi* to compare to the chemical and physical properties of the ambient waters. Abundant in south eastern Australian estuaries and also in the sediment record (Chamberlayne, 2015; Kanandjembo et al., 2001; Matthews and Constable, 2004; Semeniuk and Wurm, 2000), *A. helmsi* is an aragonitic micro-mollusc with a broad environmental tolerance (Wells and Threlfall, 1982a), short life span of ~1 year (Wells and Threlfall, 1982b), and continuous growth (Chamberlayne et al., 2020; Wells and Threlfall, 1982b). A previous geochemical analysis of this species from museum collections showed promising correlations between Sr/Ca and Mg/Ca and temperature (Chamberlayne et al., 2020), although water chemistry data were not available for that study. Consequently, there was a need for a more detailed investigation into trace element incorporation into *A. helmsi* with tighter constraints over the physical conditions and water chemistry during growth.

The objectives of this study were to: (i) determine the controls and stability of elemental chemistry in the waters of the Coorong Lagoons collected over an 18 month period; (ii) obtain high-resolution records of element-to-calcium variation within individuals of *Arthritica helmsi*; (iii) compare element-to-calcium signals within contemporary specimens; and (iv) compare carbonate elemental data to the physical and chemical properties of host waters.

## 2. Methods

### 2.1. Study site

The Coorong is a ~130 km long, narrow estuarine coastal lagoon system located at the terminus of Australia's Murray Darling Basin (Fig. 1). A constricted channel at Parnka Point separates the estuary into the North Lagoon and the South Lagoon, which are characterised by a north-south salinity gradient (Geddes and Butler, 1984; Gillanders and Munro, 2012). The North Lagoon is connected to the Murray River via Lake Alexandrina (Fig. 1) and also receives inflows of tidal marine waters, while the South Lagoon receives freshwater surface flows from the South East Drainage Network at Salt Creek. Groundwater inputs are an additional water input of varying quantity along the length of the lagoons (Haese et al., 2008; Shao et al., 2018). A series of barrages

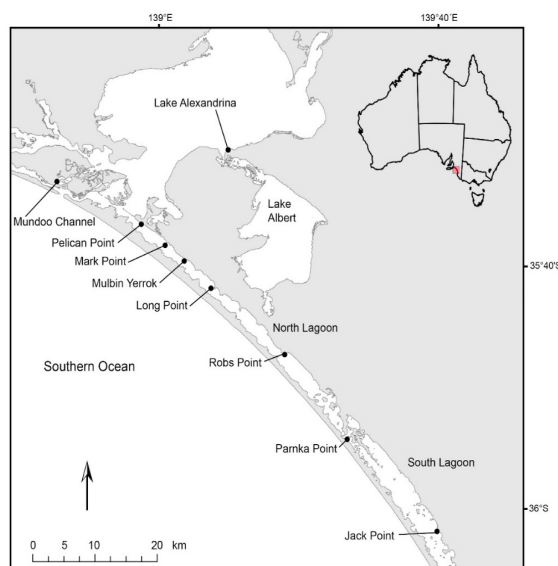


Fig. 1. Sampling locations in Lake Alexandrina and the Coorong Lagoons at the terminus of the River Murray.

constructed in the 1940s control the release of freshwater from Lake Alexandrina to the North Lagoon (Fig. 1). Daily salinity and temperature monitoring data for Pelican Point and Long Point for the sampling period were sourced from the WaterConnect website (Government of South Australia, 2020).

### 2.2. Water sampling and analysis

Surface waters were collected from 9 sites along Lake Alexandrina, the Coorong and Murray Mouth (Fig. 1) approximately monthly from November 2016 to May 2018 ( $n = 137$  samples in total). The location and date for each sample collection are summarised in Table S1. A single measurement of water temperature, salinity and pH was measured using a Hanna Instruments HI-98194 multiparameter probe at each site during each sampling time, and water samples were collected in hydrochloric acid washed 250 mL HDPE bottles for trace element analyses. Water samples were filtered through 2  $\mu\text{m}$  cellulose nitrate filters and acidified to 2% with nitric acid before being refrigerated prior to analysis.

Water samples were analysed for major and trace element concentration at Adelaide Microscopy, University of Adelaide, with an Agilent 8900x inductively coupled plasma-mass spectrometer (ICP-MS). The plasma conditions were: RF power 1550W, sample depth 10  $\mu\text{m}$  and total Ar carrier gas flow rate 1.05 L/min, with a Micro Mist nebuliser and Scott Type spray chamber. The collision cell was run in He mode (4 mL/min He gas flow) for the majority of elements (Mg, Sr and Ba). Ca was analysed with oxygen (30% flow rate) in the collision cell and the  $\text{MO}^+$  reaction products measured:  $^{44}\text{Ca} \rightarrow ^{44}\text{Ca}^{16}\text{O}$  at mass 60. On-line addition of indium was used as the internal standard. A series of mixed element calibration solutions (10, 50, 100, 200, 300, 500, 1000 ppb) were used for quantification. The IAPSO sea water reference material (OSIL) was used as a quality control standard. Samples were diluted with ultra-pure water acidified to 2% with nitric acid by a factor of 10, 20, 40, 50, 80, 100 or 120 times depending on sample salinity. 15% of samples were analysed in triplicate; the mean precision for triplicate samples was <1% for Mg and Sr; 1.8% for Ca; and 5.2% for Ba.

### 2.3. Shell collection and analysis

Shells were collected from the sediment water interface from five sites (Mundoo Channel, Pelican Point, Mark Point, Mulbin Yerrok and



Long Point) in the North Lagoon of the Coorong (Fig. 1) on six occasions between March 2017 and May 2018. Between 1 and 8 individual live shells were collected from each site at each sampling time, totalling 125 individuals (Table S2). Digital callipers were used to measure the length of the maximum growth axis. Residual organic matter was then removed via treatment with an 18% H<sub>2</sub>O<sub>2</sub> solution which was buffered to pH 8 using 0.5 M sodium hydroxide (Falster et al., 2018). The shells were then rinsed in ultra-pure water with a resistivity of 18.2 MΩ at 25 °C and a pH of 7 and dried for 12 h at 30 °C. One valve from each individual shell (n = 125) was embedded in indium spiked epoxy resin (40 ppm) and sectioned along the maximum growth axis to approximately 0.8 mm using a Buehler Isomet Low Speed Saw with diamond edge blades. Shell sections were polished to a thickness of approximately 0.5 mm on progressively finer grades of lapping film (30, 9, 3 μm) and then adhered to slides with indium spiked thermoplastic glue.

To investigate physical representations of growth increments in *A. helmsi* two sectioned shells were immersed in Mutvei's solution following the methods of Schöne et al. (2005). Briefly, the Mutvei's solution was prepared using 100 mL 1% acetic acid, 100 mL 25% glutaraldehyde and ~2 g Alcian blue powder. The solution was heated to 40 °C and the samples were immersed for 30 min under constant stirring. The samples were then rinsed with demineralised water and allowed to air-dry before examination using light microscopy.

Trace element profiles for Mg, Sr, Ba and Ca were obtained using LA-ICP-MS at Adelaide Microscopy, University of Adelaide, using a New Wave Q-Switched Nd YAG 213 nm UV laser coupled with an Agilent 7500cs ICP-MS. Beam intensities of <sup>24</sup>Mg, <sup>88</sup>Sr, <sup>138</sup>Ba and <sup>43</sup>Ca were measured, in addition to <sup>44</sup>Ca as an internal standard and <sup>115</sup>In as an indicator of resin contamination. Pre-ablation with a 40 μm diameter spot size along the outer margin of the shell preceded ablation transects of a 30 μm diameter with repetition rate of 10 Hz at 10 μm/s scan speed. Transects were collected for each individual shell (n = 125) and spanned from the ventral margin to the umbo region. The length of individual transects ranged from 1.1 mm to 2.5 mm. The glass standard NIST SRM 612 and the USGS carbonate standard MACS-3 were analysed periodically to account for instrumental drift. The mean coefficient of variation of repeated measures was 1.08% for Mg, 1.06% for Sr and 1.29% for Ba. Data reduction was performed in Iolite (Hellstrom et al., 2008; Paton et al., 2011). Transects of elemental concentrations were smoothed with a 7-point running mean and 7-point running median (Sinclair et al., 1998) and are expressed as ratios to Ca.

#### 2.4. Calculation of partition coefficients

The relationship between the chemical composition of the bivalve carbonate and the chemical composition of the ambient water in which those bivalves grew can be quantified as a partition coefficient ( $D_{Me} = R_{carb}/R_{water}$ ) where  $R_{carb}$  is the metal to calcium ratio in the shell and  $R_{water}$  is the metal to calcium ratio in the water.

As the exact lifespan and growth rate of each specimen is unknown, two methods were employed when calculating partition coefficients and when comparing to water chemistry. Firstly, we estimated the lifespan of each shell based on its size and an assumed growth rate of 0.3 mm/month as estimated by Wells and Threlfall (1982b). Average water element ratios, temperature, salinity and pH for the lifespan of each shell were then calculated to the nearest month based on this age estimation. The second approach was to take the last 10 μm of each individual shell elemental transect (n = 125) at the ventral margin as a representation of the growth occurring immediately prior to the collection of the shell. The resulting metal to calcium ratio of the shell was then used in conjunction with the metal to calcium ratio of the water measured on the day of collection to calculate coefficients which represent a more constrained time period. The partition coefficients obtained from the two approaches were compared using a one-way ANOVA in R (R Core Team, 2020).

### 3. Results

#### 3.1. Elements in water

Dissolved element concentrations for Coorong waters and their uncertainties are summarised in Table S1. Concentrations of dissolved Mg, Sr and Ca of water samples all showed conservative relations with salinity (Fig. 2; Table 1), in agreement with data previously collected for the Coorong Lagoons by Gillanders and Munro (2012). Maximum concentrations of these elements were recorded at Jack Point in the South Lagoon (Fig. 1; Table S1); Mg and Ca maximum concentrations were measured in March 2018 while the maximum Sr concentration occurred in February 2018. Minimum concentrations for Mg, Sr and Ca were all recorded at Lake Alexandrina in March 2018. In contrast to a previous study by Gillanders and Munro (2012), there was no relationship found between Ba concentration and salinity (Fig. 2). The maximum value for Ba was recorded in Lake Alexandrina in August 2017, while the minimum concentration was recorded at Pelican Point in November 2016.

Mg/Ca, Sr/Ca and Ba/Ca all exhibited non-linear relationships with salinity (Fig. 3; Table 1). Mg/Ca and Sr/Ca exhibited a positive logarithmic correlation with salinity ( $r^2 = 0.932$  and  $r^2 = 0.927$  respectively), while Ba/Ca exhibited a negative power correlation with salinity ( $r^2 = 0.906$ ; Table 1). Maximum values for Mg/Ca and Sr/Ca were measured at the South Lagoon site Jack Point in February 2018 (Table S1). Minimum values for Mg/Ca and Sr/Ca both occurred in December 2016 at Mundoo Channel and Pelican Point respectively. Both Ba/Ca maximum and minimum values were measured in the North Lagoon with the maximum value in August 2017 at Lake Alexandrina, while the minimum value was measured at Mundoo Channel in September 2017.

#### 3.2. Elements in shells

Staining with Mutvei's solution showed no evidence of incremental growth. Examination of stained sections of *A. helmsi* showed a consistent structure with no visible growth lines. The average, standard deviation, minimum and maximum values of Sr/Ca, Mg/Ca and Ba/Ca ratios measured in shells are provided in Table S2. In summary, average Sr/Ca ranged from 1.39 mmol/mol in shell LP0317-2 to 3.06 mmol/mol in shell LP1017-2. Shell LP1017-2 also recorded the highest intra-shell range of Sr/Ca (7.59 mmol/mol). The average Sr/Ca in the last 10 μm of the ventral margin ranged from 1.27 to 4.78 mmol/mol in shells LP0317-1 and MP1017-4 respectively. The average Mg/Ca ranged from 0.26 to 1.61 mmol/mol in shells MC0317-1 and MC0518-4 respectively. The intra-shell range of Mg/Ca was lowest in shell PP0317-2 (0.38 mmol/mol) and highest in shell MC0518-4 (4.45 mmol/mol). Mg/Ca in the ventral margin of shells ranged from 0.26 to 2.43 mmol/mol in shells.

MC0317-1 and PP0518-3 respectively. Ba/Ca in the ventral margin ranged from 1.9 to 30 μmol/mol in shells LP0317-1 and PP0118-7 respectively, while the average Ba/Ca ranged from 2.8 to 22 μmol/mol in shells LP0317-2 and PP0817-1 respectively. The intra-shell range of Ba/Ca values ranged from 6.1 μmol/mol in shell MC0317-1 to 75 μmol/mol in shell PP0817-3. Shells with the lowest average and range of metal/calcium ratios were all collected in March 2017 from various sites, while shells recording the highest averages and intra-shell ranges were more varied in the timing of their collection. Average and ventral margin shell elemental ratios were regressed against water metal/calcium ratios, temperature, pH and salinity to assess controls on the incorporation of elements into shells (Fig. 4; Fig. 5). Weak but statistically significant relationships were found between shell average Mg/Ca<sub>carb</sub> and Mg/Ca<sub>water</sub> ( $r^2 = 0.075$ ;  $p = 0.003$ ) and Ba/Ca<sub>carb</sub> and Ba/Ca<sub>water</sub> ( $r^2 = 0.160$ ;  $p = <0.001$ ; Table 2). Similar relationships were not observed when comparing metal/calcium ratios between waters and the ventral margin of the shells (Table 2). Both the average ( $r^2 = 0.039$ ;  $p = 0.035$ ) and the ventral margin ( $r^2 = 0.046$ ;  $p = 0.016$ ) Ba/Ca ratios were

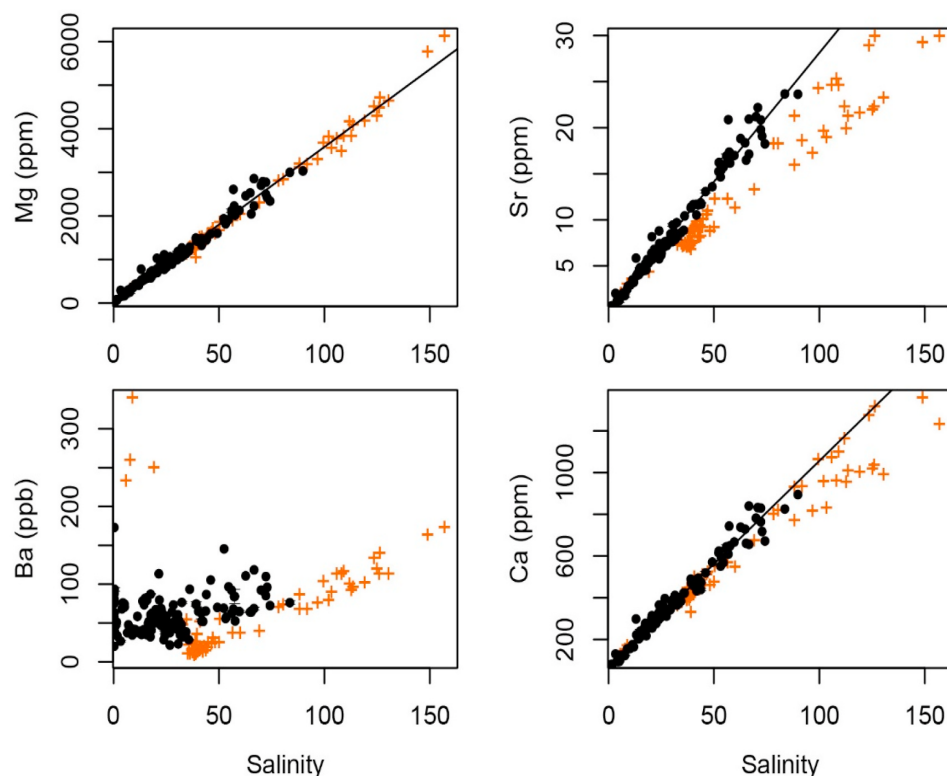


Fig. 2. Water elemental concentration against salinity for samples from all sites collected between November 2016 and May 2018 (black circles). Also depicted are elemental concentrations against salinity from Gillanders and Munro (2012) for Coorong waters collected between May 2007 and June 2008 (orange crosses). Error bars indicate  $\pm 1$  SE. (For interpretation of the references to colour in this figure legend, the reader is referred to the Web version of this article.)

Table 1

Relationships between elemental data, and salinity for all sites. Shown are the equations for the models of best fit and the corresponding r-squared values.

Vs. Salinity	Equation	$r^2$
Mg (ppm)	$y = 35.65 \times \text{salinity} + 19.58$	0.979
Sr (ppm)	$y = 0.28 \times \text{salinity} + 0.14$	0.980
Ba (ppb)	No Relationship	
Ca (ppm)	$y = 9.88 \times \text{salinity} + 68.70$	0.978
Mg/Ca (mol/mol)	$y = 0.892 \times \ln(\text{salinity}) + 1.722$	0.932
Sr/Ca (mmol/mol)	$y = 1.74 \times \ln(\text{salinity}) + 4.403$	0.927
Ba/Ca ( $\mu\text{mol/mol}$ )	$y = 466.51 \times (\text{salinity}^{-0.62})$	0.906

weakly correlated to temperature. Ventral margin Sr/Ca<sub>carb</sub> and Ba/Ca<sub>carb</sub> showed weak but significant relationships to pH. Ba/Ca<sub>carb</sub> had a weak but significant correlation to salinity for both shell averaged ( $r^2 = 0.165$ ;  $p < 0.001$ ) and ventral margin ( $r^2 = 0.036$ ;  $p = 0.029$ ) values. The intra-shell range of shell elemental ratios did not correlate to any environmental variable. In addition, there were no obvious differences between samples when separated into high ( $>35$ ) and low ( $<35$ ) salinities (Fig. 4; Fig. 5).

Continuous laser ablation transects allow the comparison of signals between contemporary specimens. As an example, trace elemental transects from four shells collected on the same occasion from Pelican Point and Long Point are compared in Fig. 6. Also shown is the salinity and temperature from nearby logging stations plotted over a period of time estimated as the maximum possible lifespan of the shells. Trace elemental transects from all shells showed a similar range of values and some but not all peaks were displayed across multiple specimens (Fig. 6). There did not appear to be similarity between any element to calcium ratio in shells from Pelican Point or Long Point and salinity or

temperature from the corresponding site (Fig. 6).

### 3.3. Partition coefficients

Strontium partition coefficients ranged from 0.14 to 0.75 for whole shell average values and from 0.13 to 0.74 for ventral margin values. The partition coefficients for average magnesium concentrations ranged from 0.00006 to 0.001, while for ventral margin values of magnesium the range was 0.00006–0.0014. The barium partition coefficients ranged from 0.007 to 0.37 and from 0.007 to 0.79 for average and ventral margin samples respectively. The strontium and magnesium partition coefficients of five shells collected from Mundoo Channel in October 2017 plotted outside 1.5 times the interquartile range for all data (Fig. 7), while the outliers in the barium data were from various sites.

## 4. Discussion

This study examined patterns in elemental concentrations in the waters of the Coorong Lagoons and of a resident bivalve species *A. helmsi*. Abundantly preserved in sediments, geochemical analyses of the fossil shells of *A. helmsi* offer a potential proxy for palaeo-environmental reconstruction, particularly due to the interest in the past environmental condition of the Ramsar listed Coorong system. Our results show that over a salinity gradient of  $\sim 0$ –90, concentrations of Mg and Sr in waters responded conservatively to changes in salinity. The Mg/Ca and Sr/Ca ratios in waters displayed a strong positive non-linear relationship with salinity, while Ba/Ca was found to have a negative non-linear relationship with salinity. These patterns remained largely consistent over time, and during wetter and drier climates, as observed when comparing the newly collected data with a previous study conducted from 2007 to 2008 by Gillanders and Munro (2012). However,

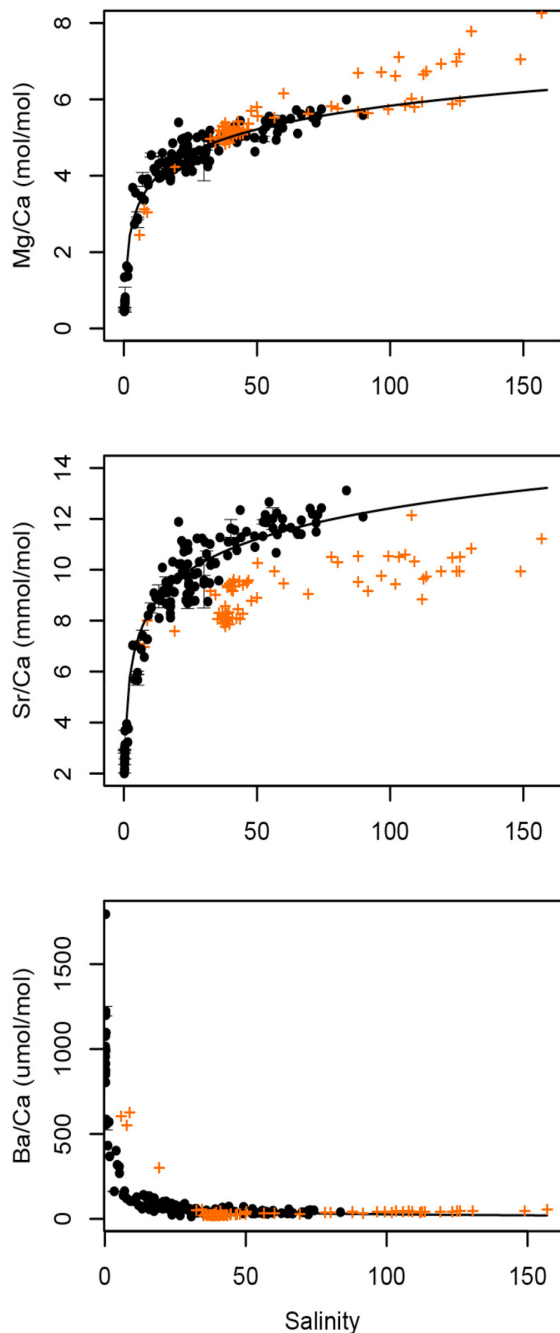


Fig. 3. Elemental ratios plotted against salinity for all samples collected in the Coorong between November 2016 and May 2018 (black circles). Also shown are elemental ratios against salinity from Gillanders and Munro (2012) for Coorong waters collected between May 2007 and June 2008 (orange crosses). Error bars indicate  $\pm 1$  SE. (For interpretation of the references to colour in this figure legend, the reader is referred to the Web version of this article.)

trace elemental ratios measured in live collected specimens of *A. helmsi* exhibited poor correlations with water chemistry. While trace element profiles across individual shells showed some synchronous peaks between shells, these patterns were not correlated with time series of water salinity or temperature. Furthermore, the spatial and temporal patterns in whole shell geochemistry, or that of the most recent carbonate deposition, exhibited poor correlations with ambient water chemistry

and temperature. This absence of environmental controls on the incorporation of Sr/Ca, Mg/Ca and Ba/Ca into *A. helmsi* are in agreement with previous studies of other bivalve taxa (Carré et al., 2006; Lorrain et al., 2005; Poulain et al., 2015; Wanamaker and Gillikin, 2018).

#### 4.1. Environmental controls over the elemental composition of contemporary Coorong waters: strontium and magnesium

The concentration of Mg, Sr and Ca in the waters of the Coorong Lagoons and Lake Alexandrina responded conservatively to salinity (Fig. 2). Previous studies have found similar linear relationships in estuaries globally (Mohan and Walther, 2015; Nelson and Powers, 2020; Surge and Lohmann, 2002), though few studies have investigated these relationships in hypersaline waters (Diouf et al., 2006). The linear response of Mg, Sr and Ca is predicted by the mixing of fresh and marine waters (Walther and Limburg, 2012) and further concentration of elements occurs alongside sodium chloride concentration by evaporation (Gibbs, 1970). Mg/Ca and Sr/Ca displayed logarithmic relationships to salinity (Fig. 3). Such non-linear relationships are mathematically predicted for the ratio of two conservative constituents if at least one of the constituents has a non-zero endmember (Walther and Limburg, 2012), as observed in the Coorong where, for example, Ca concentrations in fresh waters from Lake Alexandrina (<1 salinity) did not fall below 10 ppm. Similar relationships have been found in previous estuarine studies (Macdonald and Crook, 2010; Nelson and Powers, 2020; Surge and Lohmann, 2002). The relationship between salinity and Mg/Ca or Sr/Ca is steepest at low salinities (<30) and is therefore more likely to be a sensitive tracer for salinity in low salinity waters. It has long been thought that Mg/Ca and Sr/Ca are stable in waters above a salinity of  $\sim 10$  (Dodd and Crisp, 1982), though recent research has challenged this notion (Lebrato et al., 2020). In this study, it was clear that while the slope of the curve between Mg/Ca and Sr/Ca and salinity decreased at higher salinities, the elemental ratios did not plateau in the salinity range investigated (Fig. 3).

A previous study on major and trace element concentrations in the Coorong Lagoons in 2007/2008 was undertaken during the ‘Millennium Drought’ – a period in which the region experienced widespread rainfall deficit and evaporation (Gillanders and Munro, 2012). The Gillanders and Munro (2012) study allows a direct comparison of relationships during periods of high and low precipitation and/or river discharge (Fig. 2; Fig. 3). The conservative behaviour of Mg in the Coorong did not differ between the two studies. However, the slope of the linear element-salinity relationship was slightly steeper for Ca and Sr in the current study (Fig. 2), compared to Gillanders and Munro (2012).

One possible explanation for the differences in Sr and Ca concentrations at high salinities between the two studies is increased carbonate precipitation facilitating Sr and Ca removal during the Millennium Drought. Gillanders and Munro (2012) proposed aragonite precipitation to be the cause of increased scatter in Sr and Ca in hypersaline waters in their study. Water chemistry in the hypersaline southern lagoon is known to be altered by the precipitation of inorganic aragonite rich carbonate crusts and tufa on the sediment surface (Ford, 2007; Shao et al., 2018; 2021) and the fraction of Sr removed from the present day South Lagoon as aragonite has been recently estimated at 35–45% (Shao et al., 2021). During 2007–2008, salinity was higher than that observed during the 2016–2018 monitoring period (Fig. 2), which leads to an increased concentration of bicarbonate and carbonate mineral precipitation (Haese et al., 2009) and a subsequent decrease in ionic concentration in the residual water. Another possibility is that increased inputs of freshwater provide additional Sr into the lagoons (Beck et al., 2013; Walther and Nims, 2015). Previous studies have suggested Sr inputs from groundwater in the Coorong and Lower Lakes (Shao et al., 2018), and so changes in the relative inputs of freshwater sources (river water and groundwater) could explain the differences in water chemistry during and after drought. Overall, the comparison of water chemistry data between the 2007–2008 and 2016–2018 monitoring periods

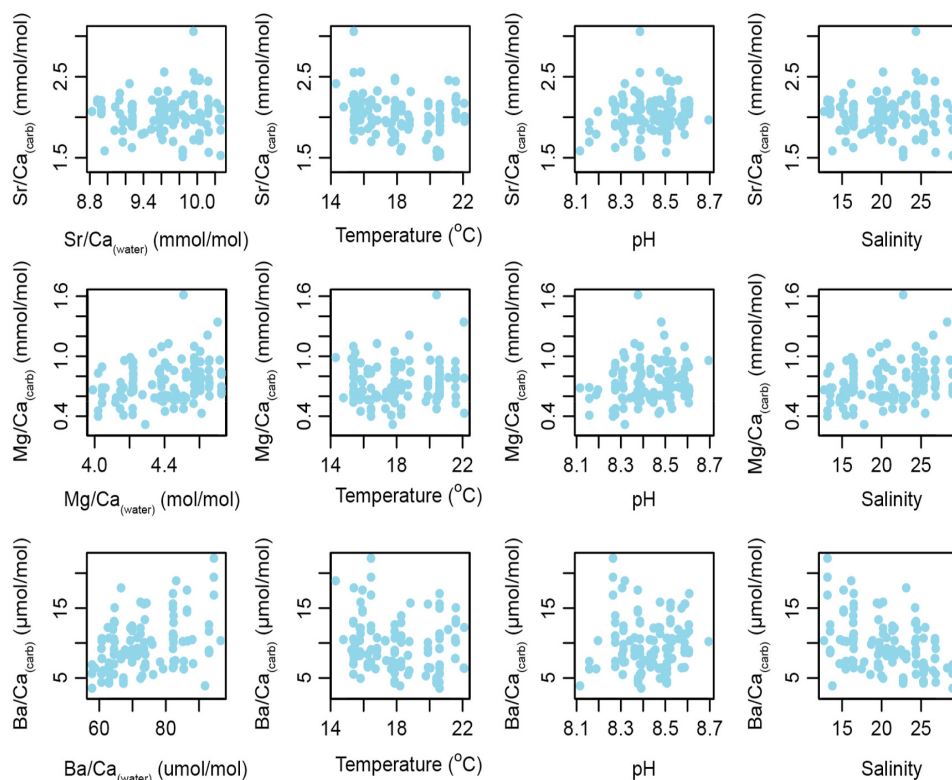


Fig. 4. Average element/calcium ratio in *A. helmsi* vs. water element/calcium ratio, temperature, pH and salinity.

suggests that Mg concentrations are more likely to be a consistent proxy for lagoonal water salinity, whereas Sr concentrations may vary in time due to changes in freshwater input vs. aragonite export. A combination of trace element and Sr or Ca stable isotope data (e.g. Shao et al., 2018) offer potential to unravel these effects through time.

#### 4.2. Environmental controls over the elemental composition of contemporary Coorong waters: barium

Barium concentrations displayed the most dissimilar patterns between the 2007–2008 and 2016–2018 monitoring periods, indicating that the drivers of Ba dynamics in the Coorong estuary have changed over time. Our current study found no relationship between Ba concentration and salinity, in agreement with previous studies in estuarine systems (Moore and Shaw, 2008; Nelson and Powers, 2020; Walther and Nims, 2015). This contrasts to the segmented linear model with a break point around a salinity of 37 found by Gillanders and Munro (2012) in the Coorong waters during the Millennium Drought. However, it is not unusual for Ba behaviour to vary greatly between estuaries and within estuaries due to factors including differences in weathering rates and river flow (Coffey et al., 1997).

There are several possible causes for the differences in Ba patterns between the two time periods, likely due to a change in flow dynamics. Low freshwater flow and associated oxygen depletion, as experienced during the Millennium Drought (Aldridge and Brookes, 2011), can increase the concentration of dissolved iron and influence primary productivity which can both impact Ba removal in estuaries (Coffey et al., 1997; Colbert and McManus, 2005). Low salinity Ba removal can occur due to absorption of Ba to flocculated iron oxyhydroxides (Coffey et al., 1997; Gillanders and Munro, 2012) which increase in concentration when oxygen levels are low (Aldridge and Brookes, 2011). Barium is then available for desorption at higher salinities (Coffey et al., 1997) and can then be concentrated by evaporation, potentially explaining the

break point linear model of Gillanders and Munro (2012). A change in hydrodynamics between 2007–2008 and 2016–2018 could also influence productivity (Lehrter et al., 2009), whereby an increase in productivity is associated with barite precipitation in estuaries (Stecher and Kogut, 1999) which in turn is a mechanism for Ba removal. Productivity in the Coorong and Lake Alexandrina was relatively stable during periods of drought, yet more variable in concert with variable freshwater flows (Murrell et al., 2007). As Ba concentrations are related to river flow, the variable releases from the barrages of the Coorong during the sampling period of the current study and the associated changes in removal/release of Ba could mask the signals observed in other estuaries (Carroll et al., 1993; Edmond et al., 1978; Stecher and Kogut, 1999).

While Ba concentrations showed no significant relationship with salinity, Ba/Ca was found to exhibit a negative power relationship with salinity (Fig. 3). Similar patterns have been observed in tank and field studies of Ba/Ca in estuarine waters where Ba and Ca concentrations are non-conservative and conservative with salinity respectively (Macdonald and Crook, 2010; Nelson and Powers, 2020; Walther and Nims, 2015).

#### 4.3. Environmental controls on Sr/Ca and Mg/Ca incorporation in *A. helmsi*

The Sr/Ca and Mg/Ca ratios measured in shells of *A. helmsi* in this study are comparable with those measured in a previous geochemical analysis of shells of this species (Chamberlayne et al., 2020). Furthermore, the Sr/Ca and Mg/Ca ratios are within the range of the values reported in other estuarine (e.g. Füllenbach et al., 2015; Poulain et al., 2015), freshwater (e.g. Geeza et al., 2018; Zhao et al., 2017) and marine bivalves (e.g. Carré et al., 2006; Elliot et al., 2009).

Temperature, salinity, pH and water trace element ratios were not strongly correlated to Sr/Ca or Mg/Ca in *A. helmsi* shells (Table 2). Temperature has been hypothesised to control Sr and Mg incorporation

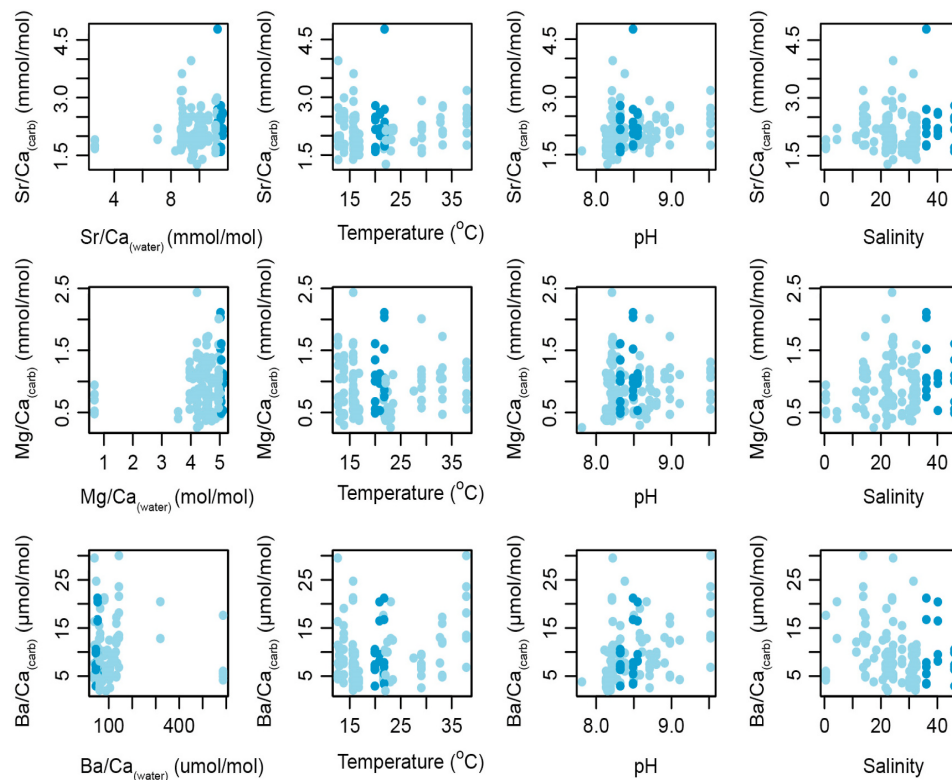


Fig. 5. Ventral margin element/calcium ratio in *A. helmsi* vs. water element/calcium ratio, temperature, pH and salinity. Light blue points represent samples where salinity <35 and dark blue points are samples where salinity is > 35. (For interpretation of the references to colour in this figure legend, the reader is referred to the Web version of this article.)

Table 2

Linear regression statistics for average and ventral margin *A. helmsi* metal/calcium ratios vs. water metal/calcium ratios, temperature and pH. Statistically significant results are presented in bold.

Relationship	Average shell x/Ca		Ventral margin x/Ca	
	r <sup>2</sup>	p	r <sup>2</sup>	p
Sr/Ca <sub>carb</sub> vs Sr/Ca <sub>water</sub>	<0.001	0.94	0.028	0.063
Mg/Ca <sub>carb</sub> vs Mg/Ca <sub>water</sub>	<b>0.075</b>	<b>0.003</b>	0.025	0.077
Ba/Ca <sub>carb</sub> vs Ba/Ca <sub>water</sub>	<b>0.160</b>	<b>&lt;0.001</b>	0.002	0.571
Sr/Ca <sub>carb</sub> vs temperature	<b>0.064</b>	<b>0.006</b>	0.021	0.215
Mg/Ca <sub>carb</sub> vs temperature	0.007	0.345	0.001	0.764
Ba/Ca <sub>carb</sub> vs temperature	<b>0.039</b>	<b>0.035</b>	<b>0.046</b>	<b>0.016</b>
Sr/Ca <sub>carb</sub> vs pH	0.034	0.051	<b>0.041</b>	<b>0.024</b>
Mg/Ca <sub>carb</sub> vs pH	0.008	0.344	0.001	0.744
Ba/Ca <sub>carb</sub> vs pH	0.002	0.642	<b>0.121</b>	<b>&lt;0.001</b>
Sr/Ca <sub>carb</sub> vs salinity	<0.001	0.939	0.005	0.411
Mg/Ca <sub>carb</sub> vs salinity	<b>0.076</b>	<b>0.003</b>	0.023	0.088
Ba/Ca <sub>carb</sub> vs salinity	<b>0.165</b>	<b>&lt;0.001</b>	<b>0.036</b>	<b>0.029</b>
D <sub>Sr</sub> vs temperature	0.004	0.453	0.011	0.254
D <sub>Mg</sub> vs temperature	0.002	0.580	0.004	0.493
D <sub>Ba</sub> vs temperature	<b>0.296</b>	<b>&lt;0.001</b>	<b>0.094</b>	<b>&lt;0.001</b>

into bivalves following the observation of a strong relationship in abiogenic aragonite (Dietzel et al., 2004). Sr/Ca has been found to be temperature controlled in some studies of aragonitic bivalve species (Hart and Blusztajn, 1998; Yan et al., 2013; Zhao et al., 2017), while Mg/Ca has been more successfully related to temperature in calcitic shells (e.g. Freitas et al., 2005; Tynan et al., 2017). A previous study of the trace elemental ratios within *A. helmsi* found significant relationships between both Sr/Ca and Mg/Ca and temperature (Chamberlayne et al., 2020). However, in that previous study water temperature was approximated from air temperature and therefore potentially subject to

uncertainties.

Most studies have concluded that Sr/Ca and Mg/Ca in bivalve shells are under physiological control (e.g. Carré et al., 2006; Gillikin et al., 2005; Lorrain et al., 2005; Vander Putten et al., 2000; Wanamaker et al., 2008; Wanamaker and Gillikin, 2018). The incorporation of elements into *A. helmsi* could be influenced by growth rate as observed in several studies of bivalve taxa (e.g. Carré et al., 2006; Freitas et al., 2006; Izumida et al., 2011; Lorrain et al., 2005) and also in inorganic aragonite (Gaetani and Cohen, 2006). A significant relationship between temperature and both Sr/Ca and Mg/Ca was observed in a study by Schöne et al. (2011) after the elimination of vital effects by age detrending Sr/Ca data and growth rate detrending Mg/Ca data. This approach could not be undertaken in *A. helmsi* due to the uncertainties around the growth rate. Staining of sections of *A. helmsi* with Mutvei's solution did not reveal growth lines. A previous study of *A. helmsi* also reported a lack of physical representations of growth on sections examined under both scanning electron microscopy and electron microprobe analysis (Chamberlayne et al., 2020).

Element concentration during reproduction could also contribute to the disequilibrium between elements and waters in *A. helmsi*. Mg enriched organic layers have been found in other bivalve species (Schöne et al., 2010; Takesue and van Geen, 2004) and can form in response to reproduction (Durham et al., 2017). A study on the estuarine bivalve *Ruditapes philippinarum* also found a suite of other elements were concentrated during reproduction (Vieira et al., 2021). Reproduction in *A. helmsi* is reported to be continuous, and young develop in a brood pouch (Wells and Threlfall, 1982c). The effect of their reproductive strategy on the incorporation of elements in *A. helmsi* is unknown and could be a target for future research. Furthermore, as *A. helmsi* inhabit the sediment-water interface, it is possible that the element concentrations in their carbonate shells may reflect the chemistry of the pore

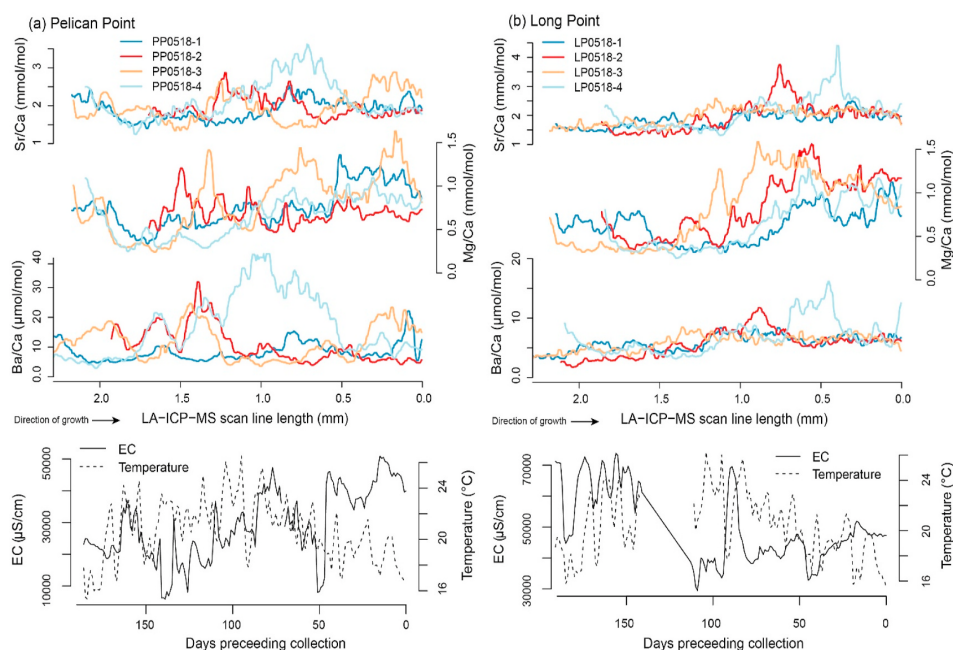


**Fig. 6.** Sr/Ca, Mg/Ca and Ba/Ca profiles of four shells of *A. helmsi* collected from (a) Pelican Point and (b) Long Point. Also shown are the temperature and salinity data for each site for the time period possibly corresponding to their lifespan. The ventral margin (0 mm) represents the most recent growth of each shell and collection times. The partition coefficients did not vary significantly when calculated from average or ventral margin element/calcium ratios for strontium ( $F = 1.29$ ,  $p = 0.26$ ) or barium ( $F = 0.024$ ,  $p = 0.88$ ). The partition coefficients for magnesium were higher when calculated using ventral margin Mg/Ca than when using average Mg/Ca ( $F = 5.31$ ,  $p = 0.022$ ). The strontium and magnesium partition coefficients were not correlated with temperature, while both average and ventral margin Ba partition coefficients showed a weak but significant relationship with temperature ( $r^2 = 0.296$ ;  $p = <0.001$  and  $r^2 = 0.094$ ;  $p = <0.001$  respectively; Table 2).

water or sediment surface chemistry in addition to the chemistry of the overlying water column (Griscom and Fisher, 2004; Schöne and Krause Jr, 2016). The distribution of elements in pore waters can be heterogeneous compared to the water column (Griscom and Fisher, 2004) and could therefore cause some variance in specimens from the same population. However, *A. helmsi* are suspension feeders (Lautenschlager et al., 2014) and so regularly access the main water column. We did not investigate the chemistry of the pore water in this study, but it could be an interesting avenue for further investigation.

Partition coefficients varied between individuals (Fig. 7), and similar to other species imply that the incorporation of Sr and Mg into the carbonate is regulated by physiological processes (Poulain et al., 2015; Schöne et al., 2011). The range of  $D_{Sr}$  and  $D_{Mg}$  found in this study were mostly well below equilibrium and the values were comparable to previous studies for both Sr (e.g.  $\sim 0.25$ , Gillikin et al., 2005;  $\sim 0.13$ – $0.28$ , Schöne et al., 2011,  $\sim 0.25$ , Poulain et al., 2015) and Mg (e.g.  $\sim 0.0003$ – $0.0008$ , Geeza et al., 2018;  $\sim 0.0003$ – $0.00042$ , Izumida et al., 2011). Five shells collected in October 2017 from Mundoo Channel had significantly higher  $D_{Sr}$  and  $D_{Mg}$  than the other shells in this study, however this appears to reflect the effects of a short term pulse of freshwater which was not representative of the growth conditions for these organisms. The salinity at Mundoo Channel on the collection day was  $<1$  (Table S1) and accordingly the concentrations of Sr/Ca and Mg/Ca were very low (Fig. 3) resulting in the apparently large partition coefficients. Mundoo Channel is located at the mouth of the estuary, near the barrages which control fresh water release from Lake Alexandrina (Fig. 1). Only weekly barrage release data are available (Government of South Australia, 2020), however it is likely that the barrages were opened on this day, releasing a pulse of low salinity water which was not recorded in the Sr/Ca or Mg/Ca ratios of the last growth recorded in these shells.

#### 4.4. Environmental controls on Ba/Ca incorporation in *A. helmsi*

The range of Ba/Ca measured in shells in this study ( $\sim 0.002$ – $0.03$  mmol/mol) was also consistent with those measured in a previous geochemical analysis of *A. helmsi* (Chamberlayne et al., 2020). Similar values have also been reported in the euryhaline Manila clam, *Ruditapes philippinarum* (Poulain et al., 2015) and estuarine mussel, *Mytilus edulis* (Gillikin et al., 2006). Carbonate Ba/Ca was very weakly correlated to salinity and temperature in both average and ventral margin analyses (Table 2). Previous studies of estuarine bivalve taxa have found strong relationships between carbonate and water Ba/Ca, suggesting their utility as an estuarine salinity proxy (Gillikin et al., 2006; Poulain et al., 2015). Other studies of marine species have directly correlated shell Ba/Ca and salinity (Izzo et al., 2016; Wanamaker and Gillikin, 2018), though in a culture study of juvenile *Arctica islandica* by Wanamaker and Gillikin (2018) the salinity interaction varied in strength with temperature highlighting the complexity of interactions during biomineralisation. Similarly, Zhao et al. (2017) in a culture study of the salinity tolerant (0–24) *Corbicula fluminea*, found that Ba/Ca in bivalve carbonate was controlled by a combination of factors including temperature, food supply, shell growth rate, and the Ba/Ca ratio of water. The controlled nature of their laboratory study allowed the factors controlling barium concentration in the shell to be identified, most of which would be difficult to disentangle in a highly variable natural environment.

Partition coefficients were variable, though the median values were similar when calculated with both the average Ba/Ca values and the ventral margin Ba/Ca values (Fig. 7). There was a weak temperature dependence observed in both average and ventral Ba partition coefficients, a pattern also observed in a previous study on otoliths (Miller, 2009). Apart from some abnormally high values calculated using the ventral margin Ba/Ca values, Ba partition coefficient values were well

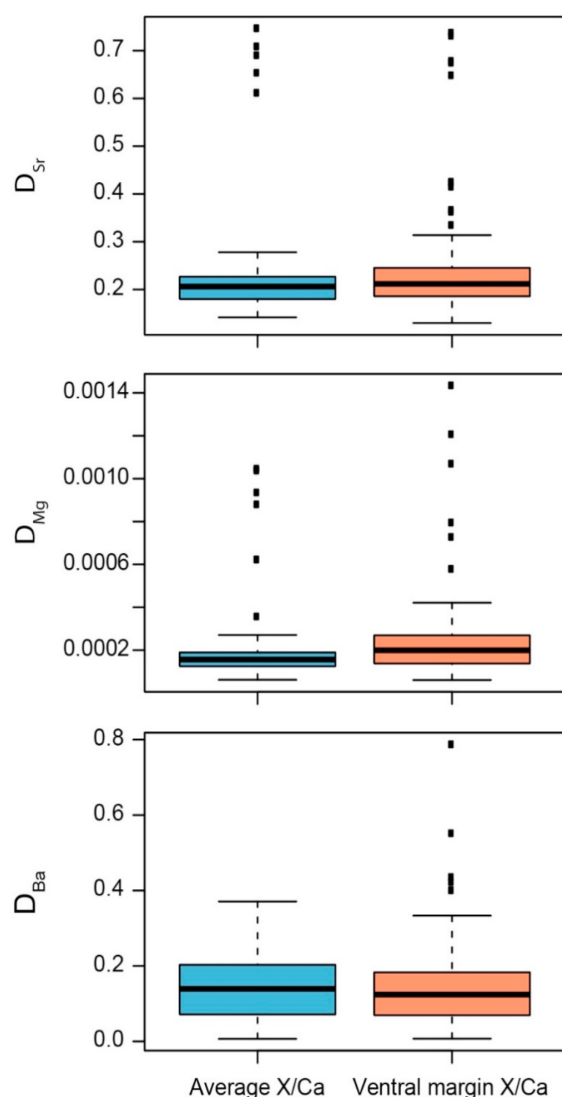


Fig. 7. Box and whisker plot of partition coefficients of Sr, Mg and Ba for average metal/Ca and ventral margin metal/Ca in *A. helmsi* shells ( $n = 125$ ).

below those observed in inorganic aragonite ( $>0.5$ ; Dietzel et al., 2004; Gaetani and Cohen, 2006), suggesting the influence of physiological or biological factors as proposed in previous studies (Geeza et al., 2018; Wanamaker and Gillikin, 2018; Zhao et al., 2017).

Ba/Ca ratios in bivalve shells have previously been characterised by a stable background interrupted by synchronous sharp peaks (e.g. Gillikin et al., 2008; Goodwin et al., 2013; Hatch et al., 2013; Thébault et al., 2009). The cause of these peaks has been attributed to phytoplankton blooms in several studies (Elliot et al., 2009; Thébault et al., 2009; Vander Putten et al., 2000), though several others have been unable to determine the cause (Gillikin et al., 2008; Goodwin et al., 2013; Hatch et al., 2013). Data recording chlorophyll or phytoplankton blooms were not available for this study, but the similarity between some peaks in Ba/Ca transects among specimens (Fig. 6) indicates that there may be a common environmental control that could be confounded by other environmental or biological factors as noted above.

## 5. Conclusions and implications for palaeoenvironmental studies

Reliable environmental reconstructions from the geochemistry of biogenic carbonate rely on an understanding of the stability of water chemistry and its correlations to environmental variables (Elsdon and Gillanders, 2006; Mohan and Walther, 2015; Nelson and Powers, 2020; Walther and Limburg, 2012). In this study, significant relationships between water trace elements and salinity were found in the Coorong Lagoons, which we primarily attribute to changes in surface water evaporation. The significant relationships between salinity and the Mg/Ca, Sr/Ca and Ba/Ca ratios in water suggested that these ratios hold potential for reconstructing past hydrological change in the Coorong. Due to the curvilinear relationships of salinity to element ratios, they would be most successfully employed as salinity proxies below marine salinities. The relationship between salinity and Mg/Ca was similar to that found in a previous study on elemental concentration in the Coorong (Gillanders and Munro, 2012). The differences in Sr/Ca and Ba/Ca behaviour alongside salinity in this study compared to the previous study by Gillanders and Munro (2012) were attributed to differences in hydrological regime over time, whereby decreased salinity and increased freshwater inputs in the present study have potentially altered carbonate precipitation dynamics from those experienced during the Millennium Drought. Therefore, Mg/Ca may serve as the most reliable salinity tracer in biogenic carbonates given the stability of these ratios across a range of hydrological states in the Coorong. However, the use of trace elemental geochemistry to reconstruct past environments requires that the geochemical properties of the water are reflected in those of contemporary carbonates, and for the bivalve *A. helmsi*, this appears not to be the case.

Controls over the incorporation of Sr/Ca, Mg/Ca and Ba/Ca into *A. helmsi* could not be constrained in this study. The occurrence of some synchronous peaks in trace elemental transects suggest the possibility of some degree of external control on element incorporation, though this signal is likely confounded by the complex interactions of environmental and biological variables as observed in previous studies (e.g. Zhao et al., 2017). Culture studies where factors such as temperature, salinity, water element chemistry and food amount can be controlled may be necessary to determine the effect of each on the element partitioning into *A. helmsi*. Laboratory or field studies using chemical tracers could also be useful in investigating the influence of physiological variables, such as growth, on element partitioning. The findings from this study indicate that Sr/Ca, Mg/Ca and Ba/Ca in *A. helmsi* are not currently reliable environmental proxies and that additional work would be required before the interpretation of these elemental ratios in (sub)fossil specimens could be made. Furthermore, this study highlights the need for contemporary investigations into the chemical and physical properties of waters prior to the interpretation of proxy data from biogenic carbonates, particularly in highly variable or altered environments.

## CRedit authorship contribution statement

**Briony K. Chamberlayne:** Conceptualization, Methodology, Formal analysis, Investigation, Data curation, Writing – original draft, Visualization, Project administration, Funding acquisition. **Jonathan J. Tyler:** Conceptualization, Methodology, Resources, Writing – review & editing, Supervision. **Bronwyn M. Gillanders:** Conceptualization, Methodology, Resources, Writing – review & editing, Supervision.

## Declaration of competing interest

The authors declare that they have no known competing financial interests or personal relationships that could have appeared to influence the work reported in this paper.

## Acknowledgements

The authors would like to thank Sarah Gilbert from Adelaide Microscopy for her assistance with water and carbonate trace elemental analyses. This research was funded by a Sir Mark Mitchell Foundation Grant, a Lirabenda Endowment Research Grant from the Field Naturalists Society of South Australia and a Conservation Biology Grant from the Nature Conservation Society of South Australia.

## Appendix A. Supplementary data

Supplementary data to this article can be found online at <https://doi.org/10.1016/j.ecss.2021.107354>.

## References

- Aldridge, K.T., Brookes, J.D., 2011. Report to the Department of Environment and Natural Resources and Department for Water, the Government of South Australia. The response of water quality and phytoplankton communities in the Northern Lagoon of the Coorong and Murray Mouth to barrage releases from the Lower Lakes, November 2010–May 2011. School of Earth & Environmental Sciences, The University of Adelaide, Adelaide.
- Beck, A.J., Charette, M.A., Cochran, J.K., Gonner, M.E., Peucker-Ehrenbrink, B., 2013. Dissolved strontium in the subterranean estuary - implications for the marine strontium isotope budget. *Geochem. Cosmochim. Acta* 117, 33–52. <https://doi.org/10.1016/j.gca.2013.03.021>.
- Carré, M., Bentaleb, I., Bruguier, O., Ordinala, E., Barrett, N.T., Fontugne, M., 2006. Calcification rate influence on trace element concentrations in aragonitic bivalve shells: evidences and mechanisms. *Geochem. Cosmochim. Acta* 70, 4906–4920. <https://doi.org/10.1016/j.gca.2006.07.019>.
- Carroll, J., Falkner, K.K., Brown, E.T., Moore, W.S., 1993. The role of the Ganges-Brahmaputra mixing zone in supplying barium and  $^{226}\text{Ra}$  to the Bay of Bengal. *Geochim. Cosmochim. Acta* 57, 2981–2990.
- Chamberlayne, B., 2015. Late Holocene Seasonal and Multicentennial Hydroclimate Variability in the Coorong Lagoon, South Australia: Evidence from Stable Isotopes and Trace Element Profiles of Bivalve Molluscs, Honours Thesis. University of Adelaide, Adelaide.
- Chamberlayne, B.K., Tyler, J.J., Gillanders, B.M., 2020. Environmental controls on the geochemistry of a short-lived bivalve in southeastern Australian estuaries. *Estuar. Coast* 43, 86–101. <https://doi.org/10.1007/s12237-019-00662-7>.
- Coffey, M., Dehairs, F., Collette, O., Luther, G., Church, T., Jickells, T., 1997. The behaviour of dissolved barium in estuaries. *Estuar. Coast. Shelf Sci.* 45, 113–121. <https://doi.org/10.1006/ecss.1996.0157>.
- Colbert, D., McManus, J., 2005. Importance of seasonal variability and coastal processes on estuarine manganese and barium cycling in a Pacific Northwest estuary. *Contin. Shelf Res.* 25, 1395–1414. <https://doi.org/10.1016/j.csr.2005.02.003>.
- Corrège, T., 2006. Sea surface temperature and salinity reconstruction from coral geochemical tracers. *Palaeogeogr. Palaeoclimatol. Palaeoecol.* 232, 408–428. <https://doi.org/10.1016/j.palaeo.2005.10.014>.
- Dietzel, M., Gussone, N., Eisenhauer, A., 2004. Co-precipitation of  $\text{Sr}^{2+}$  and  $\text{Ba}^{2+}$  with aragonite by membrane diffusion of  $\text{CO}_2$  between 10 and 50 °C. *Chem. Geol.* 203, 139–151. <https://doi.org/10.1016/j.chemgeo.2003.09.008>.
- Diouf, K., Panfili, J., Labonne, M., Aliaume, C., Tomás, J., Do Chi, T., 2006. Effects of salinity on strontium:calcium ratios in the otoliths of the West African black-chinned tilapia *Sarotherodon melanotheron* in a hypersaline estuary. *Environ. Biol. Fish.* 77, 9–20. <https://doi.org/10.1007/s10641-006-9048-x>.
- Dodd, J.R., Crisp, E.L., 1982. Non-linear variation with salinity of Sr/Ca and Mg/Ca ratios in water and aragonitic bivalve shells and implications for paleosalinity studies. *Palaeogeogr. Palaeoclimatol. Palaeoecol.* 38, 45–56.
- Durham, S.R., Gillikin, D.P., Goodwin, D.H., Dietl, G.P., 2017. Rapid determination of oyster lifespans and growth rates using LA-ICP-MS line scans of shell Mg/Ca ratios. *Palaeogeogr. Palaeoclimatol. Palaeoecol.* 485, 201–209. <https://doi.org/10.1016/j.palaeo.2017.06.013>.
- Edmond, J.M., Boyle, E.D., Drummond, D., Grant, B., Mislick, T., 1978. Desorption of barium in the plume of the Zaire (Congo) river. *Netherlands J. Sea Res.* 12, 324–328. [https://doi.org/10.1016/0077-7579\(78\)90034-0](https://doi.org/10.1016/0077-7579(78)90034-0).
- Elliot, M., Welsh, K., Chilcott, C., McCulloch, M., Chappell, J., Ayling, B., 2009. Profiles of trace elements and stable isotopes derived from giant long-lived *Tridacna gigas* bivalves: potential applications in paleoclimate studies. *Palaeogeogr. Palaeoclimatol. Palaeoecol.* 280, 132–142. <https://doi.org/10.1016/j.palaeo.2009.06.007>.
- Elsdon, T.S., Gillanders, B.M., 2006. Temporal variability in strontium, calcium, barium, and manganese in estuaries: implications for reconstructing environmental histories of fish from chemicals in calcified structures. *Estuar. Coast. Shelf Sci.* 66, 147–156. <https://doi.org/10.1016/j.ecss.2005.08.004>.
- Falster, G., Delean, S., Tyler, J., 2018. Hydrogen peroxide treatment of natural lake sediment prior to carbon and oxygen stable isotope analysis of calcium carbonate. *G-cubed* 1–13. <https://doi.org/10.1029/2018GC007575>.
- Ford, P.W., 2007. 2007. Biogeochemistry of the Coorong. Review and identification of future research requirements. CSIRO Water for a Healthy Country National Research Flagship. <https://doi.org/10.4225/08/59ae4ce808ba>. Canberra.
- Freitas, P., Clarke, L.J., Kennedy, H., Richardson, C., Abrantes, F., 2005. Mg/Ca, Sr/Ca, and stable-isotope ( $^{18}\text{O}$  and  $^{13}\text{C}$ ) ratio profiles from the fan mussel *Pinna nobilis*: seasonal records and temperature relationships. *G-cubed* 6. <https://doi.org/10.1029/2004GC000872>.
- Freitas, P.S., Clarke, L.J., Kennedy, H., Richardson, C.A., 2012. The potential of combined Mg/Ca and  $\delta^{18}\text{O}$  measurements within the shell of the bivalve *Pecten maximus* to estimate seawater  $\delta^{18}\text{O}$  composition. *Chem. Geol.* 291, 286–293. <https://doi.org/10.1016/j.chemgeo.2011.10.023>.
- Freitas, P.S., Clarke, L.J., Kennedy, H., Richardson, C.A., Abrantes, F., 2006. Environmental and biological controls on elemental (Mg/Ca, Sr/Ca and Mn/Ca) ratios in shells of the king scallop *Pecten maximus*. *Geochem. Cosmochim. Acta* 70, 5119–5133. <https://doi.org/10.1016/j.gca.2006.07.029>.
- Füllenbach, C.S., Schöne, B.R., Mertz-Kraus, R., 2015. Strontium/lithium ratio in aragonitic shells of *Cerastoderma edule* (Bivalvia) - a new potential temperature proxy for brackish environments. *Chem. Geol.* 417, 341–355. <https://doi.org/10.1016/j.chemgeo.2015.10.030>.
- Gaetani, G.A., Cohen, A.L., 2006. Element partitioning during precipitation of aragonite from seawater: a framework for understanding paleoproxies. *Geochem. Cosmochim. Acta* 70, 4617–4634. <https://doi.org/10.1016/j.gca.2006.07.008>.
- Geddes, M.C., Butler, A., 1984. Physicochemical and biological studies on the Coorong lagoons, south Australia. and the Effect of Salinity on the Distribution of the Macrobenthos. *Trans. R. Soc. South Aust* 108, 51–62.
- Geeza, T.J., Gillikin, D.P., Goodwin, D.H., Evans, S.D., Watters, T., Warner, N.R., 2018. Controls on magnesium, manganese, strontium, and barium concentrations recorded in freshwater mussel shells from Ohio. *Chem. Geol.* 1–12. <https://doi.org/10.1016/j.chemgeo.2018.01.001>.
- Gibbs, R.J., 1970. Mechanisms controlling world water chemistry. *Science* 170, 1088–1090.
- Gillanders, B.M., Munro, A.R., 2012. Hypersaline waters pose new challenges for reconstructing environmental histories of fish based on otolith chemistry. *Limnol. Oceanogr.* 57, 1136–1148. <https://doi.org/10.4319/lo.2012.57.4.1136>.
- Gillikin, D.P., 2019. Chemical sclerochronology. *Chem. Geol.* 526, 1–6. <https://doi.org/10.1016/j.chemgeo.2019.06.016>.
- Gillikin, D.P., Dehairs, F., Lorrain, A., Steenmans, D., Baeyens, W., André, L., 2006. Barium uptake into the shells of the common mussel (*Mytilus edulis*) and the potential for estuarine paleo-chemistry reconstruction. *Geochem. Cosmochim. Acta* 70, 395–407. <https://doi.org/10.1016/j.gca.2005.09.015>.
- Gillikin, D.P., Lorrain, A., Navez, J., Taylor, J.W., André, L., Keppens, E., Baeyens, W., Dehairs, F., 2005. Strong biological controls on Sr/Ca ratios in aragonitic marine bivalve shells. *Geochemistry, Geophys. Geosystems* 6. <https://doi.org/10.1029/2004GC000874>.
- Gillikin, D.P., Lorrain, A., Paulet, Y.M., André, L., Dehairs, F., 2008. Synchronous barium peaks in high-resolution profiles of calcite and aragonite marine bivalve shells. *Geo Mar. Lett.* 28, 351–358. <https://doi.org/10.1007/s00367-008-0111-9>.
- Goodwin, D.H., Gillikin, D.P., Roopnarine, P.D., 2013. Preliminary evaluation of potential stable isotope and trace element productivity proxies in the oyster *Crassostrea gigas*. *Palaeogeogr. Palaeoclimatol. Palaeoecol.* 373, 88–97. <https://doi.org/10.1016/j.palaeo.2012.03.034>.
- Government of South Australia, 2020. River Murray flow report (department for environment and water, south Australia). Available at: <https://www.waterconnect.sa.gov.au/Pages/Home.aspx>.
- Griscom, S.B., Fisher, N.S., 2004. Bioavailability of sediment-bound metals to marine bivalve molluscs: an overview. *Estuaries* 27, 826–838. <https://doi.org/10.1007/BF02912044>.
- Haese, R., Murray, E., Wallace, L., 2009. Nutrient Sources, Water Quality, and Biogeochemical Processes in the Coorong, South Australia. *Geoscience Australia Record 2009/19*. Commonwealth Government, Canberra (2009).
- Haese, R.R., Gow, L., Wallace, L., Brodie, R.S., 2008. Identifying Groundwater Discharge in the Coorong (South Australia). *AusGeo News*, pp. 1–6.
- Hart, S.R., Blusztajn, J., 1998. Clams as recorders of ocean ridge volcanism and hydrothermal vent field activity. *Science* 280, 883–886.
- Hatch, M.B.A., Schellenberg, S.A., Carter, M.L., 2013. Ba/Ca variations in the modern intertidal bean clam *Donax gouldi*: an upwelling proxy? *Palaeogeogr. Palaeoclimatol. Palaeoecol.* 373, 98–107. <https://doi.org/10.1016/j.palaeo.2012.03.006>.
- Hellstrom, J., Paton, C., Woodhead, J., Hergt, J., 2008. Iolite: software for spatially resolved LA-(quad and MC) ICPMS analysis. In: Sylvester, P. (Ed.), *Laser Ablation ICP-MS in the Earth Sciences: Current Practices and Outstanding Issues*. Mineralogical Association of Canada Short Course Volume 40, p. 343.
- Izumida, H., Yoshimura, T., Suzuki, A., Nakashima, R., Ishimura, T., Yasuhara, M., Inamura, A., Shikazono, N., Kawahata, H., 2011. Biological and water chemistry controls on Sr/Ca, Ba/Ca, Mg/Ca and  $\delta^{18}\text{O}$  profiles in freshwater pearl mussel *Hyriopsis* sp. *Palaeogeogr. Palaeoclimatol. Palaeoecol.* 309, 298–308. <https://doi.org/10.1016/j.palaeo.2011.06.014>.
- Izzo, C., Manetti, D., Doubleday, Z.A., Gillanders, B.M., 2016. Calibrating the element composition of *Donax deltooides* shells as a palaeo-salinity proxy. *Palaeogeogr. Palaeoclimatol. Palaeoecol.* 484, 89–96. <https://doi.org/10.1016/j.palaeo.2016.11.038>.
- Kanandjemo, A.N., Platell, M.E., Potter, I.C., 2001. The benthic macroinvertebrate community of the upper reaches of an Australian estuary that undergoes marked seasonal changes in hydrology. *Hydro. Process* 15, 2481–2501. <https://doi.org/10.1002/hyp.296>.
- Krause-Nehring, J., Brey, T., Thorold, S.R., 2012. Centennial records of lead contamination in northern Atlantic bivalves (*Arctica islandica*). *Mar. Pollut. Bull.* 64, 233–240. <https://doi.org/10.1016/j.marpolbul.2011.11.028>.



- Lautenschlager, A.D., Matthews, T.G., Quinn, G.P., 2014. Utilization of organic matter by invertebrates along an estuarine gradient in an intermittently open estuary. *Estuar. Coast Shelf Sci.* 149, 232–243. <https://doi.org/10.1016/j.ecss.2014.08.020>.
- Lazareth, C.E., Vander Putten, E., André, L., Dehairs, F., 2003. High-resolution trace element profiles in shells of the mangrove bivalve *Isognomon ephippium*: a record of environmental spatio-temporal variations? *Estuar. Coast. Shelf Sci.* 57, 1103–1114. [https://doi.org/10.1016/S0272-7714\(03\)00013-1](https://doi.org/10.1016/S0272-7714(03)00013-1).
- Lebrato, M., Garbe-Schönberg, D., Müller, M.N., Blanco-Ameijeiras, S., Feely, R.A., Lorenzoni, L., Molinero, J.-C., Bremer, K., Jones, D.O.B., Iglesias-Rodríguez, D., Greeley, D., Lamare, M.D., Paulmier, A., Graco, M., Cartes, J., Barcelos e Ramos, J., de Lara, A., Sanchez-Leal, R., Jimenez, P., Papparazzo, F.E., Hartman, S.E., Westernströer, U., Küter, M., Benavides, R., da Silva, A.F., Bell, S., Payne, C., Olafsdottir, S., Robinson, K., Jantunen, L.M., Korablev, A., Webster, R.J., Jones, E. M., Gilg, O., Bailly du Bois, P., Beldowski, J., Ashjian, C., Yahia, N.D., Twining, B., Chen, X.-G., Tseng, L.-C., Hwang, J.-S., Dahms, H.-U., Oschlies, A., 2020. Global variability in seawater Mg:Ca and Sr:Ca ratios in the modern ocean. *Proc. Natl. Acad. Sci.* <https://doi.org/10.1073/pnas.1918943117>, 201918943.
- Lehrter, J.C., Murrell, M.C., Kurtz, J.C., 2009. Interactions between freshwater input, light, and phytoplankton dynamics on the Louisiana continental shelf. *Continent. Shelf Res.* 29, 1861–1872. <https://doi.org/10.1016/j.csr.2009.07.001>.
- Lorrain, A., Gillikin, D.P., Paulet, Y.M., Chauvaud, L., Le Mercier, A., Navez, J., André, L., 2005. Strong kinetic effects on Sr/Ca ratios in the calcitic bivalve *Pecten maximus*. *Geology* 33, 965–968. <https://doi.org/10.1130/G22048.1>.
- Macdonald, J.I., Crook, D.A., 2010. Variability in Sr:Ca and Ba:Ca ratios in water and fish otoliths across an estuarine salinity gradient. *Mar. Ecol. Prog. Ser.* 413, 147–161. <https://doi.org/10.3354/meps08703>.
- Matthews, T.G., Constable, A.J., 2004. Effect of flooding on estuarine bivalve populations near the mouth of the Hopkins River, Victoria, Australia. *J. Mar. Biol. Assoc. U. K.* 84, 633–639.
- Miller, J.A., 2009. The effects of temperature and water concentration on the otolith incorporation of barium and manganese in black rockfish *Sebastes melanops*. *J. Fish Biol.* 75, 39–60. <https://doi.org/10.1111/j.1095-8649.2009.02262.x>.
- Mitsuguchi, T., Matsumoto, E., Abe, O., Uchida, T., Isdale, P.J., 1996. Mg/Ca thermometry in coral skeletons. *Science* 274, 961–963.
- Mohan, J.A., Walther, B.D., 2015. Spatiotemporal variation of trace elements and stable isotopes in subtropical estuaries: II. Regional, local, and seasonal salinity-element relationships. *Estuar. Coast* 38, 769–781. <https://doi.org/10.1007/s12237-014-9876-4>.
- Moore, W.S., Shaw, T.J., 2008. Fluxes and behavior of radium isotopes, barium, and uranium in seven Southeastern US rivers and estuaries. *Mar. Chem.* 108, 236–254. <https://doi.org/10.1016/j.marchem.2007.03.004>.
- Murrell, M.C., Hagy, J.D., Lores, E.M., Greene, R.M., 2007. Phytoplankton production and nutrient distributions in a subtropical estuary: importance of freshwater flow. *Estuar. Coast* 30, 390–402. <https://doi.org/10.1007/BF02819386>.
- Nelson, T.R., Powers, S.P., 2020. Elemental concentrations of water and otoliths as salinity proxies in a northern gulf of Mexico estuary. *Estuaries and coasts*. <https://doi.org/10.1007/s12237-019-00686-z>.
- O'Neil, D.D., Gillikin, D.P., 2014. Do freshwater mussel shells record road-salt pollution? *Sci. Rep.* 4 (7168) <https://doi.org/10.1038/srep07168>.
- Paton, C., Hellstrom, J., Paul, B., Woodhead, J., Hergt, J., 2011. Iolite: freeware for the visualisation and processing of mass spectrometric data. *J. Anal. At. Spectrom.* 26 (2508). <https://doi.org/10.1039/c1ja10172b>.
- Poullain, C., Gillikin, D.P., Thébault, J., Munaron, J.M., Bohn, M., Robert, R., Paulet, Y. M., Lorrain, A., 2015. An evaluation of Mg/Ca, Sr/Ca, and Ba/Ca ratios as environmental proxies in aragonite bivalve shells. *Chem. Geol.* 396, 42–50. <https://doi.org/10.1016/j.chemgeo.2014.12.019>.
- R Core Team, 2020. R: A Language and Environment for Statistical Computing. R Foundation for Statistical Computing, Vienna, Austria.
- Schöne, B.R., Dunca, E., Fiebig, J., Pfeiffer, M., 2005. Mutvei's solution: an ideal agent for resolving microgrowth structures of biogenic carbonates. *Palaeogeogr. Palaeoclimatol. Palaeoecol.* 228, 149–166. <https://doi.org/10.1016/j.palaeo.2005.03.054>.
- Schöne, B.R., Krause Jr., R.A., 2016. Retrospective environmental biomonitoring – mussel Watch expanded. *Global Planet. Change* 144, 228–251. <https://doi.org/10.1016/j.gloplacha.2016.08.002>.
- Schöne, B.R., Radermacher, P., Zhang, Z., Jacob, D.E., 2013. Crystal fabrics and element impurities (Sr/Ca, Mg/Ca, and Ba/Ca) in shells of *Arctica islandica*-Implications for paleoclimate reconstructions. *Palaeogeogr. Palaeoclimatol. Palaeoecol.* 373, 50–59. <https://doi.org/10.1016/j.palaeo.2011.05.013>.
- Schöne, B.R., Surge, D., 2014. Bivalve shells: ultra high-resolution paleoclimate archives. *Pages* 22, 20–21.
- Schöne, B.R., Zhang, Z., Jacob, D., Gillikin, D.P., Tütken, T., Garbe-Schönberg, D., McConnaughey, T., Soldati, A., 2010. Effect of organic matrices on the determination of the trace element chemistry (Mg, Sr, Mg/Ca, Sr/Ca) of aragonitic bivalve shells (*Arctica islandica*) - comparison of ICP-OES and LA-ICP-MS data. *Geochem. J.* 44, 23–37.
- Schöne, B.R., Zhang, Z., Radermacher, P., Thébault, J., Jacob, D.E., Nunn, E.V., Maurer, A.-F., 2011. Sr/Ca and Mg/Ca ratios of ontogenetically old, long-lived bivalve shells (*Arctica islandica*) and their function as paleotemperature proxies. *Palaeogeogr. Palaeoclimatol. Palaeoecol.* 302, 52–64. <https://doi.org/10.1016/j.palaeo.2010.03.016>.
- Semeniuk, V., Wurm, P.A.S., 2000. Mollusc of the Leschenault Inlet estuary: their diversity, distribution, and population dynamics. *J. Roy. Soc. West Aust.* 83, 377–418.
- Shao, Y., Farkaš, J., Mosley, L., Tyler, J., Wong, H., Chamberlayne, B., Raven, M., Samanta, M., Holmden, C., Gillanders, B.M., Kolevica, A., Eisenhauer, A., 2021. Impact of salinity and carbonate saturation on stable Sr isotopes ( $^{88}/^{86}\text{Sr}$ ) in a lagoon-estuarine system. *Geochem. Cosmochim. Acta* 293, 461–476. <https://doi.org/10.1016/j.gca.2020.11.014>.
- Shao, Y., Farkaš, J., Holmden, C., Mosley, L., Kell-Duivesteyn, I., Izzo, C., Reis-Santos, P., Tyler, J., Törber, P., Frýda, J., Taylor, H., Haynes, D., Tibby, J., Gillanders, B.M., 2018. Calcium and strontium isotope systematics in the lagoon-estuarine environments of South Australia: implications for water source mixing, carbonate fluxes and fish migration. *Geochem. Cosmochim. Acta* 239, 90–108. <https://doi.org/10.1016/j.gca.2018.07.036>.
- Sinclair, D.J., Kinsley, L., McCulloch, M.T., 1998. High resolution analysis of trace elements in corals by laser ablation ICP-MS. *Geochem. Cosmochim. Acta* 62, 1889–1901. [https://doi.org/10.1016/S0016-7037\(98\)00112-4](https://doi.org/10.1016/S0016-7037(98)00112-4).
- Stecher, H.A., Kogut, M.B., 1999. Rapid barium removal in the Delaware estuary. *Geochem. Cosmochim. Acta* 63, 1003–1012. [https://doi.org/10.1016/S0016-7037\(98\)00310-X](https://doi.org/10.1016/S0016-7037(98)00310-X).
- Surge, D.M., Lohmann, K.C., 2002. Temporal and spatial differences in salinity and water chemistry in SW Florida estuaries: effects of human-impacted watersheds. *Estuaries* 25, 393–408. <https://doi.org/10.1007/BF02695982>.
- Surge, D.M., Lohmann, K.C., Goodfriend, G.A., 2003. Reconstructing estuarine conditions: oyster shells as recorders of environmental change, Southeast Florida. *Estuar. Coast Shelf Sci.* 57, 737–756. [https://doi.org/10.1016/S0272-7714\(02\)00370-0](https://doi.org/10.1016/S0272-7714(02)00370-0).
- Takeste, R.K., van Geen, A., 2004. Mg/Ca, Sr/Ca, and stable isotopes in modern and Holocene *Protothaca staminea* shells from a northern California coastal upwelling region. *Geochem. Cosmochim. Acta* 68, 3845–3861. <https://doi.org/10.1016/j.gca.2004.03.021>.
- Thébault, J., Chauvaud, L., L'Helguen, S., Clavier, J., Barats, A., Jacquet, S., Pécuyer, C., Amouroux, D., 2009. Barium and molybdenum records in bivalve shells: geochemical proxies for phytoplankton dynamics in coastal environments? *Limnol. Oceanogr.* 54, 1002–1014. <https://doi.org/10.4319/lo.2009.54.3.1002>.
- Tynan, S., Opydyke, B.N., Walczak, M., Eggins, S., Dutton, A., 2017. Assessment of Mg/Ca in *Saccostrea glomerata* (the Sydney rock oyster) shell as a potential temperature record. *Palaeogeogr. Palaeoclimatol. Palaeoecol.* 484, 79–88. <https://doi.org/10.1016/j.palaeo.2016.08.009>.
- Vander Putten, E., Dehairs, F., Keppens, E., Baeyens, W., 2000. High resolution distribution of trace elements in the calcite shell layer of modern *Mytilus edulis*: environmental and biological controls. *Geochem. Cosmochim. Acta* 64, 997–1011.
- Vieira, S., Barrulas, P., Chaiho, P., Dias, C.B., Sroczy, K., Adão, H., 2021. Spatial and temporal distribution of the multi-element signatures of the estuarine non-indigenous bivalve *Ruditapes philippinarum*. *Biol. Trace Elem. Res.*
- Walther, B.D., Limburg, K.E., 2012. The use of otolith chemistry to characterize diadromous migrations. *J. Fish Biol.* 81, 796–825. <https://doi.org/10.1111/j.1095-8649.2012.03371.x>.
- Walther, B.D., Nims, M.K., 2015. Spatiotemporal variation of trace elements and stable isotopes in subtropical estuaries: I. Freshwater endmembers and mixing curves. *Estuar. Coast* 38, 754–768. <https://doi.org/10.1007/s12237-014-9881-7>.
- Wanamaker, A.D., Gillikin, D.P., 2018. Strontium, magnesium, and barium incorporation in aragonitic shells of juvenile *Arctica islandica*: insights from temperature controlled experiments. *Chem. Geol.* <https://doi.org/10.1016/j.chemgeo.2018.02.012>, 0–1.
- Wanamaker, A.D., Kreutz, K.J., Wilson, T., Borns, H.W., Introne, D.S., Feindel, S., 2008. Experimentally determined Mg/Ca and Sr/Ca ratios in juvenile bivalve calcite for *Mytilus edulis*: implications for paleotemperature reconstructions. *Geo Mar. Lett.* 28, 359–368. <https://doi.org/10.1007/s00367-008-0112-8>.
- Wells, F.E., Threlfall, T.J., 1982a. Salinity and temperature tolerance of *Hydrococcus brazieri* (T. Woods, 1876) and *Arthritica semen* (Menke, 1843) from the Peel-Harvey estuarine system, Western Australia. *J. Malacol. Soc. Aust.* 5, 151–156.
- Wells, F.E., Threlfall, T.J., 1982b. Density fluctuations, growth and dry tissue production of *Hydrococcus brazieri* (tenison woods, 1876) and *Arthritica semen* (menke, 1843) in peel inlet, western Australia. *J. Molluscan Stud.* 48, 310–320.
- Wells, F.E., Threlfall, T.J., 1982c. Reproductive strategies of *Hydrococcus brazieri* (tenison woods, 1876) and *Arthritica semen* (menke, 1843) in peel inlet, western Australia. *J. Malacol. Soc. Aust.* 5, 157–166.
- Yan, H., Shao, D., Wang, Y., Sun, L., 2013. Sr/Ca profile of long-lived *Tridacna gigas* bivalves from South China Sea: a new high-resolution SST proxy. *Geochem. Cosmochim. Acta* 112, 52–65. <https://doi.org/10.1016/j.gca.2013.03.007>.
- Zhao, L., Schöne, B.R., Mertz-Kraus, R., 2017. Controls on strontium and barium incorporation into freshwater bivalve shells (*Corbicula fluminea*). *Palaeogeogr. Palaeoclimatol. Palaeoecol.* 465, 386–394. <https://doi.org/10.1016/j.palaeo.2015.11.040>.

# Geochemistry, Geophysics, Geosystems

## RESEARCH ARTICLE

10.1029/2021GC009769

## Key Points:

- Oxygen and hydrogen isotope ratios in waters of the Coorong Lagoons are mostly controlled by evaporation
- A new temperature-dependent oxygen isotope fractionation equation for *Arthritica helmsi* is developed
- Fossil shells of *A. helmsi* are suitable for paleoenvironmental studies

## Supporting Information:

Supporting Information may be found in the online version of this article.

## Correspondence to:


 B. K. Chamberlayne,  
[briony.chamberlayne@adelaide.edu.au](mailto:briony.chamberlayne@adelaide.edu.au)

## Citation:

 Chamberlayne, B. K., Tyler, J. J., & Gillanders, B. M. (2021). Controls over oxygen isotope fractionation in the waters and bivalves (*Arthritica helmsi*) of an estuarine lagoon system. *Geochemistry, Geophysics, Geosystems*, 22, e2021GC009769. <https://doi.org/10.1029/2021GC009769>

 Received 12 MAR 2021  
 Accepted 26 MAY 2021

## Controls Over Oxygen Isotope Fractionation in the Waters and Bivalves (*Arthritica helmsi*) of an Estuarine Lagoon System

 B. K. Chamberlayne<sup>1</sup> , J. J. Tyler<sup>1</sup>, and B. M. Gillanders<sup>2</sup>
<sup>1</sup>Department of Earth Sciences and Sprigg Geobiology Centre, The University of Adelaide, Adelaide, SA, Australia,

<sup>2</sup>School of Biological Sciences, Southern Seas Ecology Laboratories and the Environment Institute, The University of Adelaide, Adelaide, SA, Australia

**Abstract** Oxygen isotope ratios in bivalve shells have long been used as a proxy for environmental change, reflecting both temperature and the oxygen isotope composition of host water. In estuarine systems, the oxygen isotope composition of water is complicated by variable mixing between river and seawater, as well as evaporative enrichment. In addition, due to species-specific variation in temperature-dependent fractionation into bivalve carbonate, modern calibrations are necessary prior to applications in paleoenvironmental studies. In this study, live specimens of the micromollusc *Arthritica helmsi* were collected from five sites in the Coorong Lagoon, an estuarine system at the mouth of the River Murray, Australia, on six occasions from November 2016 to May 2018. Whole shell oxygen and carbon isotope compositions ( $n = 131$ ) were measured alongside monthly temperature and oxygen and hydrogen isotope analyses of waters from the Coorong and neighboring Lake Alexandrina ( $n = 137$ ). Oxygen and hydrogen isotope ratios in water were mostly controlled by evaporation of source waters, though a period of high river water discharge was reflected in the isotopic values of the Coorong North Lagoon. A species-specific temperature-dependent oxygen isotope fractionation equation was calibrated for *A. helmsi*:  $T$  ( $^{\circ}\text{C}$ ) =  $(21.39 \pm 0.45) - (4.43 \pm 0.38) \times (\delta^{18}\text{O}_{\text{shell}} - \delta^{18}\text{O}_{\text{water}})$ . This equation is similar to other published paleotemperature equations for biogenic carbonates. These contemporary observations of the isotope hydrology of the Coorong, coupled with our contemporary calibration of oxygen isotope fractionation, lay the foundation for paleoenvironmental studies using bivalves collected from the sediments of the Coorong.

### 1. Introduction

The use of oxygen isotope ratios in bivalves and other carbonate species as a proxy for past water temperature is a well-established technique in paleoclimate studies (e.g., Carré et al., 2013; Crippa et al., 2016; Jones et al., 2005; Schöne et al., 2005). Following the initial works of Epstein et al. (1951) and Urey (1947), many studies have successfully reconstructed temperature, most commonly in marine species (e.g., Butler et al., 2012; Carré et al., 2013; Featherstone et al., 2020; Schöne et al., 2004; Surge et al., 2003). A number of studies have also examined isotope ratios in freshwater (e.g., Kelemen et al., 2017; Pfister et al., 2019; Roy et al., 2019; Schöne et al., 2020; Wurster & Patterson, 2001) and estuarine (e.g., Andrus & Rich, 2008; Dettman et al., 2004; Ingram et al., 1996) species, where the interpretation of bivalve oxygen and carbon isotopes can differ from marine species due to the added complexity of variable mixing of marine and river waters, plus evaporation, which lead to variable oxygen and hydrogen isotope compositions in water.

The ability to quantify temperature or salinity changes in paleoenvironmental studies often relies on the assumption that bivalves fractionate oxygen in accordance with well-established paleotemperature equations (Böhm et al., 2000; Epstein & Mayeda, 1953; Grossman & Ku, 1986; Kim & O'Neil, 1997). This assumption, however, does not consider the species-specific “vital effects” that are known to cause deviation from expected geochemical relationships (Owen et al., 2002). The variation among published temperature-dependent fractionation factors in bivalve studies highlights the importance of modern calibration studies. From such studies, authors have been able to validate the use of existing paleotemperature equations (e.g., Huyghe et al., 2020; Lécuyer et al., 2004), or have been able to produce species-specific equations (e.g., Carré et al., 2005; Royer et al., 2013; Tynan et al., 2014). In addition to the potential biological effects, recent

research has investigated kinetic effects on the equilibrium oxygen isotope fractionation between organic and inorganic carbonates and water (Daëron et al., 2019; Watkins et al., 2013). The effects of pH, growth rate and salinity on the carbonate-water fractionation factor have been identified in several studies (Dietzel et al., 2009; Kim et al., 2007; Zeebe, 1999) but also excluded by others (Hermoso & Lecasble, 2018; Kim et al., 2006). While there is no general scientific consensus, it is clear that the influence of biological and kinetic factors on oxygen isotope fractionation must be considered.

The oxygen isotope composition of waters are affected by several factors including the mixing of isotopically distinct inputs and subsequent modification by evaporation (Corlis et al., 2003; Epstein & Mayeda, 1953). In estuarine systems, water sources can include a complex mixture of direct precipitation, sea water, ground-water and one or more riverine inputs (e.g., Stalker et al., 2009). As such, although valuable environmental information can be gained from the oxygen isotope composition of estuarine carbonates, it is first essential to understand the effects of mixing and evaporation on water in the contemporary system. Studies in estuaries in Texas (Laguna Bay, Galveston Bay, and Mission Aransas Estuaries; Mohan & Walther, 2015), Western Australia (Shark Bay; Price et al., 2012), California (San Francisco Bay; Ingram et al., 1996), and Florida (Florida Bay; Swart & Price, 2002) have found strong linear relationships between oxygen isotope ratios and salinity despite different mixing and environmental conditions. In addition, water oxygen isotope dynamics have been successfully employed to estimate evaporation (Barrie et al., 2015; Gibson et al., 1993) and to differentiate between the sources of freshwater influxes in estuaries (Price et al., 2012; Stalker et al., 2009; Swart & Price, 2002).

This study explores the oxygen and carbon stable isotope ratios of *Arthritica helmsi* shells from the Coorong Lagoon of South Australia, alongside the oxygen and hydrogen isotope ratios of their host waters. The Coorong, at the mouth of the River Murray, is listed as a Wetland of International Significance under the Ramsar Convention (Department for Environment and Heritage, 2000), primarily for its importance for waterbird populations (Paton et al., 2009). The hydrological management of the Coorong and neighboring Lake Alexandrina is a subject of considerable debate, with uncertainties surrounding the natural or baseline hydrological state of the estuary (Kingsford et al., 2011; Reeves et al., 2015), and the sources and pathways of polluting waters which contribute to problems of eutrophication and ecosystem damage (Mosley et al., 2014). Research to gain understanding of the past hydrological and ecological conditions of the Coorong using various biomarkers in sediments has been a recent focus (Dick et al., 2011; Gell, 2017; Haynes et al., 2007; Lower et al., 2013; Reeves et al., 2015), including the use of hydrogen isotopes from sediments (McKirdy et al., 2010) and trace elemental ratios in otoliths (Disspain et al., 2011).

The sediments of the Coorong Lagoons have an abundance of bivalves, particularly *A. helmsi* (Chamberlayne, 2015), offering potential for reconstruction of past environmental change relevant to contemporary issues. Common in southern Australian estuaries (Matthews & Constable, 2004; Whisson et al., 2004; Lautenschlager et al., 2014), *A. helmsi* is an aragonitic micromollusc (Chamberlayne et al., 2020) that experiences continuous growth over a short lifespan of up to 1 year (Chamberlayne et al., 2020; Wells & Threlfall, 1982b). A monitoring study in a Western Australian estuary reported broad salinity (15–55) and temperature tolerances (18–32°C; Wells & Threlfall, 1982a). In the modern Coorong Lagoons, *A. helmsi* are abundant in the North Lagoon, but are not currently found living in the South Lagoon (Dittmann et al., 2019), likely due to the present hypersaline condition (>60; Dittmann et al., 2019) falling outside the tolerance of this species (Wells & Threlfall, 1982a). A study of museum specimens has demonstrated that stable isotope analyses of *A. helmsi* shells has potential to trace past environments, but more research is needed to better constrain the relationship between environmental change and shell chemistry (Chamberlayne et al., 2020).

To further test the reliability of *A. helmsi* as a proxy for past environmental conditions, we analyzed the isotopic composition of 135 live collected specimens and their host waters. A species-specific paleotemperature equation was developed and compared to established paleotemperature equations. In addition, we explored the principal controls over water oxygen and hydrogen isotope variability in the Coorong Lagoon, thus laying the foundation for interpreting *A. helmsi* oxygen isotope variability as a proxy for past climate and hydrological change in this significant estuarine system.

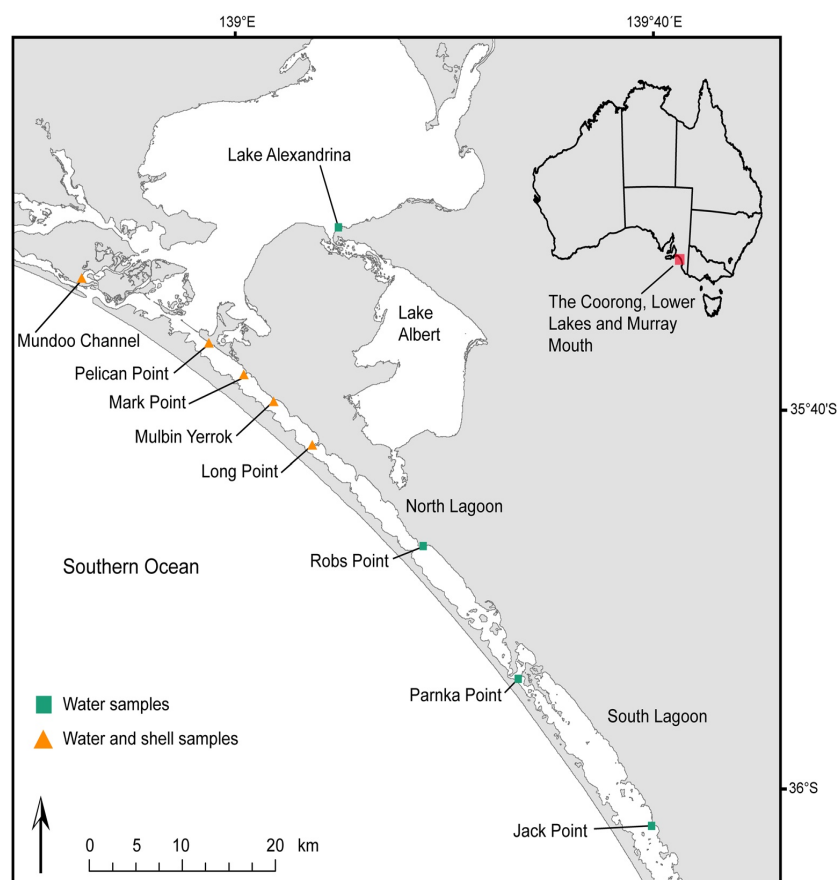


**Figure 1.** Sampling locations in Lake Alexandrina and the Coorong Lagoons at the terminus of the River Murray.

## 2. Methods

### 2.1. Study Site

The Coorong is an inverse estuary at the terminus of Australia's largest river system, the Murray Darling Basin, which drains 14% of the continent and provides water for 50% of Australia's agricultural produce (Commonwealth of Australia (Murray-Darling Basin Authority), 2020). The Coorong estuary is connected to the Murray River via Lake Alexandrina, and is separated into the North and South Lagoons which are narrowly connected at Parnka Point (Figure 1). A north-south salinity gradient, from brackish to hypersaline, has characterized the lagoon over recent decades (Geddes & Butler, 1984; Gillanders & Munro, 2012). A series of barrages erected in the 1940s control freshwater flow from the River Murray, via Lake Alexandrina and Lake Albert, into the North Lagoon which also receives marine water from the Southern Ocean via the Murray Mouth. The connectivity between the Southern Ocean and the Coorong has been maintained via dredging since 2015 (Government of South Australia, 2020). The South Lagoon receives water via the connection to the North Lagoon at Parnka Point; via the South East Drainage Network at Salt Creek; and from groundwater (Haese et al., 2008; Shao et al., 2018).

Rainfall data for the sampling period were sourced from the Australian Bureau of Meteorology's Meningie weather station (station number: 024518; BOM, 2020). Average annual rainfall at Meningie was 468 mm during the sampling period, and the mean of the annual maximum and minimum temperatures during the sampling period were 20.9°C and 10.3°C, respectively (BOM, 2020). Weekly barrage release data were sourced from the WaterConnect website (Government of South Australia, 2020). Oxygen and hydrogen

isotope compositions for local groundwater were sourced from Kell-Duivestein (2015) who sampled two groundwater wells adjacent to the North Lagoon.

### 2.2. Water Sampling and Analysis

Surface waters were collected from nine sites along Lake Alexandrina, the Coorong and Murray Mouth (Figure 1) approximately monthly from November 2016 to May 2018 (see Table S1 for collection times and locations). Water temperature and salinity was measured at each site using a Hanna Instruments HI-98194 multiparameter probe. Water samples were collected in hydrochloric acid washed 250 mL HDPE bottles with zero headspace and refrigerated until isotope analysis.

Hydrogen and oxygen isotopes in waters were determined by cavity ringdown spectroscopy using a Picarro L2130-i isotope analyzer at Flinders Analytical, Flinders University. Samples were calibrated against in-house laboratory standards consisting of desalinated water ( $\delta^2\text{H} = 0.95\text{‰}$ ,  $\delta^{18}\text{O} = 7.4\text{‰}$ ) and bottled water ( $\delta^2\text{H} = -73.8\text{‰}$ ,  $\delta^{18}\text{O} = -10.36\text{‰}$ ). An Adelaide rainwater sample ( $\delta^2\text{H} = -52.1\text{‰}$ ,  $\delta^{18}\text{O} = -8.49\text{‰}$ ) was used as an internal laboratory quality control. Oxygen and hydrogen isotope ratios are reported relative to the Vienna Standard Mean Ocean Water (VSMOW) standard using the standard delta ( $\delta$ ) notation in parts per thousand (‰):

$$\delta = \left( \frac{R_{\text{sample}} - R_{\text{standard}}}{R_{\text{standard}}} \right) \times 1,000 \quad (1)$$

where  $R$  is the isotope ratio ( $^{18}\text{O}/^{16}\text{O}$  or  $^2\text{H}/^1\text{H}$ ).

### 2.3. Shell Sampling and Analysis

Shells were collected on up to six occasions from five sites along the North Lagoon of the Coorong (Figure 1) from sediments at the sediment water interface using a 2 mm mesh sieve. In total, 135 specimens were collected (see Table S2 for details of specific collection times and locations). Each specimen was measured along its maximum growth axis using digital calipers, the length of each shell is reported in Table S2. The shells ranged from 1.30 to 2.77 mm in size and had an average of  $1.80 \pm 0.19$  mm. Shells were treated with an 18%  $\text{H}_2\text{O}_2$  solution, which was buffered to pH 8 using 0.5 M sodium hydroxide, to dissolve any residual organic matter, including the organic matrix within the bivalve, following the method of Falster et al. (2018). Shells were then rinsed in ultra-pure water with a resistivity of 18.2 M $\Omega$  at 25°C and a pH of 7 and dried for 12 h at 30°C. Due to the small size of each shell (1.30–2.77 mm), one valve of each specimen was crushed to a fine powder for whole shell isotope analysis.

A sub-sample of approximately 100  $\mu\text{g}$  of crushed whole shell carbonate powder was used for stable isotope analysis. Most (121 of 135) samples were purged with helium for 150 s at 20 ml/min and then acidified with 104% phosphoric acid and reacted at 70°C for 1 h using a Nu Instruments GasPrep system with the resultant  $\text{CO}_2$  analyzed for  $\delta^{18}\text{O}$  and  $\delta^{13}\text{C}$  with a Nu Instruments Horizon continuous flow isotope ratio mass spectrometer (IRMS). The remaining 14 samples were prepared using a Nu Instruments NuCarb system in-line connected to a Nu Instruments Perspective dual inlet IRMS. In the automated NuCarb system, samples were evacuated to high vacuum, acidified with 105% phosphoric acid at 70°C and the resultant  $\text{CO}_2$  passed through to the IRMS for  $\delta^{18}\text{O}$  and  $\delta^{13}\text{C}$  determination. Data quality for all samples were monitored using laboratory standards ANU-P3 ( $\delta^{18}\text{O} = -0.32\text{‰}$ ,  $\delta^{13}\text{C} = +2.24\text{‰}$ ), UAC-1 ( $\delta^{18}\text{O} = -18.4\text{‰}$ ,  $\delta^{13}\text{C} = -15.0\text{‰}$ ) and IAEA CO-8 ( $\delta^{18}\text{O} = -22.7\text{‰}$ ,  $\delta^{13}\text{C} = -5.76\text{‰}$ ). External reproducibility was  $\pm 0.15\text{‰}$  ( $1\sigma$ ) and  $\pm 0.1\text{‰}$  ( $1\sigma$ ) for the Nu Instruments Horizon IRMS and the Nu Instruments Perspective IRMS, respectively. Data from four samples (MP0817-1, MY0717-6, MY0817-6, and LP0817-7) were rejected due to technical problems during analysis. Carbon and oxygen isotope values are reported relative to the international standard Vienna Pee Dee Belemnite (VPDB) in parts per thousand (‰) using the delta ( $\delta$ ) notation (Equation 1).

#### 2.4. Estimation of Shell $\delta^{18}\text{O}$

As shell  $\delta^{18}\text{O}$  and  $\delta^{13}\text{C}$  ratios were measured on the whole valve of an individual specimen of *A. helmsi*, we interpret this composition to be representative of the integrated signal throughout the lifespan of the individual. A single study has investigated the growth rate and lifespan of *A. helmsi*, which reported a growth rate of 0.3 mm/month and lifespan of  $\sim 1$  year based on specimens collected in the Peel-Harvey estuary system in Western Australia (Wells & Threlfall, 1982b). Given this uncertainty in the period of time represented by the geochemistry of each shell, we made two comparisons: First, we compared  $\delta^{18}\text{O}$  value of the shells ( $\delta^{18}\text{O}_s$ ) to the temperature and  $\delta^{18}\text{O}$  value of water ( $\delta^{18}\text{O}_w$ ) measured on the date of the collection – a scenario which would assume a short lifespan for *A. helmsi* individuals, with a relatively high population turnover. Second, we estimated the lifespan of each shell based on its size and an assumed growth rate of 0.3 mm/month as estimated by Wells and Threlfall (1982b) (Table S2). Average temperature and  $\delta^{18}\text{O}_w$  values for the lifespan of each shell were then calculated to the nearest month based on this age estimation. Observed  $\delta^{18}\text{O}_s$  values were compared to estimates of  $\delta^{18}\text{O}_s$  values calculated from previously published fractionation equations. Both the temperature and  $\delta^{18}\text{O}_w$  composition measured on the date of collection, and the temperature and  $\delta^{18}\text{O}_w$  composition averaged according to the estimated lifespan, were used as parameters in the fractionation equations. Two aragonite-water fractionation equations were used: The equation from Böhm et al. (2000) who added sclerosponge data to improve the equation from Grossman and Ku (1986) which is based on data from foraminifera and gastropods:

$$T(^{\circ}\text{C}) = (20.0 \pm 0.2) - (4.42 \pm 0.10) \times (\delta^{18}\text{O}_{\text{arag./VPDB}} - \delta^{18}\text{O}_{\text{wat./VSMOW}}) \quad (2)$$

and the equation from Carré et al. (2005) which was calculated from measurements on the bivalve *Mesodesma donacium*:

$$T(^{\circ}\text{C}) = (17.41 \pm 1.15) - (3.66 \pm 0.16) \times (\delta^{18}\text{O}_{\text{arag./VPDB}} - \delta^{18}\text{O}_{\text{wat./VSMOW}}) \quad (3)$$

### 3. Results

#### 3.1. Environmental Conditions

Water temperature across the Coorong Lagoon varied seasonally (Figure 2a) with a maximum temperature of 37.9°C measured at Pelican Point in January 2018 and a minimum temperature of 10.7°C at Mundoo Channel in July 2017. Spatial variation in temperature across the lagoons was low as indicated by low between-site variance about the mean of all sites for each sampling date (standard error < 0.8), with the exception of January 2018 where the between-site standard error was 1.5. The volume of water released from Lake Alexandrina into the Coorong via barrage opening varied greatly over the sampling period (Figure 2b). Significant releases (>3,300 GL) through the summer of 2016 were followed by a prolonged period of limited releases totaling <1,100 GL for the remainder of the sampling period. The greatest monthly release was 1,421 GL in November 2016, while the releases in May 2018 totaled only 8 GL. Rainfall was less seasonal than water temperature during the sampling period (Figure 2c). The lowest monthly total rainfall of 2.8 mm was recorded in March 2018, while the highest monthly total was 106 mm in July 2017.

#### 3.2. Water Chemistry

##### 3.2.1. Salinity

Salinity ranged from 0.16 in December 2016 at Mundoo Channel and Pelican Point to 89.8 in March 2018 at Jack Point (Figure 3a). Lake Alexandrina was consistently fresh (<0.5) during the sampling period. Salinity in the North Lagoon was more variable both temporally and spatially, ranging from 0.16–26.7 at Pelican Point to 24–57.5 at Robs Point. There was no clear seasonal pattern to salinity in the North Lagoon. During November and December 2016, consistently low salinity (0.16–9.15) in the North Lagoon corresponded with a high discharge of freshwater from Lake Alexandrina (Figure 2b). In contrast, the South Lagoon, as indicated by data from Jack Point, experienced a seasonal range of salinity with highest values between January and May and lowest values between June and November (Figure 3a).

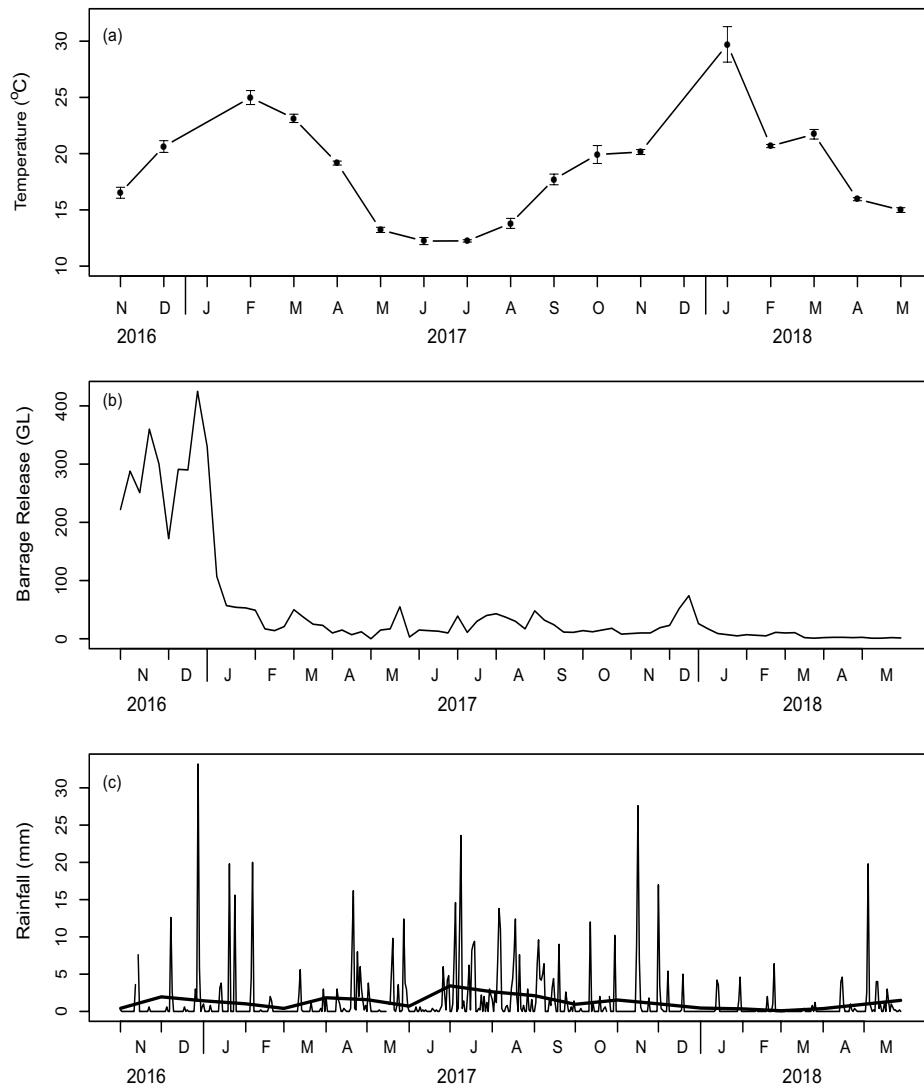


**Figure 2.** Summary of environmental data from November 2016 to May 2018. (a) Water temperature for the sampling period. The replicates were each of the nine sampling sites. Error bars indicate  $\pm 1$  SE. (b) Weekly barrage release volumes for the sampling period. (c) Daily rainfall and average monthly rainfall for the sampling period.

### 3.2.2. Oxygen and Hydrogen Isotopes in Water

The results of isotopic analyses of waters and associated uncertainties are summarized in Table S1. In summary,  $\delta^{18}\text{O}_w$  values in the Coorong Lagoons ranged from  $-2.81\text{‰}$  at Pelican Point in November 2016 to  $+5.78\text{‰}$  at Parnka Point in January 2018 (Figure 3b).  $\delta^{18}\text{O}_w$  values in Lake Alexandrina ranged from  $-0.06\text{‰}$  in April 2017 to  $+2.28\text{‰}$  measured in March of 2018. This seasonal pattern of higher  $\delta^{18}\text{O}_w$  values during the summer months was also observed in the South Lagoon including at Jack Point where the maximum value of  $+5.54\text{‰}$  was recorded in February 2018 and the minimum value of  $+1.36\text{‰}$  was recorded in August 2017. The North Lagoon also showed a similar seasonal pattern; with the exception of November and December 2016 where values ranged between  $-2.81\text{‰}$  and  $+0.02\text{‰}$  at all sites in the North Lagoon.  $\delta^{18}\text{O}_w$  values increased with distance from the Murray River mouth and Lake Alexandrina barrages. For example, in February of 2017 water samples from Pelican Point at the northern end of the North Lagoon had a  $\delta^{18}\text{O}_w$  value of  $+1.36\text{‰}$  while the waters at Robs Point at the southern end of the North Lagoon were  $+5.54\text{‰}$  (Figure 3b).

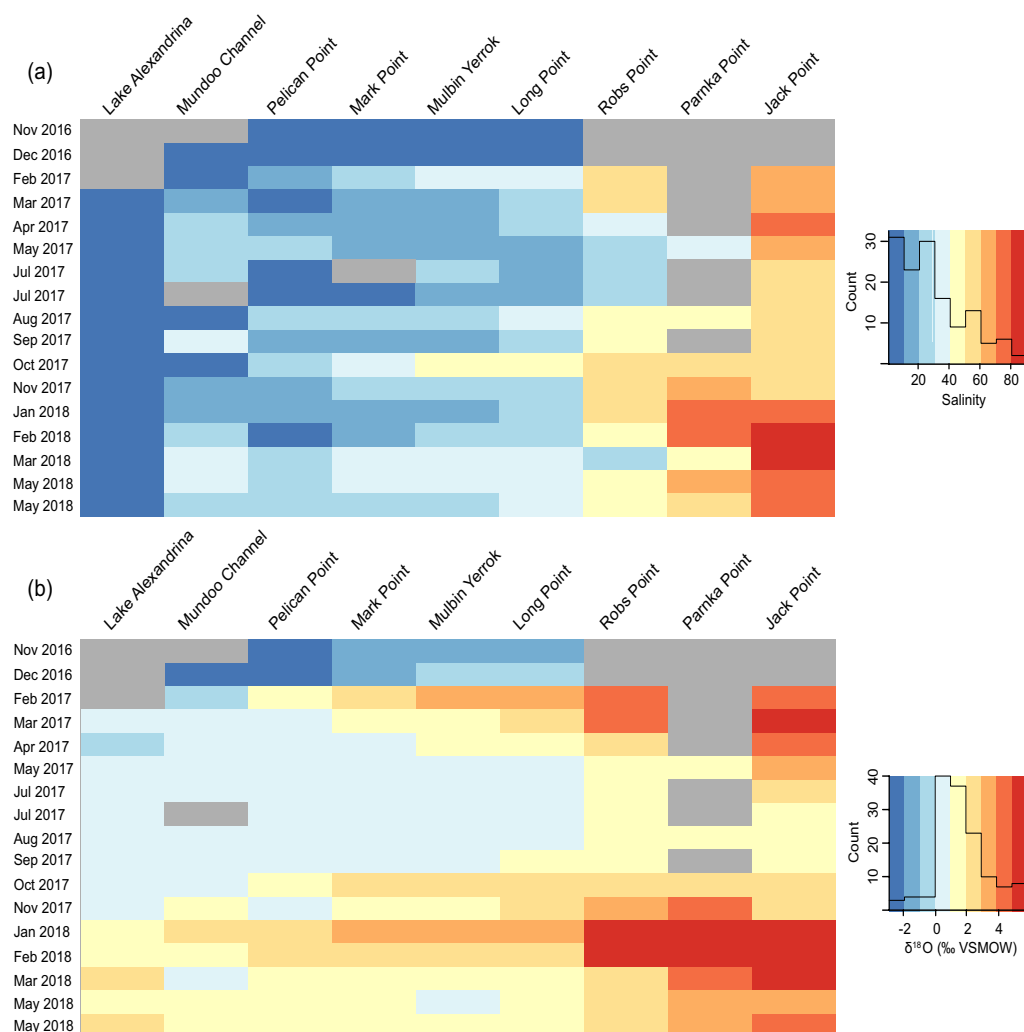


**Figure 3.** Heat maps showing water (a) salinity and (b) oxygen isotope composition of each sampling location for each sampling time. The color key is fitted with a histogram to show the distribution of values. Gray shading indicates missing data.

The  $\delta^{18}\text{O}_w$  values from all Coorong Lagoon sites (excluding Lake Alexandrina) showed a linear relationship to salinity where  $\delta^{18}\text{O}_w = 0.065 \times \text{salinity} - 2.55$  ( $R^2 = 0.629$ ,  $p < 0.0001$ ; Figure 4). However the slope, intercept, and coefficient of determination differed between sites, with the  $R^2$  of the regression varying between 0.20 at Pelican Point and 0.68 at Jack Point (Figure S1; Table S3). Low salinity waters from the North Lagoon collected in November and December 2016 have  $\delta^{18}\text{O}_w$  values lower than would be predicted by linear regression ( $< -1\text{‰}$ ). Water  $\delta^{18}\text{O}$  values displayed a linear relationship with water  $\delta^2\text{H}$  values, described by the relationship  $\delta^2\text{H} = 5.65 \times \delta^{18}\text{O} + 0.97$  ( $R^2 = 0.978$ ,  $p < 0.0001$ ; Figure 5). The slope of this line (5.65) differs from that of the Adelaide Meteoric Water Line (Adelaide MWL; slope = 7.25) as defined by the isotopic composition of Adelaide rainfall sourced from the Global Network for Isotopes in Precipitation (IAEA/WMO, 2020b). Our data are therefore consistent with a Local Evaporation Line (LEL; Gibson et al., 2016), where the LEL and Adelaide MWL intersect at  $\delta^{18}\text{O} = -4.31\text{‰}$ ,  $\delta^2\text{H} = -23.40\text{‰}$ . The slope of the relationship between water  $\delta^{18}\text{O}$  and  $\delta^2\text{H}$  differs slightly between sampling locations varying from 4.93 at Jack Point to 6.88 at Lake Alexandrina (Table S4). A slight difference was also observed between sampling times where slopes ranged from 5.12 in May 2018 to 7.59 in September 2017 (Table S5).



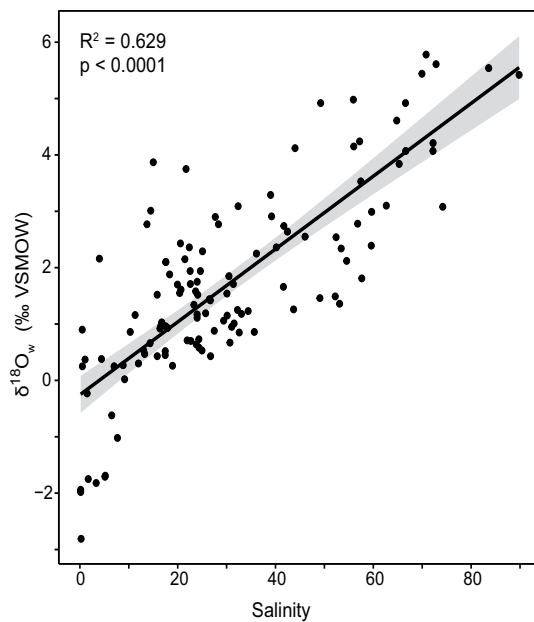


**Figure 4.**  $\delta^{18}\text{O}$  – salinity relationship for all Coorong Lagoon water samples collected between November 2016 and May 2018 with the line of best fit. The gray shaded area indicates the 95% confidence interval.

The  $\delta^{18}\text{O}_w$  and  $\delta^2\text{H}_w$  value at the intercept with zero salinity varied spatially (Figure 5; Table S3). The zero-salinity  $\delta^{18}\text{O}_w$  intercept at sites from the North Lagoon ranged from  $-0.06\text{‰}$  to  $-0.83\text{‰}$  while Lake Alexandrina and Jack Point had zero-salinity intercept  $\delta^{18}\text{O}_w$  values of  $-2.86\text{‰}$  and  $-3.88\text{‰}$  respectively (Figure 5; Figure S1; Table S3). The  $\delta^2\text{H}_w$  values at the zero intercept with salinity were also markedly different at Lake Alexandrina ( $-24\text{‰}$ ) and Jack Point ( $-17.75\text{‰}$ ) than for the other sampling locations which ranged from  $-0.91\text{‰}$  to  $-6.9\text{‰}$  (Figure 5; Figure S2; Table S3). Combined, the  $\delta^{18}\text{O}_w$  and  $\delta^2\text{H}_w$  values of the zero intercept with salinity plot closely to the LEL, with the exception of Lake Alexandrina which instead was closely aligned with a linear regression model fitted to the Murray River data from the Global Network of Isotopes in Rivers (IAEA/WMO, 2020a), and Jack Point which plotted closer to the Adelaide MWL (Figure 5).

### 3.3. Oxygen and Carbon Isotopes in Shells

The  $\delta^{18}\text{O}_s$  values of all analyzed whole shell samples ( $n = 131$ ) ranged from  $-0.36\text{‰}$  in shell MP0817-1 collected from Mark Point in August 2017 to  $+3.74\text{‰}$  in shell MP0518-6 collected from Mark Point in May 2018 (Table S2). The  $\delta^{13}\text{C}_s$  values of whole shell analyses ranged from  $-4.36\text{‰}$  in shell PP0817-4 collected from Pelican Point in August 2017 to  $+0.19\text{‰}$  in shell PP0518-5 collected from Pelican Point in May 2018. The correlation between  $\delta^{18}\text{O}$  and  $\delta^{13}\text{C}$  values in shells was weak ( $R^2 = 0.293$ ,  $p < 0.0001$ ; Figure S3). One factor ANOVA determined that  $\delta^{18}\text{O}_s$  and  $\delta^{13}\text{C}_s$  values did not differ by collection season ( $F_{3,127} = 1.55$ ,  $p = 0.21$ ;

$F_{3,127} = 1.04$ ,  $p = 0.38$ , respectively). However, when site was considered an additional variable in a two-factor ANOVA, the interaction between season and site had a significant effect on carbon isotope values ( $F_{11,112} = 5.57$ ,  $p < 0.001$ ). Shells from Pelican Point collected in winter and spring were found to have significantly different  $\delta^{13}\text{C}_s$  values than shells collected during summer and autumn (Figure S4).

### 3.4. Carbonate-Water Fractionation Factor

The carbonate-water fractionation factor ( $\delta^{18}\text{O}_{s(\text{VPDB})} - \delta^{18}\text{O}_{w(\text{VSMOW})}$ ;  $\sim\epsilon$ ) ranged from  $-2.72$  to  $+2.73$  when using the  $\delta^{18}\text{O}_w$  values from the day of collection and from  $-1.22$  to  $+2.80$  when using the  $\delta^{18}\text{O}_w$  values averaged over the estimated lifetime of each shell (Figure 6). The carbonate-water fractionation factor was linearly correlated with water temperature on the date of collection ( $R^2 = 0.509$ ,  $p < 0.0001$ ; Figure 6a) producing the following equation:  $T\text{ (}^\circ\text{C)} = (21.39 \pm 0.45) - (4.43 \pm 0.38) \times (\delta^{18}\text{O}_{\text{shell}} - \delta^{18}\text{O}_{\text{water}})$ . The slope ( $-4.43 \pm 0.38$ ) of this linear regression was within the error of that estimated by Böhm et al. (2000) (Equation 2), while the intercept ( $21.39 \pm 0.45$ ) differed slightly. The standard error for a predicted temperature value is  $\pm 5.1^\circ\text{C}$ . In contrast, there was no relationship found between  $\epsilon$  and temperature when averaged over the estimated growth period (Figure 6b).

When salinity was considered as an additional variable to temperature as determinants of the carbonate-water fractionation factor, an additional 7% of variance was explained by multiple linear regression. A significant regression equation was found ( $F = 90.36$ ,  $p < 0.0001$ ) with an  $R^2$  of 0.579 and both temperature ( $p < 0.0001$ ) and salinity ( $p < 0.0001$ ) were significant predictors of fractionation. An ANOVA test demonstrated that the two part multiple linear regression model was a significant improvement upon the single variable (temperature only) model ( $F_{1,128} = 22.41$ ,  $p < 0.001$ ). Furthermore, a variance inflation factor of 1.25 for temperature and salinity indicate that the multiple linear regression model was not adversely affected by collinearity between predictors. The predicted carbonate-water fractionation factor from the multiple linear regression was linearly correlated to the observed carbonate-water fractionation factor ( $R^2 = 0.582$ ,  $p < 0.0001$ ; Figure 7) with a slope of 1 and importantly no obvious bias with respect to the model residuals. A multiple linear regression with pH as an additional variable to temperature found that pH was not a significant predictor ( $p = 0.74$ ) of carbonate-water fractionation.

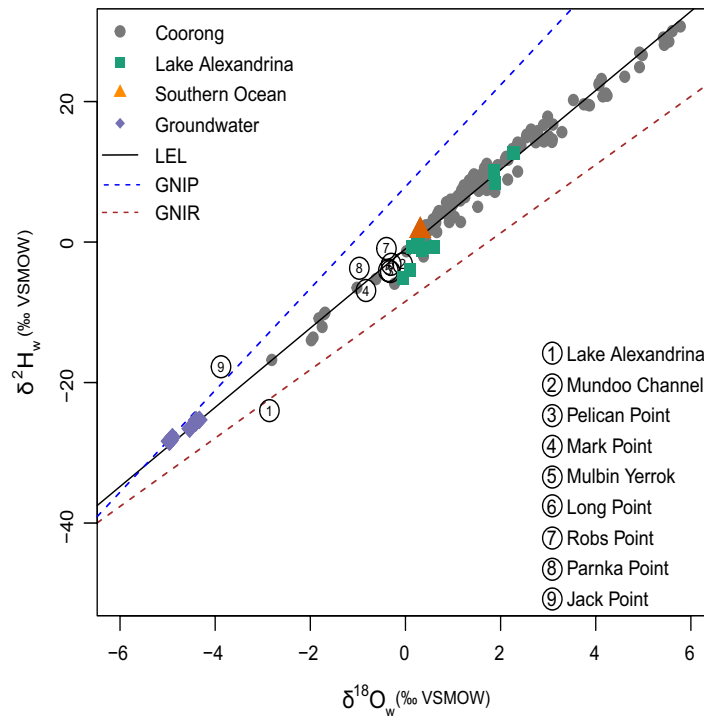


**Figure 5.** Stable isotope composition ( $\delta^{18}\text{O}$  and  $\delta^2\text{H}$ ) of waters from sampling sites in the Coorong Lagoons (gray circles) and Lake Alexandrina (green squares). Also depicted are  $\delta^{18}\text{O}$  and  $\delta^2\text{H}$  compositions for local groundwater (purple diamonds) and the Southern Ocean (orange triangle) from Kell-Duivestein (2015). The line of best fit through all samples from the Coorong Lagoons and Lake Alexandrina is shown (local evaporation line). The bold black line is the global meteoric water line. Best fit lines through the  $\delta^{18}\text{O}$  and  $\delta^2\text{H}$  values of Adelaide rainfall and the Murray River are sourced from the Global Network for Isotopes in Precipitation and the Global Network for Isotopes in Rivers, respectively. Also plotted are the  $\delta^{18}\text{O}$  and  $\delta^2\text{H}$  values for the intercept with zero salinity for each sampling location (numbered circles).

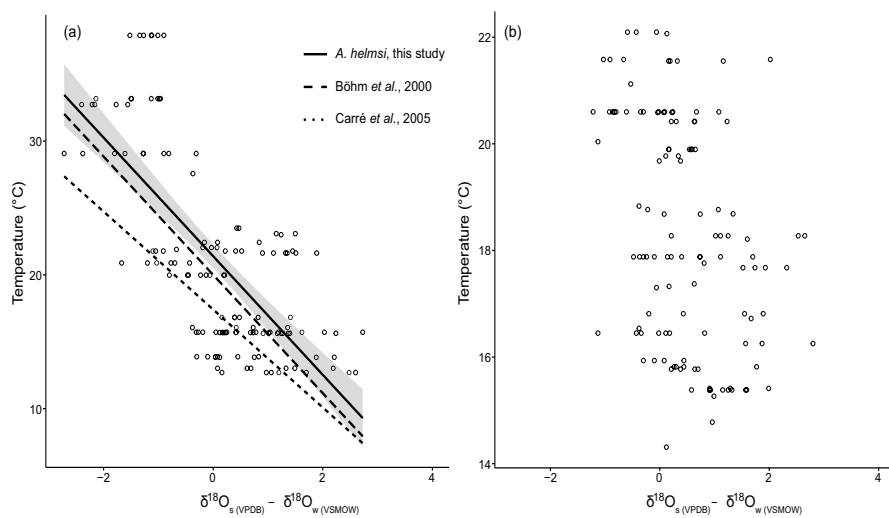


**Figure 6.** Oxygen isotope fractionation versus temperature for both (a) collection temperature and  $\delta^{18}\text{O}_w$  values and (b) averaged temperature and  $\delta^{18}\text{O}_w$  values. Included in (a) are comparisons to previous studies. The gray shaded area in (a) illustrates the 95% confidence interval for *A. helmsi*.

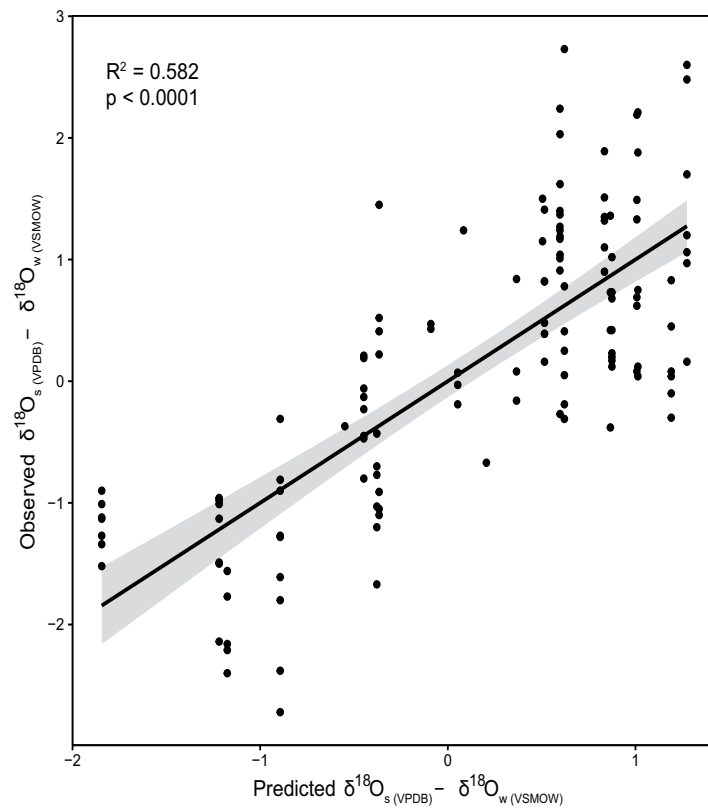


**Figure 7.** Predicted versus observed oxygen isotope fractionation in shells of *A. helmsi* collected from the Coorong Lagoon between March 2017 and May 2018. The predicted values are calculated via a multiple linear regression with temperature and salinity of the water at the time of shell collection as variables. The 1:1 line and 95% confidence interval are also illustrated.

### 3.5. Comparison of Measured Oxygen Isotope Ratios With Predicted Values

The measured  $\delta^{18}\text{O}_s$  values of *A. helmsi* were plotted against the  $\delta^{18}\text{O}_s$  values predicted by the equation developed in this study, as well as equations from Böhm et al. (2000) (Equation 2) and Carré et al. (2005); (Equation 3) in Figure 8. The predicted  $\delta^{18}\text{O}_s$  values were calculated using both the  $\delta^{18}\text{O}_w$  composition and temperature of water from the collection day and also the average values predicted over the lifetime of the shell. Figure 8 shows that there was generally overlap between measured and predicted  $\delta^{18}\text{O}_s$  values, though this pattern was inconsistent.  $\delta^{18}\text{O}$  compositions in shells from Munday Channel were not well reflected by the predicted  $\delta^{18}\text{O}_s$  values, while predicted and measured  $\delta^{18}\text{O}_s$  values in shells from Pelican Point showed good agreement. Predicted  $\delta^{18}\text{O}_s$  values at Pelican Point best reflected measured values when the average temperature and  $\delta^{18}\text{O}_w$  compositions were used. At Mulbin Yerrok and Long Point, there was more overlap in the predicted values calculated from collection day and averaged water parameters. An offset of 0.31‰ ( $\pm 0.002\%$ ) existed between  $\delta^{18}\text{O}_s$  predicted using the equation developed in this study and the equation from Böhm et al. (2000).

## 4. Discussion

Quantifying the isotope fractionation between living bivalve shells and their surrounding water is essential for the use of carbonate oxygen isotopes in paleoenvironmental studies. In this study, we examined oxygen isotope ratios in live specimens of the estuarine bivalve *A. helmsi* alongside the oxygen and hydrogen isotope compositions of ambient waters. Variability in the  $\delta^{18}\text{O}_w$  and  $\delta^2\text{H}_w$  values of Coorong and Lake Alexandrina waters was primarily linked to the evaporation of mixed waters, in addition to occasional large freshwater

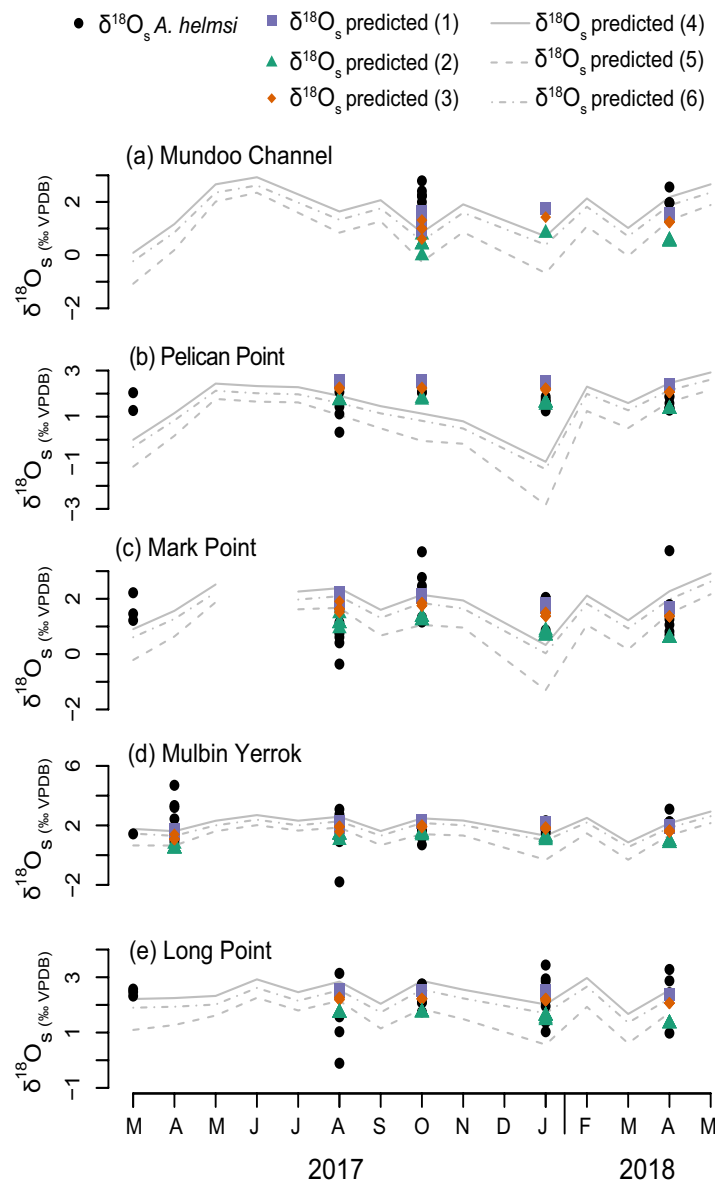


**Figure 8.** Measured  $\delta^{18}\text{O}_s$  values in *A. helmsi* and predicted  $\delta^{18}\text{O}_s$  values in aragonitic shells from each sampling location.  $\delta^{18}\text{O}_w$  values are predicted from the equations derived in this study (1 and 4), of Carré et al. (2005) (2 and 5) and Böhm et al. (2000) (3 and 6). Predicted values for 1, 2, and 3 (purple squares, orange diamonds, and green triangles) were calculated using average temperature and  $\delta^{18}\text{O}_w$  values, while the predicted values for 4, 5, and 6 (solid, dashed, and dot-dashed lines) were calculated using the temperature and  $\delta^{18}\text{O}_w$  values measured on the day of shell collection. Measured values are shown by solid black circles.

releases from the River Murray and Lake Alexandrina into the North Lagoon. A new temperature-dependent fractionation equation was developed for *A. helmsi*, which was found to have a similar slope to the relationship published by Böhm et al. (2000). A relatively high amount of scatter in this relationship could be explained by uncertainties surrounding the age of the shells, or some level of disequilibrium caused by kinetic growth rate effects. Despite these uncertainties, the development of a temperature dependent of aragonite – water fractionation equation for *A. helmsi* lays the foundation for subsequent interpretation of  $\delta^{18}\text{O}_s$  values from (sub)fossil specimens.

#### 4.1. Controls on the Oxygen and Hydrogen Isotopes of Coorong Waters

The processes that control the oxygen and hydrogen isotope composition of surface waters are well understood, with isotope ratios primarily varying as a function of evaporation and replenishment by precipitation (for comprehensive reviews see Gat, 2002; Gibson et al., 2016). However, in estuarine systems, additional complexities make interpretation of water isotope ratios more challenging, largely due to uncertainties arising from water inputs from several different sources, in addition to dynamic geomorphological variability (Cooper et al., 1997; Price et al., 2012). The Coorong and Lower Lakes system is additionally complex due to the management of river water flow through barrage structures into the Coorong. In the modern system, significant freshwater flows are only released through the barrages when Lake Alexandrina levels are high due to high River Murray discharge. During these times the  $\delta^{18}\text{O}_w$  value is expected to be lower due to the high proportion of local and headwater rainwater in the river, and due to a reduction in the water residence time, and thus evaporation, in both the river basin and Lake Alexandrina. In contrast, during dry periods, the barrages act to accentuate the effects of evaporation by restricting the flow of freshwater into the Coorong, and waters that are released will have a higher  $\delta^{18}\text{O}_w$  value due to the reduced discharge of the river and increased evaporation. The isotopic composition of Murray River waters was not measured in this study, but Simpson and Herczeg (1991) in their study of River Murray oxygen and hydrogen ratios suggest extensive evaporative enrichment of surface waters throughout the Murray Basin. They found Lake Alexandrina to have  $\delta^{18}\text{O}_w$  values 0.6–4.67 ‰ higher than those measured in the Murray River at Taillem Bend in the same time period (Simpson & Herczeg 1991).

A positive linear relationship between  $\delta^{18}\text{O}_w$  values and salinity was observed in this study in agreement with previous studies in estuaries (Figure 4; Ingram et al., 1996; Price et al., 2012; Surge & Lohmann, 2002). As salinity and  $\delta^{18}\text{O}_w$  values both increase during evaporation, this relationship would be expected in estuaries which receive relatively little, or invariable influence from fluvial sources. However, the  $\delta^{18}\text{O}_w$  – salinity relationship may depart from linearity if there are variations in the composition of the freshwater endmember (Mohan and Walther, 2015; Walther and Nims, 2015). In particular, this phenomenon could explain variable  $\delta^{18}\text{O}_w$  values in the northern reaches of the Coorong (e.g., Mundoo Channel, Pelican Point), where the barrage system accentuates evaporation of low salinity waters in Lake Alexandrina, leading to a wide range of  $\delta^{18}\text{O}_w$  values at low (<5) salinity (Figure 3; Figure S1; Table S3). The  $\delta^{18}\text{O}_w$  and  $\delta^2\text{H}_w$  analyses of Coorong and Lake Alexandrina waters exhibited a LEL typical of evaporative systems (Figure 5; Gibson et al., 1993). Previous studies of estuaries in similar climates have also found that the replenishment from either fresh or marine waters is small relative to evaporation leading to consistently enriched  $\delta^{18}\text{O}_w$  values (Stalker et al., 2009; Surge and Lohmann, 2002; Walther and Nims, 2015). During the period of high barrage release in November and December 2016, the  $\delta^{18}\text{O}_w$  values in the North Lagoon from Pelican Point to Long Point ranged from  $-2.81$  to  $+0.02$ ‰, that is, lower than average sea water (Figure 3b). The  $\delta^{18}\text{O}_w$  and  $\delta^2\text{H}_w$  of the samples from late 2016 fall between groundwater/rainwater and Lake Alexandrina waters on the LEL (Figure 5), suggesting a higher proportion of rainwater, either from the Murray River headwaters or by groundwater. Outside of this period,  $\delta^{18}\text{O}_w$  values were found to be higher than those of seawater (Figure 3b), indicating that evaporation is the primary control over water  $\delta^{18}\text{O}_w$  in the Coorong with water mixing from large freshwater releases also having an effect in the North Lagoon.

The positive linear correlations between  $\delta^{18}\text{O}_w$  values and salinity observed in this study allow the interpretation of the freshwater sources for each of the sampling locations (Price et al., 2012; Stalker et al., 2009; Swart & Price, 2002). As changes in oxygen isotope composition and salinity are both driven by evaporation, the  $\delta^{18}\text{O}_w$  value of the intercept at zero salinity can be interpreted as the  $\delta^{18}\text{O}_w$  value of the freshwater which is primarily responsible for diluting salinity (Swart & Price, 2002). In this study, the zero intercept values of  $\delta^{18}\text{O}_w$  and  $\delta^2\text{H}_w$  confirm that the Coorong North Lagoon is primarily diluted by Lake Alexandrina water, which in turn is sourced from Murray River water. Jack Point in the South Lagoon, however, appears to be primarily replenished by rain water, either direct upon the lagoon or transported via local runoff or groundwater (Figure 5). Groundwater seeps in the South Lagoon have previously been identified as an important source of fresh water both currently and historically (Haese et al., 2008; Kell-Duivesteyn, 2015). These interpretations are consistent with radiogenic strontium isotope data, which suggested that North Lagoon waters represent a mixing of seawater and freshwater from Lake Alexandrina while the South Lagoon waters are sourced primarily from continental waters, consistent with local groundwater, yet extensively salinized by

evaporation (Shao et al., 2018). These results also indicate that the large barrage release in late 2016 was not substantial or sustained enough to lower the salinity in the South Lagoon, in contrast to releases described in the 1980s (Geddes & Butler, 1984).

#### 4.2. Aragonite-Water Oxygen Isotope Fractionation in *A. helmsi* Shells

Monitoring of  $\delta^{18}\text{O}_w$  composition and water temperature alongside shell collection allowed the development of a new species-specific temperature-dependent oxygen isotope fractionation equation for *A. helmsi* for use in paleoclimate studies. The slope of the *A. helmsi* calibration was within error of the equation produced by Böhm et al. (2000), which is largely based upon the paleotemperature equation of Grossman and Ku (1986) (Figure 6). Calibration studies of several other aragonitic bivalve species from brackish environments have also found fractionation relationships similar to that of Böhm et al. (2000) (Hallmann et al., 2009; Simstich et al., 2005; Torres et al., 2011) and Grossman and Ku (1986) (Andrus & Rich, 2008; Lécuyer et al., 2004).

The inclusion of salinity in addition to temperature as a determinant of carbonate-water fractionation in *A. helmsi* explained a further 7% of variance compared to temperature alone (Figure 7). Previous studies investigating the effect of salinity on the oxygen isotope fractionation into aragonite have found no significant effect of salinity at marine salinity ranges (Kim et al., 2007). However, other authors have found a combination of temperature, salinity, precipitation rate and pH determine fractionation between aragonite and water (Wang et al., 2013). The pH of surrounding waters was not found to be a significant determinant of the carbonate-water fractionation factor in *A. helmsi*. Precipitation experiments of inorganic aragonite also found the aragonite – water fractionation factor was independent of the pH of the parent solution (Kim et al., 2006). In contrast, pH has been demonstrated to influence oxygen isotope fractionation in both inorganic (Dietzel et al., 2009; Watkins et al., 2014) and organic calcite (Zeebe, 1999). Furthermore, deviations from oxygen isotope equilibrium in the calcitic bivalve *Pecten maximus* have been hypothesized as reflecting a difference in pH between surrounding waters and the extrapallial fluid (EPF) at the site of mineralization (Owen et al., 2002). The chemistry of the EPF was not investigated in our study, but presents another possible explanation for deviation from equilibrium.

Uncertainties surrounding the growth rate and age of the *A. helmsi* specimens in this study could also be responsible for increased error in predicted temperatures and high scatter in the relationship between temperature and the fractionation factor. In a recent study, the oyster *Magallana gigas* was found to precipitate calcite in disequilibrium in the early stages of life, before a slowing in the growth rate in the adult phase resulted in equilibrium fractionation (Huyghe et al., 2020). These results were in agreement with the suggestion by Coplen (2007) and Daëron et al. (2019) that precipitation at isotopic equilibrium is possible only at very slow growth rates. As sections of juvenile and adult growth in *A. helmsi* could not be determined, the whole shell sampling of *A. helmsi* includes the juvenile portions and could therefore include periods of fast and variable growth which could result in isotopic disequilibrium. Furthermore, a study investigating fractionation between water and larval aragonite of the scallop, *Placopecten magellanicus*, demonstrated that those reared under “stressful” conditions (low salinity and temperature) exhibited a departure from oxygen isotope equilibrium (Owen et al., 2008). In our study, *A. helmsi* were at times exposed to conditions outside of their salinity and temperature tolerance (Wells & Threlfall, 1982a; Figures 2a and 3a). Temperature extremes in particular do not appear to be well recorded in *A. helmsi* (Figure 6) in agreement with findings for other bivalve species (Schöne et al., 2006). Though a range of kinetic effects could be responsible for *A. helmsi* not reaching exact equilibrium, the similarity to the paleotemperature equation from Böhm et al. (2000) suggests that the oxygen isotope ratios in *A. helmsi* shell aragonite can be useful as a tracer of past environmental change.

While water temperature was found to produce a significant correlation with  $\delta^{18}\text{O}_s - \delta^{18}\text{O}_w$  when applying the temperature and  $\delta^{18}\text{O}_w$  values measured on the day of shell collection, average temperature and  $\delta^{18}\text{O}_w$  values based on the estimated lifespan of the shells did not exhibit any correlation (Figure 6). *A. helmsi* do not show annual growth banding (Chamberlayne et al., 2020; Wells & Threlfall, 1982b) and were found to grow at a constant rate of 0.3 mm/month during a long term field study by Wells and Threlfall (1982b). As conditions on the date of collection produced a significant temperature relationship, the estimation of the shell lifespan may not have been robust. One potential explanation is that the shells in the Coorong population experienced a shorter lifespan and faster growth than those in the study by Wells and Threlfall (1982b),

and therefore reflected the temperature and  $\delta^{18}\text{O}_w$  composition close to their collection day in their carbonate. Growth rate been shown experimentally to be affected by temperature and food availability in bivalve shells (Zhao et al., 2017). While the temperatures recorded in the study by Wells and Threlfall (1982a) (18°–32°C) were similar to those recorded in this study (Figure 2a), it is possible that the nutrient rich Coorong waters (Grigg et al., 2009) contributed to higher aquatic primary productivity and thus faster bivalve growth in the Coorong population. Another potential explanation for the lack of correlation with averaged data are high variability in temperature and/or  $\delta^{18}\text{O}_w$  that was not captured by the monthly frequency of our sampling.

#### 4.3. Carbon Isotopes in *A. helmsi*

Changes in the carbon isotope composition of *A. helmsi* were not a major focus of this study. The processes that are thought to affect  $\delta^{13}\text{C}_s$  values include the carbon isotope composition of dissolved inorganic carbon (DIC) of water (Gillikin et al., 2006; McConnaughey & Gillikin, 2008; Owen et al., 2008; Poulain et al., 2010) and metabolic carbon incorporated through the diet of the bivalve (Gillikin et al., 2006, 2007; Lorrain et al., 2004; Poulain et al., 2010). Some authors have proposed the use of  $\delta^{13}\text{C}_s$  values as a salinity proxy in estuaries due to the relationship between salinity and the carbon isotope composition of DIC (Gillikin et al., 2006; Poulain et al., 2010). However, the  $\delta^{13}\text{C}$  values of DIC in the Coorong were not measured in this study and there was no correlation between  $\delta^{13}\text{C}_s$  values and salinity. Metabolic carbon has been estimated to contribute less than 10% to  $\delta^{13}\text{C}_s$  in deep sea molluscs (Gillikin et al., 2006; Lorrain et al., 2004; McConnaughey et al., 1997) and up to 35% in a freshwater species (Gillikin et al., 2009). In the Coorong, variability in  $\delta^{13}\text{C}$  values of particulate organic matter, which predominantly reflects phytoplankton, exhibited a strong north-south gradient, possibly in response to the mixing of marine and terrestrial carbon sources (Priestley pers. comm). This gradient, along with the north-south salinity gradient, was not reflected in the  $\delta^{13}\text{C}$  values of *A. helmsi* shells (Figure S4). Therefore, it is possible that  $\delta^{13}\text{C}$  values of *A. helmsi* shells reflect a complex interaction behind the bivalve diet and water DIC. A more detailed investigation into these processes would be an interesting avenue for future research.

## 5. Conclusions and Implications for Paleoclimate Studies

This study evaluated the environmental controls over oxygen and hydrogen isotope compositions of water, and oxygen isotope compositions of bivalve carbonate, in the Coorong Lagoon – an inverse estuary at the mouth of the River Murray, Australia. Variability in the oxygen and hydrogen isotope ratios of water in the Coorong is primarily affected by evaporative enrichment of  $^{18}\text{O}$  across a north-south gradient, with the majority of measured  $\delta^{18}\text{O}_w$  observations being higher than sea water. By combining  $\delta^{18}\text{O}_w$  and salinity measurements, our data suggest that waters in the North Lagoon are primarily fed by the River Murray, whereas those in the South Lagoon exhibit a closer similarity to rainfall, presumably via direct precipitation, local runoff and groundwater. With respect to the oxygen isotope composition of the aragonitic bivalve *A. helmsi*, the similarity between the species-specific paleotemperature equation developed in this study and the paleotemperature equation from Böhm et al. (2000) indicate that our equation can be applied to (sub) fossil bivalve shells to infer past hydroclimate.

From the *A. helmsi* temperature-dependent fractionation equation developed in this study, an increase in  $\delta^{18}\text{O}_s$  by 1‰ could be caused by a decrease in temperature by ~4.3°C or an increase in  $\delta^{18}\text{O}_w$  by 1‰ which is equivalent to an increase in salinity by ~15 (Figure 4). The Coorong Lagoons have highly variable salinity and temperature annually (Figures 2a and 3a) and so studies investigating  $\delta^{18}\text{O}_s$  values in the past will need to consider both changes in temperature and the isotopic composition of water as causes for carbonate isotopic shifts. Due to the short lifespan of *A. helmsi*, analysis of individual shells will likely have a seasonal bias and will only provide a limited window of temperature or water isotope variability. An approach taken to mitigate such biases in other short lived biogenic carbonates, such as ostracods, is to average several individuals from the same stratigraphic layer (e.g., Pérez et al., 2013). In addition to averaged bulk measurements providing information on long term climate trends, studies have measured the  $\delta^{18}\text{O}$  values of many individual foraminifera and ostracods to investigate the seasonal amplitude of past temperature and/or hydroclimatic change (Dixit et al., 2015; Koutavas et al., 2006). Similar approaches to the interpretation

of *A. helmsi*  $\delta^{18}\text{O}$  values in paleoenvironmental studies are recommended due to the small size and short lifespan of this species.

### Data Availability Statement

The original data from this research study are archived in the Mendeley Data repository (<http://dx.doi.org/10.17632/3fg277j4vz.1>).

### Acknowledgments

The authors would like to thank Mark Rollog, Kristine Neilson, and Robert Klæbe for assistance with carbonate isotopic analyzes; and Daniel Jardine and Jason Young from Flinders Analytical, Flinders University, for assistance with water isotope analyzes. This research study was supported by a Sir Mark Mitchell Foundation Grant, a Lirabenda Endowment Research Grant from the Field Naturalists Society of South Australia, and a Conservation Biology Grant from the Nature Conservation Society of South Australia. Funding for equipment was through an ARC LIEF grant (LE120100054).

### References

- Andrus, C. F. T., & Rich, K. W. (2008). A preliminary assessment of oxygen isotope fractionation and growth increment periodicity in the estuarine clam *Rangia cuneata*. *Geo-Marine Letters*, 28, 301–308. <https://doi.org/10.1007/s00367-008-0109-3>
- Barrie, G. M., Worden, R. H., Barrie, C. D., & Boyce, A. J. (2015). Extensive evaporation in a modern temperate estuary: Stable isotopic and compositional evidence. *Limnology & Oceanography*, 60, 1241–1250. <https://doi.org/10.1002/lno.10091>
- Böhm, F., Joachimski, M. M., Dullo, W. C., Eisenhauer, A., Lehnert, H., Reitner, J., & Wörheide, G. (2000). Oxygen isotope fractionation in marine aragonite of coralline sponges. *Geochimica et Cosmochimica Acta*, 64, 1695–1703. [https://doi.org/10.1016/S0016-7037\(99\)00408-1](https://doi.org/10.1016/S0016-7037(99)00408-1)
- BOM (Australian Bureau of Meteorology). (2020). *Climate data online [online]*. Available at <http://www.bom.gov.au/climate/data/>
- Butler, P. G., Wanamaker, A. D., Scourse, J. D., Richardson, C. A., & Reynolds, D. J. (2012). Variability of marine climate on the North Icelandic Shelf in a 1357-year proxy archive based on growth increments in the bivalve *Arctica islandica*. *Palaeogeography, Palaeoclimatology, Palaeoecology*, 373, 141–151. <https://doi.org/10.1016/j.palaeo.2012.01.016>
- Carré, M., Bentaleb, I., Blamart, D., Ogle, N., Cardenas, F., Zevallos, S., et al. (2005). Stable isotopes and sclerochronology of the bivalve *Mesodesma donacium*: Potential application to Peruvian paleoceanographic reconstructions. *Palaeogeography, Palaeoclimatology, Palaeoecology*, 228, 4–25. <https://doi.org/10.1016/j.palaeo.2005.03.045>
- Carré, M., Sachs, J. P., Schauer, A. J., Rodríguez, W. E., & Ramos, F. C. (2013). Reconstructing El Niño-Southern Oscillation activity and ocean temperature seasonality from short-lived marine mollusk shells from Peru. *Palaeogeography, Palaeoclimatology, Palaeoecology*, 371, 45–53. <https://doi.org/10.1016/j.palaeo.2012.12.014>
- Chamberlayne, B. (2015). *Late Holocene seasonal and multicentennial hydroclimate variability in the Coorong Lagoon, South Australia: Evidence from stable isotopes and trace element profiles of bivalve molluscs* honours thesis. University of Adelaide.
- Chamberlayne, B. K., Tyler, J. J., & Gillanders, B. M. (2020). Environmental controls on the geochemistry of a short-lived bivalve in south-eastern Australian estuaries. *Estuaries and Coasts*, 43, 86–101. <https://doi.org/10.1007/s12237-019-00662-7>
- Commonwealth of Australia (Murray-Darling Basin Authority). (2020). *About the basin*. Available at <https://www.mdba.gov.au/>
- Cooper, L. W., Whittleage, T. E., Grebmeier, J. M., & Weingartner, T. (1997). The nutrient, salinity, and stable oxygen isotope composition of Bering and Chukchi Seas waters in and near the Bering Strait. *Journal of Geophysical Research*, 102, 12563–12573. <https://doi.org/10.1029/97JC00015>
- Coplen, T. B. (2007). Calibration of the calcite-water oxygen-isotope geothermometer at Devils Hole, Nevada, a natural laboratory. *Geochimica et Cosmochimica Acta*, 71, 3948–3957. <https://doi.org/10.1016/j.gca.2007.05.028>
- Corlis, N. J., Veeh, H. H., Dighton, J. C., & Herczeg, A. L. (2003). Mixing and evaporation processes in an inverse estuary inferred from  $\delta^{2}\text{H}$  and  $\delta^{18}\text{O}$ . *Continental Shelf Research*, 23, 835–846. [https://doi.org/10.1016/S0278-4343\(03\)00029-3](https://doi.org/10.1016/S0278-4343(03)00029-3)
- Crippa, G., Angiolini, L., Bottini, C., Erba, E., Felletti, F., Frigerio, C., et al. (2016). Seasonality fluctuations recorded in fossil bivalves during the early Pleistocene: Implications for climate change. *Palaeogeography, Palaeoclimatology, Palaeoecology*, 446, 234–251. <https://doi.org/10.1016/j.palaeo.2016.01.029>
- Daéron, M., Drysdale, R. N., Peral, M., Huyghe, D., Blamart, D., Coplen, T. B., et al. (2019). Most Earth-surface calcites precipitate out of isotopic equilibrium. *Nature Communications*, 10, 1–7. <https://doi.org/10.1038/s41467-019-08336-5>
- Department for Environment and Heritage. (2000). *Coorong, and Lakes Alexandrina and Albert Ramsar Management Plan*. South Australian Department for Environment and Heritage.
- Dettman, D. L., Flessa, K. W., Roopnarine, P. D., Schöne, B. R., & Goodwin, D. H. (2004). The use of oxygen isotope variation in shells of estuarine mollusks as a quantitative record of seasonal and annual Colorado River discharge. *Geochimica et Cosmochimica Acta*, 68, 1253–1263. <https://doi.org/10.1016/j.gca.2003.09.008>
- Dick, J., Haynes, D., Tibby, J., Garcia, A., & Gell, P. (2011). A history of aquatic plants in the Coorong, a Ramsar-listed coastal wetland, South Australia. *Journal of Paleolimnology*, 46, 623–635. <https://doi.org/10.1007/s10933-011-9510-4>
- Dietzel, M., Tang, J., Leis, A., & Köhler, S. J. (2009). Oxygen isotopic fractionation during inorganic calcite precipitation – effects of temperature, precipitation rate and pH. *Chemical Geology*, 268, 107–115. <https://doi.org/10.1016/j.chemgeo.2009.07.015>
- Disspain, M., Wallis, L. A., & Gillanders, B. M. (2011). Developing baseline data to understand environmental change: A geochemical study of archeological otoliths from the Coorong, South Australia. *Journal of Archaeological Science*, 38, 1842–1857. <https://doi.org/10.1016/j.jas.2011.03.027>
- Dittmann, S., Lam Gordillo, O., & Baring, R. (2019). *Benthic macroinvertebrate survey 2018–2019 report. Coorong, Lower Lakes and Murray Mouth Icon site. Report for the Department for Environment and Water and the Murray-Darling Basin Authority*. Flinders University.
- Dixit, Y., Hodell, D. A., Sinha, R., & Petrie, C. A. (2015). Oxygen isotope analysis of multiple, single ostracod valves as a proxy for combined variability in seasonal temperature and lake water oxygen isotopes. *Journal of Paleolimnology*, 53, 35–45. <https://doi.org/10.1007/s10933-014-9805-3>
- Epstein, S., Buchsbaum, R., Lownstam, H., & Urey, H. C. (1951). Carbonate-water isotopic temperature scale. *Bulletin of the Geological Society of America*, 62, 417–426. [https://doi.org/10.1130/0016-7606\(1951\)62\[417:cits\]2.0.co;2](https://doi.org/10.1130/0016-7606(1951)62[417:cits]2.0.co;2)
- Epstein, S., & Mayeda, T. (1953). Variation of  $\text{O}^{18}$  content of waters from natural sources. *Geochimica et Cosmochimica Acta*, 4, 213–224. [https://doi.org/10.1016/0016-7037\(53\)90051-9](https://doi.org/10.1016/0016-7037(53)90051-9)
- Falster, G., Delean, S., & Tyler, J. (2018). Hydrogen peroxide treatment of natural lake sediment prior to carbon and oxygen stable isotope analysis of calcium carbonate. *Geochemistry, Geophysics, Geosystems*, 19, 1–3595. <https://doi.org/10.1029/2018GC007575>
- Featherstone, A. M., Butler, P. G., Schöne, B. R., Peharda, M., & Thébaud, J. (2020). A 45-year sub-annual reconstruction of seawater temperature in the Bay of Brest, France, using the shell oxygen isotope composition of the bivalve *Glycymeris glycymeris*. *The Holocene*, 30, 3–12. <https://doi.org/10.1177/0959683619865592>



- Gat, J. R. (2002). Oxygen and hydrogen isotopes in the hydrologic cycle. *Annual Review of Earth and Planetary Sciences*, 24, 225–262. <https://doi.org/10.1146/annurev.earth.24.1.225>
- Geddes, M. C., & Butler, A. (1984). Physicochemical and biological studies on the Coorong Lagoons, South Australia, and the effect of salinity on the distribution of the macrobenthos. *Transactions of the Royal Society of South Australia*, 108, 51–62.
- Gell, P. A. (2017). Paleolimnological History of the Coorong: Identifying the natural ecological character of a Ramsar wetland in crisis. In K. Weckström, K. M. Saunders, P. A. Gell, & C. G. Skilbeck (Eds.), *Applications of paleoenvironmental techniques in estuarine studies* (pp. 587–613). Springer Netherlands. [https://doi.org/10.1007/978-94-024-0990-1\\_23](https://doi.org/10.1007/978-94-024-0990-1_23)
- Gibson, J. J., Birks, S. J., & Yi, Y. (2016). Stable isotope mass balance of lakes: A contemporary perspective. *Quaternary Science Reviews*, 131, 316–328. <https://doi.org/10.1016/j.quascirev.2015.04.013>
- Gibson, J. J., Edwards, T. W. D., Bursley, G. G., & Prowse, T. D. (1993). Estimating evaporation using stable isotopes: Quantitative results and sensitivity analysis for two catchments in northern Canada. *Nord. Hydrology*, 24, 79–94. <https://doi.org/10.2166/nh.1993.0015>
- Gillanders, B. M., & Munro, A. R. (2012). Hypersaline waters pose new challenges for reconstructing environmental histories of fish based on otolith chemistry. *Limnology & Oceanography*, 57, 1136–1148. <https://doi.org/10.4319/lo.2012.57.4.1136>
- Gillikin, D. P., Hutchinson, K. A., & Kumai, Y. (2009). Ontogenic increase of metabolic carbon in freshwater mussel shells (*Pyganodon cataracta*). *Journal of Geophysical Research*, 114, 1–6. <https://doi.org/10.1029/2008JG000829>
- Gillikin, D. P., Lorrain, A., Bouillon, S., Willenz, P., & Dehairs, F. (2006). Stable carbon isotopic composition of *Mytilus edulis* shells: Relation to metabolism, salinity,  $\delta^{13}\text{C}_{\text{DIC}}$  and phytoplankton. *Organic Geochemistry*, 37, 1371–1382. <https://doi.org/10.1016/j.orggeochem.2006.03.008>
- Gillikin, D. P., Lorrain, A., Meng, L., & Dehairs, F. (2007). A large metabolic carbon contribution to the  $\delta^{13}\text{C}$  record in marine aragonitic bivalve shells. *Geochimica et Cosmochimica Acta*, 71, 2936–2946. <https://doi.org/10.1016/j.gca.2007.04.003>
- Government of South Australia. (2020). *River Murray flow report* (Department for Environment and Water, South Australia). Available at <https://www.waterconnect.sa.gov.au/Pages/Home.aspx>
- Grigg, N. J., Robson, B. J., Webster, I. T., & Ford, P. W. (2009). *Water for a healthy country nutrient budgets and biogeochemical modeling of the Coorong*. CSIRO. Water for a Healthy Country National Research Flagship.
- Grossman, E. L., & Ku, T. L. (1986). Oxygen and carbon isotope fractionation in biogenic aragonite: Temperature effects. *Chemical Geology*, 59, 59–74. [https://doi.org/10.1016/0168-9622\(86\)90057-6](https://doi.org/10.1016/0168-9622(86)90057-6)
- Haese, R. R., Gow, L., Wallace, L., & Brodie, R. S. (2008). Identifying groundwater discharge in the Coorong (South Australia). *AUSGEO News*, 1–6.
- Hallmann, N., Burchell, M., Schöne, B. R., Irvine, G. V., & Maxwell, D. (2009). High-resolution sclerochronological analysis of the bivalve mollusk *Saxidomus gigantea* from Alaska and British Columbia: Techniques for revealing environmental archives and archeological seasonality. *Journal of Archaeological Science*, 36, 2353–2364. <https://doi.org/10.1016/j.jas.2009.06.018>
- Haynes, D., Gell, P., Tibby, J., Hancock, G., & Goonan, P. (2007). Against the tide: The freshening of naturally saline coastal lakes, south-eastern South Australia. *Hydrobiologia*, 591, 165–183. <https://doi.org/10.1007/s10750-007-0802-7>
- Hermoso, M., & Lecasble, M. (2018). The effect of salinity on the biogeochemistry of the coccolithophores with implications for coccolith-based isotopic proxies. *Biogeosciences*, 15, 6761–6772. <https://doi.org/10.5194/bg-15-6761-2018>
- Huyghe, D., Emmanuel, L., de Rafelis, M., Renard, M., Ropert, M., Labourdette, N., & Lartaud, F. (2020). Oxygen isotope disequilibrium in the juvenile portion of oyster shells biases seawater temperature reconstructions. *Estuarine, Coastal and Shelf Science*, 240, 106777. <https://doi.org/10.1016/j.ecss.2020.106777>
- IAEA/WMO. (2020a). *Global Network of Isotopes in Precipitation*. The GNIP Database. Accessible at <https://nucleus.iaea.org/wiser>
- IAEA/WMO. (2020b). *Global Network of Isotopes in Rivers*. The GNIR Database. Accessible at <https://nucleus.iaea.org/wiser>
- Ingram, B. L., Conrad, M. E., & Ingle, J. C. (1996). Stable isotope and salinity systematics in estuarine waters and carbonates: San Francisco Bay. *Geochimica et Cosmochimica Acta*, 60, 455–467. [https://doi.org/10.1016/0016-7037\(95\)00398-3](https://doi.org/10.1016/0016-7037(95)00398-3)
- Jones, D. S., Quitmyer, I. R., & Andrus, C. F. T. (2005). Oxygen isotopic evidence for greater seasonality in Holocene shells of *Donax variabilis* from Florida. *Palaeogeography, Palaeoclimatology, Palaeoecology*, 228, 96–108. <https://doi.org/10.1016/j.palaeo.2005.03.046>
- Kelemen, Z., Gillikin, D. P., Graniero, L. E., Havel, H., Darchambeau, F., Borges, A. V., et al. (2017). Calibration of hydroclimate proxies in freshwater bivalve shells from Central and West Africa. *Geochimica et Cosmochimica Acta*, 208, 41–62. <https://doi.org/10.1016/j.gca.2017.03.025>
- Kell-Duivestein, I. (2015). *Tracing the groundwater inputs and water-mass mixing in the Coorong lagoons (South Australia) using strontium isotopes* honours thesis. University of Adelaide.
- Kim, S.-T., Hillaire-Marcel, C., & Mucci, A. (2006). Mechanisms of equilibrium and kinetic oxygen isotope effects in synthetic aragonite at 25°C. *Geochimica et Cosmochimica Acta*, 70, A318. <https://doi.org/10.1016/j.gca.2006.06.643>
- Kim, S.-T., & O'Neil, J. R. (1997). Equilibrium and nonequilibrium oxygen isotope effects in synthetic carbonates. *Geochimica et Cosmochimica Acta*, 61, 3461–3475. [https://doi.org/10.1016/S0016-7037\(97\)00169-5](https://doi.org/10.1016/S0016-7037(97)00169-5)
- Kim, S. T., O'Neil, J. R., Hillaire-Marcel, C., & Mucci, A. (2007). Oxygen isotope fractionation between synthetic aragonite and water: Influence of temperature and  $\text{Mg}^{2+}$  concentration. *Geochimica et Cosmochimica Acta*, 71, 4704–4715. <https://doi.org/10.1016/j.gca.2007.04.019>
- Kingsford, R. T., Walker, K. F., Lester, R. E., Young, W. J., Fairweather, P. G., Sammut, J., & Geddes, M. C. (2011). A Ramsar wetland in crisis the Coorong, Lower Lakes and Murray Mouth, Australia. *Marine and Freshwater Research*, 62, 255–265. <https://doi.org/10.1071/MF09315>
- Koutavas, A., DeMenocal, P. B., Olive, G. C., & Lynch-Stieglitz, J. (2006). Mid-Holocene El Niño-Southern Oscillation (ENSO) attenuation revealed by individual foraminifera in eastern tropical Pacific sediments. *Geology*, 34, 993–996. <https://doi.org/10.1130/G22810A.1>
- Lautenschlager, A. D., Matthews, T. G., & Quinn, G. P. (2014). Utilization of organic matter by invertebrates along an estuarine gradient in an intermittently open estuary. *Estuarine, Coastal and Shelf Science*, 149, 232–243. <https://doi.org/10.1016/j.ecss.2014.08.020>
- Lécuyer, C., Reynard, B., & Martineau, F. (2004). Stable isotope fractionation between mollusc shells and marine waters from Martinique Island. *Chemical Geology*, 213, 293–305. <https://doi.org/10.1016/j.chemgeo.2004.02.001>
- Lorrain, A., Paulet, Y. M., Chauvaud, L., Dunbar, R., Mucciarone, D., & Fontugne, M. (2004).  $\delta^{13}\text{C}$  variation in scallop shells: Increasing metabolic carbon contribution with body size? *Geochimica et Cosmochimica Acta*, 68, 3509–3519. <https://doi.org/10.1016/j.gca.2004.01.025>
- Lower, C. S., Cann, J. H., & Haynes, D. (2013). Microfossil evidence for salinity events in the Holocene Coorong Lagoon, South Australia. *Australian Journal of Earth Sciences*, 60, 573–587. <https://doi.org/10.1080/08120099.2013.823112>
- Matthews, T. G., & Constable, A. J. (2004). Effect of flooding on estuarine bivalve populations near the mouth of the Hopkins River, Victoria, Australia. *Journal of the Marine Biological Association of the United Kingdom*, 84, 633–639. <https://doi.org/10.1017/s0025315404009671h>

- McConnaughey, T. A., Burdett, J., Whelan, J. F., & Paull, C. K. (1997). Carbon isotopes in biological carbonates: Respiration and photosynthesis. *Geochimica et Cosmochimica Acta*, 61, 611–622. [https://doi.org/10.1016/S0016-7037\(96\)00361-4](https://doi.org/10.1016/S0016-7037(96)00361-4)
- McConnaughey, T. A., & Gillikin, D. P. (2008). Carbon isotopes in mollusk shell carbonates. *Geo-Marine Letters*, 28, 287–299. <https://doi.org/10.1007/s00367-008-0116-4>
- McKirdy, D. M., Thorpe, C. S., Haynes, D. E., Grice, K., Krull, E., Halverson, G. P., & Webster, L. J. (2010). The biogeochemical evolution of the Coorong during the mid- to late Holocene: An elemental, isotopic and biomarker perspective. *Organic Geochemistry*, 41, 96–110. <https://doi.org/10.1016/j.orggeochem.2009.07.010>
- Mohan, J. A., & Walther, B. D. (2015). Spatiotemporal variation of trace elements and stable isotopes in subtropical estuaries: II. Regional, local, and seasonal salinity-element relationships. *Estuaries and Coasts*, 38, 769–781. <https://doi.org/10.1007/s12237-014-9876-4>
- Mosley, L. M., Fitzpatrick, R. W., Palmer, D., Leyden, E., & Shand, P. (2014). Changes in acidity and metal geochemistry in soils, groundwater, drain and river water in the Lower Murray River after a severe drought. *The Science of the Total Environment*, 485–486, 281–291. <https://doi.org/10.1016/j.scitotenv.2014.03.063>
- Owen, E. F., Wanamaker, A. D., Feindel, S. C., Schöne, B. R., & Rawson, P. D. (2008). Stable carbon and oxygen isotope fractionation in bivalve (*Placopecten magellanicus*) larval aragonite. *Geochimica et Cosmochimica Acta*, 72, 4687–4698. <https://doi.org/10.1016/j.gca.2008.06.029>
- Owen, R., Kennedy, H., & Richardson, C. (2002). Experimental investigation into partitioning of stable isotopes between scallop (*Pecten maximus*) shell calcite and sea water. *Palaeogeography, Palaeoclimatology, Palaeoecology*, 185, 163–174. [https://doi.org/10.1016/S0031-0182\(02\)00297-3](https://doi.org/10.1016/S0031-0182(02)00297-3)
- Paton, D. C., Rogers, D. J., Hill, B. M., Bailey, C. P., & Ziembicki, M. (2009). Temporal changes to spatially stratified waterbird communities of the Coorong, South Australia: Implications for the management of heterogeneous wetlands. *Animal Conservation*, 12, 408–417. <https://doi.org/10.1111/j.1469-1795.2009.00264.x>
- Pérez, L., Curtis, J., Brenner, M., Hodell, D., Escobar, J., Lozano, S., & Schwal, A. (2013). Stable isotope values ( $\delta^{18}\text{O}$  &  $\delta^{13}\text{C}$ ) of multiple ostracode species in a large neotropical lake as indicators of past changes in hydrology. *Quaternary Science Reviews*, 66, 96–111. <https://doi.org/10.1016/j.quascirev.2012.10.044>
- Pfister, L., Grave, C., Beisel, J. N., & McDonnell, J. J. (2019). A global assessment of freshwater mollusk shell oxygen isotope signatures and their relation to precipitation and stream water. *Scientific Reports*, 9, 1–6. <https://doi.org/10.1038/s41598-019-40369-0>
- Poulain, C., Lorrain, A., Mas, R., Gillikin, D. P., Dehairs, F., Robert, R., & Paulet, Y. M. (2010). Experimental shift of diet and DIC stable carbon isotopes: Influence on shell  $\delta^{13}\text{C}$  values in the Manila clam *Ruditapes philippinarum*. *Chemical Geology*, 272, 75–82. <https://doi.org/10.1016/j.chemgeo.2010.02.006>
- Price, R. M., Skrzypek, G., Grierson, P. F., Swart, P. K., & Fourqurean, J. W. (2012). The use of stable isotopes of oxygen and hydrogen to identify water sources in two hypersaline estuaries with different hydrologic regimes. *Marine and Freshwater Research*, 63, 952–966. <https://doi.org/10.1071/MF12042>
- Reeves, J. M., Haynes, D., García, A., & Gell, P. A. (2015). Hydrological change in the Coorong estuary, Australia, past and present: Evidence from fossil invertebrate and algal assemblages. *Estuaries and Coasts*, 38, 2101–2116. <https://doi.org/10.1007/s12237-014-9920-4>
- Roy, R., Wang, Y., & Jiang, S. (2019). Growth pattern and oxygen isotopic systematics of modern freshwater mollusks along an elevation transect: Implications for paleoclimate reconstruction. *Palaeogeography, Palaeoclimatology, Palaeoecology*, 532, 109243. <https://doi.org/10.1016/j.palaeo.2019.109243>
- Royer, C., Thébault, J., Chauvaud, L., & Olivier, F. (2013). Structural analysis and paleoenvironmental potential of dog cockle shells (*Glycymeris glycymeris*) in Brittany, northwest France. *Palaeogeography, Palaeoclimatology, Palaeoecology*, 373, 123–132. <https://doi.org/10.1016/j.palaeo.2012.01.033>
- Schöne, B. R., Freyre Castro, A. D., Fiebig, J., Houk, S. D., Oschmann, W., & Kröncke, I. (2004). Sea surface water temperatures over the period 1884–1983 reconstructed from oxygen isotope ratios of a bivalve mollusk shell (*Arctica islandica*, southern North Sea). *Palaeogeography, Palaeoclimatology, Palaeoecology*, 212, 215–232. <https://doi.org/10.1016/j.palaeo.2004.05.024>
- Schöne, B. R., Meret, A. E., Baier, S. M., Fiebig, J., Esper, J., McDonnell, J., & Pfister, L. (2020). Freshwater pearl mussels from northern Sweden serve as long-term, high-resolution stream water isotope recorders. *Hydrology and Earth System Sciences*, 24, 673–696. <https://doi.org/10.5194/hess-24-673-2020>
- Schöne, B. R., Pfeiffer, M., Pohlmann, T., & Siegmund, F. (2005). A seasonally resolved bottom-water temperature record for the period AD 1866–2002 based on shells of *Arctica islandica* (Mollusca, North Sea). *International Journal of Climatology*, 25, 947–962. <https://doi.org/10.1002/joc.1174>
- Schöne, B. R., Rodland, D. L., Fiebig, J., Oschmann, W., Goodwin, D., Flessa, K. W., & Dettman, D. (2006). reliability of multitaxon, multiproxy reconstructions of environmental conditions from accretionary biogenic skeletons. *The Journal of Geology*, 114, 267–285. <https://doi.org/10.1086/501219>
- Shao, Y., Farkaš, J., Holmden, C., Mosley, L., Kell-Duivesteyn, I., Izzo, C., et al. (2018). Calcium and strontium isotope systematics in the lagoon-estuarine environments of South Australia: Implications for water source mixing, carbonate fluxes and fish migration. *Geochimica et Cosmochimica Acta*, 239, 90–108. <https://doi.org/10.1016/j.gca.2018.07.036>
- Simpson, H. J., & Herczeg, A. L. (1991). Stable isotopes as an indicator of evaporation in the River Murray, Australia. *Water Resources Research*, 27, 1925–1935. <https://doi.org/10.1029/91wr00941>
- Simstich, J., Harms, I., Karcher, M. J., Erlenkeuser, H., Stanovoy, V., Kodina, L., et al. (2005). Recent freshening in the Kara Sea (Siberia) recorded by stable isotopes in Arctic bivalve shells. *Journal of Geophysical Research*, 110, 1–11. <https://doi.org/10.1029/2004JC002722>
- Stalker, J. C., Price, R. M., & Swart, P. K. (2009). Determining spatial and temporal inputs of freshwater, including submarine groundwater discharge, to a subtropical estuary using geochemical tracers, Biscayne Bay, South Florida. *Estuaries and Coasts*, 32, 694–708. <https://doi.org/10.1007/s12237-009-9155-y>
- Surge, D. M., & Lohmann, K. C. (2002). Temporal and spatial differences in salinity and water chemistry in SW Florida estuaries: Effects of human-impacted watersheds. *Estuaries*, 25, 393–408. <https://doi.org/10.1007/BF02695982>
- Surge, D. M., Lohmann, K. C., & Goodfriend, G. A. (2003). Reconstructing estuarine conditions: Oyster shells as recorders of environmental change, Southwest Florida. *Estuarine, Coastal and Shelf Science*, 57, 737–756. [https://doi.org/10.1016/S0272-7714\(02\)00370-0](https://doi.org/10.1016/S0272-7714(02)00370-0)
- Swart, P. K., & Price, R. (2002). Origin of salinity variations in Florida Bay. *Limnology & Oceanography*, 47, 1234–1241. <https://doi.org/10.4319/lo.2002.47.4.1234>
- Torres, M. E., Zima, D., Falkner, K. K., McDonald, R. W., O'Brien, M., Schöne, B. R., & Siferd, T. (2011). Hydrographic changes in Nares Strait (Canadian Arctic Archipelago) in recent decades based on  $\delta^{18}\text{O}$  profiles of bivalve shells. *Arctic*, 64, 45–58. <https://doi.org/10.14430/arctic4079>

- Tynan, S., Dutton, A., Eggins, S., & Opdyke, B. (2014). Oxygen isotope records of the Australian flat oyster (*Ostrea angasi*) as a potential temperature archive. *Marine Geology*, 357, 195–209. <https://doi.org/10.1016/j.margeo.2014.07.009>
- Urey, H. C. (1947). The thermodynamic properties of isotopic substances. *Journal of the Chemical Society*, 562–581. <https://doi.org/10.1039/jr9470000562>
- Walther, B. D., & Nims, M. K. (2015). Spatiotemporal variation of trace elements and stable isotopes in subtropical estuaries: I. Freshwater endmembers and mixing curves. *Estuaries and Coasts*, 38, 754–768. <https://doi.org/10.1007/s12237-014-9881-7>
- Wang, Z., Gaetani, G., Liu, C., & Cohen, A. (2013). Oxygen isotope fractionation between aragonite and seawater: Developing a novel kinetic oxygen isotope fractionation model. *Geochimica et Cosmochimica Acta*, 117, 232–251. <https://doi.org/10.1016/j.gca.2013.04.025>
- Watkins, J. M., Hunt, J. D., Ryerson, F. J., & DePaolo, D. J. (2014). The influence of temperature, pH, and growth rate on the  $\delta^{18}\text{O}$  composition of inorganically precipitated calcite. *Earth and Planetary Science Letters*, 404, 332–343. <https://doi.org/10.1016/j.epsl.2014.07.036>
- Watkins, J. M., Nielsen, L. C., Ryerson, F. J., & Depaolo, D. J. (2013). The influence of kinetics on the oxygen isotope composition of calcium carbonate. *Earth and Planetary Science Letters*, 375, 349–360. <https://doi.org/10.1016/j.epsl.2013.05.054>
- Wells, F. E., & Threlfall, T. J. (1982a). Salinity and temperature tolerance of *Hydrococcus brazieri* (T. Woods, 1876) and *Arthritica semen* (Menke, 1843) from the Peel-Harvey estuarine system, Western Australia. *Journal of the Malacological Society of Australia*, 5, 151–156. <https://doi.org/10.1080/00852988.1982.10673947>
- Wells, F. E., & Threlfall, T. J. (1982b). Density fluctuations, growth and dry tissue production of *Hydrococcus Brazieri* (Tenison Woods, 1876) and *Arthritica semen* (Menke, 1843) in Peel Inlet, Western Australia. *Journal of Molluscan Studies*, 48, 310–320. <https://doi.org/10.1093/oxfordjournals.mollus.a065653>
- Whisson, C. S., Wells, F. E., & Rose, T. (2004). The benthic invertebrate fauna of the Peel-Harvey Estuary of south-western Australia after completion of the Dawesville Channel. *Records of the Western Australian Museum*, 22, 81–90. [https://doi.org/10.18195/issn.0312-3162.22\(2\).2004.081-090](https://doi.org/10.18195/issn.0312-3162.22(2).2004.081-090)
- Wurster, C. M., & Patterson, W. P. (2001). Seasonal variation in stable oxygen and carbon isotope values recovered from modern lacustrine freshwater molluscs: Paleoclimatological implications for sub-weekly temperature records. *Journal of Paleolimnology*, 26, 205–218. <https://doi.org/10.1023/A:1011194011250>
- Zeebe, R. (1999). An explanation of the effect of seawater carbonate concentration on foraminiferal oxygen isotopes. *Geochimica et Cosmochimica Acta*, 63, 2001–2007. [https://doi.org/10.1016/S0016-7037\(99\)00091-5](https://doi.org/10.1016/S0016-7037(99)00091-5)
- Zhao, L., Schöne, B. R., & Mertz-Kraus, R. (2017). Controls on strontium and barium incorporation into freshwater bivalve shells (*Corbicula fluminea*). *Palaeogeography, Palaeoclimatology, Palaeoecology*, 465, 386–394. <https://doi.org/10.1016/j.palaeo.2015.11.040>